Jeenat Aslam and Chandrabhan Verma (Eds.)

# Fiber Materials

# Also of interest

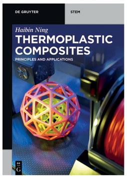

*Thermoplastic Composites.*
*Principles and Applications*
Haibin Ning, 2022
ISBN 978-1-5015-1903-1, e-ISBN 978-1-5015-1905-5

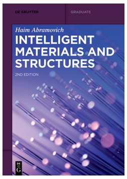

*Intelligent Materials and Structures*
Haim Abramovich, 2021
ISBN 978-3-11-072669-5, e-ISBN 978-3-11-072670-1

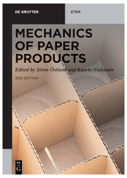

*Mechanics of Paper Products*
Sören Östlund and Kaarlo Niskanen (Eds.), 2021
ISBN 978-3-11-061741-2, e-ISBN 978-3-11-061938-6

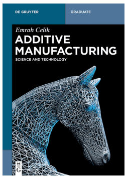

*Additive Manufacturing.*
*Science and Technology*
Emrah Celik, 2020
ISBN 978-1-5015-1877-5, e-ISBN 978-1-5015-1878-2

# Fiber Materials

## Design, Fabrication and Applications

Edited by
Jeenat Aslam and Chandrabhan Verma

DE GRUYTER

**Editors**

Dr. Jeenat Aslam
Department of Chemistry
College of Science
Taibah University
Yanbu 30799
Al-Madina
Saudi Arabia
drjeenataslam@outlook.com

Chandrabhan Verma
Interdisciplinary Research Center
for Advanced Materials
King Fahd University of Petroleum
and Minerals
Dharan 31261
Saudi Arabia
Chandraverma.rs.apc@itbhu.ac.in

ISBN 978-3-11-099274-8
e-ISBN (PDF) 978-3-11-099289-2
e-ISBN (EPUB) 978-3-11-098106-3

**Library of Congress Control Number: 2023930471**

**Bibliographic information published by the Deutsche Nationalbibliothek**
The Deutsche Nationalbibliothek lists this publication in the Deutsche Nationalbibliografie; detailed bibliographic data are available on the internet at http://dnb.dnb.de.

© 2023 Walter de Gruyter GmbH, Berlin/Boston
Cover image: marekuliasz/iStock/Getty Images Plus
Typesetting: Integra Software Services Pvt. Ltd.
Printing and binding: CPI books GmbH, Leck

www.degruyter.com

# Preface

Fiber materials are extremely important in the global economy because they are used in a variety of forms for a wide range of applications (aerospace, biomedical, energy, agriculture, civil construction, architecture, environment, waste management applications, etc.). Natural fibers (cotton, hemp, coir, flax, ramie, jute, silk and wool fiber, etc.) and synthetic fibers are the two major categories of fibers (viscose, cellulose acetate, polyester, polyamide, polyolefin, polyimide, aramid, polyurethane, glass, carbon fibers, etc.). Fibers are a remarkably old and plentiful material form. Fibers have been important in our individual lives since the beginning of time, and they have had a profound influence on the development of humanity for many thousands of years. Today, the development of fibers with unique properties is a driving force in industrial innovation, particularly in high-tech applications. Our goal is to contribute to the development of safer, more sustainable fiber in our living environment. The profoundly driven advancement of advanced fibers has the potential to find many novel applications.

The present book describes the recent advancement in the synthesis, characterization and applications of advanced fiber materials. Overall, the book is divided into two parts. Part 1 contains three chapters. Chapter 1 aims to describe the fundamentals and overview of advanced fiber materials. In Chapters 2 and 3, synthesis, characterization and properties of advanced fiber materials are described. Part 2 contains 11 chapters and each chapter reports a specific application of advanced fiber materials. In this book, pollution control, environment, energy, energy and information storage, optical and photonics, photocatalytic, textile, drug delivery, tumor therapy, and corrosion protection ability of advanced fiber materials are extensively reported and described. The last chapter talks about the state-of-art, future direction, opportunities and challenges in using advanced fiber materials for different industrial, biological, medical and environmental applications.

We editors, Dr. Jeenat Aslam and Dr. Chandrabhan Verma, would like to thank to all contributors for their great efforts. On behalf of De Gruyter, we are very thankful to the authors of all chapters for their amazing and passionate efforts in making this book. Special thanks to Dr. Christene Smith (acquisitions editor) and Ms. Stella Muller (content editor) for their dedicated support and help during this project. In the end all thanks to De Gruyter for publishing the book.

Jeenat Aslam
Chandrabhan Verma

https://doi.org/10.1515/9783110992892-202

# Contents

**Preface —— V**

**Editors’ biographies —— IX**

**List of contributing authors —— XI**

Ritika Wadhwa, Arushi Arora, Supriya Rana, Krishna K. Yadav
**Chapter 1**
**Overview of advanced fiber materials —— 1**

Omar Dagdag, Rajesh Haldhar, Seong-Cheol Kim, Elyor Berdimurodov,
Ekemini D. Akpan, Eno E. Ebenso
**Chapter 2**
**Synthesis, characterization, and properties of advanced fiber materials —— 17**

Pragnesh N. Dave and Pradip M. Macwan
**Chapter 3**
**Fabrication of advanced fiber materials —— 31**

Elyor Berdimurodov, Abduvali Kholikov, Khamdam Akbarov, Brahim El Ibrahimi,
Dakeshwar Kumar Verma, Khasan Berdimuradov, Omar Dagdag, Nuritdin Kattaev,
Nurbek Umirov
**Chapter 4**
**Advanced fiber materials in pollution control —— 89**

Gianluca Viscusi
**Chapter 5**
**Advanced fibre materials for environmental applications —— 103**

Amarpreet K. Bhatia, Shippi Dewangan
**Chapter 6**
**Advanced fiber materials in energy applications —— 149**

Aiswarya R.
**Chapter 7**
**Advanced fiber materials in information storage technology —— 171**

Ritika Wadhwa, Arushi Arora, Krishna K. Yadav
**Chapter 8**
**Advanced fiber materials in optical and photonic application —— 191**

Anastasiia Rymzhina, Nishant Tripathi, Prachi Sharma, Vladimir Pavelyev
**Chapter 9**
**Advanced fibers for photocatalysis application —— 219**

Manash Protim Mudoi, Vidushi Singh, Harroop Kaur, Asmita Choudhary
**Chapter 10**
**Advanced fiber materials in textile —— 259**

Pragnesh N. Dave and Pradip M. Macwan
**Chapter 11**
**Advanced fiber materials in drug delivery —— 273**

Shveta Sharma, Manu Sharma, Richika Ganjoo, Ashish Kumar
**Chapter 12**
**Advanced fiber material in tumor therapy —— 327**

Farhat A. Ansari and Hariom K. Sharma
**Chapter 13**
**Advanced fiber materials in corrosion protection —— 339**

Bhuvaneshwaran Mylsamy, Karthik Aruchamy, Sampath Pavayee Subramani, Sathish Kumar Palaniappan, Sanjay Mavinkere Rangappa, Suchart Siengchin
**Chapter 14**
**State of the art of advanced fiber materials: future directions, opportunities, and challenges —— 357**

**Index —— 373**

# Editors' biographies

**Dr. Jeenat Aslam** is Associate Professor at the Department of Chemistry, College of Science, Taibah University, Yanbu, Al-Madina, Saudi Arabia. She earned her PhD in Surface Science/Chemistry at the Aligarh Muslim University, Aligarh, India. Her research is mainly focused on materials and corrosion, nanotechnology and surface chemistry. Dr. Jeenat has published several research and review articles in peer-reviewed international journals of ACS, Wiley, Elsevier, Springer, Taylor & Francis, Bentham Science, etc. She has edited many books for American Chemical Society, Elsevier, Springer, Wiley, De Gruyter and Taylor & Francis, and has contributed 29 book chapters.

**Dr. Chandrabhan Verma** works at the Interdisciplinary Center for Research in Advanced Materials, King Fahd University of Petroleum and Minerals (KFUPM), Saudi Arabia. He earned his PhD in Material Science/Chemistry at the Indian Institute of Technology (Banaras Hindu University) Varanasi, India. He is a member of American Chemical Society (ACS) and also serves as a reviewer and editorial board member for various publishers of international repute: ACS, the Royal Society of Chemistry (RSC), Elsevier, Wiley and Springer. Dr. Verma is Associate Editor-in-Chief of journal *Organic Chemistry Plus*. His several research and review articles have been published by ACS, Elsevier, RSC, Wiley and Springer. He has a total citation of more than 8,456 with an H-index of 52 and i-10 index of 135. Dr. Verma has edited many books for ACS, Elsevier, RSC and Wiley. He has received several awards for his academic achievements.

https://doi.org/10.1515/9783110992892-204

# List of contributing authors

**Ritika Wadhwa**
Institute of Nano Science and Technology
Knowledge City
Sector 81
Mohali 140306
India

**Arushi Arora**
Institute of Nano Science and Technology
Knowledge City
Sector 81
Mohali 140306
India

**Supriya Rana**
Institute of Nano Science and Technology
Knowledge City
Sector 81
Mohali 140306
India

**Krishna K. Yadav**
Institute of Nano Science and Technology
Knowledge City
Sector 81
Mohali 140306
India
email: Krishnay447@gmail.com

**Omar Dagdag**
Centre for Materials Science
College of Science Engineering and Technology
University of South Africa
Johannesburg 1710
South Africa

**Rajesh Haldhar**
School of Chemical Engineering
Yeungnam University
Gyeongsan 38541
Republic of Korea

**Seong-Cheol Kim**
School of Chemical Engineering
Yeungnam University
Gyeongsan 38541
Republic of Korea

**Elyor Berdimurodov**
Faculty of Chemistry
National University of Uzbekistan
Tashkent 100034
Uzbekistan
email: elyor170690@gmail.com

**Ekemini D. Akpan**
Centre for Materials Science
College of Science
Engineering and Technology
University of South Africa
Johannesburg 1710
South Africa

**Eno E. Ebenso**
Centre for Materials Science
College of Science Engineering and Technology
University of South Africa
Johannesburg 1710
South Africa

**Pragnesh N. Dave**
Department of Chemistry
Sardar Patel University
Vallabh Vidyangar 388 120
Gujarat
India
email: pragnesh7@yahoo.com

**Pradip M. Macwan**
B. N. Patel Institute of Paramedical and Science
(Science Division)
Sardar Patel Education Trust
Bhalej Road
Anand 388001
Gujarat
India

https://doi.org/10.1515/9783110992892-205

**Abduvali Kholikov**
Faculty of Chemistry
National University of Uzbekistan
Tashkent 100034
Uzbekistan

**Khamdam Akbarov**
Faculty of Chemistry
National University of Uzbekistan
Tashkent 100034
Uzbekistan

**Brahim El Ibrahimi**
Department of Applied Chemistry
Faculty of Applied Sciences
Ibn Zohr University
86153
Morocco

**Dakeshwar Kumar Verma**
Department of Chemistry
Government Digvijay Autonomous Postgraduate College
Rajnandgaon
Chhattisgarh 491441
India

**Khasan Berdimuradov**
Faculty of Industrial Viticulture and Food Production Technology
Tashkent Institute of Chemical Technology
Shahrisabz 181306
Uzbekistan

**Omar Dagdag**
Centre for Materials Science
College of Science
Engineering and Technology
University of South Africa
Johannesburg 1710
South Africa

**Nuritdin Kattaev**
Faculty of Chemistry
National University of Uzbekistan
Tashkent 100034
Uzbekistan

**Nurbek Umirov**
Faculty of Chemistry-Biology
Karshi State University
Karshi 130100
Uzbekistan

**Gianluca Viscusi**
Department of Industrial Engineering
University of Salerno
Via Giovanni Paolo II
132 84084 Fisciano (SA)
Italy
email: gviscusi@unisa.it

**Amarpreet K. Bhatia**
Department of Chemistry
Bhilai Mahila Mahavidyalaya
Bhilai Nagar 490006
Chhattisgarh
India

**Shippi Dewangan**
Department of Chemistry
S. W. Pukeshwar Singh Bhardiya Govt. College
Nikum
Durg 491221
Chhattisgarh
India
email: shippidewangan2729@gmail.com

**Aiswarya R.**
Department of Physics and Nanotechnology
S. R. M. Institute of Science and Technology
Potheri, Kattankulathur 603203
Chengalpattu District
Tamil Nadu
India
email: aiswaryaais16@gmail.com

**Ritika Wadhwa**
Institute of Nano Science and Technology
Knowledge City
Sector 81
Mohali 140306
India

**Arushi Arora**
Institute of Nano Science and Technology
Knowledge City
Sector 81
Mohali 140306
India

**Krishna K. Yadav**
Institute of Nano Science and Technology
Knowledge City
Sector 81
Mohali 140306
India

**Anastasiia Rymzhina**
Samara National Research University
34 Moskovskoye Shosse
Samara 443086
Russia

**Nishant Tripathi**
Samara National Research University
34 Moskovskoye Shosse
Samara 443086
Russia
email: nishant.tripathi.11@gmail.com

**Prachi Sharma**
Samara National Research University
34 Moskovskoye Shosse
Samara 443086
Russia
and
School of Electronics Engineering (SENSE)
Vellore Institute of Technology (VIT)
Vellore
Tamil Nadu 632014
India

**Vladimir Pavelyev**
Samara National Research University
34 Moskovskoye Shosse
Samara 443086
Russia
and
IPSI RAS – Branch of the FSRC "Crystallography and Photonics" RAS
443001
Samara
Russia
Molodogvardeyskaya 151

**Manash Protim Mudoi**
Department of Chemical Engineering
Indian Institute of Technology
Roorkee 247667
Uttarakhand
India
and
Department of Chemical Engineering
University of Petroleum and Energy Studies
Dehradun 248007
Uttarakhand
India

**Vidushi Singh**
Department of Chemical Engineering
University of Petroleum and Energy Studies
Dehradun 248007
Uttarakhand
India

**Harroop Kaur**
Department of Chemical Engineering
University of Petroleum and Energy Studies
Dehradun 248007
Uttarakhand
India

**Asmita Choudhary**
Department of Chemical Engineering
University of Petroleum and Energy Studies
Dehradun 248007
Uttarakhand
India

**Pragnesh N. Dave**
Department of Chemistry
Sardar Patel University
Vallabh Vidyangar 388120
Gujarat
India
email: pragnesh7@yahoo.com

**Pradip M. Macwan**
B. N. Patel Institute of Paramedical and Science
(Science Division)
Sardar Patel Education Trust
Bhalej Road
Anand 388001
Gujarat
India

**Shveta Sharma**
Department of Chemistry
Government College Una
Affiliated to Himachal Pradesh University
India

**Manu Sharma**
Department of Orthopaedics
Maharishi Markandeshwar Medical College and Hospital
Solan, Himachal Pradesh
India

**Richika Ganjoo**
Department of Chemistry
School of Chemical Engineering and Physical Sciences
Lovely Professional University
Chaheru, Punjab
India

**Ashish Kumar**
Department of Chemistry
Department of Science and Technology
Government of Bihar
India
email: drashishchemlpu@gmail.com

**Farhat A. Ansari**
Department of Pharmacy
Faculty of Pharmaceutical Chemistry
Hygia Institute of Pharmaceutical Education and Research
Faizullahganj
Lucknow 226020
India
email: farhataisha@gmail.com

**Hariom K. Sharma**
Engineering Department
University of Technology and Applied Sciences (UTAS)
Salalah, Dhofar
Sultanate of Oman

**Bhuvaneshwaran Mylsamy**
Department of Mechanical Engineering
K. S. R. College of Engineering
Tiruchengode
Tamil Nadu 637215
India

**Karthik Aruchamy**
Department of Mechatronics Engineering
Akshaya College of Engineering and Technology
Coimbatore
Tamil Nadu 642109
India

**Sampath Pavayee Subramani**
Department of Mechanical Engineering
K. S. Rangasamy College of Technology
Tiruchengode
Tamil Nadu 637215
India

**Sathish Kumar Palaniappan**
Natural Composites Research Group Lab
Department of Materials and Production Engineering
The Sirindhorn International Thai-German Graduate School of Engineering (TGGS)
King Mongkut's University of Technology North Bangkok (KMUTNB)
Bangkok 10800
Thailand

**Sanjay Mavinkere Rangappa**
Natural Composites Research Group Lab
Department of Materials and Production Engineering
The Sirindhorn International Thai-German Graduate School of Engineering (TGGS)
King Mongkut's University of Technology North Bangkok (KMUTNB)
Bangkok 10800
Thailand

**Suchart Siengchin**
Natural Composites Research Group Lab
Department of Materials and Production Engineering
The Sirindhorn International Thai-German Graduate School of Engineering (TGGS)
King Mongkut's University of Technology North Bangkok (KMUTNB)
Bangkok 10800
Thailand

Ritika Wadhwa, Arushi Arora, Supriya Rana, Krishna K. Yadav*

# Chapter 1
# Overview of advanced fiber materials

**Abstract:** Fiber-based materials have shown their important role in almost all fields of science, including energy harvesting, optics, communication, water purification, and electrocatalysis. Their abundance, flexibility, structural reformation, high surface area, tunable chemical composition, and abundant composite forms make the fiber one of the most desirable materials for current and future devices. Earlier, considerable research efforts have been carried out with natural fibers, especially in the field of textiles; however, once synthetic fibers came into the picture, they changed the scenario. Synthetic fibers are nowadays highly used in wearable devices. The network of synthetic fibers facilitates charge transportation, and their large surface makes them vibrant candidates for electrochemical application. Our daily life has utilized several types of fiber materials for a long time. In the early days, natural fibers, including loops of jute, coir, and bamboo, were utilized for several applications. However, nowadays, synthetic fibers and their composites with natural fibers play a major role in making human life easy. The advanced fiber-shaped materials can be used in various applications including electronics, sensors, catalysis, and photonics. The present chapter deals with the basics of natural and advanced fibers and their few applications. Finally, the research challenges have been discussed and the prospects of fiber materials have been proposed.

**Keywords:** Natural fibers, synthetic fibers, applications, synthesis, spinning method

## 1.1 Introduction

Fibers have always been available in the history of mankind. In early days of mankind, woven textiles such as cotton, hemp, linen, silk, and wool have been used in world civilizations across the globe. Later on, synthetic fibers, nanofibers, functionalized fibers, and several fiber-based devices were developed. In the last century, fibers got a boost when silica and plastic optical fibers showed their importance in "***shrinking our world***" by contribution to the development of science and technology. Artificial fibers applications have been changing the world deeply day by day, and it is believed that in the future,

---

***Corresponding author: Krishna K. Yadav,** Institute of Nano Science and Technology, Knowledge City, Sector 81, Mohali 140306, India, e-mail: Krishnay447@gmail.com
**Ritika Wadhwa**, **Arushi Arora**, **Supriya Rana**, Institute of Nano Science and Technology, Knowledge City, Sector 81, Mohali 140306, India

https://doi.org/10.1515/9783110992892-001

fibers will change our daily life seamlessly. In recent days, fiber technology has been widely used in various fields, including chemistry, condensed matter physics, engineering, materials, polymer science, renewable and green energy, and so on. If one says that the present century is the cellulosic century, no one will wonder. Natural fiber comes from bioplants and is generally categorized into two types: primary fibers and secondary fibers. In the primary fiber, the fiber content is initially available in plants, that is, plants grown with fibers; whereas fiber is in the form of a by-product in secondary natural fibers [1]. Most research has been done on natural fibers, which do not cause any harmful impact on our environment, and they are relatively more economical than synthetic fibers, such as glass fibers and carbon fibers. The end application can be made more significant by making fiber composites. Fibers such as jute, sisal, coir, bamboo, banana, pineapple, etc. are primary natural fibers, and jute was the first material that attracted the interest of researchers in the early part of 1981. The interesting fact about jute fibers is that it very useful; the fibers are lightweight and economical but, at the same time, their low strength and modulus are obstacles to their use in various applications. The major uses of jute-reinforced plastics are in housing and in the manufacture of fishing boats. Much work has been carried out to overcome the limitations of jute-reinforced plastics [2]. After the utilization of jute fibers in the preparation of composites, bamboo fibers were used successfully in 1995. Bamboo fibers overcome the limitation of the mechanical properties (modulus and strength) of jute as well as that of reinforced plastics of glass fiber in a unidirectional orientation. Later on, coir fiber was introduced in 1998 [3]. Coir is a lingo-cellulosic fiber obtained from coconut trees and grows mostly in the tropical region. Its durability, wearing quality, low cost, and other factors make coir fiber to be utilized in rope making, yarn, and floor furnishing. The strength in coir fibers arises due to the presence of silica in its lingo-cellulosic matrix. Apart from that, it gets its properties such as not being brittle, nonhazardous, and ability to being disposed off easily from the lingo-cellulosic fiber. The low performance of the coir-reinforced composite is due to the reduced cellulose content along with high micro-fibrillar angle and hemicellulose content. Sisal is another natural fiber of a lingo-cellulosic material derived from the AgaveSisalana plant. The addition of the sisal fiber limits the cost of elastomers and plastics. The development of natural fibers has been shown in Figure 1.1 [3]. In the present

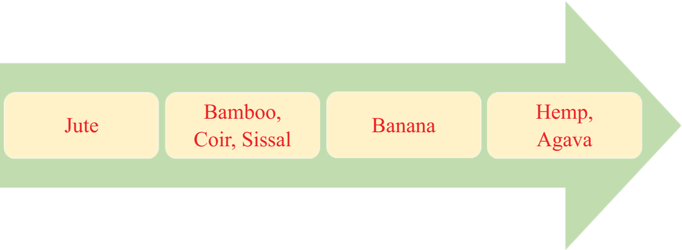

**Figure 1.1:** Development of natural fibers.

chapter, the types of fibers and a few of their applications have been discussed, which will give a further research scope to any scholar in the natural fiber composites field.

## 1.2 Types of fibers

Fibers can mostly be classified into two categories: (1) natural fibers and (2) synthetic fibers. A few examples of natural and synthetic fibers are listed below. For better clarity, Figure 1.2 has been given; it describes the progress of natural fibers to synthetic fibers. At the same time, it is very challenging to incorporate the types of fibers in one place. Fiber types can be classified based on their application or synthesis protocol.

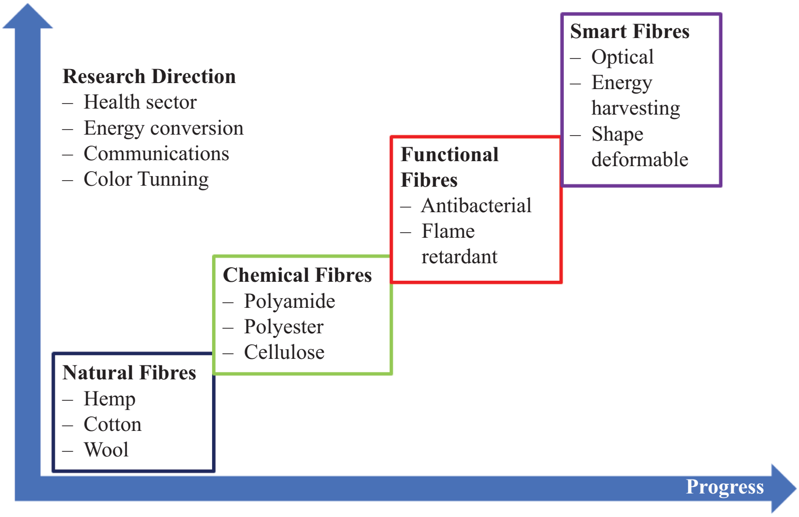
Research Direction
– Health sector
– Energy conversion
– Communications
– Color Tunning
Smart Fibres
– Optical
– Energy harvesting
– Shape deformable
Functional Fibres
– Antibacterial
– Flame retardant
Chemical Fibres
– Polyamide
– Polyester
– Cellulose
Natural Fibres
– Hemp
– Cotton
– Wool
Progress

**Figure 1.2:** Progress of fiber-based materials and their potential applications.

### 1.2.1 Natural fibers

#### 1.2.1.1 Jute

Jute fibers are natural fibers having structures of multi-cellulose, and are made up of random micro-fibrils and cross-sections [4]. Some plastics are fabricated using jute reinforcement, and they provide the plastic a high moisture retention capability; however, during the hybridization process, the density also increases. At the same time, it is a suitable reinforcement in plastic due to its economical cost and lightweight factor.

Sometimes, the limitation of jute reinforcement is overlooked by the utilization of a feasible glass solution; however, it makes the plastic brittle and leads to enhanced erosion. Conventional glass fibers are not economical; they take in too much resin. Therefore, hybrids of jute and glass have been used, which make the composite one of higher strength and stiffness than single jute-reinforced plastics [5]. Erosion occurs at the interface of fiber and the adjacent matrix. The impingement angle plays an important role in the erosion process. It has been seen that a higher strength toward erosion has been obtained with increased hybridization of the jute fiber with synthetic-specific fabric [6]. The mechanical properties can be further enhanced by the treatment of the hybrid composites (glass fiber and jute fiber) with silane and titanate. The alkali treatment of hybrids adds some additional sites for mechanical locking and for an enhanced interfacial bonding strength [7]. The treatment of jute fiber with alkali-treated fiber shows improved mechanical properties. Bio-resin, in the presence of soya milk, has been utilized for the fabrication of jute composite, and it shows higher damage tolerance and impact strength, while these composites also being completely bio-degradable [3].

#### 1.2.1.2 Bamboo

The high modulus of bamboo fiber, as compared to unidirectional glass-reinforced plastic, makes it appropriate for large-scale applications in various sectors of fibers. This fiber can be obtained from the bamboo tree. It is economical and environment friendly [8]. It is sometimes mentioned as natural glass fiber. Bamboo fibers have around 40% higher tensile strength than non-twisted fiber; however carious cells are found in bamboo [9]. The matrix of rubber with bamboo fiber enhances the stiffness of the composite. It has been seen that when natural rubber is used with bamboo, a bonding agent for bond enhancement is needed; a higher curing time will also be needed due to the filler presented in the added bonding agent [8]. The hybrid bamboo, with glass fiber, shows a higher flexural strength when glass reinforcement is on top and bamboo reinforcement is at the bottom [10].

#### 1.2.1.3 Coir

Coconut tree can be found in the tropical regions of the world, and the external part of the coconut fruit is the main source of coir fiber; it is the cheapest all-natural fiber. Various applications are found nowadays, which include usage as doormats, for water cleaning, and as active materials for supercapacitors [11]. It is hard, not brittle, and non-toxic; however, its reinforcing ability is poor and its strength is not up to mark. There are many studies available about coconut as a reinforcement fiber; however, chemically treated coir fibers have been used for reinforcing. In coir, the cellulose content is very low and its high fibrillar angle is an obstacle to its direct use. Coir itself contains hemicellulose (0.15–0.25%), cellulose (36–43%), pectins (3–4%), and lignin (41–45%) [3]. The adhesion properties of coir is very poor, and therefore it is treated with an alkaline solution before reinforcing it with rubber fiber [12]. In coir fiber, the water absorption depends on the fiber and the cellulose percentage available in materials.

#### 1.2.1.4 Sisal

Agava Sisalana fiber plant produces lingo-cellulosic extracted sisal fiber. This fiber can be recycled and reutilized several times with similar properties. It has a high stiffness and a high specific strength. Sisal fiber can be utilized in resin polymeric matrices as reinforcement materials. One sisal plant has around 250 leaves. Up to 1,200 bundles of fiber can be produced from each leaf. As in the case of coir fiber, here too the spiral angel and the cellulose define the strength and stiffness of the fiber [13]. It has been found that the fiber has a higher strength-to-stress ratio when length of fiber is large. Also, alkaline treatment favors higher moisture content [13]. The tensile properties in sisal hybrid with glass fiber can be increased by increasing the glass fiber content; the hybrid can withstand up to 68.55 MPa [14]. It has been also seen that a higher storage modulus, loss modulus, and less moisture absorption occur in 30 wt% of jute and sisal fiber reinforced epoxy composite [15]. The jute and sisal composite has a higher flexural strength, compared to the original fibers.

#### 1.2.1.5 Banana

It is also called the “abaca fiber.” It is highly resistant to seawater. Additionally, it is of the same diameter in all the commercially available cellulose fibers [1]. The presence of high cellulose content and low microfibrillar angle makes it very useful for various applications. The interlocking between phenol formaldehyde and banana is higher than that of phenol-formaldehyde resins and glass [16]. The fiber volume fraction decides the dynamic property of the reinforced polyester composite when made with short banana fiber. Banana fiber can make a composite with nylon 6 blends and high-density polyethene using the extrusion method. Generally, styrene triblock polymer is used to enhance the interfacial adhesion between the resins and the banana fiber. Jute and banana fiber, with 50% each, showed the highest mechanical and thermal properties [17].

#### 1.2.1.6 Sugar cane

Sugar cane fiber is also called “bagasse fiber.” It is available only from nature and renewable fiber. A composite of glass fiber and bagasse fiber can be prepared using compression molding and hand-layup methods. Sugar cane fibers have the potential to reinforce polymers; they offer many advantages when used as a substitute for conventional synthetic glass fiber.

### 1.2.2 Synthetic fibers

Synthetic fiber is the type of fiber that can be synthesized by humans at lab scale or at large scale. The properties of synthetic fibers can greatly be altered by changing various functions, which include the type of fiber materials, the diameter of fibers, and their functionalization. These fibers can be utilized in various advanced sectors of science such as in wearable electronics, drug delivery, the field of imaging and photonics, energy harvesting, making of smart devices, etc. Here, a few advanced types of synthetic fibers have been discussed along with their possible applications.

#### 1.2.2.1 Metals

Traditionally, most d-block elements are economical and have higher conductivity, which makes their role significant in the engineering field. For instance, the conductivity-to-cost ratio of Ni is much higher than that of graphite [18]. For applications in high-end equipment, the design of bulk materials should be such as to make the bulk materials in thin wire form. However, the problems associated with thin metal wire is their rigidity and stiffness, which should be addressed before their application in flexible devices. Nowadays, fiber materials made from low-dimensional nanostructural metals of various structures like nanoflakes, nanowires (NWs), and nanoparticles have shown their importance in making advanced conductive fibers [19]. It has been observed that when nanomaterials interact with fibers, the bonding strength between them is enhanced due to an increase in the surface energy and surface tension. Metal nanomaterials with fibers can be fabricated using several methods, including sputtering, electrodeposition, and wet spinning. Earlier, most noble metals (Ag, Au) along with copper nanowires showed their important role due to their promising character such as thermal/electrical conductivity, mechanical strength, and flexibility [20]. Here, it is important to mention that low-cost synthesis increases the utilization of metal fibers in the scale-up process. It is worth mentioning that in large-scale applications, the electrical resistance might be high at the contact surface of the fiber, and this should be overcome for their application in harsh environments [21].

Here, it might be worth to describe the synthesis of at least one metal nanowire (fiber). We will discuss the synthesis of Gold (Au) nanowires and also some of its properties. Gold is one of the chemically inert and highly conductive metals; it is sometimes considered as one of the top materials having the lowest electrical resistance. Its least electrical resistance makes the Au nanowires very versatile, and therefore several methods have been adopted for gold nanowire synthesis. One of the most adopted synthesis methods is solution-based synthesis using a micellar route. The synthesis route uses CTAB or aqueous solution with $HAuCl_4$ as the gold source, which is reduced using oleic acid/oleylamine in various pH [22]. Apart from the solution-based synthesis, gold nanowire can be also synthesized using physical deposition using lithographically patterned substrate [22]. The one limitation of using this technique is that they are polycrystalline and have rough surfaces; which makes them highly resistive as compared to bulk Au. The increased resistivity might be due to the increased contact surface of gold nanowires, which leads us to understand that these NWs may withstand at low current density [23].

#### 1.2.2.2 Liquid metals (LMs)

In recent days, one new field of metals has started to gain prominence, which is liquid metal. It adopts the traditional properties of metal, such as low resistivity, and at the same time, of a liquid, such as water-like fluids [24]. This special type of material may be either elemental metal or compounds with several other ingredients having a lower melting point. In nature, generally, five elements are regarded as low-melting liquid metals. They are mercury (Hg, −39 °C), francium (Fr, ~27 °C), caesium (Cs, 28.4 °C), gallium (Ga, ~29.8 °C), and rubidium (Rb, ~39 °C) [25]. As an example, Ga- based liquid metals show metallic properties like high electrical conductivity, superior thermal conductivity, and good corrosion resistance. At the same time, they show liquid character such as excellent fluidity, superb flexibility, and low viscosity. To understand this, one can note that the viscosity of the eutectic mixture of gallium-indium is double that of water at 20 °C. At the same time, it is less toxic than Hg. Further, no radioactivity was found, in comparison with Rb, Cs, and Fr. However, LMs hold some very interesting properties. They have some limitations such as low resolution of fabric circuits due to the inherent limitations of macroscopic LMs, but it can be enhanced by sintering conductive traces. Therefore, for practical application in flexible printed electronics, the physical size of LMs should be scaled down. It is also interesting to note in the liquid state of Ga and its alloy, it is generally coated by a thin native oxide layer due to ambient air exposure. The thin layer of gallium oxide over the liquid metal helps to preclude the particles from coalescing in the conductive pathway, and avoid short circuits due to the semiconducting nature of gallium oxide. As mentioned, the nearly room temperature melting point is the uniqueness of LMs; with high boiling temperatures, making the LMs applicable in a wide temperature range (8–2,200 °C) [25].

#### 1.2.2.3 Conductive polymer

After the discovery of doping –making composite or conjugate polymers conductive – the application of intrinsically conductive polymers (ICPs) has increased drastically. Most organic polymers are insulating; at the same time, ICPs can be tuned for electronic, electrical, magnetic, and optical properties. Based on this fact, efforts have been spent for the development of ICPs and their utilization in the field of transistors, energy harvesting (supercapacitors, battery), and field emission display devices. Ideally, the conductivity of ICPs can reach up to ~$10^9$ S/m when the dopant can be removed spatially [26]. Practically, due to the low crystallinity of ICPs, the electrical conductivities are almost similar to inorganic semiconductors and the mobility of the charge carriers is the key factor for achieving high conductivity of ICPs. Several ICPs, including polypyrrole (PPy), polyaniline(PAni), polythiophene (PTh), polyacetylene (PAc), and poly[3,4-(ethylenedioxy)thiophene]:poly(styrenesulfonate) (PEDOT:PSS), have been adopted in the last few years [27]. Out of the several ICPs, the one with lower resistance, good transparency, and higher water solubility – PEDOT:PSS – holds great promises in the field of fiber application [28]. The main challenge to ICPs is the poor thermal stability for fiber-based applications. Hence, it can be used in the RADAR and shielding techniques.

#### 1.2.2.4 Carbon-based material

Their high surface area, low electrical resistance, and their stability in a variable environment make the carbon-based materials excellent candidates as advanced fibers. Depending on their size and morphology, carbon-based materials can be categorized into 0D (carbon quantum dots and graphene quantum dots), 1D (carbon nanotubes, carbon nanofibers, carbon microfibers), 2D (Graphene, MXenes), and 3D (Graphite) [29]. Of the several advanced carbon-based materials, CNTs and graphene have been explored in almost all fields of science, including water treatment, supercapacitors, and electrochemical water oxidation [30–32]. The 1D carbon allotropes, that is, CNTs can be categorized into single-walled CNTs (SWCNTs) and multiwalled CNTs (MWCNTS), and in some textbooks, a third one – double-walled CNTs – is also mentioned. MWCNTs are a collection of SWCNTs, with concentric nature, and the interval spacing between two SWCNTs is 0.34 nm [33]. The higher covalent bond of carbon–carbon makes the CNTs promising for applications where excellent mechanical and physical properties are needed. Additionally, the high $sp^2$ nature SWCNTs shows $10^8$ S/m electrical conductivity, which is higher than bare Cu [34]. However, 1D structures do not easily allow dispersion in common solvents, which limit their practical large-scale applications; at the same time, they try to agglomerate using strong van der Waals attraction. Therefore, a suitable solvent is needed for high-performance CNT-based conductive fibers, which can make reduce the van der Waals attraction. Cellulose is the most abundantly found natural polymer having biocompatibility and biodegradability, as well as high thermal and chemical stability, making them promising materials as conductive fibers via doping or mixing with metal powders, carbon nanomaterials, and so on. Therefore, several studies have been reported on the hybrid of cellulose with CNTs.

#### 1.2.2.5 MXene

After the first report of $Ti_3C_2$MXene by Gogotsi et al., MXene emerged as an advanced 2D-type newborn material [35]. The term, MXenes, is derived analogously to graphene. MXenes may either be the framework of metal carbide or metal nitride, having two or higher layers in which transition metal is presented in a honeycomb-like 2D lattice, and intervened by carbon and/or nitrogen layers occupying the octahedral sites between the neighboring transition metal layers [36]. Generally, MXene is derived from the MAX phase. The formula for MXene is $M_{n+1}X_nT_x$ ($n = 1$–3 and $x$ is a variable), where M = transition metal site, X = carbon or nitrogen sites, and T = the terminated functionalities such as –O, –OH, –F, and –Cl. MXenes are traditionally synthesized by using a top-down approach where the A site is selectively etched to form MXene from the MAX phase. The conductivity surface area and the dispensability of MXene can be easily tuned by surface termination. MXenes are endowed with great potentiality in various applications in the field of catalysis and the energy sector. While there are some advancements in MXene, several drawbacks are also associated with MXenes, such as poor stability, low mechanical flexibility, and easy restacking, which provides us with insights to further develop MXene with higher flexibility and durability for flexible wearable electronics.

Currently, several studies are being carried out for the synthesis of MXene fibers using wet spinning, coating, electrospinning, and scrolling methods [37]. After the synthesis of MXene fibers, they have been successfully fabricated for the required electrical conductivity and mechanical properties (such as MXene/cellulose nanofibrils) [38, 39]. However, it has been observed that the fibers have lesser electrical conductivity and mechanical properties due to the inherently loose layers as compared to their original MXene structures [40]. Till now, continuous efforts have been made for compacting the layered structures that ensures a good balance between electrical conductivity, strength, and toughness.

#### 1.2.2.6 $TiO_2$

These days, the 3D networks of $TiO_2$ nanofibers, synthesized using electrospinning, are getting enhanced visibility in the scientific community, for their application in the field of catalysis, energy storage, and so on [41]. However, the problem associated with the stand-alone $TiO_2$ nanofibers is their brittleness, which limits the practical application of bare $TiO_2$ fibers. Therefore, a cohesive platform is needed in which the strength and reactivity of $TiO_2$ is not compromised, while the brittleness is lowered. It has been found that the immobilization of $TiO_2$ nanoparticles, on or within polymeric nanofibers such as cellulose or polyacrylonitrile (PAN), balanced the brittleness of $TiO_2$ [42]. For this, various routes have been adopted – such as the direct mixing of $TiO_2$ nanostructures into electrospinning precursor solutions, incorporation of Ti-containing compounds into electrospinning precursor solutions, and hydrothermal surface decoration of $TiO_2$ over fabricated nanofibers. These fabricated $TiO_2$ fibers are utilized for water treatment, air purification, and oil–water separation. In one interesting work, $TiO_2$-anchored PVDF nanofibers were electrosprayed on the substrate and used for the removal of toxic pollutants including bisphenol A (BPA), 4-chlorophenol (4-CP), and cimetidine (CMT) [43]. One more challenge arises, which is related to the synthesis. When $TiO_2$ is anchored over the surface then during the application, its stability compromise should be overcome.

## 1.3 Synthesis and application of advanced fibers in stretchable devices

Nowadays, fiber-based devices show their importance in all fields of science, including energy harvestings such as electrocatalysis, solar energy conversion, sensors for metal detection, electronics devices such as wearable electronics, piezoelectric generators, textiles, and communications. The lightweight, higher flexibility, high conductivity in conductive fibers, higher strength, and so on play a major role in their daily-life application. Recently, industrial production of fiber-shaped lithium-ion batteries has fiber gained much visibility in high-performance energy storage [44]. However, it is important to keep in mind the functionalization of fiber-enhanced conductivity and strength, as well as compliance in complicated and harsh environments [45]. The functionalization of fiber-based devices was originally developed for practical applications such as the presence of stress in wearable applications, and opened the window for stretchable fiber-shaped supercapacitors in 2013 [46]. However, delicate fiber-based devices might get damaged due to their low mechanical strength and low electrical conductivity. In the present chapter, few applications based on the fibers have been explored.

Flexibility is of great significance for future devices in almost all wearable applications. Therefore, efforts have been spent in developing fiber-based materials having high stretchability on applying stress. However, the complicated fabrication process in the preparation of stretchable electrodes as well as the coating of the conductive uniform layer is very challenging.

### 1.3.1 Electrochromic fiber devices

The term electrochromism refers to a change in the reversible optical property when materials have been electrochemically oxidized [45]. The electrochromic devices allow real-time tracking of energy storage/harvesting devices and significant attention has been employed to making wearable electrochromic devices. Multi-walled CNTs were used with PANI polymers by electrodeposition and utilized for the electrochromic component in the fiber-based supercapacitors device. They can achieve a specific capacity of 255.5 F/g or 0.189 mF/cm. The multicolor visibility of fiber devices is due to the stacking effect of the parallel electrochromic electrode configuration. For example, Au electrode of helix type was prepared using the template method, followed by gold layer deposition of polyvinyl chloride (PVC) fiber with two adhesive tapes as masks [47]. The tapes (masks) can be removed and electrochromic supercapacitors can be fabricated by depositing various electrochromic materials, such as $TiO_2$ and poly(3-methyl thiophene), onto the helix electrode. The multicolor realization occurs due to the stacking effect of the two helix electrodes, making the supercapacitors attractive to realize continuous processing. The electrochromic fibers can be used as an advanced flexible textile in military clothes where colors can be tuned based on sunlight intensity.

### 1.3.2 Triboelectric nanogenerator

The human body performs several types of actions without fail all the time, and most are a synchronization of physical movements. Taking inspiration from the human body, Triboelectric nanogenerators (TENGs) have been designed, where electrical energy can be acquired by converting mechanical energy [48]. TENGs find their applications in smart wearables due to their excellent flexibility and stretchability. In the present work, nylon fibers were wrapped over the conductive metal wire. Currently, most of the manufacturing units for the fabrication of fibrous TENGs are very new, and they have to mature for handling practical applications in e-textiles. Therefore, a highly flexible and scalable yarn was fabricated using a modified melt-spinning method that has elasticity due to silicone rubber tubes [48]. The e-textile exhibited great flexibility and stretchability, and at the same time, the self-powering system could harvest biomechanical energy.

### 1.3.3 Fibers materials for Li-ion batteries

In earlier days, energy was stored in form of batteries, named lead acid batteries; however, nowadays, Li-ion batteries are replacing lead acid batteries due to their high specific capacitance as well as portability. All the same, there is still a need to improve the lower output voltage, energy density, higher reactivity, and cycling performance. Theoretically, Li-ion has ~3,860 mAh/g, with the lowest electrochemical potential (~3.04 V) and at the same time, lower density (~0.53 g/cm$^3$). Its metal ductility makes it flexible, transportable, and light [49, 50]. Li-ion batteries consist of electrode materials, a current collector, a separator, and an electrolyte. For making flexible devices, flexible energy storage with high energy density is needed. Therefore, currently, lithium-ion batteries with 1D fibrous shape are a good choice. They can be made by the mixing anode materials with fibers, depositing on the current collector, and following up by a wrapping separator. Ultimately, the Li-ion battery can be fabricated.

### 1.3.4 Fibers for solar cells

The flexibility and low cost of fiber polymers have shown their important and unique role in solar cell manufacturing. Generally, fiber-based solar cells are similar to perovskite solar cells, where the donor–acceptor system acts as active layers made up of polymer (carbon-derivative, such as fullerene or PCBM). The electron-hole pair is created when the photons fall on the active layers. However, the high flexibility of the fiber-based solar cells, the cost, small lifetime, and low PCE limit the practical application of fiber-based solar cells. Especially, polymer solar cells (used in textiles) might be further susceptible to mechanical triggers [51, 52]. The latest work shows a 10.28% PCE for platinum-free fiber-shaped solar cells [53].

## 1.4 Conclusions and prospects

The present chapter deals with the history of fibers and their applications. The type of fiber has been also discussed along with representative preparation methods of the functional fiber. Natural and synthetic fibers have been briefly discussed. With respect to synthetic fibers, their application and a few syntheses approaches have been also summarized. MXenes, liquid metals, and carbon-based fibers have been briefly discussed. It is interesting to know that carbon-based fibers such as CNTs are widely used in fiber-based devices because of their excellent electrical conductivity, high mechanical strength, and high specific surface area. However, the inner resistance between the CNTs, in the direction of the wire length, should be further optimized to get higher electrical conductivity. In some cases, the fiber should be grown vertically to get a high current, such as in the case of field emission, and for those, we need a new processing technique [54, 55]. Earlier, the spinning method was adopted for the MWCNTs fiber synthesis; however, low electrical conductivities and high costs are the core issues. The fiber-based materials show their importance mostly for making flexible devices, which should be further enhanced due to the dramatic changes occurring in the practical application of these devices. Both, configuration and stretchability, can be tuned for getting high-performing devices. The addition of elastic rubbers can solve the problem of stretchability; however, it does not do anything to conductivity. Therefore, a balance between stretchability and electrochemical performance needs to be arrived at. Polymers having elastic properties and good electrical conductivity can be a good idea. It has been also observed that performance degradation is due to the delamination of fiber materials. Therefore, materials should have a strong bond at the interface. Apart from these know conditions, we have to explore new conditions, which can improve the fiber-based devices. For instance, the degradation of device performance due to delamination of active materials can be avoided if we could work on self-cleaning functions in fiber-based devices. Other conditions can also be made so that devices can work in high pressure, high temperature and radiation, etc. From a safety point of view, nonflammable electrodes and electrolytes would be a possibility for future fiber-based devices. Last but not the least, the scale-up production of functional fiber devices can be further explored.

## References

[1] Faruk O, Bledzki AK, Fink HP, Sain M. Biocomposites reinforced with natural fibers: 2000–2010. Prog Polym Sci. 2012;37:1552–1596.

[2] Mohan R, Kishore, Shridhar MK, Rao RMVGK. Compressive strength of jute-glass hybrid fibre composites. J Mater Sci Lett. 1983;2(3):99–102.

[3] Shireesha Y, Nandipati G. State of art review on natural fibers. Mater Today: Proc. 2019;18:15–24.

[4] Munikenche Gowda T, Naidu ACB, Chhaya R. Some mechanical properties of untreated jute fabric-reinforced polyester composites. Compos Part A Appl Sci Manuf. 1999;30:277–284.

[5] Mohan R, Kishore. Jute-glass sandwich composites. J Reinf Plast Compos. 1985;4:186–194.

[6] Dalbehera S, Acharya SK. Impact of stacking sequence on tribological wear performance of woven jute-glass hybrid epoxy composites. Tribol – Mater Surf Interfaces. 2016;9:196–201.

[7] Gassan J, Bledzki AK. Possibilities for improving the mechanical properties of jute/epoxy composites by alkali treatment of fibres. Compos Sci Technol. 1999;59:1303–1309.

[8] Ismail H, Edyham MR, Wirjosentono B. Bamboo fibre filled natural rubber composites: the effects of filler loading and bonding agent. Polym Test. 2002;21:139–144.

[9] Tong J, Ren L, Li J, Chen B. Abrasive wear behaviour of bamboo. Tribol Int. 1995;28:323–327.

[10] Samanta S, Muralidhar M, singh TJ, Sarkar S. Characterization of mechanical properties of Hybrid Bamboo/GFRP and Jute/GFRP composites. Mater Today: Proc. 2015;2:1398–1405.

[11] Yadav KK, Singh H, Rana S, Sunaina, Sammi H, Nishanthi ST, Wadhwa R, Khan N, Jha M. Utilization of waste coir fibre architecture to synthesize porous graphene oxide and their derivatives: an efficient energy storage material. J Clean Prod. 2020;124240.

[12] Geethamma VG, Mathew KT, Lakshminarayanan R, Thomas S. Composite of short coir fibres and natural rubber: effect of chemical modification, loading and orientation of fibre. Polymer (Guildf). 1998;39:1483–1491.

[13] Li Y, Mai YW, Ye L. Sisal fibre and its composites: a review of recent developments. Compos Sci Technol. 2000;60:2037–2055.

[14] John K, Naidu SV. Tensile properties of unsaturated polyester-based sisal fiber – glass fiber hybrid composites. J Reinf Plast Compos. 2004;23:1815–1819.

[15] Gupta MK, Srivastava RK. Effect of sisal fibre loading on dynamic mechanical analysis and water absorption behaviour of jute fibre epoxy composite. Mater Today: Proc. 2015;2:2909–2917.

[16] Joseph S, Sreekala MS, Oommen Z, Koshy P, Thomas S. A comparison of the mechanical properties of phenol formaldehyde composites reinforced with banana fibres and glass fibres. Compos Sci Technol. 2002;62:1857–1868.

[17] Boopalan M, Niranjanaa M, Umapathy MJ. Study on the mechanical properties and thermal properties of jute and banana fiber reinforced epoxy hybrid composites. Compos B Eng. 2013;51:54–57.

[18] Zhu C, Wu J, Yan J, Liu X. Advanced fiber materials for wearable electronics. Adv Fiber Mater 2022. 2022;1:1–24.

[19] Wang T, Bao Y, Zhuang M, Li J, Chen J, Xu H. Nanoscale engineering of conducting polymers for emerging applications in soft electronics. Nano Res. 2021;14(9):3112–3125.

[20] Zhao S, Meng X, Liu L, Bo W, Xia M, Zhang R, Cao D, Ahn JH. Polypyrrole-coated copper nanowire-threaded silver nanoflowers for wearable strain sensors with high sensing performance. Chem Eng J. 2021;417:127966.

[21] Chen M, Wang Z, Li K, Wang X, Wei L. Elastic and stretchable functional fibers: A review of materials. Fabrication Methods Appl Adv Fiber Mater. 2021;3:1–13.

[22] Wang C, Hu Y, Lieber CM, Sun S. Ultrathin Au nanowires and their transport properties. J Am Chem Soc. 2008;130:8902–8903.

[23] Aherne D, Satti A, Fitzmaurice D. Diameter-dependent evolution of failure current density of highly conducting dna-templated gold nanowires. Nanotechnology. 2007;18:125205.

[24] Wang Q, Yu Y, Liu J. Preparations, characteristics and applications of the functional liquid metal materials. Adv Eng Mater. 2018;20:1700781.

[25] Zhang M, Yao S, Rao W, Liu J. Transformable soft liquid metal micro/nanomaterials. Mater Sci Eng R Rep. 2019;138:1–35.

[26] Kim C, Kim M. Intrinsically conducting polymer (ICP) coated aramid fiber reinforced composites for broadband radar absorbing structures (RAS). Compos Sci Technol. 2021;211:108827.

[27] Bag A, Lee NE. Recent advancements in development of wearable gas sensors. Adv Mater Technol. 2021;6:2000883.

[28] Chen HW, Li C. PEDOT: Fundamentals and its nanocomposites for energy storage. Chin J Polym Sci. 2019;38(5):382019 435–448.

[29] Lee J, Llerena Zambrano B, Woo J, Yoon K, Lee T, Lee J, Llerena Zambrano B, Woo J, Yoon K, Lee T. Recent advances in 1D stretchable electrodes and devices for textile and wearable electronics: Materials. Fabrications Appl Adv Mater. 2020;32:1902532.

[30] Yadav KK, Wadhwa R, Khan N, Jha M. Efficient metal-free supercapacitor based on graphene oxide derived from waste rice. Curr Res Green Sustainable Chem. 2021;4:100075.

[31] Khan N, Yadav KK, Wadhwa R, Ankush, Jha M. One-pot green method for fabrication of MoS2 decorated graphite rod and their application in H2 evolution. Mater Lett. 2022;313:131784.

[32] Wadhwa R, Yadav KK, Goswami T, Ankush, Guchhait SK, Sunaina, Nishanthi ST, Ghosh HN, Jha M. Mechanistic insights for photoelectrochemical ethanol oxidation on black gold decorated monoclinic zirconia. ACS Appl Mater Interfaces. 2021;13:9942–9954.

[33] Yadav KK, Khan N, Jha M. Application of surface modified carbon nanotubes in energy. ACS Symp Ser. 2022;101–119.

[34] de Volder MFL, Tawfick SH, Baughman RH, Hart AJ. Carbon nanotubes: Present and future commercial applications. Science. 1979;339(2013):535–539.

[35] Naguib M, Kurtoglu M, Presser V, Lu J, Niu J, Heon M, Hultman L, Gogotsi Y, Barsoum MW. Two-dimensional nanocrystals produced by exfoliation of Ti3AlC2. Adv Mater. 2011;23:4248–4253.

[36] Jin C, Bai Z. MXene-based textile sensors for wearable applications. ACS Sens. 2022;7:929–950.

[37] Zhou T, Yu Y, He B, Wang Z, Xiong T, Wang Z, Liu Y, Xin J, Qi M, Zhang H, Zhou X, Gao L, Cheng Q, Wei L. Ultra-compact MXene fibers by continuous and controllable synergy of interfacial interactions and thermal drawing-induced stresses. Nat Commun. 2022;13(1):1–13.

[38] Cao W-T, Ma C, Mao D-S, Zhang J, Ma M-G, Chen F, Cao WT, Ma C, Chen F, Ma GM, Mao DS, Zhang J. Mxene-reinforced cellulose nanofibril inks for 3D-printed smart fibres and textiles. Adv Funct Mater. 2019;29:1905898.

[39] Shao W, Tebyetekerwa M, Marriam I, Li W, Wu Y, Peng S, Ramakrishna S, Yang S, Zhu M. Polyester@MXene nanofibers-based yarn electrodes. J Power Sources. 2018;396:683–690.

[40] Xu Z, Liu Y, Zhao X, Peng L, Sun H, Xu Y, Ren X, Jin C, Xu P, Wang M, Gao C, Xu Z, Liu YJ, Zhao XL, Peng L, Sun HY, Gao C, Xu Y, Ren XB, Jin CH, Xu P, Wang M. Ultrastiff and strong graphene fibres via full-scale synergetic defect engineering. Adv Mater. 2016;28:6449–6456.

[41] Greenstein KE, Nagorzanski MR, Kelsay B, Verdugo EM, Myung NV, Parkin GF, Cwiertny DM. Carbon–titanium dioxide (C/TiO2) nanofiber composites for chemical oxidation of emerging organic contaminants in reactive filtration applications. Environ Sci Nano. 2021;8:711–722.

[42] Lee CG, Javed H, Zhang D, Kim JH, Westerhoff P, Li Q, Alvarez PJJ. Porous electrospun fibers embedding TiO2 for adsorption and photocatalytic degradation of water pollutants. Environ Sci Technol. 2018;52:4285–4293.

[43] Ramasundaram S, Son A, Seid MG, Shim S, Lee SH, Chung YC, Lee C, Lee J, Hong SW. Photocatalytic applications of paper-like poly(vinylidene fluoride)-titanium dioxide hybrids fabricated using a combination of electrospinning and electrospraying. J Hazard Mater. 2015;285:267–276.

[44] He J, Lu C, Jiang H, Han F, Shi X, Wu J, Wang L, Chen T, Wang J, Zhang Y, Yang H, Zhang G, Sun X, Wang B, Chen P, Wang Y, Xia Y, Peng H. Scalable production of high-performing woven lithium-ion fibre batteries. Nature. 2021;597(7874):57–63.

[45] Wang S, Xu Q, Sun H. Functionalization of fiber devices: Materials. Prep Appl Adv Fiber Mater. 2022;4:324–341.

[46] Yang Z, Deng J, Chen X, Ren J, Peng H. A highly stretchable, fiber-shaped supercapacitor. Angew Chem Int Ed. 2013;52:13453–13457.

[47] Zhou Y, Fang J, Wang H, Zhou H, Yan G, Zhao Y, Dai L, Lin T. Multicolor electrochromic fibers with helix-patterned electrodes. Adv Electron Mater. 2018;4:1800104.

[48] Gong W, Hou C, Zhou J, Guo Y, Zhang W, Li Y, Zhang Q, Wang H. Continuous and scalable manufacture of amphibious energy yarns and textiles. Nat Commun. 2019;10(1):1–8.

[49] Li L, Basu S, Wang Y, Chen Z, Hundekar P, Wang B, Shi J, Shi Y, Narayanan S, Koratkar N. Self-heating -induced healing of lithium dendrites. Science. 2018;359(1979):1513–1516.

[50] Shi Q, Zhong Y, Wu M, Wang H, Wang H. High-capacity rechargeable batteries based on deeply cyclable lithium metal anodes. Proc Natl Acad Sci USA. 2018;115:5676–5680.

[51] Y. Lin, S. Dong, Z. Li, W. Zheng, J. Yang, A. Liu, W. Cai, F. Liu, Y. Jiang, T.P. Russell, F. Huang, E. Wang, L. Hou, Energy-effectively printed all-polymer solar cells exceeding 8.61% efficiency, Nano Energy. 2018;46:428–435. https://doi.org/10.1016/J.NANOEN.2018.02.035.

[52] G. Li, R. Zhu, Y. Yang, Polymer solar cells , Nat Photonics. 2012;6:153–161. https://sci-hub.se/10.1038/nphoton.2012.11.

[53] Zhang J, Wang Z, Li X, Yang J, Song C, Li Y, Cheng J, Guan Q, Wang B. Flexible platinum-free fibre-shaped dye sensitized solar cell with 10.28% efficiency. ACS Appl Energy Mater. 2019;2:2870–2877.

[54] Yadav KK, Sunaina, Sreekanth M, Ghosh S, Ganguli AK, Jha M. Excellent field emission from ultrafine vertically aligned nanorods of NdB6 on silicon substrate. Appl Surf Sci. 2020;526:146652.

[55] Yadav KK, Sreekanth M, Ankush, Ghosh S, Jha M. A new process for the stabilization of vertically aligned GdB6 nanorods and their field emission properties. Cryst Eng Comm. 2020;22:5473–5480.

Omar Dagdag*, Rajesh Haldhar, Seong-Cheol Kim,
Elyor Berdimurodov*, Ekemini D. Akpan, Eno E. Ebenso*

# Chapter 2
# Synthesis, characterization, and properties of advanced fiber materials

**Abstract:** Nowadays, advanced fiber materials of natural fiber products are interestingly investigated due to their abundance and versatility. Advanced natural fiber materials and polymer matrices have many unique properties that make them easy substitutes for synthetic fibers. To use fiber effectively, it is crucial to comprehend the fiber's characteristics. Natural fibers are easily obtainable from several plant species, including fruits, roots, leaves, bark/skin, etc. Therefore, the purpose of this chapter is to introduce some preparation and joining methods and attempt to cover various physical tests to help know the different mechanical and thermal characteristics of the fibers and analyses, and to try to discuss the numerous studies, such as FT-IR, RDX, SEM, and TGA methods, done by recent academic and industrial researchers, doctors, and clinicians to help understand the properties of natural fibers.

**Keywords:** Natural fibers, natural products, synthetic fibers, physical tests, mechanical properties

## 2.1 Introduction

Scientists around the world want to learn more about using good and environmentally friendly products that reduce pollution and benefit the society [1, 2]. In modern times, the strength of natural fibers is enhanced by various modifications. As a result, the

---

**Author Contribution Statement:** Equal contribution by all the authors.

---

***Corresponding author: Omar Dagdag**, Centre for Materials Science, College of Science, Engineering and Technology, University of South Africa, Johannesburg 1710, South Africa, e-mails: dagdao@unisa.ac.za
***Corresponding author: Eno E. Ebenso**, Centre for Materials Science, College of Science, Engineering and Technology, University of South Africa, Johannesburg 1710, South Africa, e-mail: ebensee@unisa.ac.za
***Corresponding author: Elyor Berdimurodov**, Faculty of Chemistry, National University of Uzbekistan, Tashkent, 100034, Uzbekistan, e-mail: elyor170690@gmail.com
**Rajesh Haldhar, Seong-Cheol Kim**, School of Chemical Engineering, Yeungnam University, Gyeongsan 38541, Republic of Korea
**Ekemini D. Akpan**, Centre for Materials Science, College of Science, Engineering and Technology, University of South Africa, Johannesburg 1710, South Africa

https://doi.org/10.1515/9783110992892-002

obtained products are cost-effective and more useful for mechanical use [3–5]. Figure 2.1 schematically shows the layout of the various fibers.

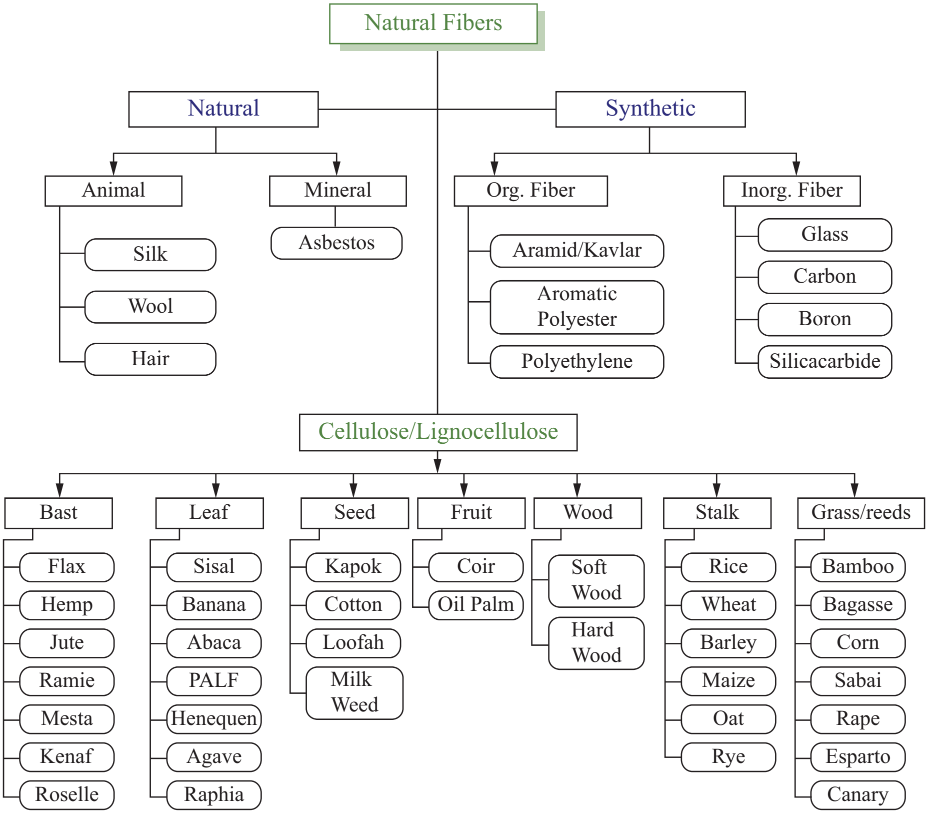
Natural Fibers
Natural
Synthetic
Animal
Silk
Wool
Hair
Mineral
Asbestos
Org. Fiber
Aramid/Kavlar
Aromatic Polyester
Polyethylene
Inorg. Fiber
Glass
Carbon
Boron
Silicacarbide
Cellulose/Lignocellulose
Bast
Flax
Hemp
Jute
Ramie
Mesta
Kenaf
Roselle
Leaf
Sisal
Banana
Abaca
PALF
Henequen
Agave
Raphia
Seed
Kapok
Cotton
Loofah
Milk Weed
Fruit
Coir
Oil Palm
Wood
Soft Wood
Hard Wood
Stalk
Rice
Wheat
Barley
Maize
Oat
Rye
Grass/reeds
Bamboo
Bagasse
Corn
Sabai
Rape
Esparto
Canary

**Figure 2.1:** Various types of synthetic and natural fibers. Reprinted with permission from [6], © 2015 Elsevier Publications.

Various plant species, their leaves, fruits, and roots can all be used to produce natural fibers from their bark/skin, etc. [7, 8]. Due to their availability in recyclability, biodegradability, abundance, improved energy recovery, high strength, less weight, low production cost, and specific modulus, and lower health risk, low density, low cost, etc. [9–12].

Natural fibers such as lignocellulosic fibers and other fibers include (a) Rosella, (o) Elephant grass, (n) Snake grass, (m) Kenaf, (i) Palm tree, (o) borassus fruit, (k) Broom corn, (j) Flax, (i) Pineapple leaves, (h) Sugar cane, (g) Banana, (f) Bamboo, (e) Hemp, (d) Coconut, (c) Cotton and (b) Sisal and etc. are displayed in Figure 2.2 [13–16]. Figure 2.2 illustrates the main natural products used for fiber processing.

(a)
(b)
(c)
(d)
(e)
(f)
(g)
(h)
(i)
(j)
(k)
(l)
(m)
(n)
(o)

**Figure 2.2:** Major plants used for fiber extraction. Reprinted with permission from [17], © 2017 Elsevier Publications.

## 2.2 The extraction and processing of natural fiber materials

Palm oil and sisal fibers were blended for one hour in a chemical solution that contained F8261, A1100, and A151 in an ethanol/$H_2O$ ratio of 6/4. After the mixing processes, the fibers were insulated from the resulting mixture, and they were then dried at high temperature for one day [18]. In other separation process, sisal fiber was added to a 4% sodium hydroxide solution that had been saturated with NaSCN for 30 min. The mixture was then reacted rapidly with $CH_2CHCN$ for 1 h at 40–45 °C. To neutralize the alkaline catalyst, it was immersed in ethanolic acid with a pH of 6–7. It was then cleaned with $H_2O$ and 95% ethanol. It was estimated that the magnitude of the cyanoethylation reaction increased by 3.7% [19]. The alpha fiber was prepared from maleic anhydride ($C_2H_2(CO)_2O$) by mixing with hot dimethyl ketone [($T = 50 \pm 5$ °C, 1:25 (w/v)]. Next, pure water and low-temperature dimethyl ketone were used to clean the obtained fiber. The hot ethane anhydride was moved into the previously provided wire flask [20]. The coconut fiber was first extracted with a 1:2 mixture of ethyl alcohol and benzene ($C_6H_6$) for 3 days, then treated with an alkaline solution and sodium hydroxide (2–10%) for 1 h at 300 °C, and copolymerized by grafting immediately with a combination of $Cu^{2+}$–$IO_4^-$ as an initiator in the water system. Coir bleaching was performed by placing the fibers in 0.7% $NaClO_2$ 1% ethanoic acid and NaOAc 50:1 at pH 4 and 65–85 °C for 120 min. Then, 2% of bisulfite ($NaHSO_3$) was used clean the fibers for 15 min [21]. In the next research work, the *Sugarcane bagasse* was functionalized with the alcohols to create a new and multifunctional polymer. In the next step, $ZrO_2.nH_2O$ in an acid solution was used to apply zirconium hydroxide to the palm fibers; $NH_4^+$ (1:3) was used as the separating compound [22]. The fibers were then cleaned and dried in a drying cabinet [23]. The roots of *Cissus quadrangularis* plants were collected and the fibers were extracted by microbial digestion. After a thorough wash in fresh water, it was dried for a week in the Sun to remove moisture. Finally, using a wire brush and the conventional combing technique, soil particles and the outer layer of the root were removed. The roots were divided into minute pieces (10 x 10 $mm^2$) and blended for one day in a solution of methanol, ethanolic acid, and ethanol (90 ml 70% ethanol + 5% ethanoic acid + 5 ml methanol). Then, they were dried in a series of tert-butyl alcohol ($(CH_3)_3COH$) and embedded in paraffin [24]. *Borassus wood* fibers were extracted from the dried fruit and soaked in water for 2 days. The resulting fibers contained short fine fibers and long coarse fibers. Both fibers are thoroughly cleaned in distilled water and then allowed to dry for seven days in the Sun. In addition to removing the water, the fibers were baked for two days at a temperature between 105 and 110 °C. A portion of the fibers was treated for 1/2 h with 5% NaOH in a 30:1 water ratio for removing hemicellulose and other impurities [7]. *Coir fibers* are described as mats and treated with an alkaline 5% sodium hydroxide solution and stored at the liquid ratio of 25:1 to insulate the mixture compounds [8]. *Napier grass* fibers are obtained by a conventional maceration method and handled with 5% and 2% of sodium hydroxide at RT for half an hour in a liquid ratio of 20:1. Subsequently, deionized water was used to wash the fibers [25]. Thespesia lampas was used to produce the lignocellulosic fibers, as shown by the results. It was cleaned with alkaline solutions for two days. In this process, other compounds are removed from the natural fiber material. Finally, hydrochloric acid was used to neutralize the product [26].

## 2.3 Characterization of natural fibers

### 2.3.1 FT-IR spectrum analysis

FT-IR results show the presence of acetyl/propionyl in wood fibers, hemp, treated flax, and due to the increased content of amorphous compounds throughout esterification; the crystallinity of the fibers gradually decreased [27]. CI was raised and amorphous material was eliminated from *Hemp* fibers after treatment with 6% sodium hydroxide [28]. *Ficus religiosa* leaf fibers are reduced to a powder and then cooled. This powder was diluted with 1% KBr [29]. FT-IR spectroscopy ($cm^{-1}$): 2925 and 2854 (C-H stretching vibrations of CH and $CH_2$ of the cellulose component of hemicellulose and ocher fibers) [30], 3500 (O-H stretching), 2900 (aliphatic C-H stretching), 1740 (($C = O$) stretching) and 1375 ($CH_3$ group). FT-IR shows no significant change in chemically treated and untreated fiber samples [31]. FT-IR spectra show that jute fiber-reinforced polypropylene composites separately from waxes and fats after sodium hydroxide treatment, as well as visible changes in fiber surface topography [32]. 1730 $cm^{-1}$, which corresponds to hemicellulosic material, was determined for dichotomous *Cordia dichotoma* /polycarbonate fibers during basecoat processing [33]. 3347 $cm^{-1}$ belongs to the alcohol group and decreases because the alkali-treated abaca fibers do not contain hemicellulose. IR spectra showed that alkali-treated *Hildegardia lignocellulosic* fibers were found to reduce hemicellulose and increase the $H_2O$ uptake. FT-IR spectra show that the hydrogen-bonded network is largely responsible for the crystalline fibril that dominates the bamboo fibers [34]. FT-IR spectra show that the spectra in the 1505–1600 $cm^{-1}$ band show a high-intensity ratio of the two peaks of softwood polymer lignin, but the ratio of $C = O$ absorption speed and absorption $C = H$ when the lignin peak is 1740 $cm^{-1}$ group is higher for hardwood polymer [35]. It is indicated that when the cotton was modified with natural fiber, the chemical composition was nearly stable [36]. FT-IR spectra show that sodium hydroxide-treated kenaf fibers lack lignin and hemicellulose, while the new fibers have more hydrogen bonds than the treated ones [37]. The OH band at 3445 $cm^{-1}$ of the FT-IR spectra shows incomplete acetylation in fibers treated with alkali and saturated with 2% $Na_2SO_3$ [38].

### 2.3.2 XRD analysis

To determine the fiber content in the *raffia textile palm* leaves, an XRD analysis was performed using an Inel square goniometer. Light, with a wavelength of 1.5405 nm, is obtained after [39] taking into account the single crystal plane of germanium and removing the Kα2 radiation. In mode 2θ, the spectra were examined at 10° and 100°. Using a linear diffractogram with a resolution of 0.015°, diffractograms were captured [40]. The crystallinity of the material was determined using X-ray diffraction. Figure 2.3 displays X-ray diffractograms of cellulose and $Nb_2O_5.nH_2O$ composites. The maximum intensity variation peaks at 2θ angles: 28°, 22.8°, 16.3° [41].

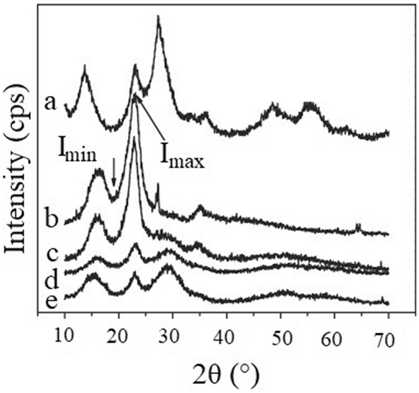

**Figure 2.3:** Results of X-ray diffractograms: (e) hybrid 50 wt.%, (d) 37.5 wt.%, (c) 16.67 wt.% and (b) cellulose and (a) $Nb_2O_5 \cdot nH_2O$ [41], © 2012 Elsevier Publications.

### 2.3.3 Microscopic analysis

SEM is the best method for finding the distribution of the individual fibers in fiber, and SEM is best for finding the layers and measuring the thickness [14]. SEM results show that the surface has changed after the fat has been removed. The SEM of esterified wood fibers, hemp, and raw flax are shown in Figure 2.4. Figure 2.4(a) demonstrates that a layer of fat covers the raw fibers; yet, this coating does not blow up and bite the fibers. However, there are regional differences in size. Figures 2.4(b) and 2.4(c) show that the surface morphology was improved with the presence of fibre-based materials [27].

### 2.3.4 Thermogravimetric analysis

One thermal technique for assessing the mass change, thermal conductivity, and composite material's stability is TGA analysis [37]. The DTA value, with and without hemp fibres, is shown in Figure 2.5, where the heating temperature of hemicellulose and pectin

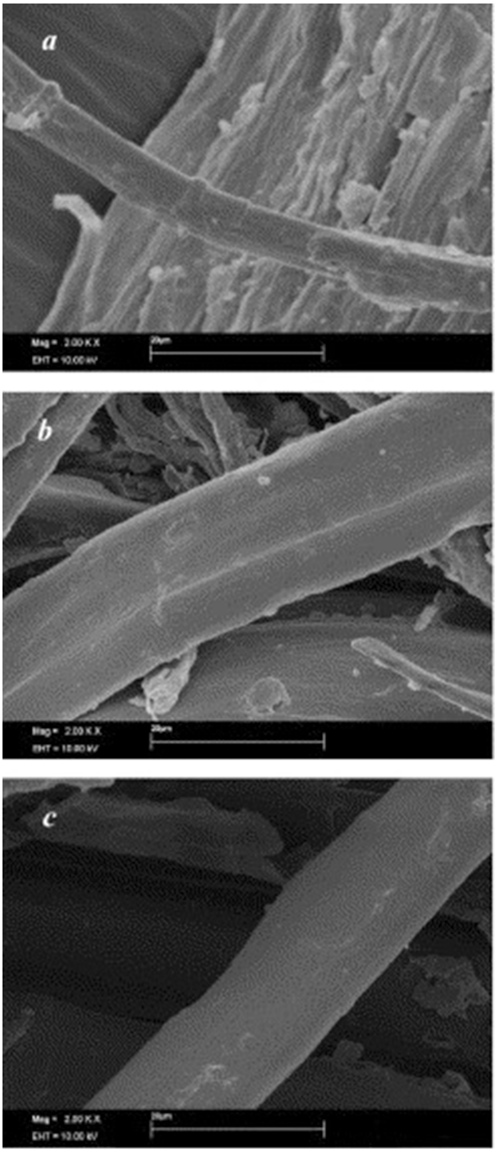
a
Mag = 2.00 K X
EHT = 10.00 kV
20µm
b
Mag = 2.00 K X
EHT = 10.00 kV
20µm
c
Mag = 2.00 K X
EHT = 10.00 kV
20µm

**Figure 2.4:** SEM of results: (a) without, (c) propionylated and (b) acetylated esterified fiber. Reprinted with permission from [27], © 2005 Elsevier Publications.

is 320 °C and 370 °C, and the heating temperature of lignin residue decomposition was high temperatures. In comparison, the cellulose was more stable at around 400 °C [28].

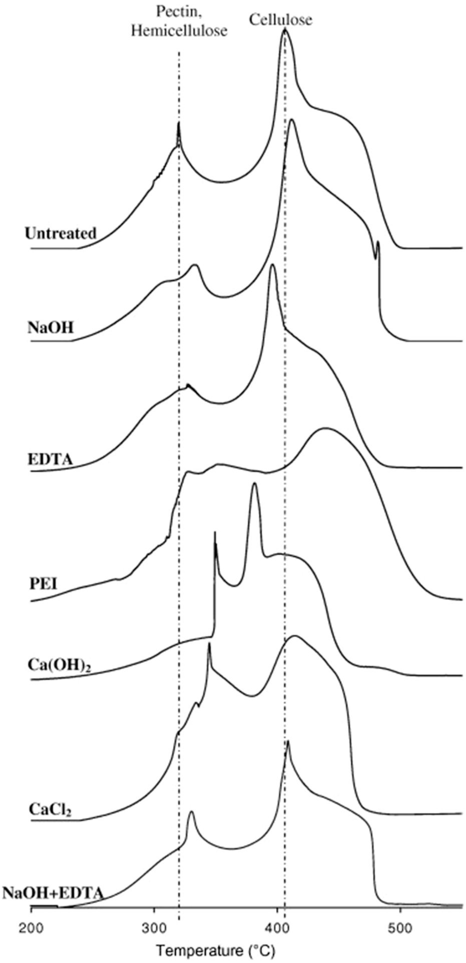

**Figure 2.5:** Results of various thermal investigations without and with hemp fiber bundles. Reprinted with permission from [28], © 2008 Elsevier Publications.

## 2.4 Mechanical properties of advanced fiber materials

This study focuses on performing any type of natural fibers, such as palm oil, bamboo, kenaf, cotton, jute, and other fibers containing resins such as polypropylene, epoxy resin (ER), and polyester. Most natural fibers and ER are made by hand because they are cost-effective and more convenient for mechanical use. Between the natural compounds, the Kenaf-ER composite, which has a fiber content of 40%, has the highest tensile strength. This type of natural fiber was produced from natural plants in South

Asia. It is used in several important industries such as medicine, pharmacology and chemical industries [42]. It is likewise expressed that with the expansion in the wt.% of support, the effective strength of the kenaf fiber increases; nonetheless, a decline in the elasticity is noticed [42]. Ramie-ER composite has good flexural strength and tensile strength. Ramie is also known as Chinese grass, which is a traditional Chinese herb [43]. As for fiber composites, composites of potato and porcelain fibers have good strength and elasticity [44]. The Henequen-ER group has the highest density (d = 1225 g/cm$^3$). Everything was done manually [45]. ER cotton composite can be produced by the compression molding process (Figure 2.6) [46], while ER palm composite can be produced by the VARTM process (Figure 2.7) [47]. The mechanical properties of the composite (tensile and flexural strength) increase with density wt.% reinforcement, which improves fiber orientation and, consequently, increases the density [48].

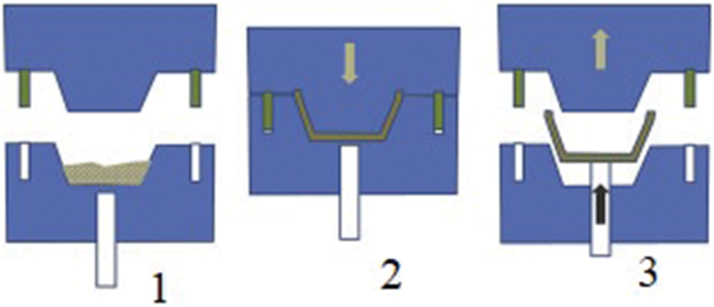

**Figure 2.6:** Schematic diagram showing compression molding. Reprinted with permission from [49], © 2019 Elsevier Publications.

The bamboo-polyester composite is strong and flexible. It contains 40.2% bamboo and 59.8% unsaturated polyester resin. It is used as a household product (source of food and many raw materials) [51]. Bamboo materials are used in many green buildings because of their durability and longevity. Due to its lightness and high density, bamboo products are more efficient than traditional fibers. Another strong point is the sycamore polyester composite with 40% unsaturated polyester resin and 60% sycamore. Sorghum, also called sorghum, is a grass grown for sorghum, which is used as food and feed, and which produces ethyl alcohol [51]. Blends of sisal, coconut, and sorghum: mainly unsaturated polyester resins have the hardest nature [44]. The polyester cotton resin as described in [52], while the combination of pumpkin polyester resin and glass fibers, described in [53], has the highest density (1.40 g/cm$^3$). This was done by hand, while the hemp-polyester and coir-polyester composites were applied mechanically [51, 54].

In the case of fibers developed with PE polymer, most composites were obtained by pressing. The compressed blend of cotton and polypropylene has high tensile and flexural strength. Cotton is a soft, airy medium that grows in a protective sheath or covering around the seeds of the *Gossypium* cotton plant, a member of the *Malvaceae* family. The

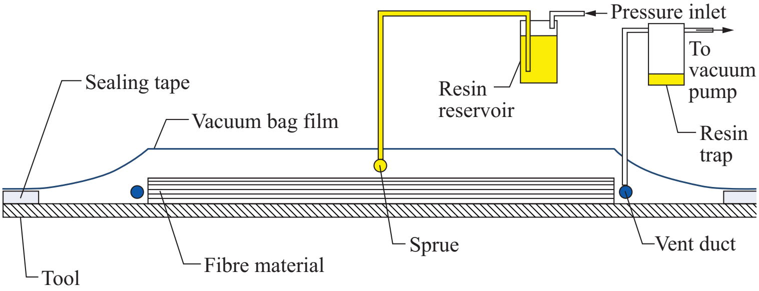

**Figure 2.7:** Illustrations of the VARTM process. Reprinted with permission from [50], © 2019 Elsevier Publications.

fiber is almost pure cellulose and is used worldwide as a raw material [55]. The thermal stability of cotton guarantees good tensile and flexural strength. Due to its low strength and water content, cotton is hydrophobic [56]. The fastest (0.98 g/cm$^3$) is a composite of bamboo and polypropylene obtained in the lamination process [57]. PALF polypropylene compound was also prepared according to the instructions [58]. Natural FRCs are used in helmets, roof panels, car interiors and exteriors, construction paper, paper boxes, mirror covers, etc. [59] The properties of various plant fibers are shown in Table 2.1.

**Table 2.1:** Mechanical characteristics of various plant fibers.

| Plant fibers | Density (g/cm$^3$) | Tensile strength (MPa) | Youngs modulus (GPa) | Ref. |
|---|---:|---:|---:|---|
| Henequen | 1.2 | 430–570 | 10.1–16.3 | [60] |
| Banana | 0.75–0.95 | 600 | 17.85 | [61] |
| Kenaf | 1.4 | 930 | 53 | [60] |
| Coir | 1.15 | 131–175 | 4–6 | [62] |
| Bamboo | 0.6–1.1 | 140–230 | 11–17 | [63] |
| Flax | 1.4–1.5 | 343–2000 | 27.6–103 | [60] |
| Hemp | 1.48 | 690 | 70 | [62] |
| Pineapple | 0.8–1.6 | 400–627 | 1.44 | [63] |
| Palm | – | 377 | 2.75 | [64] |
| Roselle | 0.75–0.8 | 147–184 | 2.76 | [61] |
| Ramie | 1.0–1.5 | 400–1000 | 24.5–128 | [60] |
| Sisal | 1.33–1.5 | 363–700 | 9–38 | [60] |
| Cotton | 1.5–1.6 | 287–597 | 5.5–12.6 | [17] |
| Jute | 1.3 | 393–773 | 26.5 | [60] |
| Abaca | 1.5 | 430–760 | 12 | [63] |
| Sugarcane | 1.25 | 290 | 17 | [63] |

## 2.5 Conclusions

This summary is based on the above data.

- Natural fibers are usually obtained by soaking and then processing using various methods to improve the surface.
- The morphology and performance of the natural fibers can be explained by SEM, FT-IR, XRD, and TGA studies – they help to understand the characteristics of natural fibers.
- Physical analyses help to understand the different mechanical characteristics of the fibers.

## Abbreviations

| | |
|---|---|
| RT | Room temperature |
| FT-IR | Fourier transform-infrared spectroscopy |
| TGA | Thermogravimetric |
| PALF | Pineapple leaf fiber |
| XRD | X-ray diffraction |
| A151 | Vinyl tri-ethoxy silane |
| A1100 | 3-Aminopropyl tri-ethoxy silane |
| F8261 | Fluoro silane |
| NaSCN | Sodium thiocyanate |
| $CH_2CHCN$ | Acrylonitrile |
| $NaClO_2$ | Sodium chlorite |
| CI | Crystallinity index |
| DTA | Differential thermal analysis |
| ER | Epoxy resin |
| VARTM | Vacuum-assisted resin transfer molding |
| PE | Polyethylene |

## References

[1] Ishak M, Leman Z, Sapuan S, Rahman M, Anwar U. Chemical composition and FT-IR spectra of sugar palm (Arenga pinnata) fibers obtained from different heights. J Nat Fibers. 2013;10:83–97.

[2] Moghaddam MK, Mortazavi SM. Physical and chemical properties of natural fibers extracted from typha australis leaves. J Nat Fibers. 2016;13:353–361.

[3] Pasquini D, de Morais Teixeira E, da Silva Curvelo AA, Belgacem MN, Dufresne A. Extraction of cellulose whiskers from cassava bagasse and their applications as reinforcing agent in natural rubber. Ind Crops Prod. 2010;32:486–490.

[4] Reddy KO, Maheswari CU, Dhlamini M, Kommula V. Exploration on the characteristics of cellulose microfibers from palmyra palm fruits. Int J Polym Anal Charact. 2016;21:286–295.

[5] Rwawiire S, Tomkova B. Morphological, thermal, and mechanical characterization of sansevieria trifasciata fibers. J Nat Fibers. 2015;12:201–210.

[6] Gurunathan T, Mohanty S, Nayak SK. A review of the recent developments in biocomposites based on natural fibres and their application perspectives. Compos Part A Appl Sci Manuf. 2015;77:1–25.

[7] Reddy KO, Guduri B, Rajulu AV. Structural characterization and tensile properties of borassus fruit fibers. J Appl Polym Sci. 2009;114:603–611.

[8] Obi Reddy K, Sivamohan Reddy G, Uma Maheswari C, Varada Rajulu A, Madhusudhana Rao K. Structural characterization of coconut tree leaf sheath fiber reinforcement. J For Res. 2010;21:53–58.

[9] Akin DE, Foulk JA, Dodd RB, Epps HH. Enzyme-retted flax using different formulations and processed through the USDA flax fiber pilot plant. J Nat Fibers. 2006;3:55–68.

[10] Biagiotti J, Puglia D, Kenny JM. A review on natural fibre-based composites-part I: Structure, processing and properties of vegetable fibres. J Nat Fibers. 2004;1:37–68.

[11] Madhu P, Sanjay M, Senthamaraikannan P, Pradeep S, Saravanakumar S, Yogesha B. A review on synthesis and characterization of commercially available natural fibers: Part-I. J Nat Fibers. 2018.

[12] Sanjay M, Arpitha G, Senthamaraikannan P, Kathiresan M, Saibalaji M, Yogesha B. The hybrid effect of Jute/Kenaf/E-glass woven fabric epoxy composites for medium load applications: Impact, inter-laminar strength, and failure surface characterization. J Nat Fibers. 2018.

[13] Baltazar-y-jimenez A, Bismarck A. Wetting behaviour, moisture up-take and electrokinetic properties of lignocellulosic fibres. Cellulose. 2007;14:115–127.

[14] Beakou A, Ntenga R, Lepetit J, Ateba J, Ayina L. Physico-chemical and microstructural characterization of "rhectophyllum camerunense" plant fiber. Compos Part A Appl Sci Manuf. 2008;39:67–74.

[15] Manimaran P, Senthamaraikannan P, Sanjay M, Marichelvam M, Jawaid M. Study on characterization of furcraea foetida new natural fiber as composite reinforcement for lightweight applications. Carbohydr Polym. 2018;181:650–658.

[16] Manimaran P, Sanjay M, Senthamaraikannan P, Jawaid M, Saravanakumar S, George R. Synthesis and characterization of cellulosic fiber from red banana peduncle as reinforcement for potential applications. J Nat Fibers. 2018.

[17] Ramesh M, Palanikumar K, Reddy KH. Plant fibre based bio-composites: Sustainable and renewable green materials. Renewable Sustainable Energy Rev. 2017;79:558–584.

[18] John MJ, Francis B, Varughese K, Thomas S. Effect of chemical modification on properties of hybrid fiber biocomposites. Compos Part A Appl Sci Manuf. 2008;39:352–363.

[19] Rong MZ, Zhang MQ, Liu Y, Yang GC, Zeng HM. The effect of fiber treatment on the mechanical properties of unidirectional sisal-reinforced epoxy composites. Compos Sci Technol. 2001;61:1437–1447.

[20] Bessadok A, Marais S, Gouanvé F, Colasse L, Zimmerlin I, Roudesli S, et al. Effect of chemical treatments of Alfa (Stipa tenacissima) fibres on water-sorption properties. Compos Sci Technol. 2007;67:685–697.

[21] Rout J, Misra M, Tripathy S, Nayak S, Mohanty A. The influence of fibre treatment on the performance of coir-polyester composites. Compos Sci Technol. 2001;61:1303–1310.

[22] Martins GA, Pereira PHF, Mulinari DR. Chemical modification of palm fibres surface with zirconium oxychloride. BioResources. 2013;8:6373–6382.

[23] Arif MF, Megat-Yusoff PS, Ahmad F. Effects of chemical treatment on oil palm empty fruit bunch reinforced high density polyethylene composites. J Reinf Plast Compos. 2010;29:2105–2118.

[24] Indran S, Raj RE, Sreenivasan V. Characterization of new natural cellulosic fiber from cissus quadrangularis root. Carbohydr Polym. 2014;110:423–429.

[25] Reddy KO, Maheswari CU, Shukla M, Rajulu AV. Chemical composition and structural characterization of napier grass fibers. Mater Lett. 2012;67:35–38.

[26] Reddy KO, Ashok B, Reddy KRN, Feng Y, Zhang J, Rajulu AV. Extraction and characterization of novel lignocellulosic fibers from thespesia lampas plant. Int J Polym Anal Charact. 2014;19:48–61.

[27] Tserki V, Zafeiropoulos N, Simon F, Panayiotou C. A study of the effect of acetylation and propionylation surface treatments on natural fibres. Compos Part A Appl Sci Manuf. 2005;36:1110–1118.

[28] Le Troedec M, Sedan D, Peyratout C, Bonnet JP, Smith A, Guinebretiere R, *et al.* Influence of various chemical treatments on the composition and structure of hemp fibres. Compos Part A Appl Sci Manuf. 2008;39:514–522.

[29] Madhu P, Sanjay M, Senthamaraikannan P, Pradeep S, Saravanakumar S, Yogesha B. A review on synthesis and characterization of commercially available natural fibers: Part II. J Nat Fibers. 2019;16:25–36.

[30] De Rosa IM, Kenny JM, Puglia D, Santulli C, Sarasini F. Morphological, thermal and mechanical characterization of okra (Abelmoschus esculentus) fibres as potential reinforcement in polymer composites. Compos Sci Technol. 2010;70:116–122.

[31] Alawar A, Hamed AM, Al-Kaabi K. Characterization of treated date palm tree fiber as composite reinforcement. Compos Part B: Eng. 2009;40:601–606.

[32] Liu X, Dai G. Surface modification and micromechanical properties of jute fiber mat reinforced polypropylene composites. Express Polym Lett. 2007;1:299–307.

[33] Jayaramudu J, Reddy GSM, Varaprasad K, Sadiku E, Ray SS, Rajulu AV. Effect of alkali treatment on the morphology and tensile properties of cordia dichotoma fabric/polycarbonate composites. Adv Polym Technol. 2013;32.

[34] HE JX, Tang Y, Wang SY. Differences in morphological characteristics of bamboo fibres and other natural cellulose fibres: studies on x-ray diffraction, solid state 13C-CP/MAS NMR, and second derivative FTIR spectroscopy data. 2007.

[35] Pandey K. A study of chemical structure of soft and hardwood and wood polymers by FTIR spectroscopy. J Appl Polym Sci. 1999;71:1969–1975.

[36] Li Y, Li G, Zou Y, Zhou Q, Lian X. Preparation and characterization of cellulose nanofibers from partly mercerized cotton by mixed acid hydrolysis. Cellulose. 2014;21:301–309.

[37] El-Shekeil Y, Sapuan S, Khalina A, Zainudin E, Al-Shuja'a O. Effect of alkali treatment on mechanical and thermal properties of kenaf fiber-reinforced thermoplastic polyurethane composite. J Therm Anal Calorim. 2012;109:1435–1443.

[38] Calado V, Barreto D, d'Almeida J. The effect of a chemical treatment on the structure and morphology of coir fibers. J Mater Sci Lett. 2000;19:2151–2153.

[39] Abdallah M, Alfakeer M, Altass H, Alharbi AM, Althagafi I, Hasan N, *et al.* The polarographic and corrosion inhibition performance of some schiff base compounds derived from 2-amino-3-hydroxypyridine in aqueous media. Egypt J Petrol. 2019;28:393–399.

[40] Elenga R, Dirras G, Maniongui JG, Djemia P, Biget M. On the microstructure and physical properties of untreated raffia textilis fiber. Compos Part A Appl Sci Manuf. 2009;40:418–422.

[41] Maschio LJ, Pereira PHF, Da Silva MLCP. Preparation and characterization of Cellulose/Hydrous niobium oxide hybrid. Carbohydr Polym. 2012;89:992–996.

[42] Mahjoub R, Yatim JM, Sam ARM, Raftari M. Characteristics of continuous unidirectional kenaf fiber reinforced epoxy composites. Mater Des. 2014;64:640–649.

[43] Irawan AP, Soemardi TP, Widjajalaksmi K, Reksoprodjo AH. Tensile and flexural strength of ramie fibre reinforced epoxy composites for socket prosthesis application. International Journal of Mechanical and Materials Engineering (IJMME), Vol.6 (2011), No.1, 46–50.

[44] Yang Y, Fahmy MF, Pan Z, Zhan Y, Wang R, Wang B, *et al.* Experimental study on basic mechanical properties of new bfrp-bamboo sandwich structure. Const Build Mater. 2020;264:120642.

[45] Yasin P, Ramana MV, Vamshi CK, Pradeep K. A study of continuous henequen/epoxy composites. Mater Today: Proc. 2019;18:3798–3811.

[46] Aruchamy K, Subramani SP, Palaniappan SK, Sethuraman B, Kaliyannan GV. Study on mechanical characteristics of woven Cotton/Bamboo hybrid reinforced composite laminates. J Mater Res Technol. 2020;9:718–726.

[47] Sarikaya E, Çallioğlu H, Demirel H. Production of epoxy composites reinforced by different natural fibers and their mechanical properties. Compos Part B: Eng. 2019;167:461–466.

[48] Sathishkumar G, Ibrahim M, Mohamed Akheel M, Rajkumar G, Gopinath B, Karpagam R, et al. Synthesis and mechanical properties of natural fiber reinforced Epoxy/Polyester/Polypropylene composites: A review. JOURNAL OF NATURAL FIBERS 2022, VOL. 19, NO. 10, 3718–3741. J Nat Fibers. 2020;1–24.

[49] Balla VK, Kate KH, Satyavolu J, Singh P, Tadimeti JGD. Additive manufacturing of natural fiber reinforced polymer composites: Processing and prospects. Compos Part B: Eng. 2019;174:106956.

[50] Hindersmann A. Confusion about infusion: an overview of infusion processes. Compos Part A Appl Sci Manuf. 2019;126:105583.

[51] Prasad A, Rao KM, Gupta A, Reddy B. A study on flexural properties of wild cane grass fiber-reinforced polyester composites. J Mater Sci. 2011;46:2627–2634.

[52] Satyanarayana K, Sukumaran K, Kulkarni A, Pillai S, Rohatgi P. Fabrication and properties of natural fibre-reinforced polyester composites. Composites. 1986;17:329–333.

[53] Sivakandhan C, Balaji R, Loganathan GB, Madan D, Murali G. Investigation of mechanical behaviour on sponge/ridge gourd (Luffa aegyptiaca) natural fiber using epoxy and polyester resin. Mater Today: Proc. 2020;22:705–714.

[54] Neves ACC, Rohen LA, Mantovani DP, Carvalho JP, Vieira CMF, Lopes FP, et al. Comparative mechanical properties between biocomposites of epoxy and polyester matrices reinforced by hemp fiber. J Mater Res Technol. 2020;9:1296–1304.

[55] Kim S-J, Moon J-B, Kim G-H, Ha C-S. Mechanical properties of polypropylene/natural fiber composites: comparison of wood fiber and cotton fiber. Polym Test. 2008;27:801–806.

[56] Ray K, Patra H, Swain AK, Parida B, Mahapatra S, Sahu A, et al. Glass/jute/sisal fiber reinforced hybrid polypropylene polymer composites: fabrication and analysis of mechanical and water absorption properties. Mater Today: Proc. 2020;33:5273–5278.

[57] Gu F, Zheng Y, Zhang W, Yao X, Pan D, Wong ASM, et al. Can bamboo fibres be an alternative to flax fibres as materials for plastic reinforcement? a comparative life cycle study on Polypropylene/Flax/Bamboo laminates. Ind Crops Prod. 2018;121:372–387.

[58] Alzebdeh KI, Nassar MM, Arunachalam R. Effect of fabrication parameters on strength of natural fiber polypropylene composites: Statistical assessment. Measurement. 2019;146:195–207.

[59] Sathishkumar T, Navaneethakrishnan P, Shankar S. Tensile and flexural properties of snake grass natural fiber reinforced isophthallic polyester composites. Compos Sci Technol. 2012;72:1183–1190.

[60] Yan L, Kasal B, Huang L. A review of recent research on the use of cellulosic fibres, their fibre fabric reinforced cementitious, geo-polymer and polymer composites in civil engineering. Compos Part B: Eng. 2016;92:94–132.

[61] Nadlene R, Sapuan S, Jawaid M, Ishak M, Yusriah L. A review on roselle fiber and its composites. J Nat Fibers. 2016;13:10–41.

[62] Mohanty A, Misra MA, Hinrichsen G. Biofibres, biodegradable polymers and biocomposites: An overview. Macromol Mater Eng. 2000;276:1–24.

[63] Faruk O, Bledzki AK, Fink H-P, Sain M. Biocomposites reinforced with natural fibers: 2000–2010. Prog Polym Sci. 2012;37:1552–1596.

[64] Srinivas K, Naidu AL, Bahubalendruni MR. A review on chemical and mechanical properties of natural fiber reinforced polymer composites. Int J Performability Eng. 2017;13:189.

Pragnesh N. Dave* and Pradip M. Macwan

# Chapter 3
# Fabrication of advanced fiber materials

**Abstract:** The revolutionary growth of the manufacturing industry and the daily lives of the social population are intimately tied to the study and applications of fiber materials. However, the demands of automation and intellectualization in contemporary society, as well as people's consumption desires in pursuit of smartness, avant-gardism, fashion, and uniqueness, cannot be met by conventional fibers and fiber products. By using well-known, ineffective textile processing techniques, several fiber structures have often been produced in ambient settings. Building electrical devices directly on the surface or inside of single fibers, which typically have a thickness of few to ten microns, is now possible due to advancements in nanotechnology. The unique benefits of elastic and stretchy functional fibers, such as their high dynamic bending elasticity, stretchability, and high mechanic strength, have attracted the interest of a vast research community. Electrospun nanofiber materials have been extensively used in a variety of fields, including environmental management, safety protection, and tissue engineering. These materials have the advantages of a large specific surface area, small pore size, high porosity, good channel connectivity, and ease of functional modification. The creation of three-dimensional (3D) fiber materials with stable structures has emerged as a crucial problem in extending application and enhancing the performance of electrospun fibers with the development of functional fiber materials.

**Keywords:** Fiber, nanofiber, electrospinning, conductive, biosensor, fabrication

## 3.1 Introduction

Fiber, a crucial component of both basic and strategic materials, not only satisfies our everyday necessities but is also being extensively used in cutting-edge industries including aerospace, the environment, and health care. When fiber is being developed, one of the crucial development trends of our day is refining textile fibers. Whenever the fiber diameter is shrunk, from micrometers to nanometers, the size impacts the surface properties. The diameter refinement's impact will endow fiber materials with several special characteristics, which can greatly enhance the performance of fiber applications material.

---

***Corresponding author: Pragnesh N. Dave,** Department of Chemistry, Sardar Patel University, Vallabh Vidyanagar 388 120, Gujarat, India, e-mail: pragnesh7@yahoo.com

**Pradip M. Macwan,** B. N. Patel Institute of Paramedical and Science (Science Division), Sardar Patel Education Trust, Bhalej Road, Anand 38800, Gujarat, India

https://doi.org/10.1515/9783110992892-003

Nanofibers, generally speaking, are fibers with a diameter of less than 1 m. Nanofibers have a considerable size effect and exhibit a variety of unique properties in the areas of light, heat, magnetism, electricity, and other phenomena. The methods for stretching, template synthesis, flash spinning, islands-in-a-sea, and electrospinning are the most common ones used to create nanofibers. Stretching and template synthesis methods are listed earlier, but their technical development is still in the laboratory stage, due to their limited raw material range and poor fiber continuity. Flash spinning and islands-in-a-sea methods, on the other hand, have high preparation efficiencies but are hindered by their wide fiber diameter distribution or difficult controllability of fiber aggregates [1].

The recent years have seen a lot of interest in one-dimensional (1D) nanomaterials with nanoscale diameter and macroscale length, which naturally connect the micro and macro worlds. One-dimensional nanomaterials have exceptional benefits over zero-dimensional (0D) or two-dimensional (2D) nanomaterials in terms of the nanosize effect of nanomaterials and macro operability, which is greater than that of a majority of materials. Electrospinning is a straightforward and adaptable method for creating 1D ultrathin fiber materials with a comparatively high level of efficiency, among the many 1D nanomaterial creation processes. Electrospinning is a technique that uses high voltage electrostatic repulsion as the driving force to stretch viscous polymeric solution into continuous ultrathin strands. Depending on the precursor materials and spinning conditions, the diameter of electrospun fibers can vary from a few nanometers to numerous micrometers. Since the turn of the century, electrospinning technology has been used in a wide range of new sectors and materials and has been improved into a highly controlled process. A variety of fibers with various morphologies can be produced, thanks to the unique spinneret design and solution composition, including porous and hierarchical fibers and nanofibers, core–shell forms, hollow structures, multichannel fibers, multiwalled structures, side-by-side fibers and yarns, necklace-shaped fibers, branched type, and several additional conformations [2].

Numerous nonstretchable polymer fibers, such as polycarbonates (PC) and polystyrene (PS), have been used in electronics, energy conversion, biomedicine, and other fields in recent years. These numerous uses highlight the promising potential of fiber technology for human-machine interface. There are limitations to these fibers present in soft and stretchy applications, such as conformal detecting, soft robotics, and textiles, despite the fact that these varied fiber materials and fiber production techniques have greatly improved human life in many ways. As a result of their distinct mechanical performance, elastic and stretchy functional fibers are in greater demand. In order to create elastomer fibers with controlled fiber shapes and designable functionality, much work has been put into discovering potential soft materials and improving processing techniques. On the basis of their distinctive features, such as great dynamic twisting elasticity, stretchability, and high mechanic strength, researchers have proven several multidisciplinary uses for elastic and stretchable fibers and made substantial progress in this field [3].

Polymeric composites offer many excellent uses in a variety of industries, including the automotive and marine sectors. Researchers have recently been interested in the idea of improving the mechanical characteristics of polymeric composites by adding nanoparticles (NPs). The mechanical behavior of polymeric composites may be considerably enhanced by adding NPs to the polymeric matrix, as is well known. The capacity of NPs to enhance the characteristics of composites at extremely low concentrations is their most significant benefit over microparticles. A family of hybrid materials known as “fiber metal laminates” (FMLs) is made up of layers of metal and fiber-reinforced polymer (FRP). The key advantages of FMLs include the benefits of both metals and polymeric composites, such as excellent wear strength, impact resistance, and fatigue resistance. FMLs have numerous excellent applications because of their exceptional characteristics, particularly in the aerospace sector. Various strengthening processes of NPs with various shapes in polymeric composites have been introduced by research. Carbon allotropes have been developed during the past ten years as suitable reinforcing materials for enhancing the mechanical characteristics of polymeric composites, including carbon nanotubes (CNTs), graphene, and nanodiamond [4].

### 3.1.1 History

While synthetic fibers (like nylon) were initially discovered around 75 years ago, man-made fibers (like rayon) have been around for almost 160 years. Natural fibers like cotton, wool, and silk are examples that have been used in clothing for a very long time. At the moment, synthetic fibers make up the great bulk of the world’s output of man-made fibers, which accounts for more than half of all fibers. There are several specialty fibers, despite the fact that they are mostly used for apparel, house and car furnishings, industrial ropes, and other things. The strongest structural materials available today are fibers. Telecommunications, energy harvesting, and medicinal applications, all make use of fibers. Fibers, now perform a wide range of functions [5].

## 3.2 Fiber fabrication

Wet spinning, dry-jet wet spinning, gel spinning, dry spinning, melt spinning, and electrospinning are just a few of the methods used to create polymer fibers [5]. Direct extrusion of polymer solution into a coagulation bath is used for wet spinning. Wet spinning is comparable to dry-jet wet spinning, except there is an air cavity between the spinneret and the coagulation bath, in the former. At DSM in the Netherlands, gel spinning was created around 1980 to produce high-strength polyethylene (PE). Low polymer concentration aids in reducing polymer entanglement, which increases drawability and leads to greater molecular alignment and modulus than is possible with most other spinning techniques. Without a coagulation bath, the solvent disappears by passing the fibers through a heated chamber in dry spinning. In melt spinning, a polymer melt rather than a solution is employed, and fibers are extruded straight from the melt. At a temperature between the melting point and the liquid crystal to isotropic transition temperature, thermotropic liquid crystalline polymers (like Vectran$^{\text{TM}}$) are spun from a melt state. Kevlar$^{\text{TM}}$ and Zylon$^{\text{TM}}$, two examples of lyotropic liquid crystals, are spun from a solution in the liquid crystalline phase. In order to spin polymer solutions or melts into fibers, high voltage (usually 10–20 kV) must be provided between the spinneret and the fiber collector. Fibers with widths ranging from around 50 nm to a few micrometers may be created using electrospinning. In contrast, the majority of textile fibers have diameters between 10 and 20 m, while carbon fibers are generally between 5 and 10 m. Other spinning techniques such as centrifugal spinning have also been created. Various spinning processes may be used to create fibers that are single-component and bicomponent.

Making a bulk preform is the initial stage in the production of optical fiber. This bulk preform has the same shape and chemical make-up as the final fiber that is required. Then, fibers are created by thermally drawing this preform. Both single component and multicomponent fibers may be produced using this method. Although polymers like PMMA [poly(methyl methacrylate)] or optical fibers with a glass core and polymer cladding can also be used, glass fibers are the primary component of optical fibers. The ultimate diameter of the core glass fibers in single-component fibers is often as tiny as 9 µm for single mode and around 50 µm for multimode, while the diameter of the cladding glass fibers is in the range of 125 µm. The diameter of multicomponent fibers is often greater than 500 µm.

## 3.3 Structural fibers

In 1855, rayon, the first synthetic material, was created using nitrocellulose solution. In 1939, nylon, the first synthetic material, was made available to the public. Since then, solution-spun synthetic fibers with high mechanical properties like poly(*p*-phenylene terephthalamide) (PPTA, a para-aramid commonly known as Kevlar$^{\text{TM}}$), poly(*p*-phenylene-2,6-benzobisoxazole) (PBO, commonly known as Zylon$^{\text{TM}}$), and ultrahigh-molecular-weight extended chain PEs (commonly known as Dyneema$^{\text{TM}}$ and Spectra$^{\text{TM}}$) have been produced. A few promising experimental fibers, such as poly(2,6-diimidazo[4,5-b:4′5′-e]pyridinylene-1,4 (2,5-dihydroxy)phenylene) (PIPD, also known as M5 fiber), are not yet manufactured commercially. Table 3.1 provides an overview of the mechanical characteristics of several fibers. Given that polymeric chains like PE, PPTA, and PBO have potential tensile strengths of 30 GPa or greater, there is tremendous space for tensile strength to rise even further. Carbon fibers made of polymers are also commonly used and will be covered later. The benefit of polymeric and carbon fibers over more conventional structural materials like metals is that they have much greater specific strength and modulus compared to the rival structural materials, up to an order of magnitude higher.

**Table 3.1:** Mechanical properties of various fibers (https://www.honeywell-spectra.com/products/fibres/).

| | Density (g/cm$^3$) | Tensile strength (GPa) | Tensile modulus (GPa) | Elongation at break (%) |
|---|---|---|---|---|
| Nylon | 1.14 | 0.4–1 | 6–10 | 18–20 |
| Kevlar™ | 1.44–1.47 | 3.4–4.1 | 130–270 | 2.0–2.8 |
| Spectra™ | 0.97 | 2.4–3.6 | 70–133 | 2.5–4.5 |
| Zylon™ | 1.54–1.56 | 5.8 | 180–270 | 2.5–3.5 |
| PIPD (M5) | 1.7 | 3.5–4.5 | 330 | 2.5 |
| PAN-based carbon fiber | 1.73–1.93 | 3.5–7.0 | 200–500 | 0.8–2.2 |
| Pitch-based carbon fiber | 1.65–2.20 | 1.1–4.0 | 150–900 | 0.3–0.9 |

For the electric light bulb, Thomas Edison employed carbon filaments produced from cotton yarn, in the nineteenth century. As a result of the high specific strength and modulus that carbon fibers now offer, their use in composites is expanding quickly. Today, polyacrylonitrile (PAN) is used to make the majority of carbon fibers. PAN fibers undergo oxidative stabilization and carbonization processes to become carbon. Both stages are completed under pressure. In air, oxidative stabilization occurs normally between 180 and 320 °C. Up to 1,700 °C, carbonization takes place in an inert environment like nitrogen or argon. The normal carbonization temperature for high-strength carbon fibers is around 1,400 °C. To further boost fiber stiffness, graphitization can also be done, if necessary, at temperatures as high as around 2,800 °C in an inert environment. The cyclization of the nitrile groups and oxidation are key components of the complicated stabilization chemistry. The potential for chain molecules to cross-link has also been covered in the literature. Figures 3.1 and 3.2 demonstrate the recommended PAN reaction strategies for stabilization and carbonization, respectively.

PAN stabilization and carbonization need a lot of energy because of external heating. The direct approach of joule heating is being investigated for fiber stabilization and probable carbonization. Before spinning the fiber, CNTs are added to the polymer solution to stabilize PAN via Joule heating. The CNTs turn the fibers into conductors of electricity and function as a Joule heating element. This allows for the electrical heating of the fibers from the inside out, possibly opening the door to the creation of a substantial energy-saving method for producing carbon fibers.

The mechanical characteristics of carbon fibers have significantly improved since the start of contemporary research on them in the late 1950s. For instance, tensile strength of carbon fibers now, is more than five times than it was in the early 1960s. Since PAN fibers offer an excellent blend of tensile and compressive characteristics, they are now the most used precursor for carbon fibers. Pitch-based carbon fibers are also accessible, and mesophase pitch-based continuous carbon fibers with more than 90% of the theoretical modulus may be produced commercially. However, these pitch-based carbon fibers have very low axial compressive strength and a rather low tensile strength (3 GPa) (200–400 MPa).

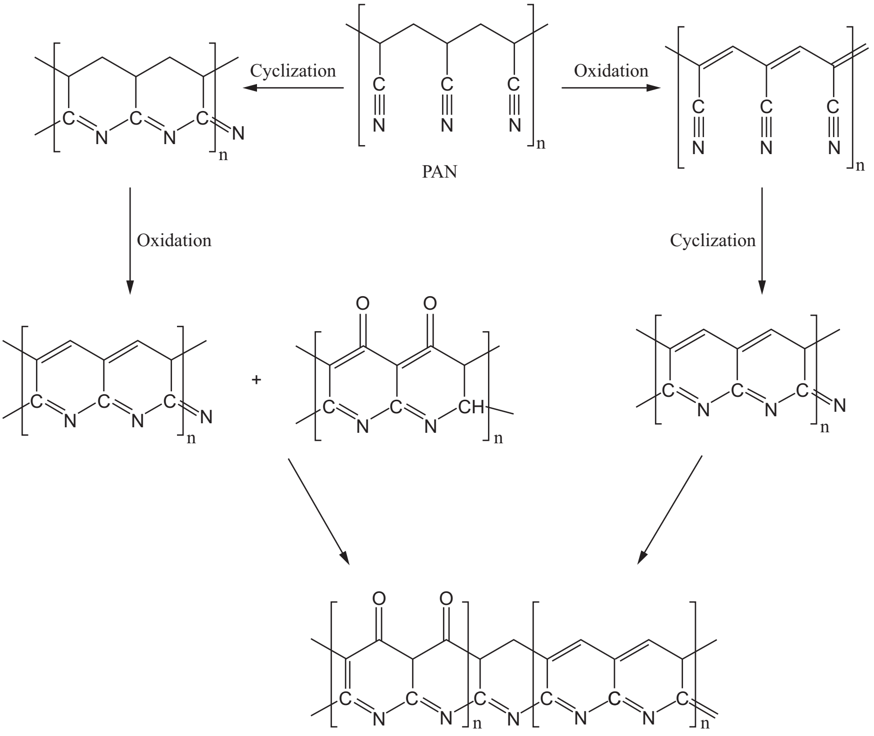

Figure 3.1: PAN chemical reaction during stabilization, as predicted [5].

PAN-based carbon fibers are among the strongest structural materials now on the market, despite having low-to-moderate tensile moduli. However, the potential strength of the carbon-carbon bond, which is thought to be between 70 and 150 GPa, is less than 10% of the tensile strength of the commercial PAN-based carbon fibers now in use. Present-day PAN-based commercial carbon fibers are produced using wet or dry-jet wet spinning technologies. At Georgia Tech, PAN-based carbon fibers with tensile strengths

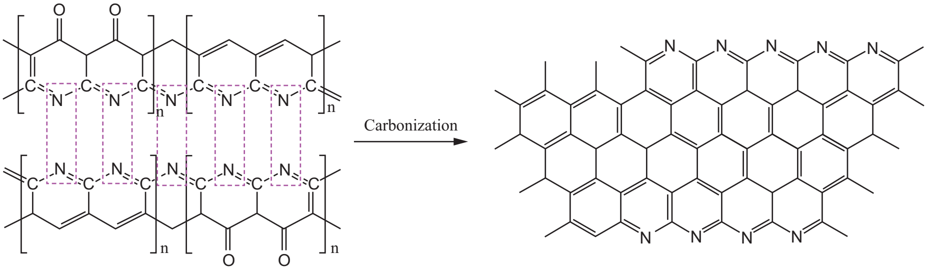

**Figure 3.2:** Proposed chemical reaction of PAN during carbonization [5].

up to 30% greater than the most advanced carbon fiber (IM7) were produced using the gel spinning technique.

Noncircular PAN-based carbon fibers have been carbonized as a 100-filament tow. When these gel-spun fibers are produced with a circular cross section and carbonized with a tow size of 6,000–12,000 filaments, it is anticipated that their tensile strength would improve even further. Tensile strength of gel-spun carbon fibers up to 12.1 GPa at a short gauge length of 100 µm has been recorded, indicating near-term promise of qualities that may be obtained in carbon fibers, with the right investment in research and development. Additionally, experimental carbon fibers made from PAN precursors incorporating CNTs have been made. The carbon fibers produced when 0.4–1 wt% of CNTs were added to PAN had a 25% increase in electrical conductivity and a 50% increase in thermal conductivity. Additionally, carbonized PAN is shaped to surround CNTs, preventing any debonding of the two materials. Making PAN/CNT-based carbon fibers with CNTs that are independently scattered rather than bundled is still difficult. The carbon fiber has a microvoid at each end of a CNT bundle, which lowers the tensile strength.

With decreasing fiber diameter, tensile strength and tensile modulus of carbon fiber rise. Hollow carbon fibers with a variety of shapes have been described for use in low-density carbon fiber production. PMMA was used for the islands and PAN for the sea polymer in a bicomponent islands-in-a-sea geometry technique to create this fiber. Stabilization and low-temperature carbonization cause PMMA to burn out, leaving the fiber hollow. This kind of hollow carbon fiber can be strong in compression and stiff in a buckling situation. The specific strength and modulus of this fiber are also anticipated to be greater than those of a solid (not hollow) fiber of equivalent diameter.

Assembling CNTs into macroscopic fibers has been done using aqueous dispersions, dispersions in strong acids, drawing from CNT forests, pulling from a CNT aerogel created in a chemical vapor deposition reactor, spinning from CNT cotton, and rolling and twisting a CNT film. Although CNT fibers are reasonably ductile and simple to knot, their tensile strength and modulus are much lower than those of commercial high-strength PAN-based carbon fibers and high-modulus pitch-based carbon fibers, respectively. Investigations on graphene-derived carbon fibers are also ongoing.

## 3.4 Conductive materials

The choice of fabrication materials and the potential to give desirable mechanical properties, safety, and environmental stability, combined with excellent overall electrical performance and great charge transport to flexible systems are important factors for fiber-based wearable electronics [6].

### 3.4.1 Materials

The development of conductive or semiconductive materials that are elastic and delicate is essential because fiber-based wearable electronics have unique electrical, chemical, and mechanical properties. Many other materials have been used and explored, including conductive polymers, metal and metal oxide NPs/nanowires, carbon-based micron/nanomaterials, such as carbon particles (CP), CNTs, carbon fiber, and graphene. For a variety of applications, including flexible optical and electrical devices, chemical and biological sensors, and more, these materials hold out a lot of potential. A steep subthreshold slope results in lower operating voltages, V, and is crucial in the construction of low-power circuits, a larger field effect, and superior mobility, and devices based on these conducting material fibers frequently show enhanced electrical performance.

#### 3.4.1.1 Conducting polymers

If all of the electrical functions could theoretically be accomplished in a fiber alone, such fibers would provide the ideal building blocks for smart clothing, since they could be seamlessly woven into fabrics. There are, currently, very few instances of such fibers due to the technological difficulty of integrating sophisticated electrical capabilities into a textile fiber. Since they are naturally flexible or may be combined with fiber to create composite materials, organic polymers and combinations of tiny molecules may be the most promising materials. Additionally, because they are created through the synthesis of fundamental building ingredients, their chemical, physical, and electrical characteristics may be precisely adjusted.

#### 3.4.1.2 Carbon-based micro/nanomaterials

The development of flexible and wearable electronics is made possible by the unique properties of 0D, 1D, and 2D carbon-based micro/nanomaterials, such as their high intrinsic carrier mobility ($10^6$ $cm^2/V$ S), electrical conductivities ($10^4$ S/cm), superior mechanical properties (elastic modulus in the order of 1 TPa), environmental stability, and the potential for production. Porous carbon materials having a large specific surface area and mechanical properties, such as CNTs, carbon fibers (including carbon microfibers and carbon nanofibers), graphene, carbon aerogels, etc., are frequently used in wearable electronics. The two most thoroughly studied carbon allotropes in materials science are CNTs and graphene. These two materials have also been identified as promising electrode materials for wearable electronics. For high-performance flexible electronics, electrodes based on these two well-known carbon compounds are now a hot issue. It has been shown that employing a polyelectrolyte-based coating with CNTs, ordinary cotton threads may be converted into smart electronic yarns and wearable fabric devices for monitoring human vital signs. Single-walled CNT (SWNT) ink was used in a straightforward “dipping and drying” procedure to create a stretchy, porous, and conductive textile fabric. These conductive fabrics may be loaded with pseudo capacitor materials, which can improve the device’s areal capacitance by a factor of 24. CPs have been used much more than CNTs and graphene because of its lesser cost, higher health and safety performance, porous structure, and ability to impart high electrical conductivity to an insulating polymer fiber or fiber-based textile substrate.

#### 3.4.1.3 Metallic nanoparticles/nanowires

As they have extremely high conductivities, low-dimensional metal nanostructures like nanowires (NWs) or NPs are particularly appealing for fiber-based flexible and wearable electronics. For instance, Kevlar fibers with Ni and Au plating can show electric conductivity levels of 6 S/cm. While nylon fiber mats plated with Ag using a commercial electrodeless plating solution exceed 1,800 S/cm when loaded with less than ~ 17 wt% Ag, silicone fibers packed with Ag flakes only achieve 470 S/cm. However, their introduction into industry has been hampered by problems of roughness, haze, and stability. Ongoing work is being done to make metallic nanowires and NPs more stable and to use them in flexible electrical applications. A unique all-fiber piezoelectric nanogenerator employing extremely stretchy silver-coated polyamide fabric as the elastic fabric electrodes illustrates the promise of metallic NWs in a recent study. In a cyclic compression test that simulates walking settings, the resulting generator displays strong durability (>1,000,000 loading cycles) and good electric power producing capability. The 3D structure of fabric electrodes provides significantly more reliable electric contact and flexibility than conventional metal foil or metal-coated thin film electrodes, which are crucial for soft and wearable generators, where the electrodes are subjected to repeated cycles of deformation.

#### 3.4.1.4 Fiber-based electrodes

Fiber-based electrodes are appropriate for wearable electronics because they are light, strong, flexible, foldable, and pleasant. They have undergone considerable research for a variety of wearable applications, including electrodes for antenna, photovoltaic cells, electric power nanogenerators, batteries, and capacitors – almost all of which are sandwich-structured wearable electronic devices. Single fibers, skeins, and other textile-structured electrodes have been produced and studied. Others are produced from textiles made of dielectric materials via surface plating, embroidery, printing, and lamination. Stainless steel, copper, silver, nickel alloys, and CNTs are the materials used to make some of them. Therefore, a variety of hybrid or composite structures exists, including reduced graphene oxide/nylon yarn, hybrid electrodes made of graphene and ferroelectric material, functional yarn coatings, stretchable hollow fibers made of a triblock copolymer, Ag-silicone fibers, fibers with liquid metal alloys like eutectic gallium indium (EGaIn) injected into the core, and SEBS resin (EGaIn in SEBS resin), a conductive composite that is mat made.

## 3.5 Fabrication technology

### 3.5.1 Fabrication methods

Fabrication techniques have a significant impact on the properties, price, and stability of fiber-based flexible and wearable electronics. In general, two categories may be used to classify different methods for creating fiber-based flexible and wearable electronics. In the first category, conducting fibers composed of conductive polymer, metal, carbon, piezoelectric materials, or regular fibers with different functional elements applied to the surface are used to create electronic devices. In order to incorporate electronics into textiles, a number of e-textile research groups have concentrated on conductive threads or yarns [6]. For the fabric keyboard and music jackets, scientists from Virginia Tech and Massachusetts Institute of Technology (MIT) looked at exploring woven metallic organza or piezoelectric materials. Cottet investigated the electrical properties of copper (Cu) fiber-twisted polyester yarns. Examples include the research done by our group, in which X–Y grids of copper wires were woven into fabrics to create connecting lines. In order to connect textiles and electronics, Locher proposed the conducting band interconnection technique. The fiber-based method has produced good wearing qualities that resemble ordinary textiles and can tolerate mechanical deformations including bending, twisting, and stretching.

The second category, which is a supplement to the first, is based on embedding prototype model, off-the-shelf electronic parts such as transducers and other components onto traditional dielectric fabrics as a motherboard or imprinting electronic features on the surface of fabrics, using coating, printing, or lamination. However, if the connecting components are inflexible, the fabric's comfort or flexibility may be jeopardized. Due to the impossibility of extensive elongation in metals and conductive polymers, many of today's flexible e-textiles cannot fully adjust to their environment, despite significant advancements over rigid devices. Additionally, it would be preferable to incorporate electrical functionalities at the fiber level in order to retain fundamental textile features like durability; nevertheless, the majority of present research is restricted to a single utility. In addition to having great conductivity, the flexible conductor's other characteristics are identical to or comparable to those of common fibers or yarns, making it simple to weave or knit a new electrically functional fabric using common yarn that has wearability, processability, and flexibility. The stretchy conductors may be knitted or woven into an electric-functioned fabric with other ordinary yarns to create a tailored electric circuit. A commercial band weaving machine weaves the electronic strands in the weft direction of a woven fabric to create flexible and wearable electronics. By adopting a commercial manufacturing process, this technique establishes a platform for the intimate integration of a wide range of flexible electronic circuits, sensors, and systems on fibers inside textile designs.

### 3.5.2 Surface mounting technology

Therefore, there is some interest in the integration of electrical functionality into fabrics with completely textile-compatible manufacturing techniques. Lamination technology, which is used in the textile business, is directly related to surface mounting technology used in the electronics sector. Thermoplastic adhesives can be used to attach the thin-film-based devices to common textile fabrics. In addition, three methods, namely screen printing, digital printing, and dip-coating, have been developed to create solution processable wearable electronics in textile substrates, for the direct production of free standing electronic devices on textile substrates. These technologies permit the employment of low-cost patterning techniques in room conditions, which is one of their main advantages. In a layer-by-layer procedure, all the layers with various functionalities are printed on top of the fabric substrate, offering a simple manufacturing path for the creation of wearable electronics. Since each structural design is immediately defined with each layer application, this approach does not require further photolithographic or chemical etching steps. Additionally, screen printing offers a path to high-volume batch fabrication since it is compatible with commercial roll-to-roll techniques. The high areal mass loading provided by the screen printing method preserves the high inherent capacitance of the activated carbon. The usual roughness of fabric surfaces is of the order of 10 µm. However, by using controlled multiple-coating processes, the surface roughness may be significantly increased to the level needed for device interfaces. The screen printing technique also gives far more design freedom and placement flexibility on textiles than other techniques like weaving and knitting, due to its outstanding adaptability to any uneven textile surface.

The advantage of digital printing technique over screen printing is the great spatial accuracy of the ink droplet. Combining desktop programmable wiring of planned patterns with inkjet printing offers an interesting potential to use on-demand material deposition. The latter has already been proven for inks made of metal, CNTs, and graphene. Additionally, digital printing technology may be used to create piezoelectric, piezoresistive, and capacitive devices for detecting fabric deformation. The use of dip-coating is an additional approach. Dip-coating poly(vinyl alcohol) (PVA)/CNT on a polyamide yarn produced conductive yarns. The surface morphology and surface tension of the textile substrate, which can differ from section to section and may lead to uneven coatings, are two factors that heavily influence this process.

### 3.5.3 Conductive nanocoating technologies

Another successful method for incorporating electrical capabilities into textiles and enhancing the performance and usefulness of wearable electronics is conductive nanocoating technology. The necessary capabilities should be imparted by a suitable coating method, which should also offer a sufficient interface layer for high durability. Coated textiles that just added different qualities would not last washing and wearing, without precise surface engineering. To induce powerful surface contacts like covalent or ionic bonding, surface modification of the fibers is necessary. Due to the large surface area-to-volume ratio and high surface energy of nanomaterials, conductive coating with discrete molecules or conductive nanomaterials can be applied to specific sites on textile materials, using thermodynamic, electrostatic, or other techniques in a particular orientation and trajectory. A few of the techniques that have been researched include thermo- and chemical vapor deposition, chemical reduction, electrochemical deposition, and pulsed laser deposition. The main question is whether it is possible to cost-effectively apply long-lasting nanoscale coatings on textiles, while still meeting the demands of electrical functions. Low-cost, low-temperature methods without a vacuum atmosphere are favored in this regard.

### 3.5.4 Self-organizing technologies

A few cutting-edge techniques using material self-organization have reportedly been used to create fiber-based gadgets. For instance, piezoelectric ZnO NWs grown radially around fibers have recently been reported to be used in a fiber-based micro-supercapacitor (SC). Two fiber electrodes make up these fiber SCs. High-quality ZnO NW arrays with one-step self-aligned dimensions are generated hydrothermally to cover both fibers. Due to their flexibility and electronic performance, Si, GaAs, GaN, and Ge are other inorganic semiconducting NWs. However, considering that the mechanisms are still unclear and that the majority of current research is empirical in nature, one would ask how effectively the self-organization, assembly, and processing processes can be managed at a scaled-up production level to produce repeatable material qualities.

## 3.6 Fabrication of electrospun porous nanofibers [2]

Various application scenarios call for certain material compositions as well as suitable pore sizes and pore shapes. The unique spatial organization of microporous materials allows the active center to be stabilized at a single spot, making them more suited for catalysis. Additionally, the microporous material is made accessible for adsorption due to its enormous specific surface area (the specific surface area of activated carbon, for instance, can reach up to 1,000 $m^2/g$). Greater molecules that are challenging for microporous zeolites to manage can be adsorbed and separated by mesoporous materials with larger pores than microporous materials. It also makes a great carrier for catalysts due to its regular and ordered pore structure, narrow pore size dispersion, and continuously changeable pore size. As macroporous materials have pores that are much bigger than molecules, this promotes the increase of substance transmission and diffusion. As a result, macroporous materials offer certain benefits as biological and energy storage materials. To get desirable porous structures in manageable ways, it is crucial to create suitable manufacturing techniques. In most cases, there are numerous techniques used to create porous architectures in electrospun nanofibers.

### 3.6.1 Phase separation

Phase separation is a method that is frequently used to create pore architectures. The condensation of water vapor occurs on the fiber surface as a result of the evaporation of volatile solvents (such as chloroform) during the electrospinning of polylactic acid from chloroform. The gap on the surface of the semidried fiber can be used as a template by the condensed water droplets. Chloroform's water immiscibility and polylactic acid's hydrophobicity allow for the condensed water droplets to stabilize and emerge on the fiber surface. Finally, water droplets and chloroform evaporate to produce pores. Contrarily, the nonvolatile solvent slowly evaporates, giving water vapor enough time to interact with the fiber surface and permeate into the fiber. Water vapor functions as a nonsolvent for the polymer, if it is hydrophobic. Liquid phase separation will encourage the creation of a porous interior structure as water permeates the polymer/solvent mixture, more and more. The same happens when the temperature of the fiber drops suddenly – thermally induced phase separation. As phase separation is driven by temperature differences, the collector's high temperature and the fiber's low temperature both help create a highly porous structure. To create porous fibers, all of the aforementioned techniques rely on phase separation. In order to produce macroporous structures in this manner, suitable solvents and polymers must be chosen.

### 3.6.2 Template method

The process of creating porous fiber via the template approach may be broken down into three parts, in accordance with the basic procedure for creating porous materials: Create the template first. In order to coat the target products onto the template, several methods were used, such as hydrothermal synthesis, precipitation, or sol–gel. The template must be removed in the last phase using a process like etching, sintering, or dissolving. Hard and soft template approaches are common categories for template methods. Materials having predictable shape and structure are often preferred by hard templates, such as polystyrene (PS) colloids, silica NPs, mesostructured silicas, and anodic aluminum oxides (AAO). Additionally, porous materials like zeolites, MOFs, and COFs are used as hard templates to add pores to already-spun fibers. After eliminating the polymer phase by calcination treatment, the mixed electrospinning solution containing porous materials and polymer is diametrically electrospun to produce porous fibers. Surfactant molecule accumulation frequently creates soft templates. Common soft templates include biopolymers, surfactants, and polymers. Although fibrous materials may be prepared using the soft template approach, there is little information available on how to create electrospun porous fibers, using this technique. The template has excellent thermal stability and is highly organized. As a result, the technique works well for producing microporous and mesoporous fibers with simple pore size control.

Gradient pyrolysis is another template approach that has gained popularity, recently. A mixture of polymers with varied molecular weights is first electrospun, and the fiber is subsequently calcinated at various temperatures to generate variable pore sizes. Instead of mixing together, the low-, middle-, and high-molecular-weight polymers, typically, are divided into three layers. There will be holes in the fiber because the thermal breakdown sequence of low-, middle-, and high-molecular-weight polymers differs, as the temperature rises. Gradient electrospinning uses a straightforward approach. However, this technique works better for creating macroporous fibers.

### 3.6.3 Multifluid electrospinning

One unique template approach that uses liquid to fill space before eliminating the liquid phase through a subsequent procedure is multifluid electrospinning. The capacity of electrospinning to produce porosity and other novel forms of nanostructures can be significantly increased by multifluid electrospinning techniques like coaxial, triaxial, quad-fluid, or side-by-side electrospinning. The outer spinneret and several inner spinnerets implanted in the outer one make up the multifluid electrospinning spinneret. A well-designed spinneret, compatibility of the working fluids, and unique operating parameters are essential for conducting multifluid electrospinning. The composite fluid is stretched and solidified by the electrostatic field's action, resulting in the formation of porous hollow fibers or multicomponent composite fibers with many internal channels. Coaxial electrospinning, the most popular type of multifluid electrospinning, can create hollow and core–shell fibers by draining the inner fluid. Choosing the proper sacrificial phase and controlling the experimental parameters during electrospinning, particularly the matched flow rate between core fluids and shell fluid, are crucial in this approach. Despite being rather consistent, the macroporous multichannel fibers made with this approach still have numerous hampering elements, and it is necessary to precisely manage the electrospinning settings.

Porosity and pore homogeneity are both important factors in the production of electrospun porous fibers. A key aspect impacting the regularity of the pore structure is the dispersibility of the polymer and additives in the spinning fluid. Adequate ultrasonic dispersion during the spinning solution preparation process followed by the addition of the polymer will improve the solution's dispersibility. Phase separation during the electrospinning process will result in uneven pores because of the solution's limited dispersibility. The homogenizer can be used to improve the dispersibility of the solution containing solid particles for the template process. The spinning solution contains no solid particles at all, and the surface of the produced fibers can also be evenly occupied.

We shall introduce several pore structures made in electrospun nanofibers, such as micropores, mesopores, macropores, and hierarchical pores, in the section that follows.

## 3.7 Microporous nanofibers

Microporous materials are porous materials having pores smaller than 2 nm. This scale is analogous to tiny molecules, which permits the size selectivity of microporous materials to various molecules. As a result, creating microporous structures is a significant and promising technique that enhances the material's performance.

Electrospinning allows for the continuous synthesis of carbon nanofibers. The microporous structure of carbon nanofibers can offer accessible active sites and contact area. Due to their distinct benefits over other types of carbon materials, electrospun carbon nanofibers have generated a lot of interest. For instance, by electrospinning, treating with iodine, and carbonizing PVA nanofibers, microporous carbon nanofibers may be produced, with pore sizes ranging from 0.55 nm to several nanometers. PVA nanofibers were first submerged for 24 h in iodine vapor (80 °C) in a sealed glass bottle. The production of carbon nanofibers can be stabilized by iodine treatment. Then, iodized PVA nanofibers were carbonized to create micropores. The specific surface area and pore size of porous carbon nanofibers may be greatly altered by adjusting the iodide insertion and the composition of the spinning solution. Additionally, using lignin/polyvinyl pyrrolidone (PVP) as the carbon precursor and zinc nitrate hexahydrate as an additive, Ma et al. [39] generated lignin-based ultrafine porous carbon nanofibers using electrospinning, pre-oxidation, carbonization, and pickling processes. Note that the purpose of the pickling operation is to etch the template. Zinc nitrate hexahydrate was pyrolyzed to yield rich micropores. The generated microporous carbon nanofibers exhibit high flexibility and can be easily cut into supercapacitor electrodes, offering useful direction for the development of microporous carbon fibers.

Zeolites are a different type of microporous material in addition to the nanoscale carbon fibers. Their microporous structure offers exceptional chemical and structural stability, as well as molecular sieving capability. In the chemical and petroleum sectors, zeolites have been widely employed as catalysts and catalytic supports. However, at high temperatures, particle zeolites easily sintered, reducing their activity and impacting performance. Making zeolite into a fibrous substance is one way to enhance its performance. By using coaxial electrospinning, Liu et al. [40] demonstrated a flexible and simple technique for creating microporous zeolite nanofibers. The outer fluid was paraffin oil with ZSM-5 nanocrystals suspended in a PVP/ethanol solution as the inner fluid. The hollow microporous zeolite fiber could be produced when the inner fluid and outer polymer of the coaxial electrospun fiber were removed by calcination. The microporous zeolite nanofibers are preferred for catalytic applications, because the reactants are more easily accessed by the catalyst's active site. Electrospun fibers are a superior catalyst carrier that may prolong the useful life and efficiency of a microporous catalyst by preventing sintering and agglomeration. Additionally, microporous structures have exceptional rate capabilities and extremely extended lifespans and can give quick kinetics of ions storage.

## 3.8 Mesoporous nanofibers

A type of porous material having pores between 2 and 50 nm in size is called mesoporous material. Mesoporous materials play a significant role in the adsorption and separation of macromolecules, particularly in catalytic processes, due to their regular and ordered pore structure, narrow pore size distribution, and constantly changeable pore size. Mesoporous materials have the ability to interact with atoms, ions, molecules, and NPs not just on their surfaces but also within the material itself. Fibers with a hierarchical structure can create cavities for mesoporous channels, which will aid in the diffusion and transmission of substances and enhance the functionality of materials.

Metal-organic framework (MOF)-based electrospun nanofibers combine the properties of MOFs (high specific surface area and adjustable form and size) with electrospun nanofibers (porous crystalline structure, coordinated metal nodes, and organic linkers), which has drawn growing interest in a variety of applications. Wang et al. recently created interconnected mesopores in zeoliticimidazolate framework-8/polyacrylonitrile (ZIF-8/PAN) nanofibers that were electrospun. Mesoporous ZIF-8/PAN fibers may be made when PVP is removed and the calcination process is completed. Mesopores were created on each fiber using the pore-forming procedure, and ZIF-8 particles were then inserted into the mesoporous channels. The $N_2$ adsorption–desorption isotherms demonstrate that ZIF-8/PAN nanofibers have the usual mesoporous characteristics. Mesoporous ZIF-8/PAN nanofibers reveal additional ZIF-8 adsorption sites and show promise for use in the treatment of water. Mesopores can also speed up pollutant molecule transport and create MOF polymer interfaces inside the fiber, which enhance adsorption capacity and rate, respectively.

Bimetallic ZIF NPs/PAN fibers with different molar ratios of Zn/Co were created by Yu et al. and used as carbonization precursors. After carbonizing MOFs nanofibers, Co/N-doped mesoporous carbon fibers with excellent electrochemical performance were produced. The thin PAN coating of the NPs shields them from irreversible Co fusion and aggregation during the pyrolysis process. Big pore volume is helpful for the quick transit of associated chemicals, and large specific surface area is useful for the adsorption of $O_2$ and electrolyte. The oxygen reduction reaction (ORR) activity of the Co/N-doped porous carbon fibers was good, even on a par with that of the Pt/C catalyst in an alkaline environment.

As electrocatalysts for ORR/OER, N-doped hierarchical porous carbon nanofibers (HPCNFs) loading $Co/Co_3O_4$ hetero-NPs were made. Phase separation was used to prepare porous polyimide (PI) fibers, in the first stage. The twofold diffusion process between the solvent in the electrospinning jet and the surrounding water vapor might be influenced by relative humidity. Phase-separated fiber pores were produced by this method. After that, $Co_3O_4$ NPs were added to the surface of the fibers using the hydrothermal technique. $Co/Co_3O_4$ NPs were added to the fibers by additional hydrothermal and pyrolysis processing. On the fiber surface, uniform mesoporous structures could be seen, and the concentration of pore sizes is primarily in the 4–7 nm region. For the design of catalysts and energy storage applications, the method of creating many cavities and mesopores on the surface of fibers may be applied to various materials. Additionally, the template approach may be used to create mesoporous structures that are more consistent. According to Nakane et al., a foaming agent-aided electrospun template approach was employed to manufacture mesoporous long $TiO_2$ nanotubes, with electrospun water-soluble PVA nanofiber serving as the template. Mesopores with a consistent spatial distribution were created on the surface of $TiO_2$ nanotubes during the template removal procedure. Additionally, several multilevel electrospun nanofibers have been generated. By employing mesoporous alumina as the shell layer and silica as the core layer, Chen et al. created core–shell nanofibers with mesopores. Due to its blooming porous structure and high adsorption capacity, the core–shell structured nanofibers demonstrated good adsorption performance, which encouraged their practical application in environmental cleanup.

Mesopores are an effective filtration and separation material because of their tunable size, which allows them to selectively filter macromolecular contaminants. Additionally, the material's organized channels can act as diffusion channels for chemicals and speed up their transfer. As a result, electrospun mesoporous nanofibers are crucial for the adsorption, separation, and catalysis of macromolecules.

## 3.9 Macroporous nanofibers

Generally speaking, macroporous materials are those that have pores greater than 50 nm. Typically, phase separation or the selective sacrifice of polymers or salts leads to the creation of macropores in electrospun nanofibers. Phase separation was employed by Wendorff et al., in 2001, to create electrospun porous nanofibers during the electrospinning process. Using volatile solvents, porous fibers with a regular pore structure were created. Then, using a similar electrospinning technique, PS and poly(D, L-lactic acid) nanofibers with macroporous structures were created. Phase separation during the electrospinning process caused the solvent to quickly evaporate, resulting in the formation of this porous morphology. Numerous electrospun macroporous nanofibers, including hollow nanofibers, nanowire-in-microtube-shaped nanofibers, and multichannel nanofibers may be created by selecting the fluid channels to be removed from the template and adjusting the number of fluid channels. The mass transfer capability of the fiber, which is extensively employed in energy storage and increases electromagnetic wave absorption, is considerably enhanced by the development of macroporous structures in electrospun nanofibers. First, composite nanofibers were created by electrospinning a precursor solution of $Ti(OBu)_4$, PVP, CTAB, and paraffin oil. The nanofibers were then calcined to create multichannel fibers. The relative amount of $Ti(OBu)_4$ and paraffin oil may be easily changed to change the pore size. Phase separation was used to create porous PS electrospun fibers in addition to the inorganic macroporous fiber. The pore size of the porous PS fibers would alter in accordance with changes in the molecular weight of the polymer, the solvent composition, the solution concentration, and other factors. Coaxial tubular electrospun nanofibers with several macroporous features have also found use in a variety of fields.

Macroporous structures are typically employed as diffusion channels. The open porous structure can speed up the transmission of charges as well as the dispersion of materials. As a result, it is often employed in battery materials, catalysis, and other fields.

## 3.10 Hierarchically porous nanofibers

Although macroporous, mesoporous, and microporous materials each has unique benefits, their uses are sometimes limited by the simple porous architectures. The macropores, for instance, cannot complete the restricted catalytic reaction or the adsorption and separation of tiny molecules if the pore size is too big. The microporous material's pores that are too small, on the other hand, will hinder the substance's transmission and diffusion. Effective mass transfer, separation, and catalytic confinement may be accomplished if the macropores, mesopores, and micropores are linked together by interconnected pores. As a result, the creation and use of hierarchically porous materials made up of micropores, mesopores, and macropores is a fast-expanding topic. Materials can frequently benefit from functional expansion and performance improvement due to hierarchical pore structure. Due to their large contact surface area, high storage volume, shape selectivity, and carefully regulated porosity, hierarchically porous materials have demonstrated substantial benefits over basic porous materials in catalysis, adsorption, sensing, and energy storage.

To create conductive hierarchically porous carbon nanofibers, Ding et al. presented a chemical cross-linking technique. Poly(tetrafluoroethylene) (PTFE) and poly (vinyl alcohol) (PVA) were cross-linked to create a hydrosol network, which was then electrospun into a fiber membrane. Boric acid was used as the cross-linking agent. The fibers were converted into B-F-N triple-doped porous carbon nanofibers with well-controlled macro-, meso-, and micropores after oxidation and pyrolysis. The fibers were transformed into porous carbon nanofibers (PCNFs) during the nitrogen pyrolysis at 1,200 °C . Small molecules were pyrolyzed to form medium micropores, whereas big PTFE NPs were decomposed to produce continuous macropores.

PCNFs demonstrated several roles in gas adsorption, sewage treatment, liquid storage, supercapacitors, and batteries while also having a significantly lower mass transfer resistance. To create mesopores by the breakdown of PVP domains, the initial phase of the thermal treatment process was performed at 900 °C in an inert environment. A sufficient amount of micropores and carbon defects may also be produced by the evaporation of Zn from ZIF-8 precursors. The active $CoN_4$ sites were added to the carbon fiber supports during the second heat treatment stage at 1,100 °C. After that, hierarchically porous Co-N-PCNF catalysts were produced. The catalyst that was created synthetically increased ORR's stability and longevity. In addition, Liang et al. created electrospun hierarchically porous ZIF-8/PAN composites that were employed as benzene adsorbents. Direct electrospinning of the ZIF-8 and PAN mixture resulted in composite fibers, which were subsequently calcined for three hours at 800 °C in an environment of $N_2$ and Ar to produce porous fibers. The abundance of N-species-containing active sites and hierarchically porous structure demonstrated good adsorption capability. The design and synthesis of various functional materials can be aided by the principles and techniques learned from this study. The hierarchically electrospun porous nanofibers have a wide variety of uses in catalysis, separation, and energy storage because of the vast pore distribution structure.

## 3.11 Carbon fibers (CFs)

Thin, long filaments consisting of more than 90% carbon, carbon fibers (CFs) have a high modulus of 200–900 GPa, large stiffness toughness of up to 3 GPa, high tensile strength of 2–7 GPa, flexibility, and customizable electrochemical performance [7]. As a result, they are used extensively in a variety of industries, including aerospace, automotive, chemical, transference, building, manure handling, and other arenas. Additionally, they can function as multifunctional hosts by easily annealing them in the air to create more oxygen-containing functional groups and higher defective edge/plane sites, which can load a variety of electrochemically active materials like noble metals, metal oxides, polymers, and MOFs. They may thus be used to create energy equipment with a high energy/power density as well as electrochemical sensors with great sensitivity and adaptability. Uniting pure CFs with metal materials, metallic oxide materials, metallic sulfide materials, carbon materials, and other materials has been found to significantly increase performance. For instance, by using solid-state mixing and thermal breakdown procedures to decorate CFs with cobalt oxide NPs, the performance improved. As a result, the capacitor’s ability to store energy increased significantly. Additionally, CFs may be put together into many other sensor-related structures. For instance, an electrode with a porous structure is easily able to produce ion diffusion and electrolyte penetration.

### 3.11.1 Preparation of CFs

More than 100 years have passed since the invention of CFs. With the ongoing advancement of technology, the present method of CF preparation has advanced significantly. Majority of the time, synthetic fibers (precursor fibers) are used to create CFs, and different fiber raw materials need the employment of various manufacturing procedures to do this. The general method, which involves controlled stretching synthesis of CFs and stable precursor fiber pyrolysis, is comparable. Presently, PAN, pitch, and rayon are the primary basic ingredients used to make CFs. About 90% of CFs are really made using PAN-based precursors, with the other 10% being created using asphalt or rayon precursors. This is due to the fact that PAN-based CFs have better strength, modulus, failure strain, and yield rates, when compared to asphalt fiber and rayon fiber. A type of high-strength material, CF is used extensively in the aerospace, automotive, chemical, general engineering, missile, nuclear, composite reinforcement, and textile industries.

## 3.12 CF classification based on precursors

### 3.12.1 PAN-based CFs

PAN-based polymer's tensile and compressive characteristics, together with its up to 68% carbon yield, make it the ideal precursor for the creation of CFs. Most PAN-based polymer precursors are employed in the commercial synthesis of CFs by wet spinning. However, dry-jet-wet spinning is gradually displacing wet spinning due to its numerous benefits, including low fiber adhesion and large specific surface area for enhancing the interlaminar shear strength of composite materials. Cortical fracture and epidermis fold essentially vanish during wet spinning, as a result of the isolation of extrusion expansion and epidermis solidification in dry-wet spinning, which modified the mechanism of fiber creation. The density of dry-wet spinning is increased, while the surface and internal flaws are reduced. Additionally, dry-wet spinning, which is the direction of development for the manufacturing of CFs, has the qualities of high spinneret drawing, high spinning speed, and ease of obtaining high strength and high orientation fiber.

### 3.12.2 Pitch-based CFs

Synthetic polymers are pyrolyzed to create pitch. Pitch has an average molecular weight of 600–1,000 g/mol and has aromatic groupings. Pitch-based CFs have a diameter between 10 and 12 mm, and their tensile strength and modulus are 3 and 960 GPa, respectively. Due to its low cost compared to other precursor fibers, pitch is an appealing precursor for producing large numbers of CFs, since it is simple to create in big quantities. In addition to these benefits, pitch-based precursors are a desirable option, since they use less energy to convert aromatic graphitized materials and include less hydrogen, nitrogen, and other noncarbon components.

### 3.12.3 Rayon-based CFs

Rayon is a synthetic material composed mostly of cellulose obtained from plants (cotton wool and pulp). A possible basic material for CFs is cellulose. Additionally, the cellulose precursor undergoes pyrolysis to produce strong CFs that are low-cost and have excellent thermal conductivity, high purity, and good mechanical toughness. Carbonization of rayon fibers into high modulus CFs filaments is necessary for the new production method. This was followed by much more yarns with high strength and high elastic modulus, in addition to the early low-strength fibers. Manufacturing of these CFs has been put off for many years due to the high cost of hot drawing, low-quality CFs spinning method, and delayed development of the qualities of cellulose precursors.

### 3.12.4 CFs based on other precursors

Other natural fibers, including silk and chitosan, are also regarded as predecessors for the development of CFs, in addition to the numerous extensively used precursors previously listed. These fibers can lower production costs but cannot create CFs with significant mechanical qualities. It has also been demonstrated that some linear and cyclic polymers can be used to create CFs, although the results suggest that these polymers produce relatively little carbon, which limits their potential for further use.

## 3.13 Functional CFs

CFs have received much research interest as nanomaterials due to their exceptional chemical and physical characteristics. However, as technology advances, more and more functional materials are blended onto the surface of CFs in order to meet the research needs of some specific performance nanomaterials. This significantly enhances the properties of composites and allows for the incorporation of precious metal nanomaterials, polymers, metal oxides, MOFs, and other materials.

### 3.13.1 Noble metal-functionalized CFs

Due to their unfilled d-electron orbitals, minimal energy level gaps, ease of forming coordination bonds, and ease of adsorbing and desorbing groups on their surface, precious metal nanomaterials may quickly generate intermediate active compounds and have high catalytic activity. Because of their outstanding stability, superior electrical conductivity, and high biocompatibility, precious metal NPs have been used often, recently, to change the surface of CFs. Metal NPs may also be created and modified in a fairly straightforward manner. Gold NPs were used to etch the surface of CFs in order to increase the specific surface area and improve the electrochemical performance of CFs. The findings demonstrate that etching not only shrinks CFs in diameter but also alters their surface shape and roughness by introducing flaws or porous structures. Additionally, it has been discovered that this etching technique may concentrate on grain boundaries or flaws rather than destroying the $sp^2$ bonding of graphite. The detection of cancer cells also uses CFs modified by Au NPs. The grapheme-based composite increased the specific surface area of CFs and improved the electrical conductivity of the material through the preparation of CFs microelectrode with hierarchical Au-$MnO_2$/GO/CF nanostructure. The $MnO_2$ on CFs then formed porous nanostructures, which provides an excellent matrix for the growth of Au NPs.

The findings demonstrate that the constructed microelectrode is capable of detecting hydrogen peroxide released by human cervical cancer cells in real time, quickly, and accurately. In order to track dopamine release and ascertain rat intracellular exocytosis, some researchers directly electrodeposited gold NPs on the surface of CFs, at the same time. Few papers on the electrochemical detection of dopamine using bimetallic NPs currently exist. Based on this, scientists have created modified CFs microelectrodes using Ag–Pt bimetallic nanomaterials to detect dopamine quickly and accurately. The study showed the sensor's benefits of quick current response, high sensitivity, wide detection range, and low detection limit, as well as its ability to successfully counteract the effects of interfering compounds on dopamine detection outcomes. Finally, precious metal composite CF NPs demonstrate the synergistic impact of diverse components, further enhancing the characteristics of the composites, particularly in the application to batteries and capacitors. Precious metals will continue to be competitive in the use of functional CFs in the future.

### 3.13.2 Metal oxide-functionalized CFs

The manufacturing of different sensors and anode materials for batteries, among other things, typically uses metal oxide NPs as the catalyst of first choice in the catalytic reaction of the oxidation–reduction process. Another usual technique for producing functionalized CFs is the mixing of metal oxides with CFs. Researchers successfully constructed a high-performance humidity sensor by mixing bismuth ferrite NPs (BFO) with CFs by hydrothermal technique after synthesizing a humidity sensor based on BFO. Composite nanomaterials demonstrate great sensitivity, low hysteresis, and outstanding stability when compared to BFO as humidity sensitive units, demonstrating the promise of BFO in humidity sensing. Due to the stringent criteria of blasting, attention of researchers has turned to the detonation ignition device, where the energy conversion element is the main area of interest. The preparation of high-quality energy conversion components can increase detonation success rates, reduce ignition delays, and improve ignition efficiency. Therefore, by mixing $Al/BiO_3$ nanomaterials on the surface of CFs, the researchers developed a novel form of ignition device, taking advantage of the superior electrical conductivity and ease of surface modification of CFs. $Al/BiO_3$ can boost the detonation ability and dependability of this device.

Due to their widespread availability and high capacitance, transition metal oxides are frequently employed as electrode materials for energy storage devices. The specific capacitance and energy density of devices have been shown to be improved by combining transition metal oxides with CFs. It will continue to be a focus of battery device research in the future.

### 3.13.3 Polymer-modified CFs

CF composites are widely employed in the domains of medicine, construction, transportation, and aerospace because of their exceptional tensile characteristics and stiffness, as well as their low weight and strong heat resistance. The key to determining the characteristics and structure of CF composites is the level of interfacial adhesion between the CFs and matrix. It is frequently stated that polymer molecules are employed to alter CFs in order to increase their interfacial stickiness. Based on this, we review recent work on certain polymer matrix modified CFs in terms of research and application. The rigid polyurethane (RPU) was combined with the polydopamine nickel-modified CFs material, and the composite's mechanical and electrochemical characteristics were investigated. Due to the chemical cross-linking at the CFs and RPU interface, the strength, toughness, and electrical characteristics of the modified CF composites are much better than those of the original CF-RPU composites. It was reported to use polyoxypropylene diamine (D400) as the coupling agent and curing agent in a green functionalization technique for the alteration of CFs in water. The polarity, lubricity, and roughness of the CFs surface were all improved by D400, which did not alter the surface structure of the CFs, according to research on the mechanical and microstructural characteristics of the modified composites.

Researchers have been paying close attention to polymer-reinforced CF composites, because they combine the outstanding mechanical and electrical conductivity of CFs with the excellent interfacial adhesion and thermoplasticity of polymers. They may also be deployed in the assembly of heavy industrial products as well as in the fabrication of microdevices such as sensors and energy storage electronics. CF-reinforced composites still have a wide range of potential applications.

### 3.13.4 Metal-organic framework (MOF)-functionalized CFs

MOFs, commonly referred to as porous coordination polymers, are novel organic porous materials (PCPs). They typically consist of two basic parts: organic ligands and metal ions or clusters, both of which are primarily joined together by obvious coordination bonds. However, due to their distinctive design, restricted purpose, and subpar performance, the potential of pure MOFs for future application is restricted. MOFs composites have emerged as a new area of scientific interest in recent years. For instance, it has been demonstrated that MOFs may be combined with inorganic materials, carbon materials, metal nanocrystals, polymers, and proteins to create novel multifunctional composites. In sensors, batteries, supercapacitors, gas storage and separation, catalysis, and other devices, MOF composites are often used. Sodium-ion and lithium-ion batteries have both been used extensively in energy storage systems, where the choice of electrode materials is almost usually the primary factor impacting battery performance. Although CFs have received a lot of attention as potential battery anode material, their limited ability to be reversed throughout the battery-making process prevents them from finding wider use. Due to this, the first porous carbon nanoarrays with $Co_3O_4$ intercalation and nitrogen doping were created on CF sheets (CFC/$Co_3O_4$-NC) and used as anode materials for lithium-ion batteries. A composite anode (CFC/Co-NC@Li), which can effectively slow down the volume change and limit the formation of Li dendrites, is created by mixing the matrix with the molten Li. Additionally, MOF-modified CF composites are employed to enhance the effectiveness of the oxygen evolution process and the interfacial characteristics. The interfacial characteristics of composites can be significantly improved by MOFs. By generating nanoflake MOFs on the surface of CFs, researchers seek to enhance the interfacial characteristics of CFs/epoxy composites. The surface structure of CFs changed by nanoflake MOFs is homogeneous, and under the influence of the MOF, the interfacial shear strength and surface energy rise by 70.30% and 69.75%, respectively.

MOFs have been successfully synthesized as a novel class of porous crystal materials. However, due to their low conductivity and poor chemical stability, they are frequently employed as precursors or templates to create other carbon-based structures. It is difficult to create distinctive MOF-based composites and to enhance their properties in the future.

## 3.14 Application of biosensor based on CFs

An electrochemical biosensor is a significant piece of technology that offers benefits including easy operation, quick analysis, great selectivity, and low cost. The need for sensors has been growing recently due to the rapid development of sensors (e.g., great biocompatibility and stability, high sensitivity, and low detection limit). It has received significant attention and is frequently used in the biomedical research, food industry, fermentation industry, and other industries, due to its exceptional qualities, including low relative density, strong mechanical strength, high-temperature endurance, and the ability to modify their structure into a variety of geometric forms to suit diverse demands. Biosensors are no longer just for the lab due to the quick development of flexible electrodes and wearable electronics. Researchers create a new class of portable, miniaturized biosensors by incorporating CF materials with flexible devices and wearable electrical gadgets. Now, wearable CF nanomaterial devices and biosensors based on flexible electrodes are widely employed in biomedicine, environmental analysis, food safety, and human health monitoring.

### 3.14.1 Conventional electrochemical biosensor based on CFs

The permeability of CF-based electrodes, which permits the entry of electrolyte and the diffusion of ions, enables the continuous conducting network to facilitate the fast transfer of charge between active compounds and metal ions. CFs have developed into a biosensing platform for the detection of biomolecules due to their superior electrical conductivity, robust mechanical qualities, and outstanding biocompatibility. Microelectrodes have also gained a lot of interest in electrochemical investigation due to their distinct electrochemical characteristics brought on by their tiny size – micron size in one dimension. For instance, an $H_2O_2$ electrochemical microsensor was created using the core–shell structure of 2D VS2@VC@N-doped carbon sheets embellished with ultrafine Pd NPs vertically grown on CFs, using a modified template-free hydrothermal approach. Because of the special rosette-like array shape, this biosensor demonstrated outstanding electron transferability, electrocatalytic activity, stability, and biocompatibility. With a high sensitivity of 152.7 µA $cm^2$/mM, a detection limit (LOD) of 50 nM (a signal-to-noise ratio of 3:1), excellent repeatability, and strong anti-interference capabilities, it might be employed for real-time in situ electrochemical detection of $H_2O_2$ in live cancer cells and cancer tissue. The monitoring of cellular active substances and human physiological indicators is another common use for CF-based biosensors. The hormone, cortisol, is thought to have a major role in the control of several physiological processes, including the stress response and bio-psychology. To identify lactate in wines and ciders, researchers created a lactate biosensor based on graphitized carbon nanofibers. Lactate oxidase (Lox) was modified by covalent immobilization onto the Pt NPs/GCNF surface using polyethyleneimine (PET) and glutaraldehyde. Graphitized carbon nanofibers supported Pt NPs composites (Pt NPs/GCNF) were prepared by chemical reduction of Pt precursors on the surface of GCNF for lactic acid sensing (GA). Excellent repeatability (RSD 4.9%, $n = 10$), sensitivity (41.302 ± 546) µA/M $cm^2$, and a good detection limit (6.9 M) are all displayed by the lactic acid sensor. Additionally, it has been demonstrated that under storage conditions of 20 °C, the sensor's activity can be maintained to an extent of around 95%, significantly enhancing the sensitivity and accuracy of lactic acid detection in drinks.

### 3.14.2 Flexible or wearable biosensor based on CFs

In recent years, wearable smart gadgets and flexible electronics have progressed quickly. They make the equipment more intelligent, portable, and compact, rather than lowering the detection accuracy and sensitivity. Therefore, there are still many opportunities for the development of flexible and wearable devices based on CF biosensors in the future. For biological physiological health markers, it is practicable to measure brain activity. A flexible biosensor probe based on CFs was inserted into mouse brain tissue, in research. We describe a micromachining technique that uses selective reactive ion etching to embed flexible, cloth-like, and polymer-derived CF pads in polyimide. One CF pad forms the whole electrocorticography (ECoG) electrode array without any joints or metal interconnections. The plane resolution of the CFs structure is decreased to 12.5 µm, and the height is increased to 3 µm during the wafer fabrication process.

The constructed superflexible neural device has high recording performance after implantation in vivo and exhibits great mechanical and electrochemical stability in vitro. Although the development of the ECoG electrode is the main focus of this work, the fabrication method of the polyimide/CF-based metal-free implantable probe may also be used in various biomedical monitoring and sensing platforms. Similarly, researchers have published a fabrication method for a hybrid flexible microelectrode based on CF using hydrothermal synthesis, which employs CF-coated gold NP-modified nitrogen hybrid CNT arrays to monitor the $H_2O_2$ released by cancer cells in vivo, in real time (NCNATs).

## 3.15 Natural components

### 3.15.1 Natural fiber

Natural fiber is categorized according to where it comes from, such as plants, animals, or minerals [8]. Cellulosic materials make up all plant fiber, which is divided into several categories, including seed fiber (cotton), bast fiber (flax, ramie), fruit fiber (coir), stalk fiber (rice), and other grass fiber. Animal hair and silk make up the animal fiber. Asbestos is the mineral fiber in question. Figure 3.3 depicts a diagram with a range of fibers. Several academics have been investigating the use of natural fibers as composite materials, during the past few years.

### 3.15.2 Natural macromolecules

Based on their purpose, function, and features, macromolecules are divided into many groups. Natural macromolecules have garnered a lot of attention in recent years from these classes, due to their environmental sustainability and biodegradability. Natural macromolecules are categorized based on the places where natural fiber polymers come from. Cellulose, hemicellulose, lignin, pectin, starch, alginate, chitin, albumin, and other macromolecules are among them. Figure 3.4 displays the categorization in detail.

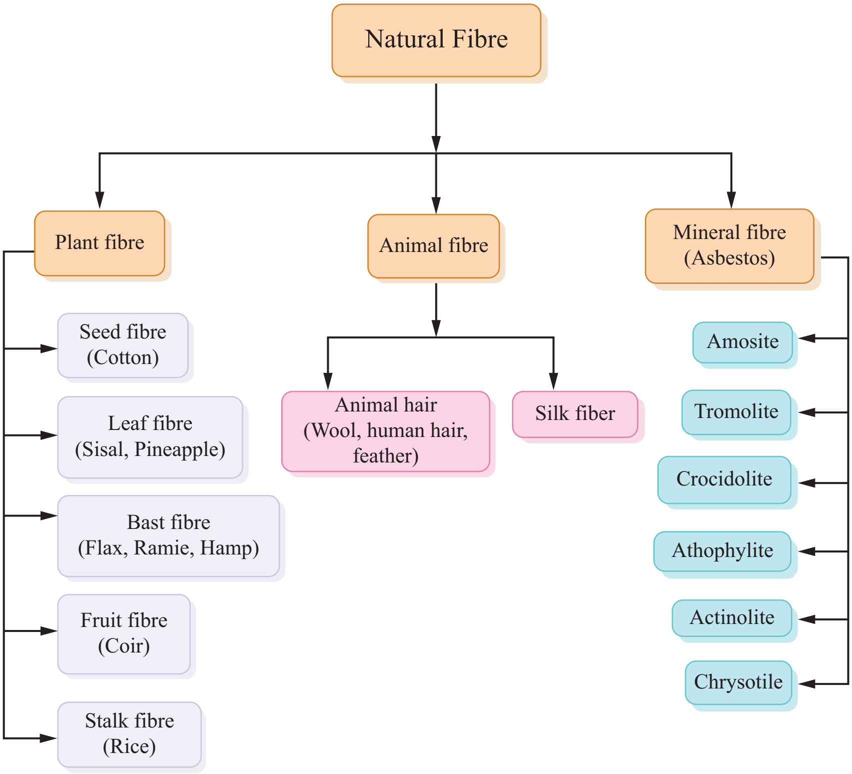
Natural Fibre
Plant fibre
Animal fibre
Mineral fibre (Asbestos)
Seed fibre (Cotton)
Leaf fibre (Sisal, Pineapple)
Bast fibre (Flax, Ramie, Hamp)
Fruit fibre (Coir)
Stalk fibre (Rice)
Animal hair (Wool, human hair, feather)
Silk fiber
Amosite
Tromolite
Crocidolite
Athophylite
Actinolite
Chrysotile

**Figure 3.3:** Classification of natural fibers [8].

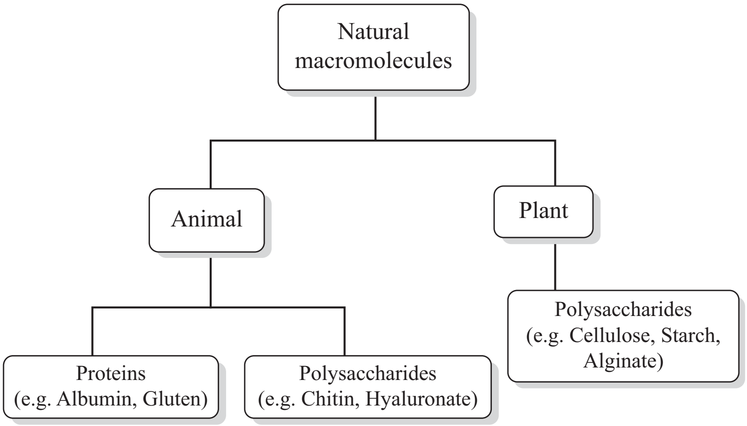
Natural macromolecules
Animal
Plant
Proteins (e.g. Albumin, Gluten)
Polysaccharides (e.g. Chitin, Hyaluronate)
Polysaccharides (e.g. Cellulose, Starch, Alginate)

**Figure 3.4:** Classification of natural macromolecules [8].

## 3.16 Fabrication of composite materials

### 3.16.1 Wood-based fabrication of composite materials

Due to their unique qualities such as environmental friendliness, renewability, and biodegradability, wood-derived composite materials have recently received a lot of attention in research and development. Thus, cellulose and lignin, the two primary natural macromolecules found in wood, have garnered a great deal of attention for both theoretical studies and real-world applications. Different forms of macromolecular engineering place an emphasis on the exact designs of well-defined polymers. The assembly into various morphologies, which depend on cellulose and lignin, to their derivatives requires the structures and compositions.

Because of their distinct structures and characteristics of cellulose and lignin, the use of wood macromolecules offers a variety of options for functionalization. Elastomers, hydrogels, aerogels, etc. are a few examples of functional polymeric materials that use macromolecular technology. These have been used in the manufacture of elastomeric composite materials. Elastomer is typically thought of as a natural or synthetic polymer with the capacity to regain its original form, following stress. It is widely used in many products, including coatings, adhesives, textiles, footwear, medical devices, and leather. Wood cellulose and lignin have been used to create elastomers. According to an elastomer design principle, elastic and glassy components make up the fundamental building blocks of elastomers. In nature, the many hydroxyl groups of cellulose may create a physically cross-linked network by hydrogen bonding, making it too stiff to be an elastomer, similar to lignin, which is sufficiently stiff and almost ever used to create elastomers directly.

### 3.16.2 Silk-based fabrication of composite materials

Animal-based silk is a natural textile made of large protein molecules of naturally occurring silk fibers made by spiders and silkworms. Silk proteins are extracted from natural silkworm or spider silks by means of chemical modification or material morphogenesis. On the basis of silk proteins, several types of composite materials have been created. *Bombyx mori* silks have been used extensively in the manufacture of composite materials for textiles because of their strength, moisture absorption, and sheen. For the creation of composite materials, the silk proteins were combined with other polymers or particles. First, the created composite made of synthetic polymers and silk proteins is combined. In this instance, silk protein and poly(acrylonitrile) were combined to create composite materials. It was noted that fibers enhanced water absorption and decreased propensity to accumulate static charge. Second, silk proteins and biopolymers were combined to create composite composites. Here, cellulose and silk fibroins are used to create the composite. Lastly, silver NPs and silk proteins are combined to create an antibacterial composite. Here, *Bombyx mori* coatings and silver ions were used to fabricate the object.

### 3.16.3 Wool-based fabrication of composite materials

When compared to other natural fibers, wool, an animal-based natural fiber, offers high strength. Macromolecules made of proteins are also included. Some investigations looked at how wool's macromolecules exhibit great capabilities for the creation of composite materials. Wool is extracted from sheep's skin, and various species have varying fiber diameters and forms. Short wool fiber and polypropylene are combined to create composite sheets. Continuous extrusion was used to fabricate the product. The composite has strong mechanical and fire resistance qualities. Numerous investigations have solidly demonstrated the mechanical behavior of wool macromolecules. These factors lead to the widespread usage of wool macromolecules in the production of composite materials. Wool protein has been employed in other investigations for the creation of reinforced polyethylene composites. Natural fibers made of lignocellulose (nettle) and protein (wool) were prepared for molding in order to create a matrix made of low density polyethylene. The composite exhibited good flexural and tensile properties.

## 3.17 Graphene-based fibers

Graphene is a 2D crystalline sheet made up of a monolayer of carbon atoms that are closely packed together in an $sp^2$-bonded honeycomb lattice [9]. It is a single layer of the graphitic film found in graphite. As each hexagonal unit cell in graphene comprises two carbon atoms and has an area of 0.052 nm$^2$, it is the thinnest nanomaterial known, and the sheet is made up of many of these cells. Many investigations have been carried out since graphene was discovered in 2004. Excellent mechanical, electrical, thermal, and optical characteristics of graphene have been proven, and transferring these features to its built macrostructures is a crucial challenge for encouraging its use in real-world applications. In order to do this, graphene-based 1D fibers (GBFs), 2D membranes (GBMs), and 3D aerogels (GBAs) have been created. Amongst them, GBAs have shown good capabilities in the cleanup of spilt oils and now hold the world record for the lightest material with a density of 0.16 mg/cm$^3$. GBMs, which are typically made via infiltration or chemical vapor deposition (CVD), have also been used in a number of other energy storage and conversion applications. However, compared to GBAs and GBMs, recently produced GBFs offer substantially better mechanical and electrical characteristics. GBFs having a 1D linear structure, in contrast to GBAs and GBMs, are flexible and weavable, suited for creating multifunctional electronic fabrics, and might be employed in some difficult-to-reach regions, such as in the case of sensing/surveillance.

## 3.17.1 Fabrication of graphene-based fibers (GBFs)

As of now, melt spinning and solution spinning are the primary methods used to fabricate GBFs. These methods were initially inspired by those used to make ordinary synthetic fibers. Solid-state polymer is melted to a gel state for fiber-filament extrusion during the melt-spinning process. As a result, this technique works well for spinning fibers from polymers like nylon and polyester that can be melted without visible deterioration. The method of solution spinning, in which the polymer is dissolved into a solvent for fiber-filament extrusion, is favored for polymers that are extensively degraded at temperatures close to their melting point. Fibers made from polyacrylic and polyaramid, for instance, can be spun using this technique. According to whether the spinning dope is coagulated in a solution bath or not and if there is an air gap between the spinneret and the coagulation bath, the solution-spinning technique also comprises wet-spinning, dry-jet wet-spinning, and dry-spinning.

According to simulation data, graphene is stable at high temperatures. Its melting point is around 4,900 K, which is greater than that of fullerene (around 4,000 K) and CNTs (4,800 K). Melt-spinning is not the best method for creating GBFs in this regard; solution-spinning is. Recent studies have shown that GBFs can be produced using any of the wet-spinning, dry-jet wet-spinning, or dry-spinning techniques. Two brand-new spinning techniques have recently been created in addition to these conventional solution-spinning techniques for creating GBFs. The electrophoretic technique is one, while film conversion is another. The specifics of the current GBF spinning techniques are examined in this chapter.

### 3.17.1.1 Wet spinning

To manufacture a graphene oxide (GO) dope for wet-spinning, GO sheets are dispersed in a stable water solution, which is then injected into a coagulation bath to create a gel-state fiber. A GO fiber may be produced by removing the gel state fiber and drying it after coagulation has taken place for a certain amount of time. When necessary, the GO fiber can be reduced to create a reduced graphene oxide (rGO) fiber. The as-coagulated fiber should maintain a certain movement speed either by spinning the bath or pulling the fiber with a collecting device in order to guarantee the uniform and continuous production of a GO gel-state fiber. The first technique produces the strongest rGO fiber, which is practical for spinning modest amounts of fiber. The fiber movement speed cannot be controlled precisely due to the fact that it varies out of proportion to the bath rotation speed and heavily depends on the friction force between the fiber surface and the coagulant. The second method, on the other hand, employs a collecting mechanism to provide as-synthesized fiber with a constant drafting force and a predetermined movement rate. As a result, it provides greater benefits for creating fibers with a precise draw ratio and potential scalability.

We will go into greater depth on the shape and structure of the spinning dope, coagulation bath, and fiber in the sections that follow.

#### 3.17.1.1.1 Spinning dope

Electrostatic repulsion plays a major role in keeping the GO spinning drug stable in water. Due to the negatively charged GO sheets in the dispersion, Xu and Gao reported that the zeta potential of the GO/$H_2O$ dispersion reached −61 ± 5 mV. It was thought that the colloid-like GO dispersion would only be stable if the zeta potential was lower than −30 mV. Although macromolecules like PAN were used to replace part of the oxygen-containing groups in the GO sheet, the zeta potential of the PAN-grafted GO dispersion in dimethyl formamide (DMF) is still as low as −32 to −22.6 mV, making it practical for continuous fiber spinning. The stabilization is adversely affected by the nonsolvent when the GO dope is injected and comes into contact with the coagulation bath. Both the lateral size of the GO sheet and the concentration of the GO solution affect the spinnability of the GO dope. At the only time the GO dope is completely in the nematic phase, long, strong GO gel-state fibers may be spun. Due to the asymmetrical form of the GO sheet, its nominal diameter (*D*), which is equal to the diameter of a circle with an equal area, is used to determine the lateral dimension of GO. The critical concentration (CC) of the GO dope for a complete nematic phase to occur in the case of $D = 37$ m is 0.75 mg/mL, which allows for continuous fiber spinning, while higher-concentration dopes exhibit comparable spinnabilities.

According to Xu et al., CC is 4 mg/mL when $D = 21$ m, and it rises to ca. 81 mg/mL (or 5.7 vol%) when *D* is further decreased to 0.91 m. The primary method for creating high-concentration GO dope is centrifugation, followed by the removal of the solvent from the top layer. Thus, it may be assumed that when the size of the GO is further reduced, it would be quite challenging to manufacture a spinnable GO dope. The dope concentration, on the other hand, cannot be less than the CC for GO of a given size, since this would only lead to unconnected segments, collapsing ribbons, or split particles. The GO dope's viscosity is thought to play a significant role in determining its spinnability. Liquid crystalline spinning is the fundamental component of wet-spinning of GO fiber (LCS). The transfer of the intrinsic structural alignment from the spinning dope to the macroscale fiber is one of the main advantages of LCS, and this, in turn, is a key factor in the exceptional fiber qualities. The continuous and robust CNT fibers spun from 1D single-walled CNTs (SWCNTs) in fuming sulfuric acid as well as polymer fibers with rigid-rod-like molecular chains, like aramid, have served as examples of this. Although 2D plate colloidal liquid crystals were found many years ago, it took the discovery of GO liquid crystals to achieve macroscopic fibers spun from pristine 2D plate.

Continuous GBFs are assembled as a result of strong sheet contacts (van der Waals, hydrogen bonds, etc.), flexibility, and high aspect ratio ($>10^4$) of individual sheets. Both in the gel stage and in dried fibers, the aligned structure of GO liquid crystals may be kept in good condition. The generation of liquid crystals and the spinnability of the ensuing solutions are rarely affected by even adding metal nanowires to the spinning dope or altering GO sheets with polymer molecules, allowing for the creation of various GO- or rGO-based composite fibers. Recently, $MoS_2$-based nanofibers have also been created by electrospinning and chemical solution methods, and potential uses for them in sodium rechargeable batteries and other products have been suggested. Therefore, it makes sense to assume that LCS would be a successful method for creating fibers based on 2D.

### 3.17.1.1.2 Coagulation bath

The coagulation bath, in addition to the spinning dope, is crucial to the processing and characteristics of GBFs. A steady aqueous dispersion of negatively charged GO sheets makes up the GO spinning dope. The stabilizing state must be eliminated in order to precipitate GO as gel or dry-state assemblies, which may then be spun into fibers. The following methods can be used to carry out this procedure while using a coagulation bath: nonsolvent precipitation; destabilization by acid, base, or salt solutions; counter-ion-neutralization- or crosslinking-induced aggregation; low-temperature freeze-drying, and so on. Since GO possesses many oxygen-containing polar groups on its surface, according to the like-dissolves-like principle, it may be dissolved in polar solvents or solvents that form hydrogen bonds with GO, such as water, DMF, acetonitrile ($CH_3CN$), or tetrahydrofuran (THF). On the other hand, the GO sheet can precipitate in nonpolar, hydrogen bond-forming solvents. An ethyl acetate bath was used, for instance, by Xiang et al. to create high-performance GO and rGO fibers. The GO precipitates as a result of the addition of additional ions from acid, basic, and salt solutions that disrupt the zeta potential's ability to stabilize the GO dispersion.

Amphiphilic or oppositely charged polymers/ions and several divalent cations ($Ca^{2+}$, $Cu^{2+}$, and $Mg^{2+}$) can be used as coagulants for GO deposition because of the negative charges of GO in the dope. In GO-fiber wet-spinning, Jalili et al. showed that a variety of coagulation methods work well and the physical and mechanical characteristics of these fibers were thoroughly investigated. For the purpose of creating GBF, a GO dispersion that was frozen in liquid nitrogen and subsequently dried under vacuum was also created. Since the coagulation system is liquid, this procedure is referred to, in this work, as wet-spinning.

### 3.17.1.2 Dry spinning

The GO dispersion, which is mostly disseminated in water, is also employed in dry-spinning of GBF in place of the coagulation bath that is no longer needed. Instead, the GO dispersion is injected into and sealed in a tube, and by heating or chemical reduction at high temperature, it precipitates in the form of a gel-state fiber. The solvent can be removed further more to get dry rGO fibers. Since the majority of the GO sheets has a diameter much larger than 100 nm, GO dispersions were thought to be a colloid (lyosol) with a large-size dispersant. On the one hand, high temperature accelerates the movement of the GO dispersant, disturbs the zeta potential's balance, and raises the likelihood of GO-sheet contact and precipitation. On the other hand, high temperatures or chemical reductions may cause the oxygen-containing groups in GO to separate, lowering the GO dispersion's absolute zeta potential value. Finally, due to insufficient electrostatic repulsion, GO sheets precipitate and unite, forming a fiber. Solvent causes the gel-state fiber to swell in its precipitated condition. According to Dong et al. and Yu et al., the fiber diameter drop reaches around 80% after drying.

It is a solvothermal technology (a hydrothermal process when water is used as the solvent of GO dispersion) that causes the GO sheet to precipitate under heating at 220–230 °C during dry spinning. Various types of tubes with 1D limited space have been used as the fiber-forming mold. As high temperatures also convert GO to rGO during precipitation, the fibers produced using this approach are truly rGO fibers (thermal reduction). At 180 °C, 27% of the oxygen in GO was said to be removable, and at 200 °C, the majority of the hydroxyl, epoxy, and carboxyl groups began to separate. As a result, GBFs produced using the hydrothermal technique exhibit high electrical conductivities (about 10 S/cm), without any post-reduction processing.

### 3.17.1.3 Dry-jet wet-spinning

Another crucial spinning technique for traditional synthetic fibers is dry-jet wet spinning. It has been shown that PAN-based carbon fibers can be spun using this technique with a high concentration of dope, and the resultant fibers have superior mechanical qualities than those produced by wet spinning. Additionally, fibers with a homogenous structure and circular cross section can be spun by dry-jet wet spinning. As a result, this technique is equally promising for the synthesis of GBF. Graphene oxide nanoribbons (GONRs) were disseminated in chlorosulfonic acid to create an LCS dope, which was then injected into diethyl ether to create the GO fiber, according to Xiang et al. For fibers with improved mechanical qualities, there was an air gap of 12 cm between the injection tip and the bath level. The rGO fiber was then created by thermal annealing. As it lowers the velocity gradient of the GO spinning dope between the injection tip and the bath and is thought to promote fiber alignment by gravity-assisted stretching, an air gap is crucial for the manufacture of high-performance fibers. Compared to fibers spun from an air gap of 2 cm, those with a 12 cm air gap had lower diameters and performed better, mechanically. It is untrue, however, that the greater the air gap, the better the performance of the fiber, as an air gap that is too long may impair fiber drawability during spinning.

## 3.18 Fabrication and performance of hybrid nanofibers

To create organic/inorganic hybrid nanofibers with desirable morphologies and improved mechanical characteristics up till now, a variety of techniques have been used [10]. The manufacture of hybrid nanofibers, which is covered in this part, has mostly used the blended electrospinning, Layer-by-Layer (LbL) self-assembly, in situ fabrication, and coaxial electrospinning techniques.

### 3.18.1 Blended electrospinning

Inorganic NPs and polymer solutions may be mixed directly to create hybrid nanofibers, which is a quick and flexible process. When two materials are simply combined in their purest forms, the resulting hybrid nanofibers have better mechanical or biological activity, which is crucial for their use in biomedical applications. In order to create a consistent and stable colloidal solution for the ensuing electrospinning process, the solid inorganic NPs were first introduced to the polymer solution while being stirred. The same blended electrospinning strategy was used in another work to produce PVA/CS/multiwalled CNT hybrid nanofibers. Hybrid electrospun nanofibers made of *n*-HA (nanohydroxyapatite)/poly(lactic-co-glycolic) (PLGA) and HNTs (Halloysite nanotubes)/PLGA were created by Zheng et al. The average diameter of the hybrid *n*-HA/PLGA nanofibers shrank when the amount of *n*-HA was increased. The average diameter of the HNTs/PLGA nanofibers rose when the number of HNTs was added. It is widely acknowledged that the addition of anionic or cationic species may alter the electrospinning solution's characteristics. The *n*-HA/PLGA hybrid nanofibers have a smaller diameter than pure PLGA nanofibers, which is likely a result of the addition of *n*-HA increasing the solution's conductivity or viscosity. Additionally, the inclusion of negatively charged HNTs may cause the spinning jet's surface charge density to drop, resulting in an increase in the diameter of the hybrid nanofibers.

### 3.18.2 Layer-by-layer self-assembly

LbL self-assembly has been widely used to deposit multilayers onto nanofiber surfaces and is one of the most significant surface modification methods. Electrospun nanofibrous mats are first created for the fiber surface functionalization, and they are then employed as a substrate for the electrostatic self-assembly-based deposition of inorganic/organic multilayers. For instance, by combining electrospinning and LbL self-assembly techniques, Luo et al. created CNT-containing nanofibrous polysaccharide scaffolds. First, electrospun cellulose acetate (CA) nanofibers were created, and then chitosan (CS)/

CNT multilayers were deposited on the CA nanofibrous mats via electrostatic LbL self-assembly. In the meantime, multilayers of CS and sodium alginate (ALG) were also applied on CA nanofibers, for comparison. According to the mechanical durability analysis, CA nanofibers formed with CS/CNT multilayers showed greater tensile stress and ultimate strain than those assembled with CS/ALG multilayers of a comparable number. Additionally, as the number of deposited CS/CNT bilayers rose, the tensile stress of the CA nanofibers did not vary considerably, and the ultimate strain began to decrease. This is likely because the mats become more brittle as more CNTs are formed onto the fiber surfaces. In order to preserve the enhanced mechanical properties of the nanofibrous scaffold, such as tensile stress, ultimate strain, and Young's modulus, fewer layers of CS/CNT deposition on the CA nanofibers were advantageous. Overall, the LbL self-assembly approach permits the production of a controlled and uniform inorganic layer on the surface of nanofibers, but its adaptability is restricted by the need that the chosen inorganic NPs be either positively or negatively charged.

### 3.18.3 In situ fabrication method

The in situ manufacturing approach may be used to produce hybrid nanofibers. In the polymer solution, the inorganic NPs can be generated in situ and then electrospun to produce hybrid nanofibers. Additionally, inorganic NPs can be grown in situ after being doped with polymer nanofibers first (for example, by adding metal ions). To prevent particle aggregation and create hybrid nanofibers with uniform particle distribution throughout the fibers, in situ approaches are useful in both situations. However, because inorganic NPs are generated in situ, this technique is primarily useful for creating hybrid nanofibers doped with metal or metal oxide NPs. For instance, $Fe_3O_4$-doped PVA nanofibers were created by Bai and colleagues. First, the study's authors combined Fe(II) and Fe(III) salts with a 6 weight percent PVA solution at 60 °C under nitrogen for 20 min. The mixture was rapidly agitated for one hour at 80 °C in an $N_2$ environment, after the pH was brought down to 11 using sodium hydroxide solution. This produced magnetic $Fe_3O_4$ NPs. The mixture was then immediately electrospun to produce $Fe_3O_4$–PVA hybrid nanofibers after being cooled to room temperature. In a different work, Pan et al. used the same in situ production technique to create hybrid nanofibers made of AgNPs/PVA and AgNPs/(PVA/PEI). Epigallocatechin gallate (EGCG) reduction was used to create an AgNPs/PVA solution, which was then electrospun to create an AgNPs/PVA nanofibrous mat. This process was used to create AgNPs/PVA hybrids.

Another technique to produce organic/inorganic hybrid nanofibers with uniform inorganic NP distribution is the in situ reduction method paired with electrospinning technology. The NPs comprising nanofibers may be created using this technique, by electrospinning a solution of a polymer and metal salt, followed by chemical or physical processing. For instance, PVA/PEI electrospun nanofibers were first produced and then functionalized by 3-mercaptopropyl triethoxysilane to introduce thiol groups together with the PVA hydroxyl groups on the surface of nanofibers in order to prepare the AgNPs/(PVA/PEI) hybrid nanofibers. Then, to create the AgNPs/(PVA/PEI) nanofibers, the functionalized nanofibers were dissolved in an $AgNO_3$ solution and reduced with EGCG.

Son and colleagues demonstrated in a separate article that electrospun nanofibers made from a CA/silver nitrate combination solution could be UV irradiated to create polymer nanofibers containing AgNPs. In a nutshell, AgNPs/CA nanofibers were produced by electrospinning a CA solution that included 0.5 wt% $AgNO_3$ to create composite CA nanofibers. AgNPs were mostly produced on the surface of the CA nanofibers, most likely as a result of the $Ag^+$ ions and Ag clusters diffusing and accumulating there during the UV irradiation.

### 3.18.4 Coaxial electrospinning

A coaxial spinneret made up of an outer and an inner needle is frequently employed in coaxial electrospinning, which has also been used to create hybrid nanofibers. It is possible to create distinct hybrid nanofibers with a variety of morphologies by altering the flow velocity of inner and outer polymer solutions with variable compositions. Composite fibers with desired mechanical characteristics can be created. For instance, Song and colleagues used poly(caprolactone) (PCL) nanofibers with coaxial electrospinning to encapsulate FePt NPs while electrospinning FePt/hexane solution, PCL/2, 2, 2-trifluoroethanol. As the inner and shell fluids, (TFE) was used. Analyses using TEM and X-ray photoelectron spectroscopy verified the FePt NP's full encapsulation PCL nanofibers inside, as opposed to mixed. Coaxial electrospinning is a kind of electrospinning that demands tighter control of the electrospinning parameters (for instance, voltage, flow rate, and electrospinning concentration solution) because core and shell fluids both are electrospun at once.

## 3.19 Preparation mechanisms of grooved micro/nanofibers

Grooved fires have demonstrated considerable promise in producing superhydrophobic surfaces and directing cell and axon development. Different polymers, including cellulose acetate butyrate (CAB), poly(vinylidene fluoride-co-hexafluoropropene) (PVDF-HFP), polystyrene (PS), poly(L-lactic acid) (PLLA), poly(vinylidene fluoride)(PVDF), and polycaprolactone (PCL) can be used to create the grooved fibers.

### 3.19.1 Grooved fiber prepared by single solute and double solvent

The preparation principle of grooved fibers can be roughly divided into four mechanisms: (I) void-based elongation, (II) wrinkle-based elongation, (III) collapsed jet-based elongation, and (IV) selective dissolution. According to Liu et al., a significant DER difference between the two solvents is necessary for the creation of groove structure in binary solvent systems. The difference between a solvent's high boiling point and low boiling point can be used to represent DER Difference in the Evaporation Rate. For Mechanism I, the quick volatilization of highly volatile solvents causes phase separation at the beginning of electrospinning, resulting in glassy skins and voids on the fiber surface. The micropores are subsequently stretched and formed into grooved fibers. Due to mechanism I, Liang et al. successfully created PLLA-grooved fibers in a solvent with a DCM (Dichloromethane)/DMF ratio of 2/1.

In the early stages of electrospinning, a glassy surface is produced on the surface of the sprayed fiber, which is subsequently stretched into groove-based fibers. Mechanism II (wrinkle-based elongation) is identical to Mechanism I. Therefore, under the influence of the jet's constant stretching, the interior pores experience transverse shrinking.

Due to the relatively slow evaporation rate and high viscosity of HBP Hyper Branched Polymers, mechanism III (compressed jet-based elongation) causes a glassy skin to develop, but the jet is collapsed and subsequently stretched into a grooved structure. Selective dissolution is the last mechanism. PVDF trench fibers were created by Zaarour et al. employing volatile DCM and challenging DMF solvents.

### 3.19.2 Brief overview of high-power laser fibers and fiber-based components

High-power fiber lasers (HPFL) were swiftly superseded by other kinds of bulk lasers as a revolutionary force in many applications [11]. Due to their unrivalled benefits of higher efficiency, little thermal degradation, and strong gain extraction, rare-earth-doped silica fibers have gained widespread use as a laser gain medium. To date, a large spectrum of laser emission has been spanned by fiber lasers using various rare-earth dopants. High-power laser production and propagation are becoming more popular due to advancements in the power management of fiber-based components for HPFLs, focusing on increased damage thresholds and steady repeatability. This section discusses the vast potential of laser fibers in broad spectrum coverage in many wavebands.

### 3.19.3 Enormous potential of high-power rare-earth-doped laser fibers

Snitzer (fiber laser) is recognized for helping launch the development of fiber lasers in the 1960s and later. His prior studies suggested that it would be feasible to use rare-earth-doped material for laser amplification within a fiber. Accordingly, the successful development of low-loss optical fiber opened the doors to developing “new” lasers using a variety of rare-earth elements that could be easily doped into the glass host, such as ytterbium (Yb), erbium (Er), thulium (Tm), holmium (Ho), praseodymium (Pr), and dysprosium (Dy). The pioneers in optical fiber and lasers, such as Maiman (laser), Snitzer (fiber laser), and Kao, predicted the constant advancements in optical fiber lasers, 60 years ago. Unprecedented power scaling of fiber lasers was sparked by the development of double-cladding fibers and the quick spread of high-power pump modules. Fiber lasers have become indispensable and have integrated themselves into a variety of applications, particularly in the fields of defense, industrial cutting, telecommunications, and surgery, thanks to their unique advantages of high-power operation, compact size, long lifetime, and uniform fabrication methods. Demand for the output power of fiber lasers rises in tandem with the ongoing growth of applications. Fiber lasers with diverse rare-earth dopants have seen distinct development trends due to the varying fiber material qualities and variable readiness levels of the relevant components in the specialty fibers.

## 3.20 Elastic and stretchable fibers

On the basis of their distinctive features, such as high dynamic bending elasticity, stretchability, and high mechanic strength, researchers have proven several multidisciplinary uses for elastic and stretchable fibers and made substantial progress in this field [12]. Here, we provide a summary of the primary processing techniques for creating soft, extensible functional fibers from a variety of generally available or newly discovered elastic materials. In order to highlight this exciting area of study and stimulate more innovative thoughts in the disciplines of functional fiber integration, soft electronics, fiber sensing, and other relevant research areas, we also show some sample uses of multifunctional elastic fibers.

### 3.20.1 Materials and fabrication methods

Elastomers offer higher conformability with the soft human skin and other irregularly shaped surfaces compared to commonly used nonstretchable polymer materials like PC and PS because of their outstanding stretchability and softness. The manufacturing processes and applications should guide the selection of elastomer materials. For instance, the most crucial characteristics of the elastomers for waveguide fibers would be their optical transparency and refractive index; thermoset elastomers like polydimethylsiloxane (PDMS) are not suitable for long-term heating processes like thermal extrusion and thermal injection. Table 3.2 lists various examples of polymeric materials, practical methods for making elastic fibers, as well as their mechanical characteristics (elongation at break/stiffness).

**Table 3.2:** Standard components for making elastic and stretchy fibers [12].

| | Material | Fabrication methods | Elongation at break/ stiffness | References |
|---|---|---|---|---|
| **Thermosets** | Polydimethylsiloxane (PDMS) | Molding, coating, printing | 80–231% | [13–18] |
| | Epoxy | | | [19] |
| **Hydrogel** | Poly(ethylene glycol) diacrylate (PEGDA)/alginate | Molding, coating | 700% | [20, 21] |
| | PEGDA-polyacrylamide (PAAm)/ alginate | | 75% | [22] |
| **TPE** | Styrene-ethylene-butylene-styrene (SEBS) | Molding, coating, thermal drawing, extrusion | 100–700% | [23–25] |
| | Cyclic olefin copolymer elastomer (COCE) | | 230% | [26] |
| **Biodegradable** | Agarose/gelatin | Thermal drawing, molding, coating, extrusion | 300% | [27–29] |
| | Poly(octamethylene maleate citrate) (POMC)/poly(octamethylene citrate) (POC) | | 58% | [30] |
| | Polylactic acid (PLA)/poly(lactic-co-glycolic) (PLGA) | | 1.94 kPa/<br>2.4 × 105 N/m | [31, 32] |
| | Silk | | >400% | [33–36] |

Preparing thermoset elastomers for fibers before cross-linking and solidification is often recommended. The thermosets would be difficult to dissolve and soften after they had cross-linked, unlike thermoplastic elastomers (TPEs), which may be melted or easily dissolved in solvents. And they might undergo various thermal processing techniques, such as thermal injection and thermal drawing. Hydrogels are made up of a network of hydrophilic, cross-linked polymer chains. They can occasionally be discovered as a colloidal gel dissolved in water. By adjusting a hydrogel's polymer concentration and cross-linking concentration, one may change the mechanical characteristics of the hydrogel. Additionally, they hold intrigue for several biological applications due to their rubber elasticity and viscoelasticity, which have both been extensively studied. The last one is composed of biodegradable substances originating from naturally occurring polymers, such as cellulose and agarose, as well as manmade degradable substances, including modified PLA and PLGA.

Starting with the conventional method of fiber manufacturing known as thermal drawing, the primary goal is to form the materials according to plan. Depending on the needs, some of the processes might be changed or skipped. For instance, if the raw material is SEBS pellets and we require a round SEBS rod, it is also possible to produce the SEBS round rod by heating the pellets, injecting them into a round tubular mold, and then chilling the form thereafter. In contrast to thermal sketching, 3D printing is a relatively new technique. This method of layer-by-layer, 3D production enables the exact printing of a wide range of materials, including metals, ceramics, thermoplastic polymers, and other polymers that might cure when exposed to stimuli. As a result, 3D printing has evolved into a flexible method of producing elastic fibers. A silicone-copper (Cu) (cladding-core) fiber with an elastomeric metal core was created by Tong et al. and used as a triboelectric nanogenerator (TENG).

A full working elastic system may be created using 3D printing in addition to elastic fiber and other elastic subassemblies. The optical lace (OL) for synthetic afferent neural networks was created by Xu et al. In order to create arbitrary 3D grids of soft, flexible light guides for spatially continuous deformation detection, they proposed a platform dubbed OL. This 3D sensory array performed tasks like those of an organism's afferent neural network. These light guide networks were dispersed within a soft scaffold that was 3D-manufactured. The rotation-translation approach is another manufacturing technique for creating the elastic conducting fiber. Co-extrusion was used to create an optical fiber with a core and cladding made of the fluorinated polymer, Daikin T-530 and the polystyrene-based polymer, Star Clear 1044 that had refractive indices of 1.52 and 1.36, respectively. It reversibly withstood tensile stresses of 300%. Another widely used technique to create elastic fibers is molding. A. Yetisen et al. reported creating a hydrogel optical fiber using post-coating procedures in molding.

### 3.20.2 Applications

For carrying and transferring information over long distances, fibers naturally have an advantage. As a result, they may be used in a natural way for tissues- and body-specific implanted biomedical sensing and monitoring. Fluorescent hydrogel fibers were used in a long-term in vivo glucose monitoring study by Heo et al. The polyacrylamide (PAM) hydrogel fibers attached to polyethylene glycol (PEG) decreased inflammation and reacted continuously to changes in blood glucose concentration for up to 140 days. A step-index optical fiber composed of biocompatible hydrogels was designated by Choi et al. to accomplish low-loss in vivo light guiding (0.42 dB/cm) over the full visible spectrum. In order to monitor spontaneous brain activity, Lu et al. created a thermally drawn flexible cyclic olefin copolymer elastomer (COCE) fiber coated with Ag nanowire (AgNW) mesh electrode layer. The elastomer materials can also be employed in soft robotics and sensing, in addition to in vivo applications. Stretchable optical waveguides as photonic strain sensors were created by H. Zhao and colleagues using a variety of elastomers. Pre-elastomers were poured into a mold, one at a time, to create the core/cladding structure for this waveguide. A light-emitting diode (LED) and a photodetector were then attached to the two ends of the optical waveguide, respectively, to complete the stretchy sensor.

## 3.21 Fiber-based materials for current energy storage applications

Fiber-based structures have shown to be one of the best possibilities for creating functionally flexible materials for applications in next-generation energy storage [37]. It is well known that fibers are much longer than they are wide, and they may also exist in the form of nanofibers, which have a diameter of less than one micrometer. The fiber morphology enables their conversion into several structures for a variety of uses, including yarns, fibrous mats, and textiles. It is also important to note that a wide variety of substances, both natural and artificial, may be used to create fibers. These characteristics enhance their flexibility in creating different battery component designs. For instance, current research has demonstrated the effective development of several electrodes employing fiber-based architectures and materials with metal, carbon, and polymer bases. The extraordinarily high surface area-to-volume ratio of fibers, which improves the contact area between the electrolyte and the electrode and helps maximize the usage of surface active sites, is one of their key benefits. Additionally, the use of fiber-structured materials with nanoengineered structures could accelerate mass transfer rates, resulting in less electrode polarization. The physical characteristics of these materials also provide unmatched advantages such as great mechanical flexibility, respectable tensile strength, acceptable stability, and desired durability in real-world applications. The textile industry has a long history of making fiber-based products, which is today backed by cutting-edge technology. For various technical applications, there are a variety of functional homogeneous or composite fiber production and modification processes. The majority of these are favorable for producing and developing high-performance zinc-ion batteries (ZIBs) made of fiber-based materials.

### 3.21.1 Fiber-based structures for energy storage applications

When building a variety of 1D, 2D, and 3D fiber assemblies, which provide considerable flexibility in creating various practical structures, fiber can be used as a unit part. In order to provide a range of purposes, functional and substrate materials in fiber-based structures have great potential for being made in varied dimensions or interlaced into diverse constructions. It is also important to note that when functional materials are used to build fiber-based structures, they are given superior electrical, mechanical, and physical characteristics than the same material in bulk forms. Numerous research studies have already documented several fiber-based active material architectures used in the manufacture of cutting-edge ZIB components. Functional materials, for instance, can be transformed into a variety of architectures, including mono or composite fibers, yarns, textiles, and fibrous mats. As a result, additional materials may be used in various ZIB components, depending on their electrochemical and physical characteristics.

Energy storage applications have been employed with functional forms of fibers that are often used, such as core–shell or coaxial structured, hierarchical structured, and helical fiber. The complementary qualities of the two types of materials, namely, those having outer and inner compartments, are present in core–shell fibers. High mass loading and rapid electron/ion transport can be facilitated by fibers having hierarchically constructed networks that are very porous. These fibers can also make energy storage devices highly flexible and adept at bending. Additionally, fiber electrodes might be coiled in sequence onto the substrate fiber to create a fiber with a helical shape and excellent tensile stability for use in ultra-stretchable energy storage.

Mangling many yarns into helical or cable structures can give yarn structures superior mechanical characteristics. For instance, tiny metal strands may be twisted into stronger, more flexible helical-structured yarns, enabling their use in more demanding working conditions. Additionally, yarns consisting of several fiber types can be combined to create a single yarn to get the benefits of synergy. A double-helix structured material can be created by twisting a functional yarn with another elastic substrate yarn. The cable yarns have superior tensile strength, homogeneity, and abrasion resistance, which allow them to be folded without breaking or losing a substantial amount of their functions. Various construction methods may be used to create fabrics, fibrous films, and fibrous porous networks, which are largely divided into woven, knitted, and nonwoven kinds. For example, to improve active material loading and enable quick electron transport, nanofibers can be woven into porous networks or textiles. Additionally, electrospinning may be used to create nanofiber films, which is a time- and money-efficient method of producing materials on a large scale. Additionally, the growth of application domains is facilitated by the varied fabric structure designs of functional materials. Knitted constructions have a notable advantage over their woven or film equivalents in terms of stretchability. The production practicality and scalability of wearable electronics may be improved by using these fiber-based fabrication techniques for functional materials, advancing the design of adaptable and robust energy storage technologies.

### 3.21.2 Demand for functional fiber-based materials for zinc-ion batteries (ZIBs)

Numerous research teams have begun to focus more attention on fiber-based functional materials due to their adaptability and suitability for aqueous ZIBs. For greater electrochemical and mechanical performances, pure metals, carbon, ceramics, polymers, and their composites have demonstrated the need to be produced in fiber-based forms or incorporated into other fiber-based substrates. This can further encourage the development of effective battery components for ZIBs.

## 3.22 Metal-based materials

### 3.22.1 Vanadium

Known to be a common cathode material used in ZIBs, vanadium oxide ($V_xO_y$), due to its superior cycle stability, high rate capacity, and rate capability, has attracted a lot of study interest. For example, $V_2O_5$ with its distinct layered structure and orthorhombic symmetry enable carrying out various redox reactions (including $V^{2+}$, $V^{3+}$, $V^{4+}$, and $V^{5+}$) and offer a significant ion transfer channel. Five O atoms and one V atom work together to produce a square pyramid chain with a common corner. Layers are formed by connecting these pyramid chain links, and layers may then be piled on the c-axis to make layered structures. The intercalation of 0.074 nm $Zn^{2+}$ ions is possible because of the 0.43 nm gap between these layers. Existing research, however, consistently demonstrates that capacity attenuation may result from poor electrical conductivity and phase transition of the $V_2O_5$ layered structure following $Zn^{2+}$ intercalation. Furthermore, according to certain research, bulk $V_2O_5$ has an unfavorable capacity loss due to its relatively less stable structure, poorer ionic and electronic conductivity, and lower ion diffusion coefficient for $Zn^{2+}$ ions. However, it is intriguing to learn that the creation of nanostructures might help overcome the restrictions.

Adopting nanostructures is one of the most efficient strategies to enhance the electrochemical performance of $V_xO_y$ cathode in aqueous ZIBs, because it plays a significant role in the activation process, capacity, and stability of electrode. Nanobelts, nanopapers, nanowires, and nanofibers are largely used in the most current study on nanostructured $V_xO_y$ cathodes. It is important to note that $V_xO_y$ in nanofiber form has distinct tunnel transport channels with bigger dimensions and results in less structural changes on $Zn^{2+}$ intercalation, which is helpful in removing the restrictions of solid-state ion diffusion in the $V_xO_y$ electrode. Additionally, these vanadium-based metal oxides may be loaded into other heterogeneous substrate materials or grown onto fiber-based templates to create hybrid fiber-based structures with defect engineering to improve electrochemical performance. After calcination, mesoporous composite nanofibers are created, which perform better than their bulk counterparts, thanks to $Zn^{2+}$ insertion and electrolyte permeability. Recent investigations on $V_xO_y$ in fiber forms have shown outstanding performance, operational stability, and manufacturing viability; this merits further study in fiber-based $V_xO_y$ cathodes.

### 3.22.2 Manganese

One of the most capable cathode materials in aqueous ZIBs is manganese oxides ($Mn_xO_y$). They may exist in a variety of valence states, which provide high specific capacity and robust ion storage ability. They can be generated as $\alpha$-$MnO_2$, $\beta$-$MnO_2$, $\gamma$-$MnO_2$, and $\delta$-$MnO_2$ among other crystallographic forms. It is noteworthy that among the several forms, $\alpha$-$MnO_2$ has the highest theoretical capacity, voltage, and abundance. However, if the battery is subjected to frequent charge-discharge cycles, the usual -$MnO_2$ may experience substantial capacity deterioration. Additionally, the manganese-based resources, such as $Mn_xO_y$ and their composites, are inexpensive, nontoxic, and renewable. However, $Mn_xO_y$'s weak proton transport, inherent electronic conductivity, and electrolyte penetration lower its specific capacitance. Therefore, before using this material for real applications, the problems with fast capacity fading and slow transport kinetics should be resolved.

### 3.22.3 Other metals and metal oxides

Another transition-metal oxide that has been widely explored is nanostructured molybdenum trioxide ($MoO_3$), which has also lately received attention as a material for electrochemical storage. Orthorhombic -$MoO_3$ has a layered structure parallel to (010) and is in a thermodynamically stable phase that permits guest atomic ions to insert splitters between the layers. As a result, $MoO_3$ has huge potential as a high-performance cathode electrode for ZIBs. Nevertheless, substantial deterioration and the dissolution of active ingredients in an aqueous electrolyte can lead to the electrochemical instability of orthorhombic $MoO_3$ nanowires. Electrolyte engineering or surface engineering of $MoO_3$, such as coating and phosphating processes, may be used to provide improved cyclic stability, faster charge transfer, and increased surface reactivity, in order to mitigate this impact. The molybdenum-based oxides may benefit from improved properties provided by fiber-based substrates. To address the inherent constraints, such as slowed faradaic kinetics and mass transfer, carbon cloth can improve the surface area and electron mobility of the coated $\alpha$-$MoO_3$. An extensive area of contact was given for the interaction between active materials and the electrolyte via porous mats made with nanobelts or nanofibers.

Metal materials are viable choices for the fabrication of battery components, since they typically have great mechanical strength and conductivity, notably current collector, and supporting framework for yarn-shaped batteries. In comparison to traditional cellulose yarns, fiber-based constructions, such as stainless steel yarn, offer greater strength, conductivity, corrosion resistance, thermal stability, and flexibility. The deposition of anode and cathode materials may therefore be carried out on them as electrode substrate, with confidence. For instance, extremely porous iron fibers can offer high conductivity at a reduced cost because they have excellent mechanical integrity and connection within their fibrous structure. Furthermore, silver fibers may be used as another effective current collector due to their exceptional conductivity and tensile qualities. A conductive and flexible electrode may be created by depositing metal material over another soft material to improve the flexibility of the yarn-shaped electrode. Structural designs of metal-based materials may be expanded by fiber-based structures, increasing the number of suitable parts for a high-performance battery.

## 3.23 Carbon and ceramic-based materials

The majority of carbon materials are robust, stable, and compatible with a wide range of materials, which is advantageous for the creation of composites. Due to their availability in a wide range of physical and chemical structures, they are a staple of ZIB components and contribute to their improved electrochemical functioning, structural adaptability, and mechanical integrity. Typically, carbon compounds behave as functional dopants, substrates, frameworks, or active surface components to enhance the battery's electrochemical performance. The fiber-based architectures of these adaptable materials offer a variety of benefits, primarily, functional improvement and more extensive practical designs. The reduction of Zn dendrite formation is one of the standout benefits of ZIB components made of carbon materials.

Recent energy storage research frequently use CNT and carbon cloth fiber-based systems, in particular, because of their exceptional electrochemical performance and mechanical benefits. The potential for wearable electronics is increased by CNT fibers made of aligned CNTs, which inherit the benefits of CNTs and also display the additional trait of macroscopical mechanical flexibility. A highly conductive 3D nitrogen-doped porous carbonaceous skeleton may also be created using CNT fibers and templates like MOFs. This core–shell hierarchical structure makes it possible to mass load active materials without the need of binders onto the fiber-shaped cathode, which benefits the ZIB system's increase in volumetric capacity, electronic conductivity, and diffusion efficiency. Additionally, a CNT-based framework for pure -$MnO_2$ can raise the tapped density of -$MnO_2$, which raises the energy density at the cellular level. Furthermore, a softer option to stainless-steel foil is carbon cloth, a 2D fabric constructed of carbon fiber. For more demanding applications, it provides exceptional mechanical strength, lightweight design, and high electrical conductivity.

Different modification techniques or assemblages of numerous materials can be used to improve the performance of carbon materials. By incorporating functional components into the carbonaceous matrix or by surface engineering with deposition methods, it is simple to modify flexible carbon nanofibers. For wearable applications, various combinations of carbon-based fibers and nanosheets may be employed as ZIB components. For instance, reduced graphene oxide (rGO) nanosheets and single-walled CNT fibers make effective complimentary materials. Mesoporous CNT fibers can increase surface area by preventing restacking between rGO nanosheets. On the other hand, rGO nanosheets can improve the electrical conductivity of CNT fibers. Fiber-based carbon materials are the best choice for creating different cathodes, anodes, and current collectors to enhance the energy storage performance and practicality of ZIBs because of their advantageous characteristics, simplicity of modification, and integrality.

Ceramic materials often have high chemical resistance, minimal thermal expansion, and good hardness. They are suited for use as ZIB components due to their wide range of physical and chemical characteristics. One of the most used separators for ZIBs is glass fiber (GF). The fibrous fabric gives GF a larger surface area for greater electrolyte absorption, which improves ionic transportation. However, the GF separator has poor mechanical strength and unevenly sized pores, making it more likely for the generated Zn dendrites to pierce through it and finally short out the cell.

## 3.24 Polymer-based materials

Using well-established processes, the majority of natural and synthetic polymeric materials are easily fabricated into a range of fiber-based architectures. The majority of these polymers are affordable to purchase commercially, making them suitable for mass manufacturing. More significantly, several studies have demonstrated its excellent modifiability in a variety of applications. Natural organic polymers like cellulose and protein are plentiful and renewable, which promotes the environment-friendly manufacture of materials made of functional fibers. The most common natural organic polymer on the globe, cellulose fibers exhibit excellent mechanical strength, acceptable hydrophilicity, a passable insulating performance, and favorable biodegradability. They are also used as separators because of their uniformly porous architecture and abundance of hydroxyl groups. The majority of synthetic polymers have the benefits of being versatile enough to modify functional groups, mechanical flexibility to withstand applied force, and good modifiability to be generated by innovative processing technologies. For making solid-state electrolytes in ZIBs, for instance, PAM and PAN can be used. For improved ionic conductivity, flexibility, and mechanical strength, most polymers are easily chemically changed and physically molded into the appropriate 3D hierarchical structures.

## 3.25 Organic materials

Moreover, because of their structural adaptability, sustainability, and light weight, organic materials are another type of desirable cathode option for ZIBs. However, the poor conductivity, significant structural damage, and dissolving issues that the organic cathode materials experience throughout the electrochemical process lead to subpar rate performance and uncertain cycle durability. Nanostructures and materials containing Quinone can be used to overcome these constraints. The organic cathode materials are given more micro and nanopores by nanofibrous membrane, which increases the interfacial contact area between the electroactive groups and electrolytes. It is important to note that organic cathodes containing Quinone compounds have greater capacity and less solubility in aqueous solutions. Another method to improve the cycle stability of organic materials is to build organic-inorganic hybrid cathode material with a dual energy storage mechanism.

## 3.26 Preparation method of fiber-based materials

Different kinds of physical and chemical manufacturing techniques are used to create useful fiber-based materials. Advanced methods including spinning, hydrothermal synthesis, deposition, and template-assisted fabrication of homogeneous or heterogeneous materials may be used to create and functionalize fiber-based forms of synthetic and organic materials. Depending on the desired material kinds and functionalities, the modification or functionalization of the raw materials may be accomplished during the pre-, mid-, or post-stages of fiber creation. As a result of their considerable research, spinning and chemical synthetic processes allow for the controlled synthesis of fiber-based materials with certain diameters, morphologies, tensile characteristics, and chemical functionalities. Additionally, a variety of methods may be used to create compositions and morphologies that are more complex. Using the aforementioned techniques, various homogeneous metals, metal oxides, carbon, ceramics, polymers, or their composites may be used to create functional materials in fiber shapes, enabling these materials to be used in a wider variety of work settings.

### 3.26.1 Spinning approach

A quick and efficient way to produce fibers on a big scale is through spinning. In recent years, electrospinning has become a popular method for creating functional nanofibers from sol–gel-derived materials for ZIB components or polymeric materials doped with active chemicals. A spinneret and injection syringe for extruding the polymeric solution at a constant rate, a high-voltage power source for charging the polymeric droplets, and a charged metal collector for collecting the nanofibers drawn by various forces such as electrostatic force, viscoelastic force, and air drag force can all be used to create electrospun materials. With the electrospinning setup's settings, it is easy to adjust the fiber diameter, material dimension, and density. Through the use of this technique, 1D nanofibers, 2D nonwoven films, and 3D frameworks with fiber sizes at the micro and nanoscale may be effectively manufactured. Additionally, it is simpler to produce fibrous films with greater porosity using haphazard electrospun nanofiber stacking. Ion migration via the network is facilitated by the porous features, which enhances the battery's conductivity performance. Additionally, by calcining electrospun polymeric fibers, carbon-based fibrous networks with rich mesoporous structures may be created. These electrospun fibers are flexible and have a high surface area-to-volume ratio, allowing for a wide range of designs. The traditional method for drawing carbon nanofiber arrays is dry spinning. Additionally, fine metal fibers may be produced by spinning at very high temperatures and then twist-bundle pulling them into yarn structures.

### 3.26.2 Synthetic chemical approach

Numerous research studies have successfully shown how to fabricate nanofibers using chemicals to increase the functioning of materials, as a consequence. One such potential technique to create nanofibers in a variety of situations is the hydrothermal approach. The hydrothermal process, which can promote the development of primary particles into nanofibers, typically entails the dissolution and recrystallization of heterogeneous substances in solvent inside of a closed reactor, at high temperature and high pressure. High-quality nanofibers were manufactured using this technology, gentle synthetic conditions, and superb uniformity being its benefits. The simple vacuum filtering approach may be used to create a nanofibrous layer after the formation of nanofibers. In order to increase electrical conductivity, the sonochemical approach can also help, with the intercalation of foreign substances such as conducting polymers and ions into the nanofiber crystal lattice of transitional metal oxide cathodes. Deposition, particularly CVD and electrodeposition, enables homogeneous synthesis of functional materials on fiber-based substrates and regulates the development of active materials in the nanofibrous form, using chemical vapor or electric current. Deposition techniques support the development of electrodes free of binders and may be applied to a variety of active and substrate materials. Additionally, for soluble or solution-processable materials, low-cost coating-based techniques like dip-coating can be used. Since they may effectively control the developing direction of active materials into predetermined morphologies, templates are frequently employed to aid in the manufacture of functional fiber-based materials. By using templates like MOFs, carbon nanofibers, nickel foams, and 3D porous copper materials, certain structures may be produced, such as a 3D hierarchical skeleton and porous structures.

## 3.27 Advanced multimaterial optoelectronic fibers

Optoelectronic gadgets play a crucial role in our daily lives. Combining semiconductors, conductors, and insulators to create optoelectronic functional units requires precise placement of these functional components in the right scales [38]. Wafer-based technologies, which are typically executed on rigid and flat substrates, have developed over decades to produce several micro- and nanoscale optoelectronic functional devices. The need for flexible and nonplanar optoelectronic devices at the micro- and nanoscale has increased in recent years. Since these cutting-edge fibers can be the perfect platforms for flexible optoelectronic devices, the method for synthesizing multimaterial, multifunctional fibers is one of the techniques for making flexible electronics that is evolving quickly.

### 3.27.1 Multimaterial optoelectronic fiber fabrication

Diverse functional materials, such as semiconductors, insulators, and conductors, must be included into the fiber design to enable more functional structures than optical waveguides, in order to create optoelectronic functional fibers. In order to fill the interior channel of glass capillaries with semiconductor materials, a high-pressure chemical vapor deposition (HPCVD) approach was first used to produce fibers containing elemental semiconductor core materials. This work was originally described in 2006. A method based on the traditional fiber-thermal drawing process was shown, soon after, and it has since been enthusiastically embraced by the community and used to fabricate new types of useful materials. However, due to their distinct thermal, mechanical, and chemical characteristics, which have an impact on the structural consistency and architectural correctness throughout the drawing process, the large diversity of materials involved adds considerable difficulty to the thermal drawing process. There are three fundamental criteria to go by, in order to get over these obstacles and attempt to simultaneously draw on many materials. In order to preserve and sustain the fiber structure throughout the heating process, the cladding components of the fiber should first be amorphous. In order to prevent component disintegration or phase change owing to high thermal heating temperatures, the melting or glass transition temperatures of the related cladding and core materials should be comparable. Thirdly, to avoid breaks and fractures in the fiber structure during the heating or cooling stages, the thermal characteristics of materials, such as the thermal expansion coefficients, should be equivalent. We may choose the functional materials depending on particular applications, pair them with the proper cladding materials, and then combine them to create a macroscale preform by adhering to these three limitations.

#### 3.27.1.1 Preform fabrication

Numerous preform manufacturing techniques have been created as a result of the fast growth of multimaterial fiber over the past few decades, expanding the options for fiber materials and architectures.

### 3.27.2 High-pressure chemical vapor deposition (HPCVD) approach

The HPCVD technique is the basis for the semiconductor production technology that is the most novel. Here, the cladding material is initially constructed into a tube structure that serves as the reaction chamber and substrate and is open to the flow of precursors, while being subject to high pressures. The chemical processes are then started, and functional materials are deposited onto the inner walls of the cladding tube. This is followed by the introduction of a thermal or photochemical treatment. By varying the deposition period, temperature, and pressure, the thickness of the deposited layers may be precisely controlled. An additional advantage of this method is that it provides a platform for the manufacturing of optoelectronic fibers, in addition to being appropriate for preform preparation. The precursor was able to directly produce the optoelectronic fiber by passing through the capillary fiber, with the aid of the high-pressure flow. Since each material is deposited separately, there is no need to be concerned about the thermal characteristics of several materials varying during a single thermal treatment or the resulting harm to the fiber structure. The HPCVD technique, however, finds it difficult to fabricate long fibers because to the poor deposition rates, which restricts its practical applicability.

#### 3.27.2.1 Rod-in-tube approach

The cladding-core structure, which may be created via the rod-in-tube method, is the most often used type of fiber structure. By drilling from the bulk materials or combining powders, the functional core materials of choice are formed into rods. The cladding material tubes composed of silica, borosilicate glass, or polymer are then placed over the functional material rods. The inserted rods can be drawn into multimaterial fibers as well as structures made of a single functional material. Multimaterial fibers, tiny glass rods, and tubes with specified structures can be inserted into other tubes to create fibers with numerous cores and an array of functional materials. For the purpose of creating a high-density functional array, the inserted multimaterial fibers share the same material. The fibers may also be combined simultaneously with other core materials, such as p- and n-doped materials or semiconductor and metal pairings, which are the fundamental components of an optoelectronic device unit. To maintain the vacuum, the stacked core-cladding structures need to be evacuated and sealed from both ends. The gaps between the fibers, rods, and tubes will close during the thermal drawing process under the drawing force and air pressure.

#### 3.27.2.2 Sandwich consolidation

The sandwich consolidation technique is created to meet the demands of highly integrated optoelectronic fibers. This preparation technique has demonstrated excellent structural correctness. Diverse functional elements, including as semiconductors, electrodes, and insulators, may be accurately implanted into the polymer cladding with well-defined topologies to enhance the functioning of the high-performance functional devices by cutting grooves with different shapes and depths onto the polymer bars. The empty grooves can also produce hollow core channels, which might be used as pipes for drawing or delivering liquids. This method has so far been used only in the fabrication of polymer-based preforms due to the limitations of the materials, such as hardness and processing challenges.

#### 3.27.2.3 Thin-film rolling approach

The polymer is a great option when looking at materials with low melting points for creating fibers. The exceptional flexibility of numerous polymer materials opens up a brand-new space for preform preparation. In this procedure, the polymer material is first formed into a thin film and then rolled into a preform shape rather than being formed into a rod or tube. The functional components can be coated or thermally evaporated onto one side of the polymer thin film and then rolled up to create the preform, if they are too bulky to be rolled up, as is. Additionally, tiny channels for inserting electrodes can be carved into the preform. To consolidate, it is necessary to evacuate and heat the rolled-up multilayer structure.

## 3.28 Applications of functional optoelectronic fibers

### 3.28.1 Photovoltaic and photodetecting fiber

The carefully crafted structures and semiconductor–insulator–conductor materials enable multimaterial fibers to capture optical energy and produce electrical charges. These fibers are perfect for photovoltaic and large-area photodetecting systems with kilometers of length and integrated optoelectronic sensors. Diverse methods have been explored to further increase the efficacy of these photovoltaic and photodetecting fibers. First, there are several options for enhancing the efficiency of light energy conversion, including the use of different semiconductor materials and in-fiber material engineering techniques. Second, the high-level performance of the device was ensured by the consistent and efficient contact between the semiconductor and electrodes over the whole fiber length. Third, very effective fiber sensing technologies have been promised by the great density of in-fiber functional units. For instance, using the break-to-contact method, it is possible to include over 104 fully packed photodetecting units per meter into the manufactured optoelectronic fibers. Recent studies have looked at the very useful optoelectronic fibers based on these principles. These multifunctional fibers can be competitive candidates for applications in long-distance and large-area optoelectronic devices, based on the fiber's extraordinary length, flexibility, and weavability.

### 3.28.2 Photoluminescence fibers

The optoelectronic fiber system may be transformed into room-temperature photoluminescence fibers by including suitable semiconductor materials, which are particularly beneficial in applications like bandgap detection, impurity level of material detection, and optical sensors. The ability of Group III–V semiconductor materials to produce light with photoluminescent properties as a result of photon absorption has been proven. The semiconductor materials having photoluminescent properties may be built into the fiber-shaped device by using the multimaterial manufacturing technique. Additionally, the development of in-fiber heterojunctions and the single crystal structure of the material produced by the in-fiber thermal treatment result in superior performance material attributes.

### 3.28.3 Highly integrated optoelectronic fiber-shaped devices

The advanced fibers have a huge potential for highly integrated optoelectronic devices operating as sensors, medical probes, and labs on fibers since they are a multimaterial platform. To sense the signal of the neurons, a flexible polymer fiber with a tiny diameter and electrodes was inserted into the brain. Thermal drawing has also been proven to be a successful method of packing electronics. This method is intended to pull together hollow polymer tubes with commercial-grade optoelectronic functional components like light emitting diodes or photonic sensors. Functional units may also be included into the polymer cladding and in contact with the in-fiber electrode cores during the thermal drawing process. The next generation of highly integrated fiber-shaped functional devices can now be developed by overcoming the limitation of the materials for a fiber's composition into more compositions that might not be suitable for the drawing process and making the in-fiber functional structures compatible with more existing devices.

### 3.28.4 Fiber-based flexible device and smart textiles

Recent developments in material science have accelerated the development of flexible electronics and smart textiles, and several of these materials are now used extensively in wearable technology, parameter monitoring, and healthcare. With their tiny diameters, modern functional fibers may be stretched out into kilometer-long lengths, which can be a suitable fundamental functionality for textiles and smart skins. When embedded into fibers with micron and nanoscale diameters, functional materials, such as a number of semiconductor materials, become robust and flexible rather than bulky and rigid. Due to their mechanical properties, fibers with sophisticated functionalities may be readily woven into fabrics and textiles or can be implanted directly into commercial cloth, enabling the performance of electrical, optoelectronic, and energy-harvesting functions on these products and making them "smart." The multimaterial fibers may also be washed and dried several times without losing their functions, since the functional elements are integrated in the cladding or coating materials, which act as the protective layers.

## 3.29 Conclusions

In conclusion, the field of fiber-based wearable electronics has seen considerable advancement and enormous application opportunities due to the present research in fiber materials. In the future, it is anticipated that electronic textiles with integrated features of distinctive structures and different functions will not only satisfy daily wear needs but also serve the developing fields of health diagnosis, human-machine interactions, and artificial intelligence, which will transform how people live their lives. With the continued efforts of researchers from many fields, functional fiber materials with unheard-of qualities will continue to play a key role in the advancement of wearable electronics, even if this sector confronts significant hurdles.

The fiber-based wearable electronics should be made from highly biocompatible and safe materials that offer no risks to the environment or humans, whether it is materials or fiber electrodes. Such issues, however, could be raised when certain materials, like CNTs or metal ions, are employed in soft and flexible wearable electronics that are placed adjacent to human skin. To reach the same or even superior performance of the present conventional fibers, fiber-based electronics urgently require suitable materials and freshly developed manufacturing techniques.

When studying the use of CFs in flexible biosensors, it was observed that the complexity and expense of the composite material manufacturing process may limit the use of CFs in flexible biosensors. Contrarily, due to their superior mechanical qualities, CFs are the most popular materials in the domains of manufacturing and electrical energy storage. CF-based biosensor probes are frequently implanted in living beings, demonstrating that they have a wide range of potential applications in the field of biomedicine. Therefore, it is still important to consider how to strike a compromise between using CFs in flexible biosensors and making composite materials.

While the electrospun nanofibrous material has demonstrated several advantages as a promising alternative for wound healing, there are still a number of difficulties. First off, the majority of the organic solvents used for electrospinning are harmful to the wound as well as the surrounding environment. The creation of a nontoxic, environment-friendly, electrospinning method is imminent in order to get around this restriction. The drug control is still unsatisfied, despite the fact that designed and functionalized fibrous scaffolds have improved regulated drug delivery. Future research should pay greater attention to how drugs are released from electrospun nanofibrous dressings with various compositions and topologies.

## References

[1] Zong D, Zhang X, Yin X, Wang F, Yu J, Zhang S, Ding B. Electrospun fibrous sponges: principle, fabrication, and applications. Adv Fibre Mater. 2022.

[2] Liu R, Hou L, Yue G, Li H, Zhang J, Liu J, Miao B, Wang N, Bai J, Cui Z, Liu T, Zhao Y, Progress of fabrication and applications of electrospun hierarchically porous nanofibres, Adv Fibre Mater. 2022;4:604–630.

[3] Chen M, Wang Z, Li K, Wang X, Wei1 L Elastic and stretchable functional fibres: A review of materials, fabrication methods, and applications. Adv Fibre Mater. 2021.

[4] Eslami-Farsani R, Aghamohammadi H, Khalili SMR, Ebrahimnezhad-Khaljiri H, Jalali H. Recent trend in developing advanced fibre metal laminates reinforced with nanoparticles: a review study. 2022.

[5] Gulgunje P, Gupta K, Kumar S. Structural and functional fibres. Fibre Soc. 2017 Fall Meet. Tech. Conf. Int. Symp. Mater. from Renewables, ISMR 2017 Adv. Smart, Sustain. Polym. Fibres, Text. 2017-Novem 2017, 1–29.

[6] Zeng W, Shu L, Li Q, Chen S, Wang F, Tao XM, Fibre-based wearable electronics: a review of materials, fabrication, devices, and applications, Adv Mater. 2014;26:5310–5336.

[7] Wenrui Z, Fanxing M, Yanan Q, Fei C, Haitao Y, Minwei Z. Fabrication and specific functionalisation of carbon fibres for advanced flexible biosensors, Front Chem. 2020;8:1–12.

[8] Mia R, Shuva IB, Al Mamun A, Bakar A, Rumman FI, Rahman M, The fabrication of composite material based on natural macromolecules: a review, OALib. 2020;07:1–9.

[9] Meng F, Lu W, Li Q, Byun JH, Oh Y, Chou TW. Graphene-based fibres: a review, Adv Mater. 2015;27:5113–5131.

[10] Huang W, Xiao Y, Shi X. Construction of electrospun organic/inorganic hybrid nanofibres for drug delivery and tissue engineering applications, Adv Fibre Mater. 2019;1:32–45.

[11] Chen X, Yao T, Huang L, An Y, Wu H, Pan Z, Zhou P. Functional fibres and functional fibre-based components for high-power lasers. 2022.

[12] Chen M, Wang Z, Li K, Wang X, Wei L. Elastic and stretchable functional fibres: a review of materials, fabrication methods, and applications. Adv Fibre Mater. 2021;3:1–13.

[13] Chang-Yen DA, Eich RK, Gale BK. A monolithic PDMS waveguide system fabricated using soft-lithography techniques. J Light Technol. 2005;23:2088–2093.

[14] Kee JS, Poenar DP, Neuzil P, Yobas L. Design and fabrication of poly(dimethylsiloxane) single-mode rib waveguide. Optics Express. 2009;17:11739.

[15] Cai Z, Qiu W, Shao G, Wang W. Sensors and actuators A : physical a new fabrication method for all-pdms waveguides. Sens Actuators A Phys. 2013;204:44–47.

[16] Missinne J, Kalathimekkad S, Van Hoe B, Bosman E, Vanfleteren J, Van Steenberge G. Stretchable optical waveguides, Optics Express. 2014;22:4168.

[17] Guo J, Niu M, Yang C. Highly flexible and stretchable optical strain sensing for human motion detection. Optica. 2017;4:1285.

[18] Guo J, Zhou B, Yang C, Dai Q, Kong L. Stretchable and temperature-sensitive polymer optical fibres for wearable health monitoring. Adv Funct Mater. 2019;29:1–8.

[19] Elmogi A, Bosman E, Missinne J, Van Steenberge G. Comparison of epoxy- and siloxane-based single-mode optical waveguides defined by direct-write lithography. Opt Mater (Amst). 2016;52:26–31.

[20] Choi M, Humar M, Kim S, Yun SH. Step-index optical fibre made of biocompatible hydrogels. Adv Mater. 2015;27:4081–4086.

[21] Guo J, Liu X, Jiang N, Yetisen AK, Yuk H, Yang C, Khademhosseini A, Zhao X, Yun SH. Highly stretchable, strain sensing hydrogel optical fibres, Adv Mater. 2016;28:10244–10249.

[22] Yetisen AK, Jiang N, Fallahi A, Montelongo Y, Ruiz-Esparza GU, Tamayol A, Zhang YS, Mahmood I, Yang SA, Kim KS, Butt H, Khademhosseini A, Yun SH. Glucose-sensitive hydrogel optical fibres functionalized with phenylboronic acid. Adv Mater. 2017;29:1–11.

[23] Cooper CB, Arutselvan K, Liu Y, Armstrong D, Lin Y, Khan MR, Genzer J, Dickey MD. Stretchable capacitive sensors of torsion, strain, and touch using double helix liquid metal fibres. Adv Funct Mater. 2017;27.

[24] Qu Y, Nguyen-Dang T, Page AG, Yan W, Das Gupta T, Rotaru GM, Rossi RM, Favrod VD, Bartolomei N, Sorin F. Superelastic multimaterial electronic and photonic fibres and devices via thermal drawing, Adv Mater. 2018;30:1–8.

[25] Zhu S, So JH, Mays R, Desai S, Barnes WR, Pourdeyhimi B, Dickey MD. Ultrastretchable fibres with metallic conductivity using a liquid metal alloy core. Adv Funct Mater. 2013;23:2308–2314.

[26] Lu C, Park S, Richner TJ, Derry A, Brown I, Hou C, Rao S, Kang J, Moritz CT, Fink Y, Anikeeva P. Flexible and stretchable nanowire-coated fibres for optoelectronic probing of spinal cord circuits. Sci Adv. 2017;3.

[27] Manocchi AK, Domachuk P, Omenetto FG, Yi H. Facile fabrication of gelatin-based biopolymeric optical waveguides. Biotechnol Bioeng. 2009;103:725–732.

[28] Sordo F, Janecek ER, Qu Y, Michaud V, Stellacci F, Engmann J, Wooster TJ, Sorin F. Microstructured fibres for the production of food. Adv Mater. 2019;31:1–10.

[29] Qin H, Owyeung RE, Sonkusale SR, Panzer MJ. Highly stretchable and nonvolatile gelatin-supported deep eutectic solvent gel electrolyte-based ionic skins for strain and pressure sensing. J Mater Chem C. 2019;7:601–608.

[30] Shan D, Zhang C, Kalaba S, Mehta N, Kim GB, Liu Z, Yang J. Flexible biodegradable citrate-based polymeric step-index optical fibre dingying. 2017.

[31] Nizamoglu S, Gather MC, Humar M, Choi M, Kim S, Kim KS, Hahn SK, Scarcelli G, Randolph M, Redmond RW, Yun SH. Bioabsorbable polymer optical waveguides for deep-tissue photomedicine. Nat Commun. 2016;7:1–7.

[32] Fu R, Luo W, Nazempour R, Tan D, Ding H, Zhang K, Yin L, Guan J, Sheng X. Implantable and biodegradable poly(l-lactic acid) fibres for optical neural interfaces. Adv Opt Mater. 2018;6:1–8.

[33] Parker ST, Domachuk P, Amsden J, Bressner J, Lewis JA, Kaplan DL, Omenetto FC. Biocompatible silk printed optical waveguides. Adv Mater. 2009;21:2411–2415.

[34] Huby N, Vié V, Renault A, Beaufils S, Lefèvre T, Paquet-Mercier F, Pézolet M, Bêche B. Native spider silk as a biological optical fibre. Appl Phys Lett. 2013;102:12–15.

[35] Applegate MB, Perotto G, Kaplan DL, Omenetto FG. Biocompatible silk step-index optical waveguides. Biomed Opt Express. 2015;6:4221.

[36] Chen G, Matsuhisa N, Liu Z, Qi D, Cai P, Jiang Y, Wan C, Cui Y, Leow WR, Liu Z, Gong S, Zhang KQ, Cheng Y, Chen X. Plasticizing silk protein for on-skin stretchable electrodes. Adv Mater. 2018;30:1–7.

[37] Jia H, Liu K, Lam Y, Tawiah B, Xin JH, Nie W, Xiang Jiang S Fibre-based materials for aqueous zinc ion batteries. Adv Fibre Mater. 2022.

[38] Zhang J, Wang Z, Wang Z, Wei L Advanced multi-material optoelectronic fibres: A review, J Light Technol. 2021;39:3836–3845.

[39] Chang Maa, Liqiang W, Mahmut D, Hui C, Junjing L, Yan S, Jingli S, Xiangwu Z, ZnO-assisted synthesis of lignin-based ultra-fine microporous carbon nanofibers for supercapacitors. Journal of Colloid and Interface Science. Doi.:10.1016/j.jcis.2020.10.105

[40] Jia L, Guiyuan J, Ying L, Jiancheng D, Yajun W, Zhen Z, Qianyao S, Chunming X, Jinsen G, Aijun D, Jian L, Yuechang W, Yong Z, Lei J. Hierarchical Macro-meso-microporous ZSM-5 Zeolite Hollow Fibers with Highly Efficient Catalytic Cracking Capability. SCIENTIFIC REPORTS; 4:7276:1–6

Elyor Berdimurodov*, Abduvali Kholikov, Khamdam Akbarov,
Brahim El Ibrahimi, Dakeshwar Kumar Verma, Khasan Berdimuradov,
Omar Dagdag, Nuritdin Kattaev, Nurbek Umirov

# Chapter 4

# Advanced fiber materials in pollution control

**Abstract:** In this book chapter, advanced nanofibers used in air pollution control for indoor environments, noise pollution control, and hybrid advanced nanofibers in air pollution control are discussed. The main properties of advanced nanofiber materials for pollution control are discussed and reviewed. In modern times, electro-spun nanofibers are introduced in advanced air filters for indoor air control. They can filter hazardous pollutants and bio aerosols in the indoor environment. The benefits of advanced nanofiber materials are good environmental impacts of disposal, high efficiency in terms of retention, ability to be easily synthesized, and cost less for air pollution control. Advanced nanofibers are potential materials for control of noise pollution. The reason for this is that modern advanced nanofibers are nontoxic, are of reasonable cost, and are bio degradable. Advanced nanofibers are interesting materials in the adsorption of volatile organic compounds. The reason for this is that these materials are ecologically effective and are easy to operate.

**Keywords:** Fiber materials, noise control, air pollution and control, nanofilters, volatile organic compounds

---

***Corresponding author: Elyor Berdimurodov,** Faculty of Chemistry, National University of Uzbekistan, Tashkent 100034, Uzbekistan, e-mail: elyor170690@gmail.com

**Abduvali Kholikov, Khamdam Akbarov, Nuritdin Kattaev,** Faculty of Chemistry, National University of Uzbekistan, Tashkent 100034, Uzbekistan

**Brahim El Ibrahimi,** Department of Applied Chemistry, Faculty of Applied Sciences, Ibn Zohr University, 86153, Morocco

**Dakeshwar Kumar Verma,** Department of Chemistry, Government Digvijay Autonomous Postgraduate College, Rajnandgaon, Chhattisgarh 491441, India

**Khasan Berdimuradov,** Faculty of Industrial Viticulture and Food Production Technology, Shahrisabz branch of Tashkent Institute of Chemical Technology, Shahrisabz 181306, Uzbekistan

**Omar Dagdag,** Centre for Materials Science, College of Science, Engineering and Technology, University of South Africa, Johannesburg 1710, South Africa

**Nurbek Umirov,** Faculty of Chemistry-Biology, Karshi State University, Karshi 130100, Uzbekistan

https://doi.org/10.1515/9783110992892-004

## 4.1 Advanced nanofibers in air pollution control for indoor environments

Indoor air pollution is a serious issue, because hazardous air is the main reason for serious health issues. Most people spent their time indoor during the coronavirus pandemic period. In addition, modern innovative technologies require more oxygen. Therefore, the air quality of the indoor environment is very important [1–3]. In modern times, electro-spun nanofibers are used in advanced air filters for indoor air control. These materials are modern in air pollution control for indoor environments. They can filter out hazardous pollutants and bio aerosols in the indoor environment. The benefits of advanced nanofiber materials are good environmental impacts of disposal, high efficiency in terms of retention, ability to be easily synthesized, and cost less for air pollution control [4–8]. Advanced nanofiber is a good adsorbent of $O_3$ (ozone), VOCs (volatile organic compounds), $NO_x$ (nitrogen oxides), $CO_2$ (carbon dioxide), and CO (carbon monoxide). Indoor air has these gases. Various biological additions are used to modify the nanofibers to enhance their efficiency, surface properties, and structural efficiency. To enhance the quality of nanofibers used in indoor air pollution control, these materials are functionalized with various organic and inorganic nanomaterials, and polymeric materials. In future, it is foreseen that the home will be designed with advanced nanofibers, improving the air quality and reducing the hazardous chemicals [9]. In the food/biotechnology industries, laboratories and hospitals, advanced types of nanofibers are mostly used. The following main nanofibers are mostly used as advanced nanofibers in air pollution control for indoor environments [10]:

(i) Polyethylene-based nanofibers offer excellent resistance to acids and bases.
(ii) Polyester-based nanofibers offer good resistance to organic solvents, offer low resistance to strong bases, and offer good acid resistance.
(iii) Polyamide-based nanofibers are degraded in the presence of heat, and concentrated with acids and bases.
(iv) Meta-aramid-based nanofibers offer good resistance to acids and bases.
(v) Poly-aramid-based nanofibers are degraded in the presence of strong mineral acids to offer good resistance to diluted acids and bases.
(vi) Cellulose-based nanofibers offer weak resistance to acids and bases.
(vii) Polyacrylonitrile-based nanofibers offer moderate resistance to weak bases and good resistance to acids (except nitric acid).
(viii) Acetate-cellulose-based nanofibers are soluble in acetone and strong bases, cause loss of mechanical strength, and offer poor resistance to strong acids.

Liu et al. [11] investigated the air filtration of new nanofibers, based on chitosan. This suggested nanofiber can filter large-size particular pollutants (dust) from indoor environments. This filter is more efficient and costs less. This filter contains two parts:

(a) chitosan is a super hydrophilic part, which promotes the large size of particular pollutants (dust) from indoor environments. The filtration efficiency is 86%.
(b) the electrospun superhydrophobic poly(methylmethacrylate)/polydimethylsiloxane is a barrier for moisture ingression.

The large-size particular pollutants are adsorbed on the surface of the suggested nanofiber with over 98% during a 100 h period. This filtrate is also an antibacterial material: 95.2% efficiency for *Staphylococcus aureus* and 96.5% for *E. coli*. The processes used by advanced nanofibers in air pollution control for indoor environments are indicated in Figure 4.1: (a) manufacturing processes of nanofiber by wire mesh; (b) filtration procedures of indoor air through the nanofibers; (c) picture of nanofiber before air cleaning; (d and e) pictures of nanofibers after the cleaning of air; (f and g) chitosan-based nanofiber after air cleaning; (h and i) pictures of filtered dust particles; (j) surface morphology of filters on the nanofiber [11]. Figure 4.2 shows the adsorption capacitance of the investigated nanofiber: (a) adsorption and desorption procedure of dust on the surface of the nanofiber; (b) recycling productivity of nanofiber after washing; (c) picture of nanofiber before adsorption; (d) picture of nanofiber after adsorption; (e) surface of nanofiber after desorption [11].

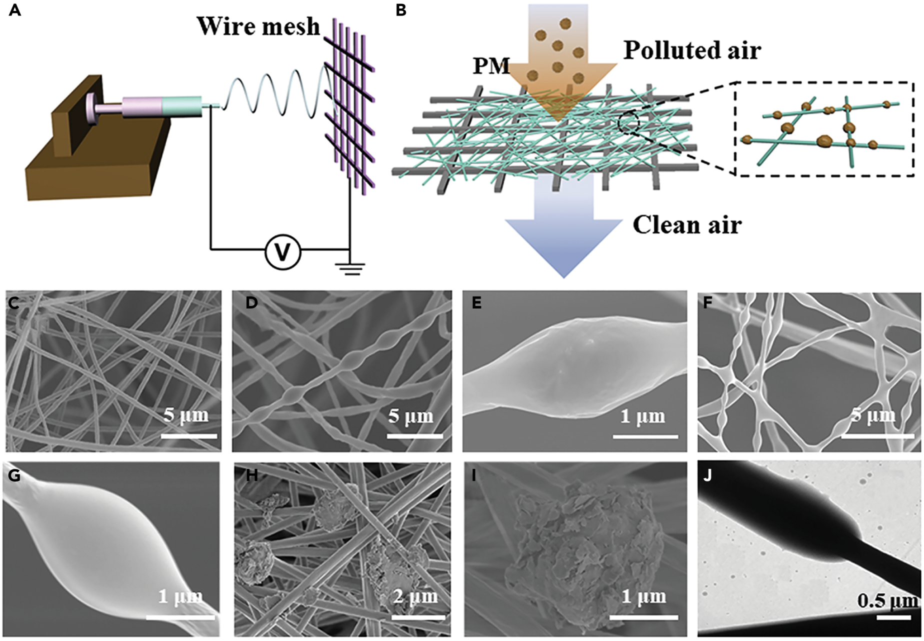

**Figure 4.1:** Processes of advanced nanofibers in air pollution control for indoor environments: (a) manufacturing processes of nanofiber by wire mesh; (b) filtration procedures of indoor air through the nanofibers; (c) picture of nanofiber before the air cleaning; (d, e) pictures of nanofibers after the cleaning of air; (f, g) chitosan-based nanofiber after air cleaning; (h, i) pictures of filtered dust particles; and (j) surface morphology of filters on the nanofiber [11].

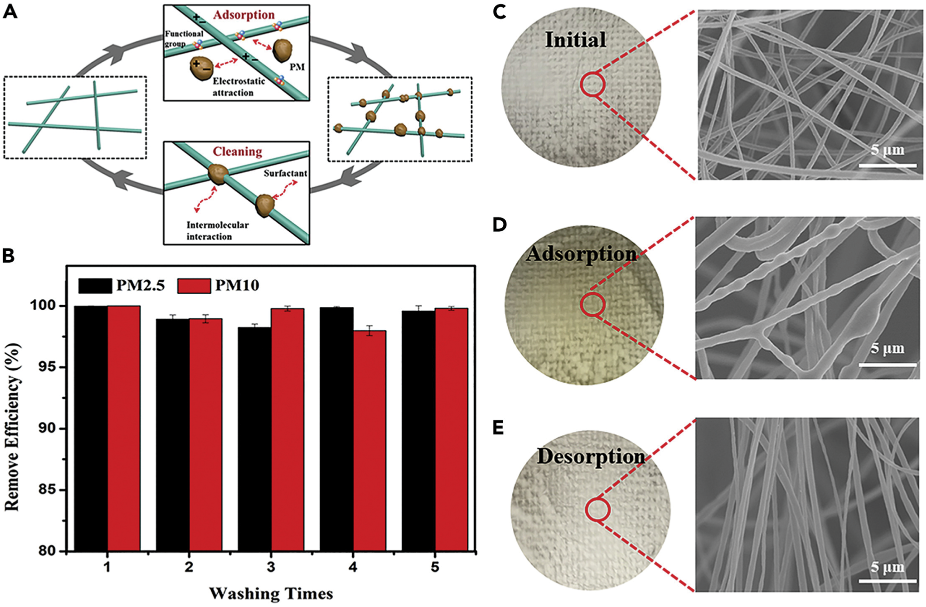

**Figure 4.2:** Adsorption capacitance of investigated nanofiber: (a) adsorption and desorption procedure of dust on the surface nanofiber; (b) recycling productivity of nanofiber after washing; (c) picture of nanofiber before adsorption; (d) picture of nanofiber after adsorption; and (e) surface of nanofiber after desorption [11].

## 4.2 Advanced nanofibers in noise pollution control

Noise is a serious problem in modern times. This is due to the many cars, people and the technologies, which are the main sources of the noise problem. Advanced nanofibers are potential materials for the control of noise pollution. The reason for this is that modern advanced nanofibers are nontoxic, cost reasonable, and are bio degradable. These properties of advanced nanomaterials make them potential materials in acoustic research [12–15]. The various modifications and functionalization of advanced nanofiber materials promote their acoustic performance, faced with the limitations of other materials. The natural jute fiber-based nanomaterials were effective and are natural control materials in noise pollution control. The density of nanofibers shows the noise properties. It has been confirmed that the lowest-density nanofiber materials are good adsorbents of noise. This depends on the structural properties. The nanofiber materials are of reasonable cost, have thermal insulation properties, are bio degradable, show nontoxic effects, are non-inflammatory, are of acceptable tensile strength, are available, are of low density, are biodegradable and are lightweight eco-friendly materials [16–19] [20].

Advanced nanofiber materials are also used in the construction and other industries because of their good economics, and environmental, mechanical, and physical properties. Various modifications have been done to nanofibers to enhance their acoustic performance through chemical, physical, and mechanical treatments. Currently, various modification treatments are used to enhance their noise adsorption ability. For example, alkali treatments are employed to enhance their mechanical properties, enhance their non-adhesion to the polymer matrix, and improve their hydrophilicity.

For example, Valipour et al. [20] investigated that alkali treatment effectively influences the acoustical and mechanical properties of natural nanofibers (jute fibers). The sound absorption performance of jute fibers was investigated. Good nanofibers effectively adsorbed noise from the environment. The impedance tube system, according to the transfer function method using the standard ISO 10,534–2, was used to estimate the values of the absorbed noise on the nanofibers. The tensile test (ASTM C1557-14 standard) and Scanning Electron Microscopy (SEM) were used to investigate the tensile and surface morphological performance. It was found that

(i) The noise reduction rate (NRC) in treated acoustic samples when compared to untreated with a thickness of 50 mm, increased from 0.66 to 0.69.
(ii) The alkali treatment enhances the noise adsorption performance of nanofibers.
(iii) The crystallinity index (CI) and tensile strength of nanofiber were enhanced to 3.26% and 61.66%, respectively.

Hassan et al. [21] suggested natural nanofiber-based panels for noise adsorption. These materials are natural and cost-effective materials, which can maximally insulate sound from outdoor activity. It is suggested that buildings are designed (household furniture, automotive body parts and building interiors) with noise resistance insulations using natural nanofibers. In this research work, the thermal, mechanical, and acoustic properties of natural fiber material with epoxy coating were investigated. The natural fiber source was sugarcane, coconut, and cotton (Figure 4.3). The thermogravimetric, coefficient of thermal expansion, diffusivity, thermal conductivity, flexural strength, impact strength, and sound absorption coefficient of these nanofiber materials were studied. Figure 4.4 shows the sound absorb efficiency of various natural nanofibers: (a) sugarcane, (b) coconut, (c) cotton, and (d) 20% fiber content composites.

## 4.3 Hybrid advanced nanofibers in air pollution control

The multifunctional and hybrid advanced nanofibers are new materials in air pollution control. Especially, metal-organic frameworks are modified with nanofibers to create hybrid nanofibers, which are good structural and multifunctional materials in

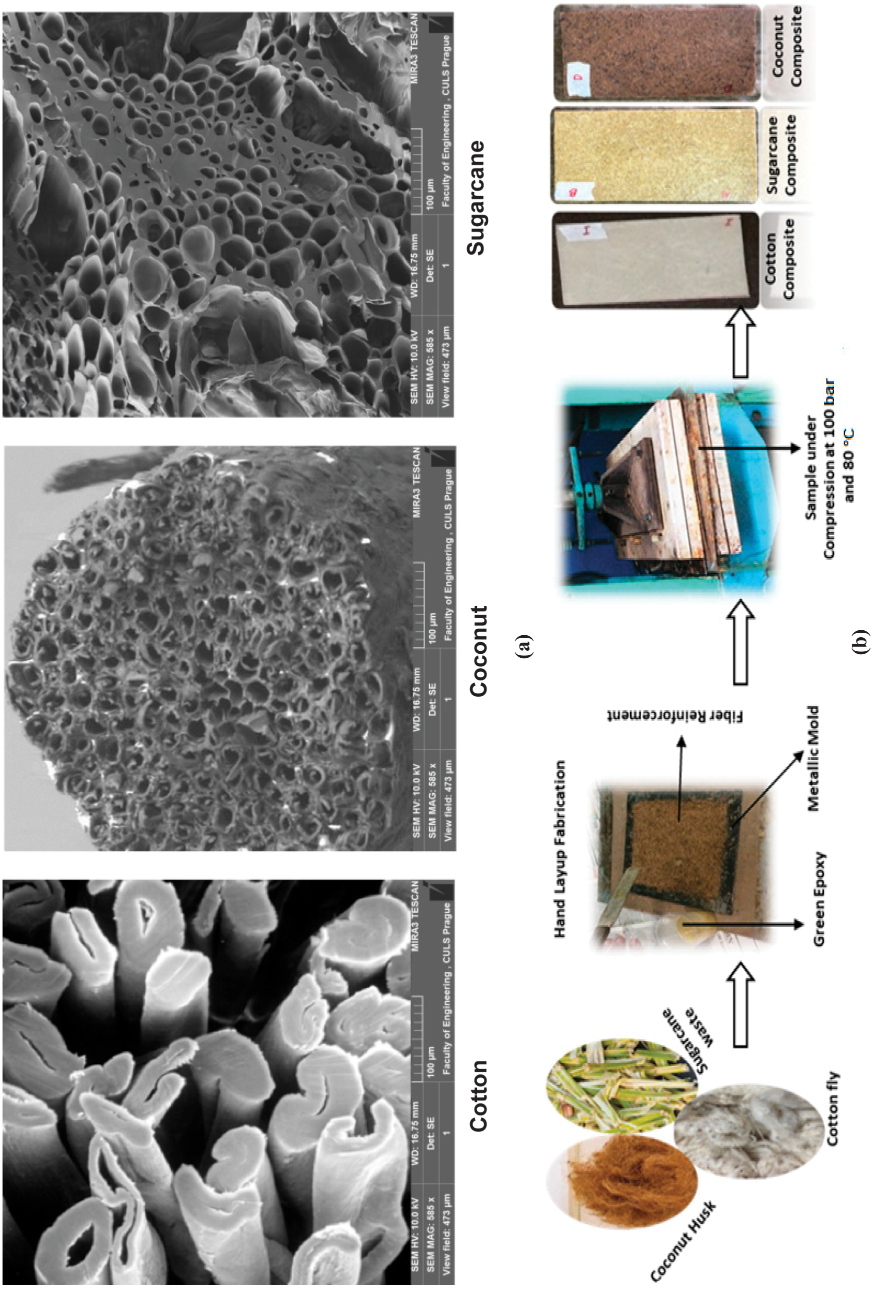
SEM HV: 10.0 kV
SEM MAG: 585 x
View field: 473 µm
WD: 16.75 mm
Det: SE
1
100 µm
Faculty of Engineering , CULS Prague
MIRA3 TESCAN
Cotton
Coconut
Sugarcane
(a)
Coconut Husk
Sugarcane waste
Cotton fly
Hand Layup Fabrication
Fiber Reinforcement
Green Epoxy
Metallic Mold
Sample under Compression at 100 bar and 80 °C
Cotton Composite
Sugarcane Composite
Coconut Composite
(b)

**Figure 4.3:** (a) Pictures of various natural nanofiber materials; (b) preparation methods of nanofiber [21].

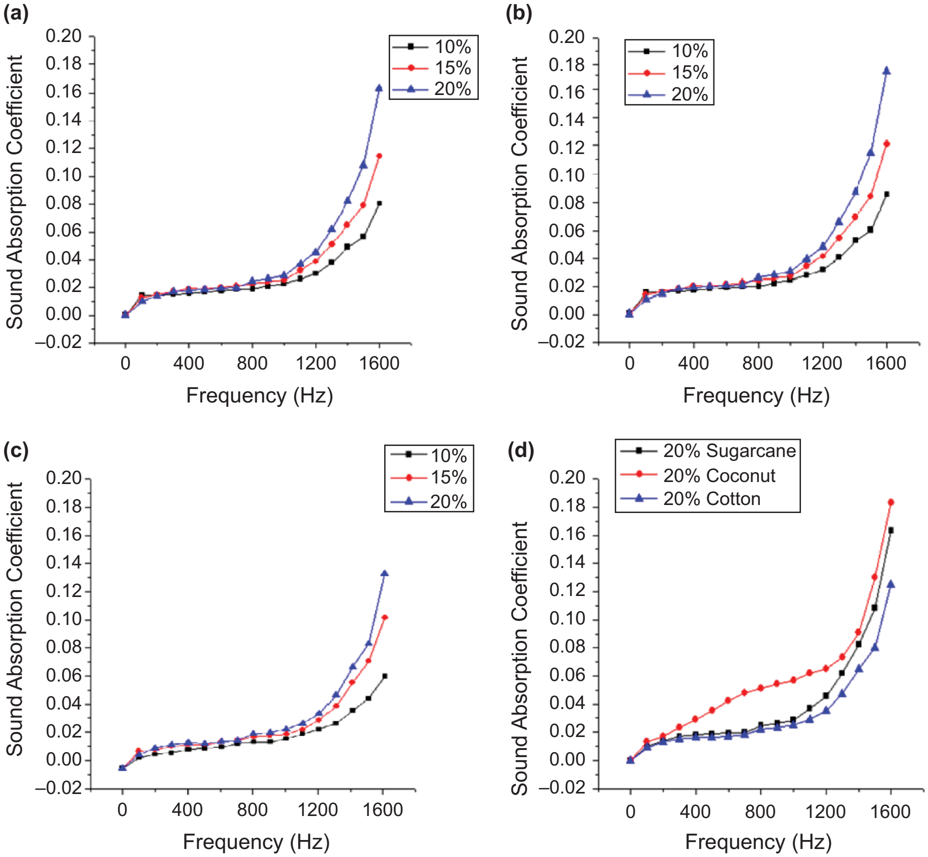

**Figure 4.4:** (a) The sound absorbs the efficiency of various natural nanofibers: (a) sugarcane, (b) coconut, (c) cotton, and (d) 20% fiber content composites [21].

air pollution control. The hybrid advanced nanofibers are more effective filters pf particulate matter (PM) in air control. Additionally, the toxic gas is also adsorbed to the surface of these types of nanomaterials. Hao and Wu [22] prepared the zeolitic imidazolate framework-polyimide (ZIF-PI) nanofibers, which have better thermogravimetric, coefficient of thermal expansion, diffusivity, thermal conductivity, flexural strength, impact strength, and sound absorption coefficient. They have a unique structure, high porosity and have a good network structure for air pollution control. The ZIF-PI nanofibers maximally filter higher PM2.5 and are a good adsorbent of $SO_2$.

Zhu et al. [23] prepared advanced nanofibers from the zeolitic imidazolate framework-8 (ZIF-8). In this process, the $SiO_2$ nanofiber membrane was fabricated by electrospinning and ZIF-8 nanocrystals were grown on the advanced nanofibers. The formed ZIF-8@$SiO_2$ nanofiber is more effective for PM particles from smoke gas, with 99.96% efficiency. The main reason for this is the electrostatic interaction between the beaded ZIF-8 nanocrystals and the PM particles, surface areas, small pores, and porosity of the ZIF-8@$SiO_2$ nanofiber. In addition to this, this material absorbed formaldehyde with 79.53% in 2 h. Therefore, it can be concluded that the ZIF-8@$SiO_2$ nanofiber membrane is more efficient for air purification. Fig. shows the structure of ZIF-8@$SiO_2$ nanofiber membrane, $SiO_2$ nanofiber membrane, air purification processes of ZIF-8@$SiO_2$ nanofiber membrane, and the structural properties of ZIF-8@$SiO_2$ nanofiber membrane (Figure 4.5).

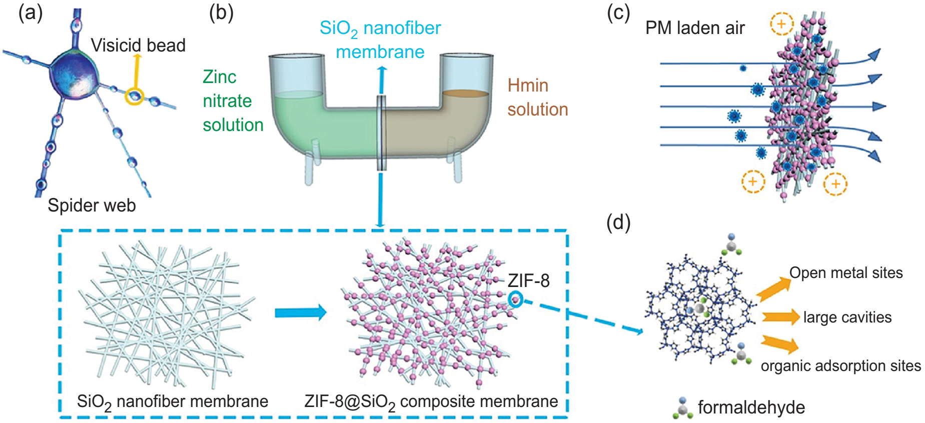
(a)
Visicid bead
Spider web
(b)
SiO2 nanofiber membrane
Zinc nitrate solution
Hmin solution
SiO2 nanofiber membrane
ZIF-8@SiO2 composite membrane
ZIF-8
(c)
PM laden air
(d)
Open metal sites
large cavities
organic adsorption sites
formaldehyde

**Figure 4.5:** (a) Structure of ZIF-8@$SiO_2$ nanofiber membrane; (b) $SiO_2$ nanofiber membrane; (c) air purification processes of ZIF-8@$SiO_2$ nanofiber membrane; and (d) structural properties of ZIF-8@$SiO_2$ nanofiber membrane [23].

The scanning electron microscope results at various times: (a and b) 30 min, (e, f) 60 min, (g, h) 120 min and transmissivity electronic microscopic results: (c, d) crystalline structure of ZIF-8@SiO2 composite membrane are shown in Figure 4.6. It is clear from Figure 4.6 that ZIF-8 is attached to the nanofibers and they can promote the adsorption capacitance of selected materials [23].

## 4.4 Advanced nanofibers in volatile organic compounds pollution control

Volatile organic compounds are serious pollutants in industrial regions. In modern times, various types of volatile organic compounds are realized in the pharmaceutical and chemical industries. These gases cause serious illnesses in the human body. Additionally, they are also the main source of hazardous gas, which is a problem for the environmental and ecological problems. The adsorption of volatile organic compounds is a very important task in material science and modern engineering. Advanced nanofibers are

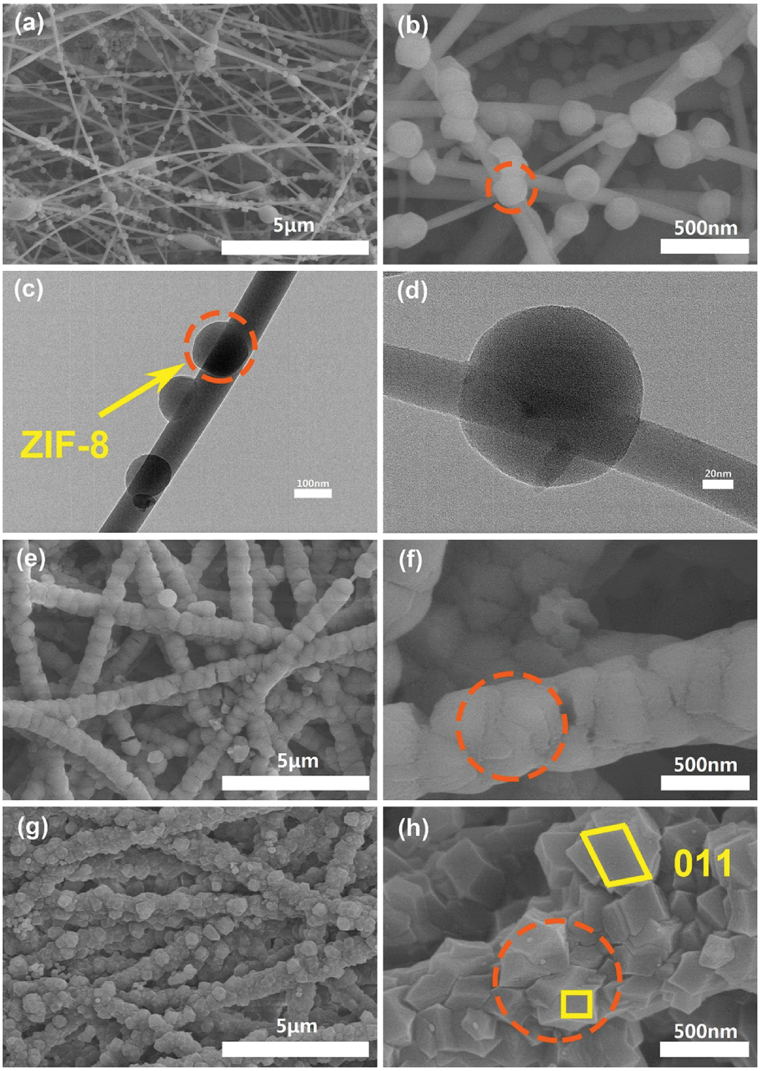

**Figure 4.6:** Scanning electron microscope results at various times: (a, b) 30 min; (e, f) 60 min; (g, h) 120 min. Transmissivity electronic microscopic results: (c, d) crystalline structure of ZIF-8@$SiO_2$ composite membrane [23].

interesting materials in the adsorption of volatile organic compounds. The reason for this is that these materials are ecologically effective and easy to operate [24–26]. Son et al. [27] prepared advanced nanofibers for the adsorption of volatile organic compounds. The suggested nanofiber-based filters could adsorb 100–900 ppmv of volatile organic compounds from air samples (Figure 4.7).

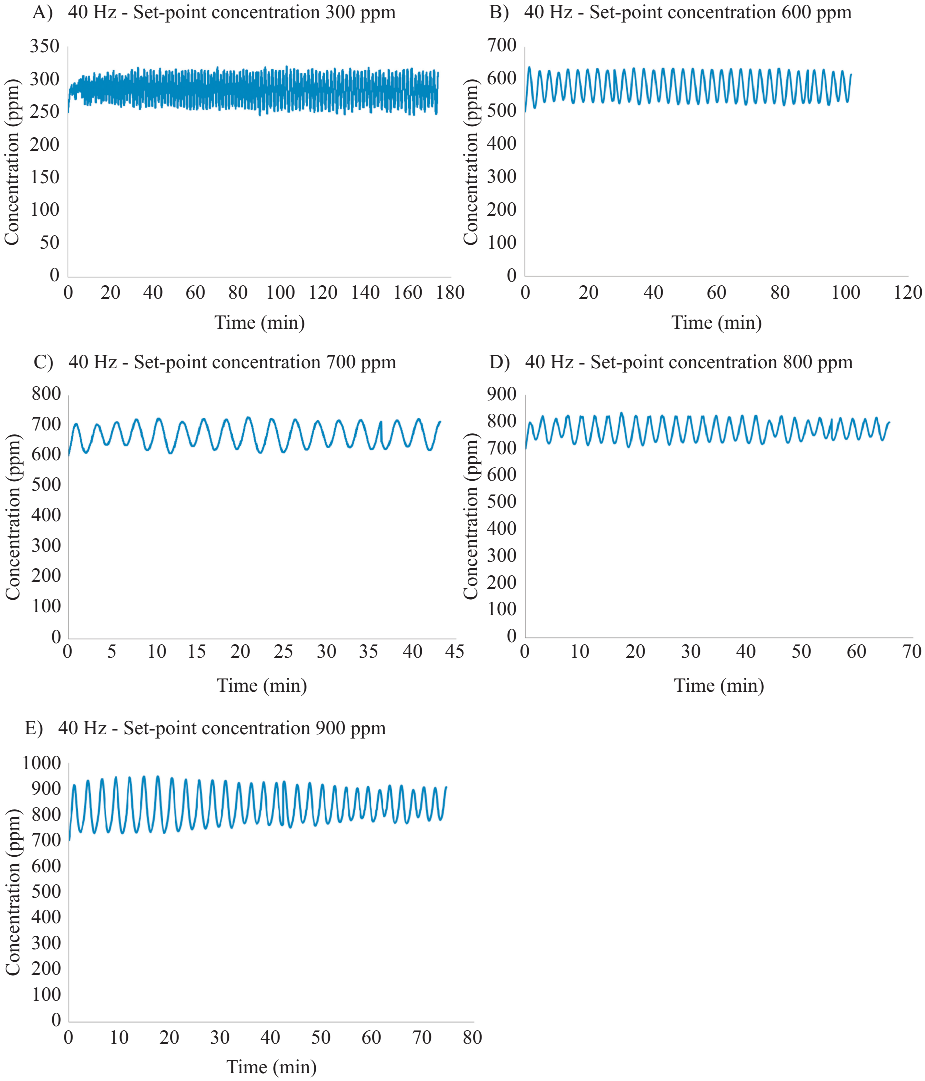

**Figure 4.7:** Desorption of total volatile organic compounds at the superficial gas velocity of 9.9 m/s and set-point concentrations of (a) 300, (b) 600, (c) 700, (d) 800, and (e) 900 ppmv [27].

The activated carbon advanced fiber cloths, based on the natural sources, were more effective for volatile organic compounds such as ammonium carbonate, metallic carbides or carbonates, carbonic acid, carbon dioxide, benzoyl, cyclohexane, and carbon monoxide. The activated carbon advanced fiber cloths are more effective in the pollution control of volatile organic compounds than the traditional methods: zeolites, silica gel, alumina, and granular activated carbons. The reason for this is that the carbon-advanced fiber cloths have increased adsorption kinetics, specific surface reactivity, have a microporous structure, show rapid adsorption/desorption rates, and have large surface areas. The carbon-advanced fiber cloths are prepared from various sources: phenolic resins, cellulosic fabric wastes, acrylic fabric wastes, viscous rayon precursors, and polymer precursors. The porosity degree, surface area, pore size, and surface characteristics are the main reasons for the emission and adsorption efficiency of volatile organic compounds [28–30].

The adsorption of volatile organic compounds depends on the environmental temperatures. The adsorption of volatile organic compounds on the surface of advanced fiber materials is exothermic. The volatile organic compounds are adsorbed on the fiber surface by the physical adsorption mechanism, in which the der Waals interaction is mainly responsible for the physical adsorption. Additionally, the volatile organic compounds chemically interact with the advanced fiber materials through the formation of covalent bonds or coordination bonds. The adsorption of volatile organic compounds decreases slowly, because, the electrostatic interactions between the components are destroyed at high temperatures. It is also indicated that the negative values of Gibbs free energy show the spontaneous adsorption of volatile organic compounds on the surface of the fiber [27].

## 4.5 Conclusions

In this book chapter, advanced nanofibers in indoor air pollution control , noise pollution control, and hybrid advanced nanofibers in air pollution control were discussed. The main properties of advanced fiber materials for pollution control were discussed and reviewed. In modern times, electrospun nanofibers are introduced in advanced air filters for indoor air control. These materials are modern in air pollution control for indoor environments. They can filter hazardous pollutants and bio aerosols in an indoor environment. The benefits of advanced nanofiber materials are good environmental impacts of disposal, high efficiency in terms of retention, can be easily synthesized and cost less with respect to air pollution control. Advanced nanofibers are potential materials for the control of noise pollution. The reason for this is that modern advanced nanofibers are nontoxic, are of reasonable cost, and are biodegradable. These properties of advanced nanomaterials make them more potential materials in acoustic research. The adsorption of volatile organic compounds is a very important task in material science and modern engineering. Advanced nanofibers are interesting materials in the adsorption of volatile organic compounds. The reason for this is that these materials are ecologically effective and are easy to operate.

# References

[1] Bian Y, et al. Metal–organic framework-based nanofiber filters for effective indoor air quality control. J Mater Chem A. 2018;6(32):15807–15814.

[2] Zhu M, et al. Electrospun nanofibers membranes for effective air filtration. Macromol Mater Eng. 2017;302(1):1600353.

[3] Bian Y, et al. Electrospun SF/PVA nanofiber filters for highly efficient PM $ _ {2.5} $ capture. IEEE Trans Nanotechnol. 2018;17(5):934–939.

[4] Homaeigohar S, Elbahri M. Nanocomposite electrospun nanofiber membranes for environmental remediation. Materials. 2014;7(2):1017–1045.

[5] Niu Z, et al. An optimization approach for fabricating electrospun nanofiber air filters with minimized pressure drop for indoor PM2. 5 control. Build Environ. 2021;188:107449.

[6] Lv D, et al. Green electrospun nanofibers and their application in air filtration. Macromol Mater Eng. 2018;303(12):1800336.

[7] Mamun A, Blachowicz T, Sabantina L. Electrospun nanofiber mats for filtering applications – technology, structure and materials. Polymers. 2021;13(9):1368.

[8] Thavasi V, Singh G, Ramakrishna S. Electrospun nanofibers in energy and environmental applications. Energy Environ Sci. 2008;1(2):205–221.

[9] de Almeida DS, Martins LD, Aguiar ML. Air pollution control for indoor environments using nanofiber filters: a brief review and post-pandemic perspectives. Chem Eng J Adv. 2022;11:100330.

[10] Hutten IM. Handbook of nonwoven filter media. Elsevier; 2007.

[11] Liu H, et al. Transparent antibacterial nanofiber air filters with highly efficient moisture resistance for sustainable particulate matter capture. iScience. 2019;19:214–223.

[12] Mohraz MH, et al. Preparation and optimization of multifunctional electrospun polyurethane/chitosan nanofibers for air pollution control applications. Int J Environ Sci Technol. 2019;16(2):681–694.

[13] Trematerra A, et al. Acoustic properties of nanofibers.

[14] Zong D, et al. Bubble templated flexible ceramic nanofiber aerogels with cascaded resonant cavities for high-temperature noise absorption. ACS Nano. 2022.

[15] Kouhnavard B. The sound adsorption of poly vinyl chloride nanocomposites, consisting of silica, zinc oxide, zeolite a to noise pollution control. Int J Occup Hyg. 2021;13(1):xxx–xxx.

[16] Xu W, et al. Laminated triboelectric acoustic energy harvester based on electrospun nanofiber towards real-time noise decibel monitoring. Nano Energy. 2022;107348.

[17] Shao H, et al. Single-layer piezoelectric nanofiber membrane with substantially enhanced noise-to-electricity conversion from endogenous triboelectricity. Nano Energy. 2021;89:106427.

[18] Davoudabadi Farahani M, Asgharian Jeddi AA, Jamshidi M. Investigation of sound absorption of warp knitted spacer fabric with nanofiber coating. J Text Sci Technol. 2021;10(2):18–25.

[19] You H, et al. Self-reinforced polymer nanofiber aerogels for multifunctional applications. Macromol Mater Eng. 2022;2100971.

[20] Valipour F, et al. Improvement of natural fiber's properties and evaluation of its applicability as eco-friendly materials in noise pollution control. J Environ Health Sci Eng. 2022;20(2), 647–656.

[21] Hassan T, et al. Acoustic, mechanical and thermal properties of green composites reinforced with natural fibers waste. Polymers. 2020;12. DOI: 10.3390/polym12030654.

[22] Hao Z, Wu J. Self-assembled zeolitic imidazolate Framework/Polyimide nanofibers for efficient air pollution control. ACS Appl Nano Mater. 2022;5(2):2343–2349.

[23] Zhu Q, et al. Zif-8@sio2 composite nanofiber membrane with bioinspired spider web-like structure for efficient air pollution control. J Membr Sci. 2019;581:252–261.

[24] De Gennaro G, et al. Indoor and outdoor monitoring of volatile organic compounds in school buildings: indicators based on health risk assessment to single out critical issues. Int J Environ Res Public Health. 2013;10(12):6273–6291.

[25] Dwivedi P, et al. Comparative study of removal of volatile organic compounds by cryogenic condensation and adsorption by activated carbon fiber. Sep Purif Technol. 2004;39(1–2):23–37.

[26] Hashisho Z, Rood M, Botich L. Microwave-swing adsorption to capture and recover vapors from air streams with activated carbon fiber cloth. Environ Sci Technol. 2005;39(17):6851–6859.

[27] Son HK, et al. Electrothermal adsorption and desorption of volatile organic compounds on activated carbon fiber cloth. J Hazard Mater. 2016;301:27–34.

[28] Li C, Moe WM. Activated carbon load equalization of discontinuously generated acetone and toluene mixtures treated by biofiltration. Environ Sci Technol. 2005;39(7):2349–2356.

[29] Fuertes AB, Marban G, Nevskaia DM. Adsorption of volatile organic compounds by means of activated carbon fibre-based monoliths. Carbon. 2003;41(1):87–96.

[30] Huang Z-H, et al. Breakthrough of methyethylketone and benzene vapors in activated carbon fiber beds. J Hazard Mater. 2003;98(1–3):107–115.

Gianluca Viscusi*

# Chapter 5
# Advanced fibre materials for environmental applications

**Abstract:** Fibre materials, widely used in industrial applications and the textile industry, represent an interesting class of materials (natural or synthetic) which is gaining a central role in the last decades. The wide application of these materials is mainly related to the beneficial properties such as mechanical toughness, resistance, stability, and lightness as well as, as far as natural fibres are concerned, renewability, eco-friendly features, biodegradability, no carcinogenicity, and lack of irritation. Apart from their use in textile applications, due to their characteristics, they have been used in many different industrial sectors such as tissue engineering, automotive, insulation, cosmetic, water remediation, building, and fine chemicals. In the last decades, the design of fibre-based materials is emerging with the possibility of exploiting them for environmental applications. Rapid urbanization and industrialization in the past decades have increased the awareness of many emerging environmental problems such as water resources pollution. The interest in fibre-based materials is related to their unique properties which could favour the adsorption of pollutants from water bodies. By stating that this chapter concerns the state of the art related to the design, fabrication, and characterization of advanced fibre materials (synthetic or natural ones) applied for environmental applications. Already-implemented technologies and emerging ones, such as electrospinning, will be considered while the applications of interest such as heavy metals, dyes, pharmaceutical residues, pesticides, inorganic ion removal, and oil adsorption will be widely discussed.

**Keywords:** fibres based materials, water pollutions, pollutant, water remediation, adsorption

## 5.1 Introduction

Clean water, free of toxic chemicals and pathogens, is known to be essential to human health. But, considering that water represents a feedstock in many industries (electronics, pharmaceuticals, and food), the rapid growth of industrialization is leading to the pollution of water sources by hazardous wastes. Among all, heavy metal and inorganic ions, dyes, oils, fluorides, pesticides, residues of care products, and other persistent organic

---

***Corresponding author: Gianluca Viscusi**, Department of Industrial Engineering-University of Salerno, Via Giovanni Paolo II, 132 84084 Fisciano, SA, e-mail: gviscusi@unisa.it

https://doi.org/10.1515/9783110992892-005

pollutants are widely present in wastewater [1, 2]. The dispersion of chemical residues, organic wastewater, and oil spills derived from industrial, agricultural, and household activities is increasing environmental pollution (water, air, soil) determining a critical problem for human health which urgently needs to be solved [3]. To overcome these issues, different classes of materials have already been tested as potential adsorbents. Among all, fibre-based materials are promising systems with great performance due to the properties of fibres to bind and remove pollutants from wastewater. But, the overuse of synthetic materials and their damage to the environment is prompting the development of eco-friendly and sustainable materials. The interest in such materials is attracting the scientific community. Since the interest in more sustainable solutions, many attempts have been made to use lignocellulosic materials (usually agro-industrial wastes and by-products) for the biosorption processes. Generally, biosorption processes can significantly reduce capital costs, operational costs, and total treatment costs concerning conventional systems [4]. Among the different adopted materials, the use of fibre materials could be adequate in environmental applications. So, different strategies have been considered to produce fibre-based materials even with a complex chemical structure able to be applied for environmental applications. Particularly, three groups of fibres can be identified:
- Natural fibres
- Synthetic fibres (organic)
- Synthetic fibres (inorganic)

The following sections summarize the design and the use of different fibre-based materials for environmental applications by diversifying the kind of fibre material and the purpose of application.

## 5.2 Natural fibre

Nowadays, there is an increasing demand for the commercial use of natural fibres in different industrial applications [5]. The plant fibres are made up of cellulose, lignin, pectin, waxes, and water-soluble substances; they can be regarded as sustainable materials which are easily available with low cost, lightweight, renewability, biodegradability, and high specific properties [6]. Currently, they are mainly used in the production of lightweight composites, automotive interior linings, construction, textile, transportation, furniture, packaging, etc. [7–9]. Moreover, the use of unmodified and modified natural fibres represents an interesting strategy to reduce the contamination of wastewater due to the presence of oil traces, metal and non-metal ions, and organic dyes as well. The use of natural fibres in environmental applications has already been explored for the detection of contaminants through the design of fibre-based sensors, separation of contaminant materials [10], and area decontamination [11]. Even if these materials show various advantages (i.e. renewability, reusability, and low cost), adsorbents based on lignocellulosic biomasslack high adsorption capacities towards organic and metallic contaminants as compared to commercial adsorbents (e.g., activated carbon or zeolite). By stating that and aiming of enhancing the adsorption potential of natural fibres, researchers have proposed different chemical modifications to introduce different types of new functionalities [12]. Hereafter, the potential applications of natural fibres for the removal of the main pollutants are discussed.

## 5.2.1 Dyes

Synthetic dyes have been widely used since they derived from different dye stuff manufacturing and industries, including the textile, leather, paper, petroleum, printing, cosmetics, paint, pigments, rubber, plastic, pesticide, wood-preserving chemicals, food, and pharmaceutical industries [13]. Dyes usually show a complex molecular structure and high stability in water [14]. Their presence in water bodies is highly hazardous for aquatic life since they inhibit sunlight penetration as well as the metabolism of some species by reducing the oxygen concentration inside the water [15]. Due to their overuse, the dispersion in wastewater is representing a critical issue [16]. The ingestion of dyes at a high concentration has many detrimental effects on human health such as allergies, asthma, and failure of the reproductive system, brain, liver, and kidneys. So, different strategies have been already employed for the removal of such substances: chemical, biological, and physical treatments. Adsorption has been proven to be an efficient and reliable alternative dye removal process to available wastewater treatment techniques because of its simple design and low initial investment cost [17]. Currently, the cost of the classical adsorbent system is substantial; so great effort has been made to produce low-cost adsorbent systems such as natural fibres. Their use to remove dyes from wastewater is gaining increasing interest in the eco-friendliness of these materials. Often, to improve the surface properties and enable the dye molecule to diffuse into the bulky fibres, chemical modifications are required.

Selambakkannu et al. [18] fabricated a novel adsorbent based on banana fibres, partially delignified using $NaClO_2$, modified with glycidyl methacrylate and trimethylamine (TMA) for the removal of acid blue (AB 80) and acid red (AR 86). The proof of the effective functionalization was demonstrated by elemental analysis, SEM, FTIR, and XRD analyses. The adsorption equilibrium was attained in 90 and 180 min for AR86 and AB80 with a $q_t$ of 292 and 319 mg/g for AB80 and AR86. Moreover, the equilibrium adsorption capacity was found to be directly related to the amine density. Desorption processes were carried out in different solvent mixtures. In all cases, the elution of AB 80 dyes is relatively higher than AR 86. So, it was demonstrated that TMA-functionalized adsorbents could be used as a promising alternative to dye removal.

Sajab et al. [14] fabricated citric acid (CA) and poleyethylenimine (PEI)-modified oil palm empty fruit bunch fibres (EFB) to produce anionic and cationic adsorbents. FTIR analysis and zeta potential measurements proved the effective modification. The modified fibres were used as adsorbent of methylene blue and anionic phenol red from aqueous solutions by changing pH, T, and dye concentrations. The maximum adsorption of MB on the CA–EFB and PEI–EFB can be achieved in pH = 7 and pH = 3, respectively, while an increase in initial dye concentration led to an increase in $q_t$. The adsorption capacity of the CA–EFB towards MB was 103.1 mg/g. However, the maximum adsorption capacity of the PEI–EFB is 158.7 mg/g in the removal of PR. The regeneration studies proved the reusability of the designed materials for more than seven cycles with a maximum adsorption capacity loss equal to 30%.

Roy et al. [12] fabricated a novel adsorbent based on lignocellulosic biomass jute fibre (JF) which was chemically modified with polyphenolic tannin in an aqueous medium by epoxy activation under mild conditions. The removal efficiency of Congo Red from aqueous solution was investigated. The adsorbent was characterized by elemental analysis, NMR, FTIR, and SEM analyses. The adsorption capacity of modified JF increased from 9.92 to 22.63 mg/g as the initial dye concentration was increased from 10 to 250 mg/L while it decreased from 4.96 to 3.59 mg/g as the temperature was increased from 30 to 50 °C proving the exothermic nature of the adsorption process. The desorption tests were carried out by using 0.1 M NaOH solution obtaining a desorption degree of 80.1%. The authors proved the performance of a new efficient and low-cost adsorbent with the potential for practical application in the treatment of wastewater.

Li et al. [19] fabricated an absorbent based on maleic anhydride-modified cellulosefibre-based beads combined with alkali-treated diatomite (MCDBs) for organic dyes removal such as methylene blue and methylene violet (MV). Calcium carbonate was added to increase the pore structure determining an improvement of adsorption capacity up to 30%. The influence of pH, shaking time, and temperature on the removal process was studied. The results indicated the high adsorption capacity towards basic dyes of the fabricated adsorbent changing from 51.6 to 116.6 mg/g for MB and from 30.5 to 61.1 mg/g for MV. The optimum pH values for MB and MV removal were 7.0 and 6.5, respectively. The adsorption of methyl violet changed as the temperature increased up to 30 °C, proving the endothermic nature of the adsorption process of dye while no changes were noted for MB removal. Concerning the reusability, the removal efficiencies under the optimal conditions were 97.1%, 88.3%, and 83.4% for MB and 93.4%, 92.6%, and 87.9%, respectively.

Viscusi et al. [20] designed a novel system based on the use of hemp fibres modified with graphite oxide for the removal of organic dye, such as methylene blue, from aqueous solutions. The amount of dye was found to be highly dependent on the pH regime, initial concentration of dye, ionic strength, and slightly dependent on temperature. Maximum adsorption capacity increased with temperature and pH changing from 54 to 58 mg/g at pH = 7.5, from 37 to 45 mg/g at pH = 3, and from 44 to 49 mg/g at pH = 12, by increasing the temperature from 20 to 80 °C indicating the endothermic nature of the process. The pH level affected the adsorption properties indicating that weak electrostatic interactions could exist between cationic dye and electron-rich sites of the surface. Regeneration studies showed a 5% drop in adsorption capacity after seven cycles.

The produced adsorbent is chemically stable, showing no noticeable leaching of GO (0.15 µg/L after 240 h of utilization). The sorption mechanism was mainly correlated to the action of electrostatic interaction, hydrogen bond, $\pi$–$\pi$ interactions, and van der Waals forces (Figure 5.1).

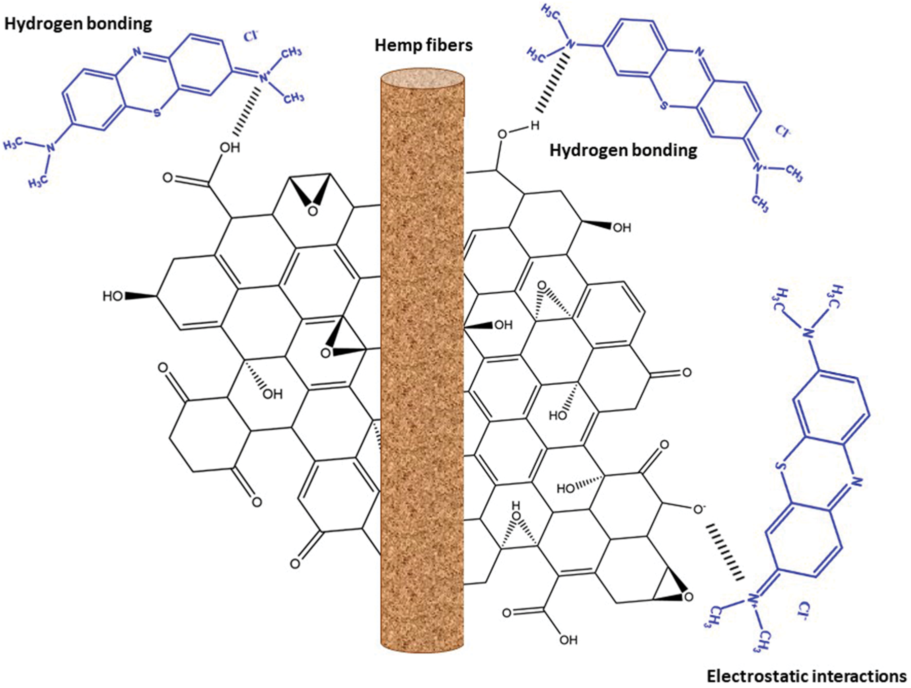

**Figure 5.1:** Adsorption mechanism of MB on GO-modified hemp fibres (reprinted with permission from [20]).

Similar systems have already been proposed and Table 5.1 reports some examples by specifying the removed dye and the investigated adsorbents.

**Table 5.1:** Comparison of maximum adsorption capacity ($q_{max}$) of different natural fibre-based adsorbents towards organic dyes.

| Adsorbent | Dye | $q_{max}$ (mg/g) | References |
|---|---|---|---|
| Graphite oxide-modified hemp fibres | Methylene blue | 200 | [20] |
| Acrylic acid-modified *Ficus carica* fibre | Methylene blue | 75.87 | [21] |
| *Luffa cylindrica* fibres | Methylene blue | 49 | [22] |

**Table 5.1** (continued)

| Adsorbent | Dye | $q_{max}$ (mg/g) | References |
|---|---|---|---|
| Methyl acrylate and acrylic acid graft copolymerization of *Luffa cylindrica* fibres | Congo red | 19.24 | [23] |
| Citric acid-modified oil palm empty fruit bunch fibres | Methylene blue | 103.1 | [14] |
| Polyethylenimine-modified oil palm empty fruit bunch fibres | Phenol red | 158.7 | [14] |
| Citric acid-modified kenaf core fibres | Methylene blue | 131.6 | [24] |
| Glycidyl methacrylate and trimethylamine-modified banana fibres | Acid red 86 | 319.35 | [18] |
| | Acid blue 80 | 292.28 | [18] |
| Ethylenediamine-modified *Populus tremula* fibres | Acid blue 25 | 67 | [17] |
| Corn fibres | Alcian blue | 159 | [25] |
| | Methylene blue | 70 | [25] |
| | Neutral red | 50 | [25] |
| | Brilliant blue | 35 | [25] |
| Sugarcane fibre | Crystal violet | 10.44 | [26] |
| Jute fibres | Congo red | 8.12 | [27] |
| Polyphenol tannin-modified jute fibres | Congo red | 27.12 | [12] |
| Beta-cyclodextrin and amino-terminated hyperbranched polymer cotton fibres | Methylene blue | 95.8 | [28] |
| | Congo red | 236.6 | [28] |
| Flax fibres | Basic yellow 37 | 512 | [29] |
| Polyacrylonitrile-coated kapok fibres | Methyl orange | 34.72 | [30] |
| Polyaniline-coated kapok fibres | Methyl orange | 75.76 | [31] |
| Oil palm trunk fibres | Malachite green | 149.35 | [32] |

## 5.2.2 Oil spills

Oil spills and leakages represent a serious source of environmental pollution becoming a great concern which is requiring the application of different methodologies for the removal of oil traces from water sources. Absorbents obtained from natural and synthetic organic and inorganic materials are efficient systems belonging to three categories: inorganic mineral materials (e.g., clays), natural organic materials (e.g., corn straw, milkweed, cotton, and kapok), and synthetic organic materials (e.g., polypropylene (PP) and polyurethane foam) [33]. Natural organic materials, such as natural fibres, are attracting interest since they are eco-friendly and cost-effective. The properties of natural fibres, such as roughness, can be exploited as adsorbents for oil sorption. Nowadays, there are different fibres which could be used as oil adsorbents. For example, Hubbe et al. [34] in their review showed that natural cellulose-based fibres can be used as oil sorbents. While wood fibres have low adsorption properties, milk weed, kapok, and cotton fibres have greater potential for oil spill clean-up, absorbing significantly more oil than commercial synthetic absorbent materials [35, 36]. In particular, the kapok fibres have been tested showing high oil adsorption characteristics towards diesel, hydraulic, and engine oil [37, 38]. Indeed, *Populus seed* fibres showed great adsorption performances when tested with high-density motor oil and diesel fuel. The unique structure consisting of hollow hydrophobic lignocellulosic microtubes coated by a hydrophobic waxy coating provides with super-absorbent behaviour with high absorption showing good adsorption values (182–211 g heavy oil per gram fibre and 55–60 g heavy oil per gram fibre as a function of the packing densities) [39]. In general, the oil uptake occurred due to the formation of van der Waals' forces and hydrophobic interactions [40].

Anjos et al. [41] tested *Calotropis procera* fibre as a novel oleophilic and hydrophobic adsorbent for oil removal. To improve the adsorption capacity, *Calotropis procera* fibres have been modified with solutions of NaOH, $NaClO_2$, and hydrothermal treatment. The effect of the treatment on the adsorption capacity of crude oil and crude oil/water system was evaluated, and the results showed that NaOH-treated fibres possessed the highest sorption capacity (103.9 g/g) fibres. The obtained results show that the modified *Calotropis procera* fibres represent a novel alternative for cleaning and removing crude oil and petroleum derivatives of their excellent selectivity of water/oil, high availability, reuse capacity, and high oil absorption.

Cao et al. [42] developed a novel oil adsorbent system based on *Calotropis gigantea* fibre (CGF) modified with metal nanoparticles of Ni and Cu via a facile in-situ growth method to create more adsorption sites. The modified fibres exhibit excellent oil–water selectivity since they can quickly absorb the model oils in oil–water mixtures. The oil-absorbing capacities of different oils and organic solvents were first investigated (Figure 5.2) including ethanol, ethyl acetate, *n*-hexane, *n*-heptane, xylene, acetone, toluene, carbon tetrachloride, kerosene, diesel fuel additives, chloroform, engine oil, soybean oil, and olive oil.

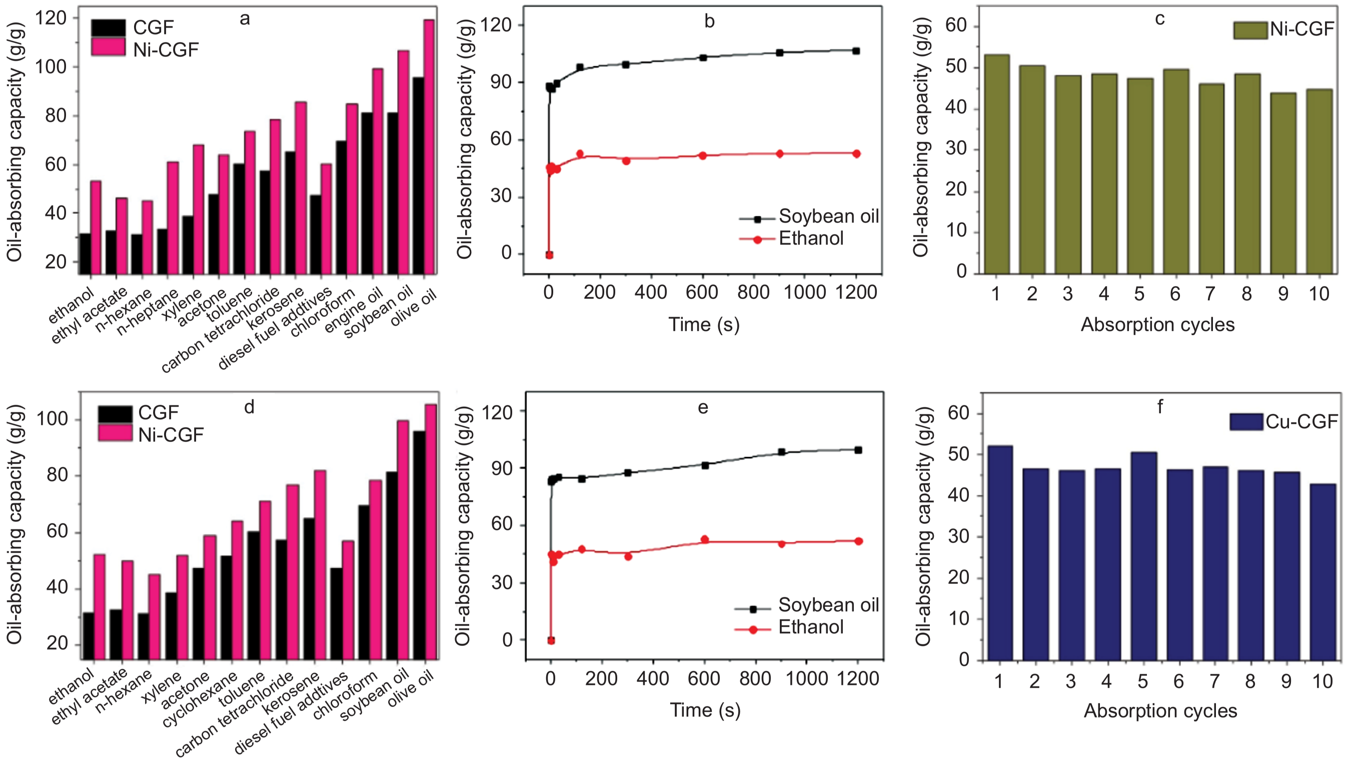

**Figure 5.2:** Oil-absorbing properties of Ni-CGF (a, c) and Cu-CGF (d, f). (a, d) Saturated absorption capacities in various oils; (b, e) oil-absorbing capacities as a function of time for soybean oil and ethanol, and (c, f) reusability using ethanol (reprinted with permission from [42]).

The raw fibre was able to absorb oils and organic solvents at 31–95 g/g to its weight, while modified fibres with Ni showed an oil-absorbing capacity of 45–120 g/g to its weight. Compared to the raw fibre, the Ni-modified fibres exhibited higher oil-absorbing capacity correlated with their roughened surface and the availability of more sites for oil storage.

Wang et al. [43] developed coated kapok fibres through a facile solution-immersion process using polybutylmethacrylate (PBMA) and polystyrene (PS) as modification agents. The as-prepared fibre can quickly absorb gasoline, diesel, soybean oil, and paraffin oil up to above 74.5%, 66.8%, 64.4%, and 47.8% of oil sorption capacity of raw fibre, respectively, while the sorption capacities of PBMA-coated fibre for gasoline, diesel, soybean oil, and paraffin oil reach were about 59.5, 64.9, 83.2, and 80.3 g/g, respectively. PS-treated fibre shows similar oil sorption capacities as PBMA-coated fibre with sorption capacities of 62.3, 67.8, 80.3, and 83.3 g/g for the above four cited oils. The recovered coated fibre, after vacuum filtration, can be used for several cycles without a noticeable loss in oil sorption capacity.

Wang et al. [44] designed a new kind of oil sorbent system based on kapok fibre coated with a mixture of PBMA and hydrophobic silica ($SiO_2$) (Figure 5.3).

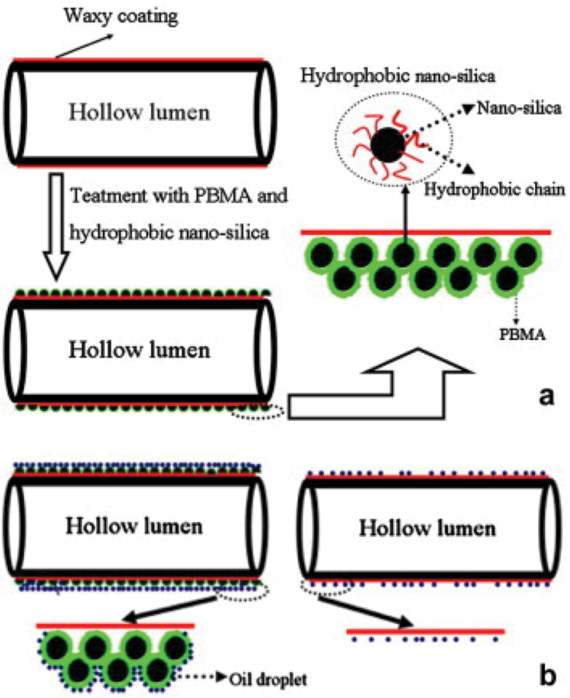
Waxy coating
Hollow lumen
Hydrophobic nano-silica
Nano-silica
Hydrophobic chain
Teatment with PBMA and hydrophobic nano-silica
PBMA
Hollow lumen
a
Hollow lumen
Hollow lumen
Oil droplet
b

**Figure 5.3:** (a) Schematic representation of the transition from raw fibre to coated kapok fibre and (b) schematic mechanism of an oil droplet on the surface of raw and coated kapok fibre (reprinted with permission from [44]).

Coated fibre showed higher oil sorption capacity than raw one in an oil/water mixture. Six types of oils, namely gasoline, diesel, soybean oil, crude oil, 150SN, and 20cst, were used to evaluate the oil sorption capabilities. The modified kapok fibre showed to possess higher performance compared to raw ones (diesel 64.5 g/g, soybean oil 87.7 g/g, crude oil 68.3 g/g, 150SN 77.9 g/g, and 20cst 82.3 g/g). These results could be ascribed to the rougher surface of the modified fibres with low surface energy can effectively prevent the oil from escaping. More than 92% of oil can be recovered from coated fibre assembly by vacuum filtration and no great loss of oil sorption capacity was observed after six cycles of sorption/desorption proving the high performances of the modified kapok fibres as a promising oil-absorbing material.

Wang et al. [45] fabricated superhydrophobic and oleophilic oil sorbent based on silica nanoparticles onto kapok fibre via sol–gel method using tetraethylorthosilicate as the precursor and subsequent hydrophobic modification using hydrolysed dodecyltrimethoxysilane (Figure 5.4).

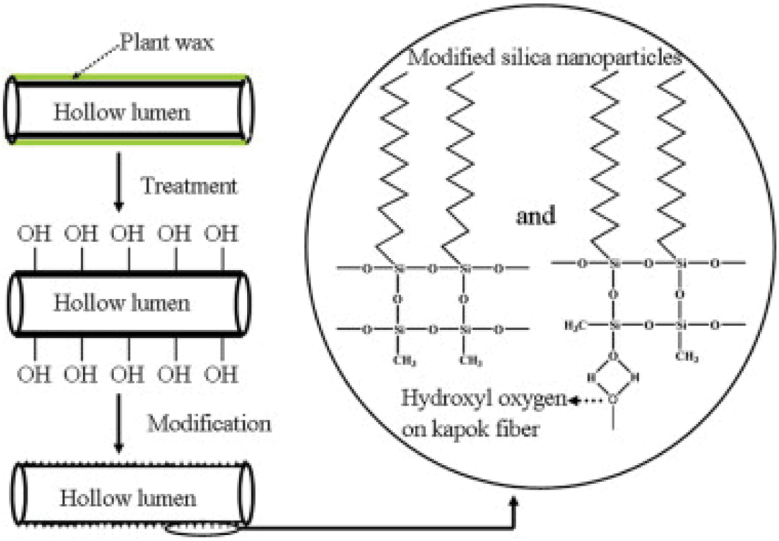

**Figure 5.4:** Schematic representation of the transition from raw kapok fibre to superhydrophobic kapok fibre (reprinted with permission from [45]).

The modified fibre exhibited good oil/water selectivity in the clean-up of oil over water. Moreover, they were able to absorb diesel and soybean oil up to above 46.9 and 58.8 g/g, with an improvement in oil sorption capacity to 46.6% and 20.2% compared with raw fibre, respectively. Owing to the high oil sorption capacity, the produced oil sorbent can be considered as a promising alternative for cleaning up the spilt oil. A comparison between the performances of the oil adsorption capacity of natural fibres is reported in Table 5.2.

**Table 5.2:** Comparison of oil adsorption capacity ($q_{\max}$) of different natural fibre-based adsorbents.

| Adsorbent | Oil | $q_{\max}$ (mg/g) | References |
|---|---|---|---|
| *Populus* seed | Heavy oil | 211 | [39] |
| *Calotropis procera* | Crude oil | 103.9 | [41] |
| | Crude oil | 92 | [41] |
| | Crude oil | 99.2 | [41] |
| *Calotropis gigantea* | Different oils | 45–120 | [42] |
| Cattail | Motor oil | 12.98 | [46] |
| | Vegetable oil | 13.47 | [46] |
| Kapok fibres | Diesel oil | 63.4 | [43] |
| | Soybean oil | 83.1 | [43] |
| | Paraffin oil | 82.3 | [43] |
| Hemp fibre boards | Vegetable oil | 8.64 | [47] |
| Oil palm empty fruit bunch | Crude oil | 6.48 | [48] |
| Silkworm cocoon | Motor oil | 52 | [49] |
| | Vegetable oil | 60 | [49] |
| Kapok fibres | Motor oil | 25.10 | [50] |
| | Diesel oil | 23.72 | [50] |
| Pomelo peel | Lubricating oil | 27 | [51] |
| 4,4′-Diphenylmethane diisocyanate-functionalized cellulosefibre | Gasoline | 214 | [52] |

### 5.2.3 Metal ions

With the rapid development of industries such as metal plating facilities, mining operations, fertilizer industries, tanneries, batteries, paper industries, and pesticides, heavy metalions are present in wastewater even at high concentrations. Since they are not biodegradable like organic pollutants in water, they tend to accumulate in living organisms [53]. They attracted more attention due to their toxicity and persistence in nature. Toxic heavy metal ions of particular concern include zinc, copper, nickel, mercury, cadmium, lead, and chromium. The long-term exposure of humans to high concentrations of some ions could cause serious health problems (damage to the circulation, immune and reproductive system, liver failure, diabetes, and irritation of the central nervous system) [54].

Among the tested adsorbent systems, lignocellulose biomass is explored as a novel biosorbent for the remediation of water contaminated with heavy metal ions [2, 55]. To enhance the adsorption performance, the original lignocellulose biomass needs to be chemically modified [56] through the introduction of different functionalities [57]. Often, some characteristic functional groups such as nitrous acid ester and carboxylic groups allow for achieving the adsorption of metal ions. The following section summarizes the principal use of natural fibre-based systems, raw, and modified for the removal of metal ions from wastewater.

### 5.2.3.1 Corn fibres

Corn fibres constitute lignin and cellulose and possess a large number of oxygen-containing functional groups, such as hydroxyl groups, carboxyl, and carbonyl on the surface. To improve the adsorption capacity, chemical modifications are needed. For example, corn fibres have been modified by Jiang et al. [58] with diluted nitric acid and applied for removing $Cu^{2+}$, $Co^{2+}$, and $Ni^{2+}$ from water. The main idea is to convert its abundant hydroxy groups into nitrous acid ester ($–O–NO_2$) groups which have a high affinity for metal ions, therefore enhancing the adsorption capacity according to the reaction shown below:

$$R - OH + HNO_3 = R - ONO_2 + H_2O$$

The increase in oxygen-containing functional groups on the surface is beneficial to the adsorption. The maximum adsorption capacities of $Cu^{2+}$, $Co^{2+}$, and $Ni^{2+}$ on $HNO_3$– corn fibres were 96.15 mg/g, 90.09 mg/g, and 76.92 mg/g, respectively. The study of the adsorption mechanism reveals the role of electrostatic attraction and coordination interaction for the adsorption of $Cu^{2+}$, $Co^{2+}$, and $Ni^{2+}$ by modified corn fibres (Figure 5.5) [58]:

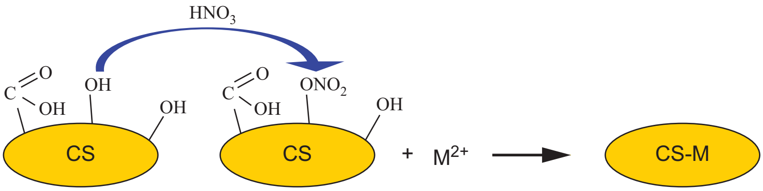

**Figure 5.5:** Schematic diagram of corn fibres modification and adsorption of $Cu^{2+}$, $Co^{2+}$, and $Ni^{2+}$ onto $HNO_3$-modified corn fibres (reprinted with permission from [58]).

### 5.2.3.2 Kapok fibres

Futalan et al. [59] proposed a review of the application of kapok fibres as adsorbents of metal ions.

Kapok (*Ceiba pentandra* L.) contains cellulose, hemicellulose, lignin, pectin, and wax with a two-layer structure (cellulose microfibrils (outer layer) and fibre axis (internal layer)) along with a small amount of waxy coating onto the surface which make them highly hydrophobic [60–62]. Kapok is usually pre-treated to alter its surface properties [63]. Different treatments have been proposed such as treating with a mixture of $NaClO_2$ and glacial acetic acid before mercury ion removal from the aqueous system [64], in situ oxidative polymerization technique to coat kapok with polyaniline for methyl orange and copper adsorption [31], polyacrylonitrile (PAN)-coated kapok fibres for the adsorption of copper [30], dopamine-coated kapok via self-polymerization for the adsorption of mercury [65], chemically modified kapok with diethylenetriamine penta-acetic acid to remove metal ions, that is, lead, cadmium, and copper from aqueous solution [66] and kapok fibre combined with polyaniline to obtain an adsorbent via in situ rapid polymerization of aniline for the removal of hexavalent chromium [67].

### 5.2.3.3 Jute fibres

JF, being rich in cellulose, can be modified through grafting with functional groups to enhance heavy metal removal after a pre-treatment process necessary to improve the accessibility of hydroxyl groups in the cellulose domains. There are very few works on graft modification of JF for adsorption towards heavy metal ions with low sorption capacities (e.g. only 8.4 mg/g for Cu(II) [68]). Shukla et al. [68] proposed the oxidation of JF with hydrogen peroxide to oxidize the hydroxyl groups of cellulose in JF to carboxyl groups, thus creating a weak cationic ion exchanger. The modified JF showed improved adsorption capacity compared to unmodified fibres ($q_t$ ($Cu^{2+}$) about 7 mg/g and $q_t$ ($Ni^{2+}$) about 5 mg/g). The metal ion adsorption on oxidized jute could be due to the ion exchange mechanism as expressed by the following mechanism:

$$2\text{Jute} - \text{COONa} + \text{M}^{2+} \rightarrow (\text{Jute} - \text{COO})_2\text{M} + 2\text{Na}^{+}$$

Du et al. [56] fabricated carboxyl-modified JF under a microwave heating process evaluating its adsorption properties towards Pb(II), Cd(II), and Cu(II) ions from aqueous solutions. More carboxylic groups were quickly introduced on the NaOH-pretreated jute surface via the formation of ester functions following microwave heating in presence of pyromellitic dianhydride (Figure 5.6).

The presence of –C=O groups (1,726 $cm^{-1}$) and the absence of the –OH band (1,338 $cm^{-1}$) in FTIR spectra prove the functionalization of JF. The adsorption performances have been evaluated by testing different pHs. The maximum adsorption capacity on Pb(II), Cd(II), and Cu(II) (155, 82, and 43 mg/g, respectively) occurred when pH was 6 while the $q_t$ values at 298 K were 157.21, 87.72, and 44.44 mg/g for Pb(II), Cd(II), and Cu(II). The enhanced metal ion adsorption capacity of the designed system may be attributed to the introduction of more single-bond COOH groups on the jute

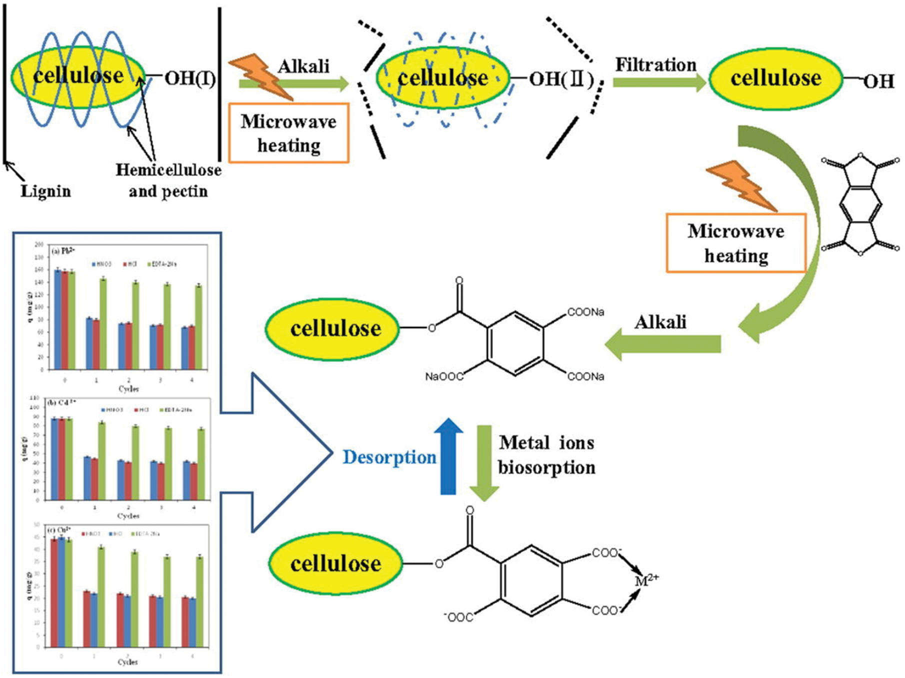
cellulose
OH(I)
Lignin
Hemicellulose and pectin
Alkali
Microwave heating
cellulose
OH(II)
Filtration
cellulose
OH
Microwave heating
Alkali
cellulose
COONa
NaOOC
COONa
Desorption
Metal ions biosorption
cellulose
COO⁻
M2+
COO⁻
⁻OOC
(a) Pb2+
(b) Cd2+
(c) Cu2+
HNO3
HCl
EDTA-2Na
Cycles
q (mg/g)

**Figure 5.6:** Scheme of jute fibre modification as proposed by Du et al. (reprinted with permission from [56]).

surface, and ion exchange could be considered the main mechanism of ions removal. Considering the main existing forms of these heavy metal ions in the aqueous solution, the probable adsorption mechanism can be expressed as

$$2(\mathrm{R-COONa}) + \mathrm{M}^{2+} \rightarrow (\mathrm{R-COO})_2\mathrm{M} + 2\mathrm{Na}^{+}$$

$$\mathrm{R-COONa} + \mathrm{MOH}^{+} \rightarrow (\mathrm{R-COO})\mathrm{MOH} + \mathrm{Na}^{+}$$

where R is the basic structure of JF and M is the metal.

### 5.2.3.4 Other natural fibres based adsorbents

Eftekari et al. [69] demonstrated the superior performance of milkweed fibres for the removal of $\mathrm{Pb}^{2+}$ ions from wastewater over $\mathrm{Ni}^{2+}$ ions. The results also revealed that the removal percentage of $\mathrm{Ni}^{2+}$ ions reached the value of 65.58% at a contact time of 60 min while the $\mathrm{Pb}^{2+}$ ions removal percentage was as high as 96.16% at a contact time of 90 min.

Wool fibres were modified by graft copolymerization with ethylacrylate using potassium persulphate and Mohr’s salt redox initiator system. The system was applied for metal ion uptake ($\mathrm{Cu}^{2+}$, $\mathrm{Hg}^{2+}$, and $\mathrm{Ni}^{2+}$). The maximum adsorption capacity for $\mathrm{Cu}^{2+}$

was higher than the values found for $Hg^{2+}$ and $Ni^{2+}$, showing the following order: $Cu^{2+}$ (142.5 mg/g) > $Hg^{2+}$ (49.33 mg/g) > $Ni^{2+}$ (46.7 mg/g) [70].

*Bombyx mori* silk, a protein fibre, is amphoteric in nature since it possesses ionizable groups on the side chain of various amino acid residues making them able to bind other charged molecules such as metal ions [71]. Silk fabrics were modified by treatment with tannic acid (TA) solution or by acylation with ethylenediamine tetraacetic (EDTA) dianhydride. The absorption of metal cations ($Ag^+$, $Cu^{2+}$) by untreated and modified silk fabrics was studied as a function of the kind of modifying agent, weight gain, and pH of the metal solution. Modification with TA or acylation with EDTA-dianhydride led to low changes in the absorption of copper ions as a function of weight gain. In basic conditions, the absorption of $Ag^+$ by silk acylated with EDTA-dianhydride remained somewhat lower than that of the divalent cation over the entire weight gain range studied. On the other hand, loading with tannic acid resulted in a sharp increase in the absorption of $Ag^+$. Finally, as far as pH is concerned, the acylation with EDTA-dianhydride enabled silk to absorb and bind metal cations even in the acidic and neutral pH range, where tannic acid had no effect [72].

Further systems concern the radiation-induced emulsion graft polymerization of glycidyl methacrylate (GMA) onto a nonwoven cotton fabric and subsequent chemical modification as adsorbent of mercury [73], grafted JF with acrylic acid by gamma irradiation for toxic heavy metalions [74], alkali-treated banana fibres grafted with GMA, and modified with Schiff base [75] and base-treated juniper fibre for cadmium sorption [76]. A summary of the natural fibre-based adsorbent for heavy metal ions removal is reported in Table 5.3.

**Table 5.3:** Comparison of maximum adsorption capacity ($q_{max}$) of different fibre-based adsorbents towards metal ions.

| Adsorbent | Metal ion | $q_{max}$ (mg/g) | References |
|---|---|---|---|
| Nitric acid-modified corn fibres | $Cu^{2+}$ | 96.15 | [58] |
| | $Co^{2+}$ | 90.09 | [58] |
| | $Ni^{2+}$ | 76.92 | [58] |
| Polyaniline-coated kapok fibres | $Cu^{2+}$ | 81.04 | [31] |
| Polyacrylonitrile-coated kapok fibres | $Cu^{2+}$ | 90.09 | [30] |
| Dopamine-coated kapok fibres | $Hg^{2+}$ | 235.7 | [65] |
| NaOH-modified kapok fibres | $Pb^{2+}$ | 23.40 | [62] |
| $NAClO_2$-modified kapok fibres | $Pb^{2+}$ | 34.63 | [62] |

**Table 5.3** (continued)

| Adsorbent | Metal ion | $q_{max}$ (mg/g) | References |
|---|---|---|---|
| Lyocell fibre modified through xanthation | $Pb^{2+}$ | 531.29 | [77] |
| | $Cd^{2+}$ | 505.64 | [77] |
| | $Cu^{2+}$ | 123.08 | [77] |
| Butyl acrylate grafting banana fibre cellulose | $Pb^{2+}$ | 209.09 | [78] |
| Imidazole-functionalized polymer graft banana fibre | $Pb^{2+}$ | 276.24 | [79] |
| | $Zn^{2+}$ | 101.52 | [79] |
| | $Cu^{2+}$ | 81.97 | [79] |
| Cellulose grafted with acrylonitrile monomer | $Cr^{6+}$ | 371.96 | [80] |
| Base-treated juniper fibre | $Cd^{2+}$ | 29.5 | [76] |
| Alkali-treated kenaf fibres | $Cu^{2+}$ | 0.38 (mmol/g) | [81] |
| Kenaf fibres/chitosan | $Ni^{2+}$ | 70.55 | [82] |
| Kenaf fibres | $Pb^{2+}$ | 50 | [83] |
| | $Cu^{2+}$ | 33.56 | [83] |
| | $Zn^{2+}$ | 13.68 | [83] |
| Thiol-modified cellulose nanofibrous composite | $Cr^{6+}$ | 87.5 | [84] |
| | $Pb^{2+}$ | 137.7 | [84] |
| 2-Hydroxyl methacrylate phosphoric acid monomer onto kenaf fibres | Th | 49.5 | [85] |
| Kapok fibre-oriented polyaniline nanofibres | $Cr^{6+}$ | 65.66 | [67] |

## 5.2.4 Inorganic ions

Wastewater derived from industrial processes may contain toxic substances such as inorganic ions.

The contamination of water sources could be mainly caused by some inorganic species such as heavy metal ions and fluoride ($F^-$). These contaminants are particularly hazardous since their high stability in the environment. Moreover, they can have adverse effects on human health (acute and chronic diseases) [86]. For example, high concentrations of fluoride occur naturally in the groundwater causing one of the main problems to be addressed in the treatment of drinking water. At high levels in drinking water, it can cause both dental and skeletal fluorosis [87]. Other pollutants could be constituted by phosphate ions (organically bound phosphates, soluble orthophosphates, and polyphosphates) [88]. The presence of phosphates in water bodies represents an environmental problem in the inducement of eutrophication, leading to the propagation of aquatic plants, algal growth, and the depletion of dissolved oxygen [89]. Arsenic (As), which could exist as inorganic forms of As(V), As(III), and organic compounds like arsanilic acid and roxarsone in the water environment [90], is one of the most hazardous contaminants in water environment, as it is originated from natural sources like soils, rocks along with volcanic activity, and anthropogenic sources like wood preservatives, pesticides, pharmaceuticals, and pigment industries [91]. Several processes have been applied for the removal of these ions from water and wastewater; however, most of them do not allow for obtaining adequate levels [92]. To accomplish that, it is necessary to design novel cost-effective measures to remove them [93]. Bioadsorbents with appropriate surface modification are known to be able to bind anions in water and, therefore, could be used for removing anionic pollutants such as orthophosphate or arsenate [94] since the presence of functional groups such as hydroxyl, carbonyl, amine, amide, carboxyl, sulfhydryl, imidazole, phosphonate, and phosphodiester [95].

For example, Eberhardt et al. [93] fabricated refined aspen wood fibre treated with ferrous chloride solution for phosphate removal. To obtain a high number of surface sites for iron complex formation, thereby improving the sorption of phosphate, a non-toxic anionic polymer carboxymethyl cellulose was used. The uptake capacities of the fabricated system and Fe-treated fibres were 4.3 and 1.8 mg/g, respectively.

Shin et al. [96] introduced lanthanum into juniper bark fibre, an organic substrate, to develop an inorganic/organic hybrid adsorbent through ion exchange with calcium. Sorption capacities of orthophosphates as a function of initial lanthanum loading varied from 0.211 to 0.351 mmol of P/g.

Other similar systems concern the use of Fe-based metal-organic frameworks (MOFs) decorated on cotton fibres via both post-synthetic method and in situ growth method for the removal of arsenic-based compounds [90], hyperbranched polyethylenimine-modified cellulosefibre as an effective biosorbent for the removal of inorganic arsenic and cellulose fibres modified by poly(*N*,*N*-dimethyl aminoethyl methacrylate) for the removal of fluoride and arsenic [97]. Table 5.4 summarizes some works regarding the use of modified natural fibres for inorganic ions removal.

## 5.2.5 Pesticides

Nowadays, the growing demand for food and the need to control a variety of new pests have led to increased production and consumption of pesticides. Since that, their presence in soil, water, and the entry into the food chain is a great concern [104]. For example, organochlorines and organophosphates are harmful insecticides, which could have a role in the inhibition of the acetylcholinesterase enzyme necessary for impulse

**Table 5.4:** Modified natural fibre systems for the removal of inorganic ions.

| Adsorbent | Removed substances | $q_{max}$ (mg/g) | References |
|---|---|---|---|
| Iron-wood fibres | Phosphate | 1.8 | [93] |
| Carboxymethyl cellulose/iron-treated wood fibres | Phosphate | 4.3 | [93] |
| Pentaethylenehexamine-functionalized cotton linter | Phosphate | 152.44 | [98] |
| Carboxymethylated bagasse fibres doped with iron ions | Phosphate | 152 | [99] |
| Hyperbranched polyethylenimine-modified cellulosefibre | As(III) | 54.13 | [100] |
| | As(V) | 99.35 | [100] |
| Poly(*N*,*N*-dimethyl aminoethyl methacrylate)-modified cellulose fibres | $F^-$ | 8.59 | [97] |
| | As(III) | 8.96 | [97] |
| | As(V) | 27.93 | [97] |
| Aluminium-impregnated coconut fibre ash | $F^-$ | 3.19 | [95] |
| Zirconium (IV) impregnated collagen fibre | $F^-$ | 2.70 mmol/g | [101] |
| Fluorescent-modified cellulose | $F^-$ | 7.5 | [87] |
| Graft polymerization of *N*-vinyl-2-pyrrolidone onto polyethene-coated polypropylene skin-core fibres | Iodine | 1237.8 | [102] |
| *N*-(3-Chloro-2-hydroxypropyl) trimethyl ammonium chloride-modified kenaf fibres | $F^-$ | 13.98 | [103] |

transmission in the human nervous system [105]. To mitigate the problem of pesticide traces presence into waters, treatments based on physical, chemical, and/or biological processes have already been explored. Some works concerning the use of natural fibres as removal systems of pesticides have been reported in Table 5.5.

**Table 5.5:** Modified natural fibre systems for the removal of pesticides.

| Adsorbent | Removed substances | $q_{max}$ (mg/g) | References |
|---|---|---|---|
| *Luffa cylindrica* fibres | Methyl parathion | 54.88 | [104] |
| | Coumaphos | 62 | [104] |
| PEI-modified cotton | Pirimiphos-methyl | 454.6 | [106] |
| | Monocrotophos | 333.3 | [106] |

**Table 5.5** (continued)

| **Adsorbent** | **Removed substances** | **$q_{max}$ (mg/g)** | **References** |
|---|---|---|---|
| PEI-modified wool | Pirimiphos-methyl | 625 | [106] |
| | Monocrotophos | 500 | [106] |
| Jute fibre carbon | Monocrotophos | 39.8 | [107] |
| Aminated cotton fibres loaded with copper(II) ions | Linuron | 0.15 mmol/g | [108] |
| Diaminododecane/hexadecylamine-modified cellulosefibres | 2-Naphthol | 867 μmol/g | [109] |
| | Chlorobenzene | 397 μmol/g | [109] |
| | Dichlorobenzene | 394 μmol/g | [109] |
| | Trichlorobenzene | 887 μmol/g | [109] |
| | Nitrobenzene | 520 μmol/g | [109] |
| | Chlorophenol | 668 μmol/g | [109] |
| Cellulose fibres grafted with aliphatic anhydrides | Nitrobenzene | 146 μmol/g | [110] |
| | Quinoline | 330 μmol/g | [110] |
| | 2-Naphthol | 320 μmol/g | [110] |
| | 1,3,4-Trichlorobenzene | 470 μmol/g | [110] |
| Amine-functionalized cellulosefibre from *Juncus acutus* L. | Linuron | 61.8 | [111] |
| $MnO_2$/cellulosefibre | Toxaphene | 5.465 | [112] |

## 5.3 Synthetic fibres

Synthetic fibres including materials are known to be a good candidate for high absorption and recyclability capacity for the sorption of different pollutants [113, 114]. Their properties such as controlled intermolecular interactions and porosity make them good adsorbents [115]. In the last decades, different methodologies are to functionalize the surface of these fibres such as irradiation-induced grafting [116]. For example, different metal ion adsorbents can be prepared by introducing the chelating functional groups to polyethylene (PE) or polypropylene (PP) fibres. It is well accepted that metal ions such as Cu, Pb, Zn, and Fe can be immobilized by chelation with an N, O, or S donor-containing ligand groups which are covalently attached to a polymer matrix [117].

Liu et al. [116] fabricated *N*,*N*-dimethylaminoethyl methacrylate covalently bonded on a commercial polyethylene-coated PP skin-core structure fibre (PE/PP) in aqueous and MeOH/$H_2O$ solutions by a one-step green reaction using radiation-induced graft polymerization. Grafting yield was correlated to the absorbed dose and solvent system. The fibre with a degree of grafting of 51.6% exhibited good adsorption capacity of Au(III) ions over a large range of concentrations (from 10 to 2.5 g/L) in both batch and flow-through adsorption tests with a maximum capacity of 949.3 mg/g and good reusability.

Kavakli et al. [118] produced *N*,*N*-dimethylaminoethyl methacrylate (DMAEMA)-grafted polyethylene/polypropylene (PE/PP) through radiation-induced graft polymerization as an adsorbent of As. The effect of some parameters such as pH, contact time, initial As(V) ion concentration, and coexisting ions was investigated through batch adsorption experiments. The adsorption of As(V) by QDMAEMA-*g*-PE/PP fibres was found to be not dependent on pH in the range of 4.00–10.00. Kinetic experiments demonstrated that the sorption data followed the pseudo-second-order kinetic model. The maximum adsorption capacity was found to be 83.33 mg As(V)/g polymer at pH 7.00.

Huang et al. [119] proposed a novel nanofibre composite hydrogel prepared by a combination of alginate, acrylic acid, and 1D titania ($TiO_2$) nanofibres prepared by the sol–gel electrospinning technique which provided a support skeleton for the formation of the 3D network of the nanofibre composite hydrogel. The high porosity and good structural stability made the produced hydrogel an efficient adsorbent for the removal of $Cd^{2+}$. The adsorption capacity of $Cd^{2+}$ on the nanofibre composite hydrogel was negligible at $pH < 2.0$ while it increased with increasing pH in the range of 2–7 (22 mg/g). The $q_{\max}$ of $Cd^{2+}$ was 76.92 mg/g at 293 K. Finally, the adsorption rate decreased from 39.75% to 38.11% after experiencing five cycles.

Other systems concern the amine-type adsorbents by radiation-induced graft polymerization for the sorption of $Cu^{2+}$ and $Pb^{2+}$ [117], amidoximated ultra-high–molecular-weight polyethylene fibre for uranium adsorption[120], methacrylic acid, and 2-hydroxyethyl methacrylate co-grafted with acrylonitrile onto polyethylene fibre for uranium adsorption [121], grafting amidoxime onto high-surface-area polyethylene fibres for uranium removal [122], macroporous fibrous polymeric adsorbent-containing amidoxime chelating functional group for uranium ions removal [123], high-surface-area polyethylene-fibre adsorbent developed by radiation-induced graft polymerization of acrylonitrile and itaconic acid for uranium removal [124], irradiated and amidoximated PAN fibres [125], and polyacrylamidoxime fibre for uranium removal [126]. Table 5.6 gathers some works concerning the use of synthetic fibres for the removal of different substances.

**Table 5.6:** Synthetic fibre-based systems for the removal of different pollutants.

| Adsorbent | Removed substances | $q_{max}$ (mg/g) | References |
|---|---|---|---|
| Methacrylic acid-*g*-poly(ethylene terephthalate) fibre reacting with tetraethylene pentamine | Congo red | 21 | [127] |
| Amide and amine-functionalized PET fibres | Congo red | 46.50 | [128] |
| *N*-Oxide-4-vinyl pyridine-*g*-poly(ethylene terephthalate) fibres | Methylene blue | 35.10 | [129] |
| Phenolate-immobilized polyacrylonitrile fibres | Brilliant cresyl blue | 890.10 | [130] |
| Sodium alginate-polyaniline nanofibres | $Cr^{6+}$ | 73.34 | [131] |
| Amidoxime-functionalized fibrous polyacrylonitrile | $Cr^{6+}$ | 250.71 | [132] |
| Polypyrrole-polyaniline nanofibres | $Cr^{6+}$ | 227 | [133] |
| Polyaniline/sepiolite nanofibres | $Cr^{6+}$ | 206.6 | [134] |
| Polyaniline nanowire/tubes | $Cr^{6+}$ | 1.67 (mmol/g) | [135] |
| Double amidoxime-containing chelating poly (ethyleneterepthalate) fibres | $Cr^{6+}$ | 125 | [136] |
| Manganese oxide nanofibres | $Cr^{6+}$ | 14.6 | [137] |
| Hydrolysed polyacrylonitrile fibres | $Cu^{2+}$ | 26.94 | [138] |
| Amidoximated ultra-high-molecular-weight polyethylene fibres | Uranium | 4.54 | [120] |
| *N*-Vinyl-2-pyrrolidone-modified polyethylene-coated polypropylene skin-core fibres | Iodine | 1,237.8 | [102] |
| Alginate, acrylic acid, and titania nanofibres hydrogel | $Cd^{2+}$ | 76.92 | [119] |
| Cellulose acetate/zeolite composite fibres | $Cu^{2+}$ | 28.57 | [139] |
| | $Ni^{2+}$ | 16.95 | [139] |

## 5.4 Fibre systems produced by electrospinning

Nowadays, the fast filtration process has attracted interest as a practical process for the purification of wastewater. The process usually requires a small amount of material and little post-treatment of the membrane, thus making this a more environmentally friendly technique [140]. To achieve that, electrospun nanofibrous systems appeared to be an effective solution for fast dynamic filtration. Electrospinning is a relatively simple methodology applied in the production of polymer fibre mats at the nano- and microscale [141]. The process is based on the production of an electrostatically driven jet of polymer solution (or polymer melt), emitted from the apex of a cone formed on the surface of a droplet of polymer. During the transit towards the collector, it solidifies leaving behind a polymer fibre to be collected. The synthetic and natural fibres are mainly processed by electrospinning which allows for fabricating micro and nanofibres with a high surface area, controlled porosity [142], and morphology. All these characteristics are advantageous for the functionalization or incorporation of additives to improve their adsorption properties [143, 144]. Owing to their remarkable feature, various electrospinning-based nanofibre adsorbents, such as single or composite inorganic nanofibres, functionalized organic nanofibres, and inorganic/organic composite nanofibres, have been investigated for treating wastewater pollution [145]. The introduction of specific functional groups onto the electrospun nanofibres was already reported for the removal/adsorption of specific materials from waste/aqueous solutions [146]. For example, the immobilization of phenolate groups in PAN fibres favours the removal of cationic dyes [130], the incorporation of NiO and ZnO in electrospun fibres favours the removal of anionic species [147], while porous membranes of poly(vinyl alcohol) and chitosan are potential candidates for the removal of direct red 80 [148].

Moreover, the electrospun fibre mats are even employed for the sorption of oil spills of the possibility of obtaining superhydrophobic structures as filtrating membranes at the water/oil interface (nanoporous electrospun fibres of PS for oil spill clean-up [149] or PAN electrospun fibres modified with dopamine for the removal of motor oil and diesel fuel [150]). By adding the required properties, electrospun systems could even be applied in the removal of metal ions. The modification of electrospun fibres of PS with the incorporation of titanium dioxide nanoparticles during the electrospinning procedure [151] is a simple strategy for the adsorption capacity for $Cu^{2+}$ ions or PAN/graphene oxide nanofibres for the adsorption capacity of Cr(VI) [152].

Wang et al. [153] fabricated calcium cross-linked sodium alginate nanofibres (SA-Ca) using low-cost materials via a low energy consumption process. The solutions of SA/PEO (w/w, 7/3) were directly used for electrospinning (Figure 5.7) obtaining a porous network structure with the average diameter and specific surface area equal to 129.6 nm and 3.409 $m^2/g$, respectively.

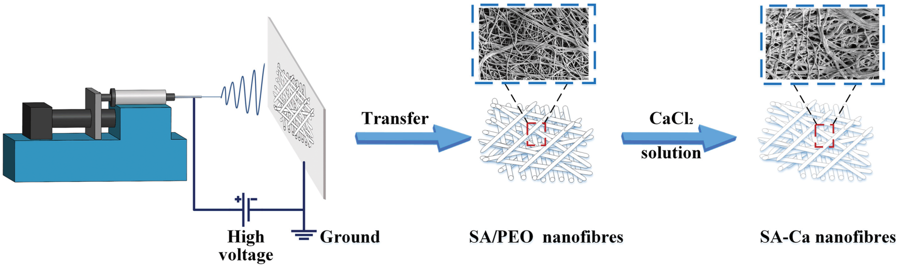

**Figure 5.7:** Schematic illustration of the fabrication of SA-Ca (reprinted with permission from [153]).

The SA-Ca nanofibres showed a high adsorption performance towards Cu(II) with an adsorption capacity of 285.5 mg/g. More importantly, SA-Ca can be regenerated using $CaCl_2$/HCl solutions based on the ion-exchange mechanism without destroying the morphology of the nanofibres. Furthermore, a low concentration of Cu(II) (10 mg/L) and other heavy metal ions [Pb(II) and Cd(II), each 10 mg/L] were successfully removed from the water, demonstrating the great application prospects in the removal of heavy metal ions. Various similar adsorbents have been developed for the removal of Cu(II) including calcium cross-linked alginate nanofibres [154], SA/GO composite fibres [155], and poly(acrylic acid)-SA nanofibrous hydrogels [156].

Li et al. [157] designed a regenerable spiral wound module of affinitive electrospun chitosan nanofibre membranes for removing Cr(VI) from contaminated water. The produced systems were cross-linked by glutaraldehyde vapour. The effect of flow rate, initial Cr(VI) concentration, chitosan nanofibre deposition density, and other metal ions on Cr(VI) adsorption was investigated in detail. The module was able to remove all the metal ions in the order of Cr(VI) > Cu(II) > Cd(II) > Pb(II). The adsorption capacity at a breakthrough point is 7.56, 3.36, 3.35, and 2.43 mg/g, respectively. In addition, compared with commercial NF membranes, the fibrous chitosan membrane had much higher Cr(VI) rejection and permeate flux, while creating no concentrated water and very small transmembrane pressure.

Efome et al. [140] fabricated Fe(III)- and Zr(IV)-based MOFs enmeshed in PAN and polyvinylidene fluoride (PVDF) electrospun nanofibre. The pristine MOFs showed high adsorption capacity for lead ions and mercury ions from aqueous solutions. The PAN-Fe bases MOF showed a $q_{\max}$ = 53.09 mg/g and 30.19 mg/g while the PAN-Zr-based MOF possesses a $q_{\max}$ = 50.88 mg/g and 23.98 mg/g for $Hg^{2+}$ and $Pb^{2+}$, respectively. The adsorption capacity of PVDF-based NMOM was found to be low. The excellent filtration performance and regenerability of the membrane coupled with the hydrostability of the MOFs suggest that the electrospun systems have the potential for water treatment through the process of membrane adsorption.

Wang et al. [158] produced zeolitic imidazolate framework-8 (ZIF-8)-based hybrid nanofibrous PAN film while poly(sodium 4-styrene sulfonate) was added to improve the stability of the hybrid film (Figure 5.8). ZIF-8, a microporous material, was in situ loaded on the PAN film by a simple strategy for heavy metal removal.

The added poly(sodium 4-styrenesulfonate) could facilitate the loading of $Zn^{2+}$ in the presence of sulfonic groups. Different parameters were considered and optimized: 1-h hydrolysis time, a two-layer film, and a 0.3 wt.% of PSS were considered as the optimum conditions. The film that was fabricated under optimum conditions was applied to remove lead from the water showing a high removal efficiency of 99.5%. In addition, this process showed a high permeation flux of 180 L/($m^2$·h·psi).

Li et al. [159] produced a novel branched polyethylenimine (bPEI)-grafted electrospun PAN fibre membrane for Cr(VI) remediation (Figure 5.9).

The experiments demonstrated that the bPEI-grafted electrospun PAN fibre adsorbent possessed an excellent adsorption capacity towards Cr(VI) ($q_{\max}$ = 637.46 mg/g),

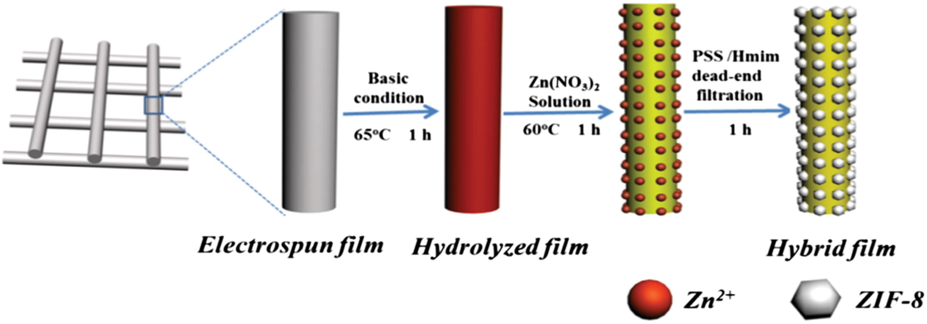
Basic condition
65°C 1 h
Zn(NO₃)₂ Solution
60°C 1 h
PSS /Hmim dead-end filtration
1 h
Electrospun film
Hydrolyzed film
Hybrid film
Zn²⁺
ZIF-8

**Figure 5.8:** Preparation of PAN-ZIF8 electrospun membranes (reprinted with permission from [158]).

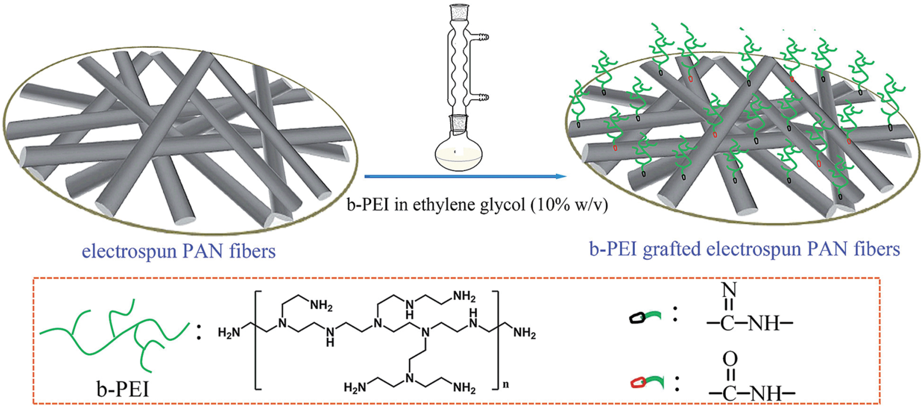
b-PEI in ethylene glycol (10% w/v)
electrospun PAN fibers
b-PEI grafted electrospun PAN fibers
b-PEI
H₂N
NH₂
N
H
n
–C–NH–
O

**Figure 5.9:** Schematic diagram of the synthesis of bPEI-grafted electrospun PAN fibres (reprinted with permission from [159]).

which was higher than many other adsorbents. The improved performance for Cr(VI) remediation is attributed to both the abundant amine groups on the adsorbent's surface and the electrospun fibrous structure. Moreover, the batch adsorption and dynamic filtration could also make the Cr(VI) concentration notably decrease from 10 or 5 mg/L to below 0.05 mg/L, which is recommended as the drinking water standard. Finally, the results showed that the adsorption is mainly based on the formation of electrostatic attractions.

Zhu et al. [160] fabricated a novel oil sorbent based on polyvinyl chloride (PVC)/PS fibre prepared by an electrospinning process. The sorption capacity, oil/water selectivity, and sorption mechanism of the PVC/PS sorbent were studied. The results showed that the sorption capacities of the PVC/PS sorbent for motor oil, peanut oil, diesel, and ethylene glycol were 146, 119, 38, and 81 g/g, respectively. It was about five to nine times that of a commercial PP sorbent. The PVC/PS sorbent also had excellent oil/water selectivity (about 1,000 times) and high buoyancy in the clean-up of oil over water.

Table 5.7 reports some scientific works concerning the use of electrospun systems for the removal of different pollutants.

**Table 5.7:** Comparison of maximum adsorption capacity ($q_{max}$) of different electrospun fibre adsorbents.

| **Adsorbent** | **Removed substances** | **$q_{max}$ (mg/g)** | **References** |
|---|---|---|---|
| Boehmite NP-impregnated PCL fibre | $Cd^{2+}$ | 0.20 | [161] |
| Boehmite NP-impregnated Nylon 6 fibre | $Cd^{2+}$ | 0.21 | [161] |
| Polystyrene fibres | Diesel oil | 7.13 | [162] |
| | Silicon oil | 81.40 | [162] |
| | Peanut oil | 112.3 | [162] |
| | Motor oil | 131.6 | [162] |
| Polypropylene fibres | Motor oil | 129 | [33] |
| | Peanut oil | 80 | [33] |
| Polystyrene fibres | Motor oil | 84.41 | [163] |
| | Sunflower oil | 79.62 | [163] |
| Poly(acrylo-amidinoethylene amine) nanofibres | As(V) | 76.92 | [164] |
| Thioamide-group chelating polyacrylonitrile fibres | Au(III) | 34.60 (mmol/g at 348 K) | [146] |
| β-Cyclodextrin-based electrospun poly(acrylic acid) fibres | Methylene blue | 826.45 | [145] |
| Poly(vinyl alcohol)/chitosan | $Pb^{2+}$ | 266.12 | [165] |
| | $Cd^{2+}$ | 148.78 | [165] |
| PEO/chitosan nanofibres | $Ni^{2+}$ | 357.1 | [166] |
| | $Cu^{2+}$ | 310.2 | [166] |
| | $Cd^{2+}$ | 248.1 | [166] |
| | $Pb^{2+}$ | 237.2 | [166] |
| Vinyl-modified mesoporous poly(acrylic acid)/$SiO_2$ nanofibres | Malachite green | 220.49 | [167] |
| Cellulose acetate/titanium oxide | $Pb^{2+}$ | 31.9 | [168] |
| | $Cu^{2+}$ | 31.4 | [168] |

**Table 5.7** (continued)

| Adsorbent | Removed substances | $q_{max}$ (mg/g) | References |
|---|---|---|---|
| Ethylenediamine-grafted-polyacrylonitrile nanofibres | Methylene blue | 94.07 | [169] |
| | Safranin T | 110.62 | [169] |
| | Rhodamine B | 138.69 | [169] |
| Polydopamine-coated poly(vinyl alcohol)/poly(acrylic acid) membranes | Methylene blue | 1147.6 | [170] |
| Poly(vinyl alcohol)/$SiO_2$ composite nanofibres | $Cu^{2+}$ | 504.89 | [171] |
| Nickel ferrite nanoparticles anchored onto silica nanofibres | Methylene blue | 1.279 | [172] |
| Amidoxime-modified polyacrylonitrile nanofibres | $Pb^{2+}$ | 263.45 | [173] |
| Chitosan nanofibres | $Pb^{2+}$ | 263.15 | [174] |
| | $Cu^{2+}$ | 485.44 | [174] |
| Wool keratose/silk fibroin | $Cu^{2+}$ | 2.88 | [175] |
| Polystyrene fibres | Motor oil | 113.87 | [149] |
| | Bean oil | 111.80 | [149] |
| | Sunflower seed oil | 96.89 | [149] |
| Chitosan/polyacrylonitrile/magnetic ZSM-5 nanofibres | Motor oil | 99.40 | [176] |
| | Lubricating oil | 95.30 | [176] |
| | Pump oil | 88.10 | [176] |
| Poly(vinylidene fluoride)/reduced graphene oxide/$TiO_2$ nanofibre | Oil | 98.46 | [177] |
| Magnetic poly(vinylidenefluoride)/$Fe_3O_4$ nanofibres | Oil | 35–46 | [178] |
| Cellulose acetate/poly(dimethyl diallyl ammonium chloride-acrylamide) nanofibrous membranes | Acid black 172 | 231 | [179] |
| Amidoxime-modified polyindole nanofibre | $Cr^{6+}$ | 404.86 | [180] |
| Diethylenetriamine-modified polyacrylonitrile fibres | $Cu^{2+}$ | 87.77 | [181] |
| Polydopamine–polyacrylonitrile fibres | Heavy motor | 148.58 | [150] |
| | Diesel fuel | 62.53 | [150] |

**Table 5.7** (continued)

| **Adsorbent** | **Removed substances** | **$q_{max}$ (mg/g)** | **References** |
|---|---|---|---|
| Polyacrylonitrile–polyamidoamine composite nanofibres | Direct red 80 | 1,666.66 | [182] |
| | Direct red 23 | 2,000 | [182] |
| Polyacrylonitrile/carbon nanotube/titanium dioxide | $Cr^{6+}$ | 527 | [183] |
| Polyester/polyacrylonitrile/GO/$Fe_3O_4$ | $Pb^{2+}$ | 799.4 | [184] |
| | $Cr^{6+}$ | 911.9 | [184] |
| Carboxymethylated and polydopamine-coated deacetylated cellulose acetate membrane | Methylene blue | 69.89 | [115] |
| | Congo red | 67.31 | [115] |
| Amidoxime-modified polyacrylonitrile nanofibres | $Cu^{2+}$ | 52.70 | [173] |
| | $Pb^{2+}$ | 263.45 | [173] |
| PVA/chitosan nanofibrous membrane | Direct red 80 | 790 | [148] |
| Polystyrene/$TiO_2$ composite nanofibre | $Cu^{2+}$ | 522 | [185] |
| Surface amidoxime-modified polyindole nanofibre | $Cr^{6+}$ | 340.14 | [186] |
| Polyacrylonitrile-CNT/$TiO_2$-$NH_2$ nanofibres | As(III) | 251 | [187] |
| | As(V) | 249 | [187] |
| Poly(acrylonitrile-*co*-maleic acid) | $Ni^{2+}$ | 243.2 | [188] |
| | $Cr^{6+}$ | 173.9 | [188] |
| Polystyrene–dithizone nanofibre | $Pb^{2+}$ | 0.016 | [189] |
| Polyacrylonitrile/polypyrrole nanofibre | $Cr^{6+}$ | 44.95 | [190] |
| Polyacrylonitrile/graphene oxide nanofibres | $Cr^{6+}$ | 382.5 | [152] |
| Polyacrylonitrile/y-AlOOH composite nanofibres | $Pb^{2+}$ | 233.10 | [191] |
| | $Cu^{2+}$ | 43.90 | [191] |
| | $Cd^{2+}$ | 144.30 | [191] |
| Poly(methyl methacrylate)/zeolite nanofibrous membranes | Methyl orange | 95.33 | [192] |
| Alginate/poly(ethylene oxide)-based nanofibrous membrane | Acid red 14 | 93 | [193] |
| | Basic blue 41 | 71 | [193] |

## 5.5 Fibre-based systems for the removal of organic substances through photocatalysis

In recent years, some substances such as pharmaceuticals, pesticides, hormones,organic acid, and personal care products have raised increasing concerns for their excessive consumption and potential threats to the ecosystem becoming emerging contaminants because of their latent risk and environmental persistence even at a low concentration [194]. For example, antibiotics could be responsible for long-term irreversible changes to micro-organism genomes [195]. Moreover, the difficulty in removing low concentrations of this kind of substance is prompting towards the application of novel methodologies such as advanced oxidation processes [196] to overcome the drawbacks of the conventional techniques. Photocatalytic oxidation, for example, can be considered a valuable process for air and water purification since the possibility of degrading organic pollutants without using chemicals to produce harmless products [197]. Up to now, many chalcogenide semiconductors such as $TiO_2$, ZnO, $ZrO_2$, CdS, $MoS_2$, $Fe_2O_3$, and $WO_3$ have been investigated as photocatalysts for the degradation of organic contaminants [198]. Sometimes, these compounds are incorporated into fibre-based systems to produce polymer-inorganic composite nanofibrous structures exploiting the advantages of polymers such as structural flexibility and lightweight with the advantages of inorganic materials (mechanical strength, high thermal stability, magnetic, optical, catalytically properties, etc.).

For example, Liu et al. [199] fabricated ZnO nanofibres starting from zinc acetate/cellulose acetate in mixed-solvent *N*,*N*-dimethylformamide/acetone by carrying out an electrospinning process.

The photo-degradations of dye molecules such as rhodamine B and acid fuchsin, under the irradiation of visible light catalysed by the ZnO nanofibre, were found to be 85% in 20 min for acid fuchsin while almost 90% of rhodamine B was degraded after 19 h.

Table 5.8 reports a summary of the main advanced fibre-based systems for the photocatalytic oxidation of the pollutant.

**Tab. 5.8:** Advanced fibre-based systems for photocatalytic oxidation of pollutants.

| Adsorbent | Pollutant | Photocatalytic activity | Referenes |
|---|---|---:|---:|
| N-Doped $TiO_2$ nanorods in regenerated cellulose | Methylene blue | 85% | [200] |
| $TiO_2$/cellulosic fibre | Paracetamol | 90 | [201] |
| ZnO-modified nylon 6,6 fibres | Rhodamine B | 93% | [202] |
| PVDF/titanium dioxide nanofibres | Bisphenol A | 84.53% | [197] |
| $TiO_2$@CNFs | Rhodamine B | 84.53% | [203] |
| Ag/$TiO_2$ | Methylene blue | 80 | [204] |

**Tab. 5.8** (continued)

| Adsorbent | Pollutant | Photocatalytic activity | Referenes |
|---|---|---|---|
| $BiVO_4/Bi_2S_3/MoS_2$ | Rhodamine B | 78 | [205] |
| Zn-doped $TiO_2$ basalt fibres | Rhodamine B | 60.45 | [206] |
| MIL-101(Fe)-decorated $TiO_2$-based junctions on carbon fibres | 17β-Oestradiol | 87.4 | [207] |
| | Tetracycline hydrochloride | 94.2 | [207] |
| $MoS_2$/CdS heterostructures on carbon fibres | Rhodamine B | 97.3 | [208] |
| | Tetracycline hydrochloride | 55.6 | [208] |
| | Hexavalent chromium | 68.4 | [208] |
| | Methylene blue | 97.3 | [208] |
| g-$C_3N_4$@Co-$TiO_2$ fibre | Tetracycline hydrochloride | 90.8 | [209] |
| g-$C_3N_4$@polyester/viscose | Tetracycline hydrochloride | 100 | [210] |
| Cotton fabrics/PDA/BiOBr | Rhodamine B | 98 | [211] |
| | Cr(VI) | 100 | [211] |
| Eu-$TiO_2$ nanocrystal-functionalized cotton | Methylene blue | 90 | [212] |
| N-carbon@N–ZnO nanofibre | 2,4-Dichlorophenol | 97 | [213] |
| $TiO_2/Ag_3PO_4$/carbon fibre | Phenol | 80.6 | [214] |
| Ag/$TiO_2$ nanofibre | Toluene | 93.4 | [215] |

## 5.6 Advanced carbon fibre materials

Activated carbon fibre belongs to a novel class of materials which could act as fibrous carbonaceous adsorbent since the excellent adsorptionproperties due to the small dimensions and concentrated pore size distribution. The carbonaceous fibres show some advantages in terms of hydrophobicity, great mechanical and physical properties, resistance to alkaline and acidic media, and structural stability even at high temperatures [216, 217]. In the last few years, this material has been widely used as a novel and efficient adsorbent for the purification of wastewater.

Li et al. [218] produced a carbon aerogel as methylene blue adsorbent prepared from abandoned cotton via a novel air-limited calcination method. The effect of calcination temperature and the loading weight of cotton on activity was studied. To the best, fabricated specimens showed a huge specific area (457.73 $m^2/g$). The adsorption properties of the as-prepared materials were evaluated by changing the experimental conditions (contact time and $T$). The maximum adsorption capacity of methylene blue decreased from 102.23 mg/g to 38.91 mg/g with the increase in the temperature from 298 to 338 K. Besides, the adsorption capacity increased with the increase of the initial concentration from 10 to 120 mg/L. The reusability test proved the efficiency of the carbon aerogel since, after five cycles, the adsorption capacities were quite high (54.3 mg/g) demonstrating that the designed system offered sustainability for the treatment of dye-containing wastewater.

Kang et al. [216] investigated the adsorption properties of commercial carbon fibres after acidic and basic treatments for the adsorption of copper and cadmium ions. The treatments led to a decrease in surface area. The performed tests highlighted that acidic pre-treatment produced many acidic groups on the surface while basic one decreased the number of carboxylic groups and increased the number of lactonic groups. The sorption capacity of $Cd^{2+}$ was about 35 mg/g after acid pre-treatment could be ascribed to an increase in the number of acidic-oxygenated functional groups and, after the basic treatment, the change of micropores led to a sorption capacity of 15 mg/g.

Tu et al. [219] reported the fabrication of sustainable oil-absorbing material, obtained through pyrolysis, by using *Calotropis gigantea* fibre with a hollow tubular structure as the starting raw material which was pre-treated with $NaClO_2$. The produced hollow carbon fibre demonstrated high performances as an adsorbent material for the removal and recovery of different oils in the industry. The big lumen was responsible for the high oil-absorbing capacity. Besides, the plant wax layer contributed to the

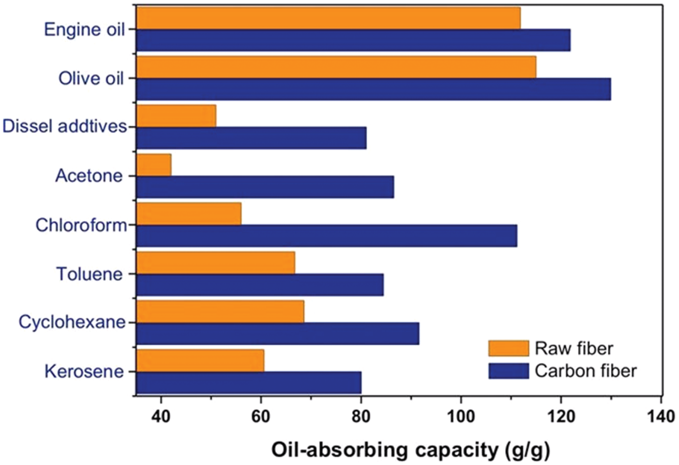

**Figure 5.10:** Absorption efficiency of carbon fibre for various model oils (reprinted with permission from [219]).

intrinsic hydrophobicity that made the fibre have a strong affinity to most organic solvents. Various substances have been tested such as kerosene, cyclohexane, toluene, chloroform, acetone, diesel fuel additives, olive oil, and engine oil (Figure 5.10).

It is evident that, compared with raw fibre, the carbon fibre exhibits a higher oil-absorbing capacity than all of the aforementioned model oils (80–130 times its weight up to 130 g/g). Reusability tests showed that the produced carbon fibres can be reused for more than 10 cycles proving the potentialities of the produced materials as a cost-effective and environmentally friendly oil-absorbing material. A similar adsorbent system for oil removal has been proposed by considering hollow carbon fibres derived from cotton [220] and carbon fibre aerogel from natural bamboo fibre [221].

Bi et al. [222] used cotton fibres to produce hydrophobic and porous aerogels based on twisted carbon fibres (TCF). The properties of the porous aerogel (hydrophobicity and mechanical resistance) make it an efficient adsorbent for the removal of pollutants such as oils and organic solvents such as commercial petroleum products fats, ketones, toluene, ethanol, and acetone (Figure 5.11).

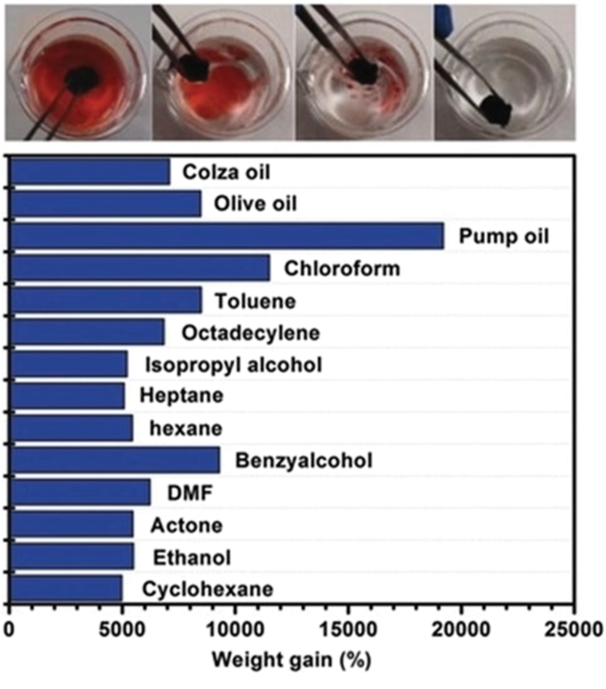

**Figure 5.11:** Sorption efficiency of the TCF aerogel for various organic liquids (reprinted with permission from [222]).

The produced adsorbent showed good sorption performances with a maximum sorption capacity of up to 192 times the weight of the neat TCF aerogel.

Table 5.9 reports a comparison of different carbon fibre-based adsorbents for the removal of organic dyes, metal ions, and inorganic ions.

**Table 5.9:** Comparison of maximum adsorption capacity of different carbon fibre-based adsorbents.

| Adsorbent | Removed substance | $q_{max}$ (mg/g) | References |
|---|---|---|---|
| Carbonaceous nanofibre membrane | Methylene blue | 818.6 | [223] |
|  | $Pb^{2+}$ | 423.7 | [223] |
|  | $Cr^{6+}$ | 221.3 | [223] |
| Nitric acid-oxidized carbon fibres from flax | $Cu^{2+}$ | 145 | [224] |
|  | $Co^{2+}$ | 72 | [224] |
| Magnetite-doped carbon fibres | As(V) | 4.18 | [217] |
| Zr NP-modified carbon fibres | As(V) | 21.74 | [225] |
| Activated carbon-jute fibres |  | 225.64 | [226] |
| Aluminium-impregnated hierarchal web of carbon fibres | $F^-$ | 3.47 | [227] |
| Carbon nanofibres/graphene oxide aerogel |  |  |  |
| Hybrid anion exchange/porous carbon fibres | $Cr^{6+}$ | 79.5 | [228] |
| Zirconium-based nanoparticle doped activated carbon fibres | As(V) | 21.7 | [229] |
| Carbon nanofibre–carbon nanotube membranes | $Cr^{6+}$ | 227 | [230] |
| Carbon fibres/NiO-ZnO nanocomposite fibres | Congo red | 613 | [147] |
| Mesoporous carbon nanofibres | Methylene blue | 119.21 | [231] |
|  | Methyl orange | 101.35 | [231] |
| Activated carbon fibre-supported titanate nanotubes | Methylene blue | 32.70 | [232] |

## 5.7 Conclusions

This chapter summarizes the use of advanced fibre systems for environmental applications by focusing on the removal of organic dyes, pesticides, oil traces, metal ions, and inorganic ions from wastewater. Performances of natural and synthetic fibres have been investigated and compared by gathering scientific works related to the investigated topic.

Apart from the use of synthetic fibres, the use of natural fibres as the adsorbent is an emerging trend in wastewater treatment technology as the fibres are abundant, readily available, and more environmentally friendly as compared to polymeric-based materials. Many types of natural fibres, especially agricultural wastes, have the potential to be utilized as absorbents (cellulose, jute, cotton, etc.). A particular focus has been focused on the use of electrospinning to produce high-performance systems with tuneable properties which could be modified to improve the adsorption capacity. Finally, fibre-based systems for the removal of pollutants through photocatalysis have been discussed prior to discuss the use of carbon fibre-based adsorbent obtained from different sources.

## References

[1] Cao Y, Li X. Adsorption of graphene for the removal of inorganic pollutants in water purification: A review. Adsorption. 2014;20(5–6):713–727. DOI: 10.1007/S10450-014-9615-Y.

[2] Abdolali A, Guo WS, Ngo HH, Chen SS, Nguyen NC, Tung KL. Typical lignocellulosic wastes and by-products for biosorption process in water and wastewater treatment: A critical review. Bioresour Technol. 2014;160:57–66. DOI: 10.1016/J.BIORTECH.2013.12.037.

[3] Molinari A, Mayacela Rojas CM, Beneduci A, Tavolaro A, Rivera Velasquez MF, Fallico C. Adsorption performance analysis of alternative reactive media for remediation of aquifers affected by heavy metal contamination. *Int J Environ Res Public Heal*. 2018;15(5):980. DOI: 10.3390/IJERPH15050980.

[4] Bulut Y, Z TEZ. Removal of heavy metals from aqueous solution by sawdust adsorption. *J Environ Sci*. 2007;19(2):160–166. DOI: 10.1016/S1001-0742(07)60026-6.

[5] Viscusi G, Barra G, Gorrasi G. Modification of hemp fibers through alkaline attack assisted by mechanical milling: Effect of processing time on the morphology of the system. Cellulose. 2020;27(15):8653–8665. DOI: 10.1007/s10570-020-03406-0.

[6] Thyavihalli Girijappa YG, Mavinkere Rangappa S, Parameswaranpillai J, Siengchin S. Natural fibers as sustainable and renewable resource for development of eco-friendly composites: A comprehensive review. Front Mater. 2019;6:226. DOI: 10.3389/FMATS.2019.00226/BIBTEX.

[7] Oksman K. High quality flax fibre composites manufactured by the resin transfer moulding process. DOI: 10.1106/CA5A-6FAX-VJRB-80P0.

[8] Lau KT, Hung PY, Zhu MH, Hui D. Properties of natural fibre composites for structural engineering applications. Compos Part B: Eng. 2018;136:222–233. DOI: 10.1016/J.COMPOSITESB.2017.10.038.

[9] Viscusi G, Pantani R, Gorrasi G. Transport properties of water vapor through hemp fibers modified with a sustainable process: Effect of surface morphology on the thermodynamic and kinetic phenomena. Appl Surf Sci. 2021;541:148433. DOI: 10.1016/j.apsusc.2020.148433.

[10] Nine MJ, Kabiri S, Sumona AK, Tung TT, Moussa MM, Losic D. Superhydrophobic/superoleophilic natural fibres for continuous oil-water separation and interfacial dye-adsorption. Sep Purif Technol. 2020;233:116062. DOI: 10.1016/J.SEPPUR.2019.116062.

[11] Sharaf El-Deen GE, Sharaf El-Deen SEA. Kinetic and isotherm studies for adsorption of Pb(II) from aqueous solution onto coconut shell activated carbon. New Pub Balaban. 2016;57(59):28910–28931. DOI: 10.1080/19443994.2016.1193825.

[12] Roy A, Adhikari B, Majumder SB. Equilibrium, Kinetic, and Thermodynamic Studies of Azo Dye Adsorption from Aqueous Solution by Chemically Modified Lignocellulosic Jute Fiber. Published online 2013. DOI: 10.1021/ie400236s.

[13] Brião GV, Jahn SL, Foletto EL, Dotto GL. Adsorption of crystal violet dye onto a mesoporous ZSM-5 zeolite synthetized using chitin as template. J Colloid Interface Sci. 2017;508:313–322. DOI: 10.1016/J.JCIS.2017.08.070.

[14] Sajab MS, Chia CH, Zakaria S, Khiew PS. Cationic and anionic modifications of oil palm empty fruit bunch fibers for the removal of dyes from aqueous solutions. Bioresour Technol. 2013;128:571–577. DOI: 10.1016/J.BIORTECH.2012.11.010.

[15] Satapathy MK, Das P. Assessment on the modelling of the kinetic parameter for the removal of crystal violet dye using Ag-soil nanocomposite: linear and non-linear analysis Desalination and Water Treatment. Published online 2016: DOI: 10.1080/19443994.2014.987179.

[16] Katheresan V, Kansedo J, Lau SY. Efficiency of various recent wastewater dye removal methods: A review. J Environ Chem Eng. 2018;6(4):4676–4697. DOI: 10.1016/J.JECE.2018.06.060.

[17] Tka N, Jabli M, Saleh TA, Salman GA. Amines modified fibers obtained from natural Populus tremula and their rapid biosorption of Acid Blue 25. J Mol Liq. 2018;250:423–432. DOI: 10.1016/j.molliq.2017.12.026.

[18] Selambakkannu S, Othman NAF, Bakar KA, Ming TT, Segar RD, Karim ZA. Modification of radiation grafted banana trunk fibers for adsorption of anionic dyes. Fibers Polym. 2019;20(12):2556–2569. DOI: 10.1007/S12221-019-9409-7.

[19] Li Y, Xiao H, Chen M, Song Z, Zhao Y. Absorbents based on maleic anhydride-modified cellulose fibers/diatomite for dye removal. J Mater Sci. 2014;49(19):6696–6704. DOI: 10.1007/S10853-014-8270-8.

[20] Viscusi G, Lamberti E, Gorrasi G. Hemp fibers modified with graphite oxide as green and efficient solution for water remediation: Application to methylene blue. Chemosphere. October 18, 2021; Published online:132614. DOI: 10.1016/J.CHEMOSPHERE.2021.132614.

[21] Gupta VK, Pathania D, Agarwal S, Sharma S. De-coloration of hazardous dye from water system using chemically modified ficus carica adsorbent. J Mol Liq. 2012;174:86–94. DOI: 10.1016/J.MOLLIQ.2012.07.017.

[22] Demir H, Top A, Balköse D, Ülkü S. Dye adsorption behavior of *Luffa cylindrica* fibers. J Hazard Mater. 2008;153(1–2):389–394. DOI: 10.1016/J.JHAZMAT.2007.08.070.

[23] Pathania D, Sharma A, Sethi V. Microwave induced graft copolymerization of binary monomers onto *Luffa cylindrica* fiber: removal of Congo red. Procedia Eng. 2017;200:408–415. DOI: 10.1016/J.PROENG.2017.07.057.

[24] Shaiful Sajab M, Hua Chia C, Zakaria S, et al. Citric acid modified kenaf core fibres for removal of methylene blue from aqueous solution. Published online 2011. DOI: 10.1016/j.biortech.2011.05.011.

[25] Mallampati R, Tan KS, Valiyaveettil S. Utilization of corn fibers and luffa peels for extraction of pollutants from water. *Int Biodeterior Biodegradation*. 2015;103:8–15. DOI: 10.1016/J.IBIOD.2015.03.027.

[26] Parab H, Sudersanan M, Shenoy N, Pathare T, Vaze B. Use of agro-industrial wastes for removal of basic dyes from aqueous solutions. Clean – Soil Air Water. 2009;37(12):963–969. DOI: 10.1002/CLEN.200900158.

[27] Roy A, Chakraborty S, Kundu SP, Adhikari B, Majumder SB. Lignocellulosic jute fiber as a bioadsorbent for the removal of azo dye from its aqueous solution: Batch and column studies. J Appl Polym Sci. 2013;129(1):15–27. DOI: 10.1002/APP.38222.

[28] Yue X, Jiang F, Zhang D, Lin H, Chen Y. Preparation of adsorbent based on cotton fiber for removal of dyes. Fibers Polym. 2017;18(11):2102–2110. DOI: 10.1007/S12221-017-1211-9.

[29] Kyzas GZ, Christodoulou E, Bikiaris DN. Basic dye removal with sorption onto low-cost natural textile fibers. Process. 2018;6(9):166. DOI: 10.3390/PR6090166.

[30] Agcaoili AR, Herrera MU, Futalan CM, Balela MDL. Fabrication of polyacrylonitrile-coated kapok hollow microtubes for adsorption of methyl orange and Cu(II) ions in aqueous solution. J Taiwan Inst Chem Eng. 2017;78:359–369. DOI: 10.1016/J.JTICE.2017.06.038.

[31] Herrera MU, Futalan CM, Gapusan R, Balela MDL. Removal of methyl orange dye and copper (II) ions from aqueous solution using polyaniline-coated kapok (*Ceiba pentandra*) fibers. Water Sci Technol. 2018;78(5):1137–1147. DOI: 10.2166/WST.2018.385.

[32] Hameed BH, El-Khaiary MI. Batch removal of malachite green from aqueous solutions by adsorption on oil palm trunk fibre: Equilibrium isotherms and kinetic studies. J Hazard Mater. 2008;154(1–3):237–244. DOI: 10.1016/J.JHAZMAT.2007.10.017.

[33] Li H, Wu W, Bubakir MM, et al. Polypropylene fibers fabricated via a needleless melt-electrospinning device for marine oil-spill cleanup. J Appl Polym Sci. 2014;131(7). DOI: 10.1002/APP.40080.

[34] Hubbe MA, Rojas OJ, Fingas M, Gupta BS. Cellulosic substrates for removal of pollutants from aqueous systems: A review. 3. Spilled oil and emulsified organic liquids. BioResources. 2013;8 (2):3038–3097. Accessed August 15, 2022: https://ojs.cnr.ncsu.edu/index.php/BioRes/article/view/BioRes_08_2_3038_Hubbe_Review_Cellulosic_Substrates_Removal_Pollutants.

[35] Sun XF, Sun RC, Sun JX. A convenient acetylation of sugarcane bagasse using NBS as a catalyst for the preparation of oil sorption-active materials. J Mater Sci. 2003;38(19):3915–3923. DOI: 10.1023/A:1026189911651.

[36] Voumbo ML, Wereme A, Gaye S, Adj M, Sissoko G. Characterization of the Thermophysical Properties of Kapok. Res J Appl Sci Eng Technol. 2010;2(2):143–148. DOI: 10.5297/SER.1201.002.

[37] Lim TT, Huang X. Evaluation of hydrophobicity/oleophilicity of kapok and its performance in oily water filtration: Comparison of raw and solvent-treated fibers. Ind Crops Prod. 2007;26(2):125–134. DOI: 10.1016/J.INDCROP.2007.02.007.

[38] Abdullah MA, Rahmah AU, Man Z. Physicochemical and sorption characteristics of Malaysian *Ceiba pentandra* (L.) Gaertn. as a natural oil sorbent. J Hazard Mater. 2010;177(1–3):683–691. DOI: 10.1016/J.JHAZMAT.2009.12.085.

[39] Likon M, Remškar M, Ducman V, Švegl F. Populus seed fibers as a natural source for production of oil super absorbents. J Environ Manage. 2013;114:158–167. DOI: 10.1016/J.JENVMAN.2012.03.047.

[40] Candido ICM, Pires ICB, de Oliveira HP. Natural and synthetic fiber-based adsorbents for water remediation. Clean – Soil Air Water. 2021;49(6):2000189. DOI: 10.1002/CLEN.202000189.

[41] Dos Anjos RB, Hilário LS, de Moraes Juviniano HB, da Silva DR. Crude oil removal using Calotropis procera. Undefined. 2020;15(3):5246–5263. DOI: 10.15376/BIORES.15.3.5246-5263.

[42] Cao E, Xiao W, Duan W, Wang N, Wang A, Zheng Y. Metallic nanoparticles roughened Calotropis gigantea fiber enables efficient absorption of oils and organic solvents. Ind Crops Prod. 2018;115:272–279. DOI: 10.1016/J.INDCROP.2018.02.052.

[43] Wang J, Zheng Y, Wang A. Coated kapok fiber for removal of spilled oil. Mar Pollut Bull. 2013;69 (1–2):91–96. DOI: 10.1016/J.MARPOLBUL.2013.01.007.

[44] Wang J, Zheng Y, Kang Y, Wang A. Investigation of oil sorption capability of PBMA/SiO2 coated kapok fiber. Chem Eng J. 2013;223:632–637. DOI: 10.1016/J.CEJ.2013.03.007.

[45] Wang J, Zheng Y, Wang A. Superhydrophobic kapok fiber oil-absorbent: Preparation and high oil absorbency. Chem Eng J. 2012;213:1–7. DOI: 10.1016/J.CEJ.2012.09.116.

[46] Dong T, Xu G, Wang F. Oil spill cleanup by structured natural sorbents made from cattail fibers. Ind Crops Prod. 2015;76:25–33. DOI: 10.1016/J.INDCROP.2015.06.034.

[47] Viscusi G, Liparoti S, Pantani R, Barra G, Gorrasi G. A layer-by-layer approach based on APTES/Cloisite to produce novel and sustainable high performances materials based on hemp fiberboards. Polym Degrad Stab. 2022;198. DOI: 10.1016/J.POLYMDEGRADSTAB.2022.109892.

[48] Onwuka JC, Agbaji EB, Ajibola VO, Okibe FG. Treatment of crude oil-contaminated water with chemically modified natural fiber. Appl Water Sci. 2018;8(3):1–10. DOI: 10.1007/S13201-018-0727-5.

[49] Moriwaki H, Kitajima S, Kurashima M, et al. Utilization of silkworm cocoon waste as a sorbent for the removal of oil from water. J Hazard Mater. 2009;165(1–3):266–270. DOI: 10.1016/J.JHAZMAT.2008.09.116.

[50] Dong T, Wang F, Xu G. Theoretical and experimental study on the oil sorption behavior of kapok assemblies. Ind Crops Prod. 2014;61:325–330. DOI: 10.1016/J.INDCROP.2014.07.020.

[51] Zou J, Chai W, Liu X, et al. Magnetic pomelo peel as a new absorption material for oil-polluted water Desalination and Water Treatment. Published online 2015: DOI: 10.1080/19443994.2015.1049958.

[52] Tursi A, Beneduci A, Chidichimo F, De Vietro N, Chidichimo G. Remediation of hydrocarbons polluted water by hydrophobic functionalized cellulose. Chemosphere. 2018;201:530–539. DOI: 10.1016/J.CHEMOSPHERE.2018.03.044.

[53] Fu F, Wang Q. Removal of heavy metal ions from wastewaters: A review. J Environ Manage. 2011;92(3):407–418. DOI: 10.1016/J.JENVMAN.2010.11.011.

[54] Naseem R, Tahir SS. Removal of Pb(II) from aqueous/acidic solutions by using bentonite as an adsorbent. Water Res. 2001;35(16):3982–3986. DOI: 10.1016/S0043-1354(01)00130-0.

[55] Abadeh ZA. Universities MICR in C. 2017 undefined. Removal of Ni and Cd ions from aqueous solution using iron dust-zeolite composite: Analysis by thermodynamic, kinetic and isotherm studies. Springer. 2017;33(2):318–326. DOI: 10.1007/s40242-017-6150-x.

[56] Du Z, Zheng T, Wang P, Hao L, Wang Y. Fast microwave-assisted preparation of a low-cost and recyclable carboxyl modified lignocellulose-biomass jute fiber for enhanced heavy metal removal from water. Bioresour Technol. 2016;201:41–49. DOI: 10.1016/J.BIORTECH.2015.11.009.

[57] Lai HT, Kim D, Park JS, Yen TF. Studies of crosslinked biopolymer structure for environmental tools in terms of the rate of weight swelling ratio, viscosity, and biodegradability: Part A. Environ Earth Sci. 2013;70(5):2405–2413. DOI: 10.1007/S12665-013-2791-3/FIGURES/4.

[58] Jiang X, Yu H, Pang J, Ai T, Liu L. Equilibrium, kinetic and mechanism studies on the biosorption of Cu2+ and Ni2+ by sulfur-modified bamboo powder biosorption of Cu 2 +, Co 2 + and Ni 2 + from aqueous solution by modified corn silk: Equilibrium, kinetics, and thermodynamic studies. J Taiwan Inst Chem Eng. 2014;62:21–30. DOI: 10.1007/s11814-014-0227-8.

[59] Futalan CM, Choi AES, Soriano HGO, Cabacungan MKB, Millare JC. Modification strategies of kapok fiber composites and its application in the adsorption of heavy metal ions and dyes from aqueous solutions: A systematic review. Int J Environ Res Public Heal. 2022;19(5):2703. DOI: 10.3390/IJERPH19052703.

[60] Prachayawarakorn J, Chaiwatyothin S, Mueangta S, Hanchana A. Effect of jute and kapok fibers on properties of thermoplastic cassava starch composites. Mater Des. 2013;47:309–315. DOI: 10.1016/J.MATDES.2012.12.012.

[61] Nilsson T, Björdal C. The use of kapok fibres for enrichment cultures of lignocellulose-degrading bacteria. Int Biodeterior Biodegradation. 2008;61(1):11–16. DOI: 10.1016/J.IBIOD.2007.06.009.

[62] Wang R, Shin CH, Park S, et al. Removal of lead (II) from aqueous stream by chemically enhanced kapok fiber adsorption. Environ Earth Sci. 2014;72(12):5221–5227. DOI: 10.1007/S12665-014-3804-6.

[63] Kalia S, Kaith BS, Kaur I. Pretreatments of natural fibers and their application as reinforcing material in polymer composites – A review. Polym Eng Sci. 2009;49(7):1253–1272. DOI: 10.1002/PEN.21328.

[64] Wang F, Zheng Y, Zhu Y, Wang A. Oriented Functionalization of natural hollow kapok fiber for highly efficient removal of toxic Hg(II) from aqueous solution. Front Environ Sci. 2016;4(FEB):4. DOI: 10.3389/FENVS.2016.00004/BIBTEX.

[65] Yang N, Shin CH, Kim D, Park JS, Rao P, Wang R. Synthesis, characterization, and mercury removal application of surface modified kapok fibers with dopamine (DA): Investigation of bidentate adsorption. Environ Earth Sci. 2020;79(11). DOI: 10.1007/S12665-020-08980-X.

[66] Duan C, Zhao N, Yu X, Zhang X, Xu J. Chemically modified kapok fiber for fast adsorption of Pb2+, Cd2+, Cu2+ from aqueous solution. Cellulose. 2013;20(2):849–860. DOI: 10.1007/S10570-013-9875-9/FIGURES/9.

[67] Zheng Y, Wang W, Huang D, Wang A. Kapok fiber oriented-polyaniline nanofibers for efficient Cr(VI) removal. Chem Eng J. 2012;191:154–161. DOI: 10.1016/J.CEJ.2012.02.088.

[68] Shukla SR, Pai RS. Adsorption of Cu(II), Ni(II) and Zn(II) on modified jute fibres. Bioresour Technol. 2005;96(13):1430–1438. DOI: 10.1016/j.biortech.2004.12.010.

[69] Eftekhari E, Hasani H, Fashandi H. Removal of heavy metal ions (Pb 2þ and Ni 2þ) from aqueous solution using nonwovens produced from lignocellulosic milkweed fibers. 2021;51(5):695–713. DOI: 10.1177/1528083719888931.

[70] Monier M, Ayad DM, Sarhan AA. Adsorption of Cu(II), Hg(II), and Ni(II) ions by modified natural wool chelating fibers. J Hazard Mater. 2010;176(1–3):348–355. DOI: 10.1016/J.JHAZMAT.2009.11.034.

[71] Shimizu F, Aida G. Adsorption behavior of copper (II) ions by silk yarns on cupric salt treatments, with reference to its inhibitory effect on photodegradatioN. Sen'i Gakkaishi. 1970;26(7):316–323. DOI: 10.2115/FIBER.26.316.

[72] Arai T, Freddi G, Colonna GM, et al. Absorption of metal cations by modified B. mori silk and preparation of fabrics with antimicrobial activity. J Appl Polym Sci. 2001;80:297–303. DOI: 10.1002/1097-4628.

[73] Sekine A, Seko N, Tamada M, Suzuki Y. Biodegradable metal adsorbent synthesized by graft polymerization onto nonwoven cotton fabric. Radiat Phys Chem. 2010;79(1):16–21. DOI: 10.1016/J.RADPHYSCHEM.2009.08.007.

[74] Hassan MS, Zohdy MH. Adsorption kinetics of toxic heavy metal ions from aqueous solutions onto grafted jute fibers with acrylic acid by gamma irradiation. 2018;15(4):506-516. https://doi.org/101080/1544047820171330721. DOI: 10.1080/15440478.2017.1330721.

[75] Kajiyama T, Sakai S, Inoue J, Kokusen H. Adsorption properties of modified banana fiber to transition metal ions. 日本イオン交換学会誌. 2014;25(4):155–159. DOI: 10.5182/JAIE.25.155.

[76] Min SH, Han JS, Shin EW, Park JK. Improvement of cadmium ion removal by base treatment of juniper fiber. Water Res. 2004;38(5):1289–1295. DOI: 10.1016/J.WATRES.2003.11.016.

[77] Bediako JK, Wei W, Kim S, Yun YS. Removal of heavy metals from aqueous phases using chemically modified waste Lyocell fiber. J Hazard Mater. 2015;299:550–561. DOI: 10.1016/J.JHAZMAT.2015.07.033.

[78] Rani K, Gomathi T, Vijayalakshmi K, Saranya M, Sudha PN. Banana fiber Cellulose Nano Crystals grafted with butyl acrylate for heavy metal lead (II) removal. Int J Biol Macromol. 2019;131:461–472. DOI: 10.1016/J.IJBIOMAC.2019.03.064.

[79] Selambakkannu S, Othman NAF, Bakar KA, Shukor SA, Karim ZA. A kinetic and mechanistic study of adsorptive removal of metal ions by imidazole-functionalized polymer graft banana fiber. Radiat Phys Chem. 2018;153:58–69. DOI: 10.1016/J.RADPHYSCHEM.2018.09.012.

[80] Hajeeth T, Sudha PN, Vijayalakshmi K, Gomathi T. Sorption studies on Cr (VI) removal from aqueous solution using cellulose grafted with acrylonitrile monomer. Int J Biol Macromol. 2014;66:295–301. DOI: 10.1016/J.IJBIOMAC.2014.02.027.

[81] Shaiful Sajab M, Chia CH, Zakaria S, Mohd Jani S, Khiew P, Chiu W. Removal of Copper(II) Ions from Aqueous Solution Using Alkali-treated Kenaf Core Fibres.

[82] Annie Kamala Florence J Chitin and Chitosan derivatives : Advances in drug discovery and development view project natural polymeric products view project. Artic J Chem Pharm Res. Published online 2015: Accessed September 3, 2022. www.jocpr.com.

[83] Shamsudin R, Abdullah H, Kamari A. Application of kenaf bast fiber to adsorb Cu(II), Pb(II) and Zn (II) in aqueous solution: Single- and multi-metal systems. Int J Environ Sci Dev. 2016;7(10):715–723. DOI: 10.18178/IJESD.2016.7.10.868.

[84] Yang R, Aubrecht KB, Ma H, et al. Thiol-modified cellulose nanofibrous composite membranes for chromium (VI) and lead (II) adsorption. Polymer (Guildf). 2014;55(5):1167–1176. DOI: 10.1016/J.POLYMER.2014.01.043.

[85] Othman NAF, Selambakkannu S, Ting TM, Zulhairun AK. Modification of kenaf fibers by single step radiation functionalization of 2-hydroxyl methacrylate phosphoric acid (2-HMPA). SN Appl Sci. 2019;1(3):1–9. DOI: 10.1007/S42452-019-0231-Z/FIGURES/10.

[86] Fernando MS, Wimalasiri AKDVK, Dziemidowicz K, et al. Biopolymer-based nanohydroxyapatite composites for the removal of fluoride, lead, cadmium, and arsenic from water. *ACS Omega*. 2021;6 (12):8517–8530. DOI: 10.1021/ACSOMEGA.1C00316/ASSET/IMAGES/LARGE/AO1C00316_0010.JPEG.

[87] Li M, Liu Z, Wang HC, et al. Dual-function cellulose composites for fluorescence detection and removal of fluoride. Dye Pigment. 2018;149:669–675. DOI: 10.1016/J.DYEPIG.2017.11.033.

[88] Ayoub GM, Koopman B, Pandya N. Iron and aluminum hydroxy (Oxide) coated filter media for low-concentration phosphorus removal. Water Environ Res. 2001;73(4):478–485. DOI: 10.2175/106143001X139533.

[89] Zhao D, Sengupta AK. Ultimate removal of phosphate from wastewater using a new class of polymeric ion exchangers. Water Res. 1998;32(5):1613–1625. DOI: 10.1016/S0043-1354(97)00371-0.

[90] Pang D, Wang CC, Wang P, Liu W, Fu H, Zhao C. Superior removal of inorganic and organic arsenic pollutants from water with MIL-88A(Fe) decorated on cotton fibers. Chemosphere. 2020;254:126829. DOI: 10.1016/J.CHEMOSPHERE.2020.126829.

[91] Hughes MF, Beck BD, Chen Y, Lewis AS, Thomas DJ. Arsenic exposure and toxicology: A historical perspective. Toxicol Sci. 2011;123(2):305–332. DOI: 10.1093/TOXSCI/KFR184.

[92] Ayoub GM, Koopman B, Pandya N. Iron and aluminum hydroxy (Oxide) coated filter media for low-concentration phosphorus removal. Water Environ Res. 2001;73(4):478–485. DOI: 10.2175/106143001X139533.

[93] Eberhardt TL, Min SH, Han JS. Phosphate removal by refined aspen wood fiber treated with carboxymethyl cellulose and ferrous chloride. Bioresour Technol. 2006;97(18):2371–2376. DOI: 10.1016/J.BIORTECH.2005.10.040.

[94] ‡ Andmandl AA. Orthophosphate Sorption onto Lanthanum-Treated Lignocellulosic Sorbents. Published online 2005. DOI: 10.1021/es048018n.

[95] Mondal NK, Bhaumik R, Datta JK. Removal of fluoride by aluminum impregnated coconut fiber from synthetic fluoride solution and natural water. Alexandria Eng J. 2015;54(4):1273–1284. DOI: 10.1016/J.AEJ.2015.08.006.

[96] Shin EW, Karthikeyan KG, Tshabalala MA. Orthophosphate sorption onto lanthanum-treated lignocellulosic sorbents. Environ Sci Technol. 2005;39(16):6273–6279. DOI: 10.1021/ES048018N/SUPPL_FILE/ES048018NSI20050605_033415.PDF.

[97] Tian Y, Wu M, Liu R, et al. Modified native cellulose fibers – A novel efficient adsorbent for both fluoride and arsenic. J Hazard Mater. 2011;185(1):93–100. DOI: 10.1016/J.JHAZMAT.2010.09.001.

[98] Du J, Dong Z, Lin Z, Yang X, Zhao L. Radiation Synthesis of Pentaethylene Hexamine Functionalized Cotton Linter for Effective Removal of Phosphate: Batch and Dynamic Flow Mode Studies. Mater. 2019;12(20):3393. DOI: 10.3390/MA12203393.

[99] Carvalho WS, Martins DF, Gomes FR, et al. Phosphate adsorption on chemically modified sugarcane bagasse fibres. Biomass and Bioenergy. 2011;35(9):3913–3919. DOI: 10.1016/J.BIOMBIOE.2011.06.014.

[100] Deng S, Zhang G, Chen S, Xue Y, Du Z, Wang P. Rapid and effective preparation of a HPEI modified biosorbent based on cellulose fiber with a microwave irradiation method for enhanced arsenic removal in water. J Mater Chem A. 2016;4(41):15851–15860. DOI: 10.1039/C6TA06051J.

[101] Liao XP, Shi B. Adsorption of fluoride on zirconium(IV)-impregnated collagen fiber. Environ Sci Technol. 2005;39(12):4628–4632. DOI: 10.1021/ES0479944/ASSET/IMAGES/LARGE/ES0479944F00007.JPEG.

[102] Ye F, Huang C, Jiang X, et al. Reusable fibrous adsorbent prepared via Co-radiation induced graft polymerization for iodine adsorption. Ecotoxicol Environ Saf. 2020;203:111021. DOI: 10.1016/J.ECOENV.2020.111021.

[103] Yusof SRM, Zahri NAM, Koay YS, Nourouzi MM, Chuah LA, Choong TSY. Removal of fluoride using modified kenaf as adsorbent. J Eng Sci Technol Spec Issue SOMCHE. Published online 2014. 11–22.

[104] Moreno-medina DA, Sánchez-salinas E, Ortiz-hernández ML. Removal of methyl parathion and coumaphos pesticides by a bacterial consortium immobilized in *Luffa cylindrica*. Rev Int Contam Ambient. 2014;30(1):51–63. Accessed September 5, 2022. http://www.scielo.org.mx/scielo.php?script=sci_arttext&pid=S0188-49992014000100005&lng=es&nrm=iso&tlng=en.

[105] Rajapaksha PP, Power A, Chandra S, Chapman J. Graphene, electrospun membranes and granular activated carbon for eliminating heavy metals, pesticides and bacteria in water and wastewater treatment processes. Analyst. 2018;143(23):5629–5645. DOI: 10.1039/C8AN00922H.

[106] Abdelhameed RM, El-Zawahry M, Emam HE. Efficient removal of organophosphorus pesticides from wastewater using polyethylenimine-modified fabrics. Polymer (Guildf). 2018;155:225–234. DOI: 10.1016/J.POLYMER.2018.09.030.

[107] Sadasivam S, Krishna SK, Ponnusamy K, Nagarajan GS, Kang TW, Venkatesalu SC. Equilibrium and thermodynamic studies on the adsorption of an organophosphorous pesticide onto “waste” jute fiber carbon. J Chem Eng Data. 2010;55(12):5658–5662. DOI: 10.1021/JE1005906/ASSET/IMAGES/LARGE/JE-2010-005906_0003.JPEG.

[108] Ghali AE, Baouab MHV, Roudesli MS. Aminated cotton fibers loaded with copper(II) ions for enhanced pesticide removal performance from water in a laboratory scale batch. Ind Crops Prod. 2012;39(1):139–148. DOI: 10.1016/J.INDCROP.2012.02.020.

[109] Alila S, Boufi S. Removal of organic pollutants from water by modified cellulose fibres. Ind Crops Prod. 2009;30(1):93–104. DOI: 10.1016/J.INDCROP.2009.02.005.

[110] Boufi S, Belgacem MN. Modified cellulose fibres for adsorption of dissolved organic solutes. DOI: 10.1007/s10570-005-9019-y.

[111] Khalfaoui M, Ghali AE, Aguir C, Mohamed Z, Baouab MHV, Lamine AB. Study on adsorption of herbicide onto functionalized cellulose extracted from *Juncus acutus* L. plant: Experimental results and theoretical modeling. Ind Crops Prod. 2015;67:169–178. DOI: 10.1016/J.INDCROP.2015.01.032.

[112] Gupta VK, Fakhri A, Agarwal S, Sadeghi N. Synthesis of $MnO_2$/cellulose fiber nanocomposites for rapid adsorption of insecticide compound and optimization by response surface methodology. Int J Biol Macromol. 2017;102:840–846. DOI: 10.1016/J.IJBIOMAC.2017.04.075.

[113] Renuka S, Rengasamy RS, Das D. Studies on needle-punched natural and polypropylene fiber nonwovens as oil sorbents. 2016;46(4):1121–1143. DOI: 10.1177/1528083715613630.

[114] Saleem J, Adil Riaz M, Gordon M. Oil sorbents from plastic wastes and polymers: A review. J Hazard Mater. 2018;341:424–437. DOI: 10.1016/J.JHAZMAT.2017.07.072.

[115] Chen W, Ma H, Xing B. Electrospinning of multifunctional cellulose acetate membrane and its adsorption properties for ionic dyes. Int J Biol Macromol. 2020;158:1342–1351. DOI: 10.1016/J.IJBIOMAC.2020.04.249.

[116] Liu X, Ao J, Yang X, et al. Green and efficient synthesis of an adsorbent fiber by preirradiation-induced grafting of PDMAEMA and its Au(III) adsorption and reduction performance. J Appl Polym Sci. 2017;134(25):44955. DOI: 10.1002/APP.44955.

[117] Ma H, Hoshina H, Seko N. Crosslinking induced by irradiation raises selectivity of polymeric adsorbent. J Appl Polym Sci. 2013;128(6):4253–4260. DOI: 10.1002/APP.38428.

[118] Kavakli C, Akkaş Kavakli P, Turan BD, Hamurcu A, Güven O. Quaternized dimethylaminoethyl methacrylate strong base anion exchange fibers for As(V) adsorption. Radiat Phys Chem. 2014;102:84–95. DOI: 10.1016/J.RADPHYSCHEM.2014.04.011.

[119] Huang X, Hu J, Huang J, et al. Preparation of ultrahigh-water-content nanofiber composite hydrogel for Cd2+ removal. J Chem Technol Biotechnol. 2021;96(5):1237–1245. DOI: 10.1002/JCTB.6636.

[120] Hu J, Ma H, Xing Z, et al. Preparation of amidoximated ultrahigh molecular weight polyethylene fiber by radiation grafting and uranium adsorption test. Ind Eng Chem Res. 2015;55(15):4118–4124. DOI: 10.1021/ACS.IECR.5B03175/ASSET/IMAGES/LARGE/IE-2015-031757_0009.JPEG.

[121] Kawai T, Saito K, Sugita K, et al. Comparison of Amidoxime Adsorbents Prepared by Cografting Methacrylic Acid and 2-Hydroxyethyl Methacrylate with Acrylonitrile onto Polyethylene. Published online 2000. DOI: 10.1021/ie990474a.

[122] Oyola Y, Janke CJ, Dai S. Synthesis, Development, and Testing of High-Surface-Area Polymer-Based Adsorbents for the Selective Recovery of Uranium from Seawater. Published online 2016. DOI: 10.1021/acs.iecr.5b03981.

[123] Zhang A, Uchiyama G, Asakura T. pH effect on the uranium adsorption from seawater by a macroporous fibrous polymeric material containing amidoxime chelating functional group. React Funct Polym. 2005;63(2):143–153. DOI: 10.1016/J.REACTFUNCTPOLYM.2005.02.015.

[124] Das S, Tsouris C, Zhang C, et al. Enhancing uranium uptake by amidoxime adsorbent in seawater: An investigation for optimum alkaline conditioning parameters. Ind Eng Chem Res. 2016;55 (15):4294–4302. DOI: 10.1021/ACS.IECR.5B02735/ASSET/IMAGES/LARGE/IE-2015-02735Z_0001.JPEG.

[125] Wongsawaeng D, Wongjaikham W, Swantomo D, Basuki KT. Innovative seawater uranium recovery agent based on low-cost polyacrylonitrile fibers. Appl Radiat Isot. 2020;158:109067. DOI: 10.1016/J.APRADISO.2020.109067.

[126] Sugasaka K, Katoh S, Takai N, Takahashi H, Umezawa Y. Recovery of Uranium from Seawater. 2006;16(9):971–985. http://dx.doi.org/101080/01496398108057594. DOI: 10.1080/01496398108057594.

[127] Arslan M, Günay K. Synthesis of amine-functionalized methacrylic acid-g-poly(ethylene terephthalate) fiber and its Congo red removal ability. Polym Bull. 2018;75(4):1701–1713. DOI: 10.1007/S00289-017-2121-0/FIGURES/11.

[128] Yiğitoğlu M, Temoçin Z. Removal of benzidine-based azo dye from aqueous solution using amide and amine-functionalized poly(ethylene terephthalate) fibers. *Fibers Polym*. 2010;11(7):996–1002. DOI: 10.1007/S12221-010-0996-6.

[129] Arslan M, Günay K. Application of 4-VP-g-PET fibers and its N-oxide derivative as an adsorbent for removal of cationic dye. Polym Bull. 2019;76(2):953–965. DOI: 10.1007/S00289-018-2400-4/FIGURES/10.

[130] Xiao J, Wang L, Ran J, Zhao J, Tao M, Zhang W. Highly selective removal of cationic dyes from water by acid-base regulated anionic functionalized polyacrylonitrile fiber: Fast adsorption, low detection limit, reusability. React Funct Polym. 2020;146:104394. DOI: 10.1016/J.REACTFUNCTPOLYM.2019.104394.

[131] Karthik R, Meenakshi S. Removal of Cr(VI) ions by adsorption onto sodium alginate-polyaniline nanofibers. Int J Biol Macromol. 2015;72:711–717. DOI: 10.1016/J.IJBIOMAC.2014.09.023.

[132] Deng S, Zhang G, Li Y, Dou Y, Wang P. Facile preparation of amidoxime-functionalized fiber by microwave-assisted method for the enhanced adsorption of chromium( vi) from aqueous solution. *RSC Adv.* 2016;6(69):64665–64675. DOI: 10.1039/C6RA11727A.

[133] Bhaumik M, Maity A, Srinivasu VV, Onyango MS. Removal of hexavalent chromium from aqueous solution using polypyrrole-polyaniline nanofibers. Chem Eng J. 2012;181–182:323–333. DOI: 10.1016/J.CEJ.2011.11.088.

[134] Chen J, Hong X, Xie Q, Li D, Zhang Q. Highly efficient removal of chromium(VI) from aqueous solution using polyaniline/sepiolite nanofibers. Water Sci Technol. 2014;70(7):1236–1243. DOI: 10.2166/WST.2014.361.

[135] Guo X, Tao Fei G, Su H, De Zhang L. High-Performance and Reproducible Polyaniline Nanowire/Tubes for Removal of Cr(VI) in Aqueous Solution. J Phys Chem C. 2011;115:1608–1613. DOI: 10.1021/jp1091653.

[136] Coşkun R, Dilci Y. Preparation of double amidoxime-containing chelating fiber for removal of chrome (VI) ions. 2014;51(10):767–782. http://dx.doi.org/101080/106013252014937122. DOI: 10.1080/10601325.2014.937122.

[137] Qusti AH. Removal of chromium(VI) from aqueous solution using manganese oxide nanofibers. J Ind Eng Chem. 2014;20(5):3394–3399. DOI: 10.1016/J.JIEC.2013.12.025.

[138] Deng S, Bai R, Chen JP. Behaviors and mechanisms of copper adsorption on hydrolyzed polyacrylonitrile fibers. J Colloid Interface Sci. 2003;260(2):265–272. DOI: 10.1016/S0021-9797(02)00243-6.

[139] Ji F, Li C, Tang B, Xu J, Lu G, Liu P. Preparation of cellulose acetate/zeolite composite fiber and its adsorption behavior for heavy metal ions in aqueous solution. Chem Eng J. 2012;209:325–333. DOI: 10.1016/J.CEJ.2012.08.014.

[140] Efome JE, Rana D, Matsuura T, Lan CQ. Metal–organic frameworks supported on nanofibers to remove heavy metals. J Mater Chem A. 2018;6(10):4550–4555. DOI: 10.1039/C7TA10428F.

[141] Araújo ES, Luis M, Nascimento F, De Oliveira HP, Araújo ES, Nascimento MLF, de Oliveira HP. Influence of Triton X-100 on PVA fibres production by the electrospinning influence of triton X-100 on PVA fibres production by the electrospinning technique. Tech Fibres Text East Eur. 2013;21 (100):39–43.

[142] Liu L, Xu W, Ding Y, Agarwal S, Greiner A, Duan G. A review of smart electrospun fibers toward textiles. Compos Commun. 2020;22:100506. DOI: 10.1016/J.COCO.2020.100506.

[143] Bhardwaj N, Kundu SC. Electrospinning: A fascinating fiber fabrication technique. Biotechnol Adv. 2010;28(3):325–347. DOI: 10.1016/J.BIOTECHADV.2010.01.004.

[144] Reneker DH, Yarin AL. Electrospinning jets and polymer nanofibers. Polymer (Guildf). 2008;49 (10):2387–2425. DOI: 10.1016/J.POLYMER.2008.02.002.

[145] Zhao R, Wang Y, Li X, Sun B, Wang C. Synthesis of β-cyclodextrin-based electrospun nanofiber membranes for highly efficient adsorption and separation of methylene blue. ACS Appl Mater Interfaces. 2015;7(48):26649–26657. DOI: 10.1021/ACSAMI.5B08403/ASSET/IMAGES/LARGE/AM-2015-08403W_0008.JPEG.

[146] Li X, Zhang C, Zhao R, et al. Efficient adsorption of gold ions from aqueous systems with thioamide-group chelating nanofiber membranes. Chem Eng J. 2013;229:420–428. DOI: 10.1016/J.CEJ.2013.06.022.

[147] Chen H, Wageh S, Al-Ghamdi AA, Wang H, Yu J, Jiang C. Hierarchical C/NiO-ZnO nanocomposite fibers with enhanced adsorption capacity for Congo red. *J Colloid Interface Sci*. 2019;537:736–745. DOI: 10.1016/J.JCIS.2018.11.045.

[148] Hosseini SA, Vossoughi M, Mahmoodi NM. Preparation of electrospun affinity membrane and cross flow system for dynamic removal of anionic dye from colored wastewater. Fibers Polym. 2017;18 (12):2387–2399. DOI: 10.1007/S12221-017-7530-Z.

[149] Lin J, Shang Y, Ding B, Yang J, Yu J, Al-Deyab SS. Nanoporous polystyrene fibers for oil spill cleanup. Mar Pollut Bull. 2012;64(2):347–352. DOI: 10.1016/J.MARPOLBUL.2011.11.002.

[150] Almasian A, Jalali ML, Fard GC, Maleknia L. Surfactant grafted PDA-PAN nanofiber: Optimization of synthesis, characterization and oil absorption property. Chem Eng J. 2017;326:1232–1241. DOI: 10.1016/J.CEJ.2017.06.040.

[151] Wanjale S, Birajdar M, Jog J, et al. Surface tailored PS/TiO2 composite nanofiber membrane for copper removal from water. J Colloid Interface Sci. 2016;469:31–37. DOI: 10.1016/J.JCIS.2016.01.054.

[152] Feng ZQ, Yuan X, Wang T. Porous polyacrylonitrile/graphene oxide nanofibers designed for high efficient adsorption of chromium ions (VI) in aqueous solution. Chem Eng J. 2020;392:123730. DOI: 10.1016/J.CEJ.2019.123730.

[153] Wang H, Wang Y, Li C, Jia L. Fabrication of eco-friendly calcium crosslinked alginate electrospun nanofibres for rapid and efficient removal of Cu(II). Int J Biol Macromol. 2022;219:1–10. DOI: 10.1016/J.IJBIOMAC.2022.07.221.

[154] Mokhena TC, Jacobs NV, Luyt A. Electrospun alginate nanofibres as potential bio-sorption agent of heavy metals in water treatment. Published online 2017: Accessed August 19, 2022. https://researchspace.csir.co.za/dspace/handle/10204/9628

[155] Pan L, Wang Z, Zhao X, He H. Efficient removal of lead and copper ions from water by enhanced strength-toughness alginate composite fibers. Int J Biol Macromol. 2019;134:223–229. DOI: 10.1016/J.IJBIOMAC.2019.05.022.

[156] Wang M, Li X, Zhang T, et al. Eco-friendly poly(acrylic acid)-sodium alginate nanofibrous hydrogel: A multifunctional platform for superior removal of Cu(II) and sustainable catalytic applications. Colloids Surf A Physicochem Eng Asp. 2018;558:228–241. DOI: 10.1016/J.COLSURFA.2018.08.074.

[157] Li L, Zhang J, Li Y, Yang C. Removal of Cr (VI) with a spiral wound chitosan nanofiber membrane module via dead-end filtration. J Memb Sci. 2017;544:333–341. DOI: 10.1016/J.MEMSCI.2017.09.045.

[158] Wang G, Zhang H, Wang J, Ling Z, Qiu J. In situ synthesis of chemically active ZIF coordinated with electrospun fibrous film for heavy metal removal with a high flux. Sep Purif Technol. 2017;177:257–262. DOI: 10.1016/J.SEPPUR.2016.11.048.

[159] Zhao R, Li X, Sun B, et al. Branched polyethylenimine grafted electrospun polyacrylonitrile fiber membrane: a novel and effective adsorbent for Cr(VI) remediation in wastewater. J Mater Chem A. 2017;5(3):1133–1144. DOI: 10.1039/C6TA09784G.

[160] Zhu H, Qiu S, Jiang W, Wu D, Zhang C. Evaluation of electrospun polyvinyl chloride/polystyrene fibers as sorbent materials for oil spill cleanup. Environ Sci Technol. 2011;45(10):4527–4531. DOI: 10.1021/ES2002343/ASSET/IMAGES/LARGE/ES-2011-002343_0007.JPEG.

[161] Hota G, Kumar BR, Ng WJ, Ramakrishna S. Fabrication and characterization of a boehmite nanoparticle impregnated electrospun fiber membrane for removal of metal ions. J Mater Sci. 2008;43(1):212–217. DOI: 10.1007/S10853-007-2142-4/TABLES/1.

[162] Wu J, Wang N, Wang L, Dong H, Zhao Y, Jiang L. Electrospun Porous Structure Fibrous Film with High Oil Adsorption Capacity. Published online 2012. DOI: 10.1021/am300544d.

[163] Lin J, Ding B, Yang J, Yu J, Sun G. Subtle regulation of the micro- and nanostructures of electrospun polystyrene fibers and their application in oil absorption. Nanoscale. 2011;4(1):176–182. DOI: 10.1039/C1NR10895F.

[164] Vu D, Li X, Wang C. Efficient adsorption of As(V) on poly(acrylo-amidino ethylene amine) nanofiber membranes. Chinese Sci Bull. 2013;58(14):1702–1707. DOI: 10.1007/S11434-013-5717-2.

[165] Karim MR, Aijaz MO, Alharth NH, Alharbi HF, Al-Mubaddel FS, Awual MR. Composite nanofibers membranes of poly(vinyl alcohol)/chitosan for selective lead(II) and cadmium(II) ions removal from wastewater. Ecotoxicol Environ Saf. 2019;169:479–486. DOI: 10.1016/J.ECOENV.2018.11.049.

[166] Aliabadi M, Irani M, Ismaeili J, Piri H, Parnian MJ. Electrospun nanofiber membrane of PEO/Chitosan for the adsorption of nickel, cadmium, lead and copper ions from aqueous solution. Chem Eng J. 2013;220:237–243. DOI: 10.1016/J.CEJ.2013.01.021.

[167] Xu R, Jia M, Zhang Y, Li F. Sorption of malachite green on vinyl-modified mesoporous poly(acrylic acid)/SiO2 composite nanofiber membranes. Microporous Mesoporous Mater. 2012;149(1):111–118. DOI: 10.1016/J.MICROMESO.2011.08.024.

[168] Gebru KA, Das C. Removal of Pb (II) and Cu (II) ions from wastewater using composite electrospun cellulose acetate/titanium oxide (TiO2) adsorbent. J Water Process Eng. 2017;16:1–13. DOI: 10.1016/J.JWPE.2016.11.008.

[169] Haider S, Binagag FF, Haider A, et al. Adsorption kinetic and isotherm of methylene blue, safranin T and rhodamine B onto electrospun ethylenediamine-grafted-polyacrylonitrile nanofibers membrane. New Pub Balaban. 2014;55(6):1609–1619. DOI: 10.1080/19443994.2014.926840.

[170] Yan J, Huang Y, Miao YE, Tjiu WW, Liu T. Polydopamine-coated electrospun poly(vinyl alcohol)/poly(acrylic acid) membranes as efficient dye adsorbent with good recyclability. J Hazard Mater. 2015;283:730–739. DOI: 10.1016/J.JHAZMAT.2014.10.040.

[171] Wu S, Li F, Wu Y, Xu R, Li G. Preparation of novel poly(vinyl alcohol) / $SiO_2$ composite nanofiber membranes with mesostructure and their application for removal of $Cu^{2+}$ from waste water. Chem Commun. 2010;46(10):1694–1696. DOI: 10.1039/B925296G.

[172] Hong F, Yan C, Si Y, He J, Yu J, Ding B. Nickel ferrite nanoparticles anchored onto silica nanofibers for designing magnetic and flexible nanofibrous membranes. ACS Appl Mater Interfaces. 2015;7(36):20200–20207. DOI: 10.1021/ACSAMI.5B05754/SUPPL_FILE/AM5B05754_SI_004.AVI.

[173] Saeed K, Haider S, Oh TJ, Park SY. Preparation of amidoxime-modified polyacrylonitrile (PAN-oxime) nanofibers and their applications to metal ions adsorption. J Memb Sci. 2008;322(2):400–405. DOI: 10.1016/J.MEMSCI.2008.05.062.

[174] Haider S, Park SY. Preparation of the electrospun chitosan nanofibers and their applications to the adsorption of Cu(II) and Pb(II) ions from an aqueous solution. J Memb Sci. 2009;328(1–2):90–96. DOI: 10.1016/J.MEMSCI.2008.11.046.

[175] Ki CS, Gang EH, Um IC, Park YH. Nanofibrous membrane of wool keratose/silk fibroin blend for heavy metal ion adsorption. J Memb Sci. 2007;302(1–2):20–26. DOI: 10.1016/J.MEMSCI.2007.06.003.

[176] Samadi S, Yazd SS, Abdoli H, Jafari P, Aliabadi M. Fabrication of novel chitosan/PAN/magnetic ZSM-5 zeolite coated sponges for absorption of oil from water surfaces. Int J Biol Macromol. 2017;105(Pt 1):370–376. DOI: 10.1016/J.IJBIOMAC.2017.07.050.

[177] Lou L, Kendall RJ, Smith E, Ramkumar SS. Functional PVDF/rGO/$TiO_2$ nanofiber webs for the removal of oil from water. Polymer (Guildf). 2020;186:122028. DOI: 10.1016/J.POLYMER.2019.122028.

[178] Jiang Z, Tijing LD, Amarjargal A, et al. Removal of oil from water using magnetic bicomponent composite nanofibers fabricated by electrospinning. Compos Part B: Eng. 2015;77:311–318. DOI: 10.1016/J.COMPOSITESB.2015.03.067.

[179] Xu Q, Peng J, Zhang W, Wang X, Lou T. Electrospun cellulose acetate/P(DMDAAC-AM) nanofibrous membranes for dye adsorption. J Appl Polym Sci. 2020;137(15):48565. DOI: 10.1002/APP.48565.

[180] Zhijiang C, Xianyou S, Qing Z, Yuanpei L. Amidoxime surface modification of polyindole nanofiber membrane for effective removal of Cr(VI) from aqueous solution. J Mater Sci. 2017;52(9):5417–5434. DOI: 10.1007/S10853-017-0786-2/FIGURES/15.

[181] Aung KT, Hong SH, Park SJ, Lee CG. Removal of Cu(II) from aqueous solutions using amine-doped polyacrylonitrile fibers. Appl Sci. 2020;10(5):1738. DOI: 10.3390/APP10051738.

[182] Almasian A, Olya ME, Mahmoodi NM. Synthesis of polyacrylonitrile/polyamidoamine composite nanofibers using electrospinning technique and their dye removal capacity. J Taiwan Inst Chem Eng. 2015;49:119–128. DOI: 10.1016/J.JTICE.2014.11.027.

[183] Mohamed A, Nasser WS, Osman TA, Toprak MS, Muhammed M, Uheida A. Removal of chromium (VI) from aqueous solutions using surface modified composite nanofibers. J Colloid Interface Sci. 2017;505:682–691. DOI: 10.1016/J.JCIS.2017.06.066.

[184] Koushkbaghi S, Jafari P, Rabiei J, Irani M, Aliabadi M. Fabrication of PET/PAN/GO/Fe3O4 nanofibrous membrane for the removal of Pb(II) and Cr(VI) ions. Chem Eng J. 2016;301:42–50. DOI: 10.1016/J.CEJ.2016.04.076.

[185] Wanjale S, Birajdar M, Jog J, et al. Surface tailored PS/TiO2 composite nanofiber membrane for copper removal from water. J Colloid Interface Sci. 2016;469:31–37. DOI: 10.1016/J.JCIS.2016.01.054.

[186] Zhijiang C, Xianyou S, Qing Z, Yuanpei L. Amidoxime surface modification of polyindole nanofiber membrane for effective removal of Cr(VI) from aqueous solution. J Mater Sci. 2017;52(9):5417–5434. DOI: 10.1007/S10853-017-0786-2.

[187] Mohamed A, Osman TA, Toprak MS, Muhammed M, Uheida A. Surface functionalized composite nanofibers for efficient removal of arsenic from aqueous solutions. Chemosphere. 2017;180:108–116. DOI: 10.1016/J.CHEMOSPHERE.2017.04.011.

[188] Allafchian AR, Shiasi A, Amiri R. Preparing of poly(acrylonitrile co maleic acid) nanofiber mats for removal of Ni(II) and Cr(VI) ions from water. J Taiwan Inst Chem Eng. 2017;80:563–569. DOI: 10.1016/J.JTICE.2017.08.029.

[189] Deng J, Kang X, Chen L, Wang Y, Gu Z, Lu Z. A nanofiber functionalized with dithizone by co-electrospinning for lead (II) adsorption from aqueous media. J Hazard Mater. 2011;196:187–193. DOI: 10.1016/J.JHAZMAT.2011.09.016.

[190] Wang J, Pan K, He Q, Cao B. Polyacrylonitrile/polypyrrole core/shell nanofiber mat for the removal of hexavalent chromium from aqueous solution. J Hazard Mater. 2013;244–245:121–129. DOI: 10.1016/J.JHAZMAT.2012.11.020.

[191] Sun B, Li X, Zhao R, et al. Hierarchical aminated PAN/γ–AlOOH electrospun composite nanofibers and their heavy metal ion adsorption performance. J Taiwan Inst Chem Eng. 2016;62:219–227. DOI: 10.1016/J.JTICE.2016.02.008.

[192] Lee JJL, Ang BC, Andriyana A, Shariful MI, Amalina MA. Fabrication of PMMA/zeolite nanofibrous membrane through electrospinning and its adsorption behavior. J Appl Polym Sci. 2017;134 (6):44450. DOI: 10.1002/APP.44450.

[193] Ghani M, Rezaei B, Ghare Aghaji A, Arami M. Novel Cross-linked Superfine Alginate-Based Nanofibers: Fabrication, Characterization, and Their Use in the Adsorption of Cationic and Anionic Dyes. Adv Polym Technol. 2016;35(4):428–438. DOI: 10.1002/ADV.21569.

[194] Wang J, Sun Y, Feng J, Xin L, Ma J. Degradation of triclocarban in water by dielectric barrier discharge plasma combined with TiO2/activated carbon fibers: Effect of operating parameters and byproducts identification. Chem Eng J. 2016;300:36–46. DOI: 10.1016/J.CEJ.2016.04.041.

[195] Rosman N, Salleh WNW, Mohamed MA, Jaafar J, Ismail AF, Harun Z. Hybrid membrane filtration-advanced oxidation processes for removal of pharmaceutical residue. J Colloid Interface Sci. 2018;532:236–260. DOI: 10.1016/J.JCIS.2018.07.118.

[196] Gaya UI, Abdullah AH. Heterogeneous photocatalytic degradation of organic contaminants over titanium dioxide: A review of fundamentals, progress and problems. J Photochem Photobiol C Photochem Rev. 2008;9(1):1–12. DOI: 10.1016/J.JPHOTOCHEMREV.2007.12.003.

[197] Nor NAM, Jaafar J, Ismail AF, et al. Preparation and performance of PVDF-based nanocomposite membrane consisting of TiO2 nanofibers for organic pollutant decomposition in wastewater under UV irradiation. Desalination. 2016;391:89–97. DOI: 10.1016/J.DESAL.2016.01.015.

[198] Konstantinou IK, Sakkas VA, Albanis TA. Photocatalytic degradation of propachlor in aqueous TiO 2 suspensions. Determination of the reaction pathway and identification of intermediate products by various analytical methods. Water Res. 2002;36:2733–2742.

[199] Liu H, Yang J, Liang J, Huang Y, Tang C. ZnO nanofiber and nanoparticle synthesized through electrospinning and their photocatalytic activity under visible light. J Am Ceram Soc. 2008;91 (4):1287–1291. DOI: 10.1111/J.1551-2916.2008.02299.X.

[200] Mohamed MA, Salleh WNW, Jaafar J, Ismail AF, Abd Mutalib M, Jamil SM. Incorporation of N-doped TiO2 nanorods in regenerated cellulose thin films fabricated from recycled newspaper as a green portable photocatalyst. Carbohydr Polym. 2015;133:429–437. DOI: 10.1016/J.CARBPOL.2015.07.057.

[201] Jallouli N, Elghniji K, Trabelsi H, Ksibi M. Photocatalytic degradation of paracetamol on TiO2 nanoparticles and TiO2/cellulosic fiber under UV and sunlight irradiation. Arab J Chem. 2017;10: S3640–S3645. DOI: 10.1016/J.ARABJC.2014.03.014.

[202] Kayaci F, Ozgit-Akgun C, Donmez I, Biyikli N, Uyar T. Polymer-inorganic core-shell nanofibers by electrospinning and atomic layer deposition: Flexible nylon-ZnO core-shell nanofiber mats and their photocatalytic activity. ACS Appl Mater Interfaces. 2012;4(11):6185–6194. DOI: 10.1021/AM3017976/ASSET/IMAGES/LARGE/AM-2012-017976_0009.JPEG.

[203] Zhang P, Shao C, Zhang Z, et al. TiO2@carbon core/shell nanofibers: Controllable preparation and enhanced visible photocatalytic properties. *Nanoscale*. 2011;3(7):2943–2949. DOI: 10.1039/C1NR10269A.

[204] Liu L, Liu Z, Bai H, Sun DD. Concurrent filtration and solar photocatalytic disinfection/degradation using high-performance Ag/TiO2 nanofiber membrane. Water Res. 2012;46(4):1101–1112. DOI: 10.1016/J.WATRES.2011.12.009.

[205] Peng LG, Wang H, Liu J, et al. Fabrication of fibrous BiVO4/Bi2S3/MoS2 heterojunction and synergetic enhancement of photocatalytic activity towards pollutant degradation. J Solid State Chem. 2021;299:122195. DOI: 10.1016/J.JSSC.2021.122195.

[206] Yang L, Li L, Li L, et al. N/Fe/Zn co-doped $TiO_2$ loaded on basalt fiber with enhanced photocatalytic activity for organic pollutant degradation. RSC Adv. 2021;11(9):4942–4951. DOI: 10.1039/D0RA10102H.

[207] Zhang Y, Xiong M, Sun A, et al. MIL-101(Fe) nanodot-induced improvement of adsorption and photocatalytic activity of carbon fiber/TiO2-based weavable photocatalyst for removing pharmaceutical pollutants. J Clean Prod. 2021;290:125782. DOI: 10.1016/J.JCLEPRO.2021.125782.

[208] Zhang Y, Luo L, Shi Z, et al. Synthesis of MoS2/CdS Heterostructures on Carbon-Fiber Cloth as Filter-Membrane-Shaped Photocatalyst for Purifying the Flowing Wastewater under Visible-Light Illumination. ChemCatChem. 2019;11(12):2855–2863. DOI: 10.1002/CCTC.201900542.

[209] Song J, Wu X, Zhang M, et al. Highly flexible, core-shell heterostructured, and visible-light-driven titania-based nanofibrous membranes for antibiotic removal and E. coil inactivation. Chem Eng J. 2020;379:122269. DOI: 10.1016/J.CEJ.2019.122269.

[210] Chen Y, Lu W, Wang X, Chen W. Graphitic carbon nitride embedded in hot-melt adhesive polyester and hydrophilic cellulose blend fibers for the efficient elimination of antibiotics under solar irradiation. Appl Surf Sci. 2018;453:110–119. DOI: 10.1016/J.APSUSC.2018.04.188.

[211] Zhao J, Chen J, Chen Z, Zhang Y, Xia D, Wang Q. Flexible cotton fabrics/PDA/BiOBr composite photocatalyst using bioinspired polydopamine as electron transfer mediators for dye degradation and Cr(VI) reduction under visible light. Colloids Surf A Physicochem Eng Asp. 2020;593:124623. DOI: 10.1016/J.COLSURFA.2020.124623.

[212] Caschera D, Federici F, de Caro T, et al. Fabrication of Eu-TiO2 NCs functionalized cotton textile as a multifunctional photocatalyst for dye pollutants degradation. Appl Surf Sci. 2018;427:81–91. DOI: 10.1016/J.APSUSC.2017.08.015.

[213] Chen X, Xu X, Cui J, et al. Visible-light driven degradation of tetracycline hydrochloride and 2,4-dichlorophenol by film-like N-carbon@N-ZnO catalyst with three-dimensional interconnected nanofibrous structure. J Hazard Mater. 2020;392:122331. DOI: 10.1016/J.JHAZMAT.2020.122331.

[214] Zhang Y, Duoerkun G, Shi Z, et al. Construction of TiO2/Ag3PO4 nanojunctions on carbon fiber cloth for photocatalytically removing various organic pollutants in static or flowing wastewater. J Colloid Interface Sci. 2020;571:213–221. DOI: 10.1016/J.JCIS.2020.03.049.

[215] Zhu X, Dai Z, Xu K, et al. Fabrication of multifunctional filters via online incorporating nano-TiO2 into Spun-Bonded/Melt-Blown nonwovens for air filtration and toluene degradation. Macromol Mater Eng. 2019;304(12):1900350. DOI: 10.1002/MAME.201900350.

[216] Kang KC, Kim SS, Choi JW, Kwon SH. Sorption of Cu2+ and Cd2+ onto acid- and base-pretreated granular activated carbon and activated carbon fiber samples. J Ind Eng Chem. 2008;14(1):131–135. DOI: 10.1016/J.JIEC.2007.08.007.

[217] Zhang S, yan LX, Chen JP. Preparation and evaluation of a magnetite-doped activated carbon fiber for enhanced arsenic removal. Carbon N Y. 2010;48(1):60–67. DOI: 10.1016/J.CARBON.2009.08.030.

[218] Li Z, Jia Z, Ni T, Li S. Adsorption of methylene blue on natural cotton based flexible carbon fiber aerogels activated by novel air-limited carbonization method. J Mol Liq. 2017;242:747–756. DOI: 10.1016/J.MOLLIQ.2017.07.062.

[219] Tu L, Duan W, Xiao W, Fu C, Wang A, Zheng Y. Calotropis gigantea fiber derived carbon fiber enables fast and efficient absorption of oils and organic solvents. Sep Purif Technol. 2018;192:30–35. DOI: 10.1016/J.SEPPUR.2017.10.005.

[220] Wang B, Karthikeyan R, Lu XY, Xuan J, Leung MKH. Hollow carbon fibers derived from natural cotton as effective sorbents for oil spill cleanup. Ind Eng Chem Res. 2013;52(51):18251–18261. DOI: 10.1021/IE402371N/SUPPL_FILE/IE402371N_SI_001.PDF.

[221] Jiao Y, Wan C, Li J. Synthesis of carbon fiber aerogel from natural bamboo fiber and its application as a green high-efficiency and recyclable adsorbent. Mater Des. 2016;107:26–32. DOI: 10.1016/J.MATDES.2016.06.015.

[222] Bi H, Yin Z, Cao X, et al. Carbon fiber aerogel made from raw cotton: A novel, efficient and recyclable sorbent for oils and organic solvents. Adv Mater. 2013;25(41):5916–5921. DOI: 10.1002/ADMA.201302435.

[223] Liang HW, Cao X, Zhang WJ, et al. Robust and highly efficient free-standing carbonaceous nanofiber membranes for water purification. Adv Funct Mater. 2011;21(20):3851–3858. DOI: 10.1002/ADFM.201100983.

[224] Fronczak M, Kowalik M, Bystrzejewski M. Carbon fibers obtained from flax and their adsorption performance in the removal of Cu(II) and Co(II) from aqueous solutions. Chem Select. 2018;3(28):8259–8269. DOI: 10.1002/SLCT.201801079.

[225] Zhao D, Yu Y, Chen JP. Fabrication and testing of zirconium-based nanoparticle-doped activated carbon fiber for enhanced arsenic removal in water. RSC Adv. 2016;6(32):27020–27030. DOI: 10.1039/C5RA25030G.

[226] Senthilkumaar S, Varadarajan PR, Porkodi K, Subbhuraam CV. Adsorption of methylene blue onto jute fiber carbon: kinetics and equilibrium studies. J Colloid Interface Sci. 2005;284(1):78–82. DOI: 10.1016/J.JCIS.2004.09.027.

[227] Kumar Gupta A, Deva D, Sharma A, Verma N. Adsorptive removal of fluoride by micro-nanohierarchal web of activated carbon fibers. DOI: 10.1021/ie801688k.

[228] Zheng W, Hu J, Han Z, et al. Interactions of Cr(VI) with hybrid anion exchange/porous carbon fibers in aqueous solution at natural pH. Chem Eng J. 2016;287:54–61. DOI: 10.1016/J.CEJ.2015.10.064.

[229] Zhao D, Yu Y, Chen JP. Fabrication and testing of zirconium-based nanoparticle-doped activated carbon fiber for enhanced arsenic removal in water. RSC Adv. 2016;6(32):27020–27030. DOI: 10.1039/C5RA25030G.

[230] Chen L, Chen N, Wu H, et al. Flexible design of carbon nanotubes grown on carbon nanofibers by PECVD for enhanced Cr(VI) adsorption capacity. Sep Purif Technol. 2018;207:406–415. DOI: 10.1016/J.SEPPUR.2018.06.065.

[231] Li S, Jia Z, Li Z, Li Y, Zhu R. Synthesis and characterization of mesoporous carbon nanofibers and its adsorption for dye in wastewater. Adv Powder Technol. 2016;27(2):591–598. DOI: 10.1016/J.APT.2016.01.024.

[232] Wang Q, Lei X, Pan F, et al. A new type of activated carbon fibre supported titanate nanotubes for high-capacity adsorption and degradation of methylene blue. Colloids Surf A Physicochem Eng Asp. 2018;555:605–614. DOI: 10.1016/J.COLSURFA.2018.07.016.

[233] Yan X, Yao Y, Zhang H, et al. Zeolitic imidazolate framework (ZIF-8)/polyacrylonitrile derived millimeter-sized hierarchical porous carbon beads for peroxymonosulfate catalysis. Environ Res. 2022;206:112618. DOI: 10.1016/J.ENVRES.2021.112618.

Amarpreet K. Bhatia, Shippi Dewangan*

# Chapter 6
# Advanced fiber materials in energy applications

**Abstract:** Energy generation from conventional fossil fuels has been identified as the main culprit of environmental quality degradation and environmental pollution. In order to address these issues, nanotechnology plays an essential role in revolutionizing the device applications for energy conversion and storage, environmental monitoring as well as green engineering of environmental friendly materials. Fiber materials like carbon nanotubes(CNTs) and their hybrid nanocomposites have received immense research attention for their potential applications in various fields due to their unique structural, electronic and mechanical properties. In this chapter, the contribution of CNTs is addressed in terms of energy generation, conversion and storage such as in supercapacitors, and renewable energy technologies. Integration of carbon nanotubes in solar cells has increased the energy conversion efficiency of these energy conversion applications, which serve as the future sustainable energy sources. Based on the literature studied, CNTs pose a great potential as a promising material for application in various environmental fields.

**Keywords:** Energy, carbon nanotubes, energy conversion, supercapacitors, renewable energy

## 6.1 Introduction

### 6.1.1 General overview about energy problem

The energy crisis during the 1970s sparked the development of renewable energy sources and energy conservation measures. As supply eventually met demand, these programs were scaled back. Ten years later, the hazards of pollution led to work on minimization and reversal of the environmental impact of fossil fuel extraction, transport and consumption [1, 2]. Over recent years, the world's energy consumption has dramatically increased because of the rapidly growing global population, improving standards of living and development of modern technologies. The US Department of

---

***Corresponding author: Shippi Dewangan,** Department of Chemistry, SW Pukeshwar Singh Bhardiya Govt. College, Nikum, Durg, 491221, Chhattisgarh, India, e-mail: shippidewangan2729@gmail.com
**Amarpreet K. Bhatia,** Department of Chemistry, Bhilai Mahila Mahavidyalaya, Bhilai Nagar, 490006, Chhattisgarh, India

https://doi.org/10.1515/9783110992892-006

Energy predicts that the world's energy demands will double by 2050 and triple by 2100. The current world energy production of ≈16.4 TW is principally met by burning fossil fuels. Damage to the environment by the fuel-burning process has become a serious problem. This has the potential for disastrous consequences, and solutions need to be pursued with urgency. Considerable developments have been made in this respect, including energy technologies based on wind power, biofuels, solar cells and fuel cells [3].

The growing concerns over the constant use of fossil fuels and its effect on climate change [4] has once again spurred research on sustainable energy development and on enhancement in renewable energy systems. Advances in energy generation, storage and conversion systems that will make our energy usage more efficient are essential if we are to meet the challenge of global warming and the finite nature of fossil fuels [4, 5]. The need for the development of efficient energy generation and storage systems is paramount in meeting the world's future energy targets, especially when energy costs are on the increase and more people need access to electricity [6, 7]. Energy generation and storage technologies can improve efficiency in supply systems by storing the energy when it is in excess, and then release it at a time of high demand [6]. Further material progression in research and development fundamentals, as well as engineering improvements need to be continued in order to create energy generation and storage systems that will help alleviate humanities energy generation, storage and conversion dilemmas. Low-grade heat (around 130 °C) is a by-product of almost all human activity, especially when energy conversion is involved. It is also known as "waste heat" because the dissipated heat into the environment is unutilized. Progress in the field of thermal energy conversion can lead to effective use of limited fossil fuels and provide supplemental power to current energy conversion systems [1]. This chapter will thus focus on the application of carbon nanotubes' (CNT) energy generation, conversion and storage such as in supercapacitors and renewable energy technologies.

### 6.1.2 Carbon nanotubes can address the issues of energy generation, storage and conversion

Nanostructured materials are of great interest in the energy generation, storage and conversion field due to their favorable mechanical and electrical properties [5, 8]. CNTs are one type of nanostructured material that possess these favorable electrical and mechanical properties due to the confinement of one dimension, combined with the surface properties that contribute to the enhanced overall behavior. The potential of nanostructured materials is not only limited to energy storage and conversion devices; but also to nanotransistors [9, 10], actuators [9, 10], electron field emission [9, 10], and biological sensing devices [11, 12]. The use of carbon-based nanomaterials as electrode materials is practical and economically viable because cheap carbon precursor materials are abundant [13]. As the research into CNTs has increased over the last 20 years, the cost of these materials has significantly reduced alongside improvements in processability and scalability [14]. The advantage of incorporating carbon materials and specifically CNTs as part of the electrode material is their excellent mechanical and electrical properties. They provide mechanical support to the substrate while enhancing the conductive and electrochemical properties. The low cost of the carbon precursor material used to synthesize CNTs makes device fabrication scalable and economically viable [15]. CNT assemblies can have extremely high specific surface areas, which are extremely important in capacitor design. CNT electrode materials can be confined to a smaller area increasing the electrode–electrolyte contact and decreasing the weight of the device therefore maximizing the overall gravimetric performance of the device [16]. CNTs are also chemically stable, which enhances the resistance to degradation of the electrode surface [1, 17].

Since the discovery of CNTs, they have eventually revolutionized the future nanotechnologies area. CNTs as reported by Sumio Iijima [18] and Bethune et al. [19] are seamless cylinder-shaped macromolecules with a radius as small as a few nanometers, and up to several micrometers in length. The walls of these tubes are constructed of a hexagonal lattice of carbon atoms and capped by fullerene-like structures. The unique structure of CNTs can be divided mainly into multiwalled CNTs (MWNTs) and single-walled CNTs (SWNTs). MWNTs are composed of two or more concentric cylindrical shells of graphene sheets coaxially arranged around a central hollow area with spacing between the layers. In contrast, SWNTs are made of a single cylinder graphite sheet held together by van der Waals bonds [20]. Current synthesis techniques including electric arc discharge, laser ablation and chemical vapor decomposition (CVD) are used commercially to produce large quantities of CNTs. CNTs' mutable hybridization states and sensitivity of the structure to perturbations in synthesis conditions exploit their unique physical, chemical and electronic properties (as shown in Table 6.1) [20, 21], which inspire innovation in new technologies and applications. Moreover, these unique

**Table 6.1:** Theoretical and experimental properties of CNTs [20, 21].

| S. no. | Properties | SWNTs | MWNTs |
|---|---|---|---|
| 1 | Specific gravity | 0.8 g/cm$^3$ | 1.8 g/cm$^3$ |
| 2 | Specific surface area | ~400–900 m$^2$/g | ~200–400 m$^2$/g |
| 3 | Thermal stability | >700 °C (in air)<br>2,800 °C (in vacuum) | >700 °C (in air)<br>2,800 °C (in vacuum) |
| 4 | Thermal conductivity | 3,000 W/m K | 3,000 W m$^{-1}$ K$^{-1}$ |
| 5 | Strength | 50–500 GPa | 10–60 GPa |
| 6 | Elastic modulus | ~1 TPa | ~0.3–1 TPa |
| 7 | Resistivity | 5–50 μΩ cm | 5–50 μΩ cm |

and tunable properties offer potential advances in environmental systems from proactive (prevention of environmental degradation, optimizing energy efficiency) to retroactive (waste water reuse, pollutant transformation) [20].

## 6.2 Supercapacitors

### 6.2.1 General overview

Electrical energy can be stored in two different forms and can best be described when considering a battery and a capacitor. In a battery, it is the available chemical energy through the release of charges that performs work when two electroactive species undergo oxidation and reduction [22]; this is termed as Faradaic reaction. In a capacitor, electrostatic forces between two oppositely charged plates will separate charge. The generated potential is due to an excess and deficiency of electron charges between the two plates without charge transfer taking place [17]. The current that is observed can be considered as a displacement current due to the rearrangement of charges [4]; this effect is termed as non-Faradaic in nature.

### 6.2.2 Supercapacitor types and its operation mechanism

There are two types of electrochemical capacitors that are referred to as (1) electric double-layer capacitors (EDLC) and (2) pseudo-capacitors. The construction of these devices can vary, with electrodes being fabricated from porous carbon materials including activated carbons, graphene, CNTs, templated carbons, metal oxides, and conducting polymers [1]. EDLC or supercapacitors have two electrodes immersed in an electrolyte solution, separated by a semipermeable dielectric that allows the movement of ions to complete the circuit but prevents a short circuit from being formed. EDLCs are advantageous as they are able to provide relatively large power densities and larger energy densities than conventional capacitors, and long life cycles compared to that of a battery and ordinary capacitor [1]. The performance of supercapacitors is affected by the power density requirements, high electrochemical stability, fast charge/discharge phenomena and low self-discharging [1]. Table 6.2 [1] shows a comparison between the three types of devices. Energy storage is achieved by the buildup and separation of electrical charge that is accumulated on two oppositely charged electrodes as shown in Figure 6.1 [1, 13].

As stated previously, no charge transfer takes place across the electrode–electrolyte interface and the current that is measured is due to a rearrangement of charges. The electrons involved in the non-Faradaic electrical double-layer charging are the conduction band electrons of the electrode. These electrons leave or enter the conduction band state

**Table 6.2:** Comparison of key parameters for a capacitor, supercapacitor, and battery [1].

| S. no. | Parameters | Capacitor | Supercapacitor | Battery |
|---|---|---|---|---|
| 1 | Charge time | $10^{-6}$–$10^{-3}$ s | 1–30 s | 0.3–3 h |
| 2 | Discharge time | $10^{-6}$–$10^{-3}$ s | 1–30 s | 1–5 h |
| 3 | Cycle life | >500,000 | >100,000 | 500–2,000 |
| 4 | Power density (W/kg) | >10,000 | 1,000–2,000 | 50–200 |
| 5 | Charge/discharge efficiency | ≈1 | 0.90–0.95 | 0.7–0.85 |
| 6 | Energy density (Wh/kg) | <0.1 | 1–10 | 20–100 |

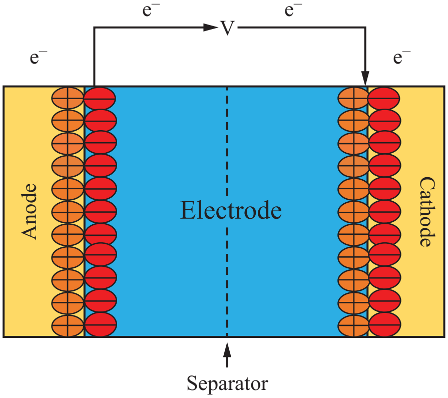

**Figure 6.1:** Schematic diagram of an EDLC supercapacitor with a positive and negative electrode, separator and porous carbon [1, 13].

depending on the energy of the least tightly bound electrons or the Fermi level of the system [1, 4]. Supercapacitors exhibit very high energy storage efficiencies exceeding 95% and are relatively stable for up to $10^4$–$10^5$ cycles [6, 7]. The energy given by the equation, $E = 0.5CV^2$, means that the operating voltage is the key in determining the energy characteristics of a supercapacitor. The choice of electrolyte when designing and fabricating a supercapacitor device dictates the operating voltage [23–24]. Operating voltages are approximately 1.2, 2.7 and 3.5 V, respectively, for aqueous, organic and ionic liquid with all of them having associated advantages and disadvantages [6, 7].

Like EDLC, a pseudo-capacitor consists of two porous electrodes with a separator between them all immersed in an electrolyte solution [25]. However, the difference is that the charge is accumulated during Faradaic reactions near to or at the surface of the electrodes [26]; hence, non-Faradaic double-layer charging and Faradaic surface processes occur simultaneously [27]. The pseudo-capacitance arises from a Faradaic reaction when some of the charge ($q$) passed in an electrode process is related to the electrode potential ($V$) via thermodynamical considerations. The two principal cases are adsorption pseudo-capacitance arising under potential deposition processes, and homogeneous redox pseudo-capacitance where the reaction is reversible. Pseudocapacitors thus combine features of both capacitors and batteries. Current commercial uses of supercapacitors include personal electronics, mobile telecommunications, back-up power storage, and industrial power and energy management. A recent application is the use of supercapacitors in emergency doors on the Airbus A380, highlighting their safe and reliable performance [1].

## 6.3 Carbon nanotube

### 6.3.1 General overview

CNTs were first discovered in 1953 through research in the Soviet Union, but the first accessible results were by Sumio Iijima [18] as a result of research into buckminster fullerenes. CNTs have a cylindrical shape that can be considered as a graphene sheet rolled up; either individually as SWNT, or concentrically as MWNT. However, these sheets can have varying degrees of twist along their length that can lead to the nanotubes to be either metallic or semiconducting as the change in chiralities induces different orbital overlaps [10]. They exhibit remarkable electrical transport and mechanical properties [8], which is why interest and research into this material has increased over the last two decades. CNT powders have the potential to be tailored to specific energy storage and conversion applications with their being an added advantage that they can be used in all electrolyte environments that encompass aqueous, organic and ionic liquids [28].

### 6.3.2 CNT synthesis overview

There are a variety of different methods for making SWNTs and MWNTs that have been developed since CNTs were first discovered. These include laser ablation, arc discharge, chemical vapor deposition (CVD), and high-pressure carbon monoxide disproportionation (HiPCO). Recently, work by Harris et al. has successfully scaled up the synthesis of CNT using a fluidized bed reactor [29]. All growing conditions for synthesizing CNTs require a catalyst to achieve high yields, where the size of the catalyst nanoparticles will determine the diameter and chirality of the CNT. The CNTs that are formed are generally in a mixture with other carbonaceous product including amorphous carbon and graphitic nanoparticles [1].

### 6.3.3 Main synthesis methods for CNT growth

Both laser ablation and arc-discharge methods for the growth of CNTs involve the condensation of carbon atoms generated from the evaporation of carbon sources. High temperature is involved, ranging from 3,000 to 4,000 °C [30]. In arc discharge, various gases such as helium or hydrogen are induced into plasma by large currents generated at a carbon anode and cathode. This process leads to the evaporation of carbon atoms which produces very high quality MWNTs and SWNTs [31, 32]. Laser ablation also produces very high quality CNTs with a high degree of graphitization by focusing a $CO_2$ laser (in pulsed or in continuous-wave mode) for a period of time onto a rotating carbon target. The HiPCO process utilizes clusters of Fe particles as catalysts to create very high quality SWNTs. Catalyst is formed in situ by thermal decomposition of iron pentacarbonyl, which is delivered intact within a cold CO flow and then rapidly mixed with hot CO in the reaction zone. Upon heating, the $Fe(CO)_5$ decomposes into atoms that condense into larger clusters. SWNTs nucleate and grow on these particles in the gas phase. The CVD method usually consists of a furnace, catalyst material, carbon source, a carrier gas, a conditioning gas and a collection device (usually a substrate). The carrier gas is responsible for taking the reacting material onto the substrate where CNT growth occurs at catalyst sites [1]. The components mentioned are essential; however, different groups and researchers have alternative experimental conditions which can contain multiple types of furnaces, and a variety of catalyst and carbon sources. The key advantage of this technique is its capability to directly deposit the CNTs onto the substrate, unlike arc discharge and laser ablation that produces a soot/powder. Recent developments by Liu et al. [29] have led to the development of a large scale batch process for fabricating MWNTs. Here, a furnace-like system called a fluidized bed reactor continuously flows a carrier gas over a porous alumina powder that is impregnated with the catalyst material, leading a to continuous creation of MWNTs where tens of grams can be synthesized in one run [1, 29].

### 6.3.4 Single-walled nanotubes

SWNTs have been studied extensively as a supercapacitor and hybrid energy material [1, 6]. The structure of an SWNT is of a cylindrical nature apparent as previously stated. Its advantage is that it has very good thermal and conductive properties where the thermal conductivity can exceed 6,000 W/m K and a potential current-carrying capacity of 109 $A/cm^2$ [1]. The maximum reported gravimetric capacitance for SWNT fabricated electrodes (PVA/PVC binder; pressed into pellet) is 180 F/g with an energy density of 7 Wh/kg and a power density of 20 kW/kg using KOH electrolyte [1]. Hu et al. [33] have recently reported a solid-state paper-based SWNT supercapacitor, which has a specific capacitance of 115 F/g, energy density of 48 Wh/kg and a large operating voltage of 3 V. The electrode preparation involved pre-processing where cotton sheets were immersed in the SWNT dispersion, annealed, then immersed in a PVA/$H_3PO_4$ electrolyte [1, 33].

### 6.3.5 Multiwalled nanotubes

Like their SWNT counterparts, MWNTs have also been studied extensively as electrode materials for supercapacitors [1, 6]. The advantages over SWNTs are their ability to be more easily synthesized on much larger scales, making them more suitable for commercial application. The maximum gravimetric capacitance attained for electrodes constructed from MWNTs range between 4 and 140 F/g with the best available commercial result at 130 F/g from Maxwell's Boost capacitor [34]. Wang et al. [35] have recently reported partially exfoliated MWNTs on carbon cloth that gave a specific capacitance in the range of 130–165 F/g with a coulombic efficiency of 98%.

### 6.3.6 Surface functionalities

The presence of surface functionalities such as oxygen, nitrogen, hydrogen, boron and catalyst nanoparticles (dependent on the synthesis environment and precursor materials) can affect the capacitive behavior of the electrode through the introduction of Faradaic reactions [1], changes in electric and ionic conductivity [25], and influencing wettability [1]. A schematic representation of $sp^2$ hybridized carbon lattice with various dopants is shown in Figure 6.2 [1].

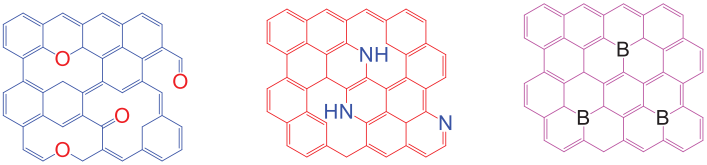

**Figure 6.2:** Schematic representation of a $sp^2$-hybridized carbon lattice that has been doped with (a) oxygen functional groups, (b) nitrogen functional groups and (c) boron [1].

#### 6.3.6.1 Oxygen

Carbon materials will have functional groups present on their surface as a result of the precursors and preparation conditions [24]. Most of these functional groups are in the form of -COOH, =CO as well as phenol, quinone and lactone groups [6, 24]. Activation procedures such as posttreatment with $H_2SO_4$ and/or $HNO_3$ also leads to acid oxygen functionalities [6]. Most of these groups are bonded with carbon atoms at the edge of hexagonal carbon layers where Faradaic reactions (via interactions with the electrolyte) lead to pseudo-capacitance such as those developed with transition metal oxides $RuO_2$ and $MnO_2$ [1, 24]. These functional groups can also be purposely added onto the surface of carbons via oxidation with $O_2$ or acid treatment with $HNO_3$ or $H_2SO_4$ [1]. In aqueous systems, the presence of oxygen containing functional groups can lead to an enhanced wettability as well as pseudo-capacitance as mentioned earlier, which maximizes the electroactive surface area leading to larger energy densities [9, 24]. It has been proposed that the pseudo-capacitative reactions for oxygen-functionalized CNTs involve carboxyl groups undergoing electron transfer [36]:

$$\mathrm{C-OH} \rightarrow \mathrm{C=O} + \mathrm{H}^+ + e^-$$

$$\mathrm{C=O} + e^- \rightarrow \mathrm{C-O}^-$$

In nonaqueous systems, however, oxygen functionalities are detrimental to device performance. Parasitic redox reactions can lead to a degradation of the electrode, as well as adverse effects relating to voltage proofing and increased leakage current [1, 6]. These redox reactions will reduce the cycle life of a device, as well as lowering the operating voltage. Shen et al. [37] reported in 2011 the effects of changing the carboxylic group concentration on SWNTs. The specific capacitance, power density and energy density 0.5 M $H_2SO_4$ electrolyte increased with carboxylic group density reaching a maximum of 149.1 F/g, 304.8 kW/kg and 20.71 Wh/kg, respectively. The 10 μm film electrodes were fabricated using vacuum filtration to create “Bucky papers” onto a mixed cellulose estate membrane [1, 37].

#### 6.3.6.2 Nitrogen

Nitrogen-containing carbons have recently attracted interest due to its n-type behavior that promotes large pseudo-capacitance, which can be obtained even if the surface area of the material is decreased [38]. In some instances, up to 3-fold increase in capacitance have been reported [39]. Typical examples of redox reactions involving nitrogen are described [40]:

$$\mathrm{C + NH} + 2e^- + 2\mathrm{H}^+ \leftrightarrow \mathrm{CH_2 - NH_2}$$

$$\mathrm{CH - NHOH} + 2e^- + 2\mathrm{H}^+ \leftrightarrow \mathrm{CH_2 - NH_2 + H_2O}$$

The chosen precursor material affects the types of functionalities that are attached to the carbon backbone. Nitrogen-containing groups may be added via various methods with compounds containing nitrogen including treatment with urea, melamine, aldehyde resins and polyacylonitrile [1, 6]. Surface areas for nitrogen-doped carbon materials are thought to be in excess of 400 $m^2/g$ [24]. This is much lower than pure SWNTs and pure MWNTs that have been reported to attain a surface area greater than 1,315 and 830 $m^2/g$, respectively, suggesting that pseudo-capacitance makes up a substantial portion of the total capacitance [1]. Zhang et al. [41] have showed that N-doped MWNTs synthesized via CVD growth exhibited a capacitance of 44.3 F/g, which was more than twice the value obtained than that of the un-doped MWNTs in a 6 M KOH electrolyte. Lee et al. [42] have shown that the nitrogen content on vertically aligned CNTs increases the capacitance until a certain point due to an increased donation of an electron by the N (N acts as an n-type dopant) and an enhanced wettability in aqueous systems. Excessive N-doping significantly reduced the conductivity and inhibited charge storage and delivery. The doped and undoped CNTs were directly grown onto a stainless steel substrate using CVD [42].

#### 6.3.6.3 Boron

Boron is another interesting material for doping CNTs due to its p-type nature which promotes CNT growth and increases the oxidation temperature of the nanotubes [43]. However, the development of boron-doped CNTs for the use as electrodes in supercapacitor devices is not well established [24]. Work by Shiraishi et al. [44] showed that boron doping MWNTs increased the capacitance per surface area from 6.5 to 6.8 $\mu F/cm^2$ in 0.5 M $LiBF_4/PC$ [44]. These electrodes were once again synthesized using CVD [44]. Wang et al. [45] reported that interfacial capacitance was increased by 1.5–1.6 times in boron-doped carbon than that in boron-free carbon with alkaline electrolyte (6 M KOH) and/or acid electrolyte (1 M $H_2SO_4$) [45]. The carbon material was made into a slurry using carbon black and PTFE binder and pasted onto a Ni mesh current collector [45].

### 6.3.7 Advantages, limitations and comparison

It can be seen that CNTs can be tailored in different ways in order to tune (to a degree) the performance of the electrode material. This control has been demonstrated by firstly, varying the chirality of the nanotube to produce the single-walled or the multiwalled variety. Both CNT types have associated advantages and disadvantages with SWNTs being able to be synthesized with a high degree of purity, while MWNTs can be synthesized on a larger scale [1]. CNTs can also have functionalities (through addition of oxygen or nitrogen containing groups) added to their structure through treatment in order to change the surface properties and hence wettability of the material. These functionalities enable enhanced compatibility to an electrolyte to maximize electroactive surface area usage and hence performance. Further doping with specific elements such boron and nitrogen can introduce a p-type/n-type behavior where electrons contribute a Faradaic response to the system and enhance capacitance and energy density [1]. However, it must be noted that when faradaic processes occur at the electrode/electrolyte interface, irreversible processes increase degradation of the electrode over time. Specific capacitance of CNTs (three electrode and device testing) is in the order of 5–165 F/g with an increase thereafter as a result of doping (i.e., due to Faradaic contribution). It must be pointed out that with electrical energy devices, there is always a trade-off between energy and power density. Therefore the electrode material has to be tailored to meet the requirements of the specific application [1].

## 6.4 Templated porous carbons

Templated porous carbons are of recent great interest in the field of energy storage due to the tenability in porosity, which is necessary to meet the materials application requirements [46, 47]. These templated carbons are commonly known as carbide-derived carbons (CDC) as the carbon materials are derived from carbon precursors through physical and/or chemical processes [46]. Briefly, the synthesis involves halogenations (usually chlorination) where the carbon is formed by selective extraction of the metal and metalloid atoms, transforming the carbide structure into pure carbon. The carbon layer is formed by inward growth, with retention of the original shape and volume of the precursor [46]. If any metal chlorides are trapped, they can be usually removed by hydrogenation or vacuum annealing [46]. The general reaction scheme is as follows where M = Si, Ti, Zr [24, 46]

$$\mathrm{MC(s) + 2Cl_2(g) \rightarrow MCl_4(g) + C(s)}$$

The advantage of forming carbon structures this way is the ability to form a tailored and narrow pore size distribution with a large surface area [46–47]. Inagaki et al. [24] in their very comprehensive review of carbon materials for electrochemical capacitors reported a maximum surface area of $S_{BET}$ of 2,000 $m^2/g$ for CDC, which gives rise to possible electrode materials with extremely large energy densities and power densities [24].

## 6.5 Composite electrode materials

Typical carbonaceous electrode materials (activated carbon, CNTs, graphene, CDC) with high surface areas used in supercapacitors have somewhat reached a limit when it comes energy storage capacity, thus restricting their possible applications [48]. Pseudo-capacitor materials that are able to meet the needs of higher energy density are currently being developed and combined with carbonaceous materials in order to create composites that when designed into hybrid supercapacitors have advantages of fast rate capability, high storage capacity, and long cyclability [48, 49].

### 6.5.1 CNT/polymer

Electrode materials comprised inherently conducting polymers (ICPs) and CNTs are promising areas of research. The conductive polymer matrix, combined with the network like structure of the CNTs provides an enhanced electronic and ionic conductivity that can considerably improve charge storage and delivery [50]. Antiohos et al. [51] reported a SWNT/Pedot-PSS composite electrode material that was fabricated into a device which had a specific capacitance of 120 F/g (1 M $NaNO_3/H_2O$), coupled with an excellent stability (~90% capacity retention) over 1,000 cycles using galvanostatic charge/discharge [51]. In SWNT/Pedot-PSS composite, SWNTs are thoroughly dispersed throughout the Pedot-PSS conducting polymer matrix. Kim et al. [52] recently fabricated a ternary composite material consisting of MWNTs, graphene, and PANI where a specific capacitance of 1,118 F/g was achieved. This electrode was stable with 85% capacity retention after 500 cycles using galvanostatic charge/discharge [52]. Hu et al. [53] have recently reported a composite electrode materials containing MWNTs coated with polypyrrole that achieved a high capacitance of 587 F/g in a 0.1 M $NaClO_4$/acetonitrile electrolyte [53].

### 6.5.2 CNT/metal oxide

Metal oxides exhibit pseudo-capacitative behavior over small rages of potentials, through redox processes which contribute electron transfer between the electrode/electrolyte interfaces (Figure 6.3) [1]. Common materials used in the construction of such devices are oxides of Mn, Ru, Ir, Pt, Rh, Pd, Au, Co and W [1]. By combining metal oxides with CNTs, composites can be formed that combine both Faradaic and non-Faradic effects enabling a larger energy density to be obtained while still holding reasonable power density. $MnO_2$ particles that have been formed (insitu) in the presence of MWNTs. Very recent work on carbon/metal oxide composites can be found in the review by Wang et al. [35]. Myoungki et al. [54] reported recently in their a $RuO_2$/MWNT, electrode material which achieved a specific capacitance of 628 F/g [54]. The electrode was fabricated by dispersing the mixture in ethanol and casting onto carbon paper [54]. Li et al. [55] reported that when MWNTs were coated with $MnO_2$, a capacitance of 350 F/g was achieved [55]. More novel materials have been created by incorporating MWNTs and $Co_3O_4$, which yielded specific capacitances of 200 F/g [56] (acetylene black/PVDF slurry on Ni gauze), while Jayalakshmi et al. reported in 2007 $V_2O_5.\ xH_2O$/CNT film with a specific capacitance of 910 F/g with the material being ground into a paste with paraffin and spread onto a graphite electrode and tested in 0.1 M KCl [57].

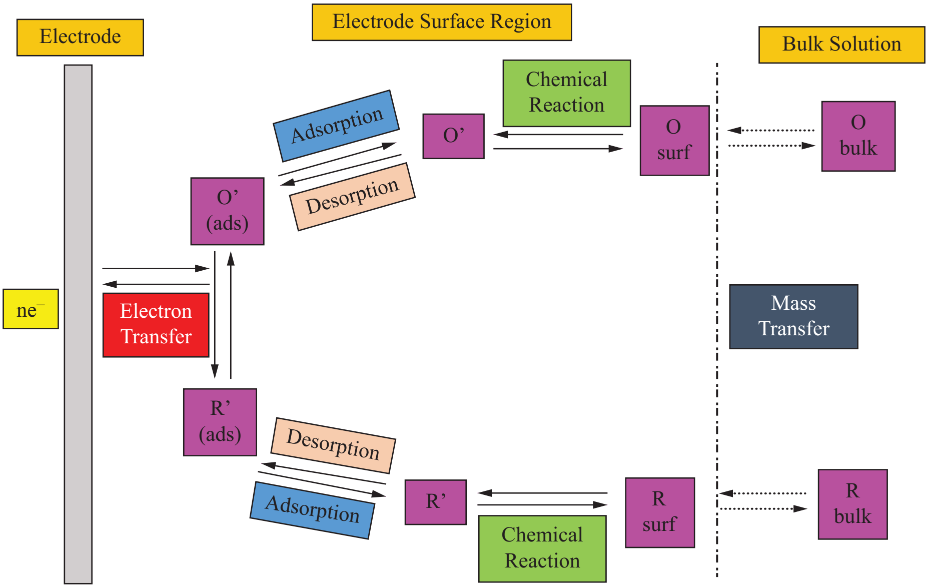
Electrode
Electrode Surface Region
Bulk Solution
Adsorption
Desorption
O’
Chemical Reaction
O surf
O bulk
O’ (ads)
ne⁻
Electron Transfer
Mass Transfer
R’ (ads)
Desorption
Adsorption
R’
Chemical Reaction
R surf
R bulk

**Figure 6.3:** Schematic diagram of a reversible redox reaction, as well as EDLC occurring at the electrode/electrolyte interface leading to pseudo-capacitance [1].

### 6.5.3 CNT/carbons

Creating composite materials from CNT and different forms of carbon such as graphene-derived carbon or CDC can be advantageous due to the fact that the CNTs provide microporosity (large surface area to maximize capacitance and hence energy density); while graphene and CDC can be used to tailor the mesoporosity which improve ions’ kinetics, enhancing the power density [1]. A composite of reduced graphene oxide coated with SWNTs is depicted that has been formed into a porous film. The edges of the graphene oxide protrude out with a uniform coating of SWNTs. Recently, Li et al. [58] fabricated different mass loadings of graphene and CNT composite electrodes by solution casting onto glass, annealing then peeling off. They reported capacitance ranges of 70–110 F/g at a scan rate of 1 mV/s in 1 M $H_2SO_4$ [58]. A CNT/graphene composite which was bound together with polypyrrole (through a filtration process) that achieved a specific capacitance of 361 F/g at a current density of 0.2 A/g in 1 M KCl. The electrode exhibited excellent stability with only a 4% capacity loss over 2000 cycles [58]. Dong et al. [59] have shown that is it possible to form SWNT/graphene oxide core shell structures and spray coat the subsequent material onto a current collector [59]. The performance of these core structures yielded a material with a specific capacitance of 194 F/g using galvanostatic charge/discharge at a high current density of 0.8 A/g in 1 M KOH [59].

## 6.6 Carbon nanotubes in renewable energy

Worldwide consumption of marketed energy is anticipated to increase by 57% between 2004 and 2030 [20]. This phenomenon foresees the requirement for advance renewable energy source technologies in order to meet the long-term energy demand challenge and protect the environmental balance. The major breakthrough contributed by CNTs in the solar energy sector lies in their application in photovoltaic devices. Photovoltaic devices generate electricity through conversion of photons absorbed from the sun. To date, several drawbacks, including high cost and low stability under illumination, have been found for commercially available silicon and semiconductor-based photovoltaic devices [20]. Therefore, CNTs are sought as an alternative material in various solar cell architectures, especially in silicon-based solar cells, organic solar cells, and dye-sensitized solar cells (DSSCs as demonstrated in Figure 6.4) [20], due to their affordability and remarkable energy conversion [20].

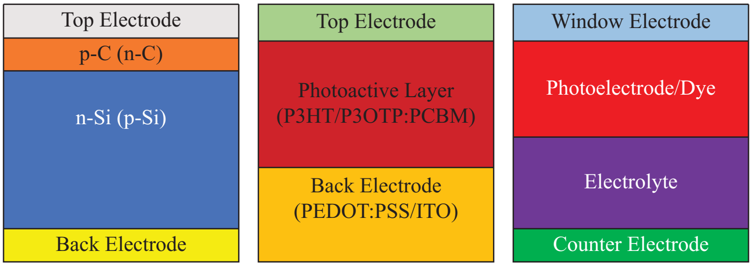

**Figure 6.4:** Basic solar cell architectures: (a) silicon-based solar cell, (b) organic solar cell and (c) dye-sensitized solar cell [20].

The nanoscale active surface area of CNTs also allows massive photon absorption for harvesting solar energy, while the presence of a delocalized π-electron system increases the mobility of the charge transfer [60]. Good alignment between CNTs can further enhance their photoconductivity upon illumination [61]. Silicon-based solar cells utilize the simplest p–n junction to separate electrons/holes and create current upon illumination. CNTs, when incorporated into silicon, serve as a heterojunction component for charge separation, as a highly conductive percolated network for charge transport, and as a transparent electrode for light illumination and charge collection [62]. Therefore, modest cell efficiency with improvement in stability was observed in CNT/Si heterojunctions [63]. As a consequence of being flexible and having low production costs compared with silicon-based solar cells, the development of organic solar cells has attracted a great deal of interest from researchers. Organic solar cells depend on a conductive organic polymer like poly(3-octylthiophene) (P3OT), poly (3-hexylthiophene) (P3HT) or [6]-phenyl-C61-butyric acid methyl ester (PCBM) for light absorption and charge transfer [64]. Current research shows an improvement in efficiency upon incorporation of CNTs in the top electrode, the photoactive layer and the back electrode of organic solar cells [20]. In the photoactive layer, CNTs serve as a photoactive material and optimize the performance of the cells by providing efficient hole or electron transport at the CNT/polymer interface. The photoactive component constructed with P3OT/CNT showed a higher open-circuit voltage by taking advantage of the high electron transport capability of CNTs. In the top and back electrodes, CNTs manage to provide a large surface area for high optical transmittance and low sheet resistance to minimize power loss. Therefore, an increase in photocurrent was observed for the design of a top electrode composed of CNT films and indium-tin oxide (ITO) [20].

DSSCs have been hailed as the promising solar cell for their low cost and simple preparation [65]. Electricity is produced in DSSC when semiconducting materials create an electron–hole pair and transfer the charge through a circuit to a counter electrode in contact with a redox couple in the electrolyte solution. Applying CNTs as photoelectrode can help to increase the mobility of carrier transport upon exposure to visible light. However, direct use of CNTs as photoelectrodes could result in modest efficiency due to ultrafast recombination of photogenerated charge carriers [20]. Hence, Brown et al. [66] suggested CNT/$TiO_2$ as a strategy to improve charge separation and promote charge flow since $TiO_2$ particles present on CNTs are capable of injecting electrons from their excited state. Besides photoelectrodes, CNTs are also a popular choice of materials for DSSC counter electrode fabrication. In addition to enhance conversion efficiency, the cells with CNT counter electrode are expected to afford several advantages including nanoscale conducting channels, lightweight and low cost, as well as improved mechanical properties and thermal stability. The use of a CNT counter electrode in an anthocyanin-sensitized cell showed an efficiency of 1.46%, which is the highest value ever reported compared to a cell using natural dye and platinum counter [67]. Other than solar energy, recent developments in hydrogen storage media have focused on CNTs as one of the ongoing strategic research areas. Hydrogen, a relatively clean fuel compared to conventional fuel, has been considered to be an attractive approach for developing technologies of green energy. The United States Department of Energy (DOE) had targeted minimum hydrogen storage of 6.5 wt% in order to meet the demand of commercial storage requirement [68]. From the investigation on strategies used to achieve hydrogen storage, CNTs have received an exceptional consideration as a potential storage material due to their affordability, recycling characteristics, low density, nanoscale pore size distribution and reasonable chemical stability [20]. Storage of hydrogen in CNTs mainly involves physisorption. Theoretical studies conducted by Wang and Johnson [69] and Dodziuk and Dolgonos [70] showed that the amount of hydrogen adsorbed depends on the nature of the array and orientation of CNTs, with the adsorption of hydrogen being preferred at the outer surface of CNTs rather than the inner core. CNTs, particularly SWNTs, outperform activated carbon for their large bulk density, which enhances volumetric storage. Experimental results indicated that storage of hydrogen in CNTs was lower than 1 wt% at ambient temperature and high pressure but reasonable storage of hydrogen could be achieved at higher pressure and lower temperature [20]. In fact, hydrogen physiosorption alone was inadequate to meet the DOE specification; hence, research has focused in the direction of hybrid CNT/metal compounds to promote chemisorption. Transition or alkali metal-doped CNTs, with s–p–d hybridization served to reinforce the notable increase in hydrogen storage via a spill-over mechanism. A nearly 30% increase in hydrogen storage capacity was reported for palladium and vanadium doped CNTs at 2 MPa under room temperature [20]. Schaller et al. [71] reinforced magnesium nickel (Mg-23.5 wt% Ni) with CNT by a powder metallurgy method and reported a hydrogen storage as high as 6.1 wt%. Another research performed by Iyakutti et al. [72] indicated that CNTs coated with aluminum hydride can bind up to four hydrogen molecules, leading to an increase of 8.3 wt% in hydrogen storage capacity. As an alternative to the metal doping methods, structural defects also appear as another potential approach to enhance chemisorptions of hydrogen in CNTs [20]. The existence of structural defects in CNTs can be anticipated with an increase in surface area and pore volume. Such structures definitely enhance the interaction between CNTs and hydrogen, which enables an increase in adsorption binding energy of up to 50%. Unfortunately, until now, there is controversy, both experimentally and theoretically, surrounding claims that CNTs possess abnormal performance as hydrogen storage, since the high storage capacity could not be reproduced by other researchers in the same field. So far, the storage capacity of CNTs still remains far from meeting the DOE target. More efforts are needed in order to prepare CNTs as the base materials for hydrogen storage technology [20].

## 6.7 Carbon nanotubes in supercapacitors

Electrochemical capacitors or supercapacitors have been considered as an alternative to replace traditional batteries given their miniature size, high power density, long cycle life and high energy density, with potential for reducing waste disposal to the environment. Supercapacitors are composed of high surface area activated capacitors that use a molecule-thin layer of electrolyte [1, 20]. Recent advancements in nanotechnology have proposed the application of CNTs as electrode material for the capacitor. Utilization of the large surface area of CNTs in the electrode couple with a thinner layer between the electrode and electrolyte enhances the ability of the capacitor to store higher energy densities. Furthermore, the use of vertically aligned CNTs with several atomic diameters in width can significantly increase the supercapacitor capacity and power density as a result of the dramatically increased surface area of the. Although they possess high surface area, stability and strong mechanical properties, CNTs are not preferable to use alone as the electrode due to their low capacitance. Therefore, CNTs have been proposed as a substrate for high specific capacitance transition metal oxides such as manganese oxides ($MnO_2$) and ruthenium oxide ($RuO_2$). Capacitances of approximately 5,000 F have been reported with supercapacitors and energy densities up to 5 Wh/kg, which is about 10-fold higher than conventional capacitors, with only 0.5 Wh/kg [1, 20].

## 6.8 Conclusions

It can be seen that there has been extensive research and development in the use of CNT as electrode materials for energy generation and storage applications. Currently, they provide an excellent platform for devices that require high power density due to the very high surface areas and fast rate capability. Further studies need to be implemented in order to better understand the relationship between electrode porosity and electrolyte. An enhanced understanding of the role of micro and mesoporosity and its effect on system performance is critical. Electrolyte selection is also critical to device performance as it is proportional to the square of the voltage. The main classes of electrolytes are aqueous-based, organic-based and room-temperature ionic liquids. Evolving work has focused on using CNT materials in conjunction with doping of various functional groups such as carboxyls, amines and elements such as boron and nitrogen in order to enhance the electrode performance through increased usage of electrode surface area and/or Faradaic contributions. The most recent work has focused on the creation of composite materials via the combination of CNTs with conducting polymers or metal oxides. CNT composites have amassed into a prevalent area of research through the search for the discovery of hybrid energy storage devices that are able to have high energy and high power density which are beneficial for creating more energy-efficient systems and providing a greater range of applications [1, 20].

## 6.9 Perspective and future developments

With energy consumption as a whole on the increase, coupled with the rapid economic development of countries such as Brazil, China, India and Russia there will be a concerted effort to improve how energy is utilized. This expansion in industrialization has already and will continue to lead to a further increase in the price of oil. Coupled to the rise in fossil fuel costs are drivers of an aging energy infrastructure system and demand for a low-carbon emission economy through the use of renewable energy [73]. To help accommodate all these factors the supply and demand challenge may be addressed by tapping into otherwise wasted energy. Low grade heat, if effectively harvested can prove to be a viable source of power. Thermal converters have the potential to increase the efficiency of current energy conversion systems. Energy storage also plays a key role in providing a solution to the energy problem. Energy must be efficiently stored, when it is in excess, and released at a time of high demand. This is extremely important for renewables that are not load-following [74]. With these energy challenges and ongoing research and development, including those that have been conducted over the last decade, the awareness of the benefits of electrochemical capacitors is increasing. As the research and development into energy storage and conversion has increased, the applications of electrochemical capacitors has increased with the technology becoming more diverse meaning that systems can better be tailored/targeted for specific applications ranging from higher energy density to high power densities where fast charge/discharge efficiencies are needed [74]. The most commonly used material for supercapacitors has been activated carbon with new nanostructured materials such as CNTs and its derivatives coming to the forefront of the current fundamental research. It can be seen that the way forward in terms of trying to improve energy density and power density is in the use of CNT with composite materials such as other carbons, and conducting polymers or metal oxides in order to take advantage of the pseudo-capacitative effects that these materials provide.

The research on thermogalvanic systems in the past has been generally limited to platinum electrodes [75]. This has enhanced the understanding of these electrochemical systems but has not advanced the research in terms of commercialization due to its cost. The use of carbon nanomaterials has improved the performance of these devices immensely because of their fast transfer kinetics and large electroactive surface area and is also economically viable. A record threefold increase in power conversion efficiency (as compared to conventional systems wherein platinum is used) has been realized with the use of MWNT electrodes [76]. Flexible electrodes are now possible due to CNTs. These can be used as scroll electrodes or for thermocells that can be wrapped around pipes will make this system more versatile in terms of its possible applications. Further increase in thermocell performance may be realized with the use of CNTs-graphene composite materials. Future development will most likely see supercapacitors and thermocells become a central part of hybrid energy storage and power delivery systems for large-scale and domestic demand strategies. The integration of these two systems into one device will allow the converted waste heat to be stored then released when deemed necessary. These future advancements will not only enable better automotive and portable electronics, but they will revolutionize the fields of medicine, defense and consumer goods, thus providing a step change in energy storage technology [1, 7].

## References

[1] Antiohos D, Romano M, Chen J, Razal JM. Carbon nanotubes for energy applications in syntheses and applications of carbon nanotubes and their composites. Intech. 2013;495–537. http://dx.doi.org/10.5772/51784.

[2] Turner JA. A realizable renewable energy future. Science. 1999;285(5428):687–689.

[3] Grace T, Shearer C, Tune D, Yu L, Batmunkh M, Biggs MJ, ALOthman ZA, Shapter JG. Use of carbon nanotubes in third generation solar cells. Ind Appl Carbon Nanotubes. 2017;201–248. http://dx.doi.org/10.1016/B978-0-323-41481-4.00008-3.

[4] Shukla AKSS, Vijayamohanan K. Electrochemical supercapacitors: energy storage beyond batteries. Current Science. 2000;79.

[5] Arico AS, et al. Nanostructured materials for advanced energy conversion and storage devices. Nat Mater. 2005;4(5):366–377.

[6] Hall PJ, et al. Energy storage in electrochemical capacitors: designing functional materials to improve performance. Energy Environ Sci. 2010.

[7] Hall PJ, Bain EJ. Energy-storage technologies and electricity generation. Energy Policy. 2008;36 (12):4352–4355.

[8] Chung J, et al. Toward large-scale integration of carbon nanotubes. Langmuir. 2004;20(8):3011–3017.

[9] Frackowiak E, et al. Supercapacitor electrodes from multiwalled carbon nanotubes. Appl Phys Lett. 2000;77(15):2421.

[10] Anantram MP, Léonard F. Physics of carbon nanotube electronic devices. Rep Prog Phys. 2010;2006:69.

[11] Pauliukaite R, et al. Electrochemical impedance studies of chitosan-modified electrodes for application in electrochemical sensors and biosensors. Electrochimica Acta. 55(21):6239.

[12] Dolatshahi-Pirouz A, et al. Bovine serum albumin adsorption on nano-rough platinum surfaces studied by QCM-D. Colloids Surf B Biointerfaces. 2008;66(1):53.

[13] Aaron D, Yu A. Material advancements in supercapacitors: From activated carbon to carbon nanotube and graphene. Can J Chem Eng. 2011;89:1342–1357.

[14] Sherman LM. Carbon Nanotubes Lots of Potential – If the Price is Right. 01/05/12], 2007, Available from: www.ptonline.com/articles/carbon-nanotubes-lots-of-potentialif-the-price-is-right.

[15] Kierzek K, et al. Electrochemical capacitors based on highly porous carbons prepared by KOH activation. ElectrochimicaActa. 2004;49(4):515–523.

[16] Izadi-Najafabadi A, et al. Extracting the full potential of single-walled carbon nanotubes as durable supercapacitor electrodes operable at 4 V with high power and energy density. Adv Mater.

[17] Kim BC, et al. Capacitive properties of $RuO_2$ and Ru-Co mixed oxide deposited on single-walled carbon nanotubes for high-performance supercapacitors. Synth Met. 2009;159(13):1389–1392.

[18] Iijima S. Helical microtubules of graphitic carbon. Nature. 1991;354(6348):56.

[19] Bethune DS, Kiang CH, De Vries MS, Gorman G, Savoy R, Vazquez J, Beyers R. Cobalt-catalysed growth of carbon nanotubes with single-atomic-layer walls. Nature. 1993;363(6430):605.

[20] Ong YT, Ahmad AL, Zein SHS, Tan SH. A review on carbon nanotubes in an environmental protection and green engineering perspective. Braz J Chem Eng. 2010;27(02):227–242.

[21] Xie XL, Mai YW, Zhou XP. Dispersion and alignment of carbon nanotubes in polymer matrix: a review. Mater Sci Eng R Rep. 2005;49(4).

[22] Bard AJ, Faulkner LR. Electrochemical methods: Fundamentals and applications, John Wiley & Sons, Inc; 2001.

[23] Bose S, et al. Carbon-based nanostructured materials and their composites as supercapacitor electrodes. J Mate Chem, 2012; 22(3), 767–784.

[24] Inagaki M, Konno H, Tanaike O. Carbon materials for electrochemical capacitors. J Power Sources. 2010;195(24):7880–7903.

[25] Subramanian VR, Devan S, White RE. An approximate solution for a pseudo-capacitor. J Power Sources. 2004;135(1-2):361–367.

[26] Yoon S, et al. Preparation of mesoporous carbon/manganese oxide materials and its application to supercapacitor electrodes. J Non-Crystalline Solids. 2009;355(4-5):252–256.

[27] Delahay P, Holub K. Coupling of charging and faradaic processes: electrode admittance for reversible processes. J Electroanal Chem. 1968;16(2):131–136.

[28] Yu B, et al. The electrolyte switchable solubility of multi-walled carbon nano-tube/ionic liquid (MWCNT/IL) hybrids. Chem Commun. 2006;22:2356–2358.

[29] Liu J, et al. Postsynthesis microwave treatment to give high-purity multi walled carbon nanotubes. AIChE J. 2008;54(12):3303–3307.

[30] Meyyappan M. Carbon nanotubes: science & applications. Boca Raton, CRC Press; 2005.

[31] Cai X, Cong H, Liu C. Synthesis of vertically aligned carbon nanotubes without a catalyst by hydrogen arc discharge. Carbon. 2012;50(8):2726–2730.

[32] Liu C, et al. Semi-continuous synthesis of single-walled carbon nanotubes by a hydrogen arc discharge method. Carbon. 1999;37(11):1865–1868.

[33] Hu S, Rajamani R, Yu X. Flexible solid-state paper based carbon nanotube supercapacitor. Appl Phys Lett. 2012;100(10).

[34] Candelaria SL, et al. Nanostructured carbon for energy storage and conversion. Nano Energy. 2012;1 (2):195–220.

[35] Wang G, Zhang L, Zhang J. A review of electrode materials for electro-chemical supercapacitors. Chem Soc Rev. 2012;797–828.

[36] Pan H, Li J, Feng Y. Carbon nanotubes for supercapacitor. Nanoscale Res Lett. 2010;5(3):654–668.

[37] Shen J, et al. How carboxylic groups improve the performance of single walled carbon nanotube electrochemical capacitors? Energy Environ Sci. 2011;4(10):4220–4229.

[38] Wu ZS, et al. Doped graphene sheets as anode materials with super high rate and large capacity for lithium ion batteries. ACS Nano. 2011;5463–5471.

[39] Babel K, Jurewicz K. Electrical capacitance of fibrous carbon composites in supercapacitors. Fuel Process Technol. 2002;77–78:181–189.

[40] Béguin F, et al. A self-supporting electrode for supercapacitors prepared by one-step pyrolysis of carbon nanotube/polyacrylonitrile blends. Adv Mater. 2005;17(19):2380–2384.

[41] Zhang Y, et al. Preparation and electrochemical properties of nitrogen-doped multi walled carbon nanotubes. Mater Lett. 2010;65(1):49–52.

[42] Lee KY, et al. Influence of the nitrogen content on the electrochemical capacitor characteristics of vertically aligned carbon nanotubes. Phys E: Low Dimension Syst Nanostruct. 2010;42 (10):2799–2803.

[43] Antal AK, et al. Comparison of structural changes in nitrogen and boron doped multi walled carbon nanotubes. Carbon. 2010;48(11):3033–3041.

[44] Shiraishi S, et al. Electric double layer capacitance of multi-walled carbon nanotubes and B-doping effect. Appl Phys A Mater Sci Process. 2006;82(4):585–591.

[45] Wang DW, et al. Synthesis and electrochemical property of boron-doped mesoporous carbon in supercapacitor. Chem Mater. 2008;20(22):7195–7200.

[46] Presser V, Heon M, Gogotsi Y. Carbide-derived carbons from porous networks to nanotubes and graphene. Adv Funct Mater. 2011;21(5):810–833.

[47] Zhang LL, Zhao XS. Carbon-based materials as supercapacitor electrodes. Chem Soc Rev. 2009;38 (9):2520–2531.

[48] Fu C, et al. Supercapacitor based on electro-polymerized polythiophene and multi walled carbon nanotubes composites. Mater Chem Phys. 2011;132(2):596–600.

[49] Wu ZS, et al. Graphene/metal oxide composite electrode materials for energy storage. Nano Energy. 2012;1(1):107–131.

[50] Crispin X, et al. The origin of the high conductivity of poly(3,4-ethylene-dioxythiophene) poly (styrenesulfonate) (PEDOT/PSS) plastic electrodes. Chem Mater. 2006;18(18):4354–4360.

[51] Antiohos D, et al. Compositional effects of PEDOT-PSS/single walled carbon nanotube films on supercapacitor device performance. J Mater Chem. 2011;21(40):15987–15994.

[52] Kim KS, Park JS. Influence of multi-walled carbon nanotubes on the electrochemical performance of graphene nanocomposites for supercapacitor electrodes. Electrochimica Acta. 2011;56(3):1629–1635.

[53] Hu Y, et al. Defective super-long carbon nanotubes and polypyrrole composite for high-performance supercapacitor electrodes. Electrochimica Acta. 2012;60(0):279–286.

[54] Myoungki M, et al. Hydrous RuO2/carbon black nanocomposites with 3D porous structure by novel incipient wetness method for supercapacitors. J Electrochem Soc. 2006;153(2):A334–A338.

[55] Li Q, et al. Structural evolution of multi-walled carbon nanotube/$mno_2$ composites as supercapacitor electrodes. Electrochimica Acta. 2011;59(0):548–557.

[56] Shan Y, Gao L. Formation and characterization of multi-walled carbon nanotubes/$co_3o_4$ nanocomposites for supercapacitors. Mater Chem Phys. 2007;103:206–210.

[57] Jayalakshmi M, et al. Hydrothermal synthesis of $sno_2$-$v_2o_5$ mixed oxide and electrochemical screening of carbon nano-tubes (CNT), $V_2O_5$, $V_2O_5$-CNT, and $SnO_2$-$V2O_5$-cnt electrodes for supercapacitor applications. J Power Sources. 2007;166(2):578–583.

[58] Li JJ, et al. Graphene/carbon nanotube films prepared by solution casting for electrochemical energy storage. IEEE Trans Nanotechnol. 2012;11(1):3–7.

[59] Dong X, et al. The formation of a carbon nanotube-graphene oxide core-shell structure and its possible applications. Carbon. 2011;49(15):5071–5078.

[60] Kamat PV. Meeting the clean energy demand: Nanostructure architectures for solar energy conversion. J Phys Chem C. 2007;111(7):2834.

[61] Liu Y, Lu S, Panchapakesan B. Alignment enhanced photoconductivity in single wall carbon nanotube films. Nanotechnology. 2009;20(3).

[62] Zhu H, Wei J, Wang K, Wu D. Applications of carbon materials in photovoltaic solar cells. Solar Energy Mater Solar Cells. 2009;93(9):1461.

[63] Jia Y, Wei J, Wang K, Cao A, Shu Q, Gui X, Zhu Y, Zhuang D, Zhang G, Ma B, Wang L, Liu W, Wang Z, Luo J, Wu D. Nanotube-silicon heterojunction solar cells. Adv Mater. 2008;20(23):4594.

[64] Janssen RAJ, Hummelen JC, Sariciftci NS. Polymer-fullerene bulk heterojunction solar cells. MRS Bulletin. 2005;30(1):33.

[65] Grätzel M. Dye-sensitized solar cells. J Photochem Photobiol C Photochem Rev. 2003;4(2):145.

[66] Brown P, Takechi K, Kamat PV. Single walled carbon nanotube scaffolds for dye-sensitized solar cells. J Phys Chem C. 2008;112(12):4776.

[67] Zhu HW, Zeng HF, Subramanian V, Masarapu C, Hung KH, Wei BQ. Anthocyanin-sensitized solar cell using carbon nanotube films as counter electrodes. Nanotechnology. 2008;19(46).

[68] U.S. Department of Energy. Multi Year Research, Development, and Demonstration Plan: Planned Program Activities for 2003–2010. Washington, DC, 2007.

[69] Wang Q, Johnson JK. Optimization of carbon nanotube arrays for hydrogen adsorption. J Phys Chem B. 1999;103(23):4809.

[70] Dodziuk H, Dolgonos G. Molecular modeling study of hydrogen storage in carbon nanotubes. Chem Phys Lett. 2002;356(1–2):79.

[71] Schaller R, Mari D, Dos Santos SM, Tkalcec I, Carreño-Morelli E. Investigation of hydrogen storage in carbon nanotube-magnesium matrix composites. Mate Sci Eng A. 2009;521–522:147.

[72] Iyakutti K, Kawazoe Y, Rajarajeswari M, Surya VJ. Aluminum hydride coated single walled carbon nanotube as a hydrogen storage medium. Int J Hydrogen Energy. 2009;34(1):370.

[73] Wilson IAG, Mc Gregor PG, Hall PJ. Energy storage in the UK electrical network: estimation of the scale and review of technology options. Energy Policy. 2010;38(8):4099–4106.

[74] Hall PJ. Energy storage: the route to liberation from the fossil fuel economy? Energy Policy. 2008;36(12):4363–4367.

[75] Quickenden TI, Mua Y. A review of power generation in aqueous thermogalvanic cells. J Electrochem Soc. 1995;142(11):3985–3994.

[76] Hu R, et al. Harvesting waste thermal energy using a carbon-nanotube based thermo-electrochemical cell. Nano Lett. 2010;10(3):838–846.

Aiswarya R.

# Chapter 7

# Advanced fiber materials in information storage technology

**Abstract:** *Advanced Fiber Materials* promotes communication between scientists working at the forefront of all fiber-related domains, including chemists, energy researchers, physicists, environmental scientists, material scientists, biological researchers, engineers, and others. Original research and reviews on fibers, fiber-related devices, and their applications are published in *Advanced Fiber Materials*. These topics include the design and synthesis of novel polymers for fibers, physics and chemistry in textiles and fibers, high-performance fibers and composites, carbon nanotube fibers, graphene fibers, and nanotechnologies in fibers and polymers. Recent years have seen a rise in interest in the study of fibers and textiles that have many materials added on or integrated into the fabric itself. Flexible electronics made from fiber and textiles have demonstrated considerable potential has varieties of applications, that include flexible circuits, pressure sensor that resemble the skin, transistors, memory devices, and displays. However, the challenge that limits the use of fibers and textiles that ensures low cost of production scale at the same time, much like other common difficulties that arise during the growth of human civilization and need to be handled.

Compared to many other material processing techniques, electrospinning is a great way to solve these issues since it is better suited for major commercial applications that continuously manufacture polymers of micro and nanofibers with increased lifespan. It also offers a lot of benefits, like being affordable, simple to use, accessible, easy to synthesize, and easy to regulate the settings. The electrospinning technology is extensively used in a variety of applications that including wearable smart devices, energy conversion and storage, medical applications and environmental applications, thanks to its sophisticated processes and tuneable properties. It has several benefits, including a high surface-to-volume ratio, increased flexibility, and high tensile strength. The use of fibers in several applications, such as energy harvesting, multifunctional sensors, biotissue development, and many more as a result of their outstanding properties.

**Keywords:** Advanced fiber materials, nanofibers, flexible electronics, multifunctional, energy harvesting

---

**Aiswarya R.**, Department of Physics and Nanotechnology, SRM Institute of Science and Technology, Potheri, Kattankulathur 603203, Chengalpattu, Tamil Nadu, India, e-mail: aiswaryaais16@gmail.com

https://doi.org/10.1515/9783110992892-007

## 7.1 Introduction

The closeness of electronics to the human body necessitates flexible energy storage solutions that can adhere to and conform to the skin. As a result, the creation of stretchable batteries and supercapacitors has received a lot of interest lately. A significant part is played by the general operating principles of batteries and supercapacitors, as well as the specifications for making these devices flexible with various methods for transforming the typically stiff electrochemical energy storage materials into stretchy shape. The issues of fiber-like geometry, stiff island geometry, and intrinsic stretchability are explored in detail [1]. Each technique works with a variety of substances, such as metals, ceramics, and polymers. By contrasting the acquired electrochemical performance and strain capacities of these distinct materials processes, we give a side-by-side evaluation of the most promising methods for enabling stretchable electrochemical energy storage. In the final section, the view for forthcoming developments and challenges for stretchable batteries and supercapacitors is provided. Smart clothing and wearable electronics are two examples of high-tech fiber-based products that may be worn as a second skin to enhance communication between individuals and their environment [2].

It is highlighted how flexible fiber-shaped multifunctional devices have made considerable advancements in terms of energy harvesting, energy storage, chromatic devices, and actuators. In particular, in-depth introductions are made to the manufacturing processes and application properties of multifunctional fiber devices such lithium-ion batteries, fiber-shaped solar cells, electrochromic fibers, and actuators [3]. Finally, we offer our opinions on the difficulties and potential advancement of useful fiber-shaped devices. The growth of the relevant revolutionary manufacturing industry and the daily lives of the social population are intimately tied to the study and applications of fiber materials. However, the demands of automation and intellectualization in contemporary society, as well as people's consumption desires in pursuit of smart, avant-garde fashion, and uniqueness, cannot be met by conventional fibers and fiber products. Over the past several years, there has been a lot of research and development done on the most cutting-edge fiber-shaped electronics with the most desired designability and integration capabilities [4].

## 7.2 Fiber materials recap

Researchers working at the cutting edge of all fiber-related domains, including chemists, physicists, material scientists, energy or environmental researchers, biomedical researchers, and engineers, are encouraged to share ideas through advanced fiber materials, fiber materials design and synthesis of novel polymers for fibers, carbon nanotube and graphene fibers, high-performance fibers and composites, and other topics related to fiber and fiber-related devices as well as their applications, like fiber and polymer nanotechnologies; the creation, production, and use of nanofibers; smart textiles; wearable technology and smart fibers; bio-inspired polymers and organic fibers; artificial problems and robots made of fiber; several uses and different materials; eco-friendly fibers and materials connected to fibers; solar cells; lithium batteries; supercapacitors; and other energy-related fibers for use in environmental applications, such as reducing pollutants and purifying water, air, and the environment [5]; fibers for biological and medical uses, including tumor treatment, medication delivery, and regenerative medicine; fibers for advanced manufacturing; laser, semiconductor, and other fiber-related materials and equipment; fibers for information technology in storage; and fibers for optical and photonics sensing [6].

The industrial community is very interested in carbon fiber composite materials. This is because they have high mechanical properties and are lighter than heavy metals like steel or titanium. Additionally, during the past 10 years, both the use and recyclable nature of this type of material have increased. However, due to the nature and anisotropy of certain materials, machining may leave behind faults. One of the most crucial factors in the machining of composite materials is the temperature generated throughout the process. Abrasive water-jet machining makes it possible to machine composite materials by significantly decreasing the temperature produced [7]. To maximize the final product, however, a number of flaws related to this unconventional machining must be taken into account. Make use of textile fiber composites in structural applications. Basic analysis and design approaches for tensile, shear, and flexural designs are necessary. The methods for conducting tests and converting the findings into design-based characteristics are covered in this [8]. In order to ascertain the basic material properties, mechanical tests are used to assess the overall load-deformation characteristics. The data is then analyzed and understood using analytical models. To characterize how the fabric, matrix, and interface perform under various loading situations, these material properties must be coupled. It includes situations like flexural, tension, impact, shear, and fast-moving ones. Additionally, the constitutive properties must be consistent with widely used analytical models, such as non-linear stress-strain models, moment-rotation structural analysis models, and finite element programs [9]. These models make it possible to study and design a variety of structural systems that include impact and blast-resistant buildings, connections between beams and columns, earthquake remediation, repairs and retrofits, strengthening of unreinforced masonry, and structural panels [10].

## 7.3 Advanced fiber materials

Advanced fiber materials, which are secured in effect by the matrix resin, add tensile strength to the finished item, improving performance characteristics like strength and stiffness while reducing weight. The method used to manufacture the fiber, together with its constituents and coating chemistries, define its qualities. There are really a number of causes for this mismatch, some of which include the fact that most materials are inhomogeneous, and have internal flaws and faults, or manufacturing flaws. This indicates that the mechanical element will have a shorter practical life than anticipated [11]. The biggest problem that designers try to prevent is component failure. Design errors, production flaws, improper material selection, overloading of the components, and inadequate maintenance are the most important causes of component failure. In order to avoid parts from failing unexpectedly, engineering parts should be appropriately designed, and planes should be configured accordingly. Numerous mechanical failure types need be taken into account in order to solve this issue, starting with the design phase and continuing throughout the components lifespan. Researchers and innovator design firms foresee most of crucial and fundamental capabilities of future smart clothes, such as the capacity to gather energy and store it effectively then change color subtly and alter shape at will. Clothing will be far more in line with demands of near future avant-garde consumers if it can have both fashion design and the aforementioned specific utility [12].

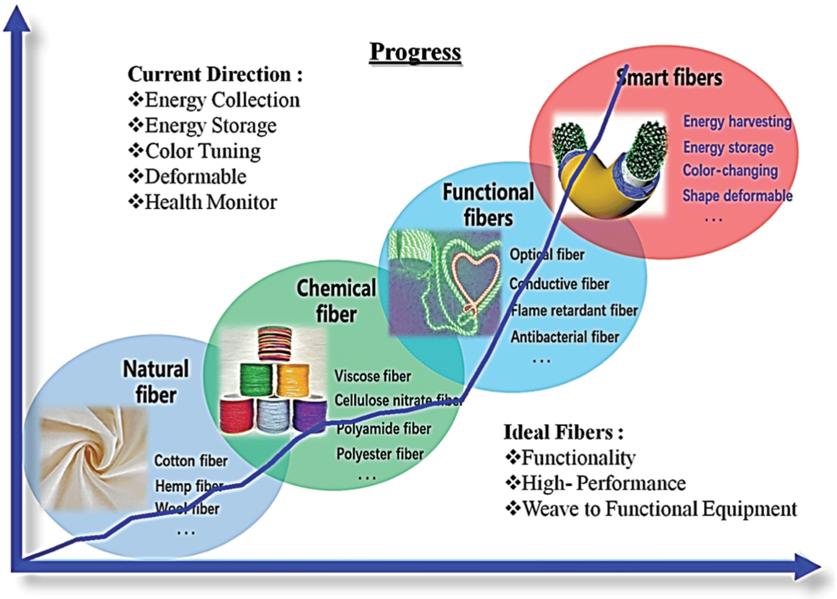
Progress
Current Direction :
❖Energy Collection
❖Energy Storage
❖Color Tuning
❖Deformable
❖Health Monitor
Smart fibers
Energy harvesting
Energy storage
Color-changing
Shape deformable
…
Functional fibers
Optical fiber
Conductive fiber
Flame retardant fiber
Antibacterial fiber
…
Chemical fiber
Viscose fiber
Cellulose nitrate fiber
Polyamide fiber
Polyester fiber
…
Natural fiber
Cotton fiber
Hemp fiber
Wool fiber
…
Ideal Fibers :
❖Functionality
❖High- Performance
❖Weave to Functional Equipment

**Figure 7.1:** A succinct history of the modern era's advances in fibers (copyrighted from ACS Publication 2022).

Actually, high-tech firms and academics have invested a significant amount of money and effort in smart clothing due to its high value-added and high-tech integration qualities. Electronics that are flexible, elastic, and stretchy are needed to support the aforementioned smart clothes, particularly for the fiber-shaped functional components. More importantly, fiber is recognized as the most fundamental component of clothing and may be utilized in weaving and knitting to create a variety of designs and styles [13].

The advanced fiber materials that are far most often employed in high-performance applications which are made of a precursors range; including rayon, polyacrylonitrile/ PAN, as well as bio-based material pitch, and carbon-rich precursors such as lignin/bio based PAN. To make the high strength fibers, the precursor fibers are chemically treated, heated, stretched, and carbonized [14]. A rayon precursor was used to create the first high-performance carbon fibers to hit the market. However, rayon's "chemdawg" cross section and high-temperature performance frequently make it the fiber of choice for carbon–carbon (C-C) composites which are ablative heat shield. PAN based carbon fibers have long ago superseded rayon in structural applications. The most adaptable and popular carbon fibers are those made from PAN.

## 7.4 Functionalization of fiber materials

The possible issues in real-world applications are what primarily drive the functionalization of fiber-shaped materials and devices. Stretchable fiber-shaped supercapacitors were created in 2013 as a result of the expectation that fiber-shaped devices would be able to withstand the frequent strain and stress in wearable applications. In wearable applications, tiny fiber-shaped devices may also sustain structural damage, necessitating rational designs to accomplish the restoration of mechanical and electrical capabilities [15]. As a result, in 2014, self-healing fiber-shaped supercapacitors were created to satisfy the aforementioned parameters. Functional component integration with fiber electrodes is a significant issue in both cases, and the resulting interfaces are essential to the stability and functionality of the resulting devices. With a focus on the various fiber electrode materials and topologies as well as the interfaces between various components that contribute to high flexibility and stability, the integration of functional guests into various fiber electrodes has attracted interest. With an emphasis on illuminating the origins, development, and practical applications of each characteristic, the discussion of functional fiber devices includes stretchability, shape memory, healability, and electrochromism, to name just a few [16]. Finally, after examining the challenges and promise of functional fiber-shaped devices, prospects and potential future methods for this expanding sector are proposed.

Tows, or groups of continuous fibers, are a common kind of high-performance carbon fiber. The number of continuous, untwisted filaments that make up a carbon fiber tow is denoted by the letter "K," which stands for multiplication by 1,000. Examples like 12 K imply that there are 12,000 filaments. Tows can be converted into unidirectional tape, fabric, and other reinforcing forms in addition to being used directly in processes like filament winding and pultrusion [17]. Spread-tow fabrics are becoming more and more popular. Each tow's filaments are spread, as the name implies, to produce very thin, wide tapes that are subsequently stitched. These materials are relatively lightweight while providing good performance. In order to improve electrochemical performance, other materials such as MXene, carbon black, and silk can also be spun into flexible nanofibers with increased surface areas. These fibers can then be coated onto other fiber substrates. For instance, a modified electrospinning method was used to equally wrap MXene/polyethylene oxide nanofibers on polyester fiber to generate a nanofibers-based fiber electrode. The thickness of the nanofibers coating was controlled in this manner by the spinning time. A considerable surface area may be provided by nanofibers coating to improve the electrode/electrolyte interface contact. Polyester fiber may be used to create composite fibers with strong mechanical properties and flexibility[18].

A sensible method for creating functional fiber electrodes is to wrap aligned multi-walled carbon nanotubes (MWCNTs) around the surface of a functional fiber. Functional fiber in the core provides functionality, and aligned MWCNTs act as conductive elements at the shell. For instance, by using the “rotation-translation” approach to wrap MWCNT sheets on the rubber fiber, a flexible electrode might be created. The aligned MWCNTs serve as the conductive and energy storage components at the shell, while the stretchability is achieved by the stretchy rubber fiber at the core [19]. The resultant fiber electrode’s stretchability is considerably improved by the highly stretchy polymer fiber and wrinkle structure, resulting in a super stretching capability with a remarkable strain. Wet spinning is an effective method for producing functional fiber electrodes on demand. For example, a typical research recommended wet spinning to produce graphene oxide (GO) fibers. The GO was thermally reduced at 90 °C after the mixed materials were put into a conduit to produce a composite fiber. More polypyrrole was electrodeposited as a thin coating on the fiber. The reduced GO-based fiber produced when twisted into a spring-shaped electrode shown a high degree of stretchability with a maximum strain [20].

## 7.5 Chemically modified fiber materials

Mercerization, acetylation, acrylation, benzoylation, silanization, and modification using carboxylic acids are examples of chemical modification processes for natural fibers. When fibers are exposed to a NaOH solution during the mercerization process, the hydrogen bonds that would normally prevent cellulose from reacting are broken. This study examines the effects of various chemical fiber surface modifications on various mechanical properties of composites made of natural fibers [21]. Along with the natural fiber constituents, such as cellulose, hemicellulose, lignin, and pectin, there are several surface modifications of the fibers, including acetylation, potassium permanganate, peroxides, and silane benzoylation. Some of the improved properties of natural fiber composites include the adhesion force between the reinforcing surface and matrix material at the surface contact as well as the fiber strength. Water absorption capabilities of composites are decreased [22].

### 7.5.1 Silane treatment

Silanes are introduced as coupling agents to the polymer matrix and glass fibers to stabilize the composite material. Silane has the chemical formula SiH4. All of the cellulose hydroxyl groups are removed by silane coupling agents at the fiber and matrix interface. Hydroxyl alcohols result in the creation of silane when moisture is present. The silanol then reacts with the hydroxyl group in the fiber, forming strong covalent bonds to the cell membrane on the fiber surface [23]. The use of silanes prevents the fibers from cramping by establishing a cross-linking infrastructure because the fiber matrix is joined to the hydrocarbon chains by covalent bonds. Below is a list of the reaction strategies for the silane treatment:

$$CH_2CHSi(OC_2H_5) \xrightarrow{H_2O} CH_2CHSi(OH)_3 + 3C_2H_5OH$$
$$CH_2CHSi(OH)_3 + Fiber - OH \rightarrow CH_2CHSi(OH)_2O - Fiber + H_2O$$

### 7.5.2 Alkaline treatment

One of the most popular surface modifications for composites on thermoplastics and thermosets is alkaline treatment. Alkaline surface treatment significantly affects hydrogen attachment in the system structure and increases the roughness of the fiber surface. This surface modification of the natural composites removes the oils, wax, and lignin that were covering the outer surface of the cell membrane. The following chemical equation can be used to illustrate how surface modification of fiber with sodium oxide/NaOH encourages the ionization of alcoholic body by hydroxyl [23]:

$$Fiber - OH + NaOH \rightarrow Fiber - O - Na + H_2O$$

### 7.5.3 Benzoylation treatment

An excellent illustration of benzoylation is the change in the production of organic compounds and benzoyl chloride. In treating fibers, it is employed. The benzoylation process and advancements in the interface between natural fiber and PS matrix reduce the water absorption capabilities of natural fibers. The reactions of the chemical alteration known as benzoylation can be expressed as below [24]. The hydroxyl components of cellulose and lignin are activated by the alkaline pretreatment. The fiber is then immersed for 15 min in a 10% benzoyl chloride and NaOH solution. After completing this step, the fibers are once more immersed in ethanol to aid in their benzoyl chloride escape before being cleansed:

$$\text{Fiber} - \text{OH} + \text{NaOH} \rightarrow \text{Fiber} - \text{ONa} + H_2O$$

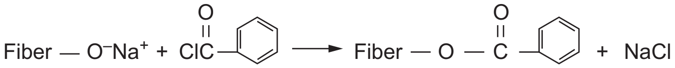

## 7.5.4 Acetylation

An interaction between an organic molecule and the acetyl ion $CH_3COO$- is known as acetylation surface modification. Esterification is taking place as a result of the plasticization of cellulosic fibers. The acetylation of natural fibers is another name for it. Ethanoic anhydride reacts with the hydroxyl groups of cellulose when it interacts with lingocellulose substance [25]. It has been demonstrated through the preparation of flax-reinforced polymer composites that flax fiber is a chemical modifying agent. Due to an 18% increase in acetylation modification, flax fiber compositions' mechanical characteristics have been significantly improved:

$$\text{Fiber} - \text{OH} + CH_3COOCOCH_3 \rightarrow \text{Fiber} - OCOCH_3 + CH_3COOH$$

## 7.5.5 Peroxide treatment

The ROOR chemical group belongs to the peroxide family in chemistry. The ion O-O is a member of the functional group ROOR. To avoid radicals, the ROOR functional group typically breaks readily. The matrix and the hydrogen-containing cellulose fibers then react with it. Alkali pretreatment fibers are subjected to one of the 6% dicummyl peroxides in acetone solution for 30 min as part of the peroxide treatment process. Thirty minutes in a deep solution at 70 °C is followed by cleaning the fibers with distilled water. Equations following illustrate a free radical reaction, for instance, where peroxide is the initiating agent between cellulose fibers and the PE matrix [26]:

$$\text{RO} - \text{OR} \rightarrow 2\text{RO}$$

$$\text{RO} + \text{Matrix (PE)} - \text{H} \rightarrow \text{RO} - \text{H} + \text{Matrix (PE)}$$

$$\text{RO} + \text{Cellulose} - \text{H} \rightarrow \text{RO} - \text{H} + \text{Cellulose}$$

$$\text{Matrix (PE)} + \text{Cellulose} \rightarrow \text{Mastrix (PE)} - \text{Cellulose}$$

### 7.5.6 Permanganate treatment

The surface modification process between potassium permanganate and cellulose produced the ions $MnO_3$ through the radical cellulose. Potassium permanganate is a member of the permanganate group ($MnO_4$). From the balanced ionic reaction, we can understand that charged $Mn^{3+}$ ion is effectively responsible for co-polymerization. The fibers with the alkali 5% concentrated surface pretreatment are submerged for 1 min in a 0.05% concentrated potassium permanganate solution with acetone. The potassium permanganate solution is drained of the fiber, which is then dried in the air [27]:

$$\text{Cellulose} - \text{H} + \text{KMnO}_4 \rightarrow \text{Cellulose} - \text{H} - \text{O} - \text{Mn}(=\text{O})_2 - \text{OK}^+$$

$$\text{Cellulose} - \text{H} - \text{O} - \text{Mn}(=\text{O})_2 - \text{OK}^+ \rightarrow \text{Cellulose} + \text{H} - \text{O} - \text{Mn}(=\text{O})_2 - \text{OK}$$

## 7.6 Advantages and disadvantages of advanced fiber materials

Advanced fiber materials made of high-performance reinforcing fibers placed in a toughened polymeric matrix to create a ply or lamina. Advanced composite fiber materials are lightweight, strong, and durable. The majority of fibers are elastic. Most synthetic textiles are resistant to wrinkling. Compared to fabrics composed of natural fibers, synthetic fabrics are often more resilient, less costly, and more easily accessible [28]. The majority of synthetic fibers can support large weights without breaking. Natural fibers, on the other hand, are not strong, have a low density, and are lightweight. They are inherently incompatible and quickly susceptible to harm because they absorb moisture and humidity. Composites are more quickly damaged than wrought metals because they are more fragile. Cast metals have a tendency to be brittle as well. Repair creates new issues because materials have short shelf life and need to be transported and stored in a refrigerator [27].

Advanced fiber material composites offer several characteristics and special abilities that result into appealing product advantages. Long fiber technology is particularly common in the car, farm, heavy truck, consumer products, and mass transportation industries because of the versatility that long fiber materials give customers. Users can choose to prepare a material to correspond to their own formulation or utilize a ready-made compound. Given its adaptability, it is easy to understand why long fiber composites are frequently employed in a range of applications [31].

**Table 7.1:** Clearly explains about the advantages and disadvantages of advanced fiber materials [27].

| Advantages | Disadvantages |
|---|---|
| – Low densities<br>– High specific strength and stiffness<br>– Durability can be improved considerably with treatment<br>– Fibers are from renewable resources<br>– Production requires little energy consumption<br>– Production involves $CO_2$ absorption, at the same time as returning oxygen to the environment<br>– Low-cost fibers<br>– Low hazard manufacturing processes<br>– Low emission of toxic fumes at end of life<br>– Less abrasive damage to processing equipment<br>– More recyclability features | – Lower durability than synthetic-fiber composites<br>– High moisture absorption, which usually results in performance deteriorations<br>– Lower strength, particularly the impact Strength compared to synthetic-fiber composites<br>– Greater variability of properties<br>– Lower processing temperatures limiting the matrix options |

## 7.7 Challenges of advanced fiber materials

Miniaturization and integration are current trends, with an increasing emphasis on advanced fiber materials. Wearables must now meet new standards for low weight, tiny size, and flexibility due to their near proximity to the human body. Due to their stiffness and mass, conventional three-dimensional and two-dimensional devices are unable to effectively satisfy these criteria. Due to their tiny diameter, lightweight, flexibility, and weavability into soft textile electronics, a new family of one-dimensional fiber-shaped devices including energy-harvesting devices, energy-storage devices, light-emitting devices, and sensing devices has risen to the challenge [32]. It is explained how fiber and textile applications encounter problems ranging from fiber-shaped devices to continuously scalable manufacture, to encapsulation and testing, to application mode discovery. The next steps that must be taken to increase their commercialization are underlined.

## 7.8 Application of advanced fiber materials in information storage technology

Advanced fiber material configurations beat planar versions in terms of excellent flexibility, outstanding comfort, high compatibility with conventional fabrics, and simple integration with a variety of devices because of their reduced size and lightweight.

The design of fibrous structure-based electrodes and devices is still being worked on in terms of polymer processing [33]. In reality, the majority of earlier investigations were susceptible to a variety of potential methodological flaws in the processing procedure because of the unfavorable mechanical strength and stability suffered by reported chemically produced conductive polymers. Future research must concentrate on materials engineering for cutting-edge processing techniques. When it comes to a variety of applications, including flexible electronic devices, miniature devices, shape-deformable fibers, energy storage devices, energy-harvesting devices, chromatic devices, and sensors [34].

Since the beginning of the previous decade, highly integrated gadgets have drawn a lot of attention. Technologies for the creation of integrated platforms are greatly needed as a result of the market need for downsized and multifunctional goods. Particularly, fibers with cooperative units of energy harvesting, energy storage, and functional modules would give the global fashion, mobile electronics, wireless interaction, and healthcare sectors a fresh lease of life and unrestricted innovation [35]. Prior to achieving this ultimate aim, there are still many important scientific and technical problems that need to be solved. These problems are extremely difficult and call for multidisciplinary approaches. Solar-powered photovoltaics have so far attained astounding efficiency for energy harvesting, directly converting sunlight to electricity. The energy-harvesting capabilities of a newly created bi-component piezoelectric textile strand were investigated. The production of fibers, weaving of the textile, high voltage polarization, installation of an outside electrode, modeling, and measurement of the piezoelectric textile's capacity to convert mechanical strain to electrical energy are all covered in this paper. According to the findings, it is feasible to salvage about 0.7 mW of electricity from the textile's fibers [36].

Compounds or combinations known as thermochromic materials undergo changes in their visual absorption spectra upon heating or cooling. Color memory is a feature of reversible thermochromic materials in particular. At a specific temperature, it discolors, revealing a new hue, and then returns to its original color when the temperature is raised to its starting point. As a result, it is possible to manufacture fibers with chromic qualities using reversible thermochromic materials. The sandwich-like shape, which consists of two transparent conductive electrodes with an interior electrochromic active layer, is thought to be a typical configuration for electrochromic devices. For various electrochromic materials, there are two main types of electrochromic active layers. One is the combination of electrolytes with electrochromic compounds [37]. The layering of electrodes, electrolytes, and electrochromic compounds is the other. However, a number of issues, including the miniaturization of electrodes, the uneven distribution of the electric field, and the poor stability during a tiny curvature radius, are faced in the fabrication of electrochromic fibers.

Shape-deformable materials can unintentionally change their position or shape in response to environmental stimuli such as magnetic fields, electricity, radiation, heat, and atmosphere. New advanced deformable materials have been extensively researched and gradually incorporated into biomimetic devices, biomimetic technologies, and fashion decoration since the turn of the twenty-first century [38]. Examples include shape memory polymers and alloys, phase change materials, and shape memory materials. Fiber, which is used to weave fabric and produce garments, is the basis for clothing. Only the design and production of controlled shape deformable fiber devices will allow the production of deformable clothes. Researchers have recently focused heavily on shape-deformable fibers and made significant advancements in this area. The unique benefits of several integrated optical systems are detailed, including optical probes of various forms and materials connected to several optical fibers. The clinical effects may be anticipated to vary in line with the major performance differences in the radiation fields of the various systems [39].

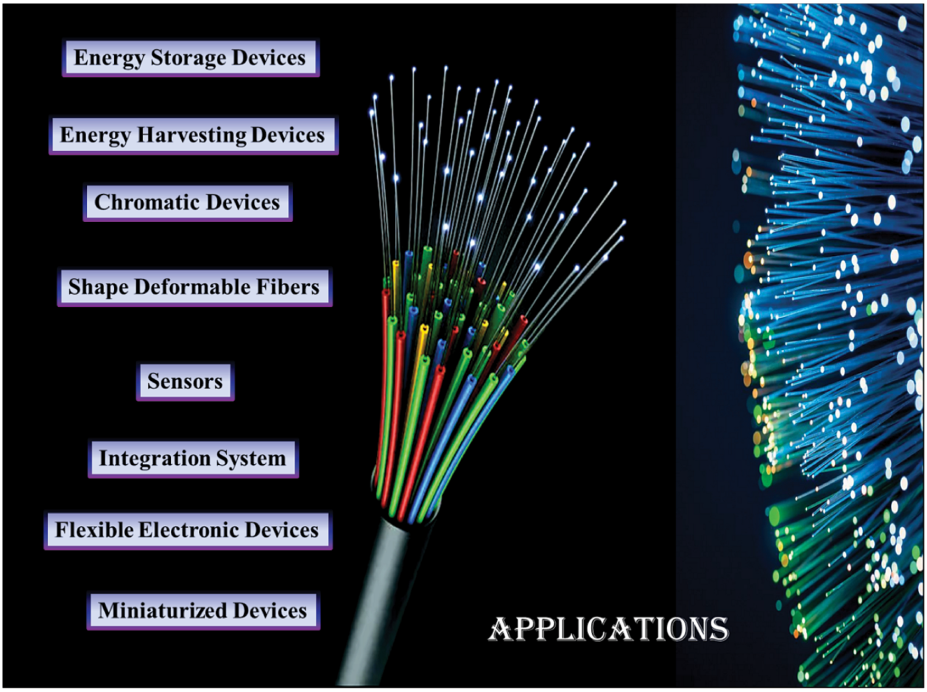
Energy Storage Devices
Energy Harvesting Devices
Chromatic Devices
Shape Deformable Fibers
Sensors
Integration System
Flexible Electronic Devices
Miniaturized Devices
APPLICATIONS

**Figure 7.2:** Application of advanced fiber materials in information storage technology.

The prospective uses for wearable electronics, portable electronics and small electronics of working fiber devices, are the advancements of man-made fibers throughout our history. The most current developments in highly functioning fiber-shaped devices including energy-harvesting and storage systems and chromatic devices are discussed. The multi-color properties of chromotropic fibers need to be researched and ascertained with regard to chromotropic fibers [40]. Eventually, these highly developed separate components will be combined into one fiber and used in downstream sectors. We have reason to assume that these intelligent items with integrated, all-purpose features and all-weather, real-time operations will exist soon, and we eagerly anticipate meeting them.

## 7.9 Patented works in advanced fiber materials

Is advanced fiber materials a core pillar of our grandfathered plan of innovations? Will you set yourself apart with distinctive product lines? Innovation drives the expansion of the textile industry, whether it is for the protection of our military personnel, the improvement of medical care, or the creation of a future that is more sustainable. Innovation is ingrained in American society, and the notion of fostering it extends back to the formulation of the U.S. Constitution, which laid the foundation for current intellectual property (IP) legislation [41]. Businesses can better recognize, safeguard, and benefit from their discoveries if they have a fundamental grasp of patents and the various kinds of IP protection that are available. Here are the some of the notable patented works in this field.

### 7.9.1 Advanced fabric technology and filters

Filter material for actively influencing the trapped particles inside the filter as well as entrapping particles. A combination of hydrophilic superabsorbent and non-superabsorbent fibers makes up the fabric, which is sufficiently porous to let gaseous passage through it. The fabric has a thickness, the hydrophilic superabsorbent fibers have an exterior coating made of a combination of a chemically or physically active substance and a liquid carrier, and the hydrophilic superabsorbent fibers have a center volume that also holds the active composition. When the concentration of active compounds in the coating is reduced to a concentration less than concentrations of the active compound within the central volume, the central volume of the hydrophilic superabsorbent fibers acts as a reservoir for replacement of the active compound into the coating; the liquid carrier is an aqueous liquid. Solution polymers can be diluted with water prior to application and given the same absorbency as granular polymers when delivered in solution form. Most substrates can be coated or saturated. The end product is a coated substrate with superabsorbent capability after drying at a particular temperature for a particular amount of time. This chemical, for instance, may be used to coat wires and cables directly, although it is best suited for components like rolled products and sheeted substrates [42].

Superabsorbent polymers (SAP) are a class of polymers that, in relation to their own mass, can absorb and hold a very high amount of liquid. The kind and strength of cross-linking to the polymer regulates the overall absorbency and swelling capacity. Low density cross-linked SAP typically has a greater capacity for absorption and swells to a greater extent. Additionally, the gel formation in these SAPs is softer and more cohesive. High cross-link density polymers swell and have a decreased capacity for absorption. Even under light pressure, the gel strength is tougher and can preserve particle structure. At least 25% of the fabric's thickness is covered by the coating on the hydrophilic superabsorbent fibers, which is present throughout the whole thickness of the fabric. When the concentration of active compounds in the coating is reduced to a concentration less than concentrations of the active compound within the central volume and the liquid carrier is an aqueous liquid, the central volume of the hydrophilic superabsorbent fibers acts as a reservoir for replacement of the active compound into the coating.

### 7.9.2 Fiber-reinforced composite materials

These materials are pertinent to fiber-reinforced composite materials reinforced with fibers made of a certain fully aromatic polyamide. The reinforced composite material with high strength, stiffness, and impact resistance as well as the reinforcing fibers with high tenacity and Young's modulus made from a specific fully aromatic polyamide are the focus of this innovation. There has been an increase in demand in recent years for the creation of composite materials with high performance, particularly high strength, stiffness, and impact strength, in a variety of industrial domains, such as those involving aeroplanes, train cars, and motor vehicles. Higher levels of properties have also been sought after from the perspective of conserving resources and energy [43].

The specified fully aromatic polyamide fibers are utilized as a reinforcing material in the fiber-reinforced composite material according to the invention. The fully aromatic polyamide fibers may be combined with other reinforcing fibers as required. Reinforcing fibers in the form of long or short fibers may be present in the invention's composite material. These fibers may also be used to create nonwoven fabrics, yarn with several filaments, plain weave, satin weave, twill weave, basket weave, etc. Instead of initially producing a sheet-like material, it is also feasible to combine and knead the matrix resin with the reinforcing fibers, preferably in the form of short fibers, and shape the combination immediately into the desired item. In addition to the previously described compression molding technique, other molding techniques include spraying, manual lay-up, lamination, transfer molding, and injection molding. Depending on the shape of the reinforcing fibers and/or the characteristics of the matrix resin, one of these techniques can be used.

### 7.9.3 Fiber with reversible enhanced thermal storage properties and fabrics made therefrom

At specific temperatures, the thermal characteristics of a fiber containing built-in microspheres packed with plastic crystals or phase-change material are improved. The fibers may be woven to create a fabric with improved thermal storage capabilities, and from that fabric, articles of manufacturing can be created. Non-woven fabrics made entirely or primarily of staple fibers, or like relatively short fibers from fleeces or layers made of fibers without cohesive properties already present or potential are distinguished by the use of specific types of fibers, provided that this use does not predominately affect the consolidation of the fleece. It is common knowledge that different compounds may be used to modify the qualities of fabrics and/or fibers. For instance, it is well known that rubber, either natural or synthetic, may be used to waterproof fabrics. There are substances in the market that, when sprayed into materials, provide stain resistance. In addition, it is well known that textiles may contain scent delivery systems. One such method of fragrance distribution involves microcapsules loaded with breakable fragrance that are attached to the surface of a fabric or fiber. When an external force is applied, the microcapsules break, releasing the scent over a prolonged period of time [44].

The aforementioned surface-mounted phase change materials do have certain drawbacks, though. For instance, it was discovered that while the phase change material was partially effective, it was not firmly bonded to the fibers and that laundering mostly destroyed the substance. With each laundering, a fraction of the phase change material was eliminated, resulting in a shift in the fabric's thermal characteristics that limited its usability. As a result, the fabric lacked repeatability in its thermal response. In order to prolong the usable life of the improved thermal characteristics, more work was done to perfect a series of binding processes for the phase change material to the fabric. The current invention will be explained in more detail, but it is important to note right away that those who are skilled in the art may change the invention as detailed here and still achieve its desirable effects. As a result, the following description is to be considered as a comprehensive educational disclosure addressed at those with suitable experience in the arts, and not as restrictive upon the present invention. Furthermore, according to the creators' knowledge, these materials' usefulness has been applied to a wider temperature range, which restricts their ability to absorb or release heat at a certain temperature range.

## 7.10 Future scope and perspectives

Since the world is experiencing a crisis of sustainable growth and environmental stability, the whole engineering community is now held accountable for change. Because of the green building movement, science in energy and environmental design, innovation for sustainability, and many other activities, the United States is ready to go in a more environmentally friendly direction. We may envision a carbon-neutral urban ecology. Research and development on paradigm-shifting technologies may have as a mid-term goal the creation of an urban habitat that can adapt to its environment while consuming the least amount of water and energy [45]. The National Science Foundation is funding a number of projects with a focus on net-zero energy buildings that maximize the heating, cooling, lighting, and influence of solar energy and other natural resources to reduce energy consumption while maintaining habitable conditions. These projects also focus on net-zero water buildings. To lower the embodied energy of these infrastructure systems, for instance, research into, and field application of green building techniques and materials will be conducted [46].

Future FRP research will also put a lot of emphasis on developing intelligent and versatile materials. Among the crucial ones are self-assessing and self-healing coatings, phase-changing materials for energy storage and release, self-cleaning and anti-pollution coatings, conductive polymers for solar cells, self-deicing materials, coatings that might be used as sensors, and many more. For instance, there will be a lot of research into ways to better use carbon fibers for sensing and detecting damage utilizing nano-fibers that include polymers. It is possible to use nano-fiber coatings as sensors to detect minor cracks, fires, and hazardous materials [47]. To identify structural threats like fire, wireless networks and electrically conductive coatings will be developed. A team at the University of Colorado at Boulder is also investigating the living wall concept with flow channels and phase change materials. To enable their practical use in the field at a reasonable cost, these subjects will be further investigated in depth. Regarding FRP composites, it is necessary to build and integrate a prefabricated modular sub-system design concept with durable, robust, and stiff composite panels composed of natural fibers and resins. These panels have ten times lower embodied energy than steel and cost four times less [48].

## 7.11 Summary

Stretchable power sources made of advanced fiber materials are generally expected to have a bright future. We anticipate that it will be feasible to find the appropriate materials to allow high-performance and practical deformable power sources by combining many of the techniques discussed in this review. To allow wearable electronics that can be worn on the skin, it will be essential to build soft, flexible, and conformal energy storage technologies. Stretchable power sources are presently being developed more slowly than wearable electronics; however there has been significant advancement in this area over the past ten years. In this analysis, we emphasized that while supercapacitors and stretchy batteries have gotten more attention than flexible energy sources, the performance of stretchable technologies is starting to catch up [49].

These deformable battery technologies would advance already available wearable technology with further research. These earlier studies have made significant progress by providing the foundational concepts for the design, fabrication, and characterization of functional fiber devices and by demonstrating the benefits of fiber-shaped devices, such as the desired miniaturization, weavability, flexibility and wearability. It encouraged the growth of research on multipurpose fiber-shaped devices. These initiatives also raise people's awareness of the potential uses for functional fiber devices, making them more eager to put them to use [50].

The advanced fiber materials reinforced composites' water absorption capabilities are decreased and the adhesive force between the natural fiber and matrix is increased thanks to the surface-modified fibers. Surface-modified fiber composites outperformed untreated fiber composites in terms of tensile strength. With the exception of the alkali approach, mixed surface modification fiber has superior mechanical qualities than single surface modification. The silane-modified surface-modified fiber composites have demonstrated good impact strength characteristics [51]. The surface changes of the advanced fiber materials can eliminate natural fiber contaminants such as lipids, lignins, and pectins.

# References

[1] Thevenaz L. Advanced fiber optics: concepts and technology. EPFL press; 2011.

[2] Hota G, Liang R Advanced fiber reinforced polymer composites for sustainable civil infrastructures. In: Proceedings of the International Symposium on Innovation & Sustainability of Structures in Civil Engineering. Xiamen University; 2011.

[3] Teixeira JG, Leite IT, Silva S, Frazão O. Advanced fiber-optic acoustic sensors. Photonic Sens. 2014; 4(3):198–208.

[4] Taheri F. Advanced fiber-reinforced polymer (FRP) composites for the manufacture and rehabilitation of pipes and tanks in the oil and gas industry. In: Advanced fibre-reinforced polymer (FRP) composites for structural applications. Elsevier; 2013. pp. 662–704.

[5] Jia H, Qiu M, Tang C, Liu H, Xu J, Tawiah B, et al. Advanced flexible carbon-based current collector for zinc storage. Adv Fiber Mater. 2022;1–11.

[6] Shi Q, Sun J, Hou C, Li Y, Zhang Q, Wang H. Advanced functional fiber and smart textile. Adv Fiber Mater. 2019;1(1):3–31.

[7] Huang W, Xiao Y, Shi X. Construction of electrospun organic/inorganic hybrid nanofibers for drug delivery and tissue engineering applications. Adv Fiber Mater. 2019;1(1):32–45.

[8] Duoerkun G, Zhang Y, Shi Z, Shen X, Cao W, Liu T, et al. Construction of n-TiO2/p-Ag2o junction on carbon fiber cloth with Vis–NIR photoresponse as a filter-membrane-shaped photocatalyst. Adv Fiber Mater. 2020;2(1):13–23.

[9] Li M, Chen X, Li X, Dong J, Zhao X, Zhang Q. Controllable strong and ultralight aramid nanofiber-based aerogel fibers for thermal insulation applications. Adv Fiber Mater. 2022;4(5):1267–1277.

[10] Meng X, Xu W, Li Z, Yang J, Zhao J, Zou X, et al. Coupling of hierarchical Al2O3/TiO2 nanofibers into 3D photothermal aerogels toward simultaneous water evaporation and purification. Adv Fiber Mater. 2020;2(2):93–104.

[11] Wang Z, You W, Wang W, Tian W, Chen F, Xiao Y, et al. Dihydromyricetin-incorporated multilayer nanofibers accelerate chronic wound healing by remodeling the harsh wound microenvironment. Adv Fiber Mater. 2022;1–16.

[12] Yang X, Li L, Yang D, Nie J, Ma G. Electrospun core–shell fibrous 2D scaffold with biocompatible poly (glycerol sebacate) and poly-l-lactic acid for wound healing. Adv Fiber Mater. 2020;2(2):105–117.

[13] Tebyetekerwa M, Xu Z, Yang S, Ramakrishna S. Electrospun nanofibers-based face masks. Adv Fiber Mater. 2020;2(3):161–166.

[14] Dong Y, Zheng Y, Zhang K, Yao Y, Wang L, Li X, et al. Electrospun nanofibrous materials for wound healing. Adv Fiber Mater. 2020;2(4):212–227.

[15] Sun Y, Mwandeje JB, Wangatia LM, Zabihi F, Nedeljković J, Yang S. Enhanced photocatalytic performance of surface-modified TiO2 nanofibers with rhodizonic acid. Adv Fiber Mater. 2020; 2(2):118–122.

[16] Zhao J, Cui W. Functional electrospun fibers for local therapy of cancer. Adv Fiber Mater. 2020; 2(5):229–245.

[17] Xiong SW, Yu Y, Wang P, Liu M, Chen SH, Yin XZ, et al. Growth of AgBr/Ag3PO4 heterojunction on chitosan fibers for degrading organic pollutants. Adv Fiber Mater. 2020;2(5):246–255.

[18] Yan C, Zhu P, Jia H, Zhu J, Selvan RK, Li Y, et al. High-performance 3-D fiber network composite electrolyte enabled with Li-ion conducting nanofibers and amorphous PEO-based cross-linked polymer for ambient all-solid-state lithium-metal batteries. Adv Fiber Mater. 2019;1(1):46–60.

[19] Fan HL, Zeng T, Fang DN, Yang W. Mechanics of advanced fiber reinforced lattice composites. Acta Mech Sin. 2010;26(6):825–835.

[20] Balilonda A, Li Q, Tebyetekerwa M, Tusiime R, Zhang H, Jose R, et al. Perovskite solar fibers: current status, issues and challenges. Adv Fiber Mater. 2019;1(2):101–125.

[21] Zhou J, Hu Z, Zabihi F, Chen Z, Zhu M. Progress and perspective of antiviral protective material. Adv Fiber Mater. 2020;2(3):123–139.

[22] Kunwar R, Harilal M, Krishnan SG, Pal B, Mariappan CR, et al. Pseudocapacitive charge storage in thin nanobelts. Adv Fiber Mater. 2019;1(3):205–213.

[23] Thostenson ET, Chou TW. Real-time in situ sensing of damage evolution in advanced fiber composites using carbon nanotube networks. Nanotechnology. 2008;19(21):215713.

[24] Li X, Chen X, Jin Z, Li P, Xiao D. Recent progress in conductive polymers for advanced fiber-shaped electrochemical energy storage devices. Mater Chem Front. 2021;5(3):1140–1163.

[25] Toutanji H. Stress-strain characteristics of concrete columns externally confined with advanced fiber composite sheets. Mater J. 1999;96(3):397–404.

[26] Cao X, Wang T, Jiao L. Transition-metal (Fe, Co, and Ni)-based nanofiber electrocatalysts for water splitting. Adv Fiber Mater. 2021;3(4):210–228.

[27] Wang G, Wang L, Meng Z, Su X, Jia C, Qiao X, et al. Visual detection of COVID-19 from materials aspect. Adv Fiber Mater. volume 4, pages 1304–1333; 2022; 1–30.

[28] Ricca SP, Huynh TC, Kong N. Impact of advanced fiber optics and ISDN technologies on PACS networking. In: Medical imaging III: PACS system design and evaluation. SPIE; 1989. pp. 140–153.

[29] Ganesh Gupta KB, Hiremath MM, Prusty RK, Ray BC. Development of advanced fiber-reinforced polymer composites by polymer hybridization technique: Emphasis on cure kinetics, mechanical, and thermomechanical performance. J Appl Polym Sci. 2020;137(43):49318.

[30] Ding B. Advanced nanofiber materials and systems: Solving global issues. Vol 2, Advanced Fiber Materials. Springer; 2020. pp. 45–45.

[31] Ma M, Yao Y, Wu Y, Yu Y. Progress and prospects of transition metal sulfides for sodium storage. Adv Fiber Mater. 2020;2(6):314–337.

[32] Yang X, Li L, Yang D, Nie J, Ma G. Electrospun core–shell fibrous 2D scaffold with biocompatible poly (glycerol sebacate) and poly-l-lactic acid for wound healing. Adv Fiber Mater. 2020;2(2):105–117.

[33] Weng W, Yang J, Zhang Y, Li Y, Yang S, Zhu L, et al. A route toward smart system integration: from fiber design to device construction. Adv Mater. 2020;32(5):1902301.

[34] Spinks GM. Advanced actuator materials powered by biomimetic helical fiber topologies. Adv Mater. 2020;32(18):1904093.

[35] Mehdipour A, Sebak AR, Trueman CW, Rosca ID, Hoa SV. Advanced carbon-fiber composite materials for RFID tag antenna applications. Appl Comput Electromagn Soc J ACES. 2010;218–229.

[36] McAlister III DD, Foulk JA, Harrison RE. Advanced fiber information system length measurement of cottons hand-sorted by length group. 2003.

[37] Vasiliev V, Morozov V, Evgeny V. Advanced mechanics of composite materials and structural elements. Newnes; 2013.

[38] Wang L, Fu X, He J, Shi X, Chen T, Chen P, et al. Application challenges in fiber and textile electronics. Adv Mater. 2020;32(5):1901971.

[39] Burchell TD. Carbon materials for advanced technologies. Elsevier; 1999.

[40] Hoffmann M, Diaz DJ Characterization of fiber materials using metallographic and image analysis techniques. In: Proceedings of the 20th annual conference on composites, advanced ceramics, materials, and structures – B: Ceramic engineering and science proceedings. Wiley Online Library; 1996. pp. 68–75.

[41] Gray DA, Hume RM, Litman MA. Advanced fabric technology and filters [internet]. US20150044267A1, 2015 [cited 2022 Oct 23]. Available from: https://patents.google.com/patent/US20150044267/en

[42] Yuzo A, Keizo S Fiber-reinforced composite materials [internet]. EP0057908B1, 1988, [cited 2022 Oct 23]. Available from: https://patents.google.com/patent/EP0057908B1/en.

[43] Bryant YG, Colvin DP. Fiber with reversible enhanced thermal storage properties and fabrics made therefrom [internet]. US4756958A, 1988 [cited 2022 Oct 23]. Available from: https://patents.google.com/patent/US4756958A/en.

[44] Burchell TD. Carbon materials for advanced technologies. Elsevier; 1999.

[45] Hoffmann M, Diaz DJ Characterization of fiber materials using metallographic and image analysis techniques. In: Proceedings of the 20th annual conference on composites, advanced ceramics, materials, and structures – B: Ceramic engineering and science proceedings. Wiley Online Library. 1996. pp. 68–75.

[46] Uddin N. Developments in fiber-reinforced polymer (FRP) composites for civil engineering. Elsevier; 2013.

[47] Petermann I, Sahlgren B, Helmfrid S, Friberg AT, Fonjallaz PY. Fabrication of advanced fiber Bragg gratings by use of sequential writing with a continuous-wave ultraviolet laser source. Appl Opt. 2002;41(6):1051–1056.

[48] Karbhari VM, Seible F. Fiber reinforced composites–advanced materials for the renewal of civil infrastructure. Appl Compos Mater. 2000;7(2):95–124.

[49] Clauss B, Schawaller D. Modern aspects of ceramic fiber development. In: Advances in science and technology. Trans Tech Publ; 2006. pp. 1–8.

[50] Okamoto M. Spinning of ultra-fine fibers. Adv Fiber Spinn Technol. 1994;187–207.

[51] Kuang, KSC, Cantwell WJ. Use of conventional optical fibers and fiber Bragg gratings for damage detection in advanced composite structures: A review. Appl Mech Rev. 2003;56(5):493–513.

Ritika Wadhwa, Arushi Arora, Krishna K. Yadav*

# Chapter 8
# Advanced fiber materials in optical and photonic application

**Abstract:** Fiber materials can directly relate to our daily life in society as well as in the development of advanced materials for their practical application which can smooth our life easy. However, conventional fibers and fiber products need modification for utilization in automation and intellectualization in modern society. The advanced fiber-shaped materials can be used in various applications including electronics, sensors, catalysis, and photonics. Recently, advanced fiber-based materials have been utilized for making wearable electronics as well as in making various photo sensing as well as making IR filters. This chapter deals with the synthesis and utilization of advanced fiber materials for optical and photonics applications.

**Keywords:** Fiber materials, photosensing, IR filters, synthesis, optical and photonic applications

## 8.1 Introduction

Fiber materials are a class of continuous filamentous materials which are distinct, elongated pieces like thread length. Mankind has long been using fiber materials in diverse fields. Fiber-based materials can be spun into distinct filaments, strings, and ropes, as a component of composite materials and can be drawn into sheets for the manufacture of products like felt, paper etc. Some of the strongest engineering materials have their basic unit as fiber, like carbon fiber and polyethene which has ultra-high molecular weight.

The category of fiber type is mainly dependent on its origin: mineral, animal, or plant. Cellulose constitutes the major structural component in plant fiber whereas protein is the main constituent in animal fiber. Although the asbestos group of minerals make up the main constituent of the mineral fiber, after crucial research, they have been found to cause health issues and hence are avoided. In general, plant fibers exhibit higher stiffness and strength than animal fibers, silk being the exception which

---

**Note:** #Equally contributed.

---

***Corresponding author: Krishna K. Yadav,** Institute of Nano Science and Technology, Knowledge City, Sector 81, Mohali, Punjab India, India, e-mails: Krishnay447@gmail.com, Krishphy25@gmail.com

https://doi.org/10.1515/9783110992892-008

has high strength but less stiffness [1]. Therefore, plant-based fibers are generally preferred to be used in composites with desired structural requirements. Another important category of important fiber materials is fiber optical. E-glass or optical fiber is a thin transparent and flexible fiber. The branch of "fiber optics" is concerned with the design and application of optical fibers. Over the years much improvement has occurred concerning improvement in the selection of fiber, treatment, extraction procedures, and engineering at the interface of fiber materials. The major constituents of fiber-reinforced composites tend to be fiber. Apart from being the largest constituent of fiber-reinforced composite materials, they also act as the largest load bearers of composite structures. Fibers have extremely small diameters which are hard to handle. The fiber materials that tend to be a bundle is the most useful form which is a collection of a large number of continuous filaments. It may be a twisted bundle which is called a yarn and untwisted form is called a strand.

### 8.1.1 History of fiber materials

The very first artificial fiber was viscose in 1894 and rayon in 1924. An analogous material discovered in 1865, was cellulose acetate. As cellulose acetate and rayon are derived from wood, they are artificial fibers but are not truly synthetic. Despite being discovered in the mid-nineteenth century, modern manufacture and processing started much later. Nylon was the first synthetic fiber which came into existence in the US at the time of World War II, as the substitute for silk. It was majorly used in parachutes, military armory, and most importantly in women's clothing. Some very common fibers along with their discovery year are given in Figure 8.1a and b. Apart from that, a few latest fiber materials that are made from older artificial materials are listed as follows:

**Glass fibers** were first made in 1936 and are used in the form of glass wool for industrial, automobile, and home insulation. Glass-reinforced plastic and glass fiber-reinforced concrete are some of the glass fiber-reinforced composite materials.

**Metallic fibers** discovered in 1946 have been widely used in the fashion industry for lustrous clothing and many heat conduction and electronic devices. Some of fiber-reinforced materials are also used in the horticulture industry as synthetics which are:
- Phenolic foam resins
- Polyurethane foam
- Urea-formaldehyde resin foam
- Expanded polystyrene flakes

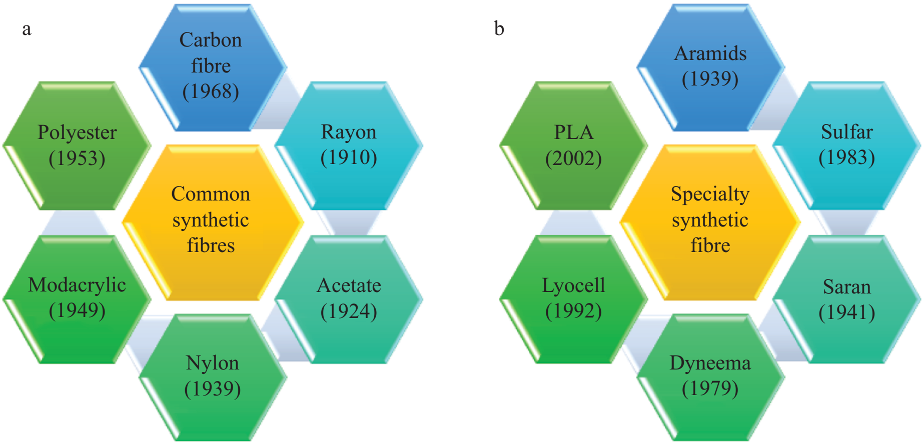
a
Carbon fibre (1968)
Polyester (1953)
Rayon (1910)
Common synthetic fibres
Modacrylic (1949)
Acetate (1924)
Nylon (1939)
b
Aramids (1939)
PLA (2002)
Sulfar (1983)
Specialty synthetic fibre
Lyocell (1992)
Saran (1941)
Dyneema (1979)

**Figure 8.1:** (a) Common synthetic fibers with their year of discovery; (b) especially synthetic fibers with their year of discovery.

## 8.2 Types of fiber materials

Although fiber materials are widely characterized the core types include natural and man-made or synthetic fibers.

### 8.2.1 Natural fibers

The fibers produced by animals, plants, and natural geological processes are classified under natural fibers and are biodegradable (Figure 8.2).

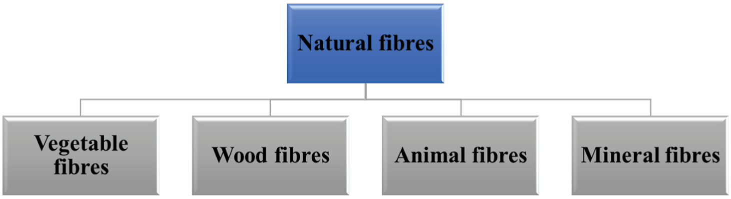
Natural fibres
Vegetable fibres
Wood fibres
Animal fibres
Mineral fibres

**Figure 8.2:** Classification of natural fibers.

#### 8.2.1.1 Vegetable fiber

Cotton, ramie, sisal, flax, and hemp constitute vegetable fiber. The thickness and strength of these fibers depend on the arrangement of cellulose. Plant fibers are mainly used in the paper and textile industry.

#### 8.2.1.2 Wood fiber

This generally comes from tree sources. Various forms of wood fiber include thermo-mechanical pulp, sulphite pulps, ground woods, and kraft pulps. The type of pulping process decides whether the pulp is kraft or sulphite. The pulping process removes the lignin bonds in the inherent wood structure. Hence, fibers are frozen for utilization in paper and wood products like fiberboard.

#### 8.2.1.3 Animal fibers

Fibers of spider silk, wool, sinew, wool, and hairs like mohair, angora, and cashmere, and furs of sheep, fox, camel, and rabbit constitute animal fiber. Fibers from birds have been also been ornamentally used in many clothing lines.

#### 8.2.1.4 Mineral fiber

The only naturally occurring long mineral fiber includes asbestos. Short mineral fiber includes attapulgite and halloysite

### 8.2.2 Man-made/synthetic fibers

Man-made or synthetic fibers are generally derived from synthetic materials such as petrochemicals. Some synthetic fibers are also derived from natural ones such as cellulose, rayon, modal etc. Pure cellulose is derived from the cupro-ammonium process and modified cellulose from cellulose acetates. These fibers are primarily the result of intuitive research by scientists over the years to improve naturally occurring fiber materials. More than half of all the fiber used in clothing and textile is procured from synthetic fibers. Almost all synthetic fibers are known to be value-added commercial products among which polyester, acrylic, and nylon stand dominant in the market. A precise brief introduction to synthetic fibers is given below.

#### 8.2.2.1 Fiberglass

It consists of extremely fine fibers of glass. It is a very common insulator which has been used as a reinforcing agent in many polymer products which is known as fiber-reinforced plastic or glass-reinforced plastic.

#### 8.2.2.2 Polymer fibers

These fibers are based on synthetic chemicals like petrochemical sources. These types of fibers can be made from polyamide nylon, polyvinyl alcohol fiber, phenol formaldehyde, spandex, polyurethane fibers, and so on.

#### 8.2.2.3 Microfibers

Sub-denier fibers constitute microfibers in textiles. These are ultrafine fibers which are majorly used in the filtration process. Modern microfibers consist of fibers that further split into ultrafine fibers.

#### 8.2.2.4 Nylon

They constitute a family of synthetic polymers known as polyamides. Nylon is one of the most used polymer fibers. The major application thrust of nylon includes applications in fabrics, textile bridal veils, ropes, and carpets.

#### 8.2.2.5 Polyethene

It is a thermoplastic polymer fiber consisting of the individual monomer of ethylene. Numerous types of polyethene classifications have been done based on density and branching.

#### 8.2.2.6 Polyester

These kinds of polymer fibers contain an ester group in their main chain. Polyethene terephthalate is the most commonly used polyester. Various classifications of polyester include aliphatic, semi-aromatic, and aromatic groups in their main chain.

## 8.3 General applications of fiber materials

For practical purposes, researchers are on their wheels to design materials with improved properties and practical usability to facilitate and match fast-paced modern living. In this regard, several factors need to be considered to achieve a low-cost stale material with excellent properties of density, hardness, machinability, durability, castability, weldability etc. The study of integrating fibers as composite materials for practical usability is at its height. The intention of making fiber-reinforced composites is to introduce the best attributes of each of the materials, to make a more efficient hybrid material.

Fibers of high strength are intercalated into a matrix of any other material to form a distinct interface. Besides retaining their individual physical and chemical properties they produce combinational superior properties unable to achieve with either of them acting alone. Fiber- reinforced composites are most commonly used as laminate, which comprise thin layers of fibers stacked into desired thicknesses. Industrial and commercial applications of fiber-reinforced composites are too wide to mention them all. Some of the general applications have been sketched down in Figure 8.3.

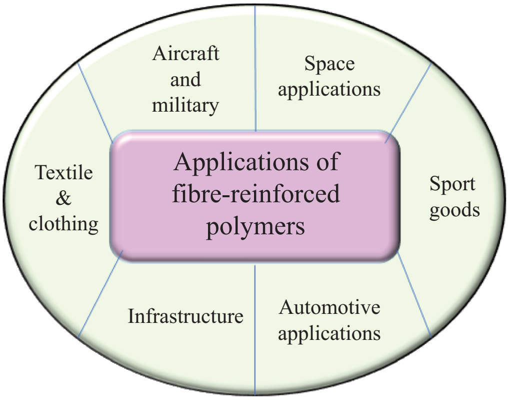

**Figure 8.3:** General applications of fiber-reinforced polymers.

### 8.3.1 Aircraft and military applications

Weight reduction for this kind of application is a major challenge for higher payloads and increased speeds. As carbon fibers were introduced in 1970, they have become an indispensable part of aircraft structures. They have indeed shown a very good performance of structural integrity and durability. The major advantage of using carbon fibers is that they mitigate the radar reflection signals and excessive heat inside the aircraft. Various materials have been used in the aircraft's body such as Boron fiber-epoxy and carbon fiber-epoxy. In rotor blades of aircraft epoxy reinforced with glass or carbon fibers are used.

### 8.3.2 Space applications

The prime reason that fiber-reinforced composites have been used in space vehicles is the weight or mass reduction. The structure and materials used in major spacecraft parts are given in Table 8.1.

**Table 8.1:** Structure and corresponding fiber-reinforced polymer materials.

| Structure | Fiber-reinforced polymer |
|---|---|
| Mid-fuselage framework structure | Tubes of aluminum fortified with boron fibers |
| Payload bay door | Epoxy face sheets fortified by sandwiched laminates of carbon fiber |
| Remote manipulator arm | Ultra-high-modulus carbon fiber-reinforced epoxy tube |
| Pressure vessels | Kevlar 49 fiber-reinforced epoxy |

### 8.3.3 Automotive applications

Chassis, body, and engine components require the use of fiber materials. Door panels and hoods of vehicles require very high damage tolerance and very high stiffness factor. E-glass fiber reinforced sheets are used for these components in which a matrix of vinyl ester resin and glass fibers are randomly dispersed. Although carbon-fiber reinforced composites are also used but using E-glass fiber composite parts is more economical.

### 8.3.4 Infrastructure applications

Polymer composites reinforced by fiber have great potential for replacing reinforced steel and concrete in various civil infrastructures, buildings, and bridges. The major advantage they offer is resistance to corrosion along with low maintenance and less repair costs. Fiber-reinforced composites tend to be lightweight too which aids its easy transportation and installation. The main component of the material used in infrastructure material is glass fiber-reinforced vinyl ester which provides improved strength.

### 8.3.5 Optical fiber communication

As optical fibers are flexible and bundled as cable they are widely used as a telecommunication medium. Optical fiber cables allow light signals to be propagated by very little attenuation compared to electrical cables they are much more suitable for long-distance communications, which restricts the use of excess repeaters. The use of fiber optics makes it immune to electrical interference and thereby offers less crosstalk with little background environment noise. Since fibers are thin materials, they occupy very less space thereby being advantageous for space saving in electrical ducts.

### 8.3.6 Textile and clothing

Fibers constitute the heart and soul of the textile and clothing industry. One of the most commonly used fiber polymers is nylon, which is a thermoplastic silky material. Its fibers are made up of repeating polyamide linkages. They are widely used in fabrics, bridal veils, ropes, and strings. Another common textile fiber is polyester which contains an ester functional group in its parent chain. Polyester fibers are extensively used in home furnishings and apparel like gym wear, waterproof clothing, and jackets. Figure 8.4 shows an SEM image of the textile sample.

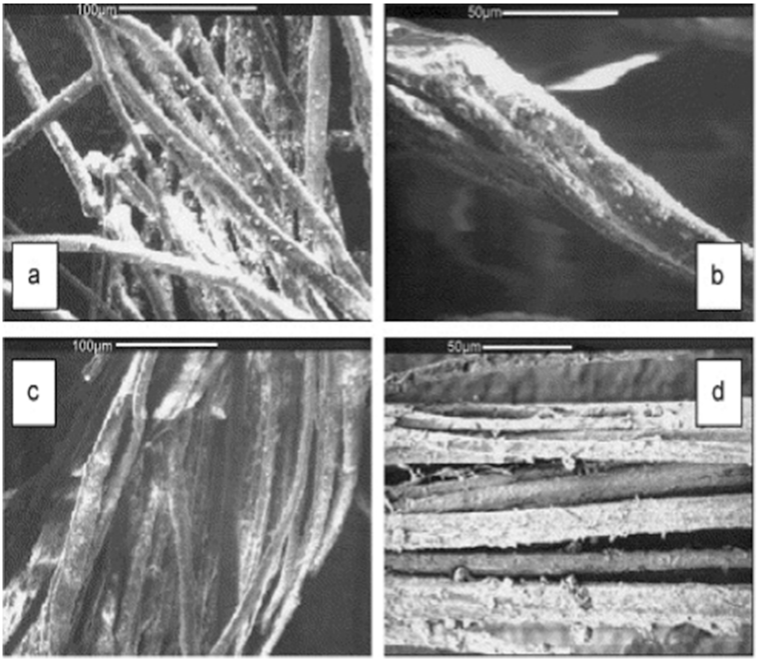

**Figure 8.4:** SEM micrographs of textile fibers [2].

# 8.4 Synthesis of a few common fiber materials

## 8.4.1 Glass fibers

The two most common types of glass fibers used in glass fibers are E and S glass. Silica is the primary ingredient of all glass fibers and some oxides such as boron oxide and alumina are used for the modification of silica matrix and improve its structure [3]. The basic steps of glass fiber manufacturing are shown in Figure 8.5.

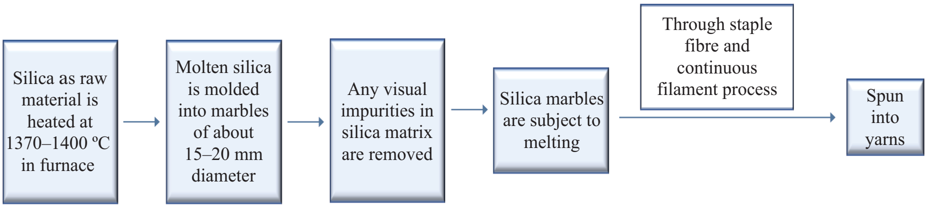
Silica as raw material is heated at 1370–1400 ºC in furnace
Molten silica is molded into marbles of about 15–20 mm diameter
Any visual impurities in silica matrix are removed
Silica marbles are subject to melting
Through staple fibre and continuous filament process
Spun into yarns

**Figure 8.5:** Steps of glass fiber manufacturing.

Figure 8.5 is a glimpse of a whole detailed process of glass fiber making. After the final step of molding to yarn, glass fibers are ready to be used in tapes, industrial fabrics, and insulators.

## 8.4.2 Carbon fibers

Carbon fiber is a very strong and light fiber-reinforced polymer, though it is expensive. Its high strength and lightweight nature allow it to be used in aerospace engineering. Considering its structure carbon fiber is an amalgam, of graphitic and amorphous carbon [4]. Two types of precursors are used in the manufacture of carbon fiber: the textile precursor (Figure 8.6) which is polyacrylonitrile (PAN) and the pitch precursor which happens to be a by-product of coking of coal.

## 8.4.3 Aramid fibers

These are highly crystalline aromatic polyamide fibers having high tensile strength and the lowest density. A typical aramid fiber under the commercial name of Kevlar 49 has amide and an aromatic ring as a repeating unit [5]. Aromatic ring contributes to a higher chain modulus and better properties. In a typical synthesis of Kevlar 49 filament, an acidic solution of *p*-phenylene diamine and terephthaloyol chloride is extruded from a spinneret. The precursors under a polycondensation reaction form the final fiber

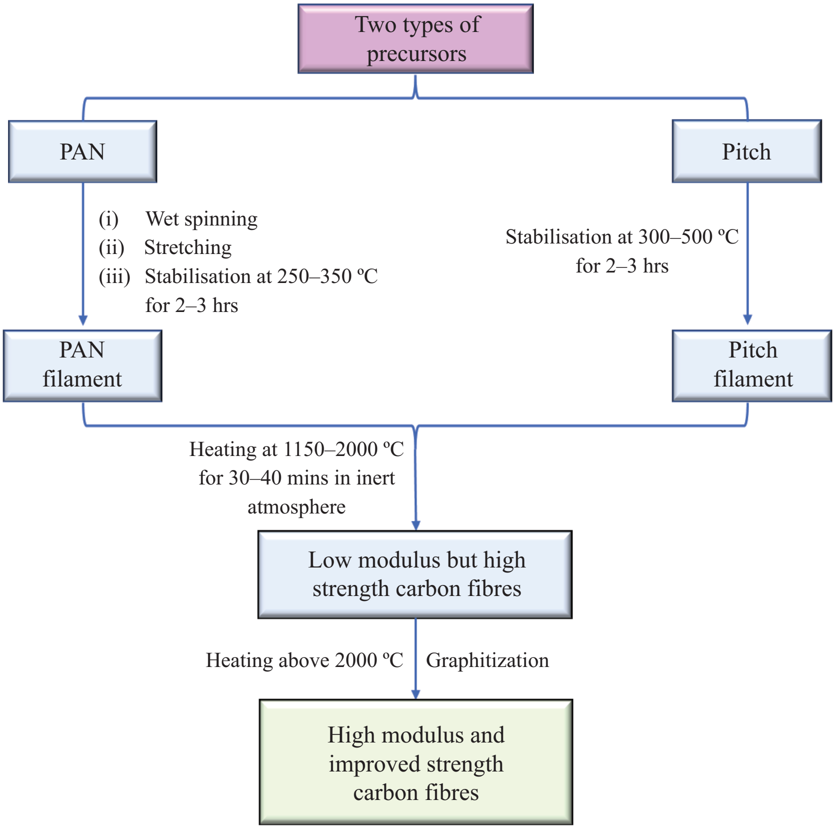
Two types of precursors
PAN
Pitch
(i) Wet spinning
(ii) Stretching
(iii) Stabilisation at 250–350 °C for 2–3 hrs
Stabilisation at 300–500 °C for 2–3 hrs
PAN filament
Pitch filament
Heating at 1150–2000 °C for 30–40 mins in inert atmosphere
Low modulus but high strength carbon fibres
Heating above 2000 °C
Graphitization
High modulus and improved strength carbon fibres

**Figure 8.6:** The basic flow of synthesis of carbon fiber from its precursor petroleum refining.

product. Frail hydrogen bonding between hydrogen and oxygen atoms holds the structure in a transverse direction. Figure 8.7 shows a sectional structure of Kevlar 49 fiber.

### 8.4.4 Extended-chain polyethene fiber

They are formed by gel spinning of high molecular weight polyethene, under the commercial name of spectra. To date spectra, polyether fiber has the highest strength-to-weight ratio among the other commercial fibers. The gel spinning technique yields fibers with excellent crystallinity of about 95–99% and is therefore a highly oriented fibrous structure.

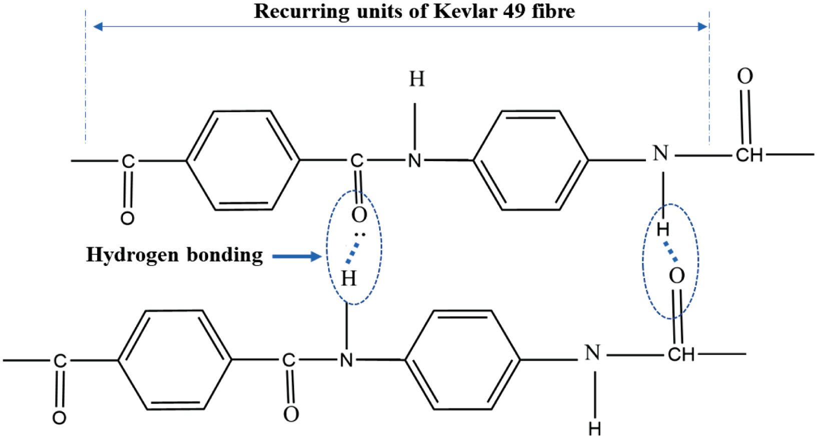

**Figure 8.7:** Repeating units of Kevlar 49 showing hydrogen bonding.

### 8.4.5 Boron fibers

Boron fibers have high compressive strength so they have been extensively used in boron-reinforced fiber composites [6]. Being expensive, these fibers have restricted themselves to aerospace engineering applications. The chemical vapor deposition method is used to manufacture boron fiber. Boron is deposited on a heated substrate which is usually a carbon filament or tungsten wire. Reaction of hydrogen with boron chloride produces boron vapors. Boron is forced into a reaction chamber of about 1,000–1,300 °C, which converts the substrate into its boride, thereby forming the basic fibers of various diameters:

$$2BCl_3 + 3H_2 \rightarrow 2B + 6HCl$$

Fiber materials can directly relate to our daily life in society as well as in the development of advanced materials for their practical application which can smooth our life easy. However, conventional fibers and fiber products need modification for utilization in automation and intellectualization in modern society. The advanced fiber-shaped materials can be used in various applications including electronics, sensors, catalysis, and photonics. Recently, advanced fiber-based materials have been utilized for making wearable electronics as well as in making various photo sensing as well as making IR filters. This chapter deals with the synthesis and utilization of advanced fiber materials for optical and photonics applications.

## 8.5 Application of fiber materials

The development of the relevant manufacturing industries and the daily life of the people has now been dependent on the application and advancement in the research related to fiber materials more than ever. Not only the natural and chemical fiber materials find application in textile and clothing but increased attention is being paid to functional fibers and smart fibers for their application in fields such as optics, healthcare, and energy harvesting [7]. The unique features of the fiber materials such as controllable architectures, tunable chemical compositions and high surface area make them suitable for their usage in a diverse range of applications including photonic and optical applications [8]. The functional and most fascinating aspect of any nanomaterial is its optical properties. The optical properties of a material can be tuned by altering the shape, particle size, surface characteristics, and other variables. Basic understanding of spectroscopic techniques and fundamental optical properties used to analyze them can help design materials for different applications. The major applications that depend on the optical properties are solar cells, photocatalysis, photoelectronic, light emission and detection [9].

Optics is a branch of physics dealing with topics related to the study of light. The subset of optics discipline that deals with the study of light, is called photonics. Light is a vital aspect of contemporary society as it is used everywhere including transportation, building, telecommunication, etc. Light is electromagnetic radiation that consists of a wide range of wavelengths and under certain circumstances shows particle behavior as well [10]. Light is used in optical fibers and optoelectronics. Light encompasses a far bigger spectrum compared to the capability of the human eye to see. When a stream of photons moves from one point to another, it refers to the particle nature of light [11]. Photons are primary particles of light and in a way are similar to electrons. Depending upon the use of light for a particular application wave or particle nature is given importance. During the use of light for optical fiber transmission, wave nature of light is of importance; while during the use of light in optoelectronics, particle nature is of importance [12].

### 8.5.1 Advanced fiber materials for optical application

Optical applications cover a wide aspect of our daily life now. Optics involves observing and analyzing properties and interaction of light with matter. Light constitutes a series of electromagnetic waves which makes up the electromagnetic spectrum including a wide range of frequencies from 1 to 1,025 Hz. In the electromagnetic spectrum, different frequency bands correspond to different electromagnetic waves which are X-rays, ultraviolet, visible light, infrared, microwave, and radio waves. During the optical fiber transmission, the electromagnetic spectrum that is used to locate the radiation used is shown in Figure 8.8.

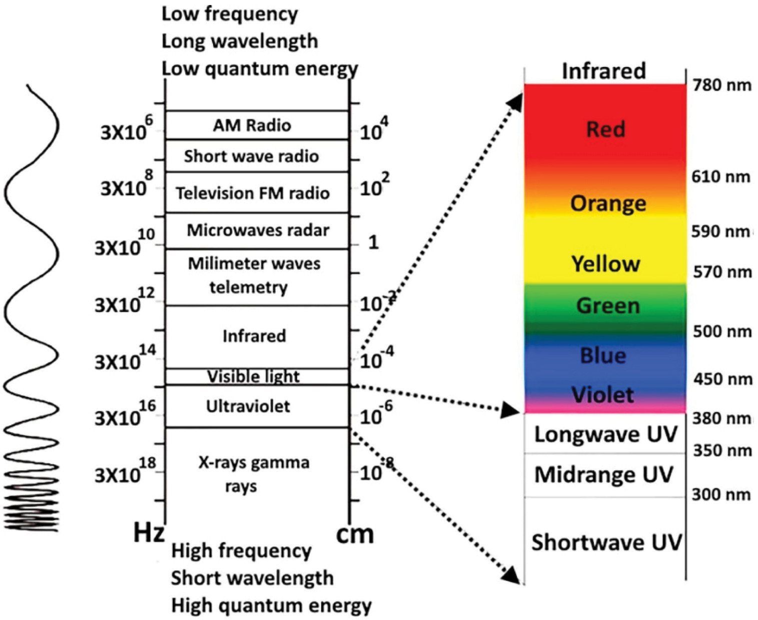
Low frequency
Long wavelength
Low quantum energy
3X10^6
3X10^8
3X10^10
3X10^12
3X10^14
3X10^16
3X10^18
Hz
AM Radio
Short wave radio
Television FM radio
Microwaves radar
Milimeter waves telemetry
Infrared
Visible light
Ultraviolet
X-rays gamma rays
10^4
10^2
1
10^-2
10^-4
10^-6
10^-8
cm
High frequency
Short wavelength
High quantum energy
Infrared
Red
Orange
Yellow
Green
Blue
Violet
Longwave UV
Midrange UV
Shortwave UV
780 nm
610 nm
590 nm
570 nm
500 nm
450 nm
380 nm
350 nm
300 nm

**Figure 8.8:** The electromagnetic spectrum involves different frequency bands (reproduced with permission [12]. Copyright 2018, Elsevier).

There is a rise in the need for optically functional and transparent materials due to the continuous expansion of the applications of optical materials. Recently certain materials have received attention for fabricating a new generation of efficient, high speed, and multifunctional optical devices. Among them, materials having long length and smaller diameter have received more attention for enhancing efficiency and miniaturization. Fiber materials have been shown great interest due to their tremendous success in optical communication in the past two decades. The invention of optical fibers in the 1960s has made them a crucial part of our daily life due to their enormous impact. With the advancement in technology, they have broadened their application from waveguides during optical transmission to sensing devices and have also become a crucial element in modern communication, manufacturing, and healthcare [13].

Optical fiber is a flexible, thin, transparent fiber that acts as a waveguide utilized for the transmission of light between the two ends of the fiber. They are mainly used in fiber-optic communication for transmission at higher bandwidths and over large distances. Fibers have the advantage over metal wires as signals travel along them without electromagnetic interference resulting in less loss. The two most significant components of optical fiber are the core and cladding. The core is the axial part of optical fiber and has a cylindrical shape. The dielectric material with distinct dielectric constant is used to make the core. Transmission of light takes place from the optical fiber core. Modification of the fiber refractive index can be done by doping elements and as a result changing the velocity of the light. The cladding section then surrounds the core section and plastic or glass with a lower refractive index than the core is used to make the cladding. The loss of light to the surrounding air is reduced by cladding section. The low refractive index of cladding allows light to remain confined inside the core as a result of total internal reflection from the core–cladding interface at a bouncing angle. As a result, the light keeps moving in the appropriate direction along the fiber length. During the process of fiber drawing a protective polymer layer known as “coating” was coated before being in contact with any surface. Further, another elastic layer as a buffer surrounds the polymer coating to reduce scattering loss occurring due to micro bending and for protection against physical damage. The last layer that is, the jacket is used to recognize the type of fiber. Figure 8.9 shows the optical fiber basic structure. Due to the purity of quartz glass, it is used to make most of the fibers.

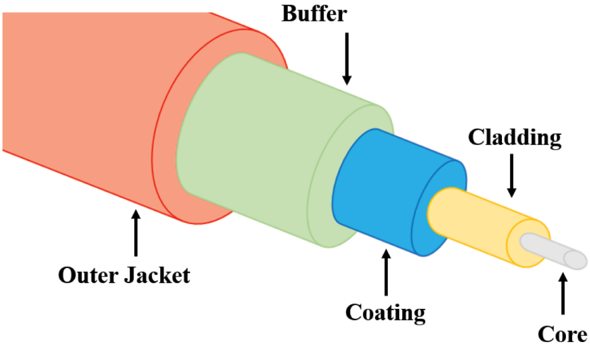

**Figure 8.9:** Fundamental constitution of optical fiber.

The principle of operation of optical fibers is total internal reflection. Inside the core of cable when incident angle exceeds the critical angle between core and cladding the phenomenon of total internal reflection comes into play. This leads to the reflection of incident light inside the core and its propagation along the fiber. When the angle at the interface exceeds the critical angle, light will not pass through the medium. The light that gets reflected at the interface is proportional to the refractive indices of the core and cladding as well as the angle of incidence. There are different types of optical fibers based on the application it is subjected to. The classification of the optical fibers based on the different aspects is shown in Figure 8.10.

Due to the innate advantages of optical fibers that include small size, ruggedness, and low cost, they have made a great impact in many fields. The chromatic dispersion of the optical fibers and the divergence of the output transmitted light limits their practical application. With the advancement in technology, chemical and functional fibers have received greater attention. Now with the growth of artificial intelligence, it is believed that these fibers should also gain intellectualization resulting in the focus being shifted toward smart fibers. Also, with the progress in meta surface technology, disruptive

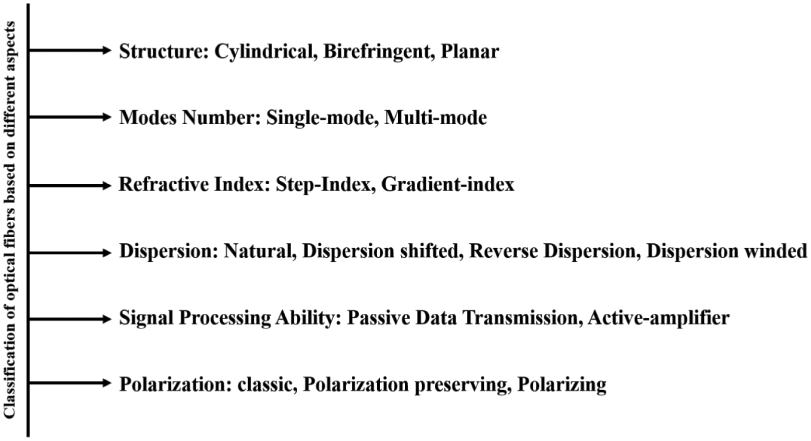
Classification of optical fibers based on different aspects
Structure: Cylindrical, Birefringent, Planar
Modes Number: Single-mode, Multi-mode
Refractive Index: Step-Index, Gradient-index
Dispersion: Natural, Dispersion shifted, Reverse Dispersion, Dispersion winded
Signal Processing Ability: Passive Data Transmission, Active-amplifier
Polarization: classic, Polarization preserving, Polarizing

**Figure 8.10:** Classification of the optical fibers.

innovations have taken place. The robustness and flexibility of the optical fibers make them an excellent platform to get linked to meta surface technology thus taking the leverage of optical fiber-based meta surface-based technologies so as to be applicable to real-time applications. A few of the optical application of fiber material is listed below.

#### 8.5.1.1 Photocatalysis

The growing process of urbanization and industrialization has led to an increase in global environmental issues such as water pollution and global warming. Semiconductors-based photocatalyst has been widely utilized for various applications such as organic pollutant removal, and hydrogen production [14].

##### 8.5.1.1.1 Organic pollutant removal

$TiO_2$ is a well-known large bandgap semiconductor used for water and air purification. $TiO_2$ nanofibers have a high surface area and offer an advantage over other morphological forms during photocatalysis. The large band gap (3.2 eV) of $TiO_2$ restricts its utilization to the UV region only and various approaches like adsorption of dye molecules, doping, and usage of plasmonic materials have been used to extend its absorption to include the visible region. Sun et al. have used Rhodizonic acid to enhance the optical properties of the $TiO_2$ nanofibers [15]. The $TiO_2$/RhA hybrid shows a significant red shift in the absorption onset due to the formation of the interfacial charge transfer (ICT) complex. In the case of the organic–inorganic hybrid, the energy alignment is such that the ICT complex ground state lies between the semiconductor; as a result red shift in absorption occurs. The $TiO_2$/RhA hybrid was then used to degrade methylene blue dye and results show faster degradation kinetics in the case of the hybrid as compared to the $TiO_2$ nanofibers as shown in Figure 8.11.

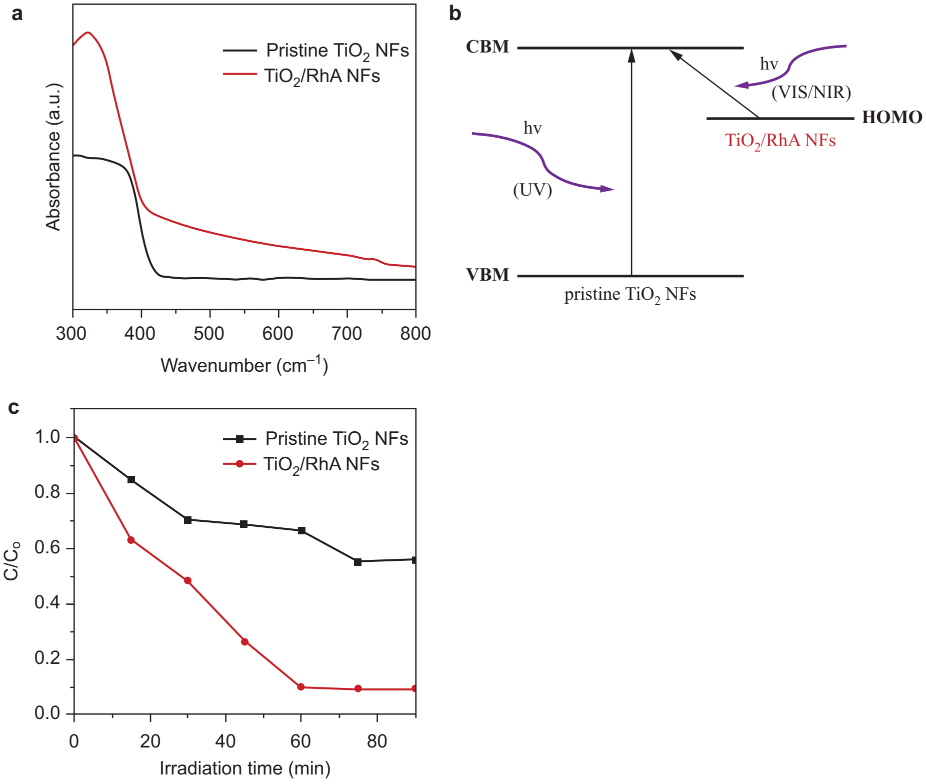

**Figure 8.11:** (a) Absorption spectra of pristine $TiO_2$ nanofibers and $TiO_2$/RhA hybrid nanofibers, (b) energy alignment in the $TiO_2$/RhA hybrid nanofibers, and (c) kinetic study of degradation of 10 ppm methylene blue over 0.1 mg/mL $TiO_2$ nanofibers and $TiO_2$/RhA hybrid nanofiber (reproduced with permission [15]. Copyright 2020, Springer Nature).

### 5.1.1.2 Photoreduction of $CO_2$

The increasing global energy demand has led researchers to look for renewable alternative sources of energy. Photoreduction of $CO_2$ to fuels using sunlight is a sustainable way to produce energy. Nguyen et al. have reported the use of the $TiO_2$–$SiO_2$, Cu/$TiO_2$–$SiO_2$, Fe/$TiO_2$–$SiO_2$, and Cu–Fe/$TiO_2$/$SiO_2$ coated optical fibers for the $CO_2$ photoreduction under natural sunlight. A circular Pyrex glass reactor (216 $cm^3$) was used to carry out the photocatalytic reaction containing a quartz window to facilitate the conduction of light irradiation. Figure 8.12a shows that the optical fibers coated with the catalyst were inserted in the reactor such that the light from the source enters along the fiber length to conduct the photocatalytic reaction on its surface [16]. When the incident light hits the internal surface of the fiber it splits into two beams because of the refractive index difference between the fiber and the $TiO_2$ film. A part of light gets reflected and is transmitted along the fiber and a part infiltrate through the interface which excites the layer of $TiO_2$. The light spreads gradually and gets diminished at the end of fiber.

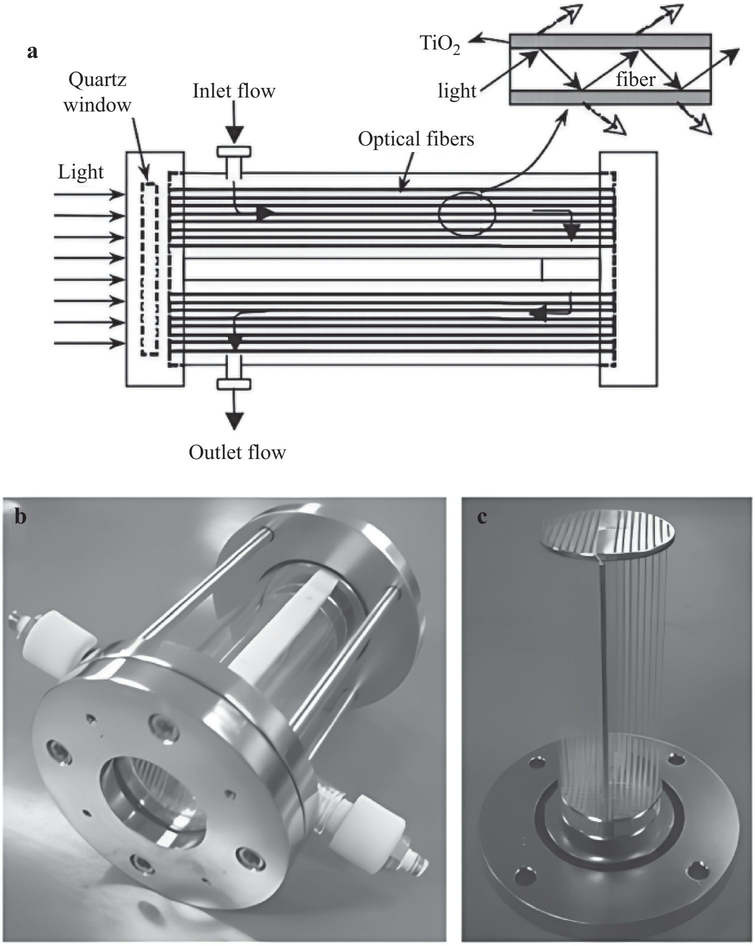

**Figure 8.12:** (a) Schematic illustration of the light transmission through the photoreactor, (b) and (c) optical fiber coated with catalyst (reproduced with permission [17]. Copyright 2008, Springer Nature).

The photocatalytic results summarized in Table 8.2 show that Cu–Fe/$TiO_2$–$SiO_2$–acac catalyst coated onto the optical fiber shows superior photoproductivity for methane production. The optical-fiber reactor shows better activity than the traditional packed-bed reactor because the light is uniformly transmitted through the reactor using optical fibers and thus providing a platform to perform photo-driven reactions. Thus, Optical

**Table 8.2:** Production rate of ethylene and methane under UVA (reproduced with permission [17]. Copyright 2008, Springer Nature).

| Photocatalyst[a] | Ethylene production rate (μmol/g h)[b] | Methane production rate (μmol/g h)[b] |
|---|---|---|
| $TiO_2$/glass plate | 0 | Trace |
| $TiO_2$–$SiO_2$/glass plate | 0 | 0.043 |
| $TiO_2$–$SiO_2$–acac/optical fiber | 0 | 0.185 |
| Cu(0.5 wt%)–Fe(0.5 wt%)/$TiO_2$/glass plate | 0.486 | 0.060 |
| Cu(0.5 wt%)–Fe(0.5 wt%)/$TiO_2$/ optical fiber | 0.575 | 0.914 |
| Cu(0.5 wt%)–Fe(0.5 wt%)/$TiO_2$–$SiO_2$/glass plate | 0.415 | 0.153 |
| Cu(0.5 wt%)–Fe(0.5 wt%)/$TiO_2$–$SiO_2$–acac/glass plate | 0.540 | 0.103 |
| Cu(0.5 wt%)–Fe(0.5 wt%)/$TiO_2$–$SiO_2$–acac/optical fiber | 0.211 | 1.860 |

[a] $TiO_2$–$SiO_2$ synthesis was done using sol–gel process with 5 wt% of $SiO_2$; acac (acetylacetone) has been used as a promoter for the preparation of $TiO_2$–$SiO_2$.

[b] The production rate of methane and ethylene production determined using average production rate in 4 h reaction time. The source of irradiation was in the UVA range (320–500 nm) with an intensity of 225 mW/cm$^2$.

fibers assist in increasing the photoactivity of the catalyst which can pave the way for the future commercial-scale viability to produce renewable fuels.

Apart from the nanomaterials coated on the surface of optical fibers, nanofiber nanomaterials themselves show enhanced activity due to improved light absorption capacity, large surface area and multiple interparticle scattering which results in improved intrinsic photocatalytic performance and light harvesting ability resulting in enhanced photocatalytic reaction rates [18]. Reñones et al. have reported $TiO_2$ nanofibers synthesized using the electrospinning technique and sol–gel method and compared them with the $TiO_2$ nanoparticles. The 1-D nanofibers containing a higher percentage of the Rutile phase show 4 and 2.5 times higher production of $H_2$ and CO respectively compared to the nanofibers containing more percentage of anatase phase due to slow recombination rate of electrons and holes [19]. Thus, the fiber-based materials and nanomaterials coated onto optical fibers can pave the way for future renewable energy production through the photoreduction of $CO_2$.

### 8.5.1.2 Biosensors

Based on the number of modes propagating through them, optical fibers can be single-mode or multimode fibers. The single mode has a small core diameter and one mode is only allowed to propagate along the fiber core, while the multimode fiber has a comparatively bigger diameter and multiple modes propagation is allowed along the fiber core. Fiber-based biosensors have nanostructures or thin metallic films along the sensing area length to excite the localized surface plasmon resonance (LSPR) or surface plasmon resonance (SPR) which are later immobilized for target-specific detection using sensing materials or antibodies [20]. Based on the LSPR or SPR effect the sensing configuration is excited with an evanescent field that extends into the cladding region and deposited metal interacts with it [21]. For the application of optical fibers in biosensors, several configurations have been developed. The exploitation of the hetero-core sensing configuration has been done for a wide range of biosensing applications such as refractive index monitoring and sensing of G proteins [22, 23]. During hetero-core sensing stubbing of MMF between two SMF or vice versa favors the excitation of cladding modes. Lokendra et al. have utilized same sensing configuration to diagnose L-cysteine in human urine. To take advantage of the LSPR phenomenon multimode section is coated with gold nanoparticles, polyvinyl alcohol-stabilized silver nanoparticles, and graphene oxide [24]. The sensing configuration used is shown in Figure 8.13. In this work two configurations for sensing were compared, one in which AuNPs/GO was coated on the optical fibers and the other in which PVA/AgNPs/GO was coated. The detection limit for AuNPs/GO was 152.5 µM having a sensitivity of 0.0012 nm/µM while for PVA/AgNPs/GO was 126.6 µM with a sensitivity of 0.0009 nm/µM.

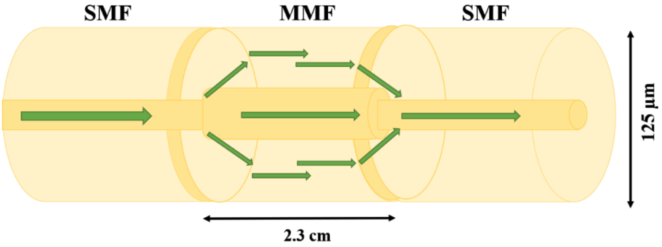

**Figure 8.13:** Illustration of a fiber hetero-core structure.

Though the sensor performs well low-light-matter interaction results in poor sensitivity and as a result limit its application. Further work has been carried out to improve the light-matter interaction by developing various other configurations such as U-shaped fiber sensors and etched/uncladded fiber sensors [25]. In the etched/uncladded fiber a small section of the fiber cladding is removed and sensing material is deposited on it that acts as a sensing head. During the propagation of light through the core, evanescent field results when some part gets extended from the core into the cladding region.

This interacts with the sensing material for the detection of changes in the surrounding. In a report on optical fiber biosensor by Qian et al., a 5 mm section was removed from the cladding and Au (50 nm) and Cr (2 nm) was deposited onto it which acts as the sensing region. For the detection of glycoprotein using a biosensor, the Au surface has been functionalized with phenyl boronic acid (PBA) using the self-assembly method. The limit of detection using an L-PBA self-assembled monolayer fiber optic sensor for Concanavalin A is 0.29 nM. Further, the evanescent field of sensing was improved by bending the structure into a U-shaped structure near the sensing region. This fiber-based SPR-biosensor has increased sensitivity and limit of detection. A U-shaped fluorescent immunosensor for microcystin-LR was reported by Jinchuan et al. The U-shaped fiber shows 16 times higher fluorescent sensitivity with light-sheet skew rays' excitation than collimated skew rays' excitation [26]. Using this feature, a sensitive and real-time microcystin-LR detection method based on the indirect competitive immunoassay principle was developed. Recovery rates between 85% and 112% were achieved using this immunosensor for the real environmental water samples spiked with microcystin-LR. The schematic diagram of the U-shaped optical fiber sensor is shown in Figure 8.14.

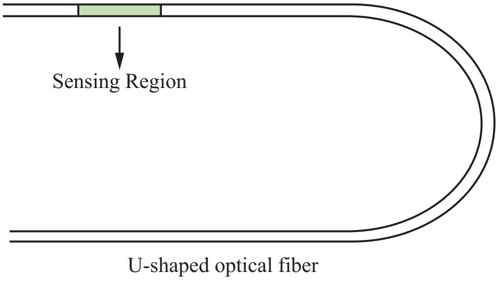

**Figure 8.14:** Illustration of the U-shaped fiber.

Research is going on developing different sensing configurations to provide portable devices with high sensitivity [25]. Researchers have also utilized D-shaped single-mode optical fiber sensors along with graphene layers, thin films, metallic nanowires, etc.

## 8.5.2 Advanced fiber materials for photonic application

Photonics deals with the science of photon (light) generation, its detection and manipulation through emission, modulation, transmission, amplification, and signal processing. Photonics emanate the best use of light as a tool for human benefit. The term "Photonics" is derived from the word "photon" which is analogous to the tiniest entity of light. Earlier, photonics was used to refer to the research field which utilizes light to perform various tasks. But with the advent of fiber optics in the late 1980s, the term became quite popular. Photonics has provided immense opportunity for manufacturing and designing devices, and integrated systems for their growing applications in the fields of high-speed data communication, laser, optoelectronic devices, aerospace, healthcare, alternative energy, and imaging. Focus has again begun to shift to light from the electrons due to the need for high system performance and high-density integration. The use of light significantly improves the transmission of information per second due to its ability to move faster [27]. With the integration of light with electronics in various systems and devices for their numerous applications optoelectronics is an emerging field in photonics. Optoelectronic devices for their application in the field of energy, communication, lighting, healthcare, and technology have been developed over the years [28]. The optoelectronic devices were produced traditionally using a wafer-based process and hence were restricted to planar geometries and rigid surfaces. But with the advancement in technology, flexible optoelectronic fibers have established themselves in diverse applications such as photo sensing, optical communication, energy storage, and chemical sensing. Now we will look at some of the photonic applications of fiber-based materials.

#### 8.5.2.1 Energy conversion and storage

Solar cells are efficient, clean, and scalable energy conversion devices for the sustainable development of alternative renewable energy sources [29]. Conventional solar cells were fabricated on rigid planar surfaces thus limiting their applications. But with the advancement in fiber technology, 1D fiber-shaped solar cells have attracted a lot of attention for their facile configuration and plausible future applications. Fabrics are like the second skin to humans and interact with the environment directly. They protect the body and can simultaneously absorb sunlight energy. Thus, a combination of fabrics and 1D fiber-shaped solar cells can effectively harvest sunlight and can be used to power up wearable electronic devices [7]. A remarkable improvement in the mechanical performance of fibrous solar cells was seen when the metal wires were substituted with the CNT fibers [30]. Li et al. have fabricated double-twisted perovskite solar cell supported by CNT fibers. One highly flexible CNT fiber was taken, and another spinnable CNT array that can be directly spun-twisted was chosen as anode. It was then coated by a thin layer of $n$-TiO$_2$, meso-TiO$_2$, $CH_3NH_3PbI_3 - xCl_x$, poly(3-hexylthiophene)/single-walled carbon nanotube (P3HT/SWNT), and silver (Ag) nanowire network from the inside out as shown in Figure 8.15a. The silver nanowire network increases the effective contact area between the two fiber electrodes. Figure 8.15b shows the power conversion efficiency (PCE) of the double-twisted perovskite solar cell that is 3.03%. The $J_{sc}$, $V_{oc}$, and FF values for this fibrous solar cell were 8.75 mA/cm$^2$, 0.615 V, and 56.4%, respectively [31]. Based on the mechanical strength and electroconductivity of the CNT fiber, the hydrophobic CNT core and hydrophilic CNT sheath have been used in the dye-sensitized solar cells which shows an outstanding PCE value of 10% [32].

Apart from energy conversion, the storage of energy and release when required is one of the demanding subjects nowadays and supercapacitors belong to those categories. Krishna et al. utilized natural coir fibers for making graphene oxide which was utilized for energy storage [33]. In this work, natural coir fibers were treated with KOH and after heat treatment, pure graphene oxide has been obtained, which was used for making a supercapacitor electrode. Apart from that, there are other works, which deal with other fiber for energy applications.

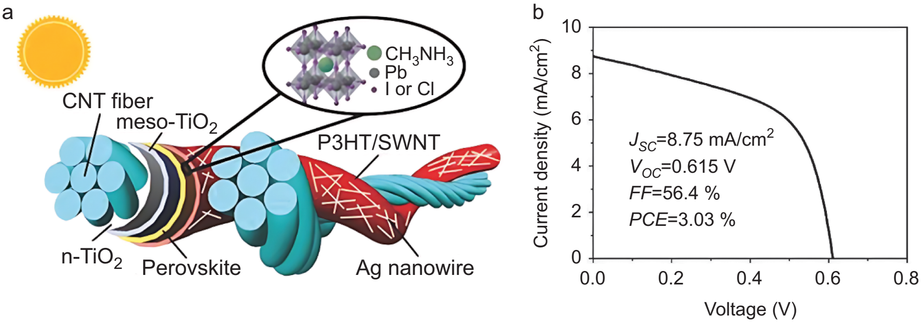

**Figure 8.15:** (a) Illustration of the double-twisted fiber-shaped solar cell structure, (b) *J–V* curve of the double-twisted perovskite solar cell (reproduced with permission [31]. Copyright 2015, Wiley-VCH).

### 8.5.2.2 Sensing application

Photoelectric sensors are optoelectrical materials being used for detection elements. The measured changes are first converted into optical signals and then by using optoelectrical elements they are converted into electrical signals.

#### 8.5.2.2.1 Chemical sensing

The detection and capturing of hazardous and toxic effluents are really important. Based on the principle of chemiluminescence optoelectronic based fibers have been fabricated for chemical sensing. The main function of the optical fibers was to collect and transmit the emissive signal at the fiber end to the detector. Fiber numerical aperture limits the sensitivity of detection and standoff distance. Gumennik et al. have introduced and demonstrated an approach for remote luminescence-based chemical detection as shown in Figure 8.6 [34]. To capture light anywhere within the hollow core, photoconductive detectors were embedded directly along the entire fiber length. The fiber electrodes immediately record the electrical signal that closely interfaces with the semiconductor ($Se_{97}S_3$) [34]. A very large noise current was generated when amorphous $Se_{97}S_3$ was used resulting in poor detection due to weak illumination from chemiluminescence. To improve the sensitivity, crystallization was induced by annealing the fiber at the temperature higher than the glass transition temperature of $Se_{97}S_3$. Trace level detection of up to 10 ppb for peroxide vapor was achieved, which was comparable to state-of-the-art commercially available vapor sensors. Thus, a platform for distributed and remote chemical sensing can be realized which extends up to several hundred meters.

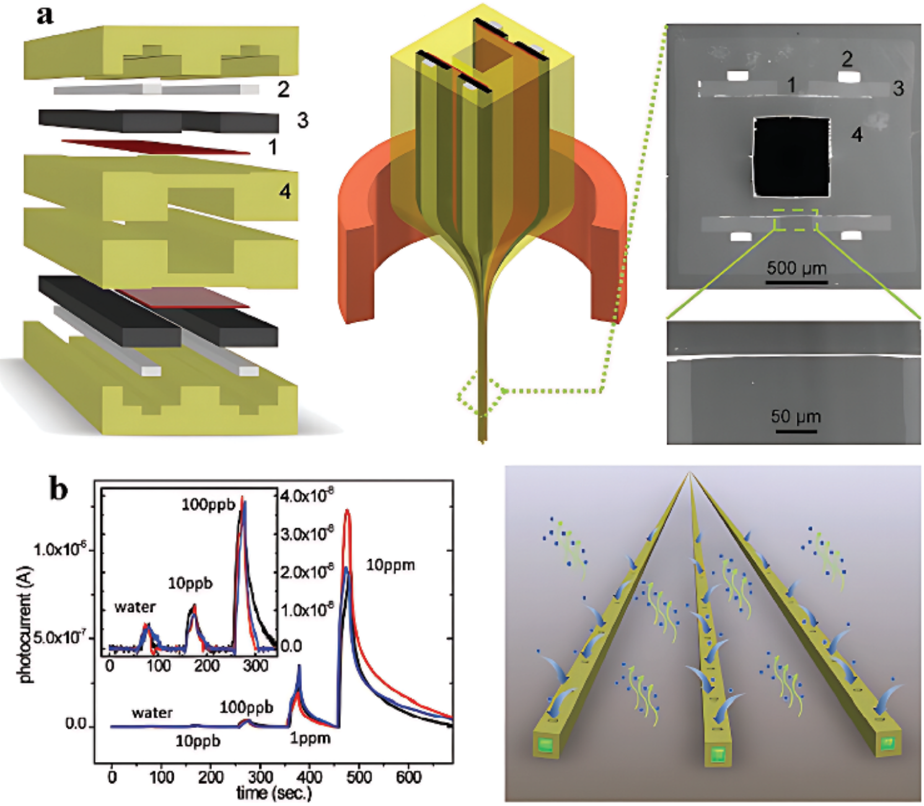
a
2
3
1
4
2
1
3
4
500 μm
50 μm
b
photocurrent (A)
1.0x10⁻⁶
5.0x10⁻⁷
0.0
water
10ppb
100ppb
1ppm
10ppm
0
100
200
300
400
500
600
time (sec.)
100ppb
10ppb
water
4.0x10⁻⁸
3.0x10⁻⁸
2.0x10⁻⁸
1.0x10⁻⁸
0.0
0
100
200
300

**Figure 8.16:** A fiber-shaped optoelectronic sensor for the detection of trace hydrogen peroxide vapor (reproduced with permission [34]. Copyright 2012 Wiley-VCH).

### 8.5.2.2.2 Photosensing

In 2004, the first metal–semiconductor–insulator optoelectronic multimaterial fiber was formed [35]. Due to the photodetecting capabilities in the visible and IR ranges, optoelectronic properties, tunability and compatibility with polymers, low-temperature chalcogenide glasses have been chosen [36]. The sensitivity of the photodetectors is measured by diving the photocurrent by noise current. For a cylindrical configuration of semiconductors in the fiber, the sensitivity is inversely proportional to the diameter of the core. So, the photodetection sensitivity can be altered by monitoring the structure and geometry of the core. Bayindir et al. have shown a fiber consisting of an $As_{40}Se_{50}Te_{10}Sn_5$ core that is interfaced by four Sn electrodes running along the fiber length and encapsulated with transparent polymer cladding as shown in Figure 8.17 [37].

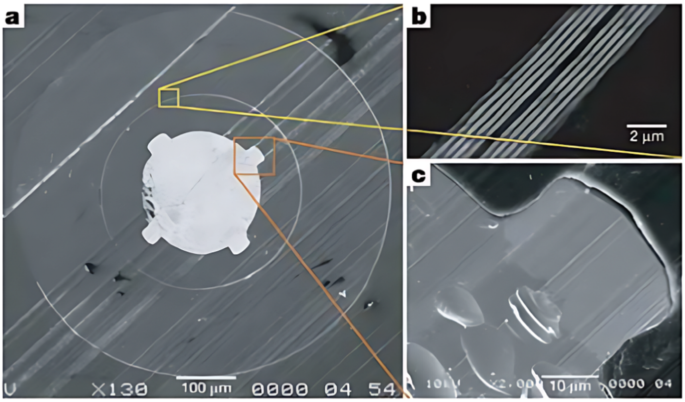

**Figure 8.17:** (a) Chalcogenide glass core ($As_{40}Se_{50}Te_{10}Sn_5$) of an optoelectronic fiber surrounded by four metallic electrodes (Sn). A PBG fiber that forms photodetecting system with narrow band surrounding the optoelectronic core (reproduced with permission [37]. Copyright 2004, Nature Publishing Group).

The metallic electrodes connected to the external circuit measure the photocurrent when external light impinges at any position on the fiber. The chalcogenide glass has a broad spectral range of photodetection. For the narrow bandgap detectors, the photodetecting domain can be surrounded by photonic bandgap structures that only allow the desired wavelength to target the core. The first-generation optoelectronic fibers have an amorphous semiconducting core. Sincere attempts have been made towards the fabrication of optoelectronic fibers with high performance. The photodetectors with ultra-high-response speed and sensitivity find application in numerous fields such as military monitoring, dissection of neural activities in the brain, and in vivo imaging. The atomic structure of semiconductor cores can be altered using different annealing strategies. The techniques used can be either laser heating, directly thermal annealing at a higher temperature, or phase transformation in chemical solutions. It is seen that ultra-large grain formation occurs in the Se-core optoelectronic fiber on laser annealing treatment [38]. The photosensitivity and photoresponsivity increase by several orders of magnitude for these fibers as compared to the fibers annealed using conventional heat treatment. In chemical solutions phase transformation occurs with the help of the solvent which modulates the surface energy of the crystal planes when they start growing from the nuclei [39]. Thus, different strategies can be employed to increase the photosensitivity of the semiconductor core in optoelectronic fiber-based photosensors.

## 8.6 Conclusions

This chapter started with the history of fiber materials. The types and their impact have been also discussed. Few synthesis routes of fiber materials have been discussed briefly. Further, their application in the field of optics and photonics has been also explored. The application discussed showed how the fibers can impact their properties. The applications have been discussed with their corresponding examples for better understanding to the readers.

## References

[1] Shah DU, Porter D, Vollrath F. Can silk become an effective reinforcing fiber? a property comparison with flax and glass reinforced composites. Compos Sci Technol. 2014;101:173–183.

[2] Müller M, Murphy B, Burghammer M, Riekel C, Roberts M, Papiz M, Clarke D, Gunneweg J, Pantos E. Identification of ancient textile fibers from khirbet qumran caves using synchrotron radiation microbeam diffraction. Spectrochim Acta Part B Atomic Spectrosc. 2004;59:1669–1674.

[3] Morampudi P, Namala KK, Gajjela YK, Barath M, Prudhvi G. Review on glass fiber reinforced polymer composites. Mater Today: Proc. 2020;43:314–319.

[4] Kobets LP, Deev IS. Carbon fibers: Structure and mechanical properties. Compos Sci Technol. 1998;57:1571–1580.

[5] Khusiafan FJ. Use of KEVLAR ® 49 in aircraft components. Eng Manage Res. 2018;7:14.

[6] Burningham NW, Rumpel WF. Properties of boron fibers and composites. PolymEng Sci. 1967;7:124–127.

[7] Shi Q, Sun J, Hou C, Li Y, Zhang Q, Wang H. Advanced functional fiber and smart textile. Adv Fiber Mater. 2019;1:3–31.

[8] Zhang F, Chen J, Yang J. Fiber materials for electrocatalysis applications. Adv Fiber Mater. 2022;4:720–735.

[9] Kumbhakar P, Chowde Gowda C, Tiwary CS. Advance optical properties and emerging applications of 2D materials. Front Mater. 2021;8:1–16.

[10] Amiri IS, Bin Azzuhri SR, Jalil MA, Hairi HM, Ali J, Bunruangses M, Yupapin P. Introduction to photonics: Principles and the most recent applications of microstructures. Micromachines (Basel). 2018;9.

[11] Lodahl P, Mahmoodian S, Stobbe S, Rauschenbeutel A, Schneeweiss P, Volz J, Pichler H, Zoller P. Chiral quantum optics. Nature. 2017;541:473–480.

[12] Addanki S, Amiri IS, Yupapin P. Review of optical fibers-introduction and applications in fiber lasers. Results Phys. 2018;10:743–750.

[13] Schuster K, Unger S, Aichele C, Lindner F, Grimm S, Litzkendorf D, Kobelke J, Bierlich J, Wondraczek K, Bartelt H. Material and technology trends in fiber optics. Adv Opt Technol. 2014;3:447–468.

[14] Mi L, Huang Y, Qin L, Seo HJ. Improved photo-degradation of dyes over Ag-loaded NiTiO3:V nanorods on visible-light-irradiation. Mater Res Bull. 2018;102:269–276.

[15] Sun Y, Mwandeje JB, Wangatia LM, Zabihi F, Nedeljković J, Yang S. Enhanced photocatalytic performance of surface-modified TiO2 nanofibers with rhodizonic acid. Adv Fiber Mater. 2020;2:118–122.

[16] Wu JCS, Lin HM, Lai CL. Photo reduction of CO2 to methanol using optical-fiber photoreactor. Appl Catal A Gen. 2005;296:194–200.

[17] Nguyen TV, Wu JCS. Photoreduction of CO2 to fuels under sunlight using optical-fiber reactor. Solar Energy Mater Solar Cells. 2008;92:864–872.

[18] Yu J, Yu H, Cheng B, Zhao X, Zhang Q. Preparation and photocatalytic activity of mesoporous anatase TiO 2 nanofibers by a hydrothermal method. J Photochem Photobiol A: Chem. 2006;182:121–127.

[19] Reñones P, Moya A, Fresno F, Collado L, Vilatela JJ, De VA, Shea PO. Hierarchical TiO 2 nano fi bres as photocatalyst for CO2 reduction : In fluence of morphology and phase composition on catalytic activity. J CO2 Util. 2016;15:24–31.

[20] Zhu G, Singh L, Wang Y, Singh R, Zhang B, Liu F, Kaushik BK, Kumar S. Tapered optical fiber-based LSPR biosensor for ascorbic acid detection. Photonic Sens. 2021;11:418–434.

[21] Pathak AK, Rahman BMA, Singh VK, Kumari S. Sensitivity enhancement of a concave shaped optical fiber refractive index sensor covered with multiple Au nanowires. Sensors (Switzerland). 2019;19.

[22] Liu Z, Liu L, Zhu Z, Zhang Y, Wei Y, Zhang Y, Yang J, Yuan L. Dual-channel surface plasmon resonance refractive index sensor based on modified hetero-core structure fiber. Opt Commun. 2017;403:290–295.

[23] Wong WC, Chan CC, Boo JL, Teo ZY, Tou ZQ, Bin Yang H, Li CM, Leong KC. Photonic crystal fiber surface plasmon resonance biosensor based on protein g immobilization. IEEE J Select Topic Quantum Electronic. 2013;19:0–6.

[24] Singh L, Singh R, Zhang B, Kaushik BK, Kumar S. Localized surface plasmon resonance based hetero-core optical fiber sensor structure for the detection of l-cysteine. IEEE Trans Nanotechnol. 2020;19:201–208.

[25] Azizur Rahman BM, Viphavakit C, Chitaree R, Ghosh S, Pathak AK, Verma S, Sakda N. Optical fiber, nanomaterial, and THz-metasurface-mediated nano-biosensors: A review. Biosensors. 2022;12:1–28.

[26] Liu J, Xing Y, Zhou X, Chen GY, Shi H. Light-sheet skew rays enhanced u-shaped fiber-optic fluorescent immunosensor for microcystin-lr. Biosens Bioelectron. 2021;176:112902.

[27] Joannopoulos JD, Villeneuve PR, Fan S. Photonic crystals [1]. Solid State Commun. 1997;102:165–173.

[28] Xing Y, Xu Y, Wu Q, Wang G, Zhu M. Optoelectronic functional fibers: Materials, fabrication, and application for smart textiles This review is dedicated to Prof. Tobin J Marks on his 75th birthday, 2021, 439–455.

[29] Peng M, Zou D. Flexible fiber/wire-shaped solar cells in progress: Properties, materials, and designs. J Mater Chem A Mater. 2015;3:20435–20458.

[30] Chen T, Qiu L, Cai Z, Gong F, Yang Z, Wang Z, Peng H. Intertwined aligned carbon nanotube fiber based dye-sensitized solar cells. Nano Lett. 2012;12:2568–2572.

[31] Li R, Xiang X, Tong X, Zou J, Li Q. Wearable double-twisted fibrous perovskite solar cell. Adv Mater. 2015;27:3831–3835.

[32] Fu X, Sun H, Xie S, Zhang J, Pan Z, Liao M, Xu L, Li Z, Wang B, Sun X, Peng H. J Mater Chem A. 2017; DOI: 10.1039/C7TA08637G.

[33] Yadav KK, Singh H, Rana S, Sunaina, Sammi H, Nishanthi ST, Wadhwa R, Khan N, Jha M. Utilization of waste coir fiber architecture to synthesize porous graphene oxide and their derivatives: An efficient energy storage material. J Clean Prod. 2020;276:124240.

[34] Alexander Gumennik CH, Stolyarov AM, Schell BR, Guillaume Lestoquoy JDJ, Sorin F, McDaniel W, Rose A, Fink Y. Advanced Materials – 2012 – Gumennik – All-in-Fiber Chemical Sensing (1).pdf. 2012, 6005–6009.

[35] Yan W, Dong C, Xiang Y, Jiang S, Leber A, Loke G, Xu W, Hou C, Zhou S, Chen M, Hu R, Shum PP, Wei L, Jia X, Sorin F, Tao X, Tao G. Thermally drawn advanced functional fi bers : New frontier of flexible electronics. Mater Today. 2020;35.

[36] Sorin F, Das Gupta T, Yan W, Martin-Monier L, Nguyen-Dang T, Gérald Page A, Qu Y. Nano-structured optical metasurfaces and multi-material fibers for IR applications. 2018 Conference on Lasers and Electro-Optics Pacific Rim, CLEO-PR 2018. 2018, 44–45.

[37] Bayindir M, Sorin F, Abouraddy AF, Viens J, Hart SD, Joannopoulos JD, Fink Y. Metal-insulator-semiconductor optoelectronic fibers. Nature. 2004;431:826–829.

[38] Yan W, Nguyen-Dang T, Cayron C, Gupta TD, Page AG, Qu Y, Sorin F. Microstructure tailoring of selenium-core multimaterial optoelectronic fibers. Opt Mater Express. 2017;4:1388–1397.

[39] Yan W, Qu Y, Gupta TD, Darga A, Nguyên DT, Page AG, Mi MR. Semiconducting nanowire-based optoelectronic fibers. Adv Mater. 2017;29:1700681.

Anastasiia Rymzhina, Nishant Tripathi*, Prachi Sharma,
Vladimir Pavelyev

# Chapter 9

# Advanced fibers for photocatalysis application

**Abstract:** Environmental pollution is a common problem in all countries. The environment is what people eat, drink, and breathe. Indifference and inaction can lead to an environmental disaster on the planet. To purify nature from pollution, photocatalysis reaction has now been actively used. This reaction requires materials that will participate in the reaction quickly purifying water or air from contaminants. Recently, transition metal dichalcogenides (TMDs) and advanced fibers made from them or other nanomaterials have become the most actively studied materials for photocatalysis. The present chapter deals with advanced fibers as well as with TMD-based photocatalysts for environmental pollution purification. We discussed in detail the physical aspects and characteristics of various materials and their hybrid structures pointing out their advantages and drawbacks for developing photocatalysts. As a result, we provided tables comparing the characteristics of the discussed materials and structures based on them. This chapter will be useful to a wide range of people involved in research in the field of photocatalysis.

**Keywords:** photocatalysis, industrial pollution, advanced fibers, TMDs, solar energy

---

**Acknowledgements:** This work was supported by the Russian Science Foundation (Grant No. 21–79–00272).

---

**Declaration of Competing Interest:** The author does not have any conflict of interest.

---

***Corresponding author: Nishant Tripathi,** Samara National Research University, 34, Moskovskoye Shosse, Samara 443086, Russia, e-mail: nishant.tripathi.11@gmail.com
**Anastasiia Rymzhina,** Samara National Research University, 34, Moskovskoye Shosse, Samara 443086, Russia
**Prachi Sharma,** Samara National Research University, 34, Moskovskoye Shosse, Samara 443086, Russia; School of Electronics Engineering (SENSE), Vellore Institute of Technology (VIT), Vellore 632014, Tamil Nadu
**Vladimir Pavelyev,** Samara National Research University, 34, Moskovskoye Shosse, Samara 443086, Russia; IPSI RAS – Branch of the FSRC “Crystallography and Photonics” RAS, 443001 Samara, Molodogvardeyskaya 151, Russia

https://doi.org/10.1515/9783110992892-009

## 9.1 Introduction

Currently, dyes and pigments are the most significant contaminants that imply a hazardous effect on the ecosystem. These organic materials, even in low concentrations, cause substantial harm in the aqueous medium [1–3]. As well, these compounds cause color changes in freshwater. Thus, the pollution can be detected easily as an indication of the existence of dye molecules in water. These pollutant molecules prevent sunlight penetration through the water surface to the aquatic plant and animal species, changing the activity of photosynthetic processes and the gas solubility in water [4]. It poses a direct threat to human beings, aqueous flora, and fauna [5–10].

Dyes play a vital role in various industry branches. It is utilized for dyeing and textile industries [11, 12]. Over 100,000 commercially available synthetic dyes are the frequently used in such industries. These dyes are a group of the most dangerous pollutants in water [1, 13–16]. They are mainly derived from coal tar and petroleum intermediates with a total annual production of more than $7 \times 10^5$ tons [17–19]. Year after year, through textile sewages, around 15% (≈1,000 tons) of these nonbiodegradable textile dyes are discharged into rivers and water bodies [20–22]. On average for every kilogram of cloth, being processed in dyeing and finishing plants, about 120–280 L of water is consumed [23]. Methylene blue (MB), methyl orange (MO), and rhodamine B (RhB) are the most applied dyes in the industry [24, 25]. MB, for example, is a material that causes many dangerous effects such as eye irritation, anemia, nausea, and vomiting [26, 27]. Therefore, the treatment of contaminated water with dyes is extremely important [28].

To date, such treatment routes like adsorption [29, 30], incineration, biotreatment, ozonation [31–34], coagulation [30–35], and membrane filtration [36–38] are utilized to clean water polluted by dyes. The main disadvantage of these methods is that the nature of the pollutant is maintained after treatment. The key point of the photocatalytic reaction is dye degradation as the result of a photocatalytic reaction so the nature of the pollutant will change and it is converted to a compound which is not harmful to the environment [39, 40]. An important issue is an energy source. The sun is the main source of clean energy. It is of uttermost importance to make use of solar energy abundance for numerous applications like energy production and environmental purification. Environmental cleanup using photocatalysts has many benefits [41]: pollutants conversion from complex molecules into simple and nontoxic compounds like $H_2O$ and $CO_2$ and avoidance of secondary treatment, disposal, or use of any expensive oxidizing chemicals with the utilization of solar energy [42].

Photocatalytic degradation is a cost-effective and progressive method which can completely degrade and mineralize hazardous organic contaminants [43, 44]. The photocatalyst-assisted reaction involves the separation of excitons upon light irradiation. The absorption of light irradiation with an energy exceeding the bandgap of a semiconductor photocatalyst stimulates the electrons transfer from the valence band to a conduction band, which causes the generation of the electron–hole pairs that take part in redox processes with adsorbed compounds resulting in the effective degradation of organic pollutants [45]. Methyl orange (MO) is a stable dye whose degradation is commonly used for examining the performance of many visible (vis) and ultraviolet (UV) light-active photocatalysts [46, 47]. A photocatalyst is a material that accelerates and enhances a light-induced reaction without being consumed [48].

The requirement to achieve mentioned application is to develop a photocatalytic material with suitable band edge positions to produce the appropriate redox species. To solve that problem, titanium dioxide ($TiO_2$) is used for many years because it is one of the well-established and renowned photocatalysts which can oxidize organic and inorganic substances in water and air through redox processes [49–51]. Along with proper band edge positions, an efficient photocatalyst should have narrow bandgap energy to absorb visible light energy, enhanced electron–hole separation to have high quantum efficiency (QE), low recombination rate to have prolonged reactions, and effective interfacial interactions to have close contact between the surrounding medium and the photocatalyst to convert the reactant. In order to overcome this issue researchers are studying properties of numerous materials for photocatalysis like ZnO [52–54], $TiO_2$ [55, 56], Ce-$TiO_2$ [57], $MoS_2$ [58], $SnO_2$ [59, 60], $WO_x$ [61], CdS [62], graphene, and graphitic carbon nitride [63–66] as well as advanced nanofibers (NFs) such as fibrous $BiVO_4$/$Bi_2S_3$/$MoS_2$ heterojunction [67], carbon fibers with various materials [68–71], PVDF/PVP/ZnO: Ln fibrous membrane [72], $TiO_2$@CMS/carbon fiber van der Waals heterostructures [73], $TiO_2$ NFs [74–76], ZnO nanorods [77], photocatalytic optical hollow fibers coated with Ag-loaded $GeO_2$ and N-doped $TiO_2$ [78], m-Bi($Er^{3+}$-$Yb^{3+}$)$VO_4$ [79], Ag@ZnO nanorods decorated on polyacrylonitrile fiber membrane [80], $TiO_2$@CNTs NFs [81], and optical and glass fibers with different materials [82–86].

Nowadays TMDs are very promising materials for photocatalysis due to their unique properties [87–90]. There are 40 different types of TMDs relying upon the combination of transition metals and chalcogen atoms [91, 92]. However, there are some limitations to these structures. Some of the major concerns are structural instability, high exciton recombination, wide bandgap, and so forth [91]. Photocatalysts' bandgap plays a crucial role in the photocatalysis process. If we use materials with a wide bandgap, we can utilize only radiation with high photon energy such as ultraviolet [93]. The narrower the material bandgap the less energy needs to be directed to the material to initiate the photocatalysis reaction. Thus, we can expand the utilizing radiation spectrum for the photocatalysis reaction by using materials with a narrower bandgap.

The main drawback of titanium oxide is that it is mainly active under ultraviolet light due to its wide bandgap ($E_g$ =3.2 eV for anatase and $E_g$ = 3.0 eV for the rutile phase) [93] and thus is not made use of the whole spectrum of sunlight which consists of 4% UV-A radiation ($\lambda$ = 320–400 nm, $E_g$ = 3.88–3.09 eV), 53% visible light ($\lambda$ = 400–800 nm, $E_g$ = 3.09–1.55 eV), and 43% IR radiation ($\lambda$ > 800 nm, $E_g$ < 1.55 eV) [65, 94, 95]. The bandgap of $TiS_3$ is $E_g$ < 1.2 eV [96, 97] and for titanium dichalcogenides ($TiS_2$, $TiSe_2$, and $TiTe_2$) it is $E_g$ < 2 eV [98], which shows that these materials can have a potential for vis or even IR-driven photocatalysis. It is shown that nonstoichiometric TiS and $TiS_3$ represent a high photocatalytic activity, especially in the presence of small amounts of hydrogen peroxide [87].

TMDs have such advantages as outstanding catalytic activity caused by better charge separation, cost-effectiveness compared to noble metals as well as easy layer separation due to weak van der Waals forces acting between these layers [89, 94, 96–98]. As for drawbacks, TMD-based composites can be easily aggregated under radiation exposure and heat which lead to a decline in the number of catalyst active states. In addition, it is necessary to carry out additional studies of TMD-based composite photocatalysis mechanisms [89].

Photocatalytic fiber-based photocatalysis is a new branch in this field. Photocatalytic fiber is a supported vis light-driven catalyst. This catalyst is constructed from active catalyst powders introduced in the stable fiber framework with a multistage pore structure and large surface area [99, 100]. This system combines the advantages of fibers with active catalyst powders, for example, superior photocatalytic efficiency, no secondary pollution after use, easy to reuse, mild reaction conditions, low cost, high resistance to stretching, bending, twisting, and folding [101–106]. In addition, the flexibility of photocatalytic fibers provides the possibility of their utilization in numerous fabric textures with variable thickness and linear density via blowing, weaving as well as twisting technologies. Moreover, photocatalytic fibers can be developed in any size and shape to fulfill the needs of a wide variety of cleaning devices and situations that need water and/or air purification as well as energy regeneration and photochemical reactions [107–112].

Based on the foregoing, we can conclude that the study of novel material properties to use them as photocatalysts for water purification is urgent.

## 9.2 Photocatalysis reaction mechanism

Photocatalysis reaction involves the $e/h$ pair's separation upon light irradiation. The absorption of light irradiation with an energy exceeding the bandgap of a semiconductor photocatalyst stimulates the electron transfer from the valence band to the conduction band, which causes the $e/h$ pairs generation [45].

Figure 9.1 shows the general semiconductor-based photocatalysis mechanism [113]. The photocatalysis mechanism includes three steps: $e/h$ pairs generation on the semiconductor surface caused by light exposition with the necessary photon's energy, $e/h$ pairs migration to the semiconductor surface, and degradation of organic pollutants by redox reactions induced by the separated $e/h$ pairs.

Schematic diagram reveals the transportation of charge carriers in semiconductor material leading to its photocatalytic activity (see Figure 9.1).

Heterostructures can dramatically improve the $e/h$ pair generation and decline recombination rate which causes much better performance of such a photocatalyst in comparison with pure semiconductor materials. Singh et al. [114] investigated the

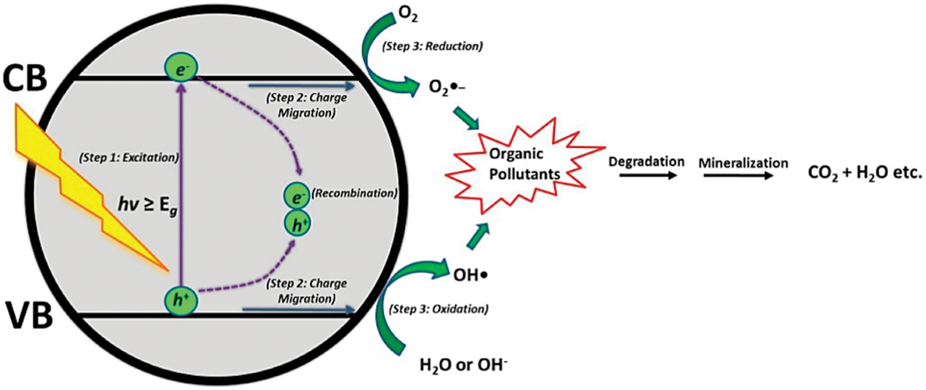
CB
VB
e⁻
h⁺
(Step 1: Excitation)
hv ≥ E_g
(Step 2: Charge Migration)
(Recombination)
(Step 2: Charge Migration)
O₂
(Step 3: Reduction)
O₂•–
Organic Pollutants
Degradation
Mineralization
CO₂ + H₂O etc.
OH•
(Step 3: Oxidation)
H₂O or OH⁻

**Figure 9.1:** Schematic diagram revealing the transportation of charge carriers in semiconductor material leading to its photocatalytic activity (figure is taken with permission from Ref. [113]).

charge transport in Ag-$TiO_2$ hybrid system for enhanced photocatalytic activity. The scheme of the photocatalysis reaction is demonstrated in Figure 9.2. When radiation of a solar spectrum exposes on a hybrid nanoparticle photocatalyst, electrons are transferred from the valence band to the conduction band of the semiconductor and create holes in the valence band. Electrons from the semiconductor conduction band flow toward metal nanoparticles joined to the semiconductor. Thus, the depletion layer between metal nanoparticles and semiconductors is formed (Schottky junctions). Therefore, the recombination rate in the semiconductor reduces as the metal nanoparticles capture photoinduced electrons. The semiconductor conduction band electrons and electrons captured by metal nanoparticles react with $O_2$ molecules to create $\cdot O_2^-$ radicals. At the same time, the interaction of holes in the valence band with water causes the ·OH radicals formation. Appeared radicals lead to the photocatalytic degradation of the organic pollutant in water. A detailed explanation of the organic pollutant degradation caused by interaction with the ·OH radicals is given in Ref. [115].

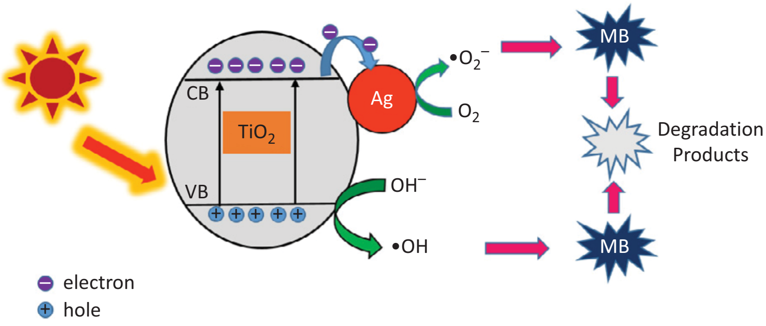
CB
TiO₂
VB
Ag
•O₂⁻
O₂
OH⁻
•OH
MB
Degradation Products
MB
⊖ electron
⊕ hole

**Figure 9.2:** Schematic diagram revealing the transportation of charge in Ag-$TiO_2$ hybrid nanoparticle system leading to its photocatalytic activity (figure is taken with permission from Ref. [114]).

Singh et al. [114] and Houas et al. [115] investigated MB degradation. The degradation mechanism of MB is as follows. In the beginning, ·OH radical led to bond cleavage in the C–S$^+$=C functional group of MB forming C–S(=O)–C and opening the central aromatic ring containing both S and N heteroatoms. After that, the reaction of the sulfoxide group with ·OH radical leads to the formation of sulfone. Subsequently, the sulfone reacts with ·OH radical forming sulfonic acid. As a final point, $SO_4^{-2}$ ions are generated due to the fourth interaction with ·OH radicals. First, in the case of mineralization of the three nitrogen-containing groups in the MB molecule, the cleavage of the –S$^+$= group induces the cleavage of the N=C double bond. Proton reduction by photoexcited electrons forms ·H radicals. These radicals lead to the saturation of the two amino bonds. The amino group can be substituted by an ·OH radical producing phenols and releasing an $\cdot NH_2$ radical which forms ammonia and ammonium ions. The two symmetrical dimethyl-phenyl-amino groups undergo progressive degrading oxidation of one methyl group due to a reaction with ·OH radical resulting in the formation of alcohol, then an aldehyde, which is spontaneously oxidized into acid and after that eliminated a carboxylic acid group from an organic compound producing $CO_2$. The phenyl-methyl-amine radical degrades as a result of the successive reactions with ·OH radicals which leads to the complete MB decomposition [114, 115].

To find out which photocatalytic material is better for application in certain circumstances, researchers evaluate many photocatalysts' parameters. Thus, to calculate photocatalytic degradation efficiency researchers are usually using the following formula [116]:

$$\mathrm{DE\%} = \left(1 - \frac{C_t}{C_0}\right) \cdot 100\% \tag{9.1}$$

where DE% is the photocatalytic degradation efficiency, $C_0$ is the absorbance value for the initial dye concentration, and $C_t$ is the absorbance value of the dye solution in various time intervals. The kinetics of the photocatalytic reaction is represented by pseudo-first-order reaction kinetics. The graph of the normalized concentration changes of the photodegraded contaminant against irradiation time must show a straight line according to the following equation [116]:

$$\ln \frac{C}{C_0} = -k_t \tag{9.2}$$

The line slope angle of the obtained straight line determines the pseudo-first-order reaction rate constant. An important role in photocatalysis plays such value as QE (identical to photonic efficiency). To find this value, the following equation is used [51, 117]:

$$\eta_{\mathrm{q}}(\%) = \frac{\langle \text{reaction rate} \rangle (\text{mol/s} \times \text{quanta/mol})}{\langle \text{photon rate} \rangle (\text{quanta/s})} \times 100 \tag{9.3}$$

where $\langle \text{reaction rate} \rangle$ is the number of photons required to produce one nontoxic molecule multiplied on generation rate and $\langle \text{photon rate} \rangle$ is the absorption rate of incident photons. The generation rate of nontoxic molecules can be obtained from the slope of the nontoxic molecules generation curve between the irradiation times. The nontoxic molecules' generation rate can be calculated using the least-squares method.

Different materials possess diverse properties which depend on numerous factors such as bandgap width, carrier density, and carrier mobility. The nature of the pollutant must also be taken into account. Therefore it is of uttermost important to investigate photocatalyst materials properties to find new materials with preeminent efficiencies for every spectral region or even better to discover such a material that will work as a photocatalyst in the entire solar spectrum range.

## 9.3 Materials for photocatalysis

Nowadays, the development of new materials for photocatalysis is urgent. It is justified by the fact that people strive to reduce the manufacturing cost of materials for photocatalysis to improve their cost-efficiency as well as to improve their parameters. Researchers are studying the properties of numerous materials for photocatalysis and trying to develop new materials with better characteristics. For example, $TiO_2$ is used for many years due to the thoroughly refined technology of its manufacturing [49–51]. But this photocatalyst has many drawbacks that researchers struggle to overcome using different materials and combinations of materials [67–86, 93, 95].

### 9.3.1 $TiO_2$ as a photocatalyst

Byrne et al. [49] prepared $TiO_2$ coatings on different substrates: tin oxide-coated glass, stainless steel, titanium metal, and titanium alloy. For sample fabrication, they used electrochemical anodization, electrophoretic (EP) coating, and spray-coating. These coated substrates were annealed at temperatures ranging from 473 to 973 K and then characterized. Catalyst stripping from the substrates was investigated as a function of annealing temperature and mixture pH. Authors noticed that catalyst stripping was nonsignificant at annealing temperatures above 573 K. Figure 9.3 shows the comparison of the photocatalytic efficiencies of the material under study on different support substrates accordingly to the annealing temperature. As we see from Figure 9.3, in the temperature range from 573 to 673 K the best result owes to the sample with a support substrate made from stainless steel and in the temperature range from 673 to 973 K. The better result gives the sample with support substrate made from titanium alloy. In comparison with the electrophoretically coated samples, the samples prepared by spray-coating gave poor photocatalytic efficiency results. As for solution pH, catalyst

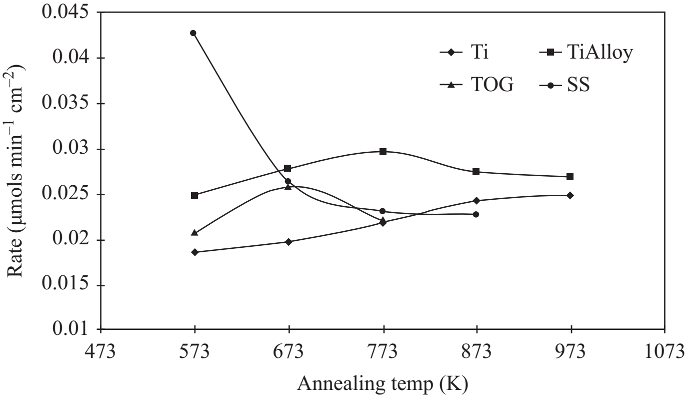

**Figure 9.3:** Comparison of the photocatalytic efficiencies of the immobilized $TiO_2$ using the EP method. The phenol rate degradation is plotted relatively to be used in the coating process annealing temperature. The graph gives the information with the following support substrates: Ti, titanium; TOG, tin oxide-coated glass; TiAlloy, titanium alloy; SS, stainless steel (figure is taken with permission from Ref. [49]).

stripping was greater with higher pH. It is shown that the film's photocatalytic efficiencies are quite similar in this work when quoted as per square centimetres of the coated supporting substrate but they are different if written as per gram of the catalyst loading. A comparison of the immobilized films' optimum photocatalytic efficiencies is given in Table 9.1.

Chen and Mao [50] described the synthesis of $TiO_2$ nanowires, nanorods, nanotubes, and mesoporous and photonic structures in detail. These nanomaterials demonstrate size-dependent as well as shape- and structure-dependent optical, electronic, thermal, and structural properties. It is reported that $TiO_2$ is widely used for the photodegradation of numerous pollutants and can be used to kill bacteria as well as to kill tumor cells in cancer treatment. Yu et al. [51] investigated photocatalytic properties of Cu(II)/$Ti_{1-3x}W_xGa_{2x}O_2$ in comparison with $Ti_{1-3x}W_xGa_{2x}O_2$. Figure 9.4 shows DOS for rutile $TiO_2$ and $Ti_{1-3x}W_xGa_{2x}O_2$ ($x = 0.125$). The values 1.75 and 1.41 eV denote the CB bottom energies in $TiO_2$ and $Ti_{1-3x}W_xGa_{2x}O_2$ ($x = 0.125$), correspondingly, when the VBs tops are assigned as 0 eV. As we can see, the bandgap decreased due to the dopants. Noticeably, the VB top was not affected by the dopants while CB changed. Also, Figure 9.4 demonstrates UV–vis absorption spectra of $Ti_{1-3x}W_xGa_{2x}O_2$ ($x$ = 0, 0.02, 0.03, and 0.05) and Cu(II)/$Ti_{1-3x}W_xGa_{2x}O_2$ ($x$ = 0, 0.02, 0.03, and 0.05) obtained by diffuse reflection method. It is shown that performed doping of rutile $TiO_2$ narrows its bandgap which causes the absorption edges to shift to a longer wavelength with increasing "$x$." This figure clearly shows that Cu(II) joining increases the absorption intensities in the wavelength regions from 420 to 550 nm and from 700 to 800 nm [51].

Data obtained during the 2-propanol decomposition tests in Ref. [51] are shown in Table 9.1. As we can see, samples with Cu(II) joining demonstrate better photocatalytic

**Table 9.1:** Comparison of the optimum photocatalytic efficiencies of different photocatalysts.

| No. | Sample | Coating method | Annealing temp. (K) | Rate of degradation (mol/min/cm$^{-2}$)·10$^{-8}$ or treated percentage in the end of the experiment | Exposure time (h) | Model pollutant | The concentration of pollutant (mmol/L) | Catalyst loading (g/L) | Source of light | Light intensity $I_0$ (W/s/m$^2$) | Wavelength (nm) | Quantum efficiency (%) | Absorbed photon number (quanta/s) | References |
|---|---|---|---|---|---|---|---|---|---|---|---|---|---|---|
| 1 | Stainless steel | Spray | 573 | 3.90 | 2 | Phenol | $1 \times 10^{-3}$ | – | Xenon lamp | 150 | 300–400 | – | – | [49] |
| 2 | Stainless steel | EP | 573 | 4.27 | 2 | Phenol | $1 \times 10^{-3}$ | – | Xenon lamp | 150 | 300–400 | – | – | |
| 3 | Ti-4V-6Al-alloy | Spray | 773 | 2.73 | 2 | Phenol | $1 \times 10^{-3}$ | – | Xenon lamp | 150 | 300–400 | – | – | |
| 4 | Ti-4V-6Al-alloy | EP | 773 | 2.96 | 2 | Phenol | $1 \times 10^{-3}$ | – | Xenon lamp | 150 | 300–400 | – | – | |
| 5 | Titanium | EP | 973 | 2.47 | 2 | Phenol | $1 \times 10^{-3}$ | – | Xenon lamp | 150 | 300–400 | – | – | |
| 6 | Titanium | Anodized | 773 | 0.90 | 2 | Phenol | $1 \times 10^{-3}$ | – | Xenon lamp | 150 | 300–400 | – | – | |
| 7 | Tin oxide-coated glass | EP | 673 | 2.58 | 2 | Phenol | $1 \times 10^{-3}$ | – | Xenon lamp | 150 | 300–400 | – | – | |
| 8 | $Ti_{1-3x}W_xGa_{2x}O_2$ ($x = 0.03$) | – | – | $2.17 \times 10^{-3}$ | – | Gaseous 2-propanol | $3 \times 10^{-3}$ | 0.6 | Xenon lamp | 10 | 400–530 | 0.093 | $1.4 \times 10^{15}$ | [51] |
| 9 | Cu(II)/$TiO_2$ | – | – | $2.83 \times 10^{-1}$ | – | Gaseous 2-propanol | $3 \times 10^{-3}$ | 0.6 | Xenon lamp | 10 | 400–530 | 15 | $1.1 \times 10^{15}$ | |
| 10 | Cu(II)/$Ti_{1-3x}W_xGa_{2x}O_2$ ($x = 0.02$) | – | – | $4.00 \times \cdot 10^{-1}$ | – | Gaseous 2-propanol | 0.003 | 0.6 | Xenon lamp | 10 | 400–530 | 14 | $1.7 \times 10^{15}$ | |
| 11 | Cu(II)/$Ti_{1-3x}W_xGa_{2x}O_2$ ($x = 0.03$) | – | – | $4.17 \cdot \times 10^{-1}$ | – | Gaseous 2-propanol | 0.003 | 0.6 | Xenon lamp | 10 | 400–530 | – | – | |

(continued)

**Table 9.1** (continued)

| No. | Sample | Coating method | Annealing temp. (K) | Rate of degradation (mol/min/cm$^{-2}$)·10$^{-8}$ or treated percentage in the end of the experiment | Exposure time (h) | Model pollutant | The concentration of pollutant (mmol/L) | Catalyst loading (g/L) | Source of light | Light intensity $I_0$ (W/s/m$^2$) | Wavelength (nm) | Quantum efficiency (%) | Absorbed photon number (quanta/s) | References |
|---|---|---|---|---|---|---|---|---|---|---|---|---|---|---|
| 12 | Cu(II)/$Ti_{1-3x}W_xGa_{2x}O_2$ ($x$ = 0.05) | – | – | $1.35 \times 10^{-1}$ | – | Gaseous 2-propanol | 0.003 | 0.6 | Xenon lamp | 10 | 400–530 | 3.1 | $2.6 \times 10^{15}$ | [51] |
| 13 | Bare $TiO_2$ | – | – | $1.83 \times 10^{-2}$ | – | Gaseous 2-propanol | 0.003 | 0.6 | Xenon lamp | 10 | 400–530 | 1.4 | $7.6 \times 10^{14}$ | |
| 14 | N-doped $TiO_2$ | – | – | $2.67 \times 10^{-1}$ | – | Gaseous 2-propanol | 0.003 | 0.6 | Xenon lamp | 10 | 400–530 | 3.9 | $4.1 \times 10^{15}$ | |
| 15 | Cu(II)/N-doped $TiO_2$ | – | – | $7.17 \times 10^{-2}$ | – | Gaseous 2-propanol | 0.003 | 0.6 | Xenon lamp | 10 | 400–530 | 0.94 | $4.6 \times 10^{15}$ | |
| 16 | ZnO(5 wt%) g-$C_3N_4$ | – | – | ≈100% | 1 | Phenol | 0.053 | 1.000 | Simulated sunlight | 80 | – | – | – | [123] |
| 17 | ZnO | – | – | 100% | 8 | Phenol | 0.797 | 2.500 | Solar lamp | – | – | – | – | [126] |
| 18 | Pt/ZnO-$SiO_2$ | – | – | 100% | 1 | Phenol | 1.063 | 1.000 | Mercury lamp | 150 | – | – | – | [127] |
| 19 | ZnO | – | – | 100% | 1.3 | Phenol | 0.531 | 2.000 | Mercury UV lamp | 6 | 253.7 | – | – | [128] |
| 20 | $Fe_3O_4$-ZnO | – | – | 80% | 2.5 | Phenol | – | 0.325 | Metal halide lamp | 575 | 315–1,050 | – | – | [129] |
| 21 | Ag/ZnO | – | – | 100% | 2.5 | Phenol | 0.266 | 1.000 | UV-C lamp | – | >254 | – | – | [130] |

| | | | | | | | | | | | | | | |
|---|---|---|---|---|---|---|---|---|---|---|---|---|---|---|
| 22 | ZnO/$Fe_3O_4$/pumice | – | – | 72% | 1 | RhB | 0.106 | 0.05 | LED | 7 | 526 | – | – | [124] |
| 23 | ZnO/$Fe_3O_4$/pumice | – | – | 85.5% | 1 | MB | 0.106 | 0.05 | LED | 7 | 526 | – | – | [124] |
| 24 | $Fe_3O_4$/ZnO/$CuWO_4$ | – | – | 99% | 3.5 | RhB | 0.010 | 0.4 | LED | 50 | – | – | – | [131] |
| 25 | $Fe_3O_4$/ZnO/$CuWO_4$ | | | 99% | 3.5 | MB | 0.013 | 0.4 | LED | 50 | – | – | – | |
| 26 | $Fe_3O_4$/ZnO/$CuWO_4$ | – | – | 98.3% | 6.75 | RhB | 0.010 | 0.4 | LED | 50 | – | – | – | [132] |
| 27 | $Fe_3O_4$/ZnO/AgCl | – | – | 99% | 2.25 | RhB | 0.025 | 0.4 | LED | 50 | – | – | – | [133] |
| 28 | $Fe_3O_4$/silica/ZnO | – | – | 99% | 1 | MB | 0.177 | 0.5 | Sunlight | – | – | – | – | [134] |
| 29 | $Fe_3O_4$/CuO/ZnO | – | – | 89% | 2 | MB | 0.213 | 0.2 | UV | 40 | – | – | – | [135] |
| 30 | rGO/$Fe_3O_4$/ZnO | – | – | 83% | 2 | MV | 1 | 0.04 | Tungsten halogen | – | – | – | – | [136] |
| 31 | (Yb, N)-$TiO_2$ | – | – | 95% | 5 | MB | 0.106 | 3 | Fluorescent lamp | 30 | 400–750 | – | – | [137] |
| 32 | $WO_3$ (W1) | – | – | 38% | 2 | MB | 0.02 | 0.05 | Halogen lamp | 300 | – | – | – | [138] |
| 33 | $WO_3$ (W2) | – | – | 31% | 2 | MB | 0.02 | 0.05 | Halogen lamp | 300 | – | – | – | [138] |
| 34 | $WO_3$ (W3) | – | – | 28% | 2 | MB | 0.02 | 0.05 | Halogen lamp | 300 | – | – | – | |
| 35 | $WO_3$@$Bi_2WO_6$/$NiWO_4$-III nanocomposites | – | – | 99.2% | 0.25 | RhB | 0.021 | 0.5 | Xenon lamp | 500 | >420 | – | – | [138] |
| 36 | $Bi_2WO_6$ hollow tubes | – | – | ≈100% | 1.5 | RhB | 0.010 | 0.5 | Xenon lamp | 500 | – | – | – | [139] |
| 37 | Bi/$Bi_2WO_6$ nanocomposites | – | – | ≈100% | >0.42 | RhB | 0.021 | 0.5 | Xenon lamp | 300 | 400 | – | – | [140] |

(continued)

**Table 9.1** (continued)

| No. | Sample | Coating method | Annealing temp. (K) | Rate of degradation (mol/min/cm$^{-2}$)·$10^{-8}$ or treated percentage in the end of the experiment | Exposure time (h) | Model pollutant | The concentration of pollutant (mmol/L) | Catalyst loading (g/L) | Source of light | Light intensity $I_0$ (W/s/m$^2$) | Wavelength (nm) | Quantum efficiency (%) | Absorbed photon number (quanta/s) | References |
|---|---|---|---|---|---|---|---|---|---|---|---|---|---|---|
| 38 | g-$C_3N_4$/$Bi_2WO_6$ nanosheets | – | – | ≈100% | >2 | MB | 0.010 | 2.5 | Xenon lamp | 400 | >450 | – | – | [141] |
| 39 | $Bi_2WO_6$ sheets | – | – | ≈100% | >0.83 | RhB | 0.010 | 1 | Xenon lamp | 300 | – | – | – | [142] |
| 40 | Thin empty-shell $Bi_2WO_6$ | – | – | ≈100% | >0.83 | RhB | 0.021 | 0.5 | Xenon lamp | 300 | >400 | – | – | [143] |
| 41 | $Bi_2WO_6$-Pd | – | – | ≈100% | >1 | RhB | 0.063 | 0.5 | Metal halide lamp | 500 | >400 | – | – | [144] |
| 42 | $Bi_2WO_6$-carbon nanofibers | – | – | ≈100% | >5 | RhB | 0.021 | 0.5 | Xenon lamp | 150 | >420 | – | – | [145] |
| 43 | Hollow $Bi_2WO_6$/RGO spheres | – | – | 99.5% | >8 | RhB | 0.125 | 1 | Sunlight | – | – | – | – | [146] |
| 44 | Hollow $Bi_2WO_6$/RGO spheres | – | – | 78.5% | >8 | MO | 0.031 | 1 | Sunlight | – | – | – | – | |
| 45 | Hollow $Bi_2WO_6$/RGO spheres | – | – | 66.5% | >8 | Phenol | 0.106 | 1 | Sunlight | – | – | – | – | [146] |
| 46 | Hollow $Bi_2WO_6$/RGO spheres | – | – | 70.9% | >8 | SMM | 0.036 | 1 | Sunlight | – | – | – | – | |
| 47 | Hollow $Bi_2WO_6$/RGO spheres | – | – | 57.6% | >8 | SN | 0.058 | 1 | Sunlight | – | – | – | – | |

| | | | | | | | | | | | | | |
|---|---|---|---|---|---|---|---|---|---|---|---|---|---|
| 48 | $Fe_3O_4$@$SiO_2$@$Bi_2WO_6$@g-$C_3N_4$ microspheres | – | – | ≈100% | >1 | RhB | 0.042 | 1 | Xenon lamp | 350 | >420 | – | – | [147] |
| 49 | BiOBr-$Bi_2WO_6$ mesoporous nanosheets | – | – | ≈100% | >0.67 | RhB | 0.021 | 1 | LED | 3 | 400–405 | – | – | [148] |
| 50 | p-Type-FeOOH/*n*-type $WO_3{\cdot}H_2O$ | – | – | ≈100% | >3.5 | RhB | 0.010 | 1 | UVA | 6 | 365 | – | – | [149] |
| 51 | $Fe_3O_4$/ZnO/$NiWO_4$ nanocomposites | – | – | ≈100% | 5 | RhB | 0.010 | 0.4 | LED | 50 | – | – | – | [150] |

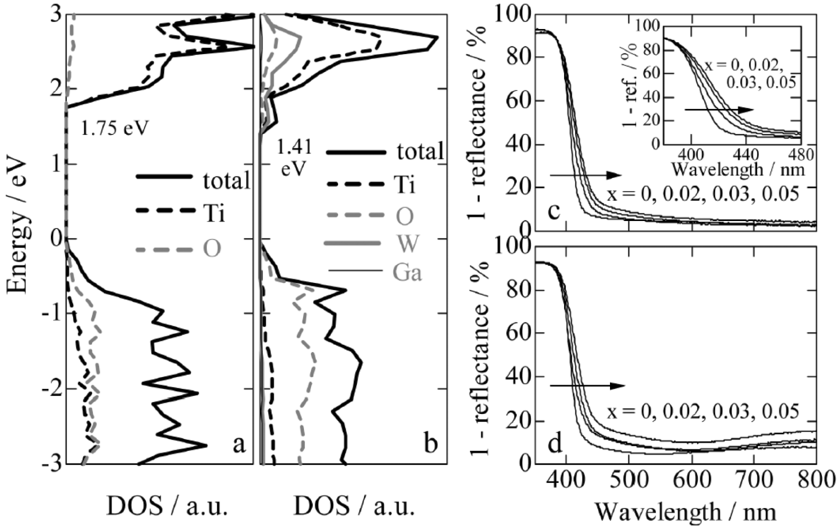

**Figure 9.4:** (a, b) DOS for a rutile $TiO_2$ and (b) $Ti1-3xW_xGa_{2x}O_2$ ($x = 0.125$); (c) $Ti1-3xW_xGa_{2x}O_2$ ($x$ = 0, 0.02, 0.03, and 0.05) UV–vis absorption spectra. The inset demonstrates zoomed-in spectra region from 380 to 480 nm. (d) Cu(II)/$Ti1-3xW_xGa_{2x}O_2$ ($x$ = 0, 0.02, 0.03, and 0.05) UV–vis absorption spectra (figure is taken with permission from Ref. [51]).

performances in comparison with samples without Cu(II). This change occurred due to a more narrow bandgap because of Cu(II) addition which was explained above.

$TiO_2$ is a well-studied material. For many years researchers are studying parameters affecting the photocatalytic degradation of dyes using $TiO_2$-based photocatalysts [118–122]. Thus, Mazierski et al. [118] studied the role of lanthanides in $TiO_2$-based photocatalysis.

## 9.3.2 ZnO as a photocatalyst

Zinc oxide has a wide bandgap ($E_g$ = 3.2 eV), which is equal to the anatase modification of titanium oxide. ZnO is a widely used photocatalyst of its high photosensitivity, environmental friendliness, and cost efficiency [123–125]. The ZnO degradation mechanism is similar to $TiO_2$. Nevertheless, ZnO has the same disadvantages as $TiO_2$. Therefore, the ZnO photocatalyst modification is conducted by numerous research groups. For that reason, Md et al. [123] prepared ZnO/g-$C_3N_4$ hybrid nanoparticles using a simple impregnation method to degrade phenol under simulated sunlight irradiation. The obtained result shown in Table 9.1 demonstrates the ZnO/g-$C_3N_4$ hybrid nanoparticles high photodegradation efficiency compared with pure ZnO because of the *e*/*h* effective separation and improved OH radicals formation. In addition, a comparison of obtained results by these researches with several other materials based on ZnO: ZnO, Pt/ZnO–$SiO_2$, $Fe_3O_4$, and Ag/ZnO is shown in Table 9.1 [126–130]. The demonstrated comparison shows the competitiveness of the developed material. Researchers found out that the amount of photocatalyst, g-$C_3N_4$ dosage, concentration at the beginning of the experiment, and solution pH influence the phenol degradation significantly. Thus, with the increase in the photocatalyst amount, first, the photocatalytic degradation of phenol increased due to an increase in the available active sites for it. However, after the achievement of a particular concentration of the photocatalysts, the photocatalytic degradation became lower because of the photocatalyst's excess suspension that intercepts light. As for g-$C_3N_4$ dosage, with the increase of g-$C_3N_4$ up to 5 wt%, the lifetime of carriers prolongs and photocatalytic activity promotes. At the same time, further g-$C_3N_4$ quantity increase can increase the recombination of *e*/*h* pairs instead of providing an electron pathway. Obviously, with the higher phenol concentration, the photocatalytic degradation of this pollutant decreased. It happened as a result of the same amount of reactive species and a decline in photons entering the solution path length. In the case of solution pH, in an acidic medium, the ZnO surface is considered positively charged, and in these conditions the $Cl^-$ possibly reduces the photocatalytic activity. On the other hand, at the natural pH = 5.7, the electrostatic attraction force takes place between phenol molecules and the ZnO surface which leads to high photocatalytic activity. At high pH, phenol molecules undergo deprotonation and become negatively charged ions. Electrostatic repulsion arising between phenol molecules and the negatively charged ZnO photocatalyst surface leads to phenol adsorption onto the photocatalyst surface decrease, resulting in a photocatalytic efficiency decline. Furthermore, the photocatalytic activity decay in an alkaline medium is also caused by the competition among adsorption sites between ions from NaOH salts and phenol molecules. In this work, it was demonstrated that the photocatalytic activity of the investigated material mainly referred to the synergetic effects between g-$C_3N_4$ and ZnO. Such a photocatalyst can be reused four times without significant decay in photoactivity [123].

Taheri-Ledari et al. [124] investigated catalytic systems based on iron oxide nanoparticles ($Fe_3O_4$ NPs), natural pumice microplates, and zinc oxide nanorods (ZnO NRs) in composite form. These photocatalysts were applied for methylene blue degradation in water under green light irradiation. It is clearly shown in Figure 9.5(a) that a significant redshift occurred after the individual ingredients composition process which means that this composition can harvest more energy from a wide spectrum of light.

Figure 9.5(b) shows the UV–vis diffuse reflectance measurement of solid samples (UV–vis DRS) which demonstrates the photoactivity enhancement and improved energy harvesting capability in comparison with the individual ZnO. Researchers found out that the absorbance maximum of the prepared composite lies in the region of ~530 nm so that is why they used green light LED. Figure 9.5(c) demonstrates that a distinguishable signal was not observed in the ESR spectrum when the ZnO/$Fe_3O_4$@pumice photocatalyst was put in the dark. Figure 9.5(d) illustrates XPS analysis where it is shown that all of the essential signals related to Al, Si, C, O, and Fe appeared. Two peaks related to Zn are there, too. In this work, researchers demonstrated that such type of photocatalyst can

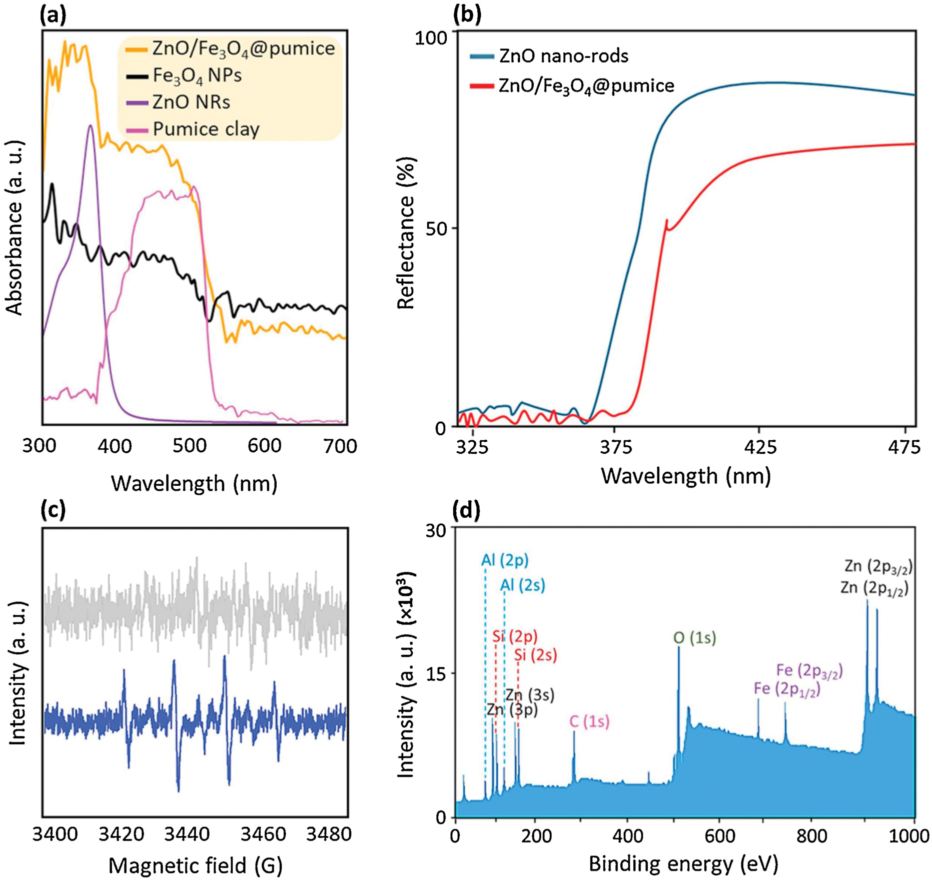

**Figure 9.5:** (a) UV–vis absorbance spectra of the fabricated $ZnO/Fe_3O_4$@ pumice photocatalyst with comparison with its individual ingredients: $Fe_3O_4$ NPs, individual ZnO NRs, and natural pumice clay, (b) UV–vis DRS spectra of the individual ZnO and $ZnO/Fe_3O_4$@pumice photocatalyst, (c) DMPO spin-trapping ESR spectra of $ZnO/Fe_3O_4$@pumice photocatalyst at ambient temperature, and (d) X-ray photoelectron spectroscopy (XPS) total spectrum of the $ZnO/Fe_3O_4$@pumice photocatalyst (figure is taken with permission from Ref. [124]).

be reused eight times without significant loss in the photoactivity. Comparison with other photocatalysts like $Fe_3O_4/ZnO/CuWO_4$, $Fe_3O_4/ZnO/AgCl$, $Fe_3O_4$/silica/ZnO, $Fe_3O_4/CuO/ZnO$, $rGO/Fe_3O_4/ZnO$, and (Yb, N)-$TiO_2$ is provided and demonstrated in Table 9.1 [124, 131–137].

### 9.3.3 $WO_x$ as a photocatalyst

$WO_x$ is a transition metal oxide with a narrow bandgap ($E_g$ = 2.8 eV) that causes effective absorption in the blue region of the solar spectrum [61]. Hao et al. [138] investigated numerous water-assisted $WO_3$ semiconductor photocatalysts to degrade methylene blue. A sample named W1 was prepared using distilled water, a sample named W2 using distilled and groundwater of an equal amount of (1:1), and a sample named W3 using groundwater. It was demonstrated that groundwater highly affects the materials' properties such as morphology and crystallinity.

Table 9.1 shows that sample W1 had the highest photocatalytic efficiency and sample W3 had the worst one even though they had equal bandgap energies and electron–hole separation times. This photocatalytic efficiency suppression could be caused by the addition of Na and Cl ions from groundwater into the catalyst [138]. To achieve better photocatalytic properties, researchers prepared $WO_3@Bi_2WO_6/NiWO_4$ nanocomposites by a simple hydrothermal method for organic dye degradation [139]. These nanocomposites consist of ultrathin $Bi_2WO_6/NiWO_4$ and ultrafine $WO_3$ nanoparticles. Obtained results show high photocatalytic activity for the RhB degradation using visible light exposure. Table 9.1 includes the comparison between some typical catalysts based on $WO_x$ in this article and reported previously [139–151]. Dong et al. [147] investigated photocatalytic activities of $Bi_2WO_6$ and $Bi_2WO_6$/RGO to degrade such pollutants as MO, rhodamine B (RhB), phenol, sulfanilamide (SN), and sulfamonomethoxine (SMM) using natural sunlight irradiation. Figure 9.6(a) shows the pollutant decomposition results without a catalyst and with it under solar light irradiation. It is demonstrated that $Bi_2WO_6$/RGO degraded mentioned organic pollutants effectively.

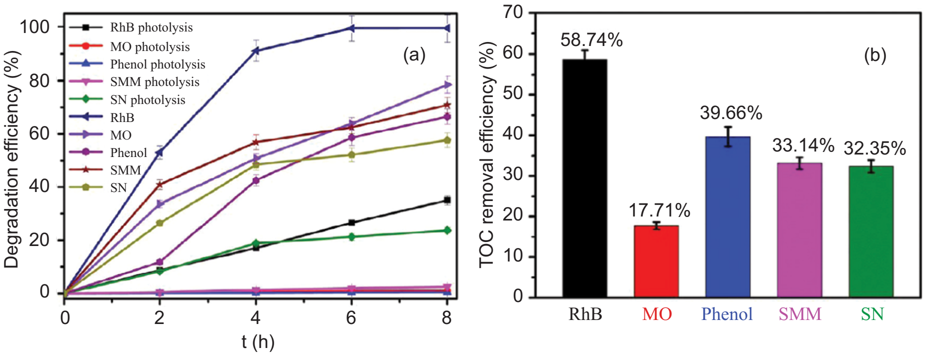

**Figure 9.6:** (a) Photocatalytic degradation efficiencies; (b) the corresponding TOC removal efficiencies of RhB, MO, phenol, SMM, and SN in the $Bi_2WO_6$/RGO presence (figure is taken with permission from Ref. [147]).

The total organic carbon (TOC) removal efficiency results demonstrated in Figure 9.6(b) revealed that the decomposition rate lies in the order of MO<<SN < SMM < phenol < RhB. The TOC removal efficiencies turned out to be lower than the degradation efficiencies. It is caused by the fact that it is easier to decompose the organic pollutant chromophore rather than to mineralize it up to carbon dioxide and pure water [147].

### 9.3.4 Advanced fibers as photocatalysts

Nowadays, there are a few types of advanced photocatalytic fibers: pure material fiber in a form of nanowires, nanorods, nanobelts, nanoneedles, and nanotubes (e.g., ZnO nanowires, $TiO_2$ nanorods/nanotubes, and carbon nanotubes) [9, 50, 76, 77]; photocatalyst micro- or nanostructure anchored/embedded in fiber surfaces (e.g., PVDF fibers embedding lanthanide-doped ZnO, $TiO_2$@CMS/carbon fiber, $TiO_2$–$MoO_3$ composite NFs, $TiO_2$@CNTs NFs, $BiVO_4/SiO_2$/rGO, cotton fibers with BiOCl, and $TiO_2$) [72, 73, 75, 81, 103, 112, 152]; photocatalyst micro- or nanostructure anchored/embedded in optical fiber surfaces (e.g., $TiO_2$-coated optical fibers and $WO_3$ heterojunction nanostructures on glass fibers) [82, 84–86]. Every photocatalytic construction possesses its advantages and drawbacks.

In most cases, fibers for photocatalysts are produced via the electrospinning technique. This technique makes it possible to manufacture continuous NFs with a huge specific surface area and a high length/diameter ratio [153]. This technique possesses such benefits as good repeatability, mass production, economical efficiency, as well as the ability of fiber dimensions to change [154]. Moreover, the electrospinning technique allows fabricating of various compositions of nanomaterials in the obtained NFs [155]. The most studied material for preparing fibers for photocatalysis is $TiO_2$. To provide a bigger active area, researchers fabricated $TiO_2$ on the surface of polymeric electrospun fiber [156]. Such photocatalytic fiber is capable of almost complete MO solution degradation (90.5%) under UV light irradiation within 50 min. Owing to the composite structure it can be separated from the reaction media without any difficulties by filtration or decantation with the aim of recycling use. Moreover, the $TiO_2$@PMMA structure prevents $TiO_2$ nanoparticles agglomeration improving the efficiency of the $TiO_2$ catalyst [156]. The comparison of obtained results with those reported previously is presented in Table 9.2 [156–160].

With the aim of photocatalysis and performance improvement, researchers fabricated $TiO_2$ NFs doped with various materials [161, 162]. Researchers calcined carbon-doped TiO2/halloysite nanotube hybrid NFs under 500 °C and found that introducing halloysite nanotubes into NFs increases MB adsorption of the obtained material because of its modified structure [162]. Another research group established that introduction of CNTs into polyacrylonitrile (PAN)/$TiO_2$ NFs improves their adsorption capability [163]. These results were obtained due to an increased surface area of the photocatalysts

**Table 9.2:** Comparison of the optimum photocatalytic efficiencies of advanced nanofibers.

| No. | Sample | Fiber diameter (nm) | Rate of degradation (mol/ min/ cm$^2$)·$10^{-8}$ or treated percentage at the end of the experiment | Exposure time (h) | Model pollutant | The concentration of pollutant (mmol/L) | Catalyst loading (g/L) | Source of light | Power of light (W) | References |
|---|---|---|---|---|---|---|---|---|---|---|
| 1 | $TiO_2$@PMMA | – | 90.5% | 0.83 | MO | 0.031 | 1 | UV | – | [155] |
| 2 | CNT–Ag/$TiO_2$ | – | ≈100% | 1.5 | MO | 0.046 | 2 | UV | – | [156] |
| 3 | $TiO_2$/PANI | – | 92% | 2.33 | MO | 0.244 | 2.5 | UV | – | [157] |
| 4 | $Fe_3O_4$@$SiO_2$@ $TiO_2$@Nd | – | 67.3% | 1.5 | MO | 0.020 | 0.6 | UV | – | [158] |
| 5 | $TiO_2$/$SiO_2$ | – | 57% | 3.33 | MO | 0.031 | 0.4 | UV | – | [159] |
| 6 | $TiO_2$ | 1,000 | 90% | 1 | MO | 0.031 | 1 | UV | 32 | [162] |
| 7 | $TiO_2$/CdS | 50–100 | 77% | 2.67 | CR | 0.061 | 0.5 | UV | 800 | [165] |
| 8 | $TiO_2$/metal (Zn, Cu, Ni, and Co) | 250–400 | 60% | 2.5 | MB | 0.031 | 0.1 | UV | 32 | [167] |
| 9 | $TiO_2$/Ag | 100 | 100% | 1.67 | RhB | 0.176 | 0.5 | UV | 350 | [169] |
| 10 | $TiO_2$/calcium acetate | 200 | 70% | 1.67 | RhB | 0.042 | 1.2 | UV | 250 | [170] |
| 11 | $TiO_2$/$SiO_2$ | 209–238 | 90% | 1 | MB | 0.031 | 1 | UV | 250 | [173] |
| 12 | $TiO_2$/$SiO_2$ | 250–300 | 20% | 2 | MO | 0.122 | 0.667 | UV | 500 | [174] |
| 13 | $TiO_2$/$BiVO_4$ | 150–250 | 10% | 4 | RhB | 0.088 | 0.5 | UV | 150 | [176] |
| 14 | $TiO_2$/GO | 120 | 57% | 1 | MO | 0.031 | 0.4 | UV | 20 | [177] |

(continued)

**Table 9.2** (continued)

| No. | Sample | Fiber diameter (nm) | Rate of degradation (mol/ min/ cm$^2$)·10$^{-8}$ or treated percentage at the end of the experiment | Exposure time (h) | Model pollutant | The concentration of pollutant (mmol/L) | Catalyst loading (g/L) | Source of light | Power of light (W) | References |
|---|---|---|---|---|---|---|---|---|---|---|
| 15 | ZnO | – | 90% | 1.42 | MB | $1.5 \times 10^{-2}$ | 1 | UV | – | [194] |
| 16 | $Mn^{2+}$/ZnO | – | 80% | 4.3 | RhB | $2.5 \times 10^{-2}$ | 1 | Vis | – | [195] |
| 17 | ZnO-ZnS | – | 73% | 1 | RhB | $2.5 \times 10^{-2}$ | 1 | UV | – | [196] |
| 18 | ZnO-$TiO_2$-CNFs | – | ≈ 95% | 2 | MB | 0.031 | 0.8 | UV | – | [197] |
| 19 | $ZnFe_2O_4$/Ag/AgBr | – | 86% | 1.67 | RhB | 0.879 | 1 | LED | – | [198] |
| 20 | $TiO_2$@ZnO | – | 95.27% | 3 | MB | – | – | UV | 125 | [199] |
| 21 | ZnTe/ZnO | – | 50% | 1 | Methylene red | $10^{-2}$ | 1 cm$^2$ | Xenon lamp | 300 W | [200] |
| 22 | ZnO/$In_2O_3$ | – | 97% | 2 | MB | 0.063 | 0.5 | Xe arc lamp | 300 W | [201] |
| 23 | $MoS_2$@ZnO nano–heterojunctions | – | 92.3% | 1.67 | MB | 0.063 | 0.2 | Daylight lamp | 18 W | [202] |
| 24 | $Cu_2O$/ZnO | – | 90% | 5 | MB | 10 | 1.5 cm$^2$ | Vis | 500 W | [203] |
| 25 | ZnO-$Cu_xO$ | – | 73.5% | 2 | RhB | 0.088 | 0.02 | Vis | 400 W | [204] |
| 26 | ZnO/ZnSe/$MoSe_2$ | – | 91.5% | 3 | MO | 0.018 | 0.03 | Vis | 300 W | [205] |
| 27 | $Cu_2O$/ZnO/$Ag_3PO_4$ | – | 85% | 3 | MO | 0.031 | 0.14 | Vis | 85 W | [206] |

| | | | | | | | | | | |
|---|---|---|---|---|---|---|---|---|---|---|
| 28 | Oxidized SWCNT | – | – | 1.67 | Basic red 46 | 0.374 | 0.05 | – | – | [234] |
| 29 | $HNO_3$-oxidized MWCNTs | – | 97% | – | Bromothymol blue | 0.048 | 0.02 | – | – | [219] |
| 30 | Functionalized CNT/ Mg(Al)O | – | 94% | 1.25 | Congo red | – | 0.03 | – | – | [235] |
| 31 | Magnetic MWCNTs-$Fe_3C$ nanocomposite | – | – | – | Direct red 23 | 0.066 | 0.04 | – | – | [236] |
| 32 | SWCNT–COOH | – | – | – | Malachite Green | 0.027 | – | – | – | [237] |
| 33 | SWCNT–$NH_2$ | – | – | – | Malachite Green | 0.027 | – | – | – | |
| 34 | SWCNT–COOH | – | – | – | MO | 0.031 | – | – | – | |
| 35 | SWCNT–$NH_2$ | – | – | – | MO | 0.031 | – | – | – | |
| 36 | Oxidized MWCNTs | – | – | – | MO | – | 0.02 | – | – | [238] |
| 37 | Functionalized-CNTs loaded $TiO_2$ | – | 100% | 0.5 | MO | 0.015 | – | – | – | [239] |
| 38 | Thiol-functionalized MWCNT (MWCNT–SH) | – | – | 1 | MB | 0.031 | – | – | – | [240] |
| 39 | KOH-modified MWCNTs | – | – | 0.08 | Bisphenol-A | 0.175 | – | – | – | [241] |
| 40 | $HNO_3$-modified MWCNTs | – | – | 0.5 | Bisphenol-A | 0.175 | – | – | – | |

(continued)

**Table 9.2** (continued)

| No. | Sample | Fiber diameter (nm) | Rate of degradation (mol/ min/ cm$^2$)·$10^{-8}$ or treated percentage at the end of the experiment | Exposure time (h) | Model pollutant | The concentration of pollutant (mmol/L) | Catalyst loading (g/L) | Source of light | Power of light (W) | References |
|---|---|---|---|---|---|---|---|---|---|---|
| 41 | $SOCl_2$/$NH_4OH$-modified CNT | – | – | – | Bisphenol-A | 0.044 | 0.125 | – | – | [242] |
| 42 | $NH_3$-treated MWCNTs | – | – | – | Chlorophenols | – | – | – | – | [243] |
| 43 | $HNO_3$ and $KMnO_4$-functionalized MWCNTs | – | 88% | – | Phenol | 5.313 | – | – | – | [244] |
| 44 | Oxidized SWNTs | – | 97.9% | 0.5 | *p*-nitrophenol | $7.18 \times 10^{-5}$ | – | – | – | [245] |
| 45 | Nitrogen-doped carbon nanotubes ($CN_x$) | – | – | – | Phenol | 0.6 | – | – | – | [246] |
| 46 | MWCNT–COOH | – | – | – | Phenol | 0.004 | 0.01 | – | – | [247] |
| 47 | MWCNT–COOH | – | 95% | – | 3-chlorophenol | 0.013 | 0.01 | – | – | [247] |
| 48 | Acid-functionalized MWCNT (MWCNT–COOH) | – | – | – | 2-nitrophenol | 0.323 | – | – | – | [248] |

resulting in improved adsorption capacity. In one recent research, the adsorption and desorption equilibrium was achieved in the dark before the photocatalytic reaction. There, PAN/$TiO_2$ NFs demonstrated a 2% MB reduction within 100 min [164]. Moreover, researchers obtained 74% and 17% solution degradation of Congo red (CR) and MB using CdS/$TiO_2$ NFs [165]. Another research group found out that the NF morphology and structure can affect the acid orange 7 adsorption. It turned out that $TiO_2$/CuO NFs can degrade 46% of dyes, whereas pure $TiO_2$ NFs can degrade only 25%. This improvement in the adsorption capacity is related to a better interaction between dye molecules and active centres of the photocatalyst [166].

The effect of different metals doping on $TiO_2$ NFs photocatalytic efficiency was discussed in detail in [167]. Researchers found that Zn and Ni doping provide higher MB decomposition efficiency using the obtained structure in comparison with pure $TiO_2$ NFs usage. On the contrary, Cu and Co doping initiates lesser MB decomposition efficiency using the obtained structure in comparison with pure $TiO_2$ NFs utilization [167]. In addition, 0.5% doping with Fe improves the MB decomposition efficiency of $TiO_2$ in comparison with bare $TiO_2$ NFs within 300 min under UV light irradiation [168]. Doping with Ag reduces the decomposition time of RhB from 100 min to 70 min compared with pure $TiO_2$ NFs [169]. It is considered that the obtained photocatalytic results are referred to the high Ag nanoparticles dispersion on individual $TiO_2$ NFs. It is worth mentioning that $TiO_2$ NFs doped with Ca exhibit 95% degradation efficiency of RhB compared with 73% obtained from pure $TiO_2$ NFs within 100 min [170]. In this structure, ions of Ca occupy the $Ti^{4+}$ positions in the $TiO_2$ resulting in an *e*/*h* recombination decay improving the photocatalytic performance. Thus, researchers established that the Ca-ion introduction in $TiO_2$ NFs leads to stability of the anatase phase modification that reduces the rutile phase modification [171, 172].

It is important to note that oxides doped with $TiO_2$ are also used for photocatalytic efficiency improving. This effect refers to grain size, heterogeneous structure, larger surface area, and, in the case of $SiO_2$, surface Si–O–H groups [173]. Important problem researchers are facing using $TiO_2$ is its phase transformation from anatase phase modification to rutile phase modification. Many researchers reported the complexity of maintaining active and stable anatase modification of $TiO_2$ at elevated temperatures. It was observed that $SiO_2$ can phase transformation preventing anatase phase modification to rutile phase modification [174]. Apart from $TiO_2$ doping with $SiO_2$, $Al_2O_3$, and $ZrO_2$ can also prolong anatase phase modification stability since they occupy the interstices, leading to distortion and decreasing the structure shrinkage in the process of transformation to rutile phase modification [174, 175].

Many researchers investigated composites of $TiO_2$ with oxides. For example, $BiVO_4$/$TiO_2$ NFs heterojunction demonstrates 90% decomposition efficiency of RhB compared with 10% decomposition efficiency using pure $TiO_2$ NFs under vis light exposure [176]. Additionally, graphene improves the photoactivity of prepared NFs. Graphene-wrapped porous $TiO_2$ NFs can touch 90% degradation efficiency of MO in contrast with 59% degradation efficiency provided by pure $TiO_2$ NFs [177]. Corresponding data of different photocatalysts compounds is presented in Table 9.2 [162, 165, 167, 169, 170, 173, 174, 176, 177].

To increase ZnO photocatalyst stability and prevent aggregation of nanoparticles researchers made ZnO/PVA nanocomposite [178, 179]. Indeed, PVA prevents aggregation of ZnO nanoparticles and increases its mechanical stability. However, PVA decreases ZnO photocatalytic activity [180]. Numerous types of research were made on ZnO/PVA fiber photocatalysis [180–184]. To degrade RhB and avoid the drawbacks of pure ZnO nanoparticles, researchers fabricated ZnO nanoparticles capped by PVA [180]. This modification leads to a drastic reduction in the ZnO photocatalytic activity. The values of chemical oxygen demand and TOC analysis results also showed a decrease in the photocatalytic efficiency after ZnO nanoparticles capping with PVA. PVA surface capping results in increasing compatibility with organic phases, hydrophobicity, and in a reduction in photocatalytic efficiency. Better photocatalytic activity is demonstrated by pure ZnO photocatalyst due to its hydrophilic condition while ZnO/PVA becomes hydrophobic and loses its photocatalytic activity [180]. A detailed study on polymer substrates' effect on photocatalysis activity was conducted in [185]. In this research, a few polymer substrates (PVA, gelatin, ethylene glycol, and polyvinylpyrrolidone) with ZnO were tested under vis light irradiation for degradation of MB. PVA turned out to be the worst choice for a substrate because of the lowest ZnO/PVA photocatalytic activity among all the samples [185].

Researchers have reported an improvement in the photocatalytic activity of ZnO/PVA by introducing various materials into the structure under consideration. For instance, chitosan/PVA/ZnO possesses better photocatalytic performance than separate compounds PVA/ZnO or chitosan/ZnO against Acid Black 1 [186]. Researchers investigated polysulfone/PVA/ZnO compound for decomposing CR dye. They revealed that such structure has enhanced hydrophilicity that leads to improvement in photocatalytic activity [187]. Curcumin-modified ZnO/PVA composite also demonstrates promising photocatalytic properties in decomposing MB [181]. Some compounds like laponite lead to an increase in the composite mechanical strength resulting in an improvement in the photocatalytic efficiency [188]. Moreover, by introducing magnetic materials into the composite, researchers managed to obtain an increment in photocatalytic efficiency and a decrement in the composite material bandgap energy [189]. It is worth mentioning that calcination greatly affects the photocatalytic activity of the photocatalyst. Calcination greatly increases the surface-to-volume ratio, thereby improving photocatalytic capabilities [184]. Moreover, some researchers obtained ZnO/PVA compound photocatalytic efficiency better than that of some commercial photocatalysts [182].

Numerous types of research were conducted on ZnO in the textile field. For example, cotton fiber surface coated with ZnO using ultrasonic energy and natural biopolymer tragacanth gum demonstrates excellent photocatalytic efficiency against MB dye [190]. Sonochemically fabricated ZnO on cotton fiber also demonstrated enhanced photocatalytic activity degrading 69% of trypan blue under solar light irradiation [191]. Furthermore, sonochemically synthesized ZnO on cotton fiber exhibited better photocatalytic properties than $TiO_2$-coated samples [192]. The causes of better photocatalytic performance of pure ZnO are interstitial oxygen atoms from acceptor states, zinc vacancies, interstitial zinc atoms from donor states, and oxygen vacancies. Researchers compared pure ZnO and doped ZnO samples as photocatalysts. They concluded that pure ZnO is better for decomposing organic pollutants, while doped ZnO is preferred for other applications such as energy and sensors [193]. A comparison of various photocatalysts' performances is presented in Table 9.2 [194–206].

One more prospective material for developing advanced NFs for photocatalysis is $MoS_2$. Double heterostructure in a form of $MoS_2$-$TiO_2$ core-shell nanosheets synthesized on a graphite fiber demonstrates improved carrier separation and efficient *e*/*h* generation [207]. Such structure decomposes 88% of MO solution within 30 min under UV light irradiation and 90% under vis light exposure. These results are considerably higher than those of graphite fiber/$TiO_2$ compound (55% degradation of MO under UV light irradiation). To improve photocatalytic performance, researchers synthesized $TiO_2$ nanobelts coated with $MoS_2$ nanosheets via hydrothermal technique [208]. $TiO_2$ nanobelts suppressed the $MoS_2$ crystal's growth along the c-axis, leading to a resulting $MoS_2$ coating of only several layers on the surface of nanobelts. Researchers compared photocatalytic activities of pure $MoS_2$, $TiO_2$, and the structure under consideration against RhB under the same conditions. They found that $TiO_2$/$MoS_2$ heterostructure completely decomposes RhB in 20 min while pure $MoS_2$ and $TiO_2$ can degrade only 86.9% and 35.3% correspondingly. To improve the photocatalysis activity of $MoS_2$, researchers developed a $TiO_2$/g-$C_3N_4$/$MoS_2$ composite using a liquid exfoliation technique and a solvothermal process [209]. Indeed, the obtained structure demonstrated better photocatalytic performance than $TiO_2$/g-$C_3N_4$, pure g-$C_3N_4$, and $TiO_2$. Improvement in the photocatalytic activity is referred to the enlarged spectral response and efficient photons utilization because of the obtained heterostructure between $TiO_2$ and g-$C_3N_4$/$MoS_2$.

One more way to improve the photocatalytic activity of $MoS_2$ is the use of noble metals. Noble metals lead to surface plasmon resonance that drastically improves optical absorption. Even though $MoS_2$ already demonstrates superior photocatalytic performance for pollutant decomposition, the use of $MoS_2$ compositions with different materials offers various advantages. For example, such composites exhibit smaller bandgap and *e*/*h* pair recombination, which additionally improves the photocatalytic activity against numerous bio and organic contaminants [210, 211–213]. Moreover, $MoS_2$ compound with graphene demonstrates quicker charge carriers separation resulting in higher MB degradation rates [211, 212]. The action of pollutant sweeping for dust particles of hydrophobic $TiO_2$/PVDF@$MoS_2$ core-shell heterostructured composite fibers is significantly reducing the maintenance costs [214]. Cauliflower-like $MoS_2$ nanoparticles synthesized on the surface of $TiO_2$/PVDF flexible fibers demonstrated excellent photocatalytic activity represented by complete color loss of RhB and MO solutions. In the same way, $MoS_2$ triple compound in the form of Pt/vertically aligned $MoS_2$/$TiO_2$ turned out to be more efficient than pure $TiO_2$ nanotube array in decomposing Rh6G under vis light exposure [215].

Other prospective materials for the creation of advanced photocatalytic fibers are carbon fibers. For example, $MoS_2/Bi_2S_3$/carbon fiber for water purification [216]. Implementation of carbon fibers contributes to an increase in surface area, improved cycling stability, increased light exploitation, and greater conductivity in comparison with materials' bulk counterparts. Heterojunction structures made from several different materials are useful for electronic structure tuning and band alignment of materials to improve the photocatalytic activity of the resulting compound. For instance, triple compound $MoS_2$/CdS/carbon fiber decomposes 97.3% of RhB and MB solutions in just 70 min [217]. Carbon fiber provides high recyclability, conductivity, and stable skeleton as well as improves electron transfer. Moreover, improvement in photocatalytic activity with the usage of carbon fibers also refers to the higher absorption efficiency caused by huge specific surface area and adjusted band alignment between CdS and $MoS_2$.

Functionalized CNTs can also be used as effective photocatalysts for contaminants removal [218]. So, MB and MO can be efficiently removed from the water with the help of oxidized MWCNTs [219, 220]. A MWCNTs/carrageenan/$Fe_3O_4$ compound is an efficient photocatalyst for crystal violet decomposition [221]. Novel nanocomposites are also useful for the functionalization of CNTs to improve their ability to adsorb cationic dyes. For instance, the adsorption of amide black was significantly improved with the help of the MWCNT–COOH–cysteamine compounds [222]. As a result, the obtained composite demonstrated an adsorption capacity of 131 mg/g, while for MWCNT–COOH it was 90 mg/g [222]. The CNT composite adsorption capacity can be reduced drastically due to competition between a few types of contaminants in a solution at the same time [223]. Nevertheless, the initial concentration of pollutants in a solution did not have any considerable impact on the CNT's degradation capacity [224]. It means that the CNT's surface tuning and functionalization can improve their selectivity in pollutant decomposition.

To decompose blue 29 dye researchers used oxidized SWCNTs with huge specific surface area and found that oxidized SWCNTs' adsorption capacity is 496 mg/g [225]. The increment in functional groups containing oxygen on the CNTs surface leads to a decay in natural organic matters due to the $\pi - \pi$ interaction decline caused by higher electrostatic repulsion [226]. Identical results were demonstrated in the case of pH increasing [226]. Organic pollutants can be absorbed by $\pi - \pi$ interactions that appear between the CNT surface and 1-naphthol aromatic rings [227].

Research groups investigate CNTs for the decomposition of pesticides as well [228]. Oxidation of CNTs results in the enlargement of their surface area, while the pore size increase leads to improved diuron adsorption [228]. It was observed that pesticides like diquat dibromide, 2,4-dichlorophenoxyacetic, and 1-pyrenebutyric were decomposed better on semiconductor CNTs rather than on metallic CNTs [229]. This result originated from the lower electron density on the semiconductor CNTs surface that offers higher adsorption ability [229]. Moreover, CNTs are useful for the nanofiltration of pollutants from aqueous solutions [230–232]. The selectivity of these structures for filtration can be adjusted by attaching various functional groups to the CNT's surface [233].

## 9.4 Conclusion

Research in the development of photocatalysts for environmental purification is rapidly advancing. Transition metal chalcogenides and advanced fibers made from them or other nanomaterials have become the most actively studied materials for photocatalysis. In this chapter, we summarized the most actively studied photocatalysts in a pure and heterostructure form as well as recent progress in improving their photocatalytic activity. We discussed in detail the physical aspects and characteristics of various materials and their hybrid structures pointing out their advantages and drawbacks for developing photocatalysts. The most prospective form of a photocatalyst today is NF since it can be separated from the reaction media without any difficulties by filtration or decantation with the aim of recycling use. Moreover, it possesses a large surface area and adjustable band structure that results in better photocatalytic activity in comparison with other materials forms. As far as we know, there have been no comprehensive studies on this topic dedicated to modern materials for water purification.

## References

[1] Robinson T, Mcmullan G, Marchant R, Nigam P. Remediation of dyes in textile effluent: a critical review on current treatment technologies with a proposed alternative. Bioresour Technol. 2001;77:247–255.

[2] Pearce CI, Lloyd JR, Guthrie JT. The removal of colour from textile wastewater using whole bacterial cells: A review. Dye Pigment. 2003;58:179–196.

[3] Talarposhti AM, Donnelly T, Anderson GK. Colour removal from a simulated dye wastewater using a two–phase Anaerobic packed bed reactor. Water Res. 2001;35(2):425–432.

[4] Hanafiah MAKM, Ngah WSW, Zolkafly SH, Teong LC, Majid ZAA. Acid Blue adsorption on base treated Shoreadasyphylla sawdust: Kinetic, isotherm, thermodynamic and spectroscopic analysis. J Environ Sci. 2012;24:261–268.

[5] Mekasuwandumrong O, Pawinrat P, Praserthdam P, Panpranot J. Effects of synthesis conditions and annealing post-treatment on the photocatalytic activities of ZnO nanoparticles in the degradation of methylene blue dye. Chem Eng J. 2010;164:77–84.

[6] Gezici O, Kucukosmanoglu M, Ayar AJ. The adsorption behavior of crystal violet in functionalized sporopollenin-mediated column arrangements. Colloid Interface Sci. 2006;304:307–316.

[7] Prado AGS, Torres JD, Faria EA, Dias SCL. Comparative adsorption studies of indigo carmine dye on chitin and chitosan. J Colloid Interface Sci. 2004;277(1):43–47.

[8] Chiou MS, Li HY. Equilibrium and kinetic modeling of adsorption of reactive dye on cross-linked chitosan beads. J Hazard Mater. 2002;93(2):233–248.

[9] Prado AGS, Costa LL. Photocatalytic discolouration of malachite green dye by application of $TiO_2$ nanotubes. J Hazard Mater. 2009;169(1–3):297–301.

[10] Clifton JII, Leikin JB. Methylene Blue. Am J Ther. 2003;10:289–291.

[11] Koyuncu I. Influence of dyes, salts and auxiliary chemicals on the nanofiltration of reactive dye baths: Experimental observations and model verification. Desalination. 2003;154(1):79–88.

[12] Bergamini RBM, Azevedo EB, Araujo LR. Heterogeneous photocatalytic degradation of reactive dyes in aqueous $TiO_2$ suspensions: Decolorization kinetics. Chem Eng J. 2009;14:9215–9220.

[13] Forgacs E, Cserháti T, Oros G. Removal of synthetic dyes from wastewaters: A review. Environ Int. 2004;30:953–971.

[14] Nakagawa K, Namba A, Mukai SR, Tamon H, Ariyadejwanich PTW. Adsorption of phenol and reactive dye from aqueous solution on activated carbons derived from solid wastes. Water Research. 2004;38:1791–1798.

[15] Hassan AF, Abdel-Mohsen AM, Fouda MMG. Comparative study of calcium alginate, activated carbon, and their composite beads on methylene blue adsorption. Carbohydr Polym. 2014;102:192–198.

[16] Hajati S, Ghaedi M, Karimi F, Barazesh B, Sahraei RDA. Competitive adsorption of direct yellow and reactive orange on ZnS: Mn nanoparticles loaded on activated carbon as novel adsorbent. J Ind Eng Chem. 2014;20:564–571.

[17] Bensalah N, Alfaro MAQ, Martínez-Huitle CA. Electrochemical treatment of synthetic wastewaters containing Alphazurine A dye. Chem Eng J. 2009;149:348–352.

[18] Turhan K, Turgut Z. Decolorization of direct dye in textile wastewater by ozonization in a semi-batch bubble column reactor. Desalination. 2009;242:256–263.

[19] Gosetti F, Gianotti V, Angioi S, Polati S, Marengo E, Gennaro MC. Oxidative degradation of food dye E133 Brilliant Blue FCF: Liquid chromatography-electrospray mass spectrometry identification of the degradation pathway. J Chromatogr A. 2004;1054:379–387.

[20] Fessenden RJ, Fessenden JS. The biological properties of silicon compounds. Adv Drug Res. 1967;4:95–132.

[21] Alaton IA, AkmehmetBalcioglu I, Bahnemann DW. Advanced Oxidation of a Reactive Dyebath Effluent: Comparison of $O_3$, $H_2O_2$/UV-C and $TiO_2$/UV-A Processes. Water Res. 2002;36:1143–1154.

[22] Houas A, Lachheb H, Ksibi M, Elaloui E, Guillard C, Herrmann JM. Photocatalytic degradation pathway of methylene blue in water. Appl Catal B Environ. 2001;31:145–157.

[23] Perkins WS. Oxidative decolorization of dyes in aqueous medium. Text Chem Color Am Dyest Rep. 1999;1:33–37.

[24] Sharma P, Kaur H, Sharma M, Sahore V. A review on applicability of naturally available adsorbents for the removal of hazardous dyes from aqueous waste. Environ Monit Assess. 2011;183:151–195.

[25] Wang C, Shao C, Liu Y, Li X. Water – Dichloromethane interface controlled synthesis of hierarchical rutile $TiO_2$ superstructures and their photocatalytic properties. Inorg Chem. 2009;48:1105–1113.

[26] Balcha A, Yadav OP, Dey T. Photocatalytic degradation of methylene blue dye by zinc oxide nanoparticles obtained from precipitation and sol–gel methods. Environ Sci Pollut Res. 2016;23 (24):25485–25493.

[27] Vieira AP, Santana SAA, Bezerra CWB, et al. Kinetics and thermodynamics of textile dye adsorption from aqueous solutions using babassu coconut mesocarp. J Hazard Mater. 2009;166:1272–1278.

[28] Konicki W, Sibera D, Mijowska E, Lendzion-Bieluń Z, Narkiewicz U. Equilibrium and kinetic studies on acid dye Acid Red adsorption by magnetic $ZnFe_2O_4$ spinel ferrite nanoparticles. J Colloid Interface Sci. 2013;398:152–160.

[29] Rafatullah M, Sulaiman O, Hashim R, Ahmad A. Adsorption of methylene blue on low-cost adsorbents: A review. J Hazard Mater. 2010;177:70–80.

[30] Lee JW, Choi SP, Thiruvenkatachari R, Shim WG, Moon H. Evaluation of the performance of adsorption and coagulation processes for the maximum removal of reactive dyes. Dye Pigment. 2006;69:196–203.

[31] Lee JK, Gu JH, Kim MR, Chun HS. Incineration characteristics of dye sludge in a fluidized bed incinerator. J Chem Eng Jpn. 2001;34(2):171–175.

[32] García-Montaño J, Domenech X, García-Hortal JA, Torrades F, Peral J. The testing of several biological and chemical coupled treatments for Cibacron Red FN-R azo dye removal. J Hazard Mater. 2008;154(1–3):484–490.

[33] Chu W, Ma CW. Quantitative prediction of direct and indirect dye ozonation kinetics. Water Research. 2000;34(12):3153–3160.

[34] Prado AGS, Miranda BS, Jacintho GVM. Interaction of indigo carmine dye with silica modified with humic acids at solid/liquid interface. Surface Science. 2003;542(3):276–282.

[35] Shi B, Li G, Wang D, Feng C, Tang H. Removal of direct dyes by coagulation: The performance of preformed polymeric aluminum species. J Hazard Mater. 2007;143:567–574.

[36] Shao P, Tian J, Duan X, et al. Cobalt silicate hydroxide nanosheets in hierarchical hollow architecture with maximized cobalt active site for catalytic oxidation. Chem Eng J. 2019;359:79–87.

[37] Hao SM, Yu MY, Zhang YJ, Abdelkrim Y, Qu J. Hierarchical mesoporous cobalt silicate architectures as high-performance sulfate-radical-based advanced oxidization catalysts. Colloid Interface Sci. 2019;545:128–137.

[38] Zhu ZS, Qu J, Hao SM, Han S, Jia KL, Yu ZZ. A-$Fe_2O_3$ Nanodisk/Bacterial cellulose hybrid membranes as high-performance sulfate-radical-based visible light photocatalysts under stirring/flowing states. ACS Appl Mater Interfaces. 2018;10:30670–30679.

[39] Prado AGS, Faria EA, SouzaDe JR, Torres JD. Ammonium complex of niobium as a precursor for the hydrothermal preparation of cellulose acetate/$Nb_2O_5$ photocatalyst. J Mol Catal A Chem. 2005;237 (1–2):115–119.

[40] Torres JD, Faria EA, SouzaDe JR, Prado AGS. Preparation of photoactive chitosan–niobium (V) oxide composites for dye degradation. J Photochem Photobiol A: Chem. 2006;182(2):202–206.

[41] Fulekar MH, Pathak B, Kale RK. Environment and Sustainable Development. New Delhi, Springer; 2014.

[42] Zhu H, Jiang R, Fu Y, et al. Effective photocatalytic decolorization of methyl orange utilizing $TiO_2$/ZnO/chitosan nanocomposite films under simulated solar irradiation. Desalination. 2012;286:41–48.

[43] Shi R, Lin J, Wang Y, Xu J, Zhu Y. Visible-light photocatalytic degradation of $BiTaO_4$ photocatalyst and mechanism of photocorrosion suppression. J Phys Chem C. 2010;114:6472–6477.

[44] Tong H, Ouyang S, Bi Y, Umezawa N, Oshikiri M, Ye J. Nano-photocatalytic materials: Possibilities and challenges. Adv Mater. 2012;24:229–251.

[45] Chu D, Mo J, Peng Q, et al. Enhanced photocatalytic properties of $SnO_2$ nanocrystals with decreased size for ppb-level acetaldehyde decomposition. ChemCatChem2011. 3:371–377.

[46] Lv J, Gong W, Huang K, et al. Effect of annealing temperature on photocatalytic activity of ZnO thin films prepared by sol–gel method. Superlattices Microstruct. 2011;50:98–106.

[47] Wahab R, Hwang IH, Kim YS, et al. Non-hydrolytic synthesis and photo-catalytic studies of ZnO nanoparticles. Chem Eng J. 2011;175:450–457.

[48] Lee J, Gouma P. Sol–Gel Processed Oxide Photocatalysts. In: Sol–Gel Processing for Conventional and Alternative Energy. vol 2012, Springer; pp. 217–237.

[49] Byrne JA, Eggins BR, Brown NMD, Mckinney B, Rouse M. Immobilisation of $TiO_2$ Powder for the Treatment of Polluted Water. Appl Catal B Environ. 1998;17(1–2):25–36.

[50] Chen X, Mao SS. Titanium dioxide nanomaterials: Synthesis, properties, modifications and applications. Cheme Rev. 2007;107:2891–2959.

[51] Yu H, Irie H, Hashimoto K. Conduction band energy level control of titanium dioxide: toward an efficient visible light-sensitive photocatalyst. J Am Chem Soc. 2010;132(20):6898–6899.

[52] Khan R, Hassan M, Jang L, et al. Low-temperature synthesis of ZnO quantum dots for photocatalytic degradation of methyl orange dye under UV irradiation. Ceram Int. 2014;40(9):14827–14831.

[53] Makita M, Harata A. Photocatalytic decolorization of rhodamine B dye as a model of dissolved organic compounds: Influence of dissolved inorganic chloride salts in seawater of the Sea of Japan. Chem Eng Process. 2008;47(5):859–863.

[54] Saleh SM. Metal Oxide Nanomaterials as Photo-Catalyst for Dye Degradation. Res Dev Mater Sci. 2019;9:990–997.

[55] Ajmal A, Majeed I, Malik RN, Idriss H, Nadeem MA. Principles and mechanisms of photocatalytic dye degradation on $TiO_2$ based photocatalysts: A comparative overview. RSC Adv. 2014;4:37003–37026.

[56] Akpan UG, Hameed BH. Parameters affecting the photocatalytic degradation of dyes using $TiO_2$-based photocatalysts: A review. J Hazard Mater. 2009;170:520–529.

[57] Pawar M, Sendoğdular ST, Gouma P. A brief overview of $TiO_2$ photocatalyst for organic dye remediation: Case study of reaction mechanisms involved in Ce–$TiO_2$ photocatalysts system. J Nanomater. 2018;2018.

[58] Splendiani A, Sun L, Zhang Y, et al. Emerging photoluminescence in monolayer $MoS_2$. Nano Lett. 2010;10:1271–1275.

[59] Chang YC, Lin JC, Chen SY, Hung LY, Lin YR, Chen CY. Complex $SnO_2$ nanoparticles and nanosheets with enhanced visible-light photocatalytic activity. Mater Res Bull. 2018;100:429–433.

[60] Manjula N, Selvan G, Balu AR. Improved photodegradation activity of $SnO_2$ nanopowder against methyl orange dye through Ag doping. J Mater Sci: Mater Electron. 2018;29(5):3657–3664.

[61] Zheng H, Ou JZ, Strano MS, Kaner RB, Mitchell A, Kalantar-Zadeh K. Nanostructured tungsten oxide – properties, synthesis, and applications. Adv Funct Mater. 2011;21(12):2175–2196.

[62] Li Q, Li X, Wageh S, Al-Ghamdi AA, Yu J. CdS/graphene nanocomposite photocatalysts. Adv Energy Mater. 2015;5(14).

[63] Mayorov AS, Gorbachev RV, Morozov SV, et al. Micrometer-scale ballistic transport in encapsulated graphene at room temperature. Nano Lett. 2011;11(6):2396–2399.

[64] Singh P, Shandilya P, Raizada P, Sudhaik A, Rahmani-Sani A, Hosseini-Bandegharaei A. Review on various strategies for enhancing photocatalytic activity of graphene based nanocomposites for water purification. Arab J Chem. 2018;13(1):3498–3520.

[65] Moser J, Barreiro A, Bachtold A. Current-induced cleaning of graphene. Appl Phys Lett. 2007;91 (16):163513.

[66] Sudhaik A, Raizada P, Shandilya P, Jeong DY, Lim JH, Singh P. Review on fabrication of graphitic carbon nitride based efficient nanocomposites for photodegradation of aqueous phase organic pollutants. J Ind Eng Chem. 2018;67:28–51.

[67] Peng LG, Wang H, Liu J, et al. Fabrication of fibrous $BiVO_4/Bi_2S_3/MoS_2$ heterojunction and synergetic enhancement of photocatalytic activity towards pollutant degradation. J Solid State Chem. 2021;299.

[68] Zhang Y, Cao W, Zhu B, et al. Fabrication of $NH_2$-MIL-125(Ti) nanodots on carbon fiber/$MoS_2$-based weavable photocatalysts for boosting the adsorption and photocatalytic performance. J Colloid Interface Sci. 2022;611:706–717.

[69] Chen X, Xu X, Cui J, et al. Visible-light driven degradation of tetracycline hydrochloride and 2,4-dichlorophenol by film-like N-carbon@N-ZnO catalyst with three-dimensional interconnected nanofibrous structure. J Hazard Mater. 2020;392:122331.

[70] Kang S, Park D, Hwang J. Hierarchical ZnO nano-spines grown on a carbon fiber seed layer for efficient VOC removal and airborne virus and bacteria inactivation. J Hazard Mater. 2022;424:127262.

[71] Triquet T, Tendero C, Latapie L, Richard R, Andriantsiferana C. The Use of Composite $TiO_2$/Activated Carbon Fibers as a Photocatalyst in a Sequential Adsorption/Photocatalysis Process for the Elimination of Ciprofloxacin. Catal Res. 2022;2:1.

[72] Pascariu P, Cojocaru C, Samoila P, Olaru N, Bele A, Airinei A. Novel electrospun membranes based on PVDF fibers embedding lanthanide doped ZnO for adsorption and photocatalytic degradation of dye organic pollutants. Mater Res Bull. 2021;141:111376.

[73] Chen HJ, Yang YL, Zou XX, Shi XL, Chen ZG. Flexible hollow $TiO_2$@CMS/carbon-fiber van der Waals heterostructures for simulated-solar light photocatalysis and photoelectrocatalysis. J Mater Sci Technol. 2022;98:143–150.

[74] Sharma HK, Sharma SK, Vemula K, Koirala AR, Yadav HM, Singh BP. CNT facilitated interfacial charge transfer of $TiO_2$ nanocomposite for controlling the electron-hole recombination. Solid State Sci. 2021;112:106492.

[75] Odhiambo VO, Le Ba T, Kónya Z, et al. Preparation of $TiO_2$-$MoO_3$ composite nanofibers by water-based electrospinning process and their application in photocatalysis. Mater Sci Semicond Process. 2022;147.

[76] Ponnamma D, Elgawady Y, Nair SS, Hassan MK, Al-Maadeed MAA. Core-Shell Nanofibers of Polyvinyl Alcohol/Polylactic Acid Containing $TiO_2$ Nanotubes for Natural Sunlight Driven Photocatalysis. Macromol Mater Eng. 2022;307:1–11.

[77] Albiss B, Abu-Dalo M. Photocatalytic degradation of methylene blue using zinc oxide nanorods grown on activated carbon fibers. Sustain. 2021;13.

[78] Zhong N, Yuan J, Luo Y, et al. Intimately coupling photocatalysis with phenolics biodegradation and photosynthesis. Chem Eng J. 2021;425, 130666.

[79] Wang JR, Shen LF, Meng ZL, Pun EYB, Lin H. Crystal filament blended m-Bi($Er_3^+$-$Yb_3^+$)$VO_4$ fibers with temperature feedback and high-efficiency photocatalysis performance. Appl Surf Sci. 2021;556:149825.

[80] Li B, Kim IS, Dai S, Sarwar MN, Yang X. Heterogeneous Ag@ZnO nanorods decorated on polyacrylonitrile fiber membrane for enhancing the photocatalytic and antibacterial properties. Colloids Interface Sci Commun. 2021;45:100543.

[81] Zhu J, Jiang Z. Electrochemical Photocatalytic Degradation of Eriochrome Black T Dye Using Synthesized $TiO_2$@CNTs Nanofibers. Int J Electrochem Sci. 2021;16:1–13.

[82] Song Y, Ling L, Westerhoff P, Shang C. Evanescent waves modulate energy efficiency of photocatalysis within $TiO_2$ coated optical fibers illuminated using LEDs. Nat Commun. 2021;12:1–9.

[83] Molino A, Hamandi M, Grosjean R, et al. Coupling of photocatalysis and catalysis using an optical fiber textile for room temperature depollution. Chemosphere. 2022;297.

[84] De Ceglie C, Pal S, Murgolo S, Licciulli A, Mascolo G. Investigation of photocatalysis by mesoporous titanium dioxide supported on glass fibers as an integrated technology for water remediation. Catalysts. 2022;12.

[85] Loka C, Lee KS. Dewetted Silver Nanoparticle-Dispersed $WO_3$ Heterojunction Nanostructures on Glass Fibers for Efficient Visible-Light-Active Photocatalysis by Magnetron Sputtering. ACS Omega. 2022;7:1483–1493.

[86] Yuan J, Xiao C, Li L, et al. Coupled microalgal biofilm production and photocatalytic removal of chlorophenol using optical fibers. Environ Chem Lett. 2021;19:3973–3979.

[87] Okeil S, Yadav S, Bruns M, Zintler A, Molina-Luna L, Schneider JJ. Photothermal catalytic properties of layered titanium chalcogenide nanomaterials. Dalton Trans. 2020;49(4):1032–1047.

[88] Biele R, Flores E, Ares JR, et al. Strain-induced band gap engineering in layered $TiS_3$. Nano Res. 2018;11:225–232.

[89] Lu Q, Yu Y, Ma Q, Chen B, Zhang H. 2D Transition-Metal-Dichalcogenide-Nanosheet-Based Composites for Photocatalytic and Electrocatalytic Hydrogen Evolution Reactions. Adv Mater. 2016;28:1917–1933.

[90] Ganguly P, Harb M, Cao Z, et al. 2D Nanomaterials for Photocatalytic Hydrogen Production. ACS Energy Lett. 2019;4:1687–1709.

[91] Coleman N, Lotya M, O'neill A, et al. Two-Dimensional Nanosheets Produced by Liquid Exfoliation of Layered Materials. Science. 2011;331(6017):568–571.

[92] Xia DD, Gong F, Pei X, et al. Molybdenum and tungsten disulfides-based nanocomposite films for energy storage and conversion: A review. Chem Eng J. 2018;348:908–928.

[93] Asahi R, Morikawa T, Irie H, Ohwaki T. Nitrogen-Doped Titanium Dioxide as Visible-Light-Sensitive Photocatalyst: Designs, Developments, and Prospects. Cheme Rev. 2014;114:9824–9852.

[94] Alonso–Vante N. Chalcogenide Materials for Solar Energy Conversion. Springer; 2018. p. 226.

[95] Moan J, Brune D, Hellborg R, Persson B, Pääkkönen R. Radiation at home, outdoors and in the workplace. Oslo, Scandinavian Science Publisher; 2001. pp. 69–85.

[96] Kang J, Sahin H, Ozaydin HD, Senger RT, Peeters FM. $TiS_3$ nanoribbons: Width-independent band gap and strain-tunable electronic properties. Phys Rev B –Condens Matter Mater Phys. 2015;92.

[97] Kang J, Wang LW. Robust band gap of $TiS_3$ nanofilms. Phys Chem Chem Phys. 2016;18:14805–14809.

[98] Rasmussen FA, Thygesen KS. Computational 2D Materials Database: Electronic Structure of Transition-Metal Dichalcogenides and Oxides. J Phys Chem C. 2015;119:13169–13183.

[99] Chen X, Peng X, Jiang L, et al. Recent advances in titanium metal-organic frameworks and their derived materials: Features, fabrication, and photocatalytic applications. Chem Eng J. 2020;395:125080.

[100] Yao C, Yuan A, Zhang H, et al. Facile surface modification of textiles with photocatalytic carbon nitride nanosheets and the excellent performance for self-cleaning and degradation of gaseous formaldehyde. J Colloid Interface Sci. 2019;533:144–153.

[101] Ding K, Wang W, Yu D, Wang W, Gao P, Liu B. Facile formation of flexible Ag/AgCl/polydopamine/cotton fabric composite photocatalysts as an efficient visible-light photocatalysts. Appl Surf Sci. 2018;454:101–111.

[102] Dong G, Wang Y, Lei H, Tian G, Qi S, Wu D. Hierarchical mesoporous titania nanoshell encapsulated on polyimide nanofiber as flexible, highly reactive, energy saving and recyclable photocatalyst for water purification. J Clean Prod. 2020;253:120021.

[103] Liu B, Lin L, Yu D, et al. Construction of fiber-based $BiVO_4/SiO_2$/reduced graphene oxide (RGO) with efficient visible light photocatalytic activity. Cellulose. 2018;25:1089–1101.

[104] Yuan Y, Dong C, Gu J, et al. A Scalable Nickel-Cellulose Hybrid Metamaterial with Broadband Light Absorption for Efficient Solar Distillation. Adv Mater. 2020;32:1–8.

[105] Zhang Y, Duoerkun G, Shi Z, et al. Construction of $TiO_2/Ag_3PO_4$ nanojunctions on carbon fiber cloth for photocatalytically removing various organic pollutants in static or flowing wastewater. J Colloid Interface Sci. 2020;571:213–221.

[106] Zhang Y, Shi Z, Luo L, et al. Construction of titanium dioxide/cadmium sulfide heterojunction on carbon fibers as weavable photocatalyst for eliminating various contaminants. J Colloid Interface Sci. 2020;561:307–317.

[107] Al–Attabi R, Rodriguez–Andres J, Schütz JA, et al. Catalytic electrospun nano-composite membranes for virus capture and remediation. Sep Purif Technol. 2019;229:115806.

[108] Chen Y, Lu W, Shen H, et al. Solar-driven efficient degradation of emerging contaminants by g-C3N4-shielding polyester fiber/$TiO_2$ composites. Appl Catal B Environ. 2019;258:117960.

[109] Ahmed T, Ling Zhang H, Bin Xu H, Zhang Y. m-$BiVO_4$ hollow spheres coated on carbon fiber with superior reusability as photocatalyst. Colloids Surfaces A Physicochem Eng Asp. 2017;531:213–220.

[110] Dzinun H, Othman MHD, Ismail AF, Puteh MH, Rahman MA, Jaafar J. Morphological study of co-extruded dual-layer hollow fiber membranes incorporated with different $TiO_2$ loadings. J Memb Sci. 2015;479:123–131.

[111] Fan J, Yu D, Wang W, Liu B. The self-assembly and formation mechanism of regenerated cellulose films for photocatalytic degradation of C.I. Reactive blue 19. Cellulose. 2019;26:3955–3972.

[112] Ferreira VC, Goddard AJ, Monteiro OC. In situ synthesis and modification of cotton fibers with bismuthoxychloride and titanium dioxide nanoparticles for photocatalytic applications. J Photochem Photobiol A Chem. 2018;357:201–212.

[113] Perovic K, Dela Rosa FM, Kovacic M, et al. Recent Achievements in Development of $TiO_2$-Based Composite Photocatalytic Materials for Solar Driven Water Purification and Water Splitting. Materials. 2020;13(1338):1–44.

[114] Singh J, Tripathi N, Mohapatra S. Synthesis of Ag–$TiO_2$ hybrid nanoparticles with enhanced photocatalytic activity by a facile wet chemical method. Nano-Struct Nano-Objects. 2019;18:100266.

[115] Houas A, Lachheb H, Ksibi M, Elaloui E, Guillard C, Herrmann JM. Photocatalytic degradation pathway of methylene blue in water. Appl Catal: B. 2001;31:145–157.

[116] Vasudevan V, Thangavel S, Nallamuthu G, Kirubakaran K, Ramasubramanian PA, Venugopal G. Enhanced photocatalytic properties of nanostructured $WO_3$ semiconductor-photocatalyst prepared via hydrothermal method. J Nanosci Nanotechnol. 2018;18(5):3320–3328.

[117] Muñoz-Batista MJ, Kubacka A, Hungría AB, Fernández-García M Heterogeneous photocatalysis: Light-matter interaction and chemical effects in quantum efficiency calculations. J Catal. 2015;330:154–166.

[118] Mazierski P, Mikolajczyk A, Bajorowicz B, Malankowska A, Zaleska-Medynska A, Nadolna J. The role of lanthanides in $TiO_2$-based photocatalysis: A review. Appl Catal B Environ. 2018;233:301–317.

[119] Zhao X, Zhang G, Zhang Z. $TiO_2$-based catalysts for photocatalytic reduction of aqueous oxyanions: State-of-the-art and future prospects. Environ Int. 2020;136:105453.

[120] Chen D, Cheng Y, Zhou N, et al. Photocatalytic degradation of organic pollutants using $TiO_2$-based photocatalysts: A review. J Cleaner Prod. 2020;268:121725.

[121] Akpan UG, Hameed BH. Parameters affecting the photocatalytic degradation of dyes using $TiO_2$-based photocatalysts: A review. J Hazard Mater. 2009;170(2–3):520–529.

[122] Zhang Z, Wang CC, Zakaria R, Ying JY. Role of Particle Size in Nanocrystalline $TiO_2$-Based Photocatalysts. Phys Chem B. 1998;102(52):10871–10878.

[123] Md RN, Sze-Mun I, Jin-Chung L, Ichikawa S, Abdul RM. Photocatalytic Performance of ZnO/g-$C_3N_4$ for Removal of Phenol under Simulated Sunlight Irradiation. J Environ Eng. 2018;144(2):1–12.

[124] Taheri-Ledari R, Valadi K, Gharibi S, Maleki A. Synergistic photocatalytic effect between green LED light and $Fe_3O_4$/ZnO-modified natural pumice: A novel cleaner product for degradation of methylene blue. Mater Res Bull. 2020;130:1–10.

[125] Vaiano V, Matarangolo M, Murcia JJ, Rojas H, Navío JA, Hidalgo MC. Enhanced photocatalytic removal of phenol from aqueous solutions using ZnO modified with Ag. Appl Catal B: Environ. 2018;225:197–206.

[126] Pardeshi SK, Patil AB. A simple route for photocatalytic degradation of phenol in aqueous zinc oxide suspension using solar energy. Sol Energy. 2008;82(8):700–705.

[127] Mohamed RM, Barakat MA. Enhancement of photocatalytic activity of $ZnO=SiO_2$ by nanosized Pt for photocatalytic degradation of phenol in wastewater. Int J Photoenergy. 2012;2012:1–8.

[128] Lathasree S, Rao AN, SivaSankar B, Sadasivam V, Rengaraj K. Heterogeneous photocatalytic mineralisation of phenols in aqueous solutions. J Mol Catal A Chem. 2004;223(1–2):101–105.

[129] Feng X, Guo H, Patel K, Zhou H, Lou X. High performance, recoverable $Fe_3O_4$–ZnO nanoparticles for enhanced photocatalytic degradation of phenol. Chem Eng J. 2014;244:327–334.

[130] Wanga R, Xin JH, Yang Y, Liu H, Xu L, Hu J. The characteristics and photocatalytic activities of silver doped ZnOnanocrystallites. Appl Surf Sci. 2004;227(1–4):312–317.

[131] Shekofteh–Gohari M, Habibi–Yangjeh A. Fabrication of novel magnetically separable visible-light-driven photocatalysts through photosensitization of $Fe_3O_4$/ZnO with $CuWO_4$. J Ind Eng Chem. 2016;44:174–184.

[132] Shekofteh–Gohari M, Habibi–Yangjeh A. $Fe_3O_4$/ZnO/$CoWO_4$ nanocomposites: Novel magnetically separable visible-light-driven photocatalysts with enhanced activity in degradation of different dye pollutants. Ceram Int. 2017;43:3063–3071.

[133] Shekofteh–Gohari M, Habibi–Yangjeh A. Novel magnetically separable $Fe_3O_4$@ZnO/AgCl nanocomposites with highly enhanced photocatalytic activities under visible-light irradiation. Sep Purif Technol. 2015;147:194–202.

[134] Atla SB, Lin WR, Chien TC, et al. Fabrication of $Fe_3O_4$/ZnO magnetite core shell and its application in photocatalysis using sunlight. Mater Chem Phys. 2018;216:380–386.

[135] Susanto IK, Taufik A, Saleh R. The influence of ZnO components on the photocatalytic activity of $Fe_3O_4$–CuO–ZnO nanocomposites. Adv Mater Res. 2015;1123, 227–32.

[136] Thangavel S, Thangavel S, Raghavan N, Krishnamoorthy K, Venugopal G. Visible-light driven photocatalytic degradation of methylene–violet by rGO/$Fe_3O_4$/ ZnO ternary nanohybrid structures. J Alloys Compd. 2016;665:107–112.

[137] Zhang J, Xu LJ, Zhu ZQ, Liu QJ. Synthesis and properties of (Yb, N)–$TiO_2$ photocatalyst for degradation of methylene blue (MB) under visible light irradiation. Mater Res Bull. 2015;70:358–364.

[138] Hao M, Fa D, Qian L, Miao Y. $WO_3$@$Bi_2WO_6$/$NiWO_4$ nanocomposites with outstanding visible-light-driven photocatalysis for the degradation of organic dyes. J Nanosci Nanotechnol. 2018;18 (7):4788–4797.

[139] Liu SJ, Hou YF, Zheng SL, Zhang Y, Wang Y. One-dimensional hierarchical $Bi_2WO_6$ hollow tubes with porous walls: Synthesis and photocatalytic property. CrystEngComm. 2013;15:4124–4130.

[140] Huang Y, Kang S, Yang Y, et al. Facile synthesis of Bi/$Bi_2WO_6$ nanocomposite with enhanced photocatalytic activity under visible light. Appl Catal B Environ. 2016;196:89–99.

[141] Wang Y, Bai X, Pan C, He J, Zhu Y. Enhancement of photocatalytic activity of $Bi_2WO_6$ hybridized with graphite-like $C_3N_4$†. J Mater Chem. 2012;22:11568–11573.

[142] Han T, Wang X, Ma Y, Shao G, Dong X, Yu C. Mesoporous $Bi_2WO_6$ sheets synthesized via a sol–gel freeze-drying method with excellent photocatalytic performance. J Sol–Gel Sci Technol. 2017;82:101–108.

[143] Li C, Chen G, Sun J, et al. A thin empty-shell bismuth tungstate hierarchical structure constructed by acid sculpture effect and improved visible-light photocatalytic activity. New J Chem. 2015;39:1–7.

[144] Zhang J, Chen T, Lu H, et al. Hierarchical $Bi_2WO_6$ architectures decorated with Pd nanoparticles for enhanced visible-light-driven photocatalytic activities. Appl Surf Sci. 2017;404:282–290.

[145] Zhang Y, Shao C, Li X, et al. Controllable synthesis and enhanced visible photocatalytic degradation performances of $Bi_2WO_6$-carbon nanofibers heteroarchitectures. J Sol–Gel Sci Technol. 2014;70:149–158.

[146] Lu D, Wang H, Shen Q, Kondamareddy KK, Neena D. Highly Efficient visible-light-induced photoactivity of magnetically retrievable $Fe_3O_4$@$SiO_2$@$Bi_2WO_6$@g–$C_3N_4$ hierarchical microspheres for the degradation of organic pollutant and production of hydrogen. J Phys Chem Solids. 2017;106:76–81.

[147] Dong S, Ding X, Guo T, Yue X, Han X, Sun J. Self-assembled hollow sphere shaped $Bi_2WO_6$/RGO composites for efficient sunlight-driven photocatalytic degradation of organic pollutants. Chem Eng J. 2017;316:778–789.

[148] Li Y, Liu Y, Wang J, et al. Titanium alkoxide induced BiOBr–$Bi_2WO_6$ mesoporous nanosheet composites with much enhanced photocatalytic activity†. J Mater Chem A. 2013;1:7949–7956.

[149] Lima LVC, Rodriguez M, Freitas VAA, et al. Synergism between n-type $WO_3$ and p-type –FeOOH semiconductors: High interfacial contacts and enhanced photocatalysis. Appl Catal B Environ. 2015;165:579–588.

[150] Habibi-Yangjeh A, Shekofteh-Gohari M. Novel magnetic $Fe_3O_4$/ZnO/$NiWO_4$ nanocomposites: Enhanced visible-light photocatalytic performance through p–n heterojunctions. Sep Purif Technol. 2017;184:334–346.

[151] Uddin MT, Nicolas Y, Olivier C, et al. Nanostructured $SnO_2$–ZnO heterojunction photocatalysts showing enhanced photocatalytic activity for the degradation of organic dyes. Inorg Chem. 2012;51 (14):7764–7773.

[152] Wang W, Zeng Z, Zeng G, et al. Sulfur doped carbon quantum dots loaded hollow tubular g-$C_3N_4$ as novel photocatalyst for destruction of Escherichia coli and tetracycline degradation under visible light. Chem Eng J. 2019;378:122132.

[153] Chang W, Xu F, Mu X, Ji L, Ma G, Nie J. Fabrication of nanostructured hollow $TiO_2$ nanofibers with enhanced photocatalytic activity by coaxial electrospinning, Mater. Res Bull. 2013;48:2661–2668.

[154] An H, Ahn HJ. Fabrication of wrinkled Nb-doped $TiO_2$ nanofibres via electrospinning. Mater Lett. 2013;93:88–91.

[155] Liu Y, Yu H, Lv Z, et al. Simulated-sunlight-activated photocatalysis of Methylene Blue using cerium-doped $SiO_2/TiO_2$ nanostructured fibers. J Environ Sci (China). 2012;24:1867–1875.

[156] Li Y, Zhao H, Yang M. $TiO_2$ nanoparticles supported on PMMA nanofibers for photocatalytic degradation of methyl orange. J Colloid Interface Sci. 2017;508:500–507.

[157] Masoud M, SA NA. Influence of modified CNT–Ag nanocomposite addition on photocatalytic degradation of methyl orange by mesoporous $TiO_2$. Inorg Nano–Metal Chem. 2017;47:1168–1174.

[158] Guo N, Liang Y, Lan S, et al. Microscale hierarchical three-dimensional flowerlike $TiO_2$/PANI composite: Synthesis, characterization, and its remarkable photocatalytic activity on organic dyes under UV-light and sunlight irradiation. J Phys Chem C. 2014;118:18343–18355.

[159] Mortazavi-Derazkola S, Salavati-Niasari M, Mazhari MP, Khojasteh H, Hamadanian M, Bagheri S. Magnetically separable $Fe_3O_4@SiO_2@TiO_2$ nanostructures supported by neodymium(III): fabrication and enhanced photocatalytic activity for degradation of organic pollution. J Mater Sci Mater Electron. 2017;28:14271–14281.

[160] Jafari H, Afshar S, Zabihi O, Naebe M. Enhanced photocatalytic activities of $TiO_2$–$SiO_2$ nanohybrids immobilized on cement-based materials for dye degradation. Res Chem Intermed. 2016;42:2963–2978.

[161] Radacsi N, Campos FD, Chisholm CRI, Giapis KP. Spontaneous formation of nanoparticles on electrospunnanofibres. Nat Commun. 2018;9:3–10.

[162] Jiang L, Huang Y, Liu T. Enhanced visible-light photocatalytic performance of electrospun carbon-doped $TiO_2$/halloysite nanotube hybrid nanofibers. J Colloid Interface Sci. 2015;439:62–68.

[163] Jung JY, Lee D, Lee YS. CNT-embedded hollow $TiO_2$ nanofibers with high adsorption and photocatalytic activity under UV irradiation. J Alloys Compd. 2015;622:651–656.

[164] Song M, Cao H, Zhu Y, et al. Electrochemical and photocatalytic properties of electrospun C/$TiO_2$ nanofibers. Chem Phys Lett. 2020;747:137355.

[165] Li X, Chen X, Niu H, et al. The synthesis of CdS/$TiO_2$ hetero-nanofibers with enhanced visible photocatalytic activity. J Colloid Interface Sci. 2015;452:89–97.

[166] Lee SS, Bai H, Liu Z, Sun DD. Novel-structured electrospun $TiO_2$/CuO composite nanofibers for high efficient photocatalytic cogeneration of clean water and energy from dye wastewater. Water Res. 2013;47:4059–4073.

[167] Park JY, Choi KI, Lee JH, Hwang CH, Choi DY, Lee JW. Fabrication and characterization of metal-doped $TiO_2$ nanofibers for photocatalytic reactions. Mater Lett. 2013;97:64–66.

[168] Park JY, Lee JH, Choi DY, Hwang CH, Lee JW. Influence of Fe doping on phase transformation and crystallite growth of electrospun $TiO_2$ nanofibers for photocatalytic reaction. Mater Lett. 2012;88:156–159.

[169] Wang T, Wei J, Shi H, et al. Preparation of electrospun Ag/$TiO_2$ nanotubes with enhanced photocatalytic activity based on water/oil phase separation. Phys E Low-Dimension Syst Nanostruct. 2017;86:103–110.

[170] Minchi L, Cao F, Xinni Z, Youqiang C. Xuhua L Photocatalytic activity of Ca–$TiO_2$ nanofibers with different concentrations of calcium. Chem Phys Lett. 2019;736.

[171] Khatun N, Anita P, Rajput D, et al. Anatase to rutile phase transition promoted by vanadium substitution in $TiO_2$: A structural, vibrational and optoelectronic study. Ceram Int. 2017;43:14128–14134.

[172] Rahimi N, Pax RA. Gray EMA Review of functional titanium oxides. I: $TiO_2$ and its modifications, Prog. Solid State Chem. 2016;44:86–105.

[173] Cao H, Du P, Song L, et al. Co-electrospinning fabrication and photocatalytic performance of $TiO_2$/$SiO_2$ core/sheath nanofibers with tunable sheath thickness, Mater. Res Bull. 2013;48:4673–4678.

[174] Cui L, Song Y, Wang F, Sheng Y. Zou H Electrospinning synthesis of $SiO_2$–$TiO_2$ hybrid nanofibers with large surface area and excellent photocatalytic activity. Appl Surf Sci. 2019;488:284–292.

[175] Hanaor DAH. Sorrell CC Review of the anatase to rutile phase transformation. J Mater Sci. 2011;46:855–874.

[176] Rafatullah M, Sulaiman O, Hashim R, Ahmad A. Adsorption of methylene blue on low-cost adsorbents: A review. J Hazard Mater. 2010;177:70–80.

[177] Lavanya T, Dutta M, Satheesh K. Graphene wrapped porous tubular rutile $TiO_2$ nanofibers with superior interfacial contact for highly efficient photocatalytic performance for water treatment, Sep. Purif Technol. 2016;168:284–293.

[178] Baruah A, Chaudhary V, Malik R, Tomer VK. Nanotechnology Based Solutions for Wastewater Treatment. vol 17, Elsevier Inc; 2018. pp. 337–368.

[179] Kakarndee S, Nanan S. SDS capped and PVA capped ZnO nanostructures with high photocatalytic performance toward photodegradation of reactive red (RR141) azo dye. J Environ Chem Eng. 2018;6:74–94.

[180] Sudha M, Senthilkumar S, Hariharan R, Suganthi A, Rajarajan M. Controlled reduction of the deleterious effects of photocatalytic activity of ZnO nanoparticles by PVA capping. J Sol–Gel Sci Technol. 2012;61:14–22.

[181] Hariharan R, Senthilkumar S, Suganthi A, Rajarajan M. Photodynamic action of curcumin derived polymer modified ZnO nanocomposites. Mater Res Bull. 2012;47:3090–3099.

[182] Lv D, Wang R, Tang G, et al. Ecofriendly electrospun membranes loaded with visible-light-responding nanoparticles for multifunctional usages: Highly efficient air filtration, dye scavenging, and bactericidal activity. ACS Appl Mater Interfaces. 2019;11:12880–12889.

[183] Hassan MS, Ali HE, Ali NM. Antibacterial activity of cotton fabrics treated with poly (Vinyl Alcohol)/ ZnO nanocomposites, photocatalyzed by UV irradiation. J Vinyl Addit Technol. 2017;23:E34–9.

[184] Sekar AD, Muthukumar H, Chandrasekaran NI, Matheswaran M. Photocatalytic degradation of naphthalene using calcined Fe–ZnO/ PVA nanofibers. Chemosphere. 2018;205:610–617.

[185] Akhil K, Jayakumar J, Gayathri G, Khan SS. Effect of various capping agents on photocatalytic, antibacterial and antibiofilm activities of ZnO nanoparticles. J Photochem Photobiol B Biol. 2016;160:32–42.

[186] Kumar S, Krishnakumar B, Ajfn S, Koh J. Bio-based (chitosan/PVA/ZnO) nanocomposites film: Thermally stable and photoluminescence material for removal of organic dye. Carbohydr Polym. 2019;205:559–564.

[187] Khumalo NP, Vilakati GD, Mhlanga SD, et al. Dual-functional ultrafiltration nano-enabled PSf/PVA membrane for the removal of Congo red dye. J Water Process Eng. 2019;31:1–8.

[188] Kim YC, Yang TY, Jeon NJ, et al. Engineering interface structures between lead halide perovskite and copper phthalocyanine for efficient and stable perovskite solar cells. Energy Environ Sci. 2017;10:2109–2116.

[189] Abdelwahab NA, Ghoneim AM. Photocatalytic activity of ZnO coated magnetic crosslinked chitosan/ polyvinyl alcohol microspheres,. Mater Sci Eng B Solid–State Mater Adv Technol. 2018;228:7–17.

[190] Ghayempour S, Montazer M. Ultrasound irradiation based in-situ synthesis of star-like Tragacanth gum/zinc oxide nanoparticles on cotton fabric,. Ultrason Sonochem. 2017;34:458–465.

[191] Chakrabarti S, Banerjee P. Preparation and characterization of multifunctional cotton fabric by coating with sonochemically synthesized zinc oxide nanoparticle-flakes and a novel approach to monitor its self-cleaning property. J Text Inst. 2015;106:963–969.

[192] Noman MT, Petru M. Effect of sonication and Nano $TiO_2$ on thermophysiological comfort properties of woven fabrics. ACS Omega. 2020;5:11481–11490.

[193] Nair MG, Nirmala M, Rekha K, Anukaliani A. Structural, optical, photo catalytic and antibacterial activity of ZnO and Co doped ZnO nanoparticles. Mater Lett. 2011;65:1797–1800.

[194] Pantò F, Dahrouch Z, Saha A, Patanè S, Santangelo S, Triolo C. Photocatalytic degradation of methylene blue dye by porous zinc oxide nanofibers prepared via electrospinning: When defects become merits. Appl Surf Sci. 2021;557:1–9.

[195] Wang Y, Hao X, Wang Z, Dong M, Cui L. Facile fabrication of $Mn_2^+$-doped ZnO photocatalysts by electrospinning. R Soc Open Sci. 2020;7:191050.

[196] Lin D, Wu H, Zhang R, Zhang W, Panw W. Facile synthesis of heterostructured ZnO–ZnS nanocables and enhanced photocatalytic activity. J Am Ceram Soc. 2010;93:3384–3389.

[197] Pant B, Ojha GP, Kuk YS, Kwon OH, Wan Park Y, Park M. Synthesis and characterization of ZnO–$TiO_2$/carbon fiber composite with enhanced photocatalytic properties. Nanomaterials. 2020;10:1–12.

[198] Sabzehmeidani MM, Karimi H, Ghaedi M, Avargani VM. Construction of efficient and stable ternary $ZnFe_2O_4$/Ag/AgBr Z-scheme photocatalyst based on $ZnFe_2O_4$ nanofibers under LED visible light,. Mater Res Bull. 2021;143:111449.

[199] Wang M, Cui L, Li S, et al. Facile fabrication hybrids of $TiO_2$@ZnO tubes with enhanced photocatalytic properties. RSC Adv. 2016;6:58452–58457.

[200] Khodami Z, Nezamzadeh-Ejhieh A. Investigation of photocatalytic effect of ZnO–$SnO_2$/nano clinoptilolite system in the photodegradation of aqueous mixture of 4-methylbenzoic acid/2-chloro-5-nitrobenzoic acid. J Mol Catal A Chem. 2015;409:59–68.

[201] Wang Z, Huang B, Dai Y, et al. Highly photocatalytic ZnO/$In_2O_3$ heteronanostructures synthesized by a coprecipitation method. J Phys Chem C. 2009;113:4612–4617.

[202] Tan YH, Yu K, Li JZ, Fu H, Zhu ZQ. $MoS_2$@ZnO nano-heterojunctions with enhanced photocatalysis and field emission properties. J Appl Phys. 2014;116:064305.

[203] Habibi MH, Rahmati MH. The effect of operational parameters on the photocatalytic degradation of Congo red organic dye using ZnO–CdS core-shell nano-structure coated on glass by doctor blade method. Spectrochim Acta – Part A Mol Biomol Spectrosc. 2015;137:160–164.

[204] Nandi P, Das D. Journal of Physics and Chemistry of Solids ZnO-$Cu_xO$ heterostructure photocatalyst for efficient dye degradation. J Phys Chem Solids. 2020;143:109463.

[205] Yang Y, Wu Z, Yang R, et al. Insights into the mechanism of enhanced photocatalytic dye degradation and antibacterial activity over ternary ZnO/ZnSe/$MoSe_2$ photocatalysts under visible light irradiation. Appl Surf Sci. 2021;539:148220.

[206] Taddesse AM, Alemu M, Kebede T. Enhanced photocatalytic activity of p-n-n heterojunctions ternary composite $Cu_2O$/ZnO/$Ag_3PO_4$ under visible light irradiation. J Environ Chem Eng. 2020;8:104356.

[207] Hu X, Zhao H, Tian J, Gao J, Li Y, Cui H. Synthesis of few-layer $MoS_2$ nanosheets-coated $TiO_2$ nanosheets on graphite fibers for enhanced photocatalytic properties,. Sol Energy Mater Sol Cells. 2017;172:108–116.

[208] Zhou W, Yin Z, Du Y, et al. Synthesis of few-layer $MoS_2$ nanosheet-coated $TiO_2$ nanobelt heterostructures for enhanced photocatalytic activities. Small. 2013;9:140–147.

[209] Zhang W, Xiao X, Li Y, Zeng X, Zheng L, Wan C. Liquid-exfoliation of layered $MoS_2$ for enhancing photocatalytic activity of $TiO_2$/g-$C_3N_4$ photocatalyst and DFT study. Appl Surf Sci. 2016;389:496–506.

[210] Islam MA, Church J, Han C, et al. Noble metal-coated $MoS_2$ nanofilms with vertically-aligned 2D layers for visible light-driven photocatalytic degradation of emerging water contaminants. Sci Rep. 2017;7:1–10.

[211] Ding Y, Zhou Y, Nie W, Chen P. $MoS_2$-GO nanocomposites synthesized via a hydrothermal hydrogel method for solar light photocatalytic degradation of methylene blue,. Appl Surf Sci. 2015;357:1606–1612.

[212] Zhao Y, Zhang X, Wang C, et al. The synthesis of hierarchical nanostructured $MoS_2$/Graphene composites with enhanced visible-light photo-degradation property. Appl Surf Sci. 2017;412:207–213.

[213] Cai Z, Dwivedi AD, Lee WN, et al. Application of nanotechnologies for removing pharmaceutically active compounds from water: Development and future trends. Environ Sci Nano. 2018;5:27–47.

[214] Zhang ZG, Liu H, Wang XX, et al. One-step low temperature hydrothermal synthesis of flexible $TiO_2$/PVDF@$MoS_2$ core-shell heterostructured fibers for visible-light-driven photocatalysis and self-cleaning. Nanomaterials. 2019;9:1–22.

[215] Dong J, Huang J, Wang A, et al. Vertically-aligned Pt-decorated $MoS_2$ nanosheets coated on $TiO_2$ nanotube arrays enable high-efficiency solar-light energy utilization for photocatalysis and self-cleaning SERS devices. Nano Energy. 2020;71:104579.

[216] Luo L, Shen X, Song L, et al. $MoS_2$/$Bi_2S_3$ heterojunctions-decorated carbon-fiber cloth as flexible and filter-membrane-shaped photocatalyst for the efficient degradation of flowing wastewater. J Alloys Compd. 2019;779:599–608.

[217] Zhang Y, Luo L, Shi Z, et al. Synthesis of $MoS_2$/CdS Heterostructures on Carbon-Fiber Cloth as Filter-Membrane-Shaped Photocatalyst for Purifying the Flowing Wastewater under Visible-Light Illumination. ChemCatChem. 2019;11:2855–2863.

[218] Zare K, Gupta VK, Moradi O, et al. A comparative study on the basis of adsorption capacity between CNTs and activated carbon as adsorbents for removal of noxious synthetic dyes: a review. J Nanostructure Chem. 2015;5:227–236.

[219] Ghaedi M, Khajehsharifi H, Yadkuri AH, Roosta M, Asghari A. Oxidized multiwalled carbon nanotubes as efficient adsorbent for bromothymol blue. Toxicol Environ Chem. 2012;94:873–883.

[220] Mahmoodian H, Moradi O, Shariatzadeha B, et al. Enhanced removal of methyl orange from aqueous solutions by poly HEMA-chitosan-MWCNT nano-composite. J Mol Liq. 2015;202:189–198.

[221] Duman O, Tunç S, Polat TG, Bozoğlan BKI. Synthesis of magnetic oxidized multiwalled carbon nanotube-κ-carrageenan-$Fe_3O_4$ nanocomposite adsorbent and its application in cationic Methylene Blue dye adsorption. Carbohydr Polym. 2016;147:79–88.

[222] Sadegh H, Zare K, Maazinejad B, et al. Synthesis of MWCNT-COOH-Cysteamine composite and its application for dye removal. J Mol Liq. 2016;215:221–228.

[223] Wang Y, Huang H, Wei X. Influence of wastewater precoagulation on adsorptive filtration of pharmaceutical and personal care products by carbon nanotube membranes. Chem Eng J. 2018;333:66–75.

[224] Ihsanullah FA, Al-Khaldi B, Abu-Sharkh AM, et al. Effect of acid modification on adsorption of hexavalent chromium (Cr(VI)) from aqueous solution by activated carbon and carbon nanotubes. Desalin Water Treat. 2016;57:7232–7244.

[225] Jahangiri-Rad M, Nadafi K, Mesdaghinia A, Nabizadeh R, Younesian M, Rafiee M. Sequential study on reactive blue 29 dye removal from aqueous solution by peroxy acid and single wall carbon nanotubes: Experiment and theory. J Environ Heal Sci Eng. 2013;10:1–8.

[226] Engel M, Chefetz B. Adsorption and desorption of dissolved organic matter by carbon nanotubes: Effects of solution chemistry. Environ Pollut. 2016;213:90–98.

[227] Yang S, Guo Z, Sheng G, Wang X. Investigation of the sequestration mechanisms of Cd(II) and 1-naphthol on discharged multi-walled carbon nanotubes in aqueous environment. Sci Total Environ. 2012;420:214–221.

[228] Sarkar C, Chowdhuri AR, Kumar A, et al. One pot synthesis of carbon dots decorated carboxymethyl cellulose- hydroxyapatite nanocomposite for drug delivery, tissue engineering and $Fe_3^+$ ion sensing, Carbohydr. Polym. 2018;181:710–718.

[229] Rocha JDR, Rogers RE, Dichiara AB, Capasse RC. Emerging investigators series: Highly effective adsorption of organic aromatic molecules from aqueous environments by electronically sorted single-walled carbon nanotubes. Environ Sci. 2017;3:203–212.

[230] Jin S, Fallgren PH, Morris JM, Chen Q. Removal of bacteria and viruses from waters using layered double hydroxide nanocomposites. Sci Technol Adv Mater. 2007;8:67–70.

[231] Srivastava A, Srivastava ON, Talapatra S, Vajtai R, Ajayan PM. Carbon nanotube filters. Nat Mater. 2004;3:610–614.

[232] Tahaikt M, El Habbani R, Ait Haddou A, et al. Fluoride removal from groundwater by nanofiltration. Desalination. 2007;212:46–53.

[233] Fornasiero F, Hyung GP, Holt JK, et al. Ion exclusion by sub-2-nm carbon nanotube pores. Proc Natl Acad Sci USA. 2008;105:17250–17255.

[234] Moradi O. Adsorption behavior of Basic Red 46 by single-walled carbon nanotubes surfaces. Fullerenes Nanotub Carbon Nanostruct. 2013;21:286–301.

[235] Yang S, Wang L, Zhang X, Yang W, Song G. Enhanced adsorption of Congo red dye by functionalized carbon nanotube/mixed metal oxides nanocomposites derived from layered double hydroxide precursor. Chem Eng J. 2015;275:315–321.

[236] Konicki W, Pełech I, Mijowska E, Jasińska I. Adsorption of anionic dye Direct Red 23 onto magnetic multi-walled carbon nanotubes-$Fe_3C$ nanocomposite: Kinetics, equilibrium and thermodynamics. Chem Eng J. 2012;210:87–95.

[237] Setareh Derakhshan M, Moradi O. The study of thermodynamics and kinetics methyl orange and malachite green by SWCNTs, SWCNT-COOH and SWCNT-$NH_2$ as adsorbents from aqueous solution. J Ind Eng Chem. 2014;20:3186–3194.

[238] Zhao D, Zhang W, Chen C, Wang X. Adsorption of Methyl Orange Dye Onto Multiwalled Carbon Nanotubes. Procedia Environ Sci. 2013;18:890–895.

[239] Ahmad A, Razali MH, Mamat M, Mehamod FSB, Anuar Mat Amin K. Adsorption of methyl orange by synthesized and functionalized-CNTs with 3-aminopropyltriethoxysilane loaded $TiO_2$ nanocomposites. Chemosphere. 2017;168:474–482.

[240] Robati D, Mirza B, Ghazisaeidi R, et al. Adsorption behavior of methylene blue dye on nanocomposite multi-walled carbon nanotube functionalized thiol (MWCNT-SH) as new adsorbent. J Mol Liq. 2016;216:830–835.

[241] Shih MW, Chin CJM, YL Y. The role of oxygen-containing groups on the adsorption of bisphenol-A on multi-walled carbon nanotube modified by $HNO_3$ and KOH, Process Saf. Environ Prot. 2017;112:308–314.

[242] Kuo CY. Comparison with as-grown and microwave modified carbon nanotubes to removal aqueous bisphenol A. Desalination. 2009;249:976–982.

[243] Liao Q, Sun J, Gao L. Adsorption of chlorophenols by multi-walled carbon nanotubes treated with $HNO_3$ and $NH_3$. Carbon N Y. 2008;46:553–555.

[244] Mubarak NM, Sazila N, Nizamuddin S, Abdullah EC, Sahu JN. Adsorptive Removal of Phenol from Aqueous Solution by Using Carbon Nanotubes and Magnetic BioChar. NanoWorld J. 2017;03:32–37.

[245] Yao YX, Li HB, Liu JY, Tan XL, Yu JG, Peng ZG. Removal and adsorption of p-nitrophenol from aqueous solutions using carbon nanotubes and their composites. J Nanomater. 2014;2014:1–10.

[246] Diaz-Flores PE, López-Urías F, Terrones M, Rangel-Mendez JR. Simultaneous adsorption of $Cd_2^+$ and phenol on modified N-doped carbon nanotubes: Experimental and DFT studies. J Colloid Interface Sci. 2009;334:124–131.

[247] Tóth A, Törocsik A, Tombácz E, László K. Competitive adsorption of phenol and 3-chlorophenol on purified MWCNTs. J Colloid Interface Sci. 2012;387:244–249.

[248] Arasteh R, Masoumi M, Rashidi AM, Moradi L, Samimi V, Mostafavi ST. Adsorption of 2-nitrophenol by multi-wall carbon nanotubes from aqueous solutions. Appl Surf Sci. 2010;256:4447–4455.

Manash Protim Mudoi*, Vidushi Singh, Harroop Kaur,
Asmita Choudhary

# Chapter 10
# Advanced fiber materials in textile

**Abstract:** Advanced fiber materials have some technological advancements in their properties. Social and industrial needs have enhanced the growth of advanced fiber materials significantly. These smart textiles have special functions such as thermal insulation, high elasticity, radiation and flame retardant, and antistatic properties. Advanced fiber textiles find use in the water treatment industry. The filter medium of filtration systems comprises double-layered satin fabrics covered by raised microfibers. The bioreaction system can use many fiber-mass blocks to sustain the microorganisms. Unlike conventional filtration systems, these systems are more compact, easy to handle, and yield a much higher quality of water. They are also used in air purification systems using air filters and bag filters. Due to their enhanced flexibility, lighter weight, and flame and heat retardant properties, smart textiles can be used in car interiors. They are employed as hollow membrane fibers for artificial kidneys, artificial lungs, and other treatments in the medical industry. The following chapter discusses the characteristics of smart textiles and their applications in various fields.

**Keywords:** Smart textile, advanced fiber, protective textile, automotive, healthcare, purification, agriculture

## 10.1 Introduction

The textile industry is gradually shifting from conventional textiles to complex and intelligent textiles. Though there will be no decline in the use of traditional textiles in the future, industries like construction, protective textiles, wound management, automobiles, and environment preservation will need more advanced technical textiles. The development of new textiles can replace plastics and metals in many applications with cheaper, lighter, and stronger properties. The use of advanced technical textiles is growing in drive belts, filters, hydraulic hoses, composite materials, and insulations

---

***Corresponding author: Manash Protim Mudoi,** Department of Chemical Engineering, Indian Institute of Technology, Roorkee 247667, Uttarakhand, India; Department of Chemical Engineering, University of Petroleum and Energy Studies, Dehradun 248007, Uttarakhand, India, e-mails: mp_mudoi@ch.iitr.ac.in, mpmudoi@ddn.upes.ac.in

**Vidushi Singh, Harroop Kaur, Asmita Choudhary,** Department of Chemical Engineering, University of Petroleum and Energy Studies, Dehradun 248007, Uttarakhand, India

https://doi.org/10.1515/9783110992892-010

[1]. Advanced technical (smart) textiles can provide excellent thermal, mechanical, electrical, and a durable performance [2]. They have a high specific area and can be easily transformed into woven and nonwoven textile structures; hence can find extensive application areas [3].

Moreover, smart textiles have a significantly more comprehensive structural range than apparel textiles. Smart textiles are growing applications in the protective textile industry [4]. Protective textiles are fibrous materials capable of performing their function under hazardous conditions. The smart textiles for such applications must possess high operating temperature, heat resistance, flame retardance capability, chemical resistance, and tensile strength. Advanced technical textiles also find a broad spectrum of applications in the healthcare industry. A bandage can be transformed into an active healing component by using technical textiles. For example, a dressing prepared with seaweed-derived alginate fibers can enhance the healing process of a wound [5]. The healing process can be termed “moist healing,” which works by forming a water-soluble gel. Apart from bandages, these textiles also find extracorporeal uses in blood dialysis, intracorporeal uses in drug delivery fabric, photodynamic therapies, and body implants, prostheses, and stents [6]. Smart textiles are also nontoxic, hemostatic, bacteriostatic, fungi-static, breathable, biocompatible, and nonallergic [7]. These essential qualities have significantly promoted the need for smart textiles in wound management in the healthcare industry. In addition, properties like insect repellence, resistance to flame, water, stain, abrasion, UV protection, and odor absorption have advanced their growth in relevant markets, covering common consumer goods and specialized applications [2]. The various application areas of technical textiles are shown in Figure 10.1.

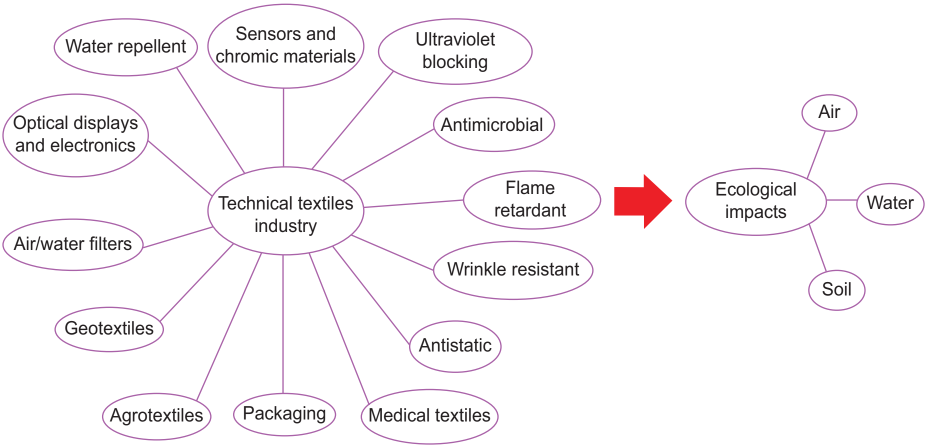
Water repellent
Sensors and chromic materials
Ultraviolet blocking
Optical displays and electronics
Antimicrobial
Technical textiles industry
Flame retardant
Air/water filters
Wrinkle resistant
Geotextiles
Antistatic
Agrotextiles
Packaging
Medical textiles
Air
Ecological impacts
Water
Soil

**Figure 10.1:** Application areas of technical textile [13]. Open access.

This chapter gives a thorough understanding of the distinct characteristics of advanced fiber materials based on their end uses, elaborates on their wide range of applications, viz. in environmental matters, automobile industry, medical and hygiene, fire and safety, E-textiles, and delves into the detailed scope of the development of the smart textile industry due to their contribution toward the technological advancement of a country.

## 10.2 Characteristics

Textile fibers can be categorized mainly into four types: (1) natural fiber (silk, cotton, hemp); (2) regenerated fiber (rayon); (c) synthetic fiber (vinyl, nylon, acrylics, polyesters); and (d) inorganic fibers (glass, asbestos, aramid) [8]. The demand for the primary uses of these fibers in decoration, comfort, and safety application will not reduce in the future. In fact, the textile industry will grow in complexity, functionality, and applications due to the increasing regulatory requirements in construction, environment protection, and the demand for better living standards. Thus, technical textiles focus on multi-directed schemes and are an active research sector in innovating new textile products (composites and specialty fibers), functionalized textile materials and their processes, biotechnologies, and developing environmentally friendly bio-based textile materials. For a better possible performance, enhancement in the various functionality characteristics of fiber- and engineering-based textile materials, and in their properties such as flexibility, durability, strength–weight ratios, insulating properties and absorption, are required. For their application in diverse areas, enchantments of textile properties, such as antibacterial and antistatic behaviour, protection from UV, insect and stain, water repellence, odor absorption, and abrasion and flame resistance, are required. Therefore, the relevant market for specialized and ordinary applications is constantly growing due to the introduction of advanced technologies in nanotechnology, plasma technology, and micro-encapsulation [2].

## 10.3 Applications

The multi-faceted properties of advanced technical textiles allow them to be of practical use in various fields as shown in Figure 10.2.

### 10.3.1 Protective textiles

The most suitable testing for protective garments and other textiles that ought to be approved is determined by the consequent workplace hazards and the protection required. Specific workplaces like foundries and firefighting consistently require both heat and flame protection. Due to rapid development, the intrigue regarding protective

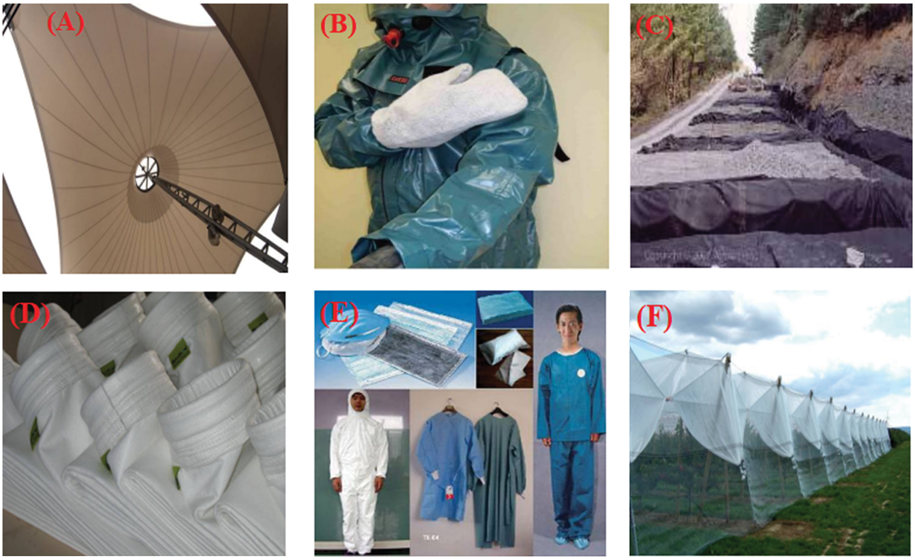

**Figure 10.2:** Technical textile usage in different fields (a) architecture, (b) personal protection, (c) geotextile, (d) filtration, (e) medical protection, and (f) agriculture [1]. Open access.

clothing has proliferated in the past 30 years. Increased utilization of fiber-blend textiles with enhanced properties like durability, comfort and heat retardance is the current area of research and interest. The structures of a fabric can be altered and manipulated. One such example is the introduction of spaces into the knit or woven structure of the fabric, which aids in lowering the overall mass and stiffness of the garment, while introducing air gaps for sufficient protection [9]. Various types of protective clothing are listed below:

#### 10.3.1.1 High-temperature protective textiles

The paramount concern in using thermal protective textiles in industries is the detrimental impact on workers' comfort. Due to the substantial material within their clothing, these protective textiles add to the wearer's thermal load. Moreover, either the breathability of the material or the capacity of water vapor diffusion is compromised to enhance protection from steam and hot water. This pronounces the need for a more high-performing fire-resistant fabric to develop thermal protective clothing. There are mainly two categories of fire-resistant fibers: inherently fire-resistant and chemically modified fiber.

In the case of chemically modified fibers, the fabrics are produced from natural or synthetic fibers, after which flame retardant finishes are applied to the fabrics. However, there also exist some synthetic fibers that can inherently resist fires by virtue of their chemical structure, and are thereby known as inherently fire-resistant [4]. For example, NXP or the Newtex Extreme Protective line, commonly utilized in firefighting and metal working, includes high-temperature protective clothing like gloves, proximity and fire entry suits, and aluminized clothing that are fabricated from other high-temperature fabrics. These utilize fabrics like aramid, Zetex, Zetex-Plus, and Z-Flex to withstand heat up to 1095 °C (2000°F), whilst providing the wearer with thermal insulation and comfort.

#### 10.3.1.2 Chemical protective textiles

Chemicals may severely damage the unprotected skin. Direct skin contact and contamination by chemicals can be prevented using protective clothing such as gloves, suits, boots, etc. Some tasks that may require advanced technical protective textiles include, working with toxic, corrosive chemicals, dust, noisy and hot environments, firefighting, welding, and rescue operation. Chemical protective clothing can provide a barrier to harmful chemicals, for example, breathable waterproof clothing used in agriculture and gas barrier clothing in military applications. These fabrics are either laminated with activated carbon or coated with nonpermeable material. The former has a significant advantage in breathability over the later. Table 10.1 discusses the advantages and disadvantages of some of the chemicals used to prepare PPE.

**Table 10.1:** Advantages and disadvantages of various chemical PPE.

| No. | Materials | Advantage | Disadvantage |
|---|---|---|---|
| 1. | Butyl Rubber | Offers good protection against compounds such as inorganic salts, ester, ketones, and the majority of alkalis and acids. | Not resistant to coal tars, oils, petroleum, or compounds that include aromatic hydrocarbons. |
| 2. | Natural rubber or latex | High tensile strength, strong temperature tolerance, and good resistance to acids and alcohols. | Moderately resistant to abrasion. |
| 3. | Neoprene | Have great resistance to aliphatic hydroxyl compounds, fluorinated heat, ozone, methanol, ethanol, and strong chain hydrocarbons. It is also resistant to aliphatic hydroxyl compounds, methanol, and ethylene glycol. | Not advised to utilize this with acetated, ketones, or strong oxidizing agents. |
| 4. | Nitrile | Saturated and unsaturated aliphatic hydrocarbons, alkali solutions, and saturated salt solutions essentially have no effect on nitrile. | Water negatively impacts it. |

**Table 10.1** (continued)

| No. | Materials | Advantage | Disadvantage |
|---|---|---|---|
| 5. | Polyvinyl Alcohol | Has strong chemical resistance to aromatic and chlorinated solvents and is extremely impermeable to gases. | |
| 6. | Viton | Petroleum-based goods, including oils, fuels, lubricants, aliphatic, aromatic, and chlorinated solvents, are particularly resistant to Viton. | |
| 7. | Polyethylene | Polyethylene offers exceptional resistance to cuts and rips and has great abrasion properties. | |

### 10.3.1.3 Ultraviolet protection finish

Depleting the stratospheric ozone layer is one of the apparent causes of growing skin cancer. Ozone can absorb UV rays excellently. Every one per cent decrease in the ozone concentration may increase the rate of skin cancer by approximately two to five per cent. Some fibers, such as linen, viscos rayon, and cotton do not provide good resistance against UV ray exposure. The structure of a technical textile and UV radiation is shown in Figure 10.3.

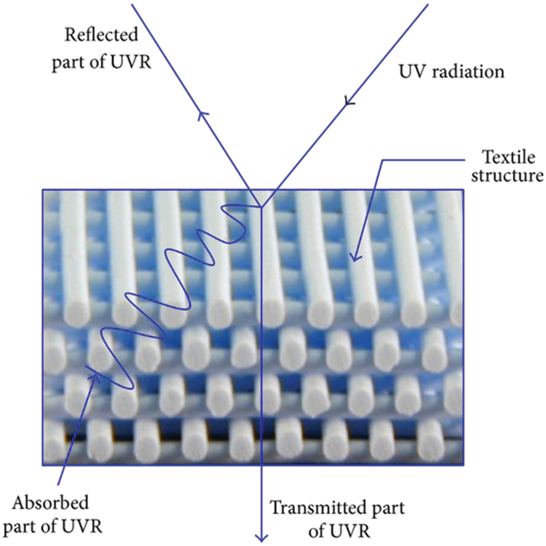

**Figure 10.3:** UV ray protection by technical textile [16].

Bleached cotton and bleached silk are transparent to UV radiation due to the removal of lignans and natural pigments. However, fibers with high porosity, like wool fiber and wool muslin, have excellent UV protection properties. Another textile material, polyester, offers less effective protection against UV radiation; however, this drawback can be solved by adding titanium dioxide, which can block the UV radiation. Therefore, polyester blends with other fibers can provide better UV protection [10].

#### 10.3.1.4 High visibility textiles

High visibility vests are made of fluorescent hues and intelligent materials to make the laborer effectively visible in all conditions. They differentiate laborers from people on foot and, at times, also distinguish which organization they work for. High visibility vest lowers the risk of fatalities and accidents in busy environments such as marshalling yards, industrial premises, and construction areas. Health and Safety regulations strictly advise using PPE (personal protective equipment) or high visibility workwear. A minimum of a reflective over vests or jackets is required in hazardous areas [4].

### 10.3.2 Healthcare industry

The main areas of utilization of advanced technical textiles in the healthcare industry are as follows:

#### 10.3.2.1 Wound management

The most advanced use of smart textiles in the treatment of wounds is seen in the use of plasma coatings used to improve the surface behaviour of textiles, like hydrophobic (water repelling) or hydrophilic (water absorbing) properties, depending on the specific requirement of the wound [11].

#### 10.3.2.2 Monitoring

Traditionally, body monitoring is extensively practiced via gel-based sensors, which are unwieldy, intrusive, and difficult to use in the case of a moving patient. However, monitoring is possible with the help of electronic technical textiles. HealthVest system of SmartLife (A British company) develops a technology to measure the body fluid flow, respiratory rate, ECG morphology, and heart rate by using dry sensors built into a garment. Researchers are trying to develop more advanced monitoring fabrics with a wearable electronic hub that can be programmed using wireless technology to monitor the various body functions[5].

### 10.3.2.3 Intracorporeal and extracorporeal treatments

One of the most established uses of intracorporeal textiles is implants. Various degenerative conditions are commonly treated by textiles, like polyethylene for artificial joints, polymethyl methacrylate for artificial corneas, and many more. The problem of incompatibility and rejection of the implant by the human body has been solved mainly by synthesizing biocompatible materials. However, deterioration of the functionality and strength of the implant due to the human body's hostile environment remains an issue that needs further research [12]. Advanced technical textiles also find application in extracorporeal treatments. This innovative technique is crucial for successfully using these machines since these filters can mimic the functions of membranes within human organs. For example, cellophane replicates the kidney's function by removing waste materials [12]. Technical textiles will drive the future of healthcare, as it is now possible to produce a greater variety of artificial body organs.

### 10.3.2.4 Innovative textiles for personalized healthcare

Smart textiles' ability to diagnose and treat ailments depends on various functionalized materials. Traditional smart textile electrodes have been made of metals (such as Ag, Cu, Ti, Au, and Ni), conducting polymers (such as poly (3, 4-ethylenedioxythiophene) polystyrene sulfonate), and certain carbon-based compounds (for example, carbon nanotubes and graphene). Smart textiles can communicate with the outside world, and semiconducting or conducting functional materials have been used to achieve this function.

Many manufacturing techniques have been created, but the most common ones are spinning, coating, printing, and thermal drawing. Spinning has been evaluated for large-scale manufacture and can be used to create standalone functional fibers or to functionalize conventional textile/fiber substrates. Continuous fibers of different diameters can be produced in parallel from one or more functional materials by adjusting the initial production procedure. Several different functional materials have been used to manufacture smart textiles, including wet spinning, dry spinning, melt spinning, and electrospinning.

Fiber architectures can offer adaptable, breathable clothing, resistant to wear and tear, and they can be materially integrated. Traditional fibers typically offer these qualities when used alone, or in combination, or in various fabric forms, or in weaving architecture design.

Access to specific therapeutic options that take patient safety margins and personal life aspects into consideration is another aspect of personalized healthcare that goes beyond diagnosis. Smart textiles with built-in therapeutic features can interact with the body to provide ongoing and one-time therapeutic benefits, tailoring treatments to the patient's changing health profile. Although they are still in the early stages of development, smart textiles for individualized therapy are anticipated to provide an alternative to the conventional one-size-fits-all therapeutic techniques.

Future development of smart textiles will necessitate crucial aspects being taken into account by both research and industry. Academic research should focus on performance standardization, functional integration, dependability and stability, and material innovation. This should involve production, clinical integration, value chain building, and product standardization in the business world.

## 10.3.3 Automobile sector

Materials used for automotive applications are selected based on "performance against cost." Steel cord is widely used as reinforcement in tire-belt plies of passenger cars due to its highest tensile modulus per cost among other available materials. However, if the requirement arises to manufacture a lightweight car, the material selection will be based on the "specific tensile modulus/cost" criteria. In that case, high-performance fiber like polyketone could be an alternative [3]. Various automobile parts like driving belts, seat belts, tires, hoses, tubes, hoses, airbags, floor coverings, seats, roof trims, noise control materials, bumper beams, and exterior body panels are manufactured with reinforcement by technical textiles.

### 10.3.3.1 Tire cords

Tire cords need materials with higher heat resistance and high modulus properties. PET multifilament is widely used in tire cords since they meet the above requirements. However, the major drawback is the lower adhesiveness of PET than matrix rubber. Fiber reinforcement can effectively improve material properties. For example, blending short fiber such as *p*-aramid with matrix rubber will meet the properties required for tire cord. Composites prepared with p-aramid nonwoven and rubber blended into the inner part of a bus or truck tire can increase the run-flat capability.

### 10.3.3.2 Driving belts

The main classifications of driving belts are metal combined belts, cogged belts, V-ribbed belts, and V-belts. In small passenger cars, speed variation can be achieved using metal-combined belts. The best suitable material for V-belts is PET fiber. The cords of V-ribbed belts, V-belts, and metal-combined belts can be prepared using *p*-aramid fiber. Figure 10.4 shows the structures of different kinds of driving belts [3].

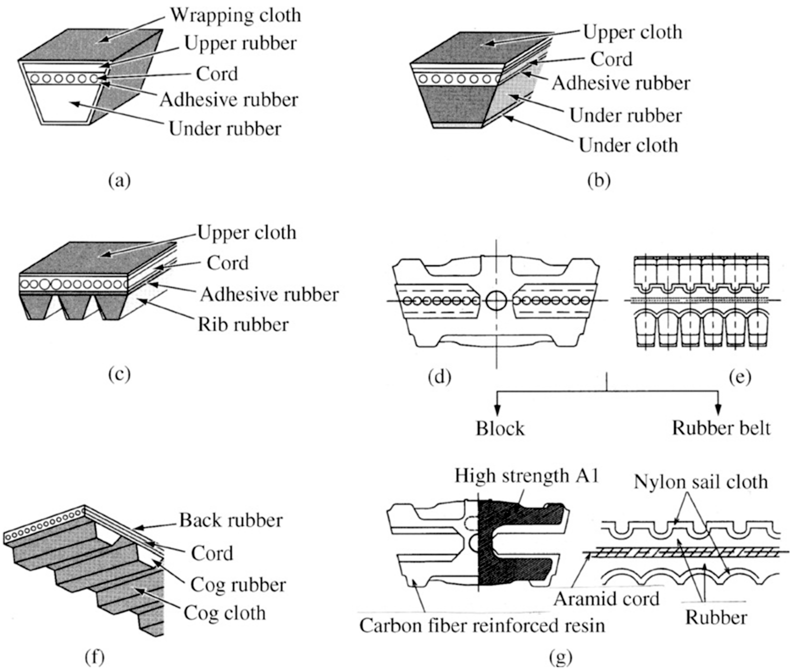
Wrapping cloth
Upper rubber
Cord
Adhesive rubber
Under rubber
(a)
Upper cloth
Cord
Adhesive rubber
Under rubber
Under cloth
(b)
Upper cloth
Cord
Adhesive rubber
Rib rubber
(c)
(d)
(e)
Block
Rubber belt
High strength A1
Nylon sail cloth
Back rubber
Cord
Cog rubber
Cog cloth
Aramid cord
Rubber
Carbon fiber reinforced resin
(f)
(g)

**Figure 10.4:** Types of driving belts: (a) wrapped V-belt, (b) raw-edge V-belt, (c) V-ribbed belt, (d) block, (e) rubber belt, (f) belt with cog, and (g) V-belt. With permission from [3], Taylor & Francis.

### 10.3.3.3 Seat belts

For the webbing of seat belts, PET woven fabrics are commonly used. PET can absorb high-impact energy and undergoes less discoloration from sunlight. Due to these capabilities, PET is more suitable for webbing than nylon. There are numerous standards for webbing; some of them are the Economic Commission for Europe, the Federal Motor Safety Standard, and the Japan Industrial Standard. The primary mechanical necessities of these standards are energy absorption ratio, strength, elongation, and width. Along with these requirements, wearing resistance, water resistance, cold and heat resistance, light-degradation resistance, and color fastness are some of the other requirements for durability.

#### 10.3.3.4 Car interior

Polyester fibers are mainly used for seat skin sheets and seat cushion material. PET fiber has high heat stability, high modulus, higher durability for sunlight degradation, high color change resistance, and is less expensive; it is sometimes also used for door trim skin materials.

Tricot fabrics and PET nonwoven materials are used for roof trim skin sheets. Needled nonwoven patterned fabric using velour is especially common, and the use of needle-punched nonwoven fabric has increased. However, stitch-bonded and spunlaced nonwovens that can be prepared by integrating with base materials are available. PET, which has been pigment-dyed, is commonly used. Sheets need to have heat resistance, formability, mechanical durability, stain resistance, light durability and color fastness for sunlight, in addition to lightness. Additionally, a specific level of heat insulation and sound-absorbing capability is required [3].

### 10.3.4 Air Purification

#### 10.3.4.1 Air filters

Air filters remove dust from the atmospheric air, recycle conditioned air, and contribute to energy savings. Generally, the filter medium is nonwoven. The removal efficiency of the filter increases with a smaller fiber diameter. However, the pressure drops simultaneously increase.

#### 10.3.4.2 Bag filters

Bag filters are widely used in the cleaning of exhaust gases from incinerators. Bag filters are usually made of synthetic needle felt fiber, glass fiber woven fabric, or a combination of woven fabrics. The synthetic fiber materials are polyimide, polyphenylenesulfide, polytetrafluorocarbon, and *m*-aramid. The surface of a tabular-shaped bag filter usually has an accumulation of dust in the exhaust gas. When the inlet pressure rises due to the accumulation of dust to the predetermined level, it is dropped off from the bag surface by mechanical vibration or by a counter-pulse jet. If activated carbon or slaked lime is used in the bag, acid and other harmful gases can also be removed.

#### 10.3.4.3 Household textiles and floor-coverings

High performance home textiles are used for furniture, internal decoration, floor and wall coverings, sun shielding, and carpeting. These are widely used in buildings, ships, caravans, and for transportation because of their fire-retardant properties. Coating the fiber with fire retardant components, like phosphorus-based pyrovatex materials, or inbuilt fire-retardant fiber (modacrylic fibers), imparts fire retardant properties. Hollow fibers having high-quality insulation find application in beds and sleep bags. Furniture packaging uses different fiber classes to avoid fires and health hazards, unlike the conventional packing materials [13].

#### 10.3.4.4 Agriculture

The characteristics of Agro-Tech textiles are biodegradation, stiffness, strength, elongation, and protection against a toxic environment and sunlight. Agricultural uses of textiles are soil erosion protection, screening from sunlight, separation of layers in fields; grass storage in windshield packing; anti-bird net; and crop protection. Thermal insulation, shading, and weed suppression are done using lightweight spunbonded fleeces.

Wind shelters and hail use heavyweight knitted, woven, and nonwoven textiles. Capillary nonwoven fibrous architectures are used in horticulture to adequately distribute moisture evenly on a growing plant. Plastic packs are replaced by woven polypropylene-based flexible vessels for the transportation of agricultural crops, fertilizers, and mass storage.

## 10.4 Future perspectives

The recent progress in advanced technical textiles consists of various applications in various industries. Various studies have also significantly contributed to the advancement of smart textile devices by opening up initial pathways for designing, preparing, and their characterization. They show various advantages, such as desired flexibility, miniaturization, wearability, and weavability. They have accelerated research in multifunctional advanced technical textiles. These initiatives and efforts raise awareness among people about the broad application potential of these smart fibers, and increase the chances of the applicability of these materials in various spheres.

The future scope of textile fiber science is very broad. New markets and new horizons for technical textiles will be opened due to the introduction of innovative products. The market for innovative technical textiles is being affected by the development of new products and creative finishes, and it is this technological evolution that integrates human science, material sciences, and information technology. It also gives people foresight in developing applications and products. Value addition through functional finishes can help to strengthen the product lines and diversify them into previously unexplored areas [14].

Regardless of the current research achievements in the fabrication of these devices, there are still many challenging problems to be solved to encourage the industrialization of smart textiles. For instance, stability of the application, safety, and scaled-up fabrication can be viewed as critical challenges for the actual implementation of functional fiber devices, particularly for the integrated framework of the functional fibers with the conventional textile industry and the related internal stress challenges in complex application environments [15]. However, the growth of technical textiles still holds potential for even greater global competitiveness, which will drive companies to develop goods with more uses at a lower cost and of higher quality, while encouraging research and trials to lessen their limitations. One of the industrial sectors with the fastest commercial growth is technical textiles. The high-performance textile industry's rapid growth has created numerous prospects for various cutting-edge applications. The US market for technical textiles is expected to reach US $251.82 billion by 2027. Currently, technical textiles are typically used for wound care and treatment products; breathing masks; diapers; wipes; bedclothes; braces; prosthetics; belts; and ropes, among other things, but in the future, innovation is anticipated to advance toward numerous and diversified end uses. More research needs to be done to determine how to lessen the ecological effects of technical fabrics on soil, water, and air. The worldwide market for high-performance textiles is more than just the manufacture and treatment of textiles [13].

## 10.5 Conclusions

The industry of advanced fibers is growing rapidly and progressively, providing stiff competition to the already established and matured traditional textile industry. Various innovative applications are emerging due to the expansion of high-performance textiles. Technical textiles are used in many applications, such as prosthetics, braces, diapers, wound-care, ropes, belts, bedclothes, breathing masks, and many more. The materials will definitely broaden the economic trend. Technical textiles will have lesser impacts on water, air, and soil. The technical textile will foresee promising stronger global production, completion and diverse application in the future. However, a proper value chain is still not established for smart textiles. Government agencies are taking some serious initiatives to assist in creating a well-defined value chain. The SmartX European Smart Textiles Accelerator has been established by the European Commission to bridge the industry-academia gap and to encourage start-up initiatives. Considering the multidisciplinary usability and the nature of advanced textiles in various applications, the collaboration and synergy between electrical engineers, materials scientists, regulatory bodies, user-interface developers, government entities, clothing industry experts, clinicians, and patients will be needed for future integration and developments.

## References

[1] Khalifa TF. Technical textile; design & methodology. Int Design J. 2013;2:57–61.

[2] Papaspyrides CD, Pavlidou S, Vouyiouka SN. Development of advanced textile materials: Natural fibre composites, anti-microbial, and flame-retardant fabrics. Proc Inst Mech Eng Part L: J Mater: Des Appl. 2009;223:91–102. https://doi.org/10.1243/14644207JMDA200.

[3] Matsuo T. Advanced technical textile products. Text Progress. 2008;40:123–181. https://doi.org/10.1080/00405160802386063.

[4] Raha S. Technical Textile Documentation on Protective Textile : Existing Technical Textile Products & New Developments, 2020. https://doi.org/10.13140/RG.2.2.14418.38089.

[5] Diane E. The impact of technical textiles on health and wellbeing current developments and future possibilities. J Text Sci Eng. 2017;07:1–4. https://doi.org/10.4172/2165-8064.1000309.

[6] de Oliveira CRS, da Silva Júnior AH, Immich APS, Fiates J. Use of advanced materials in smart textile manufacturing. Mater Lett. 2022;316:132047. https://doi.org/10.1016/j.matlet.2022.132047.

[7] Markovchick VJ, Moreira ME. Wound management. In: Legome E, Shockley LW (Eds.) Trauma: A comprehensive emergency medicine approach, Cambridge, Cambridge University Press; 2011. pp. 618–634. https://doi.org/10.1017/CBO9780511975769.037.

[8] Calamari TA, Jr, Harper Jr RJ. Flame retardants for textiles. In: Kirk-othmer encyclopedia of chemical technology, major reference works, pp. 1–23. 2014. https://doi.org/10.1002/0471238961.0612011303011201.a01.pub2.

[9] Crown EM, Batcheller JC. Technical textiles for personal thermal protection. In: Handbook of technical textiles: Technical textile applications, 2nd ed, Elsevier Ltd; 2016. https://doi.org/10.1016/B978-1-78242-465-9.00009-4.

[10] Hilfiker R, Kaufma W, Reinert G, Schmdt E. Improving sun protection factors of fabrics by applying uv-absorbers. Text Res J. 1996;66:61–70. https://doi.org/10.1177/004051759606600201.

[11] Gupta B, Saxena S, Grover N, Ray AR. Plasma-treated yarns for biomedical applications. In: Alagirusamy R, Das A (Eds.) Technical textile yarns. Woodhead Publishing; 2010. pp. 452–494. https://doi.org/10.1533/9781845699475.2.452.

[12] Morris H, Murray R. Medical textiles. Text Prog. 2020;52:1–127. https://doi.org/10.1080/00405167.2020.1824468.

[13] Aldalbahi A, El-Naggar ME, El-Newehy MH, Rahaman M, Hatshan MR, Khattab TA. Effects of technical textiles and synthetic nanofibers on environmental pollution. Polymers (Basel). 2021;13:1–26. https://doi.org/10.3390/polym13010155.

[14] Rekha R, Chauhan PD. Functional finishes on textiles. Man-Made Text India. 2005;48:339–343.

[15] Shi Q, Sun J, Hou C, Li Y, Zhang Q, Wang H. Advanced functional fiber and smart textile. Adv Fiber Mater. 2019;1:3–31. https://doi.org/10.1007/s42765-019-0002-z.

[16] Singh MK, Singh A. Ultraviolet protection by fabric engineering. J Text. 2013;1–6. https://doi.org/10.1155/2013/579129.

Pragnesh N. Dave* and Pradip M. Macwan

# Chapter 11
# Advanced fiber materials in drug delivery

**Abstract:** A drug delivery system (DDS) is in charge of influencing and determining a drug's concentration profile, the kinetics of its release, the place and time of its action, and lastly, the prevention of unfavorable side effects. An ideal DDS's job is to ensure that a drug is accessible at the place of activity at certain moments and for the required length of period. This significant part relates to the dosage frequency, the degree of drug release, and the method of administration. As a result, fresh concepts were developed for managing the pharmacokinetics, pharmacodynamics, inaccurate deadliness, responsiveness, bioreceptor, and effectiveness of drugs. These modern tactics are frequently referred to as DDSs. Controlled-release drug delivery employs drug-encapsulating devices from which therapeutic agents may be released at controlled rates for long periods ranging from days to months. A sophisticated method called electrospun has been successfully used to produce fibers and has several advantages for developing new DDSs. Electrospun has drawn the interest and attention of scientists in record numbers in recent years. When it comes to creating fibers with scales ranging from micrometers to manometers, this method is superior to others. When treating severe disease, the choice of the proper polymers, the electrospun procedures, and the electrospun parameters all play crucial roles in managing drug release. Nanofibers (NFs) are the only type of nanostructured materials that are often employed in the fields of tissue engineering (TE) and regenerative medicine. With the proper modifications, NFs may be utilized nearly for any TE technique as they can be created using a variety of different approaches. This chapter provides an overview of the key features of various DDSs as well as information on the fundamentals of electrospinning, equipment configurations, polymer/drug systems, and obstacles that must be addressed for clinical applications.

**Keywords:** Drug release, controlled release, electrospinning, nanofibers

## 11.1 Introduction

The problem of effective drug delivery has been the subject of ongoing research and study since the commencement of the twentieth century. The inefficiency of the

---

***Corresponding author: Pragnesh N. Dave,** Department of Chemistry, Sardar Patel University, Vallabh Vidyanagar 388 120, Gujarat, India, e-mail: pragnesh7@yahoo.com

**Pradip M. Macwan,** B.N. Patel Institute of Paramedical and Science (Science Division), Sardar Patel Education Trust, Bhalej Road, Anand 38800, Gujarat, India

https://doi.org/10.1515/9783110992892-011

carriers utilized in these drug delivery systems (DDSs) has slowed progress in some elements of each field despite advancements in fields like cancer therapies and drug delivery [1]. Four factors including (i) targeting the drug to the intended organ for maximum effect, (ii) avoiding the body's immune system to reach the final target, (iii) retaining the therapeutic molecules from the manufacturing process to the final target of the drug, and (iv) releasing the drug molecules at the target organ so that they can exert the envisioned therapeutic effect, contributing to the significance of the drug carrier. Therefore, the selection of the drug carrier is intrinsically linked to the success of a current or planned use of a DDS [1–3].

The process of creating a novel drug molecule is time- and money-consuming. The safety effectiveness ratio of "old" pharmaceuticals has been improved utilizing a variety of techniques including dosage titration, individualizing drug therapy, and therapeutic drug monitoring. Other extremely appealing strategies that have been actively researched include controlled drug delivery, delayed drug delivery, and targeted drug delivery. It is noteworthy that Indian scholars have produced a significant amount of work and several publications from the USA and Europe [4]. Over the last few decades, researchers have investigated a variety of carriers [5], and micro and NFs have emerged as promising potential carrier choices [6, 7]. This may be due to the characteristics of both the substance used to make the fiber and the method utilized to make it. Additionally, drug-loaded fibers are better suited for drug delivery applications due to their regulated zero-order drug-release profile and lower initial burst rate compared to spherical vesicles [1, 8].

Fibers are excellent candidates for DDSs due to their architecture. Because the fibers are cylindrical, they have a large surface area-to-volume ratio [9]. As a result, the fibers can distribute the drug into the medium over a sizable surface area. Furthermore, unlike spherical vesicles, where the surface area-to-volume ratio may be altered simply by modifying the radius, fibers allow for the modification of both the length and the cross-sectional radius. When the functioning characteristics of a DDS must be accurately regulated, adaptability is essential. Depending on the desired use, fibers with various forms and architectures, such as hollow, flat, and ribbon-shaped fibers, can also be created.

Nanometer-scale diameter describes fiber. A nanomaterial with one dimension under 100 nm is called a NF. To create NFs, a wide variety of polymers, including polyvinyl alcohol, gelatine, collagen, chitosan, and carboxy methyl cellulose, can be spun using an electrospinning (ES) method. Due to their enormous specific surface area and tiny pore size, NFs provide novel possibilities for the management of wound care applications. The production of NF layers from various polymers, the incorporation of drugs, or growth factors into various NF layers for wound care management are some advantages of NFs. NF's role in advanced wound care management includes (a) exudate absorption; (b) drug addition to the NFs; and (c) displaying antiadhesive activity. Additionally, NFs can be employed in DDSs to enhance the control of drug distribution [10].

NFs are stated as a connection between nanotechnology and the micron-size world since they differ from other fibrous structures with a diameter in the range of nanometers and length in the range of meters. To create NFs, a variety of synthetic, semisynthetic, and natural polymers have been used. As drug delivery devices, electrospun NFs offer several essential structures: (1) several solutions of both natural and synthetic polymers can be electrospun to create NFs; (2) NFs s transport both hydrophilic and hydrophobic medicines well due to their high surface-layer area-to-volume ratios; (3) by adjusting several characteristics, such as the drug-to-polymer ratio, fiber diameter, shape, and/or porosity, the drug-release profile, may be tailored to the specific therapeutic use [11]. Utilizing the electrostatic repulsions of highly charged polymer jets to create randomly oriented or aligned NFs deposition on the collector surface is the fundamental principle of ES. The Taylor cone is formed at the tip of an injecting device when an electric field is applied to a polymeric solution with a moderate viscosity value. To use electrospun NFs in biomedical applications, their surfaces have been chemically and physically altered with cell-recognizable ligands and bioactive molecules after the ES method; this subsequently provides contacting cells and tissues with biomodulating or biomimetic microenvironments. Many different electrospun NF functionalization techniques, including those using proteins, nucleic acids, and carbohydrates, have been used [12]. To improve cellular adhesion and proliferation, a range of extracellular matrix (ECM) protein components, including gelatin, collagen, laminin, and fibronectin, may be fixed onto the plasma-treated surface. Through plasma glow discharge with oxygen and gas-phased acrylic acid, electrospun NFs made of poly(glycolic acid) (PGA), poly(L-lactic acid) (PLA), or poly(lactic-*co*-glycolic acid (PLGA) were transformed with carboxylic acid groups.

Advanced fiber materials prepared this special issue on the subject of “Biomedical fibres and nano-fibres” to highlight new developments in fibers or NFs for biomedical applications. The development of fibers or NFs for biosensing, TE, and drug delivery applications is highlighted in this issue’s four contributions (one review article) and three research papers (from active professionals) in the associated domains. The use of electrospun nanofibrous materials for wound healing has recently advanced according to the report by Li and colleagues [50]. They focus on the work being done to control fiber alignment and morphology, build 3D scaffolds, create waterproof-breathable membranes, govern drug delivery performance, and control stem-cell behavior. Coaxial core–shell electrospun fibers co-loaded with levodopa and carbidopa were developed by Williams and colleagues [51] as a possible therapy for Parkinson’s disease.

In recent years, interest in protein-based biopolymers for drug delivery has grown. They benefit from being water-soluble, biocompatible, biodegradable, and nontoxic when compared to synthetic polymers. Many animal proteins found in nature, like keratin, collagen, elastin, and silk, are affordable and sustainable. They are straightforward to produce under benign conditions and are readily extracted from their natural sources. These proteins have received substantial study and offer desirable structural characteristics for a variety of biological applications. With their release behavior, degradation profile, and mucoadhesive nature, protein polymers used in drug administration are crucial components of pharmaceutical applications [13].

The highlights of several drug delivery systems are covered in the current chapter, along with the fundamentals of ES, equipment setup types, polymer/drug systems, and restrictions and hurdles that must be overcome for clinical applications. The chapter also offers a succinct introduction to the use of electrospun NFs for drug administration and lists key processing factors that may affect how well the NFs work when used for this purpose.

## 11.2 An overview of drug delivery

### 11.2.1 What is a drug delivery system?

Technologies that deliver drugs into or throughout the body are referred to as DDSs. These technologies include the mode of administration such as a pill that you swallow or an injection-based vaccine. Drug “packaging” such as a micelle or a nanoparticle may also be referred to as DDS. This packaging keeps the drug from degrading and enables it to go wherever it is needed in the body.

DDSs are polymeric or lipid carrier systems that deliver drugs to their targets or receptor sites in a way that ensures their maximum therapeutic activity, prevents drug degradation or inactivation during transportation to the target site(s), and shields the body from adverse effects resulting from inappropriate disposition. It may be described as a formulation or a tool that makes it possible to introduce a therapeutic material into the body and enhances its effectiveness and safety by managing the rate, timing, and location of drug release in the body.

### 11.2.2 Ideal characteristics of drug delivery systems

- It should boost the drug’s bioavailability.
- While avoiding the host tissue that is not sick, it should deliver the drug intact to the site of action.
- Under diverse physiological conditions, the product should be steady and delivery should be maintained.
- Significant drug dispersion.
- The same approach should work for a variety of drugs.
- It should be simple to give the patient.
- It should be safe and reliable.
- It should be affordable.

### 11.2.3 Limitations for drug preference

Specification: Preferred value
Molar mass/dimension: <1,000
Solvability: >0.1 µg/mL for pH 1 to pH 7.8
$Pk_a$Inactive molecule: >0.1% at pH 1 to pH 7.8
Observable split factor: High
Uptake technique: Dispersion
Universal absorbability: From all GI sections
Discharge: Ought not be prejudiced by pH and enzymes [14]

## 11.3 Classification of drug delivery systems

A DDS is responsible for influencing and determining a drug's concentration profile, the kinetics of its release, the place and time of its activity, and last, the prevention of unfavorable side effects [15]. An ideal DDSs job is to ensure that a medicine is accessible at the place of activity at certain moments and for the required lengths of time. This significant function relates to dosage frequency, drug-release rate, and administration route. As a result, fresh concepts were developed for managing the pharmacokinetics, pharmacodynamics, inaccurate deadliness, responsiveness, bioreceptor, and effectiveness of drugs. DDSs are a common name for these novel tactics. DDSs act as a link between a patient and a drug, to put it another way. There are two primary categories of DDSs: (1) normal DDSs and (2) novel DDSs, also known as controlled DDSs.

### 11.3.1 Normal drug delivery systems

The normal procedures of delivering a drug to the body are known as conventional DDSs. These systems are often utilized more frequently when the aim is for a drug to be absorbed fast, necessitating a quick release of the substance. Simple oral, topical, inhalation, or injectable procedures are among the common drug delivery modalities. These techniques are unable to maintain the drug engagement at a set and steady plane for a predetermined amount of period (transitory transmission). Management of numerous doses at systematic intermissions is one strategy to fight the issue of drug instability concentration (repeated doses). This approach, however, has certain drawbacks of its own. The drug's concentration in blood plasma fluctuates erratically, and patients frequently forget to take the right amount at the right time. The need for unique DDSs becomes increasingly obvious as a result of the issues described with traditional DDSs [16].

## 11.3.2 Innovative drug delivery systems

An innovative DDS (IDDS), too known as a controlled-release (CR) DDS, combines cutting-edge methodologies and new dosage procedures to improve drug effectiveness, regulate drug release, increase security, and selectively target a drug to the targeted tissue. The definition of "controlled release" extends beyond just continuous release action. Alternatively, the release kinetics of a regulated release must exhibit two characteristics such as predictability and repeatability. The cost of production is reduced and costlier drugs and excipients are used more effectively as a result of NDDSs. From the perspective of the patient, IDDS improves therapy through more comfortable DDSs that raise living standards. Four kinds of NDDSs exist: site-targeting, rate-preprogrammed, responses, and signaling pathway.

### 11.3.2.1 Site-targeting drug delivery systems

This method is built on supplying a specified region of the body with a therapeutic substance in a predetermined amount over a prolonged period (such as tumorous muscles). Therefore, the drug only works where it is intended to be released – the targeted location. Doctors are interested in targeted DDSs because they have specific characteristics that set them apart from conventional ones. Drugs taken conventionally have a shorter half-life and worse solubility, stability, and absorption additional to their smaller life span. Drugs in the normal DDSs also take lower specificity and therapeutic indices than those in the focused DDSs.

**Advantages**
- Reduces adverse effects
- Low toxicity
- Avoids drug breakdown (first-pass breakdown)
- Increased drug bioavailability
- Small variation in attentiveness
- Positive effect on protein and peptide permeability
- Reduced dose frequency
- Reduced rate of exclusive drug management

**Disadvantages**
- Requirement of innovative technology and trained personnel
- Trouble in maintaining dosage form stability

#### 11.3.2.2 Rate-preprogrammed drug delivery systems

The rate or speed of drug release in this system is regulated by a change in the framework that regulates the dispersion rate of drug molecules over the obstacle medium around it. Fick's rules of dispersion are often used to calculate diffusion rates. These systems are further classified as (a) polymer membrane permeation-controlled DDS, (b) polymer matrix diffusion-controlled DDSs, (c) polymer (membrane/matrix) hybrid-type DDSs, and (d) microreservoir partition-controlled DDSs.

**(a) Polymer membrane permeation-controlled DDSs:** A drug is wholly or partially placed into a reservoir chamber in this system (such as hard particles, a spreading of hard particles, or a concentrated solution in a liquid- or solid-type dispersing medium). Reservoirs of various forms can be covered with a polymeric laminate that regulates the rate of drug release. This form of DDS allows for preconfigured drug-release rates by adjusting the drug dispersibility and membrane width.

**(b) Polymer matrix diffusion-controlled DDSs:** To create this type of DDS, drug atoms are distributed consistently in either a oleophilic (nonswellable) or a water-loving (swellable) polymer medium. The spreading technique is accomplished by combining tiny drug particles with either thermoset or thermoplastic polymers. The resulting drug-polymer spreading is then molded or squeezed out to generate drug-delivery procedures of various forms and dimensions. The drug-release degree from this type of DDS is preprogrammed by selecting the quantity of drug placed in the polymer or altering the diffusivity of the drug interior in the polymer matrix.

**(c) Polymer (membrane/matrix) mixed-type DDSs:** This type of DDS is used to achieve the zero-order release of polymer membrane interpenetration-controlled DDSs as well as the excellent motorized characteristics of polymer matrix diffusion-controlled DDSs. As a result, a nonmedicated polymeric sheath is deposited on the external of the drug-polymer spreading to regulate drug release by membrane penetration somewhat than matrix dispersion.

**(d) Microreservoir partition-controlled DDSs:** The drug reservoir in this type of DDS is created using high-energy microdispersion methods to create a homogenous suspension of drug solid particles in an aqueous water-miscible polymer such as PEG. The resultant solution is made up of unreachable and tiny drug pools in a biocompatible polymer that may be molded or extruded into different forms and sizes. Dissolution- or matrix diffusion-controlled procedures govern the drug-release rate from this form of DDS at a preprogrammed rate.

## 11.4 Biopharmaceutics Classification System (BCS) classification of drugs

The Biopharmaceutics Classification System (BCS) (1) is an important tool not only for getting exemptions for in vivo bioequivalence research but also for making decisions in the discovery and early development of novel drugs. This is because BCS is based on a scientific framework that describes the three rate-limiting phases in oral absorption. Absorption of a drug requires three steps: (1) drug release from dosage forms, (2) maintenance of dissolved state across gastrointestinal (GI) tract, and (3) penetration of drug molecules through GI membrane into hepatic circulation. The fourth stage, enterohepatic metabolism, regulates systemic availability as well as metabolite release into systemic circulation [17].

The BCS divides drugs into four categories based on their intestinal permeability and solubility (Figure 11.1). Class I drugs have high permeability and solubility and are well absorbed; their absorption rate exceeds their excretion rate (e.g., metoprolol and paracetamol). Class II drugs have high permeability but poor solubility, and their bioavailability is limited by their rate of solvation (e.g., glibenclamide and aceclofenac). Class III drugs have low permeability but high solubility, allowing the medication to dissolve fast; nonetheless, absorption is restricted by the rate of permeation. If the formulation does not affect permeability or gastrointestinal duration, class I criteria can be used (e.g., cimetidine). Class IV drugs have limited permeability and solubility, and they are poorly absorbed via the colon, resulting in poor bioavailability with considerable variability (e.g., bifonazole) [18].

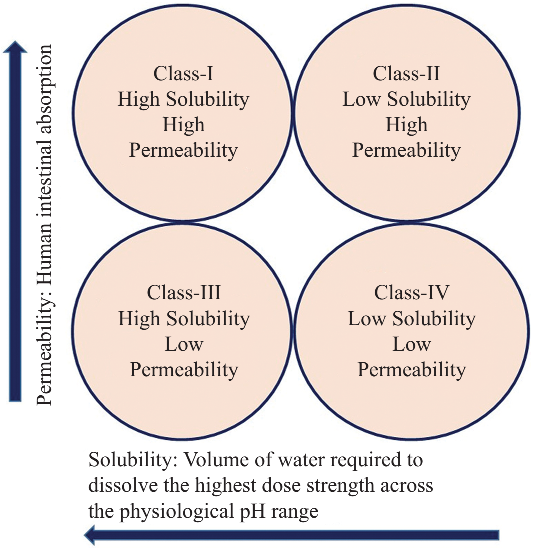
Permeability: Human intestinal absorption
Class-I
High Solubility
High
Permeability
Class-II
Low Solubility
High
Permeability
Class-III
High Solubility
Low
Permeability
Class-IV
Low Solubility
Low
Permeability
Solubility: Volume of water required to dissolve the highest dose strength across the physiological pH range

**Figure 11.1:** BCS classification of drugs [18].

When a new drug is discovered, it is generally made in the smallest dose form feasible that is effective in treating the specified ailment. Because different drugs have distinct physicochemical and biological characteristics, multiple formulations are required. This notion is shown by contrasting the oral and parenteral methods of delivery. Table 11.1 highlights some of the drug features that must be considered while looking for appropriate delivery methods. Because oral administration is the most convenient and extensively utilized method of drug administration, it is the first to be considered. Some drugs, on the other hand, have relatively poor water solubility or permeability across cells, making oral formulations challenging to manufacture. Furthermore, newer biotech drugs such as peptides, proteins, and nucleic acids are substantially bigger than classic tiny molecule pharmaceuticals. Because of their huge bulk, low stability, and short half-life, they are often administered via parenteral methods [19].

**Table 11.1:** Drugs with different properties requiring different delivery systems [19].

| | **Drugs** | | | | | | |
|---|---|---|---|---|---|---|---|
| | **Small molecules** | | | | **Large molecules** | | |
| | **BCS Class I** | **BCS Class II** | **BCS Class III** | **BCS Class IV** | **Peptides** | **Proteins** | **Nucleic acids** |
| Molecular weight | ↓ | ↓ | ↓ | ↓ | ↑ | ↑ | ↑ |
| Water solubility | ↑ | ↓ | ↑ | ↓ | ↔ | ↔ | ↔ |
| Cell permeability | ↑ | ↑ | ↓ | ↓ | ↓ | ↓ | ↓ |
| Half-life | ↕ | ↕ | ↕ | ↕ | ↓ | ↓ | ↓ |
| Main delivery route | Oral | Oral | Oral | Oral | Parenteral | Parenteral | Parenteral |

↑ : High; ↓ : Low; ↔ : Acceptable; ↕ : Individual variation from low to high

## 11.5 Controlled drug delivery

### 11.5.1 Outline

The science of sustained delivery was developed as a result of the 1940s and early 1950s discovery of edible prolonged products. For example, the sustained release of oceanic antifoulants (in the 1950s) and fertilizer (1970s) was developed, each with a single application in spiritual science. Therapeutics and pharmacokinetics have made significant strides, which have brought to light the importance of medication release rate in deciding therapeutic efficacy. This is the impetus for the creation of CR. Modified-release dose formulations are completely novel. Rhozes manufactures mucilage-coated tablets for the first time about AD 900. This technology was widely used by European countries in the tenth century in the form of gold, silver, and pearl-coated tablets; this covering affects the drug-release rates. In the late-1800s, advances in covering skill included carbohydrate and enteric coating on pills and tablets. Around 1938, the enteric coating of tablets was created, followed by the addition of another drug to the carbohydrate covering layer [14].

## 11.5.2 Terminology of controlled drug-release system

> Controlled drug delivery is one in which the drug is delivered at a predefined pace, either locally or systemically, for a certain amount of time.

Many novel chemical compounds are being generated and investigated for medicinal purposes as science and technology advance. Between 1993 and 1999, the US Food and Drug Administration authorized 22–53 novel molecular entities every year. The development of these active compounds is simply one component of the disease-fighting arsenal. When a drug molecule is administered to a patient, it requires a delivery mechanism to transport the drug to the site of action. The drugs can be delivered in a variety of dosage forms such as tablets, capsules, creams, ointments, liquids, aerosols, injections, and suppositories. The majority of traditional drug delivery methods are known to give instantaneous drug release with little or no control over the delivery rate. Several doses are required daily to produce and maintain therapeutically effective plasma concentrations, which may cause considerable swings in plasma levels (Figure 11.2). Because of these changes in drug plasma levels, the drug level may fall below or exceed the minimal effective concentration. Such oscillations cause undesired side effects or fail to provide the intended therapeutic benefit to the patient.

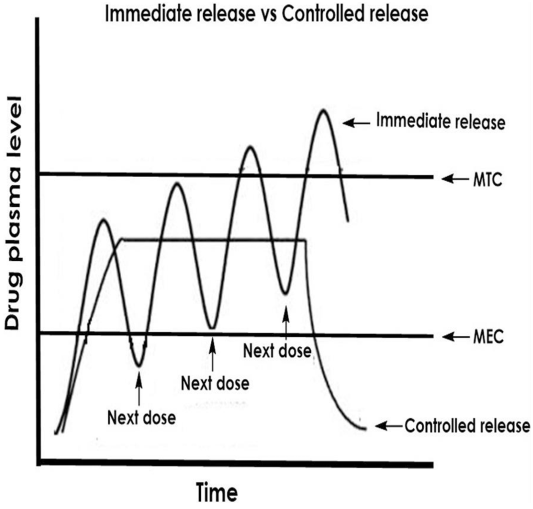

**Figure 11.2:** Therapeutic or hazardous as well as immediate versus controlled-release dose forms levels [20].

Sustained-release and CR DDSs can limit unwanted changes in medication levels, reducing adverse effects while increasing the treatment's therapeutic success (Figure 11.2). Although the phrases' continuous release and CR are sometimes used interchangeably, they relate to two distinct types of DDSs. Sustained-release dosage forms are systems that slow the release of the drug to extend the duration of effect, generally at the expense of delayed onset and pharmacological activity [20].

The CR mechanism's objective is to create a product that can continually release drugs at zero order over a longer length of time. As the technology for creating such items has advanced significantly, more vendors are now offering CR excipients. As CR, an increasing number of oral products have been created and commercialized.

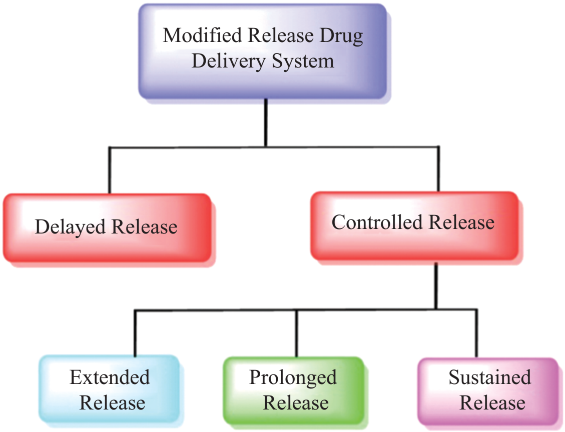

**Figure 11.3:** Classification of modified release drug delivery system [21].

Figure 11.3 depicts the classification of modified DDS. The history of CR technology is divided into three periods: the age of prolonged release of drugs from 1950 to 1970, the requirement for regulated drug delivery between 1970 and 1990, and current CR technology after 1990 (Table 11.2).

**Table 11.2:** Background on drug delivery methods and future technology since 1950 [19].

| First generation (1950–1980) | Second generation (1980–2010) | Third generation (2010–2040) |
|---|---|---|
| Basics of controlled release | Smart delivery systems | Modulated delivery systems |
| **Oral delivery**<br>– Twice a day, once a day | **Zero-order release**<br>– First-order versus zero-order | **Poorly soluble drug delivery**<br>– No toxic excipients |

**Table 11.2** (continued)

| First generation (1950–1980) | Second generation (1980–2010) | Third generation (2010–2040) |
|---|---|---|
| **Transdermal delivery**<br>– Once a day, once a week | **Peptide and protein delivery**<br>– Long-term deposits using biodegradable polymers<br>– Pulmonary delivery | **Peptide and protein delivery**<br>– Delivery for >6 months<br>– Control of release kinetics<br>– Noninvasive delivery |
| **Drug-release mechanisms**<br>– Suspension<br>– Dispersion<br>– Osmosis<br>– Ion interchange | **Smart polymers and hydrogels**<br>– Environment-sensitive<br>– Self-regulated release (working only in vitro) | **Smart polymers and hydrogels**<br>– Signal specificity and sensitivity<br>– Fast response kinetics (working in vivo) |
| | **Nanoparticles**<br>– Tumor-targeted delivery<br>– Gene transfer | **Targeted drug delivery**<br>– Nonpoisonous to non target cells<br>– Overwhelming blood–brain obstacle |
| Successful control of physicochemical properties of delivery systems | Inability to overcome biological barriers | Need to overcome both physicochemical and biological barriers |

## 11.6 Design considerations of controlled-release drug delivery systems

Various elements and characteristics must be addressed while building a CR drug delivery system. Figure 11.4 illustrates the design concerns quickly [18]. The metrics are divided into two categories: formulation-related and drug-related. The biomaterial characteristics, mode of administration, pharmacokinetics, and stability enhancement are the most important formulation-related aspects. Furthermore, drug-related factors such as drug-binding effectiveness with plasma proteins and the drug's capacity to overcome biological barriers are important considerations when developing the dosage form. It is necessary to investigate biomaterial features such as biocompatibility, surface chemistry, hydrophilicity, degradation, and mechanical and rheological qualities. Furthermore, the behavior of the biomaterials at various pH and temperature levels must be evaluated. The drug delivery routes are crucial for selecting the appropriate biomaterial and developing the dose form. Rectal administration, for example, necessitates that the biomaterial's melting point be at or above 37 °C or that it be soluble at that pH for the drug to be released. Certain drugs, such as peptides, proteins, genes (DNA), growth factors, and colloidal/noncolloidal particles, should

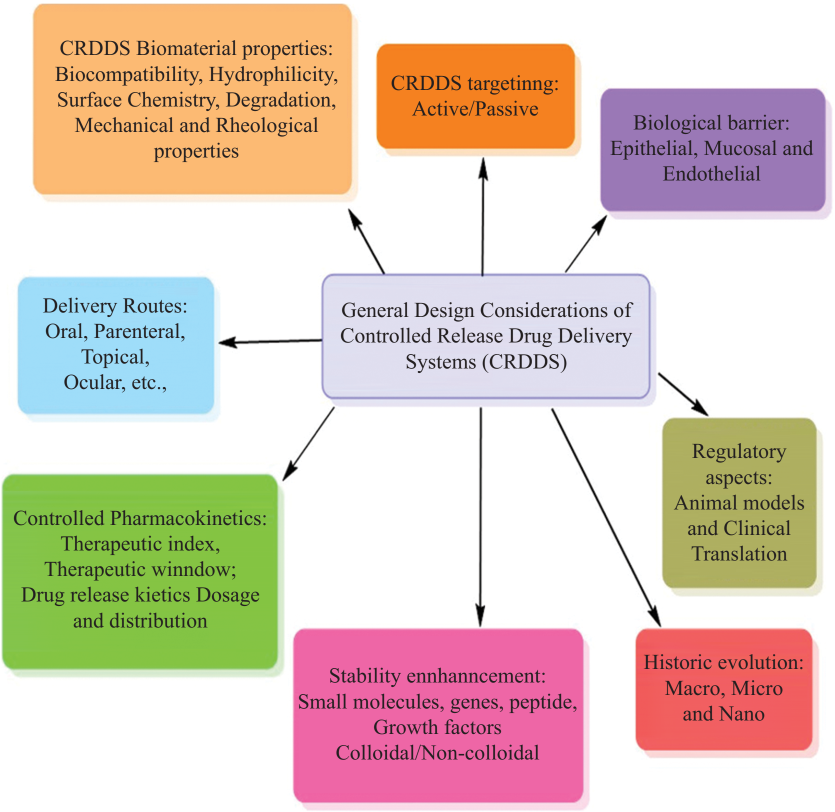
CRDDS Biomaterial properties: Biocompatibility, Hydrophilicity, Surface Chemistry, Degradation, Mechanical and Rheological properties
CRDDS targetinng: Active/Passive
Biological barrier: Epithelial, Mucosal and Endothelial
Delivery Routes: Oral, Parenteral, Topical, Ocular, etc.,
General Design Considerations of Controlled Release Drug Delivery Systems (CRDDS)
Regulatory aspects: Animal models and Clinical Translation
Controlled Pharmacokinetics: Therapeutic index, Therapeutic winndow; Drug release kietics Dosage and distribution
Stability ennhanncement: Small molecules, genes, peptide, Growth factors Colloidal/Non-colloidal
Historic evolution: Macro, Micro and Nano

**Figure 11.4:** General design considerations of CRDDS [18].

have their stability improved while the CR carrier is being designed. This can be accomplished by inserting specific drugs into customized carrier systems.

### 11.6.1 Classification of controlled-release drug delivery systems

Controlled discharge drug delivery methods are categorized as dissolution-controlled, diffusion-controlled, water penetration-controlled (osmotic pressure-controlled and swelling-controlled), chemically controlled, and nanoparticle-based systems depending on the mechanism of drug release from the dosage form [18].

#### 11.6.1.1 Dissolution-controlled drug delivery systems

Drugs are layered with or compressed inside gradually dissolving polymeric sheaths (pool systems) or mediums (monolithic systems) in dissolution-CR systems [22]. Drugs are sheltered in the interior of polymeric sheaths with deprived solubility in reservoir systems. A drug release occurs when the polymeric membranes dissolve (Figure 11.5). Drug aggregates are dispersed throughout the polymeric matrix in monolithic systems. When the matrices dissolve, the drug combinations dissolve and the dissolved drug is released. The solubility of the polymeric carriers is an important aspect of regulating drug release in dissolution-CR systems [22].

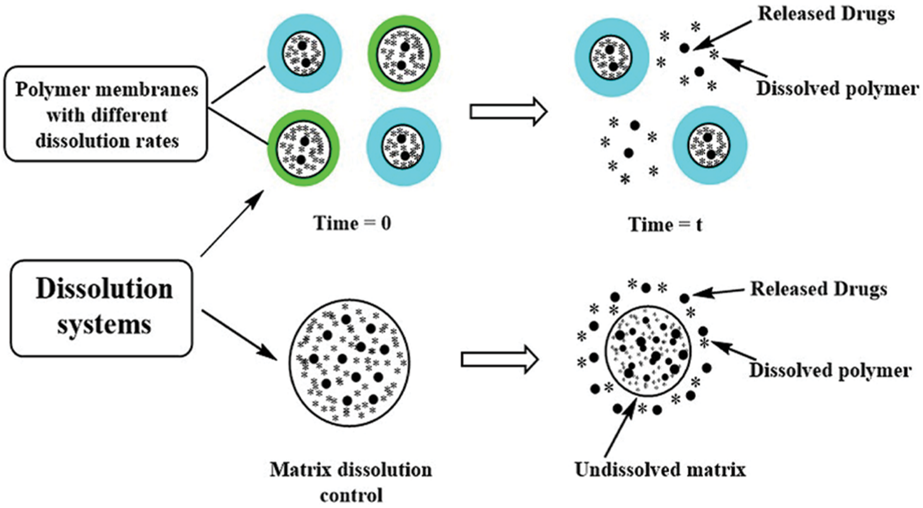
Polymer membranes with different dissolution rates
Dissolution systems
Time = 0
Time = t
Released Drugs
Dissolved polymer
Released Drugs
Dissolved polymer
Matrix dissolution control
Undissolved matrix

**Figure 11.5:** Dissolution-controlled delivery systems [22].

These systems are useful in that they can deliver high-molar-mass drugs and do not need operating exclusion. They are, however, connected with problems such as possible toxicity from dosage dumping and/or dissolved polymeric components as well as difficulties in attaining ideal zero-order release profiles.

### 11.6.1.2 Diffusion-controlled drug delivery systems

Diffusion, or the movement of a drug from a higher concentration zone to a lower concentration region, is a critical aspect in controlled discharge systems [22]. Drugs are imprisoned in and discharged by dispersion via passive water-insoluble polymeric sheaths (pool systems) or polymeric matrices (monolithic systems) in diffusion-CR systems. Diffusion-CR systems are classified into four basic categories based on their structure and drug-loading procedures as illustrated in Figure 11.6. These include (1) nonreliable supplier of drugs tank, (2) continuous drug source pool, (3) monolithic solution, and (4) monolithic spreading. Figure 11.6 depicts drug release over period in several forms of diffusion-CR systems. Loaded drugs dissolve in an aqueous solution below their saturation concentrations in nonconstant source reservoirs or monolithic solution systems (time = 0). When the drug is released, the concentration of the drug in the pools/mediums decreases with interval, causing in a drop in the quantity released at time = $t_1$ and $t_2$. An oversaturated concentration of a combination of saturated solution and undissolved sparkler/shapeless drug masses is created in the constant source reservoir or monolithic dispersion systems (time = 0). When the concentration of dissolved drug in the system falls beneath its saturation concentration, drug masses liquefy to replenish the released drug.

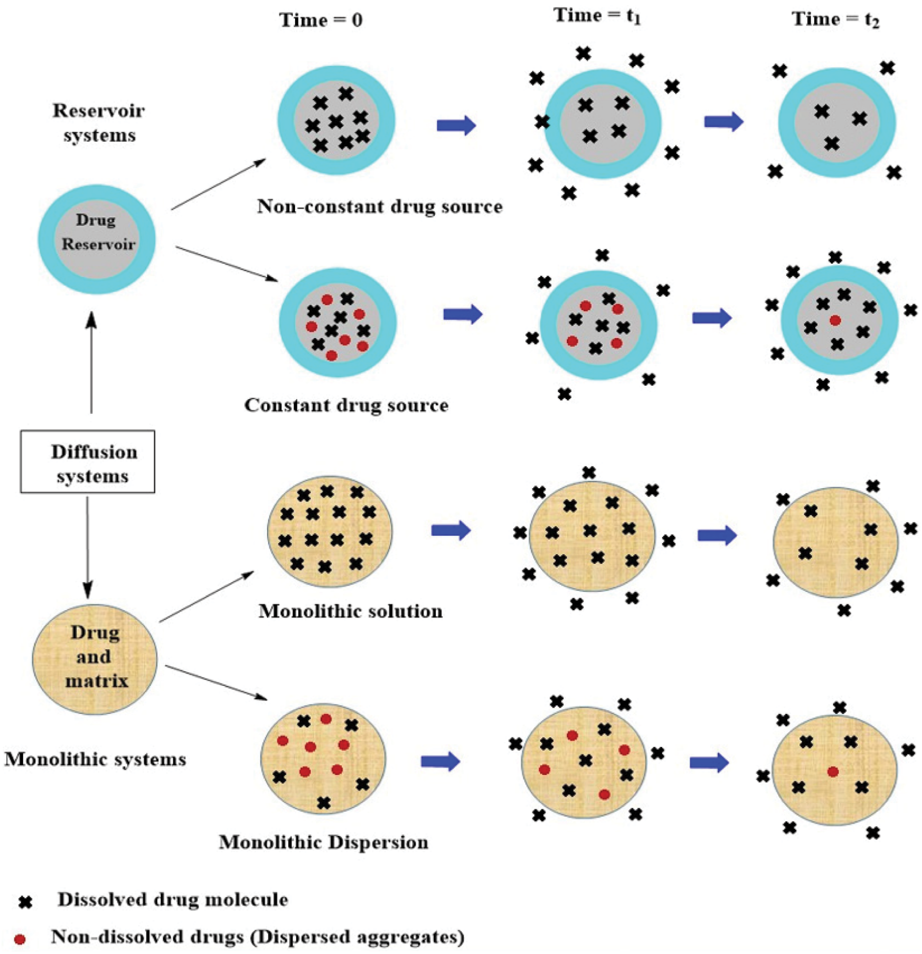
Time = 0
Time = t₁
Time = t₂
Reservoir systems
Drug Reservoir
Non-constant drug source
Constant drug source
Diffusion systems
Drug and matrix
Monolithic solution
Monolithic systems
Monolithic Dispersion
✖ Dissolved drug molecule
● Non-dissolved drugs (Dispersed aggregates)

**Figure 11.6:** Organization of diffusion-controlled release systems according to their physical assembly and drug-loading method [22].

As a consequence, at time = $t_1$ and time = $t_2$, the drug concentration in the system does not change. Drugs can therefore be delivered at a consistent pace in a regulated way using zero-order kinetics. When the drug masses in the pools/mediums dissolve fully, a nonconstant source reservoir or monolithic solution system is formed.

#### 11.6.1.3 Water trapping-controlled drug delivery systems

Drug release can be accomplished by the trapping of water or bodily liquids through water penetration CR devices. These systems are classified as enlargement-controlled systems or osmotically regulated systems [22].

**(a) Swelling-controlled systems:** Drug masses are consistently disseminated within a dehydrated swellable 3D polymeric complex in swelling-controlled systems. When submerged in water or bodily liquid, the movement of water into the 3D polymeric network hydrates the systems. As a result, the system's aqueous solvent concentration and network mesh size increase, resulting in drug dissolution and diffusion across the hydrated polymeric network. The swelling characteristic of the systems, as well as the dissolving and diffusion properties of drugs, are important elements in controlling drug release.

**(b) Osmotically controlled system:** The osmotic pressure induced by the existence of an osmotic agent (e.g., PEG and PVA) within a semipermeable membrane reservoir that is penetrable to water but not to solutes (loaded drugs) governs drug release in osmotically regulated systems. Figure 11.7 depicts a schematic representation of osmotically regulated release systems, in which drugs and osmotic agents are protected by a semipermeable membrane reservoir with tiny holes (release orifices) that allow paths for drug release into the surrounding environment. There are two kinds of osmotically regulated release systems: type A and type B. Type A has an osmotic central filled with pharmaceuticals, whereas type B has a drug pool-bounded by an osmotic core. Drugs, which might be in solution or combined constructions, are imprisoned in a semipermeable membrane pool (at time = 0) in these systems. When these devices are submerged in water or bodily liquid, water flows across the membrane to create an osmotic variance, which is used to regulate drug release through the cavities (time = *t*). The solubility and osmotic strength of osmotic agents, cavity extent, and membrane permeability all influence drug release from osmotically regulated devices. Many merits of osmotically regulated release systems include excellent drug-loading effectiveness and release ability, refillability, the ability to attain zero-order release kinetics, and freedom from drug characteristics and ambient circumstances. Nevertheless, these systems are often costlier, necessitate extra stringent excellence regulator, are incompatible with drugs having tiny half-lives in aqueous solution, and in some cases must be surgically inserted into the body.

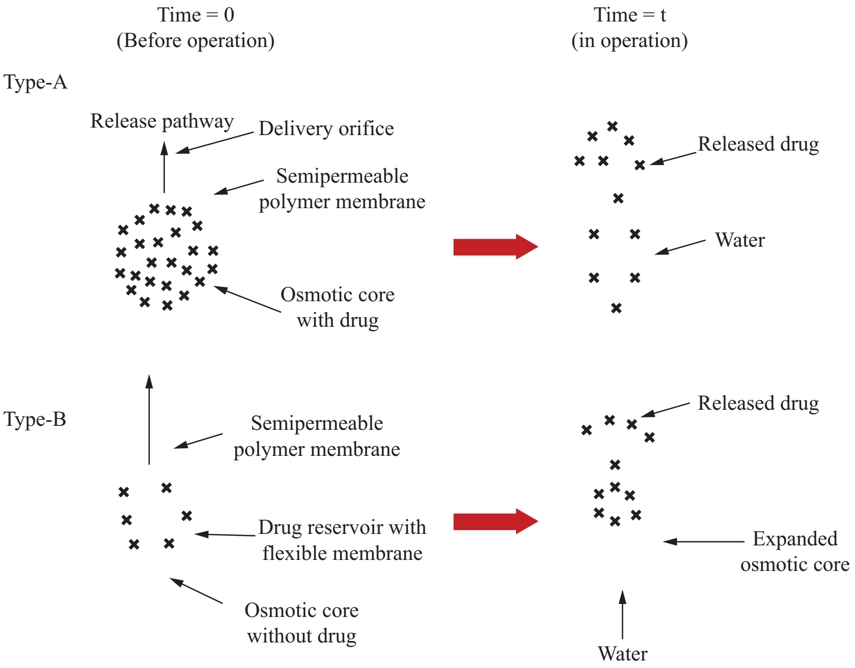
Time = 0
(Before operation)
Time = t
(in operation)
Type-A
Release pathway
Delivery orifice
Semipermeable polymer membrane
Osmotic core with drug
Released drug
Water
Type-B
Semipermeable polymer membrane
Drug reservoir with flexible membrane
Osmotic core without drug
Released drug
Expanded osmotic core
Water

**Figure 11.7:** Before and after operation of double kinds of osmotically regulated release systems at time = 0 and time = *t*, respectively. Type A has an osmotic central containing pharmaceuticals, whereas Type B has a drug pool enclosed by an osmotic core [22].

#### 11.6.1.4 Chemically controlled-release systems (erosion and polymer–drug conjugate)

Drug release in chemically measured release systems can be modified by modifying their chemical assembly (such as degradation and cluster transmission). They are classified as erosion-controlled systems or polymer–drug conjugate-controlled (dependent adjacent restraint) systems [22].

Drugs are placed in erodible polymeric mediums via dispersion and/or molar relations (hydrophobic, ionic, etc.) and can be released following matrix degradation and drug molecule dissolution and dispersion, as shown in Figure 11.8. The diffusion and dissolution of drugs, as well as the erosion of polymeric matrix, can regulate the release patterns in these systems. The release kinetics can be difficult to anticipate, and the degraded polymers may be hazardous. These systems, on the other hand, may release high-molar-mass drugs without requiring clinical exclusion and, in about situations, can permit for zero-order release kinetics. The use of recyclable injectable hydrogels for the CR of chemical or protein drugs such as doxorubicin, insulin, bovine serum albumin, and human evolution hormone has been described. These drugs can ionically relate with the hydrogel forerunner macromolecules when mixed. After injecting drug-loaded polymer solutions into mice, hydrogels formed, and the drugs were released over period as the hydrogel degraded.

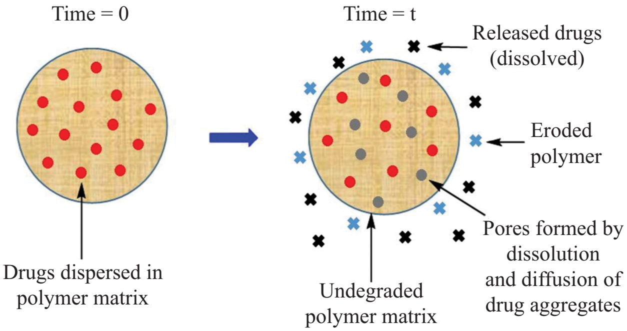
Time = 0
Time = t
Released drugs (dissolved)
Eroded polymer
Pores formed by dissolution and diffusion of drug aggregates
Drugs dispersed in polymer matrix
Undegraded polymer matrix

**Figure 11.8:** An erodible controlled-release mechanism. At time = 0, the drug is disseminated in the polymeric medium previously discharge. At time = *t*, partial release of drugs and polymeric degradation products by surface erosion of the polymeric matrix [22].

## 11.7 Preferred biopharmaceutic features of drug to be eligible for CDDS

### 11.7.1 Molecular weight or size

Convective transport allows small molecules to flow through membrane holes. This is true for both drug release from an amount custom and transport over a biological sheath. The limit for biological sheaths may be a molar mass of 150 and 400 for globular molecules and chain-like substances, correspondingly [23].

### 11.7.2 Solubility

The drug must be present in solution at the site of absorption for all processes of absorption. During the preformulation investigation, the drug's solubility at various pH levels must be determined. If the dispersibility is less than 0.1 g/mL (in acid media), the bioavailability will be varied and lowered. If the dispersibility is less than 0.01 g/mL, captivation and convenience will utmost probable become dissolution restricted. As a result, the driving power for dissemination may be insufficient. If at least 0.1–1% of the drug is in nonionized form, it appears that it is efficiently absorbed by passive diffusion from the small intestine after oral delivery.

### 11.7.3 Apparent partition coefficient

Drugs captivated by inactive diffusion must have a minimum apparent partition coefficient (APC). For many drugs, the larger the APC in an *n*-octanol/buffer combination, the greater the flow through a sheath. The APC for the full pH range in the GI tract should be determined. The APC must also be used for drug partitioning between CRDDS and biological liquid.

## 11.8 Factors influencing the design and act of controlled-release products

### 11.8.1 Physiological properties

#### 11.8.1.1 Aqueous solubility

The majority of active pharmacological moieties (API) are slightly acidic or basic in nature, which affects API water solubility [14]. It is challenging to construct controlled-release formulations for drugs that are poorly soluble in water. A drug with a high water solubility exhibits rupture release followed by a fast increase in plasma drug concentration. These drugs are excellent candidates for CRDDS. The pH-dependent solubility further complicates the formulation of CRDDS. Drugs in BCS classes III and IV are not acceptable candidates for this sort of formulation.

#### 11.8.1.2 Partition coefficient (*P*-value)

The *P*-value denotes the drug's fractionation into oil and aqueous phase, which is a crucial factor influencing passive drug diffusion through biological membranes. Drugs with high or small *P* values are not suited for CR; they should dissolve in both stages.

#### 11.8.1.3 Drug's p$K_a$

p$K_a$ is the feature that determines drug ionization in the GIT at physiological pH. High-ionized drugs, in general, are poor candidates for CRDDS. When opposed to ionized drugs, unionized/synthetic drugs are readily absorbed via biological sheaths. The p$K_a$ array for an acidic drug whose ionization is pH dependent is 3.0 to 7.5, while for a basic drug it is 7–11.

#### 11.8.1.4 Drug stability

CRDDS is a good candidate for drugs that are steady in acid/base, enzymatic degradation, and additional gastric juices. If a drug is degraded in the stomach and small intestine, it is not suitable for controlled-release formulations because the bioavailability of the concerned drug is reduced.

#### 11.8.1.5 Molecular size and molecular weight

Two important factors that influence molecular diffusibility across a biological membrane are molecular size and molecular weight. Drug diffusion is aided by molecular sizes less than 400 D, but sizes greater than 400 D cause problems.

#### 11.8.1.6 Protein binding

The drug–protein complex acts as a drug reservoir in the plasma. Drugs with high plasma protein binding are not good candidates for CRDDS because protein binding increases the biological half-life. As a result, there is no need to keep the drug flowing.

### 11.8.2 Biological factors

#### 11.8.2.1 Absorption

The homogeneity of absorption rate and degree is a significant consideration in developing the CRDDS. The rate-limiting step, however, is drugged release from the prescription form. To avoid dose dumping, the captivation speed should be faster than the release speed. Aqueous solubility, log $P$, and acid hydrolysis are all factors that influence drug absorption.

#### 11.8.2.2 Biological half-life ($t_{1/2}$)

In general, the drug has a short half-life, necessitating frequent dosing, and is a good candidate for a CR system. A drug with a long half-life necessitated dosing at regular intervals. Drugs with $t_{1/2}$ s of 2–3 h are ideal candidates for CRDDS. Drugs with $t_{1/2}$ s greater than 7–8 h are not suitable for CR systems.

#### 11.8.2.3 Dose size

Because CRDDS is designed to eliminate repeatable dosing, it must contain a higher dose than conventional dosage forms. However, the dose used in the conventional dosage form indicates the dose to be used in CRDDS. The volume of sustained dose should be as large as the acceptance criteria allow.

#### 11.8.2.4 Therapeutic window

Drugs with a slim therapeutic catalogue are ineffective against CRDDS. If the delivery system fails to control release, it will result in dose removal and eventual poisonousness.

#### 11.8.2.5 Absorption window

Drugs that show absorption from a precise section of the GI tract are poor candidates for CRDDS. Controlled-release drugs are those that are absorbed throughout the GIT.

#### 11.8.2.6 Patient physiology

The physiological state of the patient like gastrointestinal exhausting rate, private time, and GI infections impact the arrival of the medication from the measurements structure straightforwardly or on the other hand in a roundabout way.

## 11.9 Polymer used in controlled drug delivery system

Polymers are turning out to be progressively significant in the field of drug delivery [23]. The medicinal uses of polymers series from their application as covers in pills to thickness and stream-controlling specialists in fluids, suspensions, and emulsions. Polymers can be utilized as film layers to mask the horrendous flavor of a drug, to improve drug strength, and to adjust drug discharge attributes. The audit centers around the meaning of drug-polymer for controlled drug delivery applications. Sixty million patients profit from cutting-edge drug delivery frameworks today, getting more secure and more powerful portions of the prescriptions they require to battle various human diseases, including malignant growth. CDD arises when a polymer, whether natural or artificial, is carefully united with a drug or other lively agent in such a way that the lively agent is released from the material in a predetermined means. The active agent’s release may be persistent over an extended period, cyclical over an extended era, or activated by the environment or other exterior proceedings. In any case, the goal of controlling drug delivery is to attain additional actual rehabilitations while removing the possibility of together below and overdosing.

### 11.9.1 Polymers as biomaterials for delivery systems

To control the release of drugs and other active agents, a variety of materials have been used. The first of these polymers were designed for nonbiological applications and were chosen for their preferable physical properties such as [23]:

- Poly(urethanes) for bounciness
- Poly(methyl methacrylate) for toughness and clarity
- Poly(vinyl alcohol) for strength and hydrophilicity
- Poly(ethylene) for robustness and enlargement resistance
- Poly(vinyl pyrrolidone) for suspension properties

The material must be chemically passive and free of extractable impurities to be used satisfactorily in controlled drug delivery formulations. It must also have a suitable physical structure, with very little undesirable ageing, and be easily processable. The following materials are presently being used for controlled drug delivery:

- Poly(2-hydroxy ethyl methacrylate)
- Poly(*N*-vinyl pyrrolidone)
- Poly(methyl methacrylate)
- Poly(vinyl alcohol)
- Poly(acrylic acid)
- Polyacrylamide
- Poly(ethylene-*co*-vinyl acetate)
- Poly(ethylene glycol)
- Poly(methacrylic acid)

### 11.9.2 Polymers

- Insoluble, inert polyethylene, polyvinyl chloride, methyl acrylate, and ethyl cellulose
- Carnauba wax, stearyl alcohol, and castor wax are insoluble and erodible
- Hydrophilic celluloses include methyl cellulose, hydroxyl ethyl cellulose, sodium carboxy methyl cellulose, and sodium alginate

The drug is isolated as a hard particle within a permeable medium made of a water-insoluble polymer, such as polyvinyl chloride, in a matrix system.

Initially, drug particles on the exterior of the release component will be dissolved, and the drug will be quickly released. Following that, drug particles will be dissolved and released to the exterior of the release unit via diffusion in the pores at increasing distances from the surface of the release unit.

The main formulation factors that can be used to control the release speed from a medium system are the quantity of drug in the matrix, the sponginess of the release unit, and the drug's solubility. However, additional polymers designed primarily for medical applications have reached the CR arena in recent years. Several materials are intended to deteriorate within the body; a few examples contain

- PLA
- PGA
- PLGA
- Polyanhydrides
- Polyorthoesters

## 11.9.3 Advantages and disadvantages of controlled-release drug delivery

**Advantages**

1. Increasing the drug's bioavailability and duration of effect [15]
2. Little drug loss and degradation
3. Lowering the dosage frequency
4. Reduction of variations in drug concentration at the plasma level
5. A higher drug use rate
6. Patient compliance has improved
7. Keeping the drug concentration within a therapeutic range
8. Minimizing (eliminating) adverse reactions through local governance
9. Preventing the deterioration of drugs with a short half-life
10. Increasing patient adherence
11. Cheaper and more efficient drug delivery
12. Governance in disadvantaged communities becomes easier

**Disadvantages**

1. The materials' potential toxicity
2. Negative degradation products
3. The requirement for surgical intervention in the deployment or removal of systems
4. Patients' dissatisfaction with DDS device use
5. Expensive end product as a result of transportation costs or manufacturing procedures

## 11.10 Types of DDSs

Current drug delivery systems can be classified as follows [24].

### 11.10.1 Oral DDSs

Because of the apparent benefits of simplicity of administration, greater patient compliance, and convenience, the oral route is one of the most often utilized modes of drug delivery. There is little or no control over drug release from instant release (IR) dosage forms, which frequently results in continually shifting, unpredictable, and frequently sub- or supra-therapeutic plasma concentrations. A modified release (MR) dosage form is one in which the drug-release properties of time sequence and/or position are tailored to achieve healing or comfort goals that standard dosage forms do not provide. MR dosage formulations are classified as either extended-release (ER) or delayed-release (DR).

### 11.10.2 Pulmonary delivery systems

Until now, pulmonary delivery was largely employed to treat respiratory diseases. Recently, the inherent capacity of the lungs to transport chemicals into the bloodstream has been used to deliver drugs to systemic circulation. This approach is a noninvasive alternative to hurting vaccinations that can result in a speedy beginning of action and high bioavailability. There are three types of inhalation devices: pressurized metered-dose inhalers (MDIs), nebulizers, and dry powder inhalers (DPIs). MDIs include drugs in the form of a solution or a suspension of tiny particles in a highly pressurized liquid propellant. A metering valve emits the drug through an aperture. Nebulizers, on the other hand, do not require propellants and may produce vast amounts of tiny droplets that can penetrate the lung. DPI is a device that delivers the drug to the lungs in the form of a dry powder and necessitates some procedure to prepare a measured amount of powder for the patient to consume. The drug is often stored in a capsule for manual loading or in a patented form from within the inhaler itself. Once loaded or activated, the patient inserts the inhaler's mouthpiece into their mouth and takes a deep breath, effectively delivering the drug.

### 11.10.3 Transdermal drug delivery systems

During the last decade, there has been a lot of interest in systemic drug delivery by the transdermal method. Transdermal DDS (TDDS) transport drugs into the systemic circulation through the skin at a predefined pace, bypassing processing in the gastrointestinal tract and liver. As a result, the number of active components required for transdermal distribution may be much lower than for oral systems. TDDS ensures consistent blood levels for one to seven days and improves patient compliance.

### 11.10.4 Injectables

The genomics research effort is predicted to speed the identification of novel therapeutic biomolecules, putting increasing demand on the development of drug delivery methods. This drug class is distinguished by its enormous size, fragile nature, short biological half-life, and restricted ability to penetrate cell membranes. These features, as well as the methods of administration of biopharmaceuticals, may limit their therapeutic applicability to certain disease conditions that merit the price and difficulty of regular injection. Several parenteral depot formulations based on biodegradable polymers, such as microspheres and implants, are now commercially accessible to increase the effectiveness and lengthen the action of peptide and protein drugs.

### 11.10.5 Ophthalmic (ocular) drug delivery systems

Ophthalmic DDSs have recently received significant interest since they need less frequent administration than eye drops, provide continuous drug delivery, and lengthen the duration of therapeutic activity by improving corneal absorption. Viscous fluid and hydrogel delivery systems, ocular inserts, and contact lenses are all examples of ocular delivery systems.

### 11.10.6 Parenteral

Kushwaha discovered that the timeline of drug discharge and release is dependent on the amount of drug loaded into the matrix, the solution, and the medium discharge by combining polymer polyvinyl alcohol with natural macromolecule gum *Arabica*. The advantage of this system is that the plasticizer, homopolymer, and cross-linker composition can be adjusted to optimize the system’s release kinetics. Chitosan 45–300 microspheres have been used to deliver regulated progesterone.

## 11.11 Different routes of drug administration

Dosage forms can be administered via various routes depending on the target site, duration of treatment, and physicochemical properties of the drug. Tablets, capsules, pills, ointments, syrups, and injections are the most common dosage forms. Table 11.3

lists the various routes of drug administration. The preferred route of drug administration is determined by three factors: the part of the body being treated, how the drug works within the body, and the drug's solubility and permeability. Certain drugs, for example, are easily destroyed by stomach acids after oral administration, resulting in poor bioavailability. As a result, they must be administered parenterally instead. Drugs are 100% bioavailable when administered intravenously.

**Table 11.3:** Drug administration routes [18].

| | |
|---|---|
| Buccal | Held inside the cheek |
| Sublingual | Placed below the tongue |
| Enteral | Delivered directly into the stomach or intestine |
| Inhalable | Breathed in through a tube or mask |
| Nasal | Given into the nose by spray or pump |
| Ophthalmic | Given into the eye by drops, gel, or ointment |
| Otic | Given by drops into the ear |
| Rectal | Inserted into the rectum |
| Vaginal | Inserted into the vagina |
| Topical | Applied to the skin |
| Transdermal | Given through a patch placed on the skin |
| Infused | Injected into a vein with an IV line and slowly dripped in overtime |
| Intramuscular | Injected into the muscle with a syringe |
| Intravenous | Injected into a vein or an IV line |
| Subcutaneous | Injected just under the skin |

## 11.12 Nanofibers for drug delivery

In recent decades, nanofibers have become a sophisticated fiber with widespread application and potential in the biomedical fields. Innate immune response to pathophysiology, such as a wound, causes the healing process. Depending on the chronic state, the typical time for wound healing is two to three days. Pathological manifestations that could cause a delayed or ineffective palliative process are risked by air moisture and microbes. It helps to expedite the healing process when an external agent can offer balanced moisture and promote cell proliferation through microbial infiltration or antibacterial activity. In addition to these characteristics, the ideal material should be straightforward, affordable, and repeatable. The use of electrospun NFs in the treatment of wounds has proven to be a successful method. High surface area and nanoporosity NFs can load powerful drugs or enzymes. The ES procedure was first patented in 1902 by Cooley and Morton, and Formhals [25] continued to develop it in the direction of commercialization between 1934 and 1944. NFs are also used in modern cosmetics as masking agents and as tissue scaffolds, among other biomedical applications. NFs are thus excellent candidates for managing and treating wounds [26]. ES technology is appealing for TE, drug delivery, and other biomedical applications due to its ease of use, the high surface-to-volume ratio of the NF lattice, a wide variety of functioning polymers, and potential for large-scale manufacture (Figure 11.9). Table 11.4 provides a concise history of ES's development.

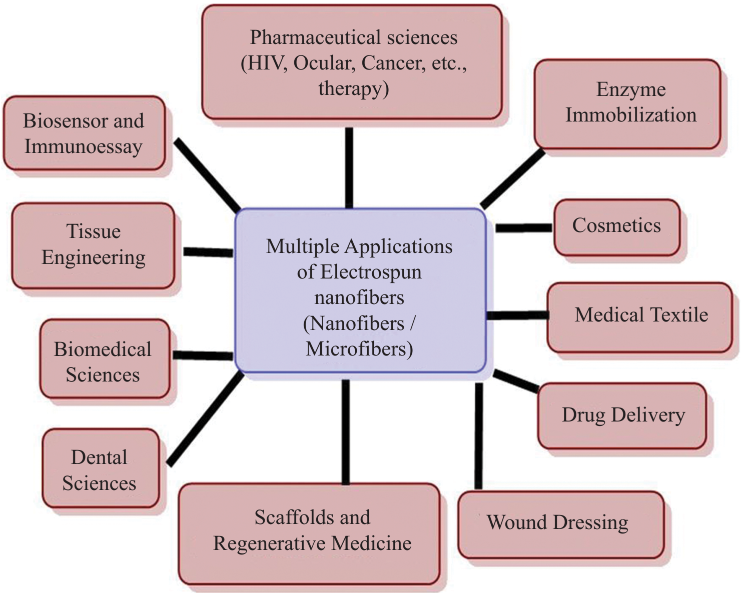
Pharmaceutical sciences (HIV, Ocular, Cancer, etc., therapy)
Biosensor and Immunoessay
Enzyme Immobilization
Tissue Engineering
Multiple Applications of Electrospun nanofibers (Nanofibers / Microfibers)
Cosmetics
Medical Textile
Biomedical Sciences
Drug Delivery
Dental Sciences
Scaffolds and Regenerative Medicine
Wound Dressing

**Figure 11.9:** Various applications of electrospun nanofibers [27].

**Table 11.4:** Short history of electrospinning development [28].

| Year | Remarks |
|---|---|
| 1600 | William Gilbert reported the formation of cone-shaped water droplets in the presence of an external electric field |
| 1700 | Stephen Gray observed the electro-hydrodynamic atomization of a water droplet. |
| 1747 | Abbe Nollet performed the electrospraying experiment during which water could be sprayed as an aerosol. |
| 1887 | Charles Boys generated electrospun fibers from a viscoelastic liquid |
| 1902 | John Cooley and William Morton filed two patents to describe a prototype of the setup for electrospinning |
| 1938 | Electrospun nanofibers were first implemented for the development of aerosol-capturing air filters |
| 1964–1969 | Geoffrey Taylor reported the formation of the Taylor cone |

**Table 11.4** (continued)

| Year | Remarks |
|---|---|
| 1980s | Donaldson Company Inc. produced and sold filters composed of electrospun fibers for air filtration |
| 1990s | Darrell Reneker and Gregory Rutledge demonstrated that many different organic polymers could be electrospun into nanofibers |
| 2000s | Development of composite and ceramic fibers, core–sheath and hollow fibers, aligned fibers, and continuous yarns of fibers |
| 2010s | Industrial production lines based on multiple-needle electrospinning and needleless electrospinning |

## 11.13 Principle of electrospinning

ES involves an electrohydrodynamic process, during which a liquid droplet is electrified to generate a jet, followed by stretching and elongation to generate fiber(s).

### 11.13.1 Fundamentals of electrospinning

The fundamental aspects of an ES system are a high-voltage power source (HV), a syringe with a needle, a metal collector, and a syringe pump. Figure 11.10 depicts a schematic illustration of a fundamental configuration. Due to the HV's electric force, the solution will draw itself out. The electric force of the solution overcomes the surface tension, and the fibers then appear at the top of the Taylor cone, a conical drop. As the solvent evaporates, the fiber stretches and lengthens on its path to the collector, resulting in the arrival of solid ultrafine fibers [29].

Different techniques can be used to collect mats that are randomly oriented or parallel-aligned; one of them to get aligned fibers is to use a cylinder collector with a fast rotation speed. Additionally, inserting an additional electrode or electrical field on the fiber trajectory will aid in the generation of aligned fibers, and using a narrow wheel with a sharp edge and a frame collector are also highly helpful in the process. The ES setup has several inherent qualities that will influence the process and have an impact on the morphology and structure of the electrospun materials. They are the needle diameter, adapted force fields, work space among the needle tip and collector, proceed degree, speed collector (if the system has one), and any rotatory drums. The kind of solvent, the concentration and molecular weight of the polymer, the conductivity, and the viscosity of the solution are other solution intrinsic factors that have a significant

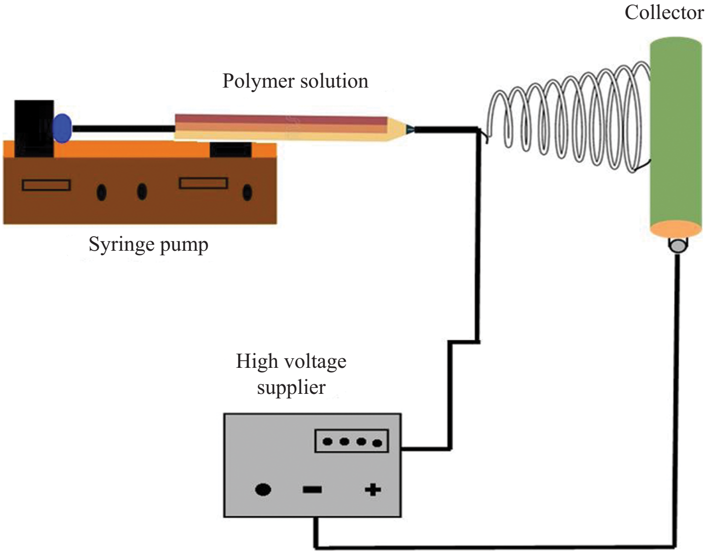

**Figure 11.10:** Pictorial view of basic electrospinning setup [29].

impact on the quality of the fibers. The third group of factors to take into account is the environmental characteristics including humidity and temperature.

## 11.14 Standard electrospinning setup

An ES system typically consists of three main parts: a high-voltage power source to charge the polymer solution, a syringe with pumps to feed the polymer solution through a capillary coupled to a syringe filled with the polymer solution, and a grounded collector to deposit NFs [30]. In this procedure, the solution (particulate suspension, polymeric, or molten solution) is extracted from the needle tip of a syringe carrying the solution at a steady pace. The typical ES setups for vertical (Figure 11.11a and b) and horizontal (Figure 11.11c) are shown schematically in Figure 11.11.

The direction of the fibers and the number of beads are the key distinctions between the upward and downward electrospinning (DWEs) setups. In contrast to the downward method's unpredictable orientation, the fiber collection from an upward ES setup will adopt a consistent pattern. On the other hand, the upward arrangement will result in a lower amount of bead creation than the descending approach. Due to its ease of optimization and operational monitoring, the downward ES setup is best suited for small-scale laboratory applications. In contrast, the upward setup has been chosen for industrial production because it is difficult to produce NFs in large quantities using a single conventional needle.

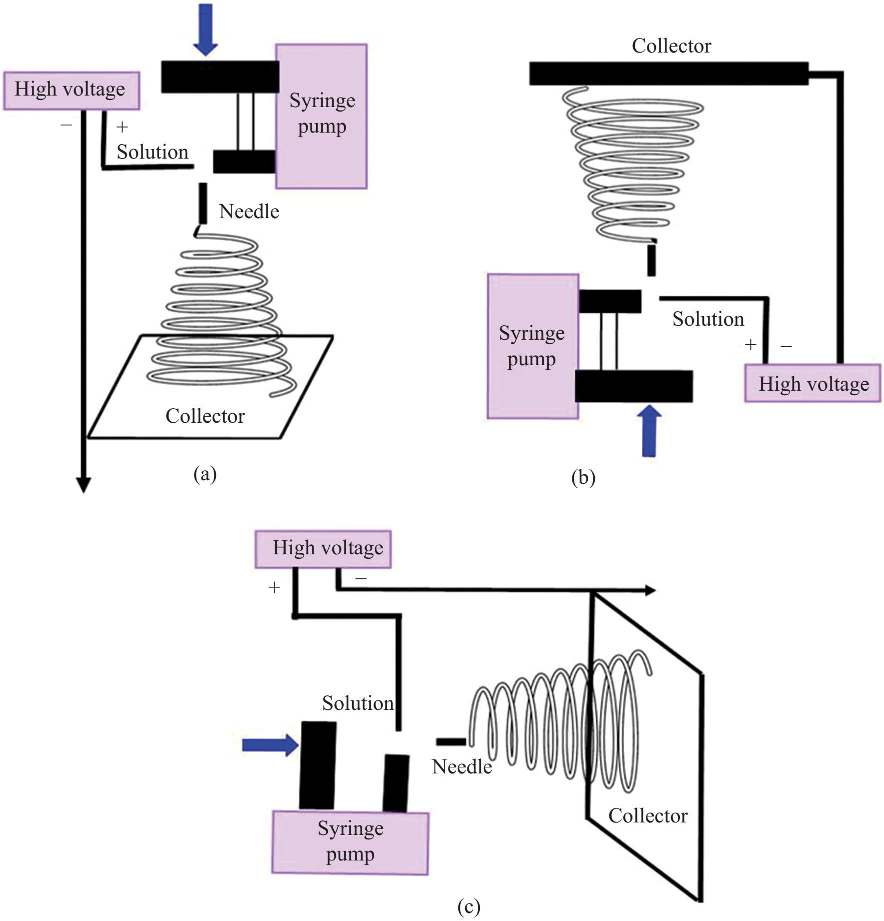
High voltage
−
+
Solution
Syringe pump
Needle
Collector
(a)
Collector
Syringe pump
Solution
+
−
High voltage
(b)
High voltage
+
−
Solution
Needle
Syringe pump
Collector
(c)

**Figure 11.11:** An illustrative outlook of (a) downward electrospinning, (b) upward electrospinning, and (c) horizontal electrospinning setup [30].

## 11.14.1 How nanofibers can be electrospun?

Electrostatic repulsion and surface tension exert opposing pressures on the droplet at the needle’s tip. The pendant droplet at the tip of the needle will change into a conical droplet known as the Taylor cone when the electrostatic repulsion begins to outweigh the surface tension of a fluid. When the electrostatic force overcomes the surface tension, a fine-charged polymeric jet of the solution will eject from the tip of the needle. The convergence of these two forces extends the jet stream and causes it to whip, which causes the solvent to evaporate. As a result, the jet stream constantly grows into a long, thin filament. A consistent fiber is created when this filament freezes and is subsequently placed onto a grounded collector.

# 11.15 Influence of the electrospinning parameters

## 11.15.1 Processing parameters

### 11.15.1.1 Applied voltage

A high voltage must be provided and regulated throughout the ES process to produce smooth, ultrafine fibers free of flaws like beads and other imperfections. Most works report applying voltages for their systems between 10 and 25 kV [29]. While many writers agree that other factors affect electrospun materials more, some claim that when the applied voltage is increased, the average diameter of the fiber will also rise, which may cause a rough surface and the development of beads. The applied voltage must be taken into account as a crucial factor in the ES process despite some authors claims that a higher applied voltage would result in fibers with a smaller diameter. This is a contentious issue that is difficult to resolve due to the wide range of systems that can be formed with a large number of polymers as well as the numerous parameters that should be controlled.

### 11.15.1.2 Flow rate

In general, a suitable flow rate that should allow for enough polarization time will result in a well-formed fiber. Zargham et al [52]. study showed that the droplet size, the trajectory of the jet, and the maintenance of the Taylor cone varied in the fabrication of nylon 6 NF as the flow rate changed, and as a result, the morphology, diameter size, and distribution of the fiber were all influenced by the flow rate of the polymer solution.

### 11.15.1.3 Work distance

The space between the needle tip and the collector should be large enough to allow the polymer to solidify before it reaches the collector, but not too large that beads rather than fibers form.

## 11.15.2 Solution parameters

### 11.15.2.1 Concentration

Another factor that is vital to ES is polymer concentration; if the concentration is below a certain level, the tensional surface cannot be maintained, preventing the creation of fibers. Smooth fiber without defects will develop at the proper concentration, but below this critical concentration, we can acquire fiber with flaws resembling beads, and the diameter of the fiber likewise rises as the polymer concentration does. According to several studies, altering the polymer concentration and voltage results in the creation of flat/ribbon morphologies.

### 11.15.2.2 Polymer molecular weight

The polymer MW measures the degree to which polymer chains are entangled in solutions or the viscosity of such solutions. It has been discovered that this has a substantial impact on the electrospun polymer's structure and also has an impact on the jet branching, elongational flow, and bending instability.

### 11.15.2.3 Viscosity

This is a crucial characteristic that provides flow resistance and, as a result, helps to define the fiber shape.

### 11.15.2.4 Conductivity

To boost the conductivity and generate fibers free of defects and with smaller diameters, the polymer jet's capacity to transfer charge depends on the ions in the solution.

# 11.16 Different methods for manufacturing nanofibers

Various methods can be used to process NFs including [31]:

### 11.16.1 Drawing

Stretching of a polymer in solution form is done while pulling a single NF. Only viscoelastic materials have been spun into NFs using this technique. A cooling mechanism is required if the polymer is in molten form to harden the fiber. On the other hand, if the polymer is a solution, a heating mechanism is required to cause the solvent to evaporate. Only a lab scale should be used for this extremely slow procedure.

### 11.16.2 Template synthesis

This approach makes use of nonporous membranes with cylindrically shaped pores. These pores have uniform diameters. Solid polymers with a diameter equivalent to the size of a porous material are created.

### 11.16.3 Phase separation

There are five processes in this procedure: solvent extraction, polymer dissolution, polymer gelation, freezing, and freeze-drying. With this method, fiber dimensions are uncontrollable. This only appears to work on a lab scale.

### 11.16.4 Self-assembly

Self-assembly is the technique used to create peptide NFs. Only lab-scale NF synthesis is suitable for this extremely complicated procedure.

### 11.16.5 Electrospinning

The following is a list of ES equipment:
1. High-voltage DC power source
2. A syringe pump
3. Spinneret (a small diameter needle connected to the syringe)
4. Metal collector

Before ES, the polymer is dissolved in a solvent, and when it is fully dissolved, it creates polymer solution. To begin the ES process, the polymer fluid is then injected into the syringe tube. The hollow needle is linked to the positive terminal of the DC power source, while the metal collector is attached to the negative terminal. The charged jet of fluid is expelled from the tip of the Taylor cone as the electric field strength increases and the repelling electrostatic force defeats the surface tension. The extruded polymer fiber's diameter decreases as a result of the discharged polymer jet's instability and elongation process, which causes the polymer in the jet to become incredibly long. The polymer in the jet is dried as the solvent used to dissolve it evaporates. The solvent evaporation is influenced by the temperature inside the chamber, the solution vapor pressure, and the distance between the tip and the collector. Therefore, stable environmental conditions are crucial for producing high-quality NFs. For a needle ES arrangement, the maximum applied voltage is typically less than 30 kV and is also strongly humidity dependent.

An ES invention that can produce NFs on a significant scale is needleless ES. ES of NFs directly from an open fluid surface is referred to as needleless ES. The needleless fiber generator (spinneret) shapes many planes simultaneously without the capillary effect that is frequently associated with needle ES. The fly started in needleless ES is a self-constructed process that occurs on a free fluid surface, making it difficult to regulate the spinning process. Numerous spinneret forms with varying degrees of productivity have been developed for the needleless ES technique.

The needle ES method's poor production rate, which is often less than 0.3 g/h, is another issue it causes. The amount of NFs produced with the needleless ES process is 250 times greater than with needle ES. The needleless ES spinneret's form has an impact on production. Production rates of 2.5–100 g/h may be reached using various spinneret designs.

## 11.17 Other methods of nanofiber production

### 11.17.1 Traditional ES

Three essential parts are required for classic ES: a high-voltage source, a syringe pump (nozzle), and a grounded collector [32]. To provide accurate observation of the Taylor cone, the nozzle is preferably a metallic needle with a blunt tip. During the ES process, a predetermined amount of polymeric solution is initially put into the appropriate syringe before being transferred to the syringe pump (ideally dissolved in a volatile solvent with a *w*:*v* ratio). The droplet's elongating conical form is then seen once a high voltage is given to the nozzle tip. When the surface tension of a droplet is overcome by electrostatic force, a Taylor Cone forms at the tip of the nozzle. A charged jet then ejects from the Taylor Cone, causing NFs to form and the solvent to quickly evaporate.

Numerous variables, including syringe pump flow rate, polymer solution concentration, collector type, solution viscosity, applied voltage, the distance between the collector, and the nozzle, nozzle diameter, etc., can affect how the generated fibers look. And each of these elements has a big impact on fiber morphology. For instance, by raising the voltage, electrospraying rather than ES might result from low polymer concentrations, and raising the flow velocity can also lower the fiber diameter. To produce fibers with the highest performance, all of these factors had to be tuned before the ES process started.

### 11.17.2 Multijet electrospinning

In the literature, this technique is often referred to as “Multi Needle ES.” Its creation was driven by a need to increase production and create composite fibers that are impervious to ordinary solvents. In this method as in the other ES methods, the needle arrangement, needle number, and needle diameter all play a significant influence. Unfortunately, this approach has one significant flaw: the multineedle system causes a high repulsion among the jets. This repulsion, which is brought on by the Coulomb force, may result in poor fiber quality and lower fiber deposition. Needles must be positioned at the proper distance to prevent this issue.

### 11.17.3 Coaxial electrospinning

By utilizing either several syringe pumps or a single syringe pump with various feeding systems, the coaxial ES technique is utilized to create core–shell NFs. A polymer and a composite solution, one of which is used to create the shell and the other to create the core sections, can primarily be used separately, or two distinct polymer solutions can be utilized as precursor solutions. The polymer solution, which will constitute the shell portion of the composite NFs, will be stretched and will produce viscous tension under the control of the electrostatic repulsions between the surface charges. The polymer solution, which will eventually become the core component, will immediately be stretched when this tension is applied to the core layer. As a consequence, composite jets with coaxial structures will be created.

### 11.17.4 Melt electrospinning

The melt ES approach needs a heating source in addition to the standard ES setup such as heat guns, lasers, or electrical heating equipment. A steady heat source is required to maintain the molten condition of the polymer solution. The process of fiber creation is the main distinction between melt ES and the traditional ES approach. In melt ES, a molten polymer is utilized in place of a solution, and the required result is achieved after cooling; in traditional ES, fibers are created by the solvent evaporation process. The factors that determine the fiber diameter, fiber quality, and ES procedure using the traditional ES method are the same except for this distinction. The lack of a solvent system and the fast flow rate of the polymer are the main benefits of this approach. The polymers that lack a suitable solvent at room temperature can be processed using this approach.

### 11.17.5 Centrifugal electrospinning

The terms force spinning and rotary spinning are also used to describe centrifugal ES. Centrifugal ES differs from traditional ES in that the electric field is substituted by a centrifugal force in this approach. With one small exception, fiber formation is nearly identical to that of conventional ES. Instead of an electric field, a Taylor cone is formed when the rotation speed exceeds the critical point and a liquid jet is subsequently blasted from the needle. Therefore, along with the nozzle configuration, collector type, temperature, etc., the rotation speed is one of the crucial factors that affects the quality of the fibers. Due to the system's usage of centrifugal force rather than the electric field, there are various benefits. With this technique, a wide range of conductive and nonconductive polymers may be electrospun. This technology considerably reduces safety-related problems because the high-voltage is not required.

### 11.17.6 Magnetic-field-assisted electrospinning

By adding magnetic nanoparticles to the polymer solution or employing polymers that can react to magnetic fields, magnetic characteristics are obtained in this approach. Helmholtz coils, magnetic field responder systems, or two parallel permanent magnets can all produce this magnetic field. Another method for using magnetic-field-assisted ES is to incorporate nonpolymeric materials (such as metals and ceramics) in addition to mixing various polymers. This procedure reportedly results in more consistent fiber maintenance. Because of the magnetic field's direction, fiber splitting from the jet may be avoided by applying a magnetic field. Smaller fiber diameter is supported by the process's high speed.

### 11.17.7 Emulsion electrospinning

Emulsion ES is developed to produce fibers from two immiscible solutions. A strong swirling motion is necessary to emulsify these immiscible liquids. A glass syringe fitted with a needle and a high-voltage source is then filled with this emulsion. Due to the characteristics and immiscible phases of the two immiscible solutions present in this emulsion, fiber production is challenging. Nanoparticles and surfactants like detergents and sodium dodecyl sulfate are typically utilized to get around these problems. A significant downside of this approach is the ongoing requirement for the emulsion to maintain stability during the ES process.

### 11.17.8 Wet spinning

An alternate technique for creating NFs from polymers produced from natural sources is wet spinning (WS). Compared to any ES approach, it is considerably more affordable and straightforward. The spectrum of polymers from natural or synthetic sources handled by WS is increased since it is much simpler to load therapeutic chemicals into fibers without the utilization of a high-voltage source. Wet-spun NFs can be combined to create biodegradable and biocompatible scaffolds with a 3D network for regenerative medicine techniques; however this method is still under development. The essential component of this technology is the extrusion of a polymeric solution into a solvent- or solvent–nonsolvent-containing coagulation bath.

The primary objective is to produce coagulating fibers in the coagulation bath that, as the extrusion process progresses, solidify as a constant fiber. The typical WS setup consists of a needle, a syringe pump, a coagulation medium, and a polymeric solution. For fiber coagulation to begin, the needle has to be fully submerged in the medium.

## 11.18 Characterization techniques for electrospun nanofibers

An important step in evaluating if electrospun NFs are effective at delivering drugs is their characterization [33]. The difficulty of drug diffusion from NFs may be visualized using scanning electron microscopy and field emission scanning electron microscopy. These techniques can show the fiber diameter, degree of smooth surface, structure, and pore density. For instance, a layered construction creates a steady release while reducing the burst release. The differential scanning calorimeter and X-ray powder diffraction have both been used to determine whether the drug is crystallized or not. The ability of electrospun NFs as a possible solid dispersion and noncrystal form of the drug is advantageous for the drug's steady release. Fourier transform infrared spectroscopy (FTIR) has been used in the spectroscopic investigation to confirm the structure and stability of fibers. By speculating on hydrogen bonding, FTIR demonstrates compatibility between the elements and offers a method to compare different polymers and choose one that is more suitable.

## 11.19 Stimuli-responsive nanofibers in drug delivery applications

For many therapeutic applications, a smart system is offered by a stimuli-responsive nanocarrier [27]. Typically, in response to triggering signals, stimuli-responsive systems can accelerate or initiate the release of therapeutic drugs (intrinsic or extrinsic).

pH, temperature, enzyme activity, and oxidative stress are examples of internal signals, whereas magnetic field, light, and heat are examples of external stimuli. These stimuli are used as a prompting component in drug delivery systems for nanocarriers. Therapeutic molecule release is regulated both spatially and temporally. Here, we provide a concise description of the many triggers used to cause NFs to release drugs. Table 11.5 depicts the delivery methods that release active molecules in reply to particular stimuli at the target region.

### 11.19.1 pH-responsive systems

Drug delivery devices have been programmed to release drugs when the pH varies. To release therapeutic compounds in response to variations in ambient pH, polymers having ionizable groups (carboxylic, sulphonate, and amino) go through structural and/or solubility variations. Thermolabile drugs work well in pH-responsive systems. With pH-sensitive polymers like poly(ε-caprolactone), PLGA, and silk, several NF systems have been created. Weak polyacids and weak polybases are two different categories for polymers containing ionizable groups. While poly(*N*,*N*-dimethylaminoethyl methacrylate) and poly(*N*,*N*-diethylaminoethylaminoethyl methacrylate) are pH-responsive polymeric bases, poly(acrylic acid) and poly(methacrylic acid) are often utilized as pH-responsive polyacids.

### 11.19.2 Light-activated systems

Since it is possible to accurately adjust the intensity of light, it may be utilized as an external stimulus. Drug delivery methods have frequently employed light-sensitive materials. These delivery methods include the formulation of light-sensitive groups that react to a certain wavelength, such as azobenzene, stilbene, and triphenylmethane, the biodegradable, hydrophilic, and biocompatible light-sensitive polymers. Nevertheless, the drawbacks of light-sensitive polymers contain uneven reactions brought on by chromophores being dissolved during system expansion or contraction and a sluggish response to stimuli. Based on the wavelength that causes the phase change, these polymers may be classified as ultraviolet (UV)- and visible-light-sensitive systems. Due to their accessibility, safety, and convenience of use, visible light-sensitive polymers are chosen over UV-sensitive ones.

### 11.19.3 Thermoresponsive systems

Increased body temperature has been linked to several diseases including cancer. A modest change in temperature causes thermosensitive polymers to abruptly shift in solubility in thermo-responsive drug delivery devices. At a temperature below the lower critical solution temperature, thermosensitive polymers show a phase shift in the solution. The polymer material may undergo conformational changes as a result of this mechanism, triggering drug release. The most commonly used thermosensitive polymers include poly (*N*-isopropyl acrylamide), poly(*N*,*N*-diethylacrylamide), poly(*N*-vinylalkylamide), poly(*N*-vinyl caprolactam), pluronics, polysaccharide, chitosan, and PLGA/polyethylene glycol (PEG) triblock/pentablock copolymers. The elimination of hazardous organic solvents, the capacity to deliver both hydrophilic and lipophilic drugs, and prolonged drug release are the main benefits of thermosensitive polymeric systems.

### 11.19.4 Ultrasound-responsive systems

A tiny part of the body can be treated with ultrasonic energy at various intensities. A medium that concentrates, reproduces, and diverts the ultrasonic waves is part of the ultrasound mechanism. The capacity of ultrasound-sensitive vehicles to penetrate far into the human body, their invasive nature, and their controllability make them potentially useful in the treatment of cancer. However, repeated usage of this technology may still be necessary for clinical application, which has several drawbacks such as patient nonconformity, a higher hazard of adverse effects from sonication, and a corresponding expense.

### 11.19.5 Enzyme-responsive systems

In the control of cells, enzymes are essential. These proteins are crucial for formula formation in addition to serving as significant therapeutic targets. Drugs can be delivered or released via drug delivery systems, particularly nanocarriers, through enzymatic conversion of the vehicles. For instance, a target location may release more drugs if the amount of an enzyme is higher there or if the activity of an enzyme is higher in sick tissue.

### 11.19.6 Oxidative stress-responsive systems

Hydrogen peroxide ($H_2O_2$) build-up is the primary source of oxidative stress and may catalyze the delivery of certain drugs. Oxidation-responsive polymers have a lot of promise for use in drug delivery and the biomedical industry. Although oxidative stress-responsive NF systems are still developing slowly, future stimuli-sensitive treatments for oxidative stress-related illnesses such as posterior eye segment disorders can target this stimulus.

**Table 11.5:** Stimuli-sensitive nanofiber delivery systems in pharmaceutical and biomedical applications [27].

| Stimulus | Active moiety | Polymer | Target diseases | Comments | References |
|---|---|---|---|---|---|
| pH | Doxorubicin | Silk | Breast cancer | Thixotropic silk hydrogels offer better injectability to facilitate prolonged release, pointing to interesting uses for localized chemotherapy. | [34] |
| | Doxorubicin | Poly(ε-caprolactone) (PCL) | Gastric cancer and vaginal delivery of antiviral drugs or anti-inflammatory drugs | It may be possible to administer anticancer drugs physically for the treatment of gastrointestinal cancer and antiviral or anti-inflammatory drugs vaginally while minimizing their potentially harmful side effects with the use of pH-responsive drug delivery systems based on PCL nanofibers. | [35] |
| | Etravirine and TDF | Cellulose acetate phthalate (CAP) | Human immunodeficiency virus (HIV) | We demonstrate that the antiviral medications released along with the CAP, which has been known to have intrinsic antimicrobial action, effectively neutralize HIV in vitro by carefully examining the pH-dependent release profile. | [36] |
| | | Polyurethane (PU) and CAP | HIV | For men who are sensitive to endoscopic drug delivery, CAP makes the fiber's core–shell structure pH-responsive. | [37] |
| | Paracetamol | Triblock copolymers | Various applications | These fibers are possible implanted drug carriers and useful coverings for medical devices due to their local delivery and regulated release patterns. | [38] |

| | | | | | |
|---|---|---|---|---|---|
| Temperature | Paclitaxel | PCL | Liver cancer | The strategy described here combines nanoparticles and nanofibers to cure cancer. | [39] |
| | Ibuprofen | Poly(*N*-isopropylacrylamide) and PCL | Various applications | For future pharmaceutical applications, composite design can offer a cutting-edge method to decrease the burst effect in drug delivery systems. | [40] |
| | Ketoprofen | Poly(*N*-isopropylacrylamide), ethyl cellulose | Various applications | This work showed PNIPAAm/EC fibers electrospun in a composite are useful and biocompatible materials for tissue engineering and drug delivery systems. | [41] |
| Light | Polymethylmethacrylate (PMMA) nanofibers doped with silver nanoparticles (AgNPs) and meso-tetraphenylporphyrin (TPP) | PMMA nanofibers doped with AgNPs and TPP | Antibacterial | The described material provides a potential choice for the photodynamic inactivation of bacteria according to the results. | [42] |
| | Fluorescein isothiocyanate-bovine serum albumin | Poly(*N*-isopropylacrylamide-*co*-polyethylene glycol acrylate) | | These findings imply that applications like drug delivery can make use of light-responsive fibrous nanocomposites. | [43] |
| Moisture | Maraviroc | Polyvinylpyrrolidone or poly (ethylene oxide) | HIV | When exposed to moisture, moisture electrospun materials can release maraviroc quickly, and when the drug is electrospun into polyvinylpyrrolidone fiberswith an excipient wetting agent, the drug is delivered more quickly (in less than 6 min under sink circumstances). | [44] |

(continued)

**Table 11.5** (continued)

| Stimulus | Active moiety | Polymer | Target diseases | Comments | References |
|---|---|---|---|---|---|
| Hydrogen peroxide | Rhodamine B | Polyvinyl alcohol (PVA)/ polyoxalate (PVA/POX NFs) blended | Inflammatory diseases | The overproduction of hydrogen peroxide by a variety of inflammatory disorders can be targeted with nanofibrous PVA/POX, which also has the potential to be employed as a local drug delivery system. | [45] |
| pH + glucose | Lectins | ConA and Jacalin | Removal of toxins from the solution | As a result of their simplicity of modification, these functional nanofibers can be utilized to quickly remove particular proteins or toxins from a solution. | [46] |
| pH + temperature | Nifedipine (NIF) | Poly(*N*-isopropylacrylamide)-*co*-poly(acrylic acid) [P(NIPAAmco-AAc)] |  | By modifying the aqueous medium’s temperature or pH value and adding the hydrophobic PU, it is possible to effectively control the amount of NIF released from the nanofibers. | [47] |

### 11.19.7 Carbohydrate-responsive systems

Drug delivery methods that are sensitive to carbohydrates have gained popularity. These systems are built to induce the release of a drug in response to particular molecules, such as carbohydrates (glucose, fructose, and mannose). Due to their usage in both sensing and delivery (insulin) applications, these polymers have attracted a lot of attention. Despite these benefits, the main drawbacks include biocompatibility problems and a short response time.

### 11.19.8 Multiresponsive systems

Exciting advancements in the realm of stimuli-sensitive drug delivery include dual- or multiresponsive nanocarriers. In general, these systems can react orthogonally to two or more inputs. pH and ionic strength, pH and thermo-responsiveness, or pH and carbohydrates are all involved in the combination. These two monomers that are responsive to various stimuli are combined to create these dual-responsive systems. The pH- and temperature-responsive NFs are the most researched multiresponsive systems. One possible benefit of dual-responsive systems is the ability to load the carrier with one stimulus while triggering the release with a different stimulus.

## 11.20 The application of electrospun nanofibers in drug delivery systems design

Creating nanofibers for use as drug carriers in DDSs has drawn a lot of interest in ES [48]. Electrospun nanofibers have two key characteristics that make them desirable as DDSs. First off, when taking into account the porosity of the electrospun nanofibers, the already high surface area to volume ratio of nanofibers is considerably boosted. Higher drug uptake, which is often linked with other traditional methods, is overcome by larger surface areas. Second, altering the processing variables allows for the control and "tailoring" of matrix parameters including diameter, porosity, and morphology. The drug-release profile can be controlled by the type of materials used. Several drugs, including antibiotics and cancer treatments proteins, anti-inflammatory substances, and agents and DNA have been added to electrospun yarn carpets and sent to the body's intended objectives. Additionally, carriers can provide site-specific distribution of many drug consumption.

Numerous reports on the use of drug-loaded electrospun nanofibers as drug delivery devices and some in vivo studies conducted in the field of cancer research. Xu and associates, as well as Ranganath and Wang, have created drug delivery implants that offer a site-specific continuous release of an anticancer medication to a tumor. Another illustration is the targeted administration of heparin using electrospun nanofibers to the location of a vascular graft. Additionally, the potential use of electrospun fiber mats as wound dressings or transdermal drug delivery devices has been explored. Utilizing electrospun fibrous scaffolds that are loaded with antibiotics, the prevention of postoperative abdominal adhesions and infection has been studied.

### 11.20.1 Drug loading and drug release from electrospun nanofibers

To manage the drug-release kinetics, it has been reported to load drugs into electrospun nanofibrous matrices utilizing a variety of techniques, including coating, embedding, and encapsulation. If the drug and polymer are soluble in the same solvent, the drug can be dissolved right into the polymer solution; if not, the drug can be presolubilized in a tiny amount of another solvent before being added to the polymer solution. When such solutions are electrospun, the drug is embedded in the created nanofiber scaffold. A different strategy for drugs and polymers insolubility in a common solvent, the drug can be dissolved in a solvent that is immiscible with the polymer's solution, and the two solutions can be loaded in separate capillaries to be electrospun coaxially. Alternatively, the two solutions can be blended to create an emulsion that can be electrospun. This method results in the drug being encapsulated in the polymeric matrix. After ES, there is still another method for loading the drug. By soaking the electrospun nanofibers in a drug solution, the drug is absorbed into the nanofibers in this approach. Drugs are primarily released from nanofiber matrices by one of three mechanisms: desorption off the nanofiber surface, diffusion through the nanofibers' channels and pores, or matrix disintegration. By altering the numerous processing factors during ES, it is possible to manage the nanofiber diameter, porosity, geometry, and morphology as well as the drug-release kinetics.

## 11.21 Other applications of electrospun nanofibers

### 11.21.1 Electrospun nanofibers in tissue engineering

The creation of TE scaffolds has been mentioned using a wide range of techniques in the literature [27]. Excellent cell-growing capabilities have been demonstrated using electrospun NF scaffolds. Because they may offer a natural environment for tissue regeneration, biocompatible and biodegradable NFs are typically selected over traditional scaffolds. Cellular attachment to the matrix or nearby cells causes it to start. A natural ECM covers or surrounds the majority of tissues and cells (ECM). These tissues can assist cell migrations, activate signal transduction pathways, arrange cells into the ECM, and synchronize cellular activities. The capacity of NFs to replicate the ECM of target cells and tissues is something special. The fact that PLGA is biodegradable, easily spinnable and has several focal attachment locations makes it the best synthetic polymer for tissue regeneration. The outcomes showed that MC3T3-E1 preosteoblast cell adhesion and proliferation, as well as support inside the cell, may be improved using PCL electrospun NF scaffolds. By creating a 3D environment rather than a 2D one, the drawbacks of electrospun NF in TE can be eliminated.

### 11.21.2 Skin tissue engineering

Innovative skin grafting scaffolds were developed mainly attributed to an electrospun NF. For instance, electrospun NFs with high porosity could offer more structural room for grafted cells. In the process of healing a wound, it also promotes cell migration, cell proliferation, oxygen exchange, and nutrition delivery. Nanofibrous scaffolds' tiny pores help to dry up the wound and prevent infection. Additionally, upon implantation, wound contraction is prevented by the adjustable mechanical characteristics of electrospun NFs. Collagen, gelatin, silk, chitosan, and fibrinogen are just a few examples of natural polymers that have been transformed into NFs for wound curing. According to research, the specific adhesion characteristics and strong multiplication of human dermal fibroblasts are represented by electrospun cellulose acetate/gelatin (25:75) NFs. Low resistance to enzymatic breakdown and poor mechanical characteristics are two drawbacks of natural polymers. Conversely, biodegradable synthetic polymers, such as PGA, PLA, PCL, and their copolymers, are extensively employed for skin and another TE owing to their excellent mechanical qualities.

The wound is covered from microbes by the dressing. Exudates are absorbed, hastening the healing process. Burns, diabetic ulcers, and split-skin graft donor sites all have a slower wound-healing process. Exudates may be effectively absorbed by electrospun NFs, which can also regulate wound wetness. The large porosity of nanofibrous membranes adds to air permeability essential for cell respiration. The comparatively tiny pore size of NFs helps prevent bacterial infections by protecting the wound. The NF dressings provide several benefits, including improved homeostasis, dressing flexibility, mechanical strength, and functionalization, with different bioactive compounds. By carrying out the typical skin cell proliferation, an NF also has the benefit of scar-free regeneration.

### 11.21.3 Bone tissue engineering

Physically, bone is a strong, inflexible, and hard connective tissue. Microscopically, there are not very many cells in it. ECM in the form of collagen NFs and stiffening inorganic substrates like hydroxyapatite (HAp) are plentiful in this tissue. Osteocytes can therefore act inside the particular organic–inorganic nanofibrous composite that makes up the bone. Numerous studies are being conducted on scaffolds that imitate the bone ECM, electrospun composite NFs made of biodegradable polymers and calcium phosphate. By soaking electrospun PLLA or PLLA/collagen NFs in calcium chloride solution and disodium phosphate solution, polymeric mineralized nanofibrous composites are created. The researchers found that while bone-like nano-HAp may be effectively deposited on both NFs, PLLA/collagen NFs generate nano-HAp more quickly and uniformly than PLLA NFs. Additionally, nano-HAp-deposited NFs exhibit improved human fetal osteoblast cell capture efficiency in just 20 min.

Nano-HAp incorporation into electrospun NFs may increase osteogenic differentiation of mesenchymal stem cells as well as cell adhesion and proliferation. The development of brand-new nano-HAp/PLGA composite scaffolds with high porosity and carefully regulated pore topologies. In bone TE, these newly created composite scaffolds could make ideal 3D substrates for cell adhesion and migration. In addition to HAp, other calcium salts have been incorporated into polymeric nanofibers for bone TE, including β-tricalcium phosphate, calcium carbonate, and even calcium phosphate cement. This suggests that polymer/bioceramics nanofibrous composites are promising scaffolds for accelerating bone healing.

### 11.21.4 Cardiac tissue engineering

Cardiac TE has drawn interest since it might completely alter how patients with advanced heart failure are treated. Due to their adaptable mechanical characteristics, electrospun NFs have been regarded as potential scaffolds. Myocardial regeneration may result from fiber orientation. The expression and functionality of cardiac cells are significantly influenced by cell alignment in the myocardial tissues and an aligned ECM. A tissue-engineered cardiac graft has been created by concurrently ES elastic polyurethane NFs and electrospraying mesenchymal stem cells to imitate the cell alignment of the heart and improve cardiac differentiation.

### 11.21.5 Nerve tissue engineering

Nerve regeneration is another use for electrospun NFs. The goal is to create a neural network capable of filling in the gaps left by injured peripheral or central neurons. The purpose of neural scaffolds is to control axonal sprouting and to encourage the diffusion of neurotrophic factors. Since electrospun NFs replicate the neural fibrous ECM in addition to providing substrate topographical guidance to drive neural cell proliferation, they are excellent materials for nerve TE. A new strategy to encourage neurite development and differentiation is the use of electrical stimulation in nerve TE. The development of electrically conductive NFs has made them an essential substrate for electrical stimulation. Therefore, during ES, conductive polymers, including carbon nanotubes, polypyrrole, polyaniline, poly(3,4-ethylenedioxythiophene), and even poly (3,4-ethylenedioxythiophene), may be introduced into NFs.

### 11.21.6 Electrospun nanofibers in biomedical application

In addition to having a high surface-to-volume ratio, electrospun NF scaffolds also can connect pores with cell adhesion, infiltration, migration, and proliferation while allowing the free interchange of nutrients and wastes [27]. In addition to mechanical strength, biocompatibility, and biodegradability, other properties of the electrospun NF include surface modification of bioactive compounds, cell-recognized ligands, and the capacity to mimic natural ECM. Medical implants, biosensors, wound dressing, drug delivery, and oral surgery all demonstrate impressive applications for electrospun nanofiber. A low-cost way to simulate native ECM, which is made up of an interlocking meshwork of proteins and glycosaminoglycans, is using electrospun NF. The raw ingredients PCL, PLA, PGA, PLGA, and PLCL are also significant. These copolymers are ideal due to how simple they are to produce, how strong they are, and how biocompatible they are. Collagen, gelatin, chitosan, and silk fibroin are examples of natural polymers that have been electrospun into NF scaffolds for biological uses.

### 11.21.7 Electrospun nanofibers applications in dentistry

A good method for creating TE scaffolds in dentistry is ES. For TE of oral and dental tissues, such as pulp dentin complex, guided tissue regeneration for periodontium, caries prevention, modification of resin composites, implant surface modification, and cartilage regeneration, a variety of materials including natural polymers (silk, collagen, chitosan), synthetic polymers (PVA, polydioxanone), and nanocomposites (HAp blends) have been electrospun. The primary benefit of ES is its capacity to create nanofibrous scaffolds with complicated shapes for dentin-pulp complex regeneration. Regeneration of the dentin-pulp complex aims to bring back the mechanical and physical characteristics of the tooth structure. For the healing of deficiencies in periodontal tissues such as alveolar bone, periodontal ligament, and cementum, electrospun NF has been of attention. The drawbacks of biodegradable polymers including collagen, PLGA, PLA, and PCL include low porosity, uneven surface alignment, and a lack of biological functioning. A significant study has been done on electrospun NF, which offers improved porosity, cell attachment, and fiber alignment for use in periodontal regeneration, to solve these disadvantages.

### 11.21.8 Cancer therapy

Medical science faces enormous challenges while treating cancer. To treat different forms of cancer, a vast range of therapeutic agents have so far been created. These therapeutic agents have several disadvantages, including poor solubility and instability in the biological setting, the low concentration at the site of the tumor, negative effects on healthy tissues, low effectiveness in solid tumors, and rapid rate of clearance by the reticuloendothelial system. Innovative delivery technologies such as liposomes, nanomicelles, hydrogels, and nanoparticles have been researched as solutions to these problems. These electrospun materials that are infused with anticancer drugs seem like a viable method. For instance, it is challenging to achieve continuous release of active drug molecules at acceptable concentrations for a long enough length of time using very hydrophobic anticancer drugs because of their low solubility and instability. Using 2-hydroxypropyl-*b*-cyclodextrin as a solubilizer, hydroxyl camptothecin, an insoluble and unstable anticancer drug, has been loaded in poly (D,L-lactic acid)–PEG electrospun NFs to address these issues.

## 11.22 Protein-based fiber materials in medicine

We will talk about several types of proteins, such as keratin, collagen, silk, elastin, zein, and soybean. These proteins are among the most popular protein polymers used to create fibers for use in biomedicine [49].

### 11.22.1 Elastin

The ECM, which is a naturally occurring protein, contains elastin, which keeps the connective tissue in the human body elastic. The rough endoplasmic reticulum of cells initially produces tropoelastin, a 72 kDa precursor of elastin that has alternating hydrophobic and hydrophilic domains. The lysine oxidase enzyme can tetra-functionally crosslink tropoelastin molecules, thanks to the lysine and alanine residues that make up the hydrophilic domains. The self-assembly of the hydrophobic domains, which are composed of repetitive motifs of nonpolar residues of glycine, valine, and proline, strengthens the crosslinking of tropoelastin molecules even more. It is thought that after engaging with extracellular microfibrils close to the cell surface, tropoelastin molecules align and crosslink. Although these microfibrils serve as a crucial scaffolding for the synthesis of elastin, when elastin-rich tissue develops, they can only be seen at the edges of the protein structures. Depending on where the tissue is located, the elastin-based fibers are then organized in a variety of configurations. Elastin fibers, for instance, are grouped in parallel-oriented structures in ligaments, but they are found in a honeycomb-like arrangement in cartilage.

### 11.22.2 Collagen and gelatin

The major constituent of the ECM is collagen, a fibrous protein. As many as 29 distinct forms of collagen have been discovered, however, types I, II, or III collagen make up the bulk of the collagen in the body. A repeating X-Y-Gly amino acid sequence, with glycine always present as the third residue, is found in all collagen. Proline and hydroxyproline are the two most prevalent amino acids; however, X and Y can stand for any amino acid. Collagen may form a stable secondary structure called a triple helix, which is made up of three strands that are wound around one another by the glycine residue. Depending on the kind of collagen, these triple helices can then organize themselves into various quaternary configurations.

Gelatin may create a thermally reversible network in water and is also amphoteric due to the residues of alkaline and acidic amino acids. Similar to collagen, gelatin-based materials' mechanical characteristics can be further altered by chemical or physical crosslinking, which is frequently required because the native biopolymer is unstable in water at body temperature. The promotion of eye, bone, cardiovascular, nerve, and skin regeneration has been demonstrated for cross-linked gelatin-based materials and fibers created by dissolving gelatin in polar solvents to avoid aggregation.

### 11.22.3 Silk

Due to its accessibility and affordability, silk fibroin produced by the *Bombyx mori* silkworm is one of the most widely utilized biomaterials. The capacity to regenerate bone, cartilage, heart valves, and nerves using silk-based fibers has been demonstrated to have great biocompatibility, bioactivity, biodegradability, tunability, mechanical stability, and minimal immunogenicity. Silk's permeability to oxygen and water vapor makes it useful for wound healing, cartilage, heart valve, and neuron regeneration. Silk's permeability to oxygen and water vapor promotes its usage in wound healing.

### 11.22.4 Keratin

The main component of the adnexa of the epidermis, including hair, horns, and fingernails, is keratin, an insoluble structural protein. Depending on the order of its amino acids, the protein can also be classified as either soft or hard keratin. But both soft and hard keratin has secondary structures with two chains and a core α-helical domain in common. Keratin is a perfect natural polymer to employ in the development of biomaterials for tissue regeneration since it has cell-binding motifs and can self-assemble. Keratin is frequently mixed with other natural or synthetic polymers to produce composite fibers despite its low mechanical stability. These composites have been utilized to regenerate bone, cartilage, and skin tissue.

## 11.23 Future perspectives

Electrospun is a straightforward, adaptable, and affordable method that creates ultrafine continuous polymer nanofibers with a high surface-area-to volume ratio, high porosity, and other desirable properties. Unlike electrospraying, electrospun might have significant impacts from a variety of factors. It is vital to note that polymer is crucial in determining the solution properties, cytotoxicity of fibers, the drug-release kinetics of nanofibers, solubility of drugs, and therapeutic impact. However, before electrospun nanofibers are strong enough for industrial-level applications, numerous methodological concerns still need to be overcome. To start, more theoretical modeling and practical research are needed to better regulate the size and shape of electrospun fibers. Particularly, at this point it is still exceedingly challenging to manufacture consistent electrospun nanofibers with diameters below 30 nm. To improve the capabilities of nanofibers, a lot of work has to be invested in creating new procedures that can be integrated with ES. With greater study and development, it is believed that ES will emerge as the century's most important nanotechnology and that electrospun nanofibers will be used more widely across a range of sectors.

## 11.24 Conclusions

Controlled DDSs have become a viable alternative to traditional methods for maintaining drug plasma levels within the therapeutic range while increasing bioavailability, extending drug release, and minimizing adverse effects. Controlled drug delivery delivers selective drug administration with a known rate and mechanism to particular organs, tissues, and cells while increasing the solubility and stability of the drug. The numerous kinds of controlled DDSs include diffusion, water penetration, dissolution, and chemically controlled DDSs. The primary responsibility of a DDS is to ensure that the drug is administered in an adequate quantity and at the right pace to the site of action. However, it must also satisfy other vital requirements including chemical and physical stability and the capacity to be mass-produced in a way that ensures content consistency.

Due to its flexibility and convenience in producing low-cost polymer nanofibers for several applications, ES has emerged as a viable approach for DDS. By using various polymers and solvents as well as by managing and adjusting the many equipment settings and environmental factors, the fundamental understanding of the manufacture of tiny fibers with the capacity to release a variety of medications has been established. Although significant progress has been made, there are still many ES systems for biomedical research that need to be developed. These challenges include the efficient and uniform production of electrospun materials, environmental safety, reproducibility, high accuracy, and scalability to industrial production to meet market demand. First and foremost, the choice of the ES material determines the bulk and surface characteristics of electrospun nanofibers. There is still a need for substantial study on various ES parameters and the development of methods for ES novel polymer combinations, even though new DDSs based on ES are being developed. To meet the rising demand for DDSs, it is necessary to further explore novel techniques for loading various drugs and other bioactivities in electrospun nanofibers.

Hopefully, this chapter will give readers some quick details on the production processes of ES, WS, drawing, and so on.

## References

[1] Sharifi F, Sooriyarachchi AC, Altural H, Montazami R, Rylander MN, Hashemi N. Fiber based approaches as medicine delivery systems. ACS Biomater Sci Eng. 2016;2:1411–1431.

[2] Mitra S, Gaur U, Ghosh PC, Maitra AN. Tumour targeted delivery of encapsulated dextran-doxorubicin conjugate using chitosan nanoparticles as carrier. J Control Release. 2001;74:317–323.

[3] Kumbar SG, Nair LS, Bhattacharyya S, Laurencin CT. Polymeric nanofibers as novel carriers for the delivery of therapeutic molecules. J Nanosci Nanotechnol. 2006;6:2591–2607.

[4] Tiwari G, Tiwari R, Bannerjee S, Bhati L, Pandey S, Pandey P, Sriwastawa B. Drug delivery systems: An updated review. Int J Pharm Investig. 2012;2:2.

[5] Acar H, Banerjee S, Shi H, Jamshidi R, Hashemi N, Cho MW, Montazami R. Transient biocompatible polymeric platforms for long-term controlled release of therapeutic proteins and vaccines. Materials (Basel). 2016;9.

[6] Ahn SY, Mun CH, Lee SH. Microfluidic spinning of fibrous alginate carrier having highly enhanced drug loading capability and delayed release profile. RSC Adv. 2015;5:15172–15181.

[7] Garg T, Rath G, Goyal AK. Biomaterials-based nanofiber scaffold: Targeted and controlled carrier for cell and drug delivery. J Drug Target. 2015;23:202–221.

[8] Huang X, Brazel CS. On the importance and mechanisms of burst release in matrix-controlled drug delivery systems. J Control Release. 2001;73:121–136.

[9] Lim D, Lee E, Kim H, Park S, Baek S, Yoon J. Multi stimuli-responsive hydrogel microfibers containing magnetite nanoparticles prepared using microcapillary devices. Soft Matter. 2015;11:1606–1613.

[10] Sasikanth K, Nama S, Suresh P, Brahmaiah B. Nanofibers - A New Trend in Nano Drug Delivery Systems Systems. 2013;3:47–55.

[11] Fattahi FS, Khoddami A, Avinc O. Poly (lactic acid) nano-fibers as drug-delivery systems: Opportunities and challenges. Nanomedicine Res J. 2019;4:130–140.

[12] Yoo HS, Kim TG, Park TG. Surface-functionalized electrospun nanofibers for tissue engineering and drug delivery. Adv Drug Deliv Rev. 2009;61:1033–1042.

[13] Jao D, Xue Y, Medina J, Hu X. Protein-based drug-delivery materials. Materials (Basel). 2017;10:1–24.

[14] Zamrodah Y. Novel drug delivery systems. 2016;15:1–23.

[15] Reza Rezaie H, et al. Classification of drug delivery systems. Springer Briefs Appl Sci Technol. 2018;9–25.

[16] Paquin F, Rivnay J, Salleo A, Stingelin N, Silva C. Multi-phase semicrystalline microstructures drive exciton dissociation in neat plastic semiconductors. J Mater Chem C. 2015;3:10715–10722.
[17] Ku MS. Use of the biopharmaceutical classification system in early drug development. AAPS J. 2008;10:208–212.
[18] Adepu S, Ramakrishna S. Controlled drug delivery systems: Current status and future directions. Molecules. 2021;26.
[19] Yun YH, Lee BK, Park K. Controlled drug delivery: Historical perspective for the next generation. J Control Release. 2015;219:2–7.
[20] Shade DM, Johnson AT. Source : Standard Handbook Of Biomedical Engineering And Design Chapter 21 Design Of Respiratory Devices, Most. 2004, 1–30.
[21] Hussain S, Kaur G, Pamma P. Overview of Controlled Drug Delivery System Adv Biores. 2021. Volume 12, p.p 248–255.
[22] Huynh CT, Lee D. Encyclopedia of polymeric nanomaterials. Encycl Polym Nanomater. 2015.
[23] Heng PWS. Controlled release drug delivery systems. Pharm Dev Technol. 2018;23:833.
[24] Skrinda A. J Teach Educ Sustain. 2012;14(1):14.
[25] Cui W, Zhou Y, Chang J. Electrospun nanofibrous materials for tissue engineering and drug delivery. Sci Technol Adv Mater. 2010;11:014108.
[26] Abdelhady S, Honsy KM, Kurakula M. Electro spun- nanofibrous mats: A modern wound dressing matrix with a potential of drug delivery and therapeutics. J Eng Fiber Fabr. 2015;10:155892501501000.
[27] Agrahari V, Agrahari V, Meng J, Mitra AK. Electrospun nanofibers in drug delivery : Fabrication. Adv Biomed Appl. 2017 Its a book chapter with ISBN 978-0-323-42978-8, pp. 189–215.
[28] Xue J, Wu T, Dai Y, Xia Y. Electrospinning and electrospun nanofibers: Methods, materials, and applications. Cheme Rev. 2019;119:5298–5415.
[29] Martínez-Pérez CA. Electrospinning: A promising technique for drug delivery systems. Rev Adv Mater Sci. 2020;59:441–454.
[30] Alghoraibi I, Alomari S. Different methods for nanofiber design and fabrication. Handbook of Nanofibers, Springer International Publishing AG 2018, pp. 1–46. 2019.
[31] Waqas Munir M, Ali U. Classification of electrospinning methods. Nanorods Nanocompos. 2020;1–19.
[32] Bayrak E. Nanofibers: Production, characterization, and tissue engineering applications, twenty-first century nanostructured mater. Phys Chem Classif Emerg Appl Ind Biomed Agric. 2022;1–67.
[33] Liu M, Zhang Y, Sun S, Khan AR, Ji J, Yang M, Zhai G. Recent advances in electrospun for drug delivery purpose. J Drug Target. 2019;27:270–282.
[34] Wu H, Liu S, Xiao L, Dong X, Lu Q, Kaplan DL. Injectable and pH-responsive silk nanofiber hydrogels for sustained anticancer drug delivery. ACS Appl Mater Interfaces. 2016;8:17118–17126.
[35] Jiang J, Xie J, Ma B, Bartlett DE, Xu A, Wang CH. Mussel-inspired protein-mediated surface functionalization of electrospun nanofibers for ph-responsive drug delivery. Acta Biomater. 2014;10:1324–1332.
[36] Huang C, Soenen SJ, van Gulck E, Vanham G, Rejman J, Van Calenbergh S, Vervaet C, Coenye T, Verstraelen H, Temmerman M, Demeester J, De Smedt SC. Electrospun cellulose acetate phthalate fibers for semen induced anti-hiv vaginal drug delivery. Biomaterials. 2012;33:962–969.
[37] Hua D, Liu Z, Wang F, Gao B, Chen F, Zhang Q, Xiong R, Han J, Samal SK, De Smedt SC, Huang C. Ph responsive polyurethane (core) and cellulose acetate phthalate (shell) electrospun fibers for intravaginal drug delivery. Carbohydr Polym. 2016;151:1240–1244.
[38] Qi M, Li X, Yang Y, Zhou S. Electrospun fibers of acid-labile biodegradable polymers containing ortho ester groups for controlled release of paracetamol. Eur J Pharm Biopharm. 2008;70:445–452.

[39] Che HL, Lee HJ, Uto K, Ebara M, Kim WJ, Aoyagi T, Park IK. Simultaneous drug and gene delivery from the biodegradable poly(ε-caprolactone) nanofibers for the treatment of liver cancer. J Nanosci Nanotechnol. 2015;15:7971–7975.

[40] Tran T, Hernandez M, Patel D, Wu J. Temperature and ph responsive microfibers for controllable and variable ibuprofen delivery. Adv Mater Sci Eng. 2015;2015.

[41] Hu J, Li HY, Williams GR, Yang HH, Tao L, Zhu LM. Electrospun poly(N-isopropylacrylamide)/ethyl cellulose nanofibers as thermoresponsive drug delivery systems. J Pharm Sci. 2016;105:1104–1112.

[42] Elashnikov R, Lyutakov O, Ulbrich P, Svorcik V. Light-activated polymethylmethacrylate nano fi bers with antibacterial activity. 2016;64:229–235.

[43] Ramanan VV, Hribar KC, Katz JS, Burdick JA. Nanofiber-nanorod composites exhibiting light-induced reversible lower critical solution temperature transitions. Nanotechnology. 2011;22.

[44] Ball C, Woodrow KA. Electrospun solid dispersions of maraviroc for rapid intravaginal preexposure prophylaxis of HIV. Antimicrob Agents Chemother. 2014;58:4855–4865.

[45] Phromviyo N, Lert-Itthiporn A, Swatsitang E, Chompoosor A. Biodegradable poly(vinyl alcohol)/polyoxalate electrospun nanofibers for hydrogen peroxide-triggered drug release. J Biomater Sci Polym Ed. 2015;26:975–987.

[46] Wang Y, Kotsuchibashi Y, Uto K, Ebara M, Aoyagi T, Liu Y, Narain R. PH and glucose responsive nanofibers for the reversible capture and release of lectins. Biomater Sci. 2015;3:152–162.

[47] Lin X, Tang D, Yu Z, Feng Q. Stimuli-responsive electrospun nanofibers from poly(N-isopropylacrylamide)-*co*-poly(acrylic acid) copolymer and polyurethane. J Mater Chem B. 2014;2:651–658.

[48] Pillay V, Dott C, Choonara YE, Tyagi C, Tomar L, Kumar P, Du Toit LC, Ndesendo VMK. A review of the effect of processing variables on the fabrication of electrospun nanofibers for drug delivery applications. J Nanomater. 2013;2013.

[49] Defrates KG, Moore R, Borgesi J, Lin G, Mulderig T, Beachley V, Hu X. Protein-based fiber materials in medicine: A review. n.d.

[50] Yuping D, Yuqi Z, Keyan Z, Yueming Y, Lihuan W, Xiaoran Li, Jianyong Y, Bin Ding. Electrospun Nanofibrous Materials for Wound Healing. Advanced Fiber Materials. 2020;2:212–227.

[51] Haitham B, Gareth RW, Mine O, Fabrication of Electrospun Levopada-Carbidopa Fixed-Dose Combinations. Advanced Fiber Materials. 2020;2:194–203.

[52] Shamim Z, Saeed B, Amir T, Abo Saied R, Rogheih D, The Effect of Flow Rate on Morphology and Deposition Area of Electrospun Nylon 6 Nanofiber. Journal of Engineered Fibers and Fabrics. 2012;7:42–49.

Shveta Sharma, Manu Sharma, Richika Ganjoo, Ashish Kumar*

# Chapter 12
# Advanced fiber material in tumor therapy

**Abstract:** Even though there has been a lot of research done and a lot of progress made in the treatment of cancer, tumor recurrence and metastasis are still significant concerns. Recent developments in biomaterials have made it easier to create a local therapy for cancer. Nano-sized medicines have the potential to advantageously improve circulation time, targeted activities, and safe drug administration, all with the goal of reducing the risks and side effects associated with chemotherapy. Among them, nanofiber frameworks are the most important due to the porosity they possess, which consequently results in increased surface area and high loading of drug. In this chapter, recent researches on nano fibrous material to be used in tumor therapy have been summarized.

**Keywords:** Tumor, tumor therapy, nanofibrous material

## 12.1 Introduction

Cancer is one of the major causes of mortality worldwide, and it starts with the gradual change of healthy cells into malignant tumor cells. Increased molecular profiling of growths in our bodies has aided our understanding of cancer in general, and has offered novel approaches to managing them. The intricacy of cancer as well as the vast differences between the various cancer kinds have made it impossible to determine an optimal solution and a remedy that is applicable across the board. Generally, chemotherapy or radiotherapy is the popular technique to cure cancer, but these techniques are associated with a poor selection of cancer cells. Therefore, research is ongoing on to improve the target selection [1–3]. The photon-stimulated response is also an effective avenue for malignant cell treatments such as photothermal therapy and photodynamic therapy. Photodynamic therapy focuses on the targeted stimulation of photosensitizers within tumors to trigger chemical damage, and thus, the death of cancerous tumor

---

***Corresponding author: Ashish Kumar**, Department of Chemistry, NCE, Department of Science and Technology, Government of Bihar, India, e-mail: drashishchemlpu@gmail.com
**Shveta Sharma**, Department of Chemistry, Government College Una, Affiliated to Himachal Pradesh University, India
**Manu Sharma**, Department of Orthopaedics, Maharishi Markandeshwar Medical College and Hospital, Solan, Himachal Pradesh, India
**Richika Ganjoo**, Department of Chemistry, School of Chemical Engineering and Physical Sciences, Lovely Professional University, Punjab, India

https://doi.org/10.1515/9783110992892-012

cells, and this method has been implemented in clinical practice for over forty years for the treatment of a wide variety of malignancies. The effectiveness of photothermal treatment agents, which can be used to boost the efficacy of localized light-based heating and ablation of the tumor present in the body, has not yet been investigated in the context of large clinical studies [4–6]. Light has established itself as a good alternative to cancer theranostics because it confers extraordinary advantages, such as being ionization-free, having a microscopic invasion, having only minor side effects, having a high degree of adaptability, and reducing both the expense and the mental strain [7]. Again, there are a few drawbacks like scattering of light and low power of penetration, which cause hindrance to treatment. Therefore, researchers are also trying to use optical fibers and this technique provides a new opportunity to inspire the design of optical fiber medications [8]. Conventional photothermal substances, such as nanostructures made up of gold metal and carbon, are restricted. This is due to the fact that gold nanoparticles have properties such as cytotoxic effects [9]. One of the most successful clinical procedures for the treatment of cancer is surgical intervention, which aims to remove the tumor tissue [10]. For the treatment of breast cancer, for instance, breast-conserving surgery is quickly becoming the treatment of choice because that it is less intrusive and more likely to result in fewer difficulties during surgery. On the other hand, the local persistent tumor cells and the recurrence of tumor, following surgical excision, continue to be the most important clinical concerns [11]. In the localized way of treating, the use of drug delivery systems that are based on hydrogels is also becoming increasingly common as a result of the high drug absorbing capacity and outstanding compatibility with the human body [12–14]. Direct loading of medicines on the hydrogels may have some issues like diffusion on long incubations. But here, the usage of core-shell fibers, in which the shell of the fibers entraps the drug, provides a platform for regulated drug delivery, with limited uncontrolled diffusion of medicines. Core-shell fibers can also reduce the quantity of drugs that diffuse into the body uncontrollably. [14–16]. Various ways are developed by researchers to form the fibers on a nano or microscale, such as co-axial electrospinning, microfluidics generation, and core-shell 3D printing [17–19]. Drug delivery at a specific region can be attained by putting the fibrous materials, encapsulated with a drug, to the tumor site, thus providing unique benefits for the curing of cancer, including increased dosage at the tumor site, fewer effects on the surrounding organs, as well as better controlled drug release profiles. In general, drug delivery is not specific and to work on the particular tumor cell, fabrication of stimuli-responsive systems can be used [20, 21]. The stimuli can be broken down into two categories: endogenous and exogenous (as given in Figure 12.1). Endogenous stimuli are those that are caused by changes in the immediate environment, such as a decrease in pH; exogenous stimuli are those that are related to changes in the extracorporeal physical conditions, such as temperature, magnetic fields, and light [21, 22].

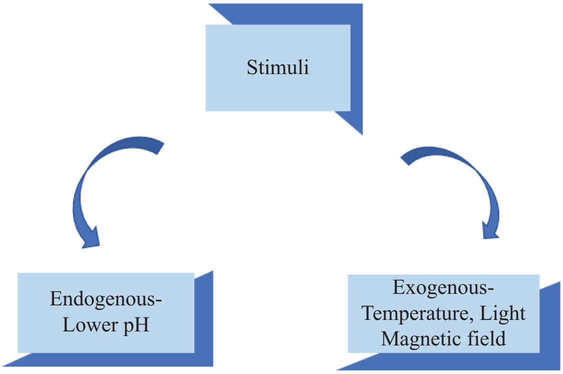

**Figure 12.1:** Various types of stimuli.

## 12.2 Usage of fibrous material in the treatment of tumor

Huang et al. [3] worked on electrospun fiber webs that are highly filled with particles sized at 50 nm and smaller – Iron oxide nanoparticles (IONPs). The study was carried out because IONPs continue to struggle with significant obstacles, including limited capacity to target tumors, high degree of variation IONPs that are absorbed by the tumor, and IONP leakage from cancer cells that have died into the healthy tissues that surround them. For the formation of fibers, polystyrene solution (DMF/ THF as solvent) was added into IONPs and then electrospun into fibers. When the matter is spun, the solvent, which may be harmful to cells, disappears entirely. Scanning electron microscopy was employed to check the morphology of fibers and the uniform diameter was confirmed by the SEM, and only 20% of the IONPs could be seen in clear detail; the rest of them were embedded inside the fibers. It has also been demonstrated that magnetic fibers may readily be functionalized with collagen, which makes it possible for cells to adhere to them. When web-bound cells are heated to 45 degrees Celsius, either in a warm water bath or in an alternating magnetic field, the temperature-dependent elimination of ovarian cancer cells occurs. Results revealed that the use of a magnetic field appeared to be significantly more effective in cell killing, than the use of water. Ran et al. [8] utilized functional fibers, such as fluorescent fibers and fibers made up of rare earth metals, to accurately explore and attack tumors without the need for an extra injection of photoreporters and photosensitizers. To test the viability of the photoinduced heat technique, the two distinct varieties of optical fibers that were used were a regular single-mode fiber and Er-/Yb-codoped fiber. The results of the measurements showed that Er-/Yb-codoped fiber performed significantly better than single-mode fiber by thermalizing to temperatures as high as 140° Celsius. Chen et al. [9] developed a composite, combining both orthotopic treatment and photothermal therapy, by using an electrospinning technique. In this process, fibers of Polyaniline were made by merging Polyaniline in poly (ε-caprolactone)) and gelatin in nano dimensions. The multifunctional spinning bits that were produced as a result can be implanted directly into the tumor site of mice through medical interventions to carry out orthotopic photothermal therapy in vivo. According to the findings of the experiments conducted in vivo, polyaniline PG has the potential to effectively limit the growth of tumors by transforming the optical energy into the thermal energy needed to kill tumor cells. Wei et al. [14] created a core-shell fiber with the help of PDA/alginate and gelatin, where the first component is used for the shell and the second component is used to form the core. Following irradiation with a NIR laser, PDA with a strong cause a rise in temperature in core-shell fibers. This increased temperature prompted the dissemination of core hydrogels from the fibers, which in turn led to the release of drugs into the surrounding environment. After the laser was turned off, the hydrogels proceeded through a process called sol-gel transition, and both the gels and the loaded pharmaceuticals were able to be kept in the fibers. Drugs that were placed in the inner part of the fibers and the frameworks accomplished release at regular intervals of time and in an on-demand manner because the sol-gel transition of the hydrogel can be reversed by turning the laser on and off. To check the controlled drug release, the fibers loaded with the drug were kept in the simulated body fluid and radiation of 808 nm was applied for three minutes. Radiation was given seven times with an interval of seventeen minutes every time. Next, UV was employed to find out the concentration of the drug. To explore the in vivo release of DOX from fibers, DOX-loaded core/shell fibers of 1 centimeter in length and 18/25 G were implanted into the subcutaneous region of mice that had been given anesthesia. Next, various cycles of radiation were given and colored images were analyzed. In vivo tumor therapy was also investigated. Results revealed that photothermal effects and the controlled release of the drug successfully cleared the breast cancer cells and stopped the spreading of the tumor. After the surgical resection of breast cancer, it was seen that the core-shell fiber framework could be candidates for further treatment in a confined setting. Chen et al. [23] worked on designing nanofibrous fabrics by using an electrospinning technique. For that, antitumor drug doxorubicin was added in $Cu_9S_5$@m$SiO_2$, and then merged into poly(ε-caprolactone) and gelatin to form nanofibrous fabrics. Following surgical operations, the multifunctional spinning pieces that were produced were implanted directly into the area of the tumor present in mice. Transmission electron microscopy (TEM) was then utilized to get an idea about the nanoparticles. Morphological investigations also indicated the mesoporous nature of the material – $Cu_9S_5$@m$SiO_2$ – which is helpful in further loading. Experiments involving photothermal radiation were carried out so that the photothermal effect of DOX- $Cu_9S_5$@m$SiO_2$ PG fiber could be studied. After applying radiation, there was a drastic color change and rise in temperature, which was enough to kill the tumor in vivo. Then, the experiment was started in seven different groups where each group had four mice. Groups in which nanofibrous fabrics were incorporated showed an unexpected decrease in tumor. In the case of DOX- $Cu_9S_5@mSiO_2$ PG + light, the growth inhibition was up to 95%. According to the findings, composite fibers are an excellent choice for the treatment of orthotopic cancer since they combine synergistic photothermal therapy with chemotherapy to cure tumors. After the therapy, the findings of the gross anatomy and pathomorphology examinations were analyzed, and it has been determined that all of the organs, including the heart, spleen, liver, and kidneys, are healthy and show no signs of inflammation, necrosis, or lesions. This is something that may be clarified in the following manner. In the process of electrospinning, the composite fibers undergo a process in which they gradually inflate and then break when exposed to normal environmental conditions. This means that the organs of the animals that were subjected to the experiment were in perfect working order. Zhang et al. [24] in their study formulated the composite of cisplatin by loading it into fibers/sponge, and for that they utilized the electrospun and freeze-drying techniques. First, the gelatin/poly(lactic-co-glycolic acid) fibers were put into gelatin/chitosan. The sponge layers had the potential to successfully treat leaking blood or bleeding from locations that were difficult to access, thereby dramatically reducing the amount of blood lost during the operation. In addition to this, the dispersed tumor cells in the blood could be contained in the sponge, preventing an increase in the quantity of CTC. During this time, the cisplatin that has been released from the fibers could be further limited in the sponge for prolonged release. Then, cisplatin would be able to destroy any cancer cells that were still there, as well as any cells in the sponge that had been absorbed from the surrounding environment, thereby lowering the likelihood of recurrence and metastasis, while causing the least amount of damage to any healthy organs. Niiyama et al. [25] developed a sophisticated anti-cancer fiber mesh that is capable of precisely controlling malignant cells' action against lung adenocarcinoma. The mesh has the advantage of being able to carry huge loads of the chemotherapeutic medicine paclitaxel as well as magnetic nanoparticles. Heat is produced by the mesh as a result of the activation of the loaded nanoparticles in an alternating magnetic field. The heat that is created can potentially be utilized to act as a catalyst for the release of PTX from the mesh. The mesh is generated through the use of an electrospinning technique with a copolymer of N-isopropylacrylamide and N-hydroxymethylacrylamide. Both are mixed in 30 and 0.75 w/w%, and electrospinning is used to transform the solution into fibers. A voltage of 20 kV is applied, and the needle and collection plate are kept at a distance of 13 centimeters from one another [26]. The fibers are then kept at a high temperature to remove the solvents. Fabricated mesh is illustrated in Figure 12.2.

When treating hyperthermia, radiofrequency, microwaves, and focused ultrasound waves are frequently employed as means for producing heat [27]. The ability of the AMF to generate heat at a distance makes it an appealing therapeutic option for the removal of tumors that are difficult to reach or located in deep tissue. Both in vitro and in vivo studies were conducted to investigate the antitumor effects of the fiber mesh. Results revealed that the mesh with drug molecule was able to kill 43%, and when containing both the drug and nanoparticles, it was able to kill 66%. In vivo investigations

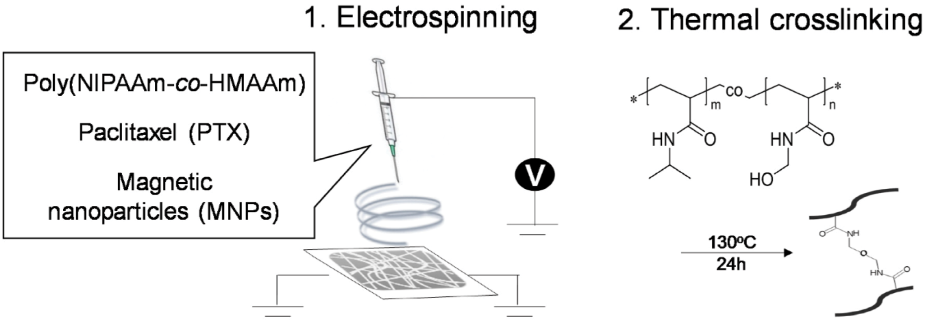

**Figure 12.2:** Fabrication of thermally cross-linkable temperature-responsive fiber mesh by electrospinning and thermal curing processes by self-condensation.
Source: Reproduced from the reference 25 [CC By 4.0].

were carried out on mice. Figure 12.3 illustrates the comparison for two months and reveals the increased tumor size after two months in control. When the mesh was loaded with only one drug, the tumor was not controlled. The tumor growth was significantly controlled when the mesh was loaded with both drug and nano particles.

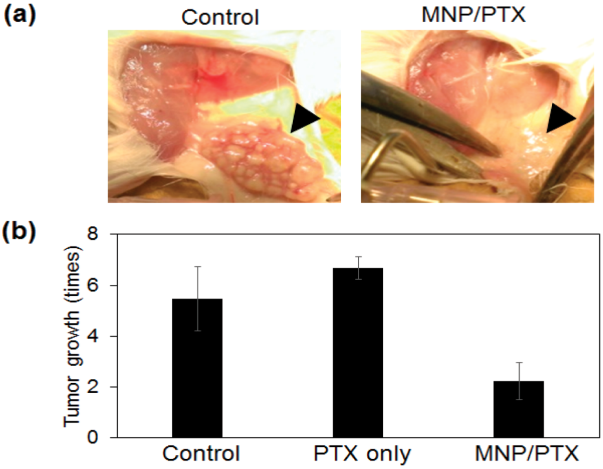

**Figure 12.3:** (a) Pictorial presentation of tumors after the treatment with (right) and without (left) fiber. (b) Growth comparison of tumor after the treatment with fiber containing PTX and MNP/PTX.
Source: Reproduced from the reference 25 [CC By 4.0].

In one more study by Yusef et al. [28], different techniques (dewaxing, bleaching, etc.) were used to decompose lignin and hemicellulose present in rice straw to liberate CF containing ordered nanofibrils. These modifications were carried out to release CF and then synthesize bio nanocomposites from chitosan and the rice straw cellulose encapsulated 5-Fluorouracil (CS-CF/5FU BNCs). Figure 12.4 depict the formation of a composite for in vitro study. NaCl and KOH solutions helped to break lignin and hemicelluloses of the rice straw waste, respectively [29]. After that, rice straw from which the lignin has been removed was again exposed to 5% KOH to separate the CF, and the isolated CF with a diameter on the nanoscale had a nearly consistent structure. Literature also suggested that variation in KOH percentage affected the CF, as its quality of CF got reduced and many researchers have also reached comparable conclusions, making use of this methodology [30–32]. Further, ionic gelation method was employed to solve two purposes – first, to trap the drug under investigation in the dual polysaccharide, and second, to enhance the extent of crosslinking between polysaccharides [33]. Studies also reported that there was a strong possibility of the presence of weak forces like Van der Waals forces, etc. in composite fibers, resulting in strong interactions [34, 35]. Techniques like FTIR and XRD were employed to confirm the formation of the composite. XRD results showed the structure with the same cellulose structure, confirming that after exposure to varied environmental conditions, it remains unaltered, and the diffraction peaks shown were the same as that in unexposed cellulose [29]. When XRD was performed for the composite, it confirmed the peak for the drug molecule, which validated the encapsulation of the drug in the fiber, and such a peak was identified in the pre-drug molecule [36]. Further SEM analysis was performed, which confirmed the rod- like structure of cellulose. The size of the rice straw was reduced after an experimental exposure. CF was uniform in appearance and chitosan nanoparticles were spherical in shape. SEM also verified the coating of CS NPs on the cellulose and composite fibers, with a diameter of 48.73 ± 1.5 nm. Both techniques confirmed the synthesis of fiber and encapsulation of the drug under study. Dynamic light scattering was also used to find out the particle size in the solution. With the increased pH, the size of the composite fibers showed an increase, which may be attributed to the fact that chitosan got affected by the variation in pH [37]. The extent of loading of drug into the fibrous material was studied using UV. Alkali-treated cellulose had excellent swelling characteristic along with open bonds, and the composite has OH bonds, which helped in interacting with the drug molecules. This was confirmed by the aromatic character and low molecular weight; so it easily gets encapsulated [38–40]. The chemical structure of the composite and the changes that occurred on crosslinking were investigated by FTIR. Results revealed the stretching vibrations of O-H and C-H in cellulose, and because glycosidic linkage appeared as a result of chemical treatments, a minor peak at 887 $cm^{-1}$ appeared [41, 42]. The varied absorption peaks in chitosan and the composite of chitosan-cellulose was due to the varied bonding between OH and NH, the different extent of Vander Wals, hydrogen bonding, etc. [43] Only a few peaks of drug molecules confirmed that there was proper encapsulation of the drug molecule in the fibrous framework of chitosan and cellulose.

Swelling analysis of the fibrous material loaded with the drug was performed, because swelling properties are somehow related to drug load and the drug release property of the composite. In the first four hours, the swelling ratio was maximum, which was attributed to the porous nature of the fibers [44], and a state of equilibrium was

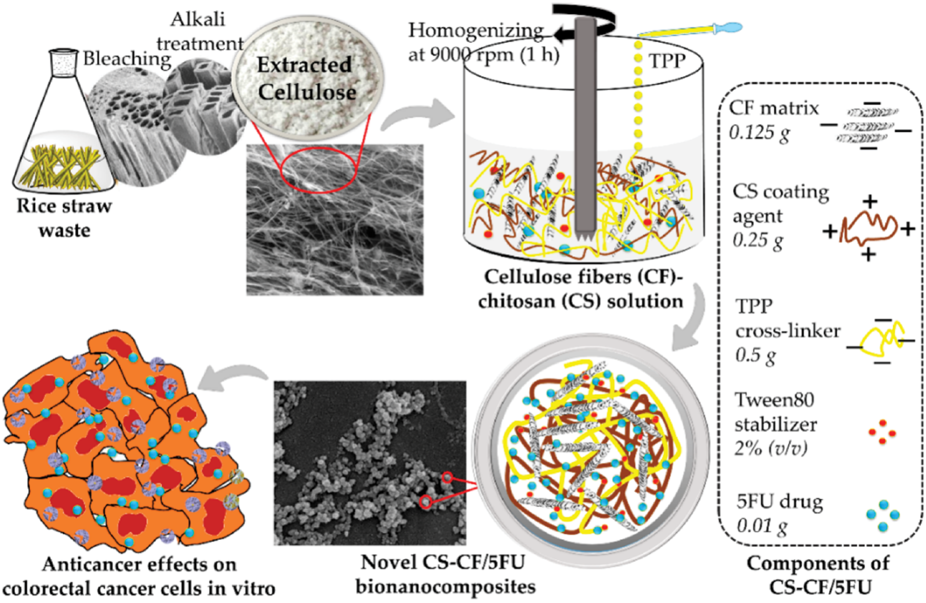
Alkali treatment
Bleaching
Extracted Cellulose
Rice straw waste
Homogenizing at 9000 rpm (1 h)
TPP
Cellulose fibers (CF)-chitosan (CS) solution
CF matrix 0.125 g
CS coating agent 0.25 g
TPP cross-linker 0.5 g
Tween80 stabilizer 2% (v/v)
5FU drug 0.01 g
Components of CS-CF/5FU
Novel CS-CF/5FU bionanocomposites
Anticancer effects on colorectal cancer cells in vitro

**Figure 12.4:** Scheme of cellulose-chitosan composite formation.
Source: Reproduced from the reference 28 [CC By 4.0].

achieved after twelve hours, which was also there in the literature [45, 46]. Finally, the amount of drug molecule loaded in the fibers was estimated with the encapsulation efficiency, and the calculated value came out to be 86% (approx.). The kinetics of the drug was also studied to get an idea about the releasing capacity of fiber with the help of UV-IR, and the study confirmed that it was safe to use the examined fibrous composite to put into the human body. Kim et al. [47] studied fiber-based microplasma in cancer therapy. Generally, plasmas have been employed in cancer therapy; however, single-cell treatments cannot be administered because the delivery systems are too large [48]. Plasma-based cancer therapies that function at atmospheric pressure have been developed in recent years. These therapies expose the tumor cells to free radicals, which in turn causes cell death at an accelerated rate [49]. It would be preferable to have a plasma device that can treat tumor cells at the single-cell level to establish the mechanism by which plasma induces apoptosis in cancer cells. In this work, a hollow-core optical fiber was employed to develop a microplasma jet, and this microplasma jet was with positive points of smaller inner diameter. When compared to traditional endoscopy, this micrometer-scale, flexible plasma jet technology can allow for the treatment of smaller groups of tumor cells through fewer incisions. Murine melanoma B16F0 tumor cells and murine fibroblast CL cells were exposed to a microplasma jet, generated in a hollow-core optical fiber, to ascertain the treatment's specific impact. The microplasma caused the B16F0 tumor cells, and not the CL.7 fibroblast cells, to go through the process of apoptosis at a dose duration of two seconds. On the other hand, when the dose duration was raised to 5 s, the plasma therapy appeared to produce equivalent levels of apoptosis in B16F0 tumor cells and CL.7 fibroblast cells. Results revealed that a flexible microplasma device that was based on hollow-core optical fibers produces apoptosis in cultured murine tumor cells as well as in non tumor fibroblast cells in a dose-dependent way.

## 12.3 Conclusion

Surgery is currently the most common treatment option for most solid tumors. There are still many obstacles to overcome in the treatment, but therapy of some malignant tumors cannot be removed surgically, in addition to the prevention of residual tumor recurrence in some cases. Exciting new developments in the treatment of cancer locally have been demonstrated through the use of fibrous scaffolds. Studies have been carried out on different fiber frameworks and the effects of heat, light, etc. have also been analyzed. The usage of fibers in treating the tumor came out to be beneficial but whenever such type of frameworks has been used, it is necessary to do in-depth research on the inflammatory response as well as the healing process that is brought on by the accumulation of chemotherapeutic medicines and polymers. Lots of other points need to be taken care of as living organisms are involved here. The fibers employed should be nontoxic; its degradation should not result in any reaction with the neighboring tissue or blood. The repercussions of the reaction that occurs at the interface between the tissue and the substance can modify the microenvironment of the tumor, which can speed up the return of tumor cells. In-depth study and careful investigations are required to avoid any kind of damage to any organ.

## References

[1] Trevino V, Tadesse MG, Vannucci M, Al-Shahrour F, Antczak P, Durant S, . . . Falciani F. Analysis of normal-tumour tissue interaction in tumours: prediction of prostate cancer features from the molecular profile of adjacent normal cells. PloS One. 2011;6(3):e16492.

[2] Dong Y, Wu WKK, Wu CW, Sung JJY, Yu J, Ng SSM. MicroRNA dysregulation in colorectal cancer: A clinical perspective. Br J Cancer. 2011;104(6):893–898.

[3] Huang C, Soenen SJ, Rejman J, Trekker J, Chengxun L, Lagae L, . . . De Smedt SC. Magnetic electrospun fibers for cancer therapy. Adv Funct Mater. 2012;22(12):2479–2486.

[4] Li X, Lovell JF, Yoon J, Chen X. Clinical development and potential of photothermal and photodynamic therapies for cancer. Nat Rev Clin Oncol. 2020;17(11):657–674.

[5] Jiang Y, Huang J, Xu C, Pu K. Activatable polymer nanoagonist for second near-infrared photothermal immunotherapy of cancer. Nat Commun. 2021;12(1):1–14.

[6] Karges J, Kuang S, Maschietto F, Blacque O, Ciofini I, Chao H, Gasser G. Rationally designed ruthenium complexes for 1-and 2-photon photodynamic therapy. Nat Commun. 2020;11(1):1–13.

[7] Shi H, Sadler PJ. How promising is phototherapy for cancer? Br J Cancer. 2020;123(6):871–873.

[8] Ran Y, Xu Z, Chen M, Wang W, Wu Y, Cai J, . . . Guan BO. Fiber-optic theranostics (FOT): Interstitial fiber-optic needles for cancer sensing and therapy. In: Advanced science. 2022. p. 2200456.

[9] Chen Y, Li C, Hou Z, Huang S, Liu B, He F, . . . Lin J. Polyaniline electrospinning composite fibers for orthotopic photothermal treatment of tumors in vivo. New J Chem. 2015;39(6):4987–4993.

[10] Findlay-Shirras LJ, Outbih O, Muzyka CN, Galloway K, Hebbard PC, Nashed M. Predictors of residual disease after breast conservation surgery. Ann Surg Oncol. 2018;25(7):1936–1942.

[11] Gooch JC, Schnabel F. Locoregional recurrence of breast cancer. In: Clinical algorithms in general surgery. Cham, Springer; 2019. pp. 97–100.

[12] Norouzi M, Nazari B, Miller DW. Injectable hydrogel-based drug delivery systems for local cancer therapy. Drug Discovery Today. 2016;21(11):1835–1849.

[13] Li J, Mooney DJ. Designing hydrogels for controlled drug delivery. Nat Rev Mater. 2016;1(12):1–17.

[14] Wei X, Liu C, Wang Z, Luo Y. 3D printed core-shell hydrogel fiber scaffolds with NIR-triggered drug release for localized therapy of breast cancer. Int J Pharm. 2020;580:119219.

[15] Sperling LE, Reis KP, Pranke P, Wendorff JH. Advantages and challenges offered by biofunctional core–shell fiber systems for tissue engineering and drug delivery. Drug Discovery Today. 2016;21 (8):1243–1256.

[16] Chen C, Chen X, Zhang H, Zhang Q, Wang L, Li C, . . . Sun D. Electrically-responsive core-shell hybrid microfibers for controlled drug release and cell culture. Acta Biomater. 2017;55:434–442.

[17] Lu Y, Huang J, Yu G, Cardenas R, Wei S, Wujcik EK, Guo Z. Coaxial electrospunfibers: applications in drug delivery and tissue engineering. Wiley Interdiscip Rev Nanomed Nanobiotechnol. 2016;8 (5):654–677.

[18] Onoe H, Okitsu T, Itou A, Kato-Negishi M, Gojo R, Kiriya D, . . . Takeuchi S. Metre-long cell-laden microfibres exhibit tissue morphologies and functions. Nat Mater. 2013;12(6):584–590.

[19] Akkineni AR, Ahlfeld T, Lode A, Gelinsky M. A versatile method for combining different biopolymers in a core/shell fashion by 3D plotting to achieve mechanically robust constructs. Biofabrication. 2016;8(4):045001.

[20] Yang KN, Zhang CQ, Wang W, Wang PC, Zhou JP, Liang XJ. pH-responsive mesoporous silica nanoparticles employed in controlled drug delivery systems for cancer treatment. Cancer Biology Med. 2014;11(1):34.

[21] Zhao J, Cui W. Functional electrospunfibers for local therapy of cancer. Adv Fiber Mater. 2020;2 (5):229–245.

[22] Mura S, Nicolas J, Couvreur P. Stimuli-responsive nanocarriers for drug delivery. Nat Mater. 2013;12 (11):991–1003.

[23] Chen Y, Hou Z, Liu B, Huang S, Li C, Lin J. DOX-Cu 9 S 5@ mSiO 2-PG composite fibers for orthotopic synergistic chemo-and photothermal tumor therapy. Dalton Trans. 2015;44(7):3118–3127.

[24] Zhang Z, Kuang G, Zong S, Liu S, Xiao H, Chen X, . . . Huang Y. Sandwich-like Fibers/Sponge composite combining chemotherapy and hemostasis for efficient postoperative prevention of tumor recurrence and metastasis. Adv Mater. 2018;30(49):1803217.

[25] Niiyama E, Uto K, Lee CM, Sakura K, Ebara M. Alternating magnetic field-triggered switchable nanofiber mesh for cancer thermo-chemotherapy. Polymers. 2018;10(9):1018.

[26] Kim YJ, Ebara M, Aoyagi T. A smart hyperthermia nanofiber with switchable drug release for inducing cancer apoptosis. Adv Funct Mater. 2013;23(46):5753–5761.

[27] Chicheł A, Skowronek J, Kubaszewska M, Kanikowski M. Hyperthermia–description of a method and a review of clinical applications. Rep Pract Oncol Radiother. 2007;12(5):267–275.

[28] Yusefi M, Chan HY, Teow SY, Kia P, Lee-Kiun Soon M, Sidik NABC, Shameli K. 5-fluorouracil encapsulated chitosan-cellulose fiber bionanocomposites: Synthesis, characterization and in vitro analysis towards colorectal cancer cells. Nanomaterials. 2021;11(7):1691.

[29] Srasri K, Thongroj M, Chaijiraaree P, Thiangtham S, Manuspiya H, Pisitsak P, Ummartyotin S. Recovery potential of cellulose fiber from newspaper waste: An approach on magnetic cellulose aerogel for dye adsorption material. Int J Biol Macromol. 2018;119:662–668.

[30] Lu P, Hsieh YL. Preparation and characterization of cellulose nanocrystals from rice straw. Carbohydr Polym. 2012;87(1):564–573.

[31] Cai M, Takagi H, Nakagaito AN, Katoh M, Ueki T, Waterhouse GI, Li Y. Influence of alkali treatment on internal microstructure and tensile properties of abaca fibers. Ind Crops Prod. 2015;65:27–35.

[32] Kunjachan S, Jose S, Lammers T. Understanding the mechanism of ionic gelation for synthesis of chitosan nanoparticles using qualitative techniques. Asian J Pharm (AJP). 2010;4(2).

[33] Hps AK, Saurabh CK, Adnan AS, Fazita MN, Syakir MI, Davoudpour Y, . . . Dungani R. A review on chitosan-cellulose blends and nanocellulose reinforced chitosan biocomposites: Properties and their applications. Carbohydr Polym. 2016;150:216–226.

[34] Anirudhan TS, Christa J. Multi-polysaccharide based stimuli responsive polymeric network for the in vitro release of 5-fluorouracil and levamisole hydrochloride. New J Chem. 2017;41 (20):11979–11990.

[35] Anirudhan TS, Nima J, Divya PL. Synthesis, characterization and in vitro cytotoxicity analysis of a novel cellulose based drug carrier for the controlled delivery of 5-fluorouracil, an anticancer drug. Appl Surf Sci. 2015;355:64–73.

[36] Zhu W, Wan L, Zhang C, Gao Y, Zheng X, Jiang T, Wang S. Exploitation of 3D face-centered cubic mesoporous silica as a carrier for a poorly water soluble drug: influence of pore size on release rate. Mater Sci Eng C. 2014;34:78–85.

[37] Pech-Cohuo SC, Canche-Escamilla G, Valadez-González A, Fernández-Escamilla VVA, Uribe-Calderon J. Production and modification of cellulose nanocrystals from Agave tequilana weber waste and its effect on the melt rheology of PLA. Int J Polym Sci. 2018;2018.

[38] Illangakoon UE, Yu DG, Ahmad BS, Chatterton NP, Williams GR. 5-fluorouracil loaded eudragit fibers prepared by electrospinning. Int J Pharm. 2015;495(2):895–902.

[39] Sun B, Zhang M, Shen J, He Z, Fatehi P, Ni Y. Applications of cellulose-based materials in sustained drug delivery systems. Curr Med Chem. 2019;26(14):2485–2501.

[40] Roman M. Toxicity of cellulose nanocrystals: A review. Ind Biotechnol. 2015;11(1):25–33.

[41] Chen X, Yu J, Zhang Z, Lu C. Study on structure and thermal stability properties of cellulose fibers from rice straw. Carbohydr Polym. 2011;85(1):245–250.

[42] Kavaz D, Kirac F, Kirac M, Vaseashta A. Low releasing mitomycin c molecule encapsulated with chitosan nanoparticles for intravesical installation. J Biomater Nanobiotechnol. 2017;8(4):203–219.

[43] Area MC, Ceradame H. Paper aging and degradation: recent findings and research methods. 2011.

[44] Yang J, Duan J, Zhang L, Lindman B, Edlund H, Norgren M. Spherical nanocomposite particles prepared from mixed cellulose–chitosan solutions. Cellulose. 2016;23(5):3105–3115.

[45] Bullo S, Buskaran K, Baby R, Dorniani D, Fakurazi S, Hussein MZ. Dual drugs anticancer nanoformulation using graphene oxide-PEG as nanocarrier for protocatechuic acid and chlorogenic acid. Pharm Res. 2019;36(6):1–11.

[46] Nugraheni AD, Purnawati D, Rohmatillah A, Mahardika DN, Kusumaatmaja A. Swelling of PVA/ chitosan/TiO2 nanofibers membrane in different pH. In: Materials science forum. Vol 990, Trans Tech Publications Ltd; 2020. pp. 220–224.

[47] Kim JY, Ballato J, Foy P, Hawkins T, Wei Y, Li J, Kim SO. Single-cell-level cancer therapy using a hollow optical fiber-based microplasma. Small. 2010;6(14):1474–1478.

[48] Lee HJ, Shon CH, Kim YS, Kim S, Kim GC, Kong MG. Degradation of adhesion molecules of G361 melanoma cells by a non-thermal atmospheric pressure microplasma. New J Phys. 2009;11 (11):115026.

[49] Stoffels E, Sakiyama Y, Graves DB. Cold atmospheric plasma: charged species and their interactions with cells and tissues. IEEE Trans Plasma Sci. 2008;36(4):1441–1457.

Farhat A. Ansari* and Hariom K. Sharma

# Chapter 13
# Advanced fiber materials in corrosion protection

**Abstract:** The widespread usage, simpler accessibility, more cost-effectiveness, and improved moisture resistance fiber-reinforced polymer composites are employed in the automobile, electrical-electronics, cycle, and aviation industries. The composite materials are a complex blend of at least two separate materials at the microlevel, with novel properties distinct from those of its components and typically a nearly uniform structure at the macroscopic level. It is strong, durable, resistance to corrosion, lightweight, and affordable. In general, composite materials are a complex blend of at least two separate materials at the microlevel, with novel properties distinct from those of its components and typically a nearly uniform structure at the macroscopic level. The fibers, textiles, or fillers make up the reinforced composites. In this chapter, the objective is to identify the components, advanced fiber-reinforced polymer composite's characteristics, and their use as an improved fiber composite for corrosion resistance.

**Keywords:** fiber composite, reinforcement, corrosion, corrosion resistance

## 13.1 Introduction

Composites made of fiber-reinforced polymer (FRP) are utilized in virtually all technologically advanced structural components, including aeroplanes, choppers, satellites, offshore platforms, sporting goods, machinery for processing chemicals, and civil infrastructures like bridges and buildings. The creation of new cutting-edge forms of FRP materials has been a major element in the growth of composite use in recent decades. This also brings fresh reinforcement techniques, like using nanoparticles and materials, as well ass improvement in greater resin systems. FRP composites can be customized to meet performance needs as it is lightweight, anticorrosive, have high specific toughness, and are simple to produce. Due to its advantageous features, composites (FRP) have been used in both constructional design and structural maintenance,

---

***Corresponding author: Farhat A. Ansari,** Department of Pharmacy, Faculty of Pharmaceutical Chemistry, Hygia Institute of Pharmaceutical Education and Research, Faizullahganj, Lucknow 226020, India, e-mail: farhataisha@gmail.com

**Hariom K. Sharma,** Engineering Department, University of Technology and Applied Sciences (UTAS), Salalah, Dhofar, Sultanate of Oman

https://doi.org/10.1515/9783110992892-013

including their use in reinforced concrete (RC), bridges, modular buildings, scaffolding, and external reinforcement for stiffening and seismic improvement [1].

Fabricated or naturally present composite materials are formed of a number of components that have distinctly different physicochemical features. In most composites, strong, rigid fibers are enclosed by a smoother, less flexible matrix. Creating a material that is strong, rigid, and frequently low in density is the common goal. Glass or carbon fibers are frequently found in commercial materials that are made of thermoplastic plastics like epoxy or synthetic polymer. Even though other fibers, such as paper, timber, or asbestos, have rarely been utilized, glasses, carbonaceous, or fiberglass reinforced are the most commonly used fibers.

The broad definition of matrix composites is a heterogeneous mixture of at least two separate materials at the microlevel, with novel properties distinct from those of its components and typically a nearly uniform structure at the macroscopic scale. The ability to adjust a composite material's qualities to the needs of the intended application is the most distinctive feature that results from the combination of such a range of properties. Fiber-reinforced composites are those in which the reinforced component typically is composed of fibers, textiles, or fillers. The fibers and matrix, which are the core components of the hybrid, as well as the interfacial region make up the substructure of fiber-reinforced composite materials.

FRP reinforcements in structural concrete are being used as an alternative to metal bars. The benefits of FRP reinforcements are their tolerance to corrosion, non-magnetic qualities, superior tensile strength, lightweight, and simplicity of handling. Furthermore, this conclusion needs to be considered in the context of the possible advantages of employing FRP composites, accounting for things like [2]:

- Higher sturdiness
- Lightweight
- Higher performance
- Lasts longer
- Reconstructing existing systems and extending increasing their lives

### 13.1.1 Market prognosis for the present and future

The market for finished products created with such composite "fiber materials is anticipated to reach $78 billion by 2016, with the composite materials industry estimated to reach $27.4 billion." In Europe, the manufacturing of glass fiber-reinforced plastics is anticipated to reach 1.1 million tons in 2016. Carbon fiber demand is expected to reach 100.5k tons in 2020 and 120k tons in 2022, with a fair value of $4.2 billion. In contrast, it is predicted that the need for carbon FRP (CFRP) would be 155,000 tons in 2020 and 191,000 tons in 2022 [3].

## 13.1.2 Constituents of fiber-reinforced polymers

According to the nature, shape, and alignment of the reinforcing phase, two-phase different composite materials are divided into three types as shown in Figure 13.1.

(i) Particulate composites are composed of small particles that are randomly arranged inside the matrices and come in a variety of shapes and sizes. These mixtures can be thought of as semi-homogeneous due to the typical irregularity of grain structure. Particulate composites include nonmetal particles in a non-metallic matrix (e.g., cement, glass reinforced with mica particles, fragile polymers supplemented with rubber-like particles, polymer/clay nanostructured materials, and ceramic).

(ii) Discrete or short-fiber composite materials use nanotubes, bristles, or thin fibers as their reinforcing phase. These thin fibers, which can have a significant aspect ratio (i.e., be quite long due to their width), can be arbitrarily orientated or all aligned in the same orientation. The composite material tends to be somewhat texturizing, or asymmetric, in the initial case, whereas it may be considered quasi-isotropic in the latter.

(iii) Fiber with continuity composites, which are strengthened by particularly long fibers, are among the most efficient composites in respect of stiffness and strength. The continuous fibers may be aligned in many directions or at sharp angles to one another (cross-ply or weaved fabric continuous fiber), or they may be entirely concurrent (single direction) (multidirectional continuous-fiber composite.

In the fiber-reinforced composites (FRP), the reinforcing fiber, matrix, coupling agents, coating, and fillings are the main components [4]. The primary load-bearing elements are fibers. They are more rigid and durable than when utilized in mass. They are shaped like very fine grains and exhibit high molecular symmetry [5]. The majority of the composite's volume is made up of fibers. The four broader categories into which FRP composites fall are (i) metal matrix composites, (ii) polymer matrix composites, (iii) ceramic matrices, and (iv) carbon–carbon composites.

### 13.1.2.1 Glass fiber

Glass fiber is the fiber that is most frequently utilized in PFRCs. It is inexpensive, has a high breaking strength, has less chemical tolerance, and is very insulating. There are two different types of glass fibers: E-glass and S-glass. S-glass has a 33% better tensile strength and a 20% higher percentage of elongation than E-glass.

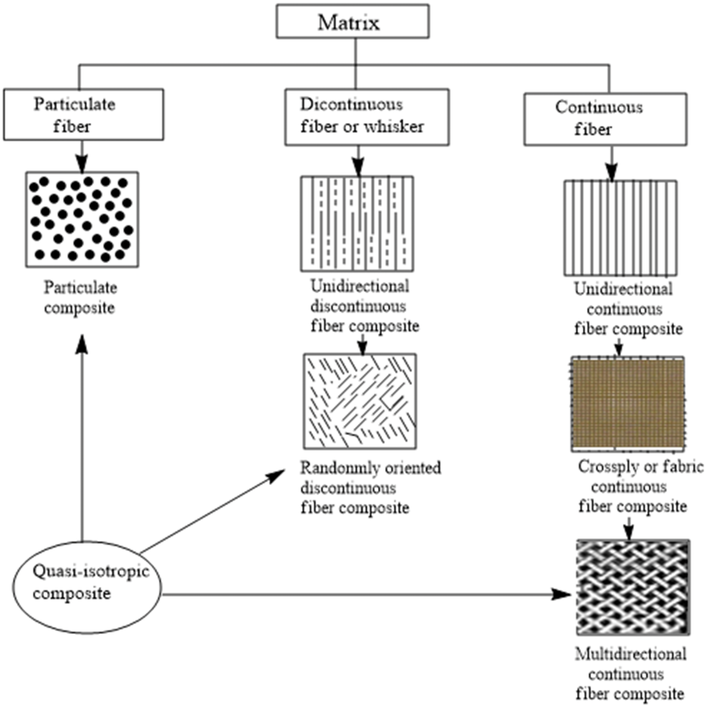
Matrix
Particulate fiber
Dicontinuous fiber or whisker
Continuous fiber
Particulate composite
Unidirectional discontinuous fiber composite
Unidirectional continuous fiber composite
Randonmly oriented discontinuous fiber composite
Crossply or fabric continuous fiber composite
Quasi-isotropic composite
Multidirectional continuous fiber composite

**Figure 13.1:** The classification of the fiber composite material system.

### 13.1.2.2 Carbon fiber

Carbon fiber is extremely strong, rigid, and lightweight. Polymeric fiber antecedents are used to produce carbon fibers. Most often, it is used in the aviation industry. Carbon fiber has an elastic strength ranging from 207 to 802 GPa.

### 13.1.2.3 Aramid fiber

Aramids are aliphatic polyamides are aromatic compounds whose constituent parts are inextricably linked by the amide (NH-CO) connection. They are low in density, lightweight, resonant, damage-resistant, highly tensile, and economical. Kevlar, the first poly-aramid material, was created by Du Pont [6].

#### 13.1.2.4 Boron fiber

Boron fiber has a huge diameter; it can tolerate high compressive stress, and has superior buckling resistance. It has a high tensile modulus ranging from 379 to 414 GPa.

#### 13.1.2.5 Ceramic fiber

The two most common types of ceramic fibers utilized at high temperatures are $Al_2O_3$ (aluminum oxide) and SiC (silicon carbide). They are immune to environmental damage, possess good strength, and have high mechanical properties at high temperatures.

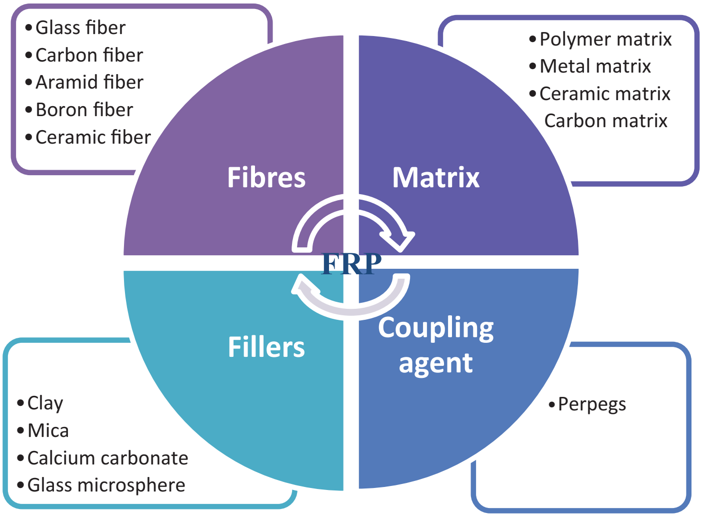
• Glass fiber
• Carbon fiber
• Aramid fiber
• Boron fiber
• Ceramic fiber
• Polymer matrix
• Metal matrix
• Ceramic matrix
Carbon matrix
Fibres
Matrix
FRP
Fillers
Coupling agent
• Clay
• Mica
• Calcium carbonate
• Glass microsphere
• Perpegs

**Figure 13.2:** The constituents of fiber-reinforced polymers.

### 13.1.3 Matrix

The matrix maintains the fibers in position and keeps them oriented in the main stress axis. Through the use of shear force and the matrix, the weight is transmitted through the fibers. The lattice shields the fiber from environmental harm brought on by high temperatures and people [7]. The various matrix materials are further described.

#### 13.1.3.1 Matrix materials of polymers

It is lightweight and possesses advantageous mechanical characteristics. Thermosets and thermoplastics are two forms of polymer matrix structures. Thermosets are best suited for fiber composites because they have a three-dimensional crystal structure after hardening. Epoxy resin, which is employed in aircraft structures for high-performance applications, polyester or phenolic resin, vinyl ester resin, and polyamides are the principal thermoset polymers. Thermoplastics melt at high temperatures and feature a one-dimensional or two-dimensional molecular structure.

**(i) Metal matrix material**
The impact strength and rigidity of metal matrices are higher. The three main metal matrix components are Ti, Al, and Mg (titanium, aluminum, magnesium).

**(ii) Materials for ceramic matrix**
In addition, to possessing a high melting temperature, being corrosion-resistant, and exhibiting sizable strength properties, it also has covalent and ionic bonding.

**(iii) Materials in a carbon matrix**
They are extraordinarily strong, stiff, and temperature-insensitive matrix materials that can withstand high temperatures of up to 23,000 °C [8].

### 13.1.4 Coupling agent and prepregs

Cross-link agents, which also enable binding all over the fiber–matrix junction simpler, increase the hydration of the fibers with the matrix. If matrix and fiber were commercially available as a single product, it would eliminate the need to purchase fiber. Half-cured matrix polymeric resins are used to bind a system of carefully prepared fibers. Prepregs are the label given to these fibers [9].

### 13.1.5 Fillers

To lower the cost, boost elasticity, manage fluidity, and provide a smoother finish, fillers are added to the matrix material. $CaCO_3$ (calcium carbonate) is a typical filler used in polyester and vinyl ester resins. Conventional fillers include glass, mica, and clay microparticles [10].

## 13.2 Corrosion

Through the process of corrosion, a metal or alloy reacts with its surroundings to change into a steady state (i.e., hydroxides, oxides, or sulfides. Large financial losses are incurred by corrosion, which also puts many industries' safety at risk.

A metallic/ non-metallic substance degrades or loses its properties as a result of the chemical/ electrochemical activity of the surroundings to which it is subjected, based on the definitions of corrosion that are most frequently used. When metals deteriorate through an electrochemical process or over time as a result of an aggressive environment, this is referred to as corrosion [11]. One of the biggest issues in the industry is corrosion, which puts plant safety at risk, lowers plant productivity, results in plant shutdowns and economic losses, and can also lead to product contamination [12, 13]. Anodic reaction (dissolution of the metal) and cathodic reduction of oxidizing agents present in the electrolyte solution, such as $H^+$ or $O_2$, constitute the fundamental mechanism of metallic corrosion in aqueous solutions [14]:

$$\mathrm{M_{(s)}} \rightarrow \mathrm{M}^{n+}{}_{\mathrm{(aq)}} + ne^- \quad \text{(oxidation at anode)} \tag{13.1}$$

$$\mathrm{Ox_{(aq)}} + ne^- \rightarrow \mathrm{Red_{(aq)}} \qquad \text{(reduction at cathode)} \tag{13.2}$$

Typically, corrosion is random reaction mechanism that has a chemical/electrochemical characteristic and tends to alter the physicochemical properties of the materials. There is a sizable need for corrosion-resistant items due to the global technological advancement [15].

There are several causes of metal and alloy corrosion. These elements, which also include salts, liquid chemicals, sharp metal polishes, bases or acidic media, salts, and potentially hazardous gases that might encourage corrosion on the metal surface, are listed in Figure 13.4 [16]. In conjunction with the elements listed in Figure 13.4, corrosion is also affected by the temperature as well [17]. Additionally, the development of specific bacterial species within a biofilm on steel can hasten the corrosion process and foster it [18, 19].

Corrosion causes massive economic losses on a global scale. It significantly affects the world economy. The manufacturing, chemical, oil, and many other metal-using industries are currently dealing with expensive issues as a result. Most corrosion-related issues can be brought on by corroded chemical leaking, broken oil pipelines, and even fire when exposed to electrical components and materials [20]. Numerous sectors have recognized how expensive poor corrosion management can be. It is possible to reduce costs by managing corrosion effectively.

Some constructions suffer major structural collapse due to corrosion, such as those made of metals that corrode quickly and can be expensive to repair. Additionally, system shutdowns during maintenance consume time. According to reports, the need to replace damaged systems as well as higher costs for issues like repair, maintenance, and reconstruction was caused by a lack of corrosion protection. Corrosion of these metallic-based

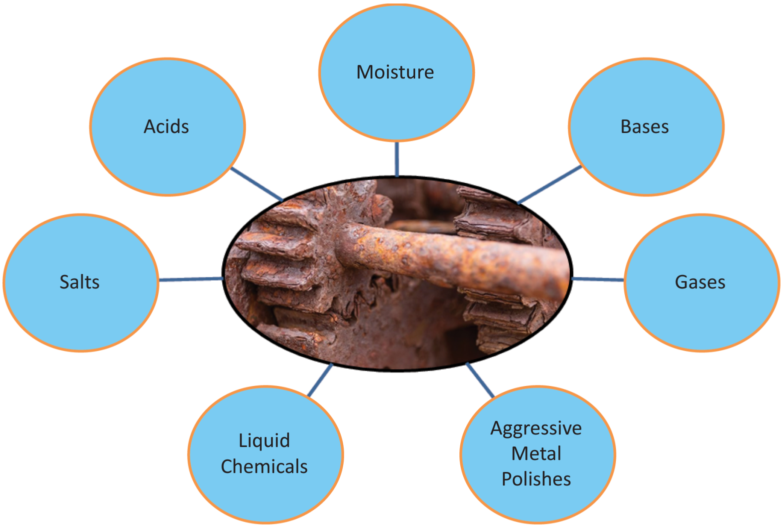
Moisture
Acids
Bases
Salts
Gases
Liquid Chemicals
Aggressive Metal Polishes

**Figure 13.3:** Causes of corrosion of metals and alloys.

items has a considerable economic effect. The total economic losses brought on by corrosion are projected to be over US $2.5 trillion, or roughly 3.4% of the global GDP, according to a recent NACE research [21]. Corrosion in the oil and gas industry is expected to cost roughly US $1372 per year globally [22].

Numerous measures are taken as shown in Figure 13.4 to maintain the surface of these materials in order to prolong their lifespan and lessen this monetary loss, including the use of anticorrosion coatings, cathodic and anodic protection, corrosive-resistant alloys, fiber materials, and inhibitors.

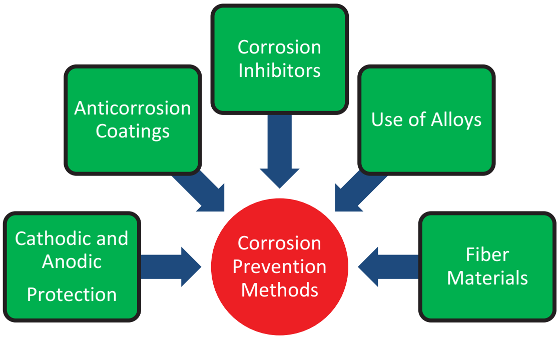
Corrosion Inhibitors
Anticorrosion Coatings
Use of Alloys
Cathodic and Anodic Protection
Corrosion Prevention Methods
Fiber Materials

**Figure 13.4:** Corrosion prevention methods for the metals and alloys.

Numerous studies have been carried out to look into, the role of FRP affecting corrosion reduction [23]. The majority of the studies [24–31] concentrated on corrosion damage in RC elements in cold climates induced by saltwater runoff from defective expansion joints. Fewer research was conducted on corrosion mitigation in tidal waters during hot, humid conditions [32–35], when the corrosion rates are much greater. These applications are only viable because novel resins which can cure in water are now available [36–39]. In a time-lapse research to gauge the effectiveness of FRP in reducing corrosion, for approximately 3 years, one-third-scale models of prestressing piles encased in CFR (carbon fiber-reinforced) polymer and GFR (glass fiber-reinforced) polymer were exposed to modeled tide cycles in external ambiance settings. The efficacy of the reinforced polymer was compared to similar uncontrolled specimens placed in the same surroundings using weight loss testing [35].

Polymer fiber materials exhibit a number of remarkable properties as their diameters decrease to submicron or nanometers from micrometers, including a high surface area to volume ratio, flexibility in surface functionalities, and superior mechanical performance (e.g., stiffness and tensile strength) compared to any other form of the material that is currently known. Due to their exceptional qualities, polymer nanofibers are the best choice for a variety of crucial applications. In recent years, polymer nanofibers have been created using a variety of processing methods, including drawing [36], template synthesis [37], phase separation [38], self-assembly [39], and electrospinning [40]. Nanostructured coatings can be created in a variety of ways, such as super-lattice coatings, nanoscale multilayer coatings, nanocomposite coatings, and nano-graded coatings. By altering or adding a thin layer to the surface of a substrate material, coatings give it special technical qualities. A coating that contains at least one component with nanoscale dimensions is referred to as a nanocoating. The usage of ecologically friendly coatings is becoming increasingly important due to legislation’s demands to reduce environmental harm. By electrospinning deposition of polyvinyl chloride nanofiber on aluminum, stainless steel, and brass substrates, a novel application of a polymeric material for the preparation of corrosion-resistant coatings has been investigated.

## 13.3 Corrosion protection by reinforced fiber material

The right materials and reagents to cure reinforcements is one of the defence barriers against corrosion invasions in hostile situations. There are numerous different reinforcing treatment techniques, such as fusion-bonded epoxy coating and anticorrosive protection employing acid or alkali agents.

Products composed of matrix composites offer long-lasting resilience to extreme climatic and biochemical environments. In corrosive, outside, as well as other harsh conditions including industrial production sites, petroleum and natural gas refineries, paper mills, and wastewater treatment plants, composites are frequently the preferred material for various applications. Cabinetry, pipes, blowers, grates, hoods, compressors, and tankers are examples of common usage [41–43]. For everything from sewage renovations and drainage developments to desalination, petroleum, and gas uses, fiber-reinforced various polymeric pipes are now used. FRP is a remedy for corrosion control in pipes constructed of conventional materials [41, 43].

In a solution of 3–5 wt% NaCl, CFR aluminum shows poor protection to corrosive environment [44]. Diamond-like carbon (DLC) coverings have characteristics that make them appealing substances for matrix material composites for surface corrosion prevention. In a 35 wt% alkaline solution, the various electrochemical performance of untreated and DLC-coated CFR aluminum was evaluated. It has been observed that the encapsulating DLC covering considerably shifts the pitting potential towards the anode and greatly reduces the corrosion current. Further, scratch tests and scanning electron microscopy research were done to assess that, effectively the DLC films adhered to the heterogeneous metal composites.

The purpose of the research [45] was to determine precorroded steel reinforcement in RC columns through passive and active protection. Active protection is a unique method for preventing corrosion, by using the CFRP wrap as the anode of the impressed current cathodic protection (ICCP). The CFRP fabric's anticorrosion behavior is known as passive protection.

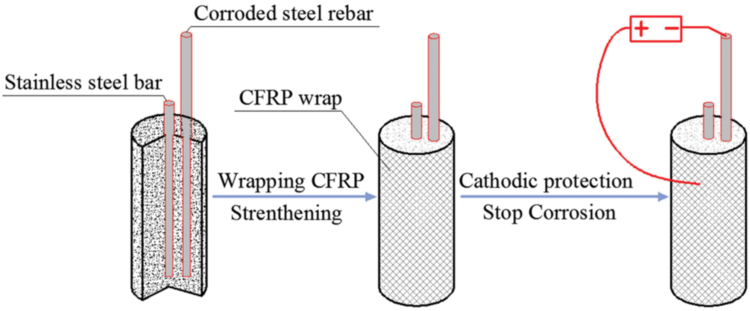

**Figure 13.5:** Details of the corroded and protected specimen.

In this study, CFRP wraps that were externally bonded were used in an electrochemical study to investigate both active and passive reinforcing steel prevention in well before corroded RC columns (Figure 13.5). By employing the CFRP sheets as the anode of the ICCP and connecting them using a conductive adhesive, active protection was obtained. The protective methods (no shielding, passive prevention, and active prevention), the precorroding levels (1%, 3%, and 6% hypothetical mass loss), and other factors were taken into consideration. It was concluded from the observations of steel's potential, linear polarization, and impedance study reactions of all examined specimens (Figure 13.6):

(1) The early corrosion condition of the protected samples and the effectiveness of prevention were closely correlated. In comparison to the control sample, active prevention demonstrated adverse impacts on corrosion growth for specimens that were 1% precorroded. The active protection worked well and outperformed passive protection for the 3% of specimens which was corroded before.
(2) The concrete resistance and $R_{ct}$ (charge transfer resistance) were enhanced even during active prevention process. But these advantages of active protection mostly emerged in the initial phases of prevention. In other words, active protection's effectiveness decreased over time. As a conclusion, the active prevention in this investigation using the CFRP anode is inadequate in preventing the corrosion rate of the steel reinforcement in concrete.
(3) In all situations examined, the rate of corrosion was substantially decreased by the passive protection offered by the CFRP covers. Passive protection can only decrease corrosion; it cannot eradicate it. This was demonstrated by the stable steel potential and decreasing rate of corrosion of passively shielded samples over time.

A comparatively recent class of fiber nanocomposites known as fiber metal laminates (FMLs) or "fiber-reinforced metal laminates" (FRMLs) has received a lot of interest nowadays [46–48]. FMLs are a type of composite material mix that consists of stacks of FRP (fiber-reinforced plastic) and metal sheets joined together. Since CFR plastic (CFRP) has so many benefits over AFRP (Aramid fiber-reinforced plastics) and GFRP (glass fiber-reinforced plastic), like greater effective stiffness and tensile strength, it was also taken into consideration as an effective composite layer in the early stages of the research of FMLs when blended with aluminum alloy to create "carbon fiber reinforced aluminum layer" (CFRP/Al-FRML).

The term for blended CFRP/Al-FRML was named as "CARALL" in this work [49]. Over the years, a large number of scientists have worked hard to create CARALL. The synthesis methods and evaluation of CARALL, in particular, have benefited greatly from the work of experts at the Delft University of Technology and the University of Sydney. Focusing on nanocomposite layer, a novel CARALL that resists the corrosion process has been created. The hybrid sol–gel coating with silica nanoparticle reinforcement and sulfuric acid anodized finish make up the nanocomposite coating. Investigated are the nanocomposite coating's microstructures. The findings of electrochemical tests and corrosive tests that involved submerging the CARALL sample in 3% NaCl aqueous solution for an extended period show that the nanocomposite coating significantly increases the corrosion resistance of Aluminum alloy 2024-T3.

Epoxy coatings that had been treated with polyaniline (PANI) fibers and epoxy fillers were used for testing mild steel in 12% NaCl. After being submerged in the harsh electrolyte for more than 3 months, the coatings still exhibit corrosion protection. The better corrosion resistance is a result of the surface passivation abilities of the PANI nanofibers and the sustained release of the epoxy fillers. Additionally, the

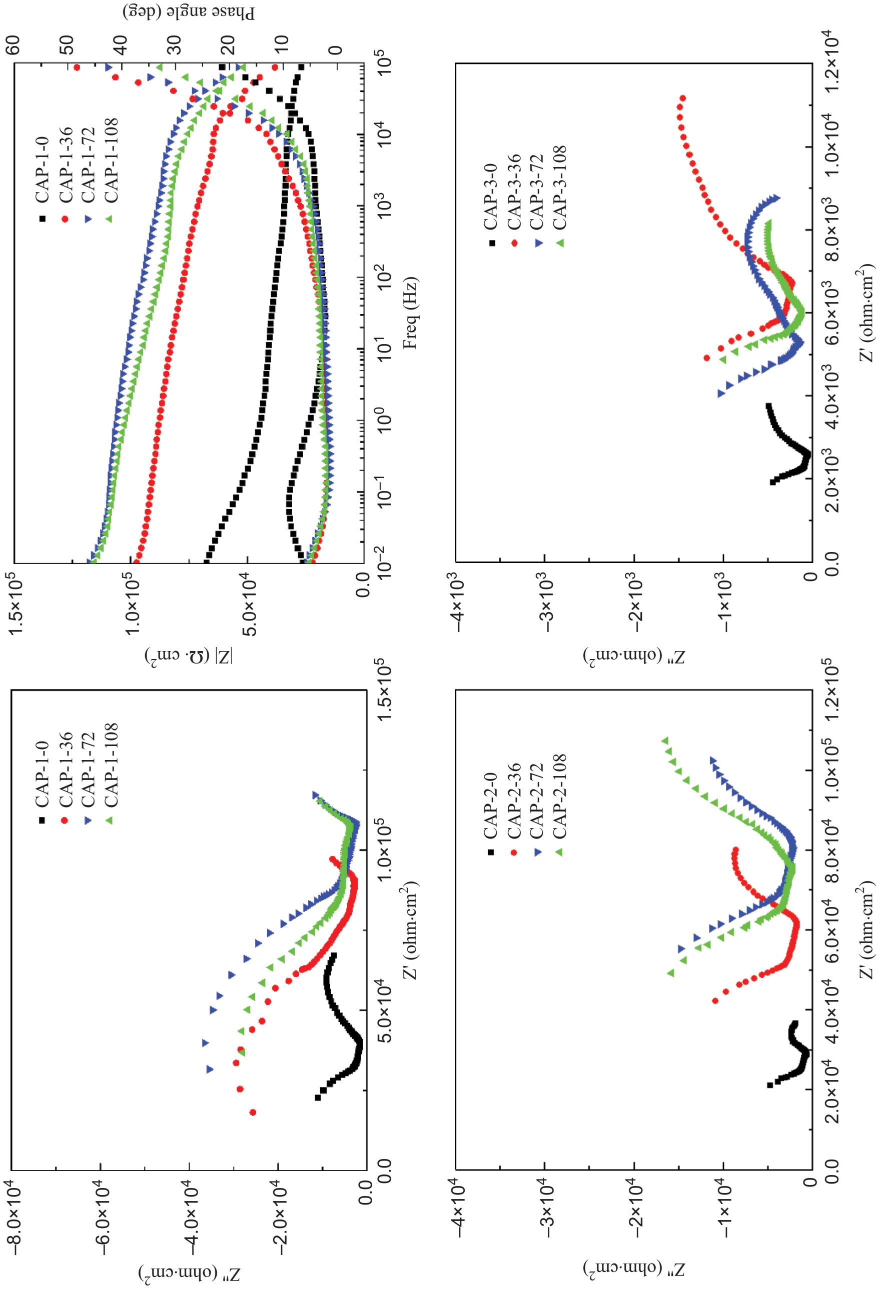

**Figure 13.6:** Elecrochemical impedance spectroscopy response after 108 days of wet–dry exposure in Nyquist and Bode format for: (a) specimens with a 1% theoretical mass loss; (b) specimens with 3% theoretical mass loss; and (c) specimens with a 6% theoretical mass loss.

PANI fibers might enlarge, improving the shielding of affected parts [50]. Steel corrosion prevention using PANI coatings with water-repellent behavior has also been suggested. Measurements of the corrosion potential of cold-rolled steel using PDP and EIS (potentiodynamic and electrochemical impedance spectroscopy) show a switch toward more positive values and higher polarization resistances. The creation of a protective surface made of iron oxides covered in a water-repellent PANI layer explains the prevention of corrosion [51].

In the substrate polymeric matrices, the distribution of tiny PANI nanoparticles or PANI nanofibers can produce nanostructured frameworks that improve protection against corrosion while also changing the conductivity of the substrate. The introduction of dopants [52, 53, 57] or the creation of nanocomposites with additional nanoparticles produces more thick, durable, and improved barrier characteristics [51, 54, 55].

The higher corrosion protection to steel and steel-RC as well as their higher decaying durability to the lumber, GFR polymer composites have become increasingly popular for usage in the building of concrete blocks in coastal locations in addition to interior uses. According to a paper [56], installing a GFRP composite seawall structure may not involve massive equipment, which would drastically shorten construction time when compared to seawalls made of conventional concrete.

The demand for building civil infrastructure systems with FRP composites in aggressive environments has grown due to their exceptional material properties such as high strength, lightweight, and excellent fatigue and corrosion resistance [57–65]. Recent developments in metal fibers have led to the introduction of a good potential type of stainless-steel fiber that can be used in steel FRPs and has good strength, a depth of less than 100 m (0.00394 in).It is unknown how the degradation of fiber composites of stainless-steel fibers encased in a polymer substrate relates to that of substantial steel components (such as steel plates) because there have been few studies that investigate the characteristics of stainless-steel fiber composites in corrosive media.

Furthermore, due to their tiny size and the larger surface area of the reinforcing steel, steel fibers are intrinsically more prone to corrosion than conventional stainless-steel plates. Caitlin O'Brien et al. [66] focused their research on evaluating the corrosive characteristics of SFRP (stainless-steel FRP) composites in comparison to other types of stainless-steel plates. Because of the chemical makeup of the grade 430 SS sample, which is a broad type of steel, it turned out to be the one most prone to corrosion attack. These corroded specimens showed the greatest weight loss as well as a significant decrease in stiffness and stress. In these specimens, pitting was also more common than usual.

Type 174 was among the most vulnerable varieties of stainless steel evaluated, yet it outperformed Type 430 in tensile testing efficiency and loss of weight following corrosion. Although Type 304 lost weight similarly to Type 174, it was really able to keep more of its power and stress from failure.

The composites tended to be the least prone to pitting. They were capable of holding onto their strength and stress the longest. The composites lost weight at a rate comparable to that of the Type 316 SS samples. The results of this investigation support the idea that SFRP composites are a practical corrosion-resistant alternative to traditional metals.

Hai Fang et al. [67] reviewed and compared for environmental consequences on FRP composites, primarily for connectors and junctions, comprising high ambient temperatures, moisture, submersion in water, and UV exposure. The conclusion drawn to further support design and industry adoption of such FRP applications for civil infrastructure in hostile settings, it is anticipated that such approaches may exhibit application and improvement for other similar attributes.

## 13.4 Conclusion

In contrast to other synthetic matrix composites, fiber-reinforced composites have a lower density, good stiffness are inexpensive, and readily harden. FRP is thus utilized in the construction and renovation commodities industries, the automobile industry, the aerospace industry, the marine industry, and other industrial uses. Polymer mechanical performance is enhanced by FRP composite structures.

While the composition is crucial in determining the variety of uses that these substances are suitable, it is also crucial that the finished products are developed to maximize the benefits of these materials' intrinsic characteristics. This chapter includes corrosion and its aspect. Several FRP techniques use the simplest form of fabrication for a variety of uses, including corrosion control. It also examines the features and attributes of FRP composites. Last but not least, it emphasizes the significance of FRP in the mechanical area and the most recent developments in the composites industry for corrosion control.

## References

[1] Jain R, Lee L. Fiber reinforced polymer (FRP) composites for infrastructure applications: Focusing on innovation, technology implementation and sustainability. Springer; 2012.

[2] Masuelli MA. Chapter 1: Introduction of fibre-reinforced polymers – polymers and composites: Concepts, properties and processes, fiber reinforced polymers, Intechopen, Published; 2013. 3–40.

[3] Witten E, Kraus T, K€uhnel M. Composites market report, 2016.

[4] Pamington D. (Ed.). Carbon and high performance fibers directory, 4th ed, U. K, Pammac Directories Ltd.; 1988.

[5] Rout AK, Singh JK. An overview of advanced fiber reinforced polymer composites and it's applications. Int J Mech Prod Eng Res Dev. 2018;8:311–318.

[6] Datoo MH. Mechanics of fibrous composites, London, Elsevier applied science; 1991.

[7] Rosen BW. Mechanics of composite strengthening in fiber composite materials, Ohio, USA, American Society of Metals; 1965.

[8] Luben G. (Ed.). Handbook of composites, New York, Van Nastrand Inc; 1986.

[9] Hull D. An introduction to composites materials, U. K, Cambridge University Press; 1981.

[10] James JA, KilduffT F. Engineering materials technology- structure, processing, properties and selection. 3rd ed, 1997.

[11] Adewuyi A, Göpfert A, Wolff T. Succinyl amide gemini surfactant from adenopus breviflorus seed oil: A potential corrosion inhibitor of mild steel in acidic medium. Ind Crop Prod. 2014;52:439–449.

[12] Heakal FET, Fouda AS, Radwan MS. Inhibitive effect of some thiadiazole derivatives on c-steel corrosion in neutral sodium chloride solution. Mater Chem Phys. 2011;125:26–36.

[13] Uerdingen M, Treber C, Balser M, Schmitt G, Werner C. Corrosion behaviour of ionic liquids. Green Chem. 2005;7:321–325.

[14] Sato N. Basics of corrosion chemistry. In: Sharma SK (Ed.). Green corrosion chemistry and engineering: Opportunities and challenges, John Wiley & Sons; 2011. 1–2.

[15] Alcântara S, Ramosa F, Sennaa LFD, Lagoa Dz CBD. Evaluation of aqueous coffee husks extracts as s corrosion inhibitor of 1020 carbon steel in 1 Mol L-1 HCl solution. Mater Res. 2019;22:e20180839.

[16] Raja PB, Ismail M, Ghoreishiamiri S, Mirza J, Ismail MC, Kakooei S, Rahim AA. Reviews on corrosion inhibitors: A short view. Chem Eng Commun. 2016;203:1145–1156.

[17] Goyal M, Kumar S, Bahadur I, Verma C, Ebenso EE. Organic corrosion inhibitors for industrial cleaning of ferrous and non-ferrous metals in acidic solutions: A review. J Mol Liq. 2018;256:565–573.

[18] Lin J, Ballim R. Biocorrosion control: Current strategies and promising alternatives. Afr J Biotechnol. 2012;11:15736–15747.

[19] Rubio C, Ott C, Amiel C, Dupont-Moral I, Travert J, Mariey L. Sulfato/ Thiosulfato reducing bacteria characterization by FT-IR spectroscopy: A new approach to biocorrosion control. J Microbiol Methods. 2006;64:287e296.

[20] Fayomi OSI, Akande IG, Odigie S. Economic impact of corrosion in oil sectors and prevention: An overview. J Phys Conf Ser. 2019;1378:022037.

[21] Koch G, Varney J, Thompson N, Moghissi O, Gould M, Payer J. International measures of prevention, application, and economics of corrosion technologies study. NACE Int. 2016;216.

[22] Perez TE. Corrosion in the oil and gas industry: An increasing challenge for materials. Jom. 2013;65:1033–1042.

[23] Sen R. Advances in the application of FRP for repairing corrosion damage. Prog Struct Eng Mater. 2003;5(2):99–113.

[24] Sheikh S, Pantazoupoulou S, Bonacci J, Thomas M, Hearn N. Repair of delaminated circular pier columns with advanced composite materials. Ontario Joint Transportation Research Report No. 31902, Ministry of Transportation of Ontario, Aug. 1997, 75.

[25] Neale KW, Labossiere P. Fiber composite sheets in cold climate rehab. Concr Int. 1998;20(6):22–24.

[26] Bonacci J. Rehabilitation of corrosion-damaged RC infrastructure using externally bonded FRP. Proceedings of ACMBS 2000, CSCE. Montreal, Quebec, Canada, 2000, 561–568.

[27] Baiyasi M, Harichandran R. Corrosion and wrap strains in concrete bridge columns repaired with FRP wraps, *paper* no. 01-2609. 80th Annual Meeting. Washington, D.C., Transportation Research Board; 2001.

[28] Debaiky A, Green M, Hope B. Carbon fiber-reinforced polymer wraps for corrosion control and rehabilitation of reinforced concrete columns. ACI Mater J. 2002;99(2):129–137.

[29] Wootton I, Spainhour L, Yazdani N. Corrosion of steel reinforcement in CFRP wrapped concrete cylinders. J Compos Constr. 2003;7(4):339–3 47.

[30] Wheat HG, Jirsa JO, Fowler DW. Monitoring corrosion protection provided by fibre reinforced composites. Int J Mater Prod Technol. 2005;23:372–388.

[31] Mullins G, Sen R, Torres-Acosta A, Goulish A, Suh K, Pai N, Mehrani A. Load capacity of corroded pile bents. Final Report submitted to the Florida Department of Transportation. 2001, 327.

[32] Suh KS, Mullins G, Sen R, Winters D. Use of FRP for corrosion strengthening applications in a marine environment. Final Report submitted to Florida/U.S. Tallahassee, Fla., Department of Transportation; 2005, 406.

[33] Bazinet S, Cereone L, Worth F. Composite FRP moves into underwater repair applications. Sampe J. 2003;39(3):8–16.

[34] Mullins G, Sen R, Suh K, Winters D. Underwater FRP repair of prestressed piles in the allen creek bridge. J Compos Constr ASCE. 2005;9(2):136–1 46.

[35] Sen R, Mullins G, Suh KS, Winters D, FRP application in underwater repair of corroded piles. In: Shield C, Busel J, Walkup S, Gremel D (Eds.). 7th international symposium on fiber-reinforced (FRP) polymer reinforcement for concrete structures, SP-230. Farmington Hills, Mich, American Concrete Institute; Vol. 2, 2005, 1139–1156.

[36] Mullins G, Sen R, Suh K, Winters D. A demonstration of underwater FRP repair. Concr Int. 2006;28:70–73.

[37] Ondarcuhu T, Joachim C. Drawing a single nanofibre over hundreds of microns. Europhys Lett. 1998;42:215.

[38] Ma PX, Zhang R. Synthetic nano-scale fibrous extracellular matrix. J Biomed Mat Res. 1999;46:60.

[39] Whitesides GM, Grzybowski B. Self-assembly at all scales. Science. 2002;295:2418.

[40] Fong H, Reneker DH, Salem DR (Eds.). Structure formation in polymeric fibers. Munich, Hanser; 2001, 225–246.

[41] Available from: http://compositeslab.com/composites-101/history-ofcomposites/.

[42] Available from: https://www.compositesworld.com.

[43] Hu N. Composites and their applications. Croatia, IntechOpen; 2012. DOI: 10.5772/3353.

[44] Wielage B, Dorner A, Shu¨rer C, Kim JH. Corrosion protection of carbon fibre reinforced aluminium composite by diamond like carbon coatings. Mater Sci Technol. 2000;16:344–348.

[45] Lu YY, Hu JY, Li S, Tang WS. Active and passive protection of steel reinforcement in concrete column using carbon fibre reinforced polymer against corrosion. Electrochimica Acta. 2018;278:124–136.

[46] Asundi A, Choi AYN. Fiber metal laminates: an advanced material for future aircraft. J Mater Process Technol. 1997;63:384–394.

[47] Vogelesang LB, Vlot A. Development of fiber metal laminates for advanced aerospace structures. J Mater Process Technol. 2000;103:1–5.

[48] Vlot A, Gunnink JW. Fiber metal laminates: An introduction, Kluwer Academic Publishers. L. B; 2001, 14–21.

[49] Wang WX, Takao Y, Matsubara T. Galvanic corrosion-resistant carbon fiber metal laminates. 16th International Conference On Composite Materials. 2007, 1–10.

[50] Zhang H, Wang J, Liu X, Wang Z, Wang S. Facile fabrication of superhydrophobic sponge with selective absorption and collection of oil from water. Ind Eng Chem Res. 2013;52:10172–10180.

[51] Peng CW, Chang KC, Weng CJ, Lai MC, Hsu CH, Hsu SC, Hsu YY, Hung WI, Wei Y, Yeh JM. Superhydrophobic surfaces for corrosion protection: a review of recent progresses and future directions. Electrochim Acta. 2013;95:192–199.

[52] Gupta G, Birbilis N, Cook AB, Khanna AS. Polyaniline-lignosulfonate/epoxy coating for corrosion protection of AA2024-T3. Corros Sci. 2013;67:256–267.

[53] Arefinia R, Shojaei A, Shariatpanahi H, Neshati J. Anticorrosion properties of smart coating based on polyaniline nanoparticles/epoxy-ester system. Prog Org Coat. 2012;75:502–508.

[54] Navarchian AH, Joulazadeh M, Karimi F. Clay nanocomposites on steel surfaces. Prog Org Coat. 2014;77:347–353.

[55] Huang TC, Su YA, Yeh TC, Huang HY, Wu CP, Huang KY, Chou YC, Yeh JM, Wei Y. Physico-mechanical and electrochemical corrosion behavior of soy Alkyd/Fe3O4 nanocomposite coatings. El Ectrochim Acta. 2011;56:6142–6149.

[56] Ashpiz ES, Egorov AO, Ushakov AE. Application of composite materials for the protection of sea shores and engineering structures against the impact of waves. WIT Trans Ecol Envir. 2010;130:231–238.

[57] Pour A, et al. In situ synthesis of polyaniline-camphorsulfonate particles in an Epoxy matrix for corrosion protection of mild steel in NaCl solution. Corros Sci. 2014;85:204–214.

[58] Fang Y, Wang K, Hui D, Xu FJ, Liu WQ, Yang SL, Wang L. Monitoring of seawater immersion degradation in glass fibre reinforced polymer composites using quantum dots. Compos Part B: Eng. 2017;112:93–102.

[59] Fang H, Sun HM, Liu WQ, Wang L, Bai Y, Hui D. Mechanical performance of innovative GFRP-bamboo-wood sandwich beams: Experimental and modelling investigation. Compos Part B: Eng. 2015;79:182–196.

[60] Wu C, Bai Y, Zhao XL. Improved bearing capacities of pultruded glass fibre reinforced polymer square hollow sections strengthened by Thin-Walled steel or CFRP. Thin-Wall Structure. 89 (201):67–75.

[61] Manalo AC, Aravinthan T, Karunasena W. Flexural behaviour of glue-laminated fibre composite sandwich beams. Compos Struct. 2010;92:2703–2711.

[62] Fang H, Zou F, Liu WQ, Wu C, Bai Y, Hui D. Mechanical performance of concrete pavement reinforced by CFRP grids for bridge deck applications. Compos Part B: Eng. 2017;110:315–335.

[63] Yang X, Shi Liu WQ, Fang H, Bai Y, Hui D. Flexural responses and pseudo-ductile performance of lattice-web reinforced GFRP-wood sandwich beams. Compos Part B Eng D. 2017;108:364–376.

[64] Yang X, Fang H, Shi HY, Liu WQ, Qi YJ, Bai Y. Bending performance of GFRP-wood sandwich beams with lattice-web reinforcement in flatwise and sidewise directions. Construct Build Mater. 2017;156:532–545.

[65] Fang H, Xu X, Liu WQ, Qi YJ, Bai Y, Zhang B, Hui D. Flexural behavior of composite concrete slabs reinforced by FRP grid facesheets. Composites Part B Eng. 2016;92:46–62.

[66] O'Brien C, McBride A, Zaghi AE, Burke KA, Hill A. Mechanical behavior of stainless steel fiber- reinforced composites exposed to accelerated corrosion. Materials. 2017;10:772.

[67] Fang H, Bai Y, Liu W, Qi Y, Wang J. Connections and structural applications of fibre reinforced polymer composites for civil infrastructure in aggressive environments. Compos Part B: Eng. 2019;164:129–143.

Bhuvaneshwaran Mylsamy*, Karthik Aruchamy,
Sampath Pavayee Subramani, Sathish Kumar Palaniappan,
Sanjay Mavinkere Rangappa, Suchart Siengchin

# Chapter 14
# State of the art of advanced fiber materials: future directions, opportunities, and challenges

**Abstract:** The most investigated issues over the past several years have been the use of natural fibers in replacing man-made fibers. This is a result of their natural qualities, which are superior to synthetic fibers in terms of biodegradability, renewability, and abundance of availability. Since synthetic fibers are made of limited resources (fossil fuels), they are primarily impacted by changes in oil prices and their build up mostly in the environment. Even synthetic fibers replace natural fibers in terms of their mechanical and thermal characteristics. Combining these fibers/fillers as reinforcing for different polymeric composite materials provides the potential for developing structures and materials with multiple functions for leading applications. Since biological and synthetic materials individually have benefits and drawbacks, different materials have been utilized in combination and in a composite form to enhance the physicochemical, mechanical, and biological qualities.

**Keywords:** Hybrid composite materials, mechanical properties, moisture absorption, biological durability, flame resistance, applications of composite materials

## 14.1 Introduction

Environmental protection, along with energy, is one of the biggest issues facing the present generation. More than ever, novel approaches are needed to either safeguard the environment or produce environmentally friendly products. The superior characteristics of

---

***Corresponding author: Bhuvaneshwaran Mylsamy,** Department of Mechanical Engineering, K.S.R. College of Engineering, Tiruchengode 637 215, Tamil Nadu, India, e-mail: bhuvansparks@gmail.com
**Karthik Aruchamy**, Department of Mechatronics Engineering, Akshaya College of Engineering and Technology, Coimbatore 642 109, Tamil Nadu, India
**Sampath Pavayee Subramani**, Department of Mechanical Engineering, K.S.Rangasamy College of Technology, Tiruchengode 637 215, Tamil Nadu, India
**Sathish Kumar Palaniappan, Sanjay Mavinkere Rangappa, Suchart Siengchin,** Natural Composites Research Group Lab, Department of Materials and Production Engineering, The Sirindhorn International Thai-German Graduate School of Engineering (TGGS), King Mongkut's University of Technology North Bangkok (KMUTNB), Bangkok 10800, Thailand

https://doi.org/10.1515/9783110992892-014

the renewable plant fibers such as their lower compactness, higher strength, biodegradability, and sustainability in nature [1–5] have paved the way to be a promising alternative to replace artificial man-made fibers. Natural fibers are distinctive in that they are inexpensive, widely available, and made from renewable resources that absorb carbon dioxide to less harmful emissions. Natural fibers do not produce any toxic fumes when they are processed, and they do not wear down the machinery either. Natural fibers' primary drawbacks are their inherited hydrophilic and high flammability, which hinders their use as reinforcement in polymers. Due to their hydrophilic nature, they absorb a lot of moisture and have weak matrix–fiber interface adhesion and fiber dispersion. To get around these restrictions, a large amount of study has been carried out on the surface treatment of natural fibers [1–7]. As described in these review studies [1, 2, 4, 5], it can be argued that numerous investigations on treating plant fibers to enhance the general characteristics of the final product have been carried out. Several fire-resistance coatings have been experimentally investigated to improve the nonflammable property of the fibers. However, given their better qualities than those of natural fibers, artificial/man-made fibers merit extra attention [8–14].

It is acknowledged that several factors, including growth conditions, harvesting techniques, and maturity, frequently alter the qualities of natural fibers [7–11]. Figure 14.1 shows the classification of fibers [12].The drawbacks of artificial fibers include their exorbitant price, nonbiodegradable property and the fact that they are made from limited available non–renewable sources [1]. Numerous gases, such as $CO_2$, methane, and nitrous oxide, are produced only by the refining of fossil fuels and add to unwelcome environmental contamination. In addition, toxic gases that cause dreadful diseases such as cancer are released during the manufacture of composites. These gases can also be abrasive to the machinery used for processing the materials. The durability of synthetic fibers, on the other hand, makes them more advantageous for wide applications [1–5]. These fibers are very strong and can be created with specific functions needed for the desired use.

Carbon fibers have excellent strength, thermal stability, low or no moisture content, good electrical and thermal conductivity. These characteristics give composite laminates as-prepared a chance to be used in high-end applications including thermal energy storage, wind turbines, and aerospace [6].

A hybrid composite is formed by the mixture of one or more fillers with a common matrix [3] including ceramic, polymer or steel. The term "hybrid" can also refer to a mixture of two or more polymer materials that have been strengthened with one or more fillers when referring to polymer composite materials. The term "auto-hybrid" is generally used when the same form of filler has varied sizes or proportions. The usage of polymer composite materials can be improved due to hybridization, particularly in high-end applications. The qualities of the final hybrid composite product are significantly influenced by three main parameters. The first is the composition of the components (matrix and filler), which varies depending on the usage. For instance, jute/glass hybrids showed better reinforcement than bamboo/glass composites under compressive stresses but their behavior was the opposite when subjected to tensile load [7].

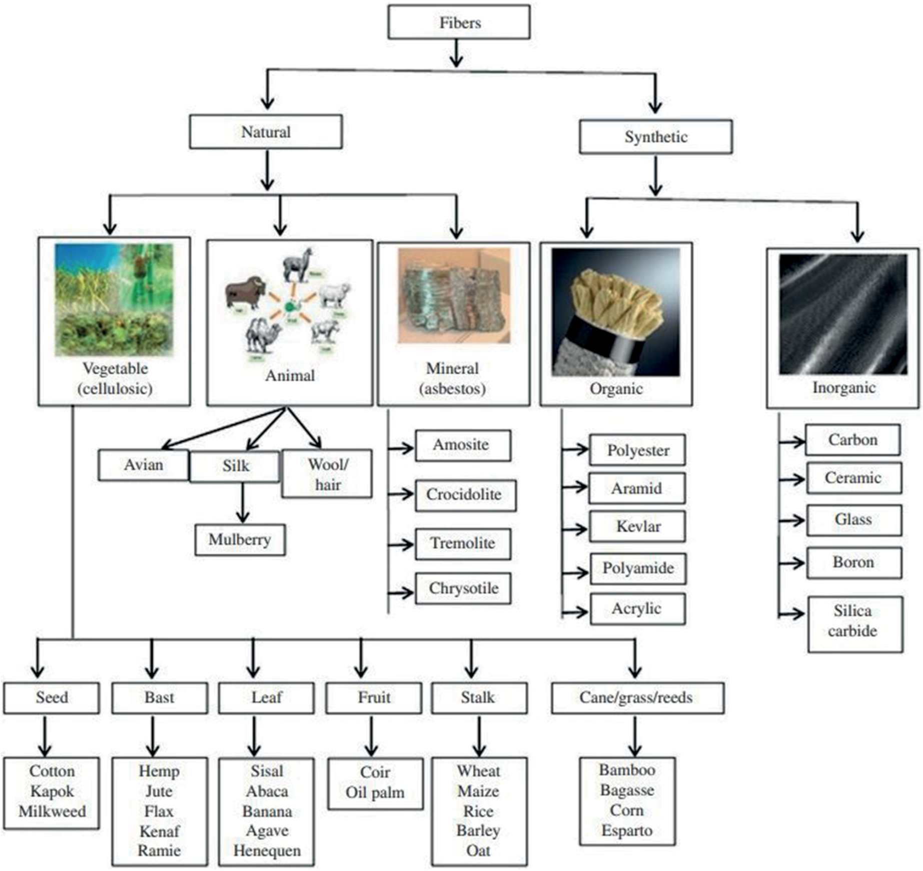
Fibers
Natural
Synthetic
Vegetable (cellulosic)
Animal
Mineral (asbestos)
Organic
Inorganic
Avian
Silk
Wool/ hair
Mulberry
Amosite
Crocidolite
Tremolite
Chrysotile
Polyester
Aramid
Kevlar
Polyamide
Acrylic
Carbon
Ceramic
Glass
Boron
Silica carbide
Seed
Bast
Leaf
Fruit
Stalk
Cane/grass/reeds
Cotton Kapok Milkweed
Hemp Jute Flax Kenaf Ramie
Sisal Abaca Banana Agave Henequen
Coir Oil palm
Wheat Maize Rice Barley Oat
Bamboo Bagasse Corn Esparto

**Figure 14.1:** Classification of fibers [12].

In general, a “hybrid effect” is a comparison between a hybridized composite and a single fiber-reinforced composite that can either be positive or negative. In comparison to the single reinforced composite, the hybridized composite material performs better, based on the definition of the positive hybrid effect, while the negative hybrid effect has the opposite impact. There has been more focus on using different fibers/ fillers that are lighter, more widely available, and less expensive in replacement of a certain percentage of traditional fibers utilized for the intended application [15, 16].

Every application may need a certain set of characteristics to accomplish its objectives, it can be argued. To blend (individually) natural fibers with glass fiber to create an automotive brake lever, Mansor et al. [17] utilized the analytical hierarchy method to select the best natural fibers among 13 possibilities. When compared to other fibers, they observed that kenaf fibers produced the highest score. The other factor is the making technique which mostly depends on the subject matrix and filler. It is important to note many requirements must be satisfied while designing a new product, such as the environment (e.g., whether it will be utilized indoors or outside). This must be accomplished by conducting research, comparing it to available commercially products on the market, and formulating their requirements.

It is also important to strike a balance between the product's performance and sustainability to satisfy both the requirements of the customer and the ecosystem. There are still other things to consider. Mechanical strength, weight, disability, density, recyclability water absorption, production costs, cost of raw materials, compatibility with the already-existing recycling system, and test procedures are the factors that must be considered to make the final product (depending on the intended application). The relationship between the matrix and fillers is the third most crucial characteristic. Moreover, the bonding strength of these components can be substantially increased if the fibers are treated or a coupling agent is used, particularly for natural fibers. In most cases, this will enhance the overall characteristics of the hybrid material.

Hybrid polymer matrix composites reinforced by artificial and natural fibers have been utilized to improve the material strength, decrease moisture content, optimize the fiber cost, minimize the ill effect on the environment, and reduce energy and carbon footprints [18]. Because they have hydroxyl groups on the surface of natural fibers, are hydrophilic by nature, and swell when exposed to moisture or water, providing them undesirable characteristics. The above-mentioned issue has been minimized by the use of surface modification techniques, but most of these techniques involve the application of harsh chemicals that are not ecologically friendly. Combining natural fibers with artificial hydrophobic fibers in a process known as hybridization provides an alternative to chemical treatment [18]. With this technique, the moisture content is decreased while the material's characteristics are also improved.

## 14.2 Properties of composite materials

### 14.2.1 Thermomechanical characteristics of hybrid composites

The thermomechanical characteristics of a hybrid composite material are a function of time, frequency, and temperature. The property of the composites depends on the storage modulus and loss modulus and tan also known as the damping factor. Ridzuan et al. [19] studied the thermal and mechanical characteristics of hybrid polymers, reinforced with raw and treated grass fibers and glass fibers. The polymer chains began to move freely as the temperature increased, as was expected, and the storage modulus reduced. The storage modulus of each hybrid was higher than that of neat epoxy. The maximum storage modulus and loss modulus were found in hybrid composite with 5% NaOH-treated grass fibers and glass fibers, followed by hybrid polymer composite with 10% NaOH-treated grass fibers and glass fibers, and finally hybrid polymer composite with untreated grass fibers and glass fibers. Romanzini et al. [20] claim that the increased molecular mobility restriction the fibers placed on the polymer matrix was what caused the improvement in storage modulus in the hybrid composites.

Hybrid polymer composites' mechanical characteristics are influenced by several variables. These factors consist of the distribution and dispersion of fibers in the selected matrix; the reinforcements and polymer bond strength; the size and aspect ratio of the reinforcement materials; the mechanical characteristics of the reinforcements; the impact of loading; surface modification; and, in the case of natural fibers, the dimension and orientation of the fiber [21–25]. The formation of hybrid polymer composites from thermoplastics and thermosets using artificial and plant fibers, fibers and nanomaterials, have all been the subject of numerous studies and their mechanical and thermomechanical properties have been clarified [18, 23, 25, 26].

Additionally, there is a huge market potential to bring in use such materials, as they satisfy the specifications for a variety of products, including door panels and vehicle interiors [23]. The material parameters, such as the mechanical characteristics of the reinforcements (fibers or particles), matrix mechanical characteristics, distribution and dispersion of reinforcement material, the fiber volume fraction of reinforcements, and test conditions, all affect the prediction of the mechanical characteristics of hybrid materials. To forecast the mechanical characteristics of hybrid materials, the rule of mixture is frequently used.

### 14.2.2 Moisture absorption

One of the key issues with natural fiber-reinforced polymer composites is water absorption. This can have a significant negative impact on the effective use of natural fibers in durable composites, which are not just confined to nonstructural and interior uses. Because natural fibers are hydrophilic, they absorb more moisture than synthetic materials. There are several hydroxyl groups (-OH) in cellulose and hemicellulose, which make up natural fibers, however not all of these components are involved in moisture absorption. For example, lignin has a low ratio of -OH to carbon (C) and is hydrophobic by nature. However, as cellulose is semicrystalline and forms up the majority of natural fibers, its ratio of OH-to-C is high, with a meager amount of its -OH groups being exposed to or available to water molecules. Water molecules can penetrate the amorphous region of the cellulose but not in the crystalline portion. Hemicellulose is primarily amorphous. The -OH-to-C ratio is high and is highly sensitive to moisture [27, 28]. As a result, it is very accessible to water molecules. Water molecules fill the temporary microcapillary network, which is the area between the microfibrils, when natural fibers absorb water molecules, causing the fibers to inflate. The water molecules, absorbed within the fibers can either form a monolayer that closely connects with the available -OH groups or a multilayer where only a few water molecules are in close contact with them. Several variables affect how water is absorbed by natural fiber-reinforced polymer composites. These variables include fiber type, fiber volume fraction, variations in water penetration in the composite, temperature, crosslinking and level of crystallinity, diffusivity, and the reaction of water and the polymer [29, 30]. One key mechanism, called diffusion, is what propels water absorption into composite laminates. In diffusion, the molecules spontaneously translate from a high-concentration region to a region of low concentration with the same system. In composite materials water molecules diffuse directly into the microgaps between polymer chains, indirectly through matrix microcracks caused by fiber swelling, and also via capillary transport into gaps present in the fiber-polymer interface caused by inadequate or incomplete impregnation and wetting [31–33]. As a result, natural fiber-based polymer-reinforced composites are prone to moisture absorption. This absorption characteristic is due to the polar nature of the fibers resulting in the water absorption and thereby swelling of the fibers. The swelling that results from molecules of water penetrating the fiber-polymer contact causes dilapidation, the formation of fractures, and debonding. Figure 14.2 shows the effect of water absorption on fiber–matrix interface [28]. The formation of osmotic pressure pockets at the fiber surface is caused on by the partitioning of water-soluble materials [33–35]. Additionally, the absorbed molecules may function as a plasticizer, resulting in areas of low transfer efficiency and a decrease in the mechanical characteristics of the composite. The tensile strength of injection molded hemp/glass fiber hybrid polypropylene composites was studied by Panthapulakkal and Sain [31] for their water absorption capabilities and their impact. At varying temperatures, namely 40, 60, and 80 °C, the moisture absorption by immersion technique was assessed. Due to the development of micro-cracks and the dissolving of lower molecular weight material from the natural fibers, the composite exhibited a diffusion behavior that vanished when it was subjected to high temperatures.

In addition, the moisture absorption caused the fiber–matrix interface to debone, which significantly reduced the mechanical strength and stiffness of the hemp fiber composite. Hybridized natural and glass fibers showed a reduction in their water absorption characteristics by 40%. The tensile modulus and strength of hemp fiber and hemp/glass fiber hybrid composites, however, were adversely affected by the water absorbed. The modulus and strength retention of pultruded hybrid composites made of jute-glass fibers and unsaturated polyester, as opposed to jute composites, were superior especially in the temperature range of 50–80 °C after being submerged in water [36]. As moisture resistance increased as a result of the addition of glass fibers, the hybrid composites also showed a propensity to deviate from Fickian behavior. The findings indicate that it is possible to adjust the durability of natural fiber composites while balancing economic effectiveness and environmental impact by appropriately blending them with synthetic fibers.

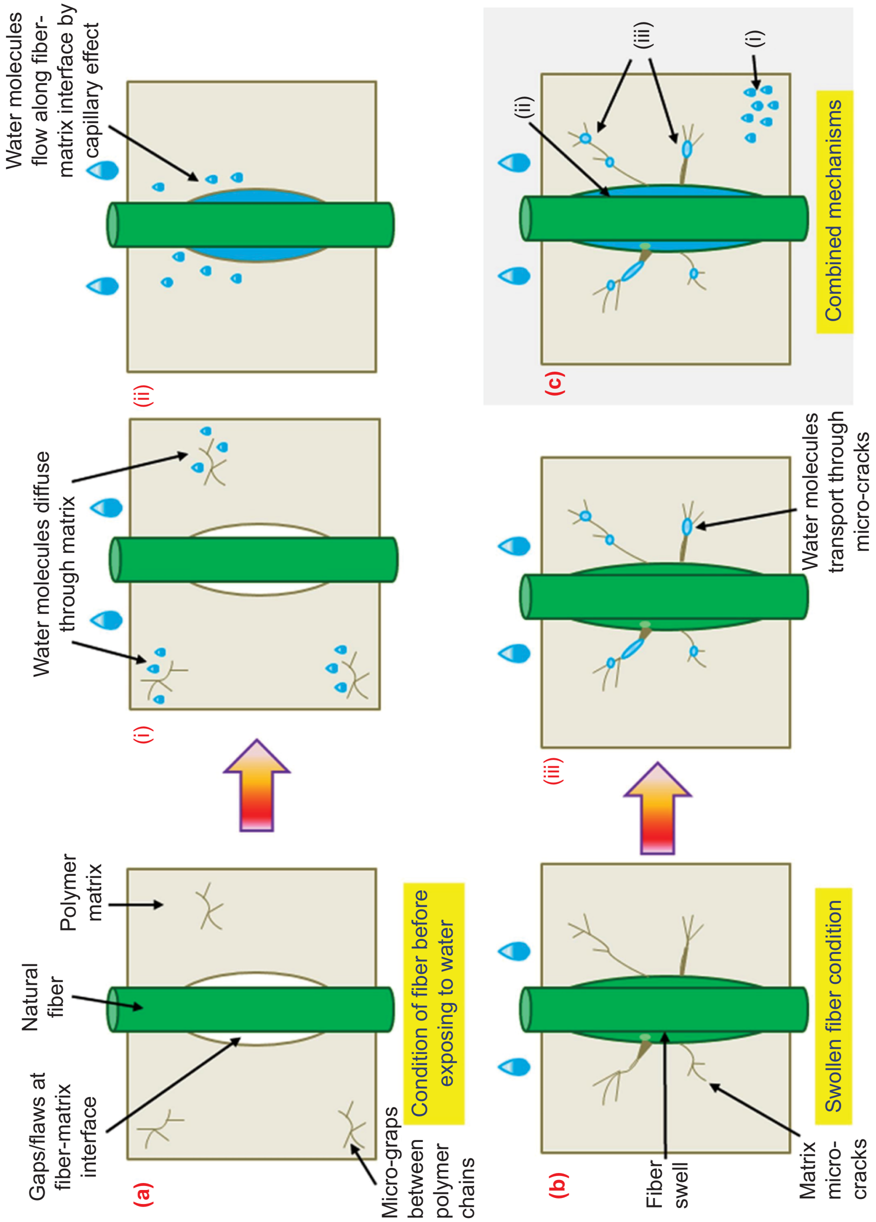
(a)
Gaps/flaws at fiber-matrix interface
Natural fiber
Polymer matrix
Micro-graps between polymer chains
Condition of fiber before exposing to water
(i)
Water molecules diffuse through matrix
(ii)
Water molecules flow along fiber-matrix interface by capillary effect
(b)
Fiber swell
Matrix micro-cracks
Swollen fiber condition
(iii)
Water molecules transport through micro-cracks
(c)
(ii)
(iii)
(i)
Combined mechanisms

**Figure 14.2:** Effect of water absorption on fiber–matrix interface [28].

### 14.2.3 Biological durability

According to the environment they are subject to while performing their function, natural fibers can be identified by their propensity to degrade (i.e., chemical, thermal, mechanical, and biological) [36, 37]. This is related to the various components of the natural fiber that was used. For instance, it has been found that hemicelluloses are responsible for moisture absorption, biological degradation and, whereas lignin is responsible for UV degradation [37–41]. Although their employment as reinforcement for certain polymeric materials is justified by this attribute, their degradation may be undesired in other situations. The ability of fibers to resist biological deterioration can be increased by treating them to inhibit -OH and other polar groups on their surface [37]. It is identified that the resin and interfacial treatment have a significant role in the biological degradation of composites, and that the loss of interfacial strength can have a significant impact on the overall composite's susceptibility to biological deterioration [42]. Thus MA-g-PP was used to incorporate Caraua fiber into a biodegradable polyester-based blend. This reduced the volume of water absorbed, which increased the amount of composite mass retained during biodegradation experiments [44–46]. Investigated the influence of weathering on polyethylene/wood composites when nano zinc oxide was present. Due to its propensity to absorb UV rays, zinc oxide's presence reduced surface degradation during weathering. Conditions to which the materials are exposed generally have an impact on how quickly a hybrid composite degrades. According to the hybrid composite developed micro- and macro-cracks as a result of UV radiation, rainwater, and high temperatures, which sped up the biodegradation of the soil and the growth of fungi [46].

### 14.2.4 Flame resistance

The properties of composite materials smoke production and flame retardancy are serious problems. As most of the composite materials developed for domestic applications are made from natural fibers, they must comply with fire safety regulations. Natural fiber composites undergo thermal disintegration and combustion when subjected to fire or high temperature. It is quite crucial to comprehend how different parts of the finished composite burn and thus it is a real challenge to meticulously bring changes in materials until the flame-resistant property is attained, without sacrificing the characteristic of a high strength-to-weight ratio. Utilizing measurements from the limiting oxygen index (LOI), cone calorimeter, and UL 94 burning rates, researchers have examined the flammability qualities of hybrid natural fiber composites. The flammability will usually be lower for the material with a higher value of LOI and higher for the material with a lower value of LOI. The cone calorimeter instrument works on the principle that the amount of oxygen consumed by a substance during the combustion performance test is what determines the quantity of energy released [47].

## 14.3 Applications of composite materials

### 14.3.1 Transportation applications

Implementation of the proposed product design parameters, an analytical hierarchy process (AHP) was used to select a hybrid of natural and glass fiber-reinforced composite to create car brake levers [17]. Among the 13-hybridized glass fiber reinforced composites, kenaf fiber was found to be a good choice to fabricate a Light Motor Vehicle (LMV) car body and the hand brake lever. The resulting composite material must satisfy several requirements before it can be used in aircraft. Safety and weight are the two most crucial factors in aircraft. As a result, the flammability of the composite material also qualifies it for use in aerospace, in addition to its mechanical characteristics. The use of flame retardants in combination with fibers to develop hybridization composites that are highly fire resistant has become a popular research area in recent years [48, 49]. The interior wall panels, ceiling panels, galley structures, partitions, overhead stowage bins, huge cabinet walls, and structural flooring, are frequently made of reinforced composites. The most widely used composite is made of carbon fiber-reinforced thermosets, which are very flammable. As a result, there has been an increased study on thermosets with strong flammability resistance; however, due to the high cost and their low mechanical strength, attention has been shifted toward the development of composites that have good fire resistance properties and mechanical strength. Hybrid composites made of basalt/sisal, glass/sisal, and basalt/glass/sisal were compared by Alexander and Churchill [50]. According to studies, basalt/sisal/epoxy composites exhibited a better bond strength between the fibers compared to other combinations, thereby becoming a potential material for aircraft structural applications. As a result, a hybrid composite that can be used in automobiles is created, with a performance-to-weight ratio that is balanced. However, when the glass fibers were added to the hybrid system, the moisture absorption was also decreased, it is significant to note.

### 14.3.2 Energy generation

Researchers, governments, and environmentalists are increasingly focused on renewable energy sources. Two of the most popular renewable energy sources that have attracted a lot of interest as alternatives to energy sources are wind and solar energy. In the instance of solar energy, hybridized composites have lately been used as a component of the parabola for harnessing the sun's energy [51]. Despite a composite collector having the advantage of less weight, the commercial feasibility is not there due to the higher fabrication cost owing to the high mold cost. This disadvantage can be overcome by the use of natural fibers to significantly offset the overall cost of the collector. Recent research has shown that adding natural fibers and synthetic fillers as the reinforcing phase of the continuous phase can lower the cost of trough collectors [51].

The performance of a wind turbine relies on the design and strength of the blades and wind rotor; the components that make up these key parts determine the cost and efficiency of electricity generation. The most popular fillers in turbine blades are hybrids of carbon and glass fibers both of which are highly expensive making them a major drawback. The effectiveness of wind turbines can be increased by using fillers that are much lower and more affordable than carbon fibers. According to a recent study, basalt fibers may replace 20–30% of carbon fibers in turbine blade applications without significantly affecting the composite product's characteristics [52]. A combination of woven, silicon, and mesoporous silica demonstrated potential for usage in wind turbines in another study [53].

### 14.3.3 Electromagnetic interference shielding

In a variety of disciplines, including the army, aircraft, and communications, electromagnetic interference (EMI) has been a major topic [54–56]. Various instruments and electronic equipment that produce a lot of electrical and magnetic fields were introduced because of the rapid advance technologies. Electronic device signals are impacted by electromagnetic pollution, which also has the potential to harm internal parts and reduce overall performance. Additionally, magnetic fields interact strongly with biological systems and change the DNA structure of humans. It may also result in headaches and sleeplessness. According to recent study kenaf and magnetite fiber mixed as polyester matrix reinforcements has a significant EMI shielding property [56]. Another method to generate high EMI shielding hybrid polymer composites material and prevent corrosion of metal films is to protect them with natural fibers [57]. Xia et al. [57] coated the aluminum sheets with hemp fiber mat to produce a composite using vacuum-assisted resin transfer molding with epoxy matrix. The newly added aluminum sheets raised the EMI shielding to 20 dB, which is above its being required for commercial use.

### 14.3.4 Armor systems

To investigate their suitability for application in armor systems, synthetic fibers including glass, aramid, and carbon have been frequently used as reinforcement of resins [58, 59]. The armor system is known to typically consist of two layers. High-strength metals that have been rolled into homogeneous armor material make up the outer layer (titanium or uranium). For protection against heavy bullet impacts, the interior (second) layer (spall liners) is frequently placed. It has been investigated whether using more widely available, less expensive fibers could compromise safety or protection. Kevlar, glass, and carbon fibers, as well as their hybrids, were investigated as potential candidates. The nonwoven kenaf fiber layer and the Kevlar layer were studied by Yahaya et al. [60] using various sequences, including kenaf at alternating layers, the outermost layers, and the innermost layers. When kenaf was used in the outer layers, the resultant composite acquired a higher V50 (i.e., velocity of ballistic impact, with 50% likelihood of penetration and 50% of nonperforation) than other systems. Compared to their earlier investigation with randomly oriented kenaf fibers. their next study with woven kenaf fiber-Kevlar hybrid, showed better characteristics [61]. These investigations showed the possibility of combining natural and synthetic fibers in armor systems.

## 14.3.5 Emerging applications

By 2025, it is projected that the worldwide economy for biocomposites would be worth $41 billion [62]. Natural fiber-reinforced polymer composites (NFRPCs) offer a lot of potential uses, including 3D printing [63], tribological, packaging, and automotive [64–66]. Table 14.1 presents the typical applications of NFRC composites in various industries [67].

**Table 14.1:** Different applications of natural fiber reinforced composites in various industries [67].

| S. no. | Industry/sector | Name of the parts |
|---|---|---|
| 1 | Household | Door panels, food trays, tables, chairs, interior panels, lampshades, shower and bath units, suitcases |
| 2 | Aerospace, automotive and transport | Seat backs, floor mats, interior door panels, dash boards, spare tire covers, spare-wheel pans, automobile and railway coach interior, interior carpets, boats, and architectural moldings |
| 3 | Electronics | Mobile and laptop cases |
| 4 | Construction and building | Partition boards, false ceiling and panels for partition, windows, and door frames |
| 5 | Storage and materials handling | Postboxes, biogas containers, fuel containers, and storage silos |
| 6 | Sports | Boats, tennis racket, bicycle, frames, snowboards, fork, ball, and seat post |

## 14.4 Conclusions

This review examines hybrid composites, focusing on their water absorption, thermo-mechanical, mechanical, flammability, and applications. Hybridization has become popular due to both the enhanced performance of the end products and the potential to get around the obstacles that prevent the use of natural fibers in technical structures. From an economic and environmental perspective, it is quite likely that a significant portion of natural fibers will be included in standard synthetic reinforced composite products. However, there is still inconsistency in the quality of hybrid composite products due to the uncertainty in the quality of the natural fibers, which solely depends on the growing environment and the level of maturity attained by the plant. The commercialization of natural fibers can unquestionably undergo a revolution when more attention is focused on controlling fiber quality. However, some of the limitations of the composites can be solved by using a second filler, either in the form of a micro or nano-filler. Engineering polymers may be eligible for high-end applications since the inclusion of flame-retardants increases their heat stability and flammability. It is important to note that hybrid composites made from natural fibers have a huge potential in making a wide range of industrial products.

## 14.5 Challenges and future directions

A research gap is identified in the fields such as NFRPC safety, endurance, and recycling in particular. Composite products when used in an open environment are more prone to various elements and biological attacks, thereby being at risk of degradation always. Composites made of natural fibers though by definition recyclable, are still facing recycling technological challenges.

## References

[1] Kiruthika A. A review on physico-mechanical properties of bast fiber reinforced polymer composites. J Build Eng. 2017;9:91–9. DOI: 10.1016/j.jobe.2016.12.003.
[2] Ahmad F, Choi HS, Park MK. A review: Natural fiber composites selection in view of mechanical, light weight, and economic properties. Macromol Mater Eng. 2015;300:10–24. DOI: 10.1002/mame.201400089.
[3] Saba N, Paridah MT, Abdan K, Ibrahim NA. Dynamic mechanical properties of oil palm nano filler/kenaf/epoxy hybrid nanocomposites. Constr Build Mater. 2016;124:133–8. DOI: 10.1016/j.conbuildmat.2016.07.059.
[4] Karthik A, Sampath PS. Analysis of thrust force in drilling cotton with bamboo blended fiber-reinforced composites using Box-Behnken methodology. Indian J Fiber Text Res. 2020;45(3):267–73. DOI: 10.56042/ijftr.v45i3.27238.

[5] Aruchamy K, Subramani SP, Palaniappan SK, Sethuraman B, Kaliyannan GV. Study on mechanical characteristics of woven cotton/bamboo hybrid reinforced composite laminates. J Mater Sci Technol. 2020;9(1):718–26. DOI: 10.1016/j.jmrt.2019.11.013.

[6] Mylsamy B, Palaniappan SK, Subramani SP, Pal SK, Aruchamy K. Impact of nanoclay on mechanical and structural properties of treated Coccinia indica fiber reinforced epoxy composites. J Mater Sci Technol. 2019;8(6):6021–8. DOI: 10.1016/j.jmrt.2019.09.076.

[7] Bhuvaneshwaran M, Subramani SP, Palaniappan SK, Pal SK, Balu S. Natural cellulosic fiber from Coccinia indica stem for polymer composites: Extraction and characterization. J Nat Fibers. 2021;18 (5):644–52. DOI: 10.1080/15440478.2019.1642826.

[8] Ramesh M, Rajeshkumar L, Balaji D, Sivalingam S. Mechanical and viscoelastic properties of wool composites. In: Thomas S (Ed.). Wool fiber reinforced polymer composites, Seiko Jose 2nd ed. Elsevier; 2022. 299–318. DOI: 10.1016/B978-0-12-824056-4.00001-7.

[9] Balaji D, Rajeshkumar L, Bhuvaneswari V, Sanjay MR, Suchart Siengchin G. Additive manufacturing of jute fiber reinforced polymer composites – a concise review of material forms and methods. Polym Compos. 2022. Online Published. DOI: 10.1002/pc.26789.

[10] Priyadharshini M, Balaji D, Bhuvaneswari V, Rajeshkumar L, Sanjay MR, Siengchin S. Fiber reinforced composite manufacturing with the aid of artificial intelligence – a state-of-the-art review. Arch Comput Methods Eng. 2022;1–14. DOI: 10.1007/s11831-022-09775-y.

[11] Ramesh M, Tamil Selvan M, Rajeshkumar L, Deepa C, Ahmad A. Influence of vachellia nilotica subsp. indica tree trunk bark nano-powder on properties of milkweed plant fiber reinforced Epoxy composites. J Nat Fibers. 2022. Online Published. DOI: 10.1080/15440478.2022.2106341.

[12] Puttegowda M, Rangappa SM, Jawaid M, Shivanna P, Basavegowda Y, Saba N. Potential of natural/synthetic hybrid composites for aerospace applications. In: Jawaid M, Thariq M (Eds). Sustainable composites for aerospace applications, Woodhead Publishing; 2018, 315–351. DOI: 10.1016/B978-0-08-102131-6.00021-9.

[13] Mylsamy B, Chinnasamy V, Palaniappan SK, Subramani SP, Gopalsamy C. Effect of surface treatment on the tribological properties of Coccinia indica cellulosic fiber reinforced polymer composites. J Mater Sci Technol. 2020;9(6):6423–34. DOI: 10.1016/j.jmrt.2020.11.100.

[14] Bhuvaneshwaran M, Sampath PS, Sagadevan S. Influence of fiber length, fiber content and alkali treatment on mechanical properties of natural fiber-reinforced epoxy composites. Polimery. 2019;64 (2):93–99. DOI: 10.14314/polimery.2019.2.2.

[15] Chinnasamy V, Subramani SP, Palaniappan SK, Mylsamy B, Aruchamy K. Characterization on thermal properties of glass fiber and kevlar fiber with modified epoxy hybrid composites. J Mater Sci Technol. 2020;9(3):3158–67. DOI: 10.1016/j.jmrt.2020.01.061.

[16] Samanta S, Muralidhar M, Signh TJ, Sarkar S. Characterization of mechanical properties of hybrid bamboo/GFRP and jute/GFRP composites. Mater Today: Proc. 2015;2:1398–405. DOI: 10.1016/j.matpr.2015.07.059.

[17] Mansor MR, Sapuan SM, Zainudin ES, Nuraini AA, Hambali A. Hybrid natural and glass fibers reinforced polymer composites material selection using analytical hierarchy process for automotive brake lever design. Mater Des. 2013;51:484–92. DOI: 10.1016/j.matdes.2013.04.072.

[18] Safri SNA, Sultan MTH, Jawaid M, Jayakrishna K. Impact behaviour of hybrid composites for structural applications: A review. Compos B Eng. 2017;133:112–21. DOI: 10.1016/j.compositesb.2017.09.008.

[19] Ridzuan MJM, Majid MSA, Afendi M, Mazlee MN, Gibson AG. Thermal behaviour and dynamic mechanical analysis of pennisetum purpureum/glass reinforced epoxy hybrid composites. Compos Struct. 2016;152:850–9. DOI: 10.1016/j.compstruct.2016.06.026.

[20] Romanzini D, Lavoratti A, Ornaghi Jr HL, Amico SC, Zattera AJ. Influence of fiber content on the mechanical and dynamic mechanical properties of glass/ramie polymer composites. Mater Des. 2013;47:9–15. DOI: 10.1016/j.matdes.2012.12.029.

[21] Bisaria H, Gupta MK, Shandilya P, Srivastava RK. Effect of fiber length on mechanical properties of randomly oriented short jute fiber reinforced epoxy composite. Mater Today: Proc. 2015;2:1193–9. DOI: 10.1016/j.matpr.2015.07.031.

[22] Gupta MK, Srivastava RK. Effect of sisal fiber loading on dynamic mechanical analysis and water absorption behaviour of jute fiber epoxy composite. Mater Today: Proc. 2015;2:2909–17. DOI: 10.1016/j.matpr.2015.07.253.

[23] Kureemun U, Ravandi M, Tran LQN, Teo WS, Tay TE, Lee HP. Effects of hybridization and hybrid fiber dispersion on the mechanical properties of woven flax-carbon epoxy at low carbon fiber volume fractions. Compos B Eng. 2018;134:28–38. DOI: 10.1016/j.compositesb.2017.09.035.

[24] Shanmugam D, Thiruchitrambalam M. Static and dynamic mechanical properties of alkali treated unidirectional continuous palmyra palm leaf stalk fiber/jute fiber reinforced hybrid polyester composites. Mater Des. 2013;50:533–42. DOI: 10.1016/j.matdes.2013.03.048.

[25] Ramana MV, Ramprasad S. Experimental investigation on jute/carbon fiber reinforced epoxy based hybrid composites. Mater Today: Proc. 2017;4:8654–64. DOI: 10.1016/j.matpr.2017.07.214.

[26] Akil HM, Santulli C, Sarasini F, Tirillo J, Valente T. Environmental effects on the mechanical behaviour of pultruded jute/glass fiber-reinforced polyester hybrid composites. Compos Sci Technol. 2014;94:62–70. DOI: 10.1016/j.compscitech.2014.01.017.

[27] Mokhothu TH, John MJ. Review on hygroscopic aging of cellulose fibers and their biocomposites. Carbohydr Polym. 2015;131:337–54. DOI: 10.1016/j.carbpol.2015.06.027.

[28] Arman NSN, Chen RS, Ahmad S. 2021. Review of state-of-the-art studies on the water absorption capacity of agricultural fiber-reinforced polymer composites for sustainable construction. Constr Build Mater. 302:124174. DOI: 10.1016/j.conbuildmat.2021.124174.

[29] Deshpande S, Rangaswamy T. A comparative study on dry sliding wear characteristics of Al2O3 and bone powder filled hybrid composites. J Met Mater Miner. 2016;4(2):164–80. DOI: 10.4236/jmmce.2016.42016.

[30] Zhang D, Milanovic NR, Zhang Y, Su F, Miao M. Effects of humidity conditions at fabrication on the interfacial shear strength of flax/unsaturated polyester composites. Compo B Eng. 2014;60:186–92. DOI: 10.1016/j.compositesb.2013.12.031.

[31] Panthapulakkal S, Sain M. Studies on the water absorption properties of short hemp–glass fiber hybrid polypropylene composites. J Compos Mater. 2007;41:1871–83. DOI: 10.1177/0021998307069900.

[32] Zhou J, Lucas JP. The effects of a water environment on anomalous absorption behavior in graphite/epoxy composites. Compos Sci Technol. 1995;53:57–64. DOI: 10.1016/0266-3538(94)00078-6.

[33] Balu S, Sampath PS, Bhuvaneshwaran M, Chandrasekar G, Karthik A, Sagadevan S. Dynamic mechanical analysis and thermal analysis of untreated Coccinia indica fiber composites. Polimery. 2020;65(5):357–62. DOI: 10.14314/polimery.2020.5.3.

[34] Azwa ZN, Yousif BF, Manalo AC, Karunasena W. A review on the degradability of polymeric composites based on natural fibers. Mater Des. 2013;47:424–42. DOI: 10.1016/j.matdes.2012.11.025.

[35] Ashik KP, Sharma RS, Guptha VLJ. Investigation of moisture absorption and mechanical properties of natural/glass fiber reinforced polymer hybrid composites. Mater Today: Proc. 2018;5:3000–7. DOI: 10.1016/j.matpr.2018.01.099.

[36] Xia C, Shi SQ, Cai L, Hua J. Property enhancement of kenaf fiber composites by means of vacuum assisted resin transfer molding (VARTM). Holzforschung. 2015;69:307–12. DOI: 10.1515/hf-2014-0054.

[37] Marques AR, de Oliveira Patricio PS, Dos Santos FS, Monteiro ML, de Carvalho Urashima D, de Souza Rodrigues C. Effects of the climatic conditions of the southeastern Brazil on degradation the fibers of coir geotextile: Evaluation of mechanical and structural properties. Geotext Geomembr. 2014;42:76–82. DOI: 10.1016/j.geotexmem.2013.07.004.

[38] Nagappan S, Subramani SP, Palaniappan SK, Mylsamy B. Impact of alkali treatment and fiber length on mechanical properties of new agro waste Lagenaria Siceraria fiber reinforced epoxy composites. J Nat Fibers. 2021. Online Published. DOI: 10.1080/15440478.2021.1932681.

[39] Bhuvaneshwaran M, Sampath PS, Balu S, Sagadevan S. Physicochemical and mechanical properties of natural cellulosic fiber from Coccinia indica and its epoxy composites. Polimery. 2019;64 (10):656–64. DOI: 10.14314/polimery.2019.10.2.

[40] Aruchamy K, Subramani SP, Palaniappan SK, Pal SK, Mylsamy B, Chinnasamy V. Effect of blend ratio on the thermal comfort characteristics of Cotton/Bamboo blended fabrics. J Nat Fibers. 2021;19 (1):105–14. DOI: 10.1080/15440478.2020.1731903.

[41] Mochane MJ, Mokhena TC, Mokhothu TH, Mtibe A, Sadiku ER, Ray SS, Ibrahim ID, Daramola OO. Recent progress on natural fiber hybrid composites for advanced applications: A review. Express Polym Lett. 2019;13(2):159–98. DOI: 10.3144/expresspolymlett.2019.15.

[42] Terzi E, Kartal S, Muin M, Hassanin A, Hamouda T, Kiliç A, Candan Z. Biological performance of novel hybrid green composites produced from glass fibers and jute fabric skin by the VARTM process. BioResources. 2018;13(1):662–77. DOI: 10.15376/biores.13.1.662-677.

[43] Tufan M, Akbas S, Aslan M. Decay resistance, thermal degradation, tensile and flexural properties of sisal carbon hybrid composites. Maderas Cienc Tecnol. 2016;18(4):599–606. DOI: 10.4067/S0718-221X2016005000052.

[44] Harnnecker F, Dos Santos Rosa D, Lenz DM. Bio -degradable polyester-based blend reinforced with curaua fiber: Thermal, mechanical and biodegradation behaviour. J Polym Environ. 2012;20:237–244. DOI: 10.1007/s10924-011-0382-5.

[45] Rasouli D, Dintcheva NT, Faezipour M, La Mantia FP, Farahani MRM, Tajvidi M. Effect of nano zinc oxide as UV stabilizer on the weathering performance of wood-polyethylene composite. Polym Degrad Stab. 2016;133:85–91. DOI: 10.1016/j.polymdegradstab.2016.08.004.

[46] Catto AL, Montagna LS, Almeida SH, Silveira RMB, Santana RMC. Wood plastic composites weathering: Effects of compatibilization on biodegradation in soil and fungal decay. Int Biodeterior Biodegradation. 2016;109:11–22. DOI: 10.1016/j.ibiod.2015.12.026.

[47] Pei B, Song G-Y, Lu C. The application of cone calorimeter on the study of burning performance of liquorices. Procedia Eng. 2014;71:291–95. DOI: 10.1016/j.proeng.2014.04.042.

[48] Dorez G, Taguet A, Ferry L, Cuesta J-ML. Phosphorous compounds as flame retardants for polybutylene succinate/flax biocomposite: Additive versus reactive route. Polym Degrad Stab. 2014;102:152–59. DOI: 10.1016/j.polymdegradstab.2014.01.018.

[49] Szolnoki B, Bocz K, Soti PL, Bodzay B, Zimonyi E, Toldy A, Morlin B, Bujnowicz K, Wladyka-Przybylak M, Marosi G. Development of natural fiber reinforced flame retarded epoxy resin composites. Polym Degrad Stab. 2015;119:68–76. DOI: 10.1016/j.polymdegradstab.2015.04.028.

[50] Alexander J, Churchill SJE. Mechanical characterization of baslat based natural hybrid composites for aerospace applications. IOP Conf Ser Mater Sci Eng. 2017;197(1):1–012008/8. DOI: 10.1088/1757-899X/197/1/012008.

[51] Reddy KS, Singla H. Optimization of woven jute/glass fiber-reinforced polyester hybrid composite solar parabolic trough collector. IOP Conf Ser Mater Sci Eng. 2017;222:1–012016/8. DOI: 10.1088/1757-899X/222/1/012016.

[52] Chikhradze NM, Marquis FDS, Abashidze GS. Hybrid fiber and nanopowder reinforced composites for wind turbine blades. J Mater Sci Technol. 2015;4:60–7. DOI: 10.1016/j.jmrt.2015.01.002.

[53] Hua C, Mazlan N. Investigation on the flexural properties and glass transition temperature of kenaf/epoxy composite filled with mesoporous silica for wind turbine applications. Pertanika J Sci Technol. 2017;25:1261–74.

[54] Xia C, Zhang S, Ren H, Shi SQ, Zhang H, Cai L, Li J. Scalable fabrication of natural-fiber reinforced composites with electromagnetic interference shielding properties by incorporating powdered activated carbon. Materials. 2015;9:1–9. DOI: 10.3390/ma9010010.

[55] Xia C, Ren H, Shi SQ, Zhang H, Cheng J, Cai L, Chen K, Tan HS. Natural fiber composites with EMI shielding function fabricated using VARTM and Cu film magnetron sputtering. Appl Surf Sci. 2016;362:335–40. DOI: 10.1016/j.apsusc.2015.11.202.

[56] Borba PM, Tedesco A, Lenz DM. Effect of reinforcement nanoparticles addition on mechanical properties of SBS/curaua fiber composites. Mater Res. 2014;17(2):412–19. DOI: 10.1590/S1516-14392013005000203.

[57] Xia C, Yu J, Shi SQ, Qiu Y, Cai L, Wu HF, Ren H, Nie X, Zhang H. Natural fiber and aluminum sheet hybrid composites for high electromagnetic interference shielding performance. Compos B Eng. 2017;114:121–27. DOI: 10.1016/j.compositesb.2017.01.044.

[58] Zhang D, Sun Y, Chen L, Zhang S, Pan N. Influence of fabric structure and thickness on the ballistic impact behavior of ultrahigh molecular weight polyethylene composite laminate. Mater Des. 2014;54:315–22. DOI: 10.1016/j.matdes.2013.08.074.

[59] Bandaru AK, Ahmad S, Bhatnagar N. Ballistic performance of hybrid thermoplastic composite armors reinforced with kevlar and basalt fabrics. Compos Part A Appl Sci. 2017;97:151–65. DOI: 10.1016/j.compositesa.2016.12.007.

[60] Yahaya R, Sapuan SM, Jawaid M, Leman Z, Zainudin ES. Quasi-static penetration and ballistic properties of kenaf–aramid hybrid composites. Mater Des. 2014;63:775–82. DOI: 10.1016/j.matdes.2014.07.010.

[61] Yahaya R, Sapuan SM, Jawaid M, Leman Z, Zainudin ES. Measurement of ballistic impact properties of woven kenaf–aramid hybrid composites. Measurement. 2016;77:335–43. DOI: 10.1016/j.measurement.2015.09.016.

[62] Zwawi M. A review on natural fiber bio-composites, surface modifications and applications. Molecules. 2021;26(2):404–32. DOI: 10.3390/molecules26020404.

[63] Bhagia, et al. Critical review of FDM 3D printing of PLA biocomposites filled with biomass resources, characterization, biodegradability, upcycling and opportunities for biorefineries. Appl Mater Today. 2021;24:101078. DOI: 10.1016/j.apmt.2021.101078.

[64] Keskisaari A, Karki T. The use of waste materials in wood-plastic composites and their impact on the profitability of the product. Resour Conserv Recycl. 2018;134:257–61. DOI: 10.1016/j.resconrec.2018.03.023.

[65] Mylsamy B, Palaniappan SK, Subramani SP, Pal SK, Sethuraman B. Innovative characterization and mechanical properties of natural cellulosic Coccinia indica fiber and its composites. Mater Test. 2020;62(1):61–7. DOI: 10.3139/120.111451.

[66] Sethuraman B, Subramani SP, Palaniappan SK, Mylsamy B, Aruchamy K. Experimental investigation on dynamic mechanical and thermal characteristics of Coccinia indica fiber reinforced polyester composites. J Eng Fibers Fabr. 2020;15:1–10. DOI: 10.1177/1558925020905831.

[67] Balla VK, Kate KH, Satyavolu J, Singh P, Tadimeti JGD. Additive manufacturing of natural fiber reinforced polymer composites: Processing and prospects. Compos B Eng. 174:106956. DOI: 10.1016/j.compositesb.2019.106956.

# Index

0D 8
1981 2
2D 8–9

abaca fibre 5
abrasion 260–261, 263–264
absorption 260–261, 268, 357, 360–365, 368
Acetate-cellulose-based nanofibers 90
Acetylation 178
achieving 8
acrylic acid 275, 294, 310, 314
activated 263, 269
activated carbon fibre 131, 134
actuators 172
adhesion properties 5
administration 273, 276–277, 281, 284, 296–298, 315, 322
adsorption 103, 105–107, 109, 112–117, 122, 124–125, 127, 131–132, 134–135
Adsorption capacitance 92
Advanced Fiber Materials 171–173, 179–180, 182–183
advancement 172, 186, 261, 270
Advantages 179–180
Agave Sisalana 2
agriculture 259, 262–263
air pollution control 89–91, 93, 99
Alkali treatment 4
Alkaline Treatment 177
alternative 267
application 359–360, 366
applications 149, 151, 154, 159, 165–166, 171–173, 175, 179–181
Aramid 342, 349
asbestos 191, 194
attapulgite 194
automotive 259, 267

bamboo 1–2, 4
batteries 10–11
benzoylation 176–177
billion 340
bioaerosols 89–90, 99
biocompatible 260, 266
biosensing 209
biosorption 104
blend 339
Boron fiber 196
breathability 262–263
brittle 2, 4

capacitance 153, 155–158, 160–161, 164
capacitors 152, 154, 159, 164, 166
carbon fibers 196
Carbon materials 156
carbon nanotubes 149, 151–152, 166
catalysis 1, 191, 201
cellulose 104, 106, 109, 113–115, 118–121, 129–130, 135, 191
Cellulose-based 90
Cellulosic century 2
challenges 180
charge transfer resistance 349
chemical resistance 260, 264
chemical vapor deposition 201
chemically modified 262
chemiluminescence 212
chemotherapy 327, 331
chitosan 90–91
chromatic devices 172, 181–182
cladding 203–204, 209, 214
CNTs 149–151, 154–155, 157–166
communication 171–172
composite 357–360, 362, 364–368
composite’s 339, 341
compressive strength 201
conductivity 6–10, 12
construction 259, 261, 265
contaminants 104, 118, 130
contamination 104, 118
continuous 341
Controlled-release 273, 293
conventional 149, 152, 163, 165
conversion 149–150, 154, 162–163, 165–166
core 193, 203–204, 209, 211–214
corrosion 339, 345–347
CTAB 7

degenerative 266
degradation 13
diffusion 279, 285–292, 295, 309, 316, 318, 322
Disadvantages 179–180

https://doi.org/10.1515/9783110992892-015

discolouration 268
Discrete 341
Dissolution 279, 285–286
drug administration 327
drug delivery 273–279, 281–285, 293–298,
  310–315, 319, 322–323
durability 9, 260–262, 268–269
dye 105–107, 130, 132
dyes and pigments 220
dynamic 5

E and S glass 199
efficiency 149, 152–153, 156, 162–163, 165–166
E-glass 192, 197
electrical 150, 152, 154, 159, 260, 271
electrical resistance 6–8
electrocatalysis 1, 10
electrochemical 1, 8, 12–13, 151–152, 159, 166, 345,
  348–349, 351
electrochromism 175
electrode materials 175
electrode potential 153
electrodes 152–153, 155–158, 161, 163, 166
electrolytes 13
electromagnetic radiation 202
electromagnetic waves 202
electronics 1, 191, 201, 211
electrospinning 176, 266
electrospinning method 274–275, 306
electrospun 273, 275–276, 298–300, 302–304,
  308–309, 313, 315–320, 322–323, 329
energy 149–150, 152–155, 157–166
energy harvesting 1, 6, 8, 171, 202
energy sources 149
energy storage materials 172
environment 357, 360, 364, 368
environmental 149, 152, 162
environmental applications 103–104, 134
environmental pollution 104, 219
environmentally 17
epoxy 5
excellent 7–8, 11–12
extracorporeal 260, 266

Faradaic reaction 152–153
feasible glass 4
fiber 149, 171–180, 182, 184–187, 259–262, 264–271,
  327–329, 331–335, 341
fiber cloths 98
fiber materials 17, 20, 24
fiber optical 192
Fiber-reinforced 184
fiber-reinforced polymer 339 *See*
fibers 273–274, 300–301, 303–304,
  306–309, 312–313, 320–322, 357–362,
  364–366, 368
fiber-shaped 172, 174–175, 180, 182, 187
fibre application 8
fibre based systems 130, 135
fibre materials 103
fibre synthesis 12
fibres 275
fibrillar angle 2, 5
filaments 191–192
firefighting 261, 263
flame resistance 261
flame retardancy 260
flexibility 1, 6–7, 9–12, 171, 175–176, 180, 187, 259,
  261, 270
Flexible Electronics 171
flexural strength 4–5
FRP 339–341, 347, 349, 351–352
FTIR 333
fullerene 12
Functional component 175
functionalized fibers 1
future devices 1, 10
Future scope 185

Ga 7
generation 149–150, 165
Glass fibers 192
graphene oxide 176
graphite 6

halloysite 194
harsh environments 6, 10
hazardous 89–90, 96, 99
healability 175
healthcare 259–260, 265–267
heavy metal 103, 113–118, 125
helix 11
high energy 12
higher conductivity 6
hybrid composite 358, 360, 364–365, 368
hybridization 3

hydrogen production 205
hydrothermal 10

immunosensor 210
impedance 348, 351
indoor environments 89–91, 99
inherently 9
insulating 261
insulation 259, 263, 269–270
insulators 199
interfacial charge transfer (ICT) 205
IR filters 191, 201

jute fibre 4

Kevlar 49 199
kinetics 273, 277–278, 284, 288–289, 297, 316, 322
kraft pulps 194

laminate 196
lignin 194
lignocellulosic 18, 21
lignocellulosic biomass 105–106
Li-ion 11
lingo-cellulosic 2, 5
liquid metals 7, 12
lithographically 7
low-cost 196

Matrix 343–344
MAX 9
mechanical 2, 4–6, 8–12, 260, 268–269
membrane 123, 125, 129, 134
metal 340, 344–345, 348–349, 351
Metallic fibers 192
methylene blue 205–206
micro-encapsulation 261
micro-fibrillar 2
microfibrillar angle 5
micrometers 273
morphology 8
multi walled carbon nanotubes 151
multi-cellulose 3
multifunctional 171
Multi-walled 11
MWCNTs 8, 12, 176
MWNTs 154–158, 160
MXenes 8–9, 12

nanocomposites 149, 351
Nanofibers 171, 273, 275, 298, 309, 315–316, 319
nanofibres 1, 8–9
nanoflakes 6
nanotechnology 149, 164, 261
nanowires 6–7
Natural 17–18, 20–21, 24, 26–27
natural fiber 93
natural fibres 1–3
natural jute fiber-based nanomaterials 92
noble 6
noise adsorption 93

oil spills 109
optical communication 203, 211
optical fibers 1, 203
optics 192, 198, 202, 210, 215
optoelectronic devices 211
organic pollutant removal 205

Patented Works 183
perovskite solar cell 211
petrochemicals 194
pharmacodynamics 273, 277
pharmacokinetics 273, 277, 281, 284
phenol formaldehyde 195
phenylboronic acid 210
photocatalysis 202, 205, 219, 221–225, 232, 236, 242–243, 245
photocurrent 213–214
photoelectronic 202
photonics 1, 191, 201–202, 210, 215
photonics sensing 173
photoreduction 206
photoresponsivity 214
photosensing 211
photosensitivity 214
photosynthetic processes 220
physical deposition 7
plasma 261, 265
plasma technology 261
plastics 259
playing 10
pollutants 103–105, 113, 118, 121, 123, 127, 130, 133, 135
pollution 89–93, 96, 99, 103, 109, 124
polyacrylonitrile 199
polyacrylonitrile-based nanofibers 90

polyamides 195
polyester fibers 198
polyethylene-based nanofibers 90
poly(glycolic acid) 275, 317
poly(lactic-*co*-glycolic acid (PLGA) 275
poly(L-lactic acid) 275
polymer 17, 20–21, 25
polymeric matrices 5
polyurethane fibers 195
polyvinyl chloride 11
potential 171–172, 175, 181, 185, 187
potentiality 9
potentiodynamic 351
*p*-phenylene diamine 199
production 10, 13
progress 3
properties 149–151, 154–155, 158, 163–164
pseudo-capacitor 153
pultrusion 175
purification 123, 130–131, 219–220, 222, 244–245, 259

RADAR 8
radiation 13
radiotherapy 327
rayon 192, 194
refractive index 203
reinforced plastics 2, 4
resistivity 7

self-cleaning 13
self-healing 175, 186
SEM 329, 333
semiconducting 266
semiconductor 173
Semiconductors 205
sensors 1, 191, 201, 209–210, 212–213
*shrinking our world* 1
silanes 177
silica 199
single-walled carbon nanotubes 151
sintering 7
sisal fibre 2, 5
smart textile 259
solar cells 172, 186
spandex 195
stimuli-responsive 309
storage 149–150, 152–154, 158–160, 163, 165–166
storage properties 185
storage technology 171, 180, 182
strength 2, 4–5, 6, 9–10, 12, 191, 194, 196–197, 199–200, 211, 358, 360–362, 364–366
strength–weight ratios 261
stretchability 172, 175–176
stretchable 10
stretchable batteries and supercapacitors 172
Sugar cane 6
suitable 3, 8
supercapacitors 149–150, 152, 154, 156, 159, 164, 166
surface energy 6
surface functionalities 156
surface plasmon resonance 209
surface tension 6
susceptible 12
sustained-release 283
swellable 279, 288
swelling 288
SWNTs 154–158, 160–161
synthesis 151, 154, 156, 159
synthesized 6–7, 9
synthetic 17–18
synthetic fibres 1, 3, 6, 12

target 274, 276, 278, 284, 297, 310–311, 317
technical textiles 259–261, 265–267, 270–271
techniques 339, 347, 352
TENGs 11
tensile 4–5
tensile strength 260, 263
terephthaloyol chloride 199
textile 259–262, 264–266, 270–271
thermal 259–260, 262–263, 266
thermal load 262
Thermo Mechanical 360
thermomechanical pulp 194
thermoplastic 195, 198
$Ti_3C_2$ 9
$TiO_2$ 9, 11, 205
total internal reflection 204
transition metal dichalcogenides (TMDs) 219
treatment 177–179, 358, 360, 364
Triboelectric Nanogenerator 11
tumor 327, 329, 332, 334–335

vinyl ester 197
volatile organic compounds 89–90, 96, 98–99

wastewater 104–106, 113–114, 116, 119, 123, 131–132, 134
water 1, 4, 7–8, 10
water purification 1
water repellence 261
weak forces 333

XRD 333

ZIF-8@$SiO_2$ nanofiber membrane 96